Identifying alterations in adipose tissue-derived islet GPCR peptide ligand mRNAs in obesity: implications for islet function

Ashik, Tanyel

Awarding institution:
King's College London

Identifying alterations in adipose tissue-derived islet GPCR peptide ligand mRNAs in obesity: implications for islet function

Tanyel Ashik

Department of Diabetes
King's College London

A thesis submitted for the degree of
Doctor of Philosophy

September 2023

Dedication

♡

This thesis is wholeheartedly dedicated to my beloved parents, Tülin and Gürkan, whose inspirational strength and sacrifice, and endless love, support and encouragement have made my every success possible.

Sizi çok seviyorum.

Acknowledgements

I would like to thank my supervisor, Professor Shanta J. Persaud, who has been a constant source of guidance, support, and mentorship since my arrival at King's as an undergraduate and as her personal tutee. Since that day in 2014, she has shaped me into the researcher I am today. Shanta has been an incredible role model – a strong and formidable leader in science – whom I will continually look up to for the remainder of my career. Special thanks to Doctor Patricio Atanes for not only teaching me all the ways of being a good scientist, inside and outside of the lab, but for being the most beautiful friend.

I extend my utmost gratitude to all members of the Department of Diabetes, past and present. Thank you to Doctor Klaudia Toczyska for introducing and teaching me new techniques with such patience, and for always bringing a warm and friendly presence in the department. Thank you to Doctor Vivian Lee for collecting adipose tissue samples during the coronavirus pandemic closures. Thank you to Doctor Ed Olaniru and Doctor Matilda Passmore (Kennard) for maintaining high-fat diet mouse cohorts, and to Doctor Tim Pullen and Maya Wilson for maintaining the *db/db* mouse cohort, all for the collection of adipose tissue samples used in this thesis. Thank you to Doctor Naila Haq for her partnership and help during mouse islet proliferation experiments, and for always having kind and encouraging words to say. Thank you to Zekun Lye for his help with bioinformatic data interpretations and accepting human fat samples on my behalf. Thank you to Doctor Hannah Rosa for fighting all "fires" in the department (keeping Jeremy the poltergeist away), for being the best Head of Elf and Safety, and for always making time for our very important business meetings (walkies). Thank you to the members of my thesis progression committee, Doctor Aileen King, Doctor Tim Pullen, and Doctor Paul Caton, for helping ensure my continued development throughout my PhD.

Many thanks to Mitacs and UKRI for honouring me with the Globalink Research Award to undertake an international research placement in Canada. I would like to thank Doctor Gareth Lim for inviting me to join his lab at the Centre de recherche du CHUM (CRCHUM) to advance my expertise in adipose tissue biology. I also have great appreciation for the members of the Lim lab, Frederic Abou Azar, Doctor Sabri Ahmed Rial, Frédéric Paré, and Siyi He, who welcomed and supported me so warmly. Thank you to Doctor Catherine Arden for her gift of MIN6 β-cells, to Doctor Edward Westcott for providing human adipose tissue samples, and to Doctor Bryan Roth for his gift of HTLA cells. I thank the Medical Research Council for funding my studies and making this all possible.

Lastly, I would like to thank my beautiful family – my mum and dad, my brother, Tekin, and my partner, Adam – as well as my amazing friends (you know who you are!) I love you all deeply for sustaining me and making this PhD an experience I will cherish forever.

Abstract

In addition to acting as an energy reservoir, white adipose tissue is a vital endocrine organ involved in the modulation of cellular function and the maintenance of metabolic homeostasis through the synthesis and secretion of peptides, known as adipokines. It is known that some of these secretory peptides play important regulatory roles in glycaemic control by acting directly on islet β-cells or on insulin-sensitive tissues. Excess adiposity causes alterations in the circulating levels of some adipokines which, depending on their mode of action, can have pro-inflammatory, pro-diabetic or anti-inflammatory, anti-diabetic properties. Some adipokines that are known to act at β-cells have actions that are transduced by binding to G protein-coupled receptors (GPCRs). This large family of receptors represents ~35% of all current drug targets for the treatment of a wide range of diseases, including type 2 diabetes (T2D). Islets express ~300 GPCRs, yet only one islet GPCR is currently directly targeted for T2D treatment. This deficit represents a therapeutic gap that could be filled by the identification of adipose tissue-derived islet GPCR peptide ligands that increase insulin secretion and overall β-cell function. Thus, by defining their mechanisms of action, there is potential for the development of new pharmacotherapies for T2D. Therefore, this thesis describes experiments which aimed to compare the expression profiles of adipose tissue-derived islet GPCR peptide ligand mRNAs under lean and obese conditions, and to characterise the functional effects of a selected candidate of interest on islet cells.

Visceral fat depots were retrieved from high-fat diet-induced and genetically obese mouse models, and from human participants. Fat pads were either processed as whole tissue, or mature adipocyte cells were separated from the stromal vascular fraction (SVF) which contains several other cell populations, including preadipocytes and macrophages. The expression levels of 155 islet GPCR peptide ligand mRNAs in whole adipose tissue or in isolated mature adipocytes were quantified using optimised RNA extraction and reverse transcription-quantitative polymerase chain reaction (RT-qPCR) protocols. Comparisons between lean and obese states in mice models and humans revealed significant modifications in the expression levels of several adipokine mRNAs. As expected, mRNAs encoding the positive control genes, *Lep* and *AdipoQ* were quantifiable, with the expression of *Lep* mRNA increasing and that of *AdipoQ* mRNA decreasing in obesity. Expression of *Ccl4* mRNA, encoding chemokine (C-C motif) ligand 4, was significantly upregulated in whole adipose tissue across all models of obesity compared to their lean counterparts. This coincided with elevated circulating Ccl4 peptide levels. This increase was not replicated in isolated mature adipocytes, indicating that the source of upregulated *Ccl4* expression in obesity was the SVF of adipose tissue. Based on this significant increase in *Ccl4* mRNA expression within visceral fat and its undetermined effects on β-cell function, Ccl4 was selected for further investigation in MIN6 β-cells and mouse islets.

PRESTO-Tango β-arrestin reporter assays were performed to determine which GPCRs were activated by exogenous Ccl4. Experiments using HTLA cells expressing a protease-tagged β-arrestin and transfected with GPCR plasmids of interest indicated that 100ng/mL Ccl4 significantly activated Cxcr1 and Cxcr5, but it was not an agonist at the previously identified Ccl4-target GPCRs Ccr1, Ccr2, Ccr5, Ccr9 and Ackr2. RNA extraction and RT-qPCR experiments using MIN6 β-cells and primary islets from lean mice revealed the expression of Cxcr5 mRNA in mouse islets, but it was absent in MIN6 β-cells. The remaining putative Ccl4

receptors (*Ccr1*, *Ccr2*, *Ccr5*, *Ccr9*, *Cxcr1* and *Ackr2*) were either absent or present at trace levels in mouse islets and MIN6 β-cells.

Recombinant mouse Ccl4 protein was used for functional experiments at concentrations of 5, 10, 50 and 100ng/mL, based on previous reports of biological activities at these concentrations. Trypan blue exclusion testing was initially performed to assess the effect of exogenous Ccl4 on MIN6 β-cell viability and these experiments indicated that all concentrations (5-100ng/mL) were well-tolerated. Since β-cells have a low basal rate of apoptosis, cell death was induced by exposure to the saturated free fatty acid, palmitate, or by a cocktail of pro-inflammatory cytokines (interleukin-1β, tumour necrosis factor-α and interferon-γ). In MIN6 β-cells, Ccl4 demonstrated concentration-dependent protective effects against palmitate-induced and cytokine-induced apoptosis. Conversely, while palmitate and cytokines also increased apoptosis of mouse islets, Ccl4 did not protect islets from either inducer. Quantification of bromodeoxyuridine (BrdU) incorporation into β-cell DNA indicated that Ccl4 caused a concentration-dependent reduction in proliferation of MIN6 β-cells in response to 10% fetal bovine serum (FBS). In contrast, immunohistochemical quantification of Ki67-positive mouse islet β-cells showed no differences in β-cell proliferation between control- and Ccl4-treated islets. Whilst the number of β-cells and δ-cells were unaffected, α-cells were significantly depleted by Ccl4 treatment. Exogenous Ccl4 had no effect on nutrient-stimulated insulin secretion from both MIN6 β-cells and primary mouse islets. The 3T3-L1 preadipocyte cell line was used to assess potential Ccl4-mediated paracrine and/or autocrine signalling within adipose tissue. Ccl4 did not alter the mRNA expression of *Pparγ*, a master regulator of adipocyte differentiation, but did significantly downregulate the mRNA expression of the crucial adipogenic gene, adiponectin. Oil Red O staining and Western blotting were performed to assess lipid accumulation, and insulin and lipolytic signalling, respectively, and these experiments indicated that the observed Ccl4-induced decrease in adiponectin expression failed to correlate with any changes in adipocyte function.

In summary, these data demonstrated anti-apoptotic and anti-proliferative actions of the adipokine, Ccl4, on MIN6 β-cells that were not replicated in mouse islets. The absence of any anti-apoptotic, insulin secretory and/or pro-proliferative effects of Ccl4 in islet β-cells suggests that it is unlikely to play a role in regulating β-cell function via crosstalk between adipose tissue and islets. The divergent functional effects highlight that whilst MIN6 cells are a useful primary β-cell surrogate for some studies, primary islets should always be used to confirm physiological relevance. On the other hand, significant α-cell depletion following Ccl4 treatment suggests a cell-specific function within the islets. Furthermore, Ccl4 impaired adiponectin mRNA expression in adipocytes, although, how adipocyte function is affected as a result requires further investigation. Collectively, these data have contributed increased understanding of the role of obesity in modifying the expression of adipose tissue-derived islet GPCR peptide ligands.

List of abbreviations

$[Ca^{2+}]_i$	Intracellular calcium ion concentration
2D	2-dimensional
3D	Three-dimensional
AA	Arachidonic acid
AB	Antibody
AC	Adenylate cyclase
ACh	Acetylcholine
Actb	β-actin
ADD1/SREBP1	Adipocyte determination and differentiation-dependent factor 1
AdipoQ	Adiponectin
AE	Adverse event
AG	Antigen
aGPCR	Adhesion G protein-coupled receptor
AKAP	A-kinase anchoring protein
ALDH1A3	Aldehyde dehydrogenase 1A3
AMPK	AMP-activated protein kinase
AP	Action potential
APAF-1	Apoptotic protease-activating factor-1
APC	Antigen-presenting cell
APJ	Apelin receptor
ARC	Arcuate nucleus
ASC	Adipose tissue-derived stromal cell
AST	Astaxanthin
Bcl-2	B-cell lymphoma-2
B-CLL	B-chronic lymphocytic leukemia
BMI	Body mass index
BrdU	5-bromo-2′-deoxyuridine
BRET	Bioluminescence resonance energy transfer
BSA	Bovine serum albumin
C/EBP	CCAAT/enhancer binding protein
CA	Catecholamine
Ca^{2+}	Calcium ion
CaMK	Ca2+/calmodulin-dependent protein kinase
cAMP	Cyclic AMP
CaR	Calcium receptor
CB1R	Cannabinoid type 1 receptor
CBP	CREB-binding protein
CCL	Chemokine (C-C motif) ligand
cDNA	Complementary DNA
Chm3/M3R	Carbachol receptor
CHO	Chinese hamster ovary
CNS	Central nervous system
CPM	Counts per minute
CREB	cAMP-responsive element binding protein
CTRP	Complement 1Q factor/TNF-related peptide
CVD	Cardiovascular disease
Cx36	Connexin-36
CXCL	Chemokine (C-X-C motif) ligand

Cyt c	Cytochrome c
DAG	Diacylglycerol
dATP	Deoxyadenosine triphosphate
DEX	Dexamethasone
dH_2O	Distilled water
DISC	Death-inducing signalling complex
DM	Diabetes mellitus
DMEM	Dulbecco's modified Eagle's medium
DMH	Dorsomedial hypothalamus
DMSO	Dimethyl sulfoxide
dNTP	Deoxynucleoside triphosphate
DPP-4	Dipeptidyl peptidase-4
DTT	Dithiothreitol
eCB	Endocannabinoid
ECM	Extracellular matrix
EDTA	Ethylenediaminetetraacetic acid
ELISA	Enzyme-linked immunosorbent assay
EPAC	Exchange protein activated by cyclic AMP
ER	Endoplasmic reticulum
ERK	Extracellular signal-regulated protein kinase
ETC	Electron transport chain
EV	Extracellular vesicle
Ex4	Exendin-4
FACS	Fluorescence-activated cell sorting
FADD	FAS-associated death domain protein
FAS	Fatty acid synthase
FBS	Foetal bovine serum
FFA	Free fatty acid
FoxM1	Foxhead box M1
FoxO1	Forkhead box protein O1
FRET	Fluorescence resonance energy transfer
GCGR	Glucagon receptor
GCK	Glucokinase
GD	Gestational diabetes
GH	Growth hormone
GI	Gastrointestinal
GIP	Glucose-dependent insulinotropic peptide
GLP-1	Glucagon-like peptide-1
GLP-1RA	Glucagon-like peptide-1 receptor agonists
GLUT	Glucose transporter
GPCR	G protein-coupled receptor
GRK	GPCR kinase
GST	Glutathione S-transferase
GWAS	Genome-wide association studies
HbA1c	Glycated haemoglobin A1c
HBSS	Hanks' Balanced Salt Solution
HIV	Human immunodeficiency virus
HLA	Human leukocyte antigen
HNF	Hepatocyte nuclear factor
HNF1A	Hepatocyte nuclear factor 1-α
HOMA-IR	Homeostasis model assessment for insulin resistance

HRP	Horseradish peroxidase
HSL	Hormone-sensitive lipase
I^-	Iodide ion
I^{125}	Iodine-125
IBMX	3-isobutyl-1-methylxanthine
ICDI	Ca2+-dependent inactivation
IFN-γ	Interferon-γ
IGF-1R	Insulin-like growth factor 1 receptor
IL-1R	Interleukin-1 receptor
IL-1RA	Iinterleukin-1 receptor antagonist
IL-1β	Interleukin-1β
iNOS	Nitric oxide synthase
IP_3	Inositol 1,4,5-triphosphate
IR	Insulin receptor
IRS	Insulin receptor substrate
JAK2	Janus kinase 2
JNK	JUN N-terminal kinase
K^+	Potassium ion
K_{ATP}	ATP-sensitive potassium
KIC	α-ketoisocaproic acid
KRBH	Krebs-Ringer bicarbonate HEPES
L	Litre
LDHA	Lactate dehydrogenase
Lep	Leptin
LEP-R	Leptin receptor
LPA	Lysophosphatidic acid
LPAR	Lysophosphatidic acid receptor
LPL	Lipoprotein lipase
LPS	Lipopolysaccharide
m	Milli
M	Molar
Mafa	V-maf musculoaponeurotic fibrosarcoma oncogene homolog A
MAPK	Mitogen-activated protein kinase
MB	Maximum binding
MC4R	Melanocortin-4 receptor
MCP-1	Monocyte chemoattractant protein-1
MEM	Minimum Essential Media
MHC	Major histocompatibility complex
MIP-1β	Macrophage inflammatory protein-1β
MODY	Maturity-onset diabetes of the young
MOMP	Mitochondrial outer membrane permeabilisation
MyD88	Myeloid differentiation factor-88
n	N-number
Na^+	Sodium ion
NCS	Newborn calf serum
Neurog3	Neurogenin-3
NF-κB	Nuclear factor-κB
NK	Natural killer
nm	Nanometre
NOR	Non-obese diabetes-resistant
NSB	Non-specific antigen binding

OEA	Oleoylethanolamide
ORO	Oil Red O
PAD	Peripheral arterial disease
Pax4	Paired box 4
PBS	Phosphate Buffered Saline
PCK1	Phosphoenolpyruvate carboxykinase 1
PCOS	Polycystic ovarian syndrome
Pdx1	Pancreatic duodenal homeobox gene 1
PFA	Paraformaldehyde
PGC-1α	Peroxisome proliferator-activated receptor-γ co-activator-1α
PI3K	Phosphatidylinositol 3-kinase
PIP_2	Phosphatidylinositol 4,5 bisphosphate
PKA	Protein kinase A
PKB	Protein kinase B
PKC	Protein kinase C
PL	Placental lactogen
PLA_2	phospholipase A2
PLC	Phospholipase C
PMN	Polymorphonuclear
PP	Pancreatic polypeptide
PPARγ	Peroxisome proliferator-activated receptor-γ
PRESTO	Parallel Receptor-ome Expression and Screening via Transcriptional Output
PRL	Prolactin
PVH	Paraventricular hypothalamus
RAS	Renin-angiotensin system
RCT	Randomised controlled trial
RLU	Relative luminescence unit
ROS	Reactive oxygen species
RP	Reserve pool
RPMI	Roswell Park Memorial Institute
RRP	Rreadily releasable pool
RT	Reverse transcription
S.E.M	Standard error of the mean
SAA	Serum amyloid A
SAPK	Stress-activated protein kinase
SARS-CoV-2	Severe acute respiratory syndrome coronavirus 2
SNARE	Soluble N-ethylmaleimide-sensitive factor attachment protein receptor
SNP	Single nucleotide polymorphism
SSTR	Somatostatin receptor
STZ	Streptozotocin
SUR	Sulphonylurea
SV40	Simian virus 40
SVF	Stromal vascular fraction
T	Total
T1D	Type 1 diabetes
T2D	Type 2 diabetes
Tango	Transcriptional activation following arrestin translocation
TEMED	Tetramethylethylenediamine
TEV	Tobacco Etch Virus
TLR4	Toll-like receptor 4
TMB	Tetramethylbenzidine

TNF-α	Tumour necrosis factor-α
tTA	Tetracycline transactivator
TZD	Thiazolidinedione
UCP1	Uncoupling protein 1
UKRI	UK Research and Innovation
UPR	Unfolded protein response
UV	Ultraviolet
VEGF	Vascular endothelial growth factor
α	Alpha
α-MSH	α-melanocyte-stimulating hormone
β	Beta
β-ME	β-mercaptoethanol
γ	Gamma
δ	Delta

Table of contents

List of tables

List of figures

Chapter 1: Introduction

1.1 Diabetes mellitus

Diabetes mellitus (DM) is a group of complex metabolic diseases characterised by a state of abnormally high plasma glucose levels, known as hyperglycaemia. This results from dysfunction in the secretion and/or action of insulin – a peptide hormone produced by pancreatic β-cells to reduce plasma glucose levels. Chronic hyperglycaemia fuels the development of severe microvascular and macrovascular complications, such as diabetic nephropathy, neuropathy, and retinopathy, and cardiovascular disease (CVD), which are main contributors to diabetic-related morbidity and mortality (Banday et al., 2020). For this reason, glycaemic control is a primary focal point for diabetes treatment and management. Sustained hyperglycaemia can be detected by measuring the level of glycated haemoglobin (HbA1c) within the blood. HbA1c reflects the average glycaemic level across the preceding 8 to 12 weeks, and, therefore, can be used as both a diagnostic test for diabetes and as an indication of glycaemic management (Nathan et al., 2007). Non-diabetic individuals fall within a HbA1c range of 4.0-5.6%, whilst those with prediabetes have HbA1c levels of 5.7-6.4%, and levels of 6.5% or greater indicate a diabetic state (Sherwani et al., 2016).

The latest estimation of global prevalence shows 537 million adults are currently affected by diabetes; this is expected to rise to 783 million by 2045 equating to an estimated $845 billion in annual health expenditure on diabetes (Kumar et al., 2023; Williams et al., 2020). Thus, the disease burden of diabetes and its related complications is a growing health challenge that highlights an urgent need for more efficacious and sustainable prevention, treatment, and management strategies.

Diabetes varies in its aetiology, pathogenesis, and presentation, and can be classed into five main types: type 1 diabetes (T1D), type 2 diabetes (T2D), gestational diabetes (GD), monogenic diabetes, and secondary diabetes.

1.1.1 Type 1 diabetes

1.1.1.1 Aetiology

Type 1 diabetes (T1D) is characterised by the autoimmune, T-cell-mediated destruction of β-cells leading to insulin deficiency and hyperglycaemia. Its exact aetiology remains unclear, however, a polygenic component is widely recognised with a strong link to human leukocyte antigen (HLA) loci (Giwa et al., 2020). The immune system uses the HLA complex, also known as the major histocompatibility complex (MHC), as a recognition system to discriminate between foreign invaders, such as viruses and bacteria, and self-peptides. The complex consists of genes that encode cell-surface peptides, or antigens, for presentation to immune cells. The genes are categorised into three groups: class I, class II, and class III (Liu et al., 2021). According to genome-wide association studies (GWAS), single nucleotide polymorphisms (SNPs) within HLA class II accounts for 50% of the genetic risk for T1D development (Warshauer et al., 2020). This is because of their role in insulin autoantibody production, T-cell activation, and macrophage infiltration into the islets (Burrack et al., 2017).

Environmental factors are also thought to be implicated in the individual risk of T1D development. For example, some studies have identified certain viral infections, including Coxsackie virus, enterovirus, and SARS-CoV-2, as influencing factors on T1D incidence (Rahmati et al., 2022; Zorena et al., 2022). Other potential risk factors include vitamin D deficiency (Bener et al., 2009), exposure to air pollution (Elten et al., 2020; Hathout et al., 2006; Malmqvist et al., 2015), cold seasons (Moltchanova et al., 2009) and high latitude (Weng et al., 2018). Conversely, breastfeeding (Lampousi et al., 2021), a delayed introduction of gluten, fruit and cow's milk (Lampousi et al., 2021), and polyunsaturated fatty acid supplementation (Norris et al., 2007; Stene et al., 2000) may be protective.

1.1.1.2 Epidemiology

Approximately 8.4 million people were living with T1D worldwide in 2021 and this is expected to rise to between 13.5-17.4 million by 2040 (Gregory et al., 2022). T1D is the most common type of diabetes affecting children and young people (Dowling, 2021), however, onset can occur at any age and common misdiagnosis of adults can lead to inappropriate treatment and life-threatening diabetic complications (Muñoz et al., 2019; Thomas et al., 2019). There is considerable geographic variation in the incidence of T1D with the highest observed in Northern Europe, Australia, New Zealand and North America, and the lowest reported in Melanesia, Western Africa and South America for the 0-14-year age group (Gomber et al., 2022). High-income countries show greater incidence rates compared to low- and middle-income countries, but this observation may be inaccurate due to deficits in published studies for incidences in the latter countries (Gomber et al., 2022).

1.1.1.3 Pathogenesis

As previously described in Section 1.1.1.1, mutations within HLA Class II genes confer the greatest genetic risk for the development of T1D. Class II molecules are expressed mainly on antigen-presenting cells (APCs), such as B cells, dendritic cells, macrophages and monocytes (Choo, 2007). In T1D, insulin autoantigens are generated, leading to the activation of CD4+ T cells followed by CD8+ T cells. The actions of CD8+ T cells cause direct β-cell damage through the production of pro-inflammatory cytokines, such as tumour necrosis factor-α (TNF-α) and interferon-γ (IFN-γ). Islet inflammation is exacerbated via recruitment of islet-resident macrophages and other immune cells. Their release of additional cytokines propagates β-cell destruction as a positive feedback loop is stimulated (Calderon et al., 2008). For example, IFN-γ can induce β-cell release of CXCL10, a chemokine which promotes further T-cell infiltration and autoimmune islet destruction (Bender et al., 2017; Calderon et al., 2008). This T-cell-mediated pathology is known as insulitis and is present in 85% of patients alongside a 70-80% reduction in β-cell mass at diagnosis (Cnop et al., 2005; Hackett et al., 2013). Resulting insulin deficiency and hyperglycaemia cause common clinical presentations, such as polydipsia (excessive thirst), polyuria (excessive urine production) and weight loss (Kahanovitz et al., 2017).

1.1.1.4 Treatment

Administration of exogenous insulin is the main therapy for T1D. Since the use of animal-sourced insulin, human analogues which mimic the biological actions of insulin have emerged. These are delivered daily via subcutaneous injection or insulin infusion pump. The

pharmacokinetics of available insulin analogues vary with aspart, lispro and humulin being rapid/short-acting, and levemir and lantus being long-acting (Pathak et al., 2019). The action of short-acting insulin analogues peaks between 20-30 minutes and must be administered three times a day. Long-acting insulin analogues have a more prolonged pharmacodynamic action that provides a constant insulin level over 24-36 hours (Pathak et al., 2019). This provides patients with a more convenient delivery option as only once-daily injections are required. Insulin replacement therapy may be complemented with adjunctive therapies. Metformin, for example, reduces the insulin dose requirement likely through its insulin-sensitising and glucose-lowering effects (see Section 1.1.2.4) (Priya & Kalra, 2018). A newly approved humanised monoclonal antibody, teplizumab, has also proven effective in delaying the onset of T1D and reducing the use of exogenous insulin by decreasing T-cell activation, T-cell replication, and cytokine release (Herold et al., 2023). As well as pharmacological strategies, islet transplantation, artificial pancreas and stem cell therapies are under continuous development (Inoue et al., 2021). These present major challenges, immunosuppression being a peak of concern, but further research may pave the way for new promising treatments for T1D.

1.1.2 Type 2 diabetes

1.1.2.1 Aetiology

T2D is a progressive disease with both peripheral insulin resistance and β-cell failure at the core of the underlying pathophysiology (Chaudhury et al., 2017). Several factors have been identified as major drivers for the current T2D epidemic: lifestyle factors (diet, physical activity, smoking, alcohol consumption, etc.); an ageing population; intrauterine environment and developmental components; socioeconomic factors and Westernisation; and genetic predisposition which governs susceptibility of T2D on an individual level (Zheng et al., 2018). Obesity remains the most significant risk factor for T2D development, with 90% of diabetic patients classified as overweight or obese (Grant et al., 2021). This is further supported by the inverse linear relationship between body mass index (BMI) and the age of diabetes diagnosis (Hillier & Pedula, 2003), and adiposity being a strong predictor of T2D risk (Wang et al., 2005). As noted above, genetic factors can strongly influence the individual risk of T2D (Fuchsberger et al., 2016). However, despite the fact that T2D is highly heritable, only a fraction of this can be explained by known genetic variants, perhaps implicating rare variants beyond the detectable limit even with large-scale genomic studies, or epigenetic factors (Fuchsberger et al., 2016).

1.1.2.2 Epidemiology

T2D accounts for the majority of global diabetes diagnoses contributing over 95% of the total diabetes prevalence (World Health Organisation, 2023). The disease was once associated with adult onset, however, the frequency of paediatric cases is growing rapidly in parallel with childhood obesity (Wu et al., 2022). Whilst the prevalence of T2D is rising worldwide, the rate increase is greater in developed countries within Western Europe, possibly reflecting the Western dietary pattern and sedentary lifestyle associated with these regions (Khan et al., 2020). On the other hand, low- and middle-income countries, such as India and China, also display upward trends in diabetes incidence and mortality (Liu et al., 2022). Several public health challenges may be contributing to the increased disease burden in these countries,

including limited access to resources, lower educational attainment, and environmental risk factors (Khan et al., 2020; Liu et al., 2022). Overall, the epidemiology of T2D is governed by genetics and the environment, with both interacting to contribute to disease prevalence.

1.1.2.3 Pathogenesis

The progression of T2D reflects the slow decline in pancreatic β-cell function and its eventual inability to secrete sufficient insulin in response to peripheral insulin resistance (Chaudhury et al., 2017) (Figure 1). The development of T2D begins with excess accumulation of adipose tissue. The risk of diabetes development correlates with not only the presence but also the duration of excess adiposity (Torgerson et al., 2004). This fact establishes a simple but definitive link between fat accumulation and a state of defective glycaemic control. Interestingly, distinct fat distribution patterns can pose differing levels of diabetic risk (Yamazaki et al., 2022). Epidemiological studies have associated visceral adiposity, i.e. fat depots surrounding internal organs within the abdominal cavity, with insulin resistance, increased metabolic risk and mortality (Yamazaki et al., 2022). In contrast, subcutaneous fat depots, i.e. those situated below the skin surface, are inversely associated with insulin resistance, suggesting possible protective properties (McLaughlin et al., 2011).

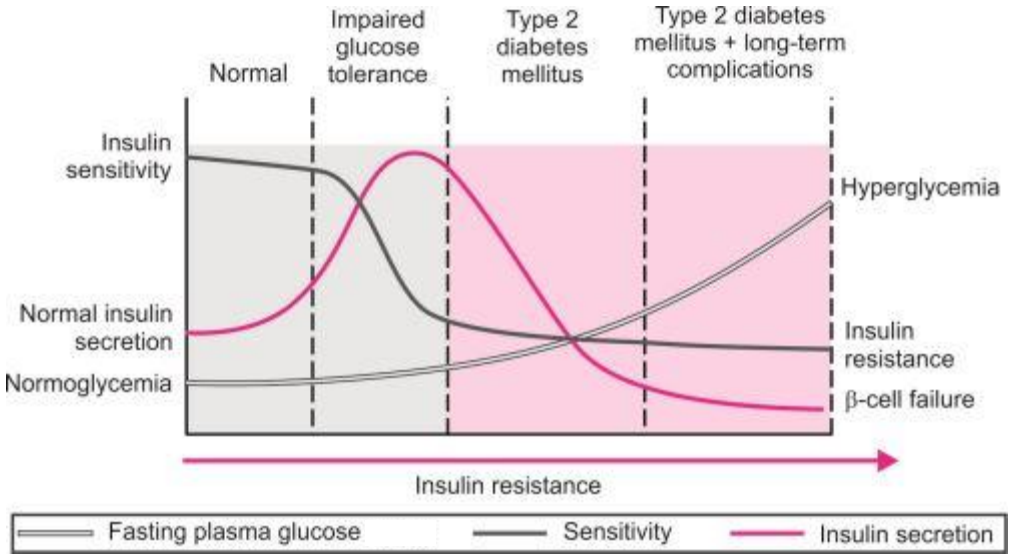

Figure 1. The progression of T2D. As adiposity grows, the sensitivity of peripheral tissues to insulin declines. In response to impaired glucose tolerance and hyperglycaemia, the islets undergo compensatory adaptations to expand β-cell mass and increase insulin secretion. However, continued expansion of fat mass exacerbates insulin resistance and β-cell function declines. Once the level of insulin secretion is insufficient to overcome hyperglycaemia, T2D develops. As hyperglycaemia worsens, long-term complications arise. (Moses et al., 2017).

As visceral fat accumulates, the insulin sensitivity of peripheral tissues (skeletal muscle and adipose tissue) declines. Insulin-resistant tissues are less responsive to insulin action which leads to reduced glucose uptake and an enhanced insulin demand. Initially, the systemic insulin resistance observed in obesity is countered by several compensatory mechanisms in β-cells. Examples include upregulated β-cell proliferation (hyperplasia), enlargement of cell size (hypertrophy), and sensitised insulin secretory response to glucose (Wortham & Sander, 2016). This adaptative response to a greater workload increases insulin secretion and helps

maintain normoglycaemia in obesity. However, as insulin resistance worsens and hyperglycaemia amplifies over time, β-cell function declines to a point of exhaustion, dysfunction, and failure. Furthermore, dysfunction in several other key cells and organs exacerbates hyperglycaemia and drives T2D progression: 1) elevated glucose production in the liver; 2) increased glucagon secretion from α-cells (see Section 1.2.3.2); 3) diminished insulinotropic and appetite-suppressing hormone release from the brain and gut; 4) increased renal glucose reabsorption; and 5) upregulated lipolysis in adipose tissue (DeFronzo, 2009). Overall, β-cell dysfunction, insulin resistance and chronic hyperglycaemia mark the onset of overt T2D. The later stages of the disease are compounded by long-term complications which are largely responsible for the increased risk of morbidity and mortality in diabetic patients (Nellaiappan et al., 2022).

1.1.2.4 Treatment

Lifestyle interventions, including increased physical activity, dietary modifications, and health education, are initially implemented for T2D management. Whilst these interventions can be challenging, diabetes remission can be achieved with intense calorie restriction and primary care support (Lean et al., 2018). If significant and durable improvements to glycaemic control are not observed, monotherapy in the form of pharmacology intervention is prescribed. Current pharmacotherapies for T2D harness one of four mechanisms of action; 1) increase insulin secretion from β-cells; 2) enhance insulin sensitivity and action at peripheral tissues; 3) stimulate urinary glucose excretion; or 4) inhibit carbohydrate absorption from the small intestine. Regardless of the mechanism, all converge towards the same objective of lowering plasma glucose to a desirable range (4-6mM) (Atanes & Persaud, 2020).

The first line and most widely used pharmacotherapy for diabetes is metformin which acts as an insulin sensitising agent (Gunton et al., 2003). Metformin belongs to the biguanide group of oral diabetes medications which inhibit hepatic gluconeogenesis, i.e. glucose production in the liver, and enhance insulin-mediated glucose uptake into skeletal muscle (Pernicova & Korbonits, 2014). There are several reported cellular responses to metformin, including inhibition of the mitochondrial electron transport chain (ETC), activation of the energy sensor, AMP-activated protein kinase (AMPK), changes in the expression of mRNAs associated with gluconeogenesis, and upregulated translocation and action of glucose transporters (GLUTs) (Gunton et al., 2003). Together, the anti-diabetic actions of metformin consequently reduce fasting blood glucose and insulin levels, and improve insulin resistance (Salpeter et al., 2008). In addition to its glucose-lowering properties, successful repurposing of metformin has led to treatment of other diseases, including cardiovascular disease (Han et al., 2019), cancer (Bowker et al., 2010; Currie et al., 2012; Franciosi et al., 2013), and polycystic ovarian syndrome (PCOS) (Diamanti-Kandarakis et al., 1998; Nestler et al., 1998).

Similar to metformin, thiazolidinediones (TZDs), also known as “glitazones”, are a group of insulin sensitisers which enhance insulin action at metabolic tissues (Eggleton & Jialal, 2023). The main function of this drug class, which now only comprises of pioglitazone, is to modulate the expression of peroxisome proliferator-activated receptor-γ (PPARγ), a master regulator of adipocyte differentiation. PPARγ activates the transcription of target genes involved in nutrient metabolism and energy homeostasis (Eggleton & Jialal, 2023). Examples include adiponectin, an adipose tissue-specific insulin-sensitising peptide (Kubota et al., 2006), and the GLUT4 transporter (Armoni et al., 2003). The TZD-induced reductions in blood glucose and HbA1c

ameliorates insulin resistance in T2D (Lebovitz et al., 2001). Unfortunately, however, there are several adverse side effects associated with the long-term use of TZDs, such as weight gain, oedema (Chilcott et al., 2001), and congestive heart failure (Singh et al., 2007), which could counteract their glucose-lowering benefits.

Whilst the actions of biguanides and TZDs improve insulin resistance, most pharmacotherapies for T2D treatment aim to enhance insulin secretion from β-cells. The sulphonylureas (SURs), such as tolbutamide and glibenclamide, stimulate insulin secretion by directly binding to and inhibiting ATP-sensitive potassium (K_{ATP}) channels within the β-cell membrane. (Costello et al., 2023). This is followed by membrane depolarisation, the opening of voltage-gated calcium (Ca^{2+}) channels, and an influx of Ca^{2+} ions. The subsequent stimulation of insulin secretion is independent of plasma glucose levels; thus, hypoglycaemia is the most common severe adverse event (AE) associated with sulphonylurea administration. As a result, the popularity of this drug class has dramatically declined (Costello et al., 2023).

An alternative, well-established treatment modality that stimulates insulin secretion are the glucagon-like peptide-1 (GLP-1) receptor agonists (GLP-1RAs), which are synthetic peptide analogues of the naturally occurring gut hormone, GLP-1. In response to orally administered glucose, GLP-1 is released from enteroendocrine L-cells situated within the ileum and colon of the gastrointestinal (GI) tract (Drucker & Nauck, 2006). It acts on β-cells via cell surface receptors within the membrane to potentiate the insulin secretory response, resulting in augmented release. This phenomenon is known as the “incretin effect” and accounts for 50-70% of total insulin secreted following an oral glucose load (Chaudhury et al., 2017). The insulinotropic properties of GLP-1, both direct and indirect, have been confirmed through numerous *in vitro* and *in vivo* experiments, including clinical trials involving diabetic patients (Drucker et al., 1987; Quddusi et al., 2003; Scrocchi et al., 1996; Siegel et al., 1992). Furthermore, appetite suppression and weight loss in healthy subjects (Flint et al., 1998) and patients with T2D (Zander et al., 2002) support anorectic effects of GLP-1. Coupled with the insulinotropic activity of the peptide, as well as other metabolically beneficial actions summarised in Figure 2, it comes as no surprise that the GLP-1R is a target for T2D and obesity therapies.

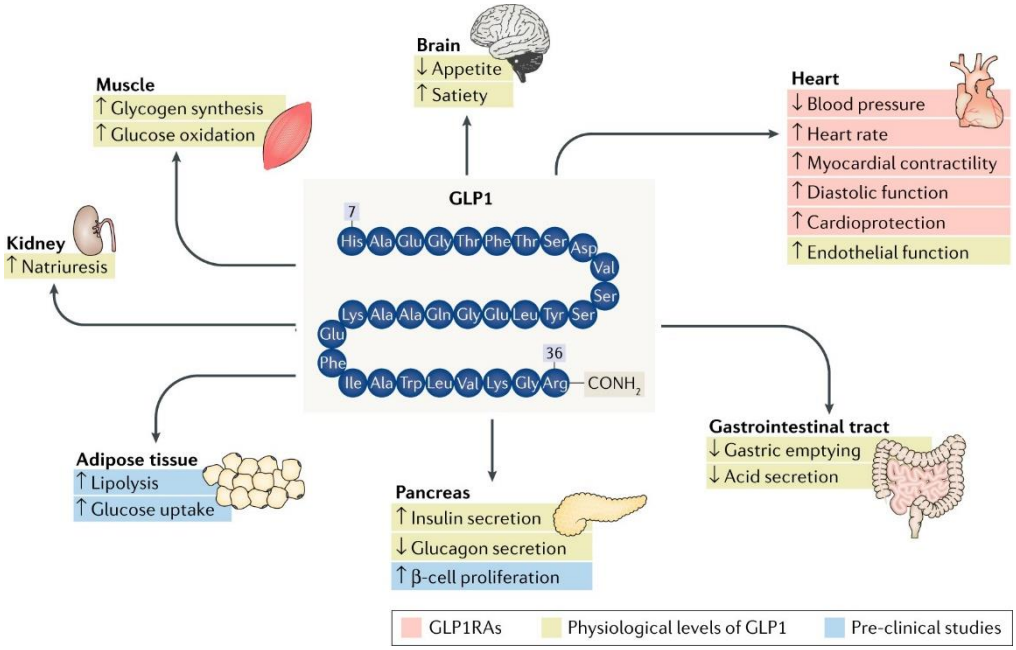

Figure 2. A schematic illustrating the tissue-specific effects of native GLP-1 at physiological levels (yellow) and of pharmacological GLP-1RAs (red), including effects observed during pre-clinical studies (blue). Numerous metabolic benefits of GLP-1 action are mediated by widespread distribution of GLP-1Rs: 1) upregulated metabolism and insulin sensitivity in skeletal muscle and adipose tissue; 2) induced satiety within the CNS; 3) cardioprotective effects coupled to enhanced sodium excretion; 4) delayed gastric emptying; and 5) increased β-cell mass and improved counterregulatory mechanisms involving islet hormones. (Andersen et al., 2018).

Due to a short half-life of ~1-2 minutes (Chaudhury et al., 2017), native GLP-1 is inappropriate as a therapeutic agent. This rapid breakdown is attributable to the actions of dipeptidyl peptidase-4 (DPP-4), which initiates enzymatic degradation of endogenous GLP-1 immediately following its release into the circulation (Alarcon et al., 2006). Inhibitors of DPP-4 activity have been developed to block the breakdown of GLP-1, increase its availability, and subsequently promote its metabolically beneficial actions to improve glycaemic control (Monami et al., 2011). However, there are concerns regarding the safety of DPP-4 inhibitors, such as saxagliptin and sitagliptin, as their use is associated with an increased risk of heart failure and acute pancreatitis (Packer, 2018; Rehman et al., 2017). Fortunately, the exploitation of the GLP-1 system remains possible due to the development of numerous degradation-resistant GLP-1RAs; one of which is exendin-4 (Ex4). Subcutaneous administration of Ex4 to individuals with diabetes leads to reductions in hyperglycaemia and improved glycaemic control (Kolterman et al., 2005), reduced HbA1c (Riddle et al., 2006), an associated enhancement in insulin secretion (Kolterman et al., 2003) and progressive weight loss (Riddle et al., 2006). Correspondingly, Ex4 has become a successful pharmacotherapy for T2D and obesity. Continued advancement of the GLP-1RA class has led to the development of long-acting compounds, such as dulaglutide and liraglutide (Chun & Butts, 2020), and the orally administered GLP-1RA, semaglutide (Avgerinos et al., 2020). However, the most common side effect of GLP-1RAs is nausea and other GI adverse events (Fehse et al., 2005; Kolterman et al., 2003). 30-50% of T2DM patients who utilise GLP-1RAs experience nausea (Jones et al., 2018), making it the most frequent of all AEs contributing to the discontinuation rate of this class of drug (Horowitz et al., 2017).

If monotherapy fails to achieve adequate control of glycaemia and relief of symptoms, combination therapy is typically adopted. A persistent inability to control hyperglycaemia ultimately leads to the introduction of insulin replacement therapy, although insulin treatment is often met with high risks of hypoglycaemia and weight gain (Edelman et al., 2008).

Despite the extensive range of drugs available, the most effective treatment for both obesity and T2D is bariatric surgery (Chukir et al., 2018). A large number of randomised controlled trials (RCTs) have established the long-term success of bariatric surgery for weight loss, remission of T2D and improvements in multiple metabolic parameters including blood pressure and plasma lipids, with consequent reductions in mortality also demonstrated (Adams et al., 2017; Schauer et al., 2012). The success can be attributed to several physiological and behavioural changes that arise from surgery, such as increased post-prandial energy expenditure (Werling et al., 2013), enhanced release of satiety hormones, oxyntomodulin (Laferrère et al., 2010) and GLP-1 (Salehi et al., 2011), and diminished neuronal hedonic responses including reduced reward, palatability, and appeal for energy-dense foods (Scholtz et al., 2014). However, whilst bariatric surgery is highly effective for resolution of T2D and obesity, the procedure has a relatively high up-front cost, has a small but definite mortality rate, is associated with several acute and long-term complications, and some bariatric surgeries are irreversible. Furthermore, bariatric surgery is clinically appropriate for only a small portion of individuals who meet strict patient criteria: a BMI>40 without comorbidities, a BMI between 35-39.9 with a minimum of one serious comorbidity, or a BMI between 30-34.9 with uncontrolled metabolic syndrome or diabetes (Benalcazar & Cascella, 2023).

Given obesity is a major risk factor for T2D development, it is worth noting the limited availability of anti-obesity drugs to patients. The only anti-obesity pharmacotherapies currently available on the National Health Service is semaglutide, the orally administered GLP-1RA, and orlistat, a lipase inhibitor which blocks the action of gastric and pancreatic lipases (Jain et al., 2011) and produces modest weight loss, along with reduced risk of diabetes and improvements in cardiovascular risk factors (Torgerson et al., 2004). Other weight loss medications have been developed but significant concerns remain about their use. Examples include sibutramine and phentermine-fenfluramine, both withdrawn from the market following increases in cardiovascular disease and blood pressure risk (Jain et al., 2011) and valvular heart disease (Hopkins & Polukoff, 2003), respectively.

Although a wide range of diabetes treatments are available, a significant portion of patients still fail to achieve adequate glycaemic control (Fonseca, 2009). Therefore, there is a considerable need to develop additional, more efficacious pharmacotherapies for T2D.

1.1.3 Gestational diabetes

Gestational diabetes (GD) is defined by the onset of glucose intolerance and hyperglycaemia during pregnancy. During normal gestation, maternal metabolism is altered via the development of progressive insulin resistance to facilitate the availability of fuel to the growing fetus in the form of glucose, amino acids, essential fatty acids, and ketones (Freemark, 2010). As a result, there is a high demand for insulin production that must be met by adaptative changes in the islets. These long-term structural and functional adaptations include expansion of β-cell mass, enhanced cell-cell communication, and increased nutrient metabolism (Green

et al., 1973; Green & Taylor, 1972; Xue et al., 2010). Further details regarding the mechanisms of islet dynamics during pregnancy can be found in Section 1.4.3.1. However, much like the failure of islet adaptation in obesity causing the development of T2D, the inability of maternal islets to do the same results in GD. The disease is associated with an increased incidence of neonatal hypoglycaemia, congenital anomalies, a larger than average new born birth weight (macrosomia), and maternal hyperglycaemia (Hod et al., 1991), all of which are detrimental complications to mother and child. Furthermore, there is a growing body of evidence supporting the increased risk for obesity, insulin resistance and T2D in offspring of women with GD (Garcia-Vargas et al., 2012).

1.1.4 Monogenic diabetes

T1D, T2D and GD are polygenic forms of diabetes meaning several gene variants, combined with environmental factors, contribute to the susceptibility and pathophysiology. Each genetic variant has a small effect on an individual's disease risk, however, combining multiple variants greatly enhances the genetic predisposition of a given disease. Polygenic diabetes is far more common than monogenic diabetes which is caused by a single, highly penetrant genetic mutation in a dominant autosomal gene (Zhang et al., 2021). Monogenic diabetes can be further subdivided into three categories: neonatal diabetes, maturity-onset diabetes of the young (MODY), and syndromic diabetes (Zhang et al., 2021).

Despite accounting for ~80% of monogenic diabetes cases (De Franco et al., 2015), neonatal diabetes remains an extremely rare disease affecting 1:500,000-400,000 live births globally (Iafusco et al., 2012). Diagnosis, which occurs within the first 6 months of age, can be confirmed by genetic testing, and it is important in clinical practice to differentiate between neonatal diabetes and T1D (Rubio-Cabezas et al., 2011). The most common pathogenic variants which cause neonatal diabetes are *ABCC8* and *KCNJ11* encoding subunits of the β-cell K_{ATP} channel (De Franco et al., 2020). K_{ATP} channels represent a key component in the insulin secretory pathway, thus, mutation in either gene leads to impaired glucose-stimulated insulin secretion. Due to their actions at these channels, sulfonylureas offer an effective treatment strategy over insulin supplementation in infants who carry *ABCC8* or *KCNJ11* gene mutations (Stanik et al., 2007; Taberner et al., 2016).

MODY is a rare form of monogenic diabetes diagnosed outside of the neonatal period. There are currently 14 causal genetic variants for MODY described in the literature, with *GCK* (glucokinase), *HNF1A* (hepatocyte nuclear factor 1-α), and *HNF4A* being the most prevalent (Zhang et al., 2021). Patients with heterozygous *GCK* mutations exhibit mild, stable hyperglycaemia that slightly exceeds the desirable range for fasting plasma glucose levels (5.5-8.0mM) (Urakami, 2019). This may be due to the overexpression of the functioning allele (Sturis et al., 1994), or the activity of other glucokinase isozymes that can compensate for glucokinase deficiency. *HNF1A* and *HNF4A* encode transcription factors implicated in β-cell identity, maturation, and function (Legøy et al., 2020). Mutations in these genes lead to reduced insulin secretion and β-cell dedifferentiation, but also increase insulin sensitivity which heightens sensitivity to sulfonylureas (Colclough et al., 2013; Miyachi et al., 2022). Depending on the mutation and disease severity, treatment options range from simple diet modification to low-dose sulfonylurea administration in combination with GLP-1 agonists to offset the risks of hypoglycaemia (Haliyur et al., 2019).

Syndromic diabetes is a less common form of monogenic diabetes and has differing aetiology to neonatal and MODY. Non-autoimmune extra-pancreatic features, such as developmental delays and defects, microcephaly, cardiomyopathy and optic atrophy (Sanchez Caballero et al., 2021; Zhang et al., 2021), distinguish syndromic diabetes from the other monogenic forms. In addition, patients are more likely to be treated with insulin replacement therapy vs sulfonylurea medication (Colclough et al., 2022).

1.1.5 Secondary diabetes

Secondary diabetes can develop as a result of steroid treatment, substance abuse, and other acquired medical conditions, such as Cushing's syndrome, acromegaly, and pancreatic cancer (Nomiyama & Yanase, 2015; Ojo et al., 2018; Störmann & Schopohl, 2020). The pathophysiology of the disease is dependent on the associated condition. Early stages of secondary diabetes induced by endocrine disease is typically characterised by insulin resistance followed by insulin deficiency in the later stages (Nomiyama & Yanase, 2015). In contrast, secondary diabetes induced by pancreatic disease results from β-cell destruction and insulin deficiency which is managed with insulin therapy (Nomiyama & Yanase, 2015). The complexity of its varying aetiologies can present challenges for diagnosis and treatment. Furthermore, patients with secondary diabetes have heightened vulnerability and risk compared to patients with T1D and T2D because of their primary condition (Yang et al., 2022).

1.1.6 Complications of chronic hyperglycaemia

As previously mentioned, chronic hyperglycaemia paves the way for microvascular and macrovascular complications that manifest in multiple organ systems. As chronic hyperglycaemia is shared in both T1D and T2D, the types of complications are similar (Deshpande et al., 2008). Microvascular complications include damage to the renal (nephropathy), nervous (neuropathy), and ocular (retinopathy) systems, and are more prevalent than macrovascular complications which constitute cardiovascular disease, stroke, and peripheral arterial disease (PAD). PAD is characterised by poor circulation and blood flow and increases the risk of developing non-healing sores, or ulcers, in the lower extremities. In severe cases, this can cause tissue death (gangrene) and if necessary, amputation of the affected foot or leg. Miscellaneous complications include dental disease, diminished resistance to infection, birth complications in pregnant women with GD (Deshpande et al., 2008), cancers, liver disease, and age-related conditions, such as dementia (Harding et al., 2019).

Infection has recently been identified as a complication of diabetes in light of the global coronavirus pandemic. The severity of coronavirus in the diabetes community is triple that in the healthy population, and diabetic patients exhibit an increased susceptibility to severe disease caused by coronavirus infection (Gregory et al., 2021). Research studies have implicated SARS-CoV-2 (severe acute respiratory syndrome coronavirus 2) in impaired glucose homeostasis and hyperglycaemia (Ben Nasr et al., 2022; Müller et al., 2021; Tang et al., 2021; Wu et al., 2021). The underpinning cellular mechanisms involve viral infection of β-cells followed by decreased numbers of insulin secretory granules, defective glucose-stimulated insulin secretion (Müller et al., 2021), β-cell transdifferentiation (Tang et al., 2021), and β-cell apoptosis (Wu et al., 2021). As a result, patients are at greater risk of further perturbations, such as diabetic ketoacidosis and pancreatitis (Gęca et al., 2022). Further

studies are required to improve current knowledge and understanding of SARS-CoV-2 infection in relation to diabetes, and to determine the best management approach for patients with diabetes and coronavirus (Gęca et al., 2022).

1.2 Islets of Langerhans

1.2.1 Pancreas

The pancreas is a retroperitoneal gland that sits in the upper abdominal cavity (Atkinson et al., 2020). The head is located near the duodenum of the small intestine, whilst the body and tail extend towards the spleen (Figure 3). The pancreas is a heterocrine gland as it is composed of two systems: the exocrine and the endocrine. The exocrine pancreas functions to synthesise, store, and secrete proenzymatic peptides, such as trypsin and lipase. It is formed of acini and a complex ductal network that connects to the duodenum in which pancreatic enzymes are activated to aid food digestion. Acinar cells secrete digestive enzymes into intercalated ducts which converge to form intralobular and interlobular ducts. These, in turn, drain into the main pancreatic duct which either empties into the duodenum as the accessory pancreatic duct or joins with the common bile duct near the ampulla of Vater (Atkinson et al., 2020). Clusters of hormone-producing cells are located between acinar cells and form the endocrine compartment of the pancreas. These clusters are known as the islets of Langerhans, and comprise 2-3% of the total pancreatic volume (Jones & Persaud, 2017). The human pancreas contains approximately 1 million individual islets, each with an arterial supply and nerve innervation.

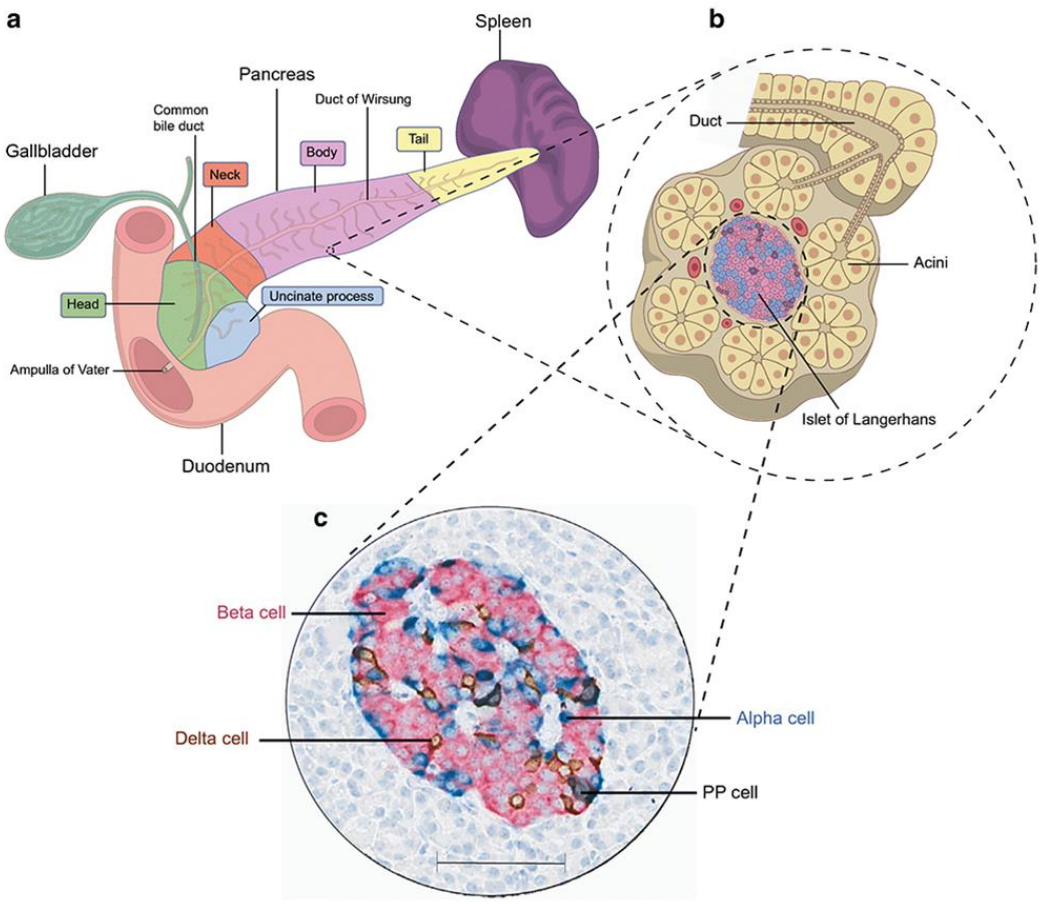

Figure 3. The anatomical organisation and structure of the pancreas. a) The gross anatomy of the pancreas in relation to surrounding organs. b) The exocrine pancreas composed of acinar cells and ductal branches to synthesise and supply enzymatic peptides to the duodenum. c) A single human islet displaying four endocrine cell types: β-cell (pink), α-cell (blue), δ-cell (red) and PP cell (grey). Scale bar = 100µm. Figure sourced from Atkinson et al. (2020).

1.2.2 Islet morphology

The islets of Langerhans are highly dynamic and efficient heterogeneous bodies of cells, whose functions are essential in the regulation of glucose homeostasis. These small micro-organs consist of four main types of endocrine cell which express and secrete their own exclusive hormone: 1) the insulin-containing β-cells; 2) the α-cells containing glucagon; 3) the δ-cells containing somatostatin; and 4) the pancreatic polypeptide (PP)-producing cells (Jones & Persaud, 2017). The cells are arranged in such a way that gives the islets a unique cytoarchitecture within the human pancreas (Cabrera et al., 2006). The anatomical organisation of islet cells has several implications on islet cell function, for example, paracrine interactions and access to islet microcirculation (Cabrera et al., 2006). Interestingly, the composition and cytoarchitecture of islets vary between species (Figure 4). The insulin-secreting β-cell is the most abundant cell type in both rodent and human islets, followed by the glucagon-secreting α-cell as the second most abundant. However, in rodent islets, the β-cell population clusters to form a central core which is encircled by a mantle of α-and δ-cells at the periphery. Conversely, cells appear randomly distributed within the human islet. This intermingled arrangement parallels the vascularisation pattern in human islets (Cabrera et al., 2006) whereby cells are positioned adjacent to islet microcirculation, allowing for intimate

contact with blood and the systematic monitoring and detection of changes in plasma glucose levels. Real-time imaging of mouse islet blood flow revealed a contrasting inner-to-outer and top-to-bottom perfusion pattern (Nyman et al., 2008). Both rodent and human pancreases are richly innervated by sympathetic, parasympathetic, and afferent nerve fibres, however, there are differences in the distribution throughout the pancreas and contacts with particular islet cells (Dolenšek et al., 2015).

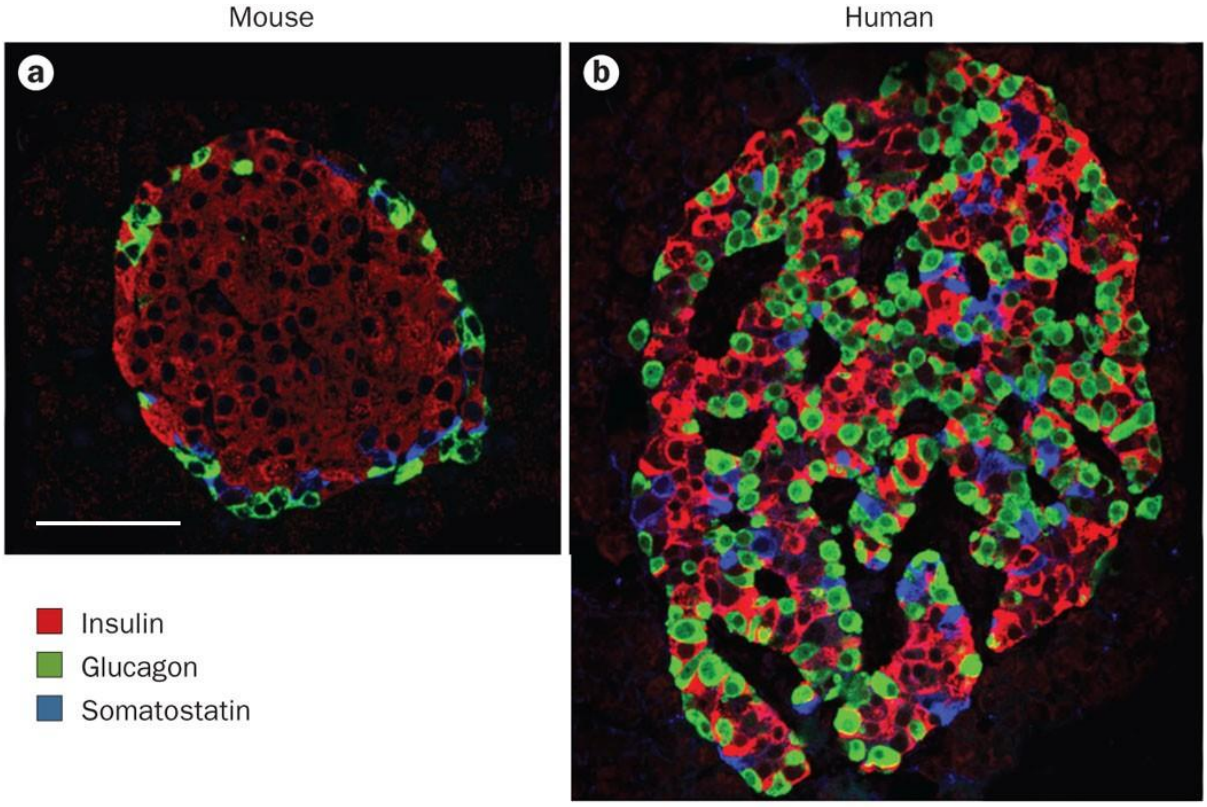

Figure 4. Immunolabelling of insulin (red), glucagon (green), and somatostatin (blue) in mouse (a) and human (b) islets. Scale bar = 50µm. Figure sourced from Cabrera et al. (2006) and Wang et al. (2015).

Differences in cellular composition accompany the contrasting morphologies between rodent and human islets. Despite single islets being of a similar size, ranging from 100-500µm, islet number is considerably lower in mice than in humans (1,000-5000 vs 1.0-1.5 million islets) (Dolenšek et al., 2015). The proportion of β-cells is greater (60-80 vs 50-70%) whereas the proportion of α-cells is lower (10-20 vs 20-40%) in mouse compared to human islets (Cabrera et al., 2006; Dolenšek et al., 2015).

Overall, the contrast between rodents and humans in terms of islet composition and architecture should be considered in the design and interpretation of basic research experiments, as this may have implications on clinical application.

1.2.3 Islet cell types and functions

1.2.3.1 β-cells

The primary function of the β-cell is to produce, store, and secrete insulin in response to metabolic demand. Insulin synthesis begins with the transcription of the preproinsulin gene, followed by RNA splicing and translation into a 11.5kDa preproinsulin polypeptide (Jones & Persaud, 2017). Once transported to the rough endoplasmic reticulum (ER), proteolytic enzymes cleave an N-terminal signal sequence to generate proinsulin. This 9kDa molecule consists of A and B insulin chains linked by a C-peptide. By aligning the disulfide bridges that join the A and B chains together, the C-peptide ensures correct protein folding and cleavage. Proinsulin is transferred to the Golgi apparatus where it is packaged into membrane-bound vesicles known as secretory granules. Endopeptidases, prohormone convertase 2 and 3, and carboxypeptidase H mediate the conversion of proinsulin to insulin within maturing secretory granules. Their actions cleave the C-peptide chain to yield insulin, and both are stored in late-stage secretory granules to await release by exocytosis. Rapid nutrient-stimulated insulin secretion is accompanied by the relatively slow production of insulin to maintain intracellular stores (Jones & Persaud, 2017).

β-cells secrete insulin in response to nutrients, hormones, and neurotransmitters to maintain circulating glucose levels within a narrow physiological range (4-6mM). To limit fluctuations in plasma glucose levels, insulin secretion is subject to tight mechanistic control. The key physiological stimulus for insulin secretion is a change in the circulating concentration of glucose and other nutrients, including amino acids and free fatty acids (FFAs) (Jones & Persaud, 2017). All have the capacity to elicit an insulin secretory response, prompting the uptake, metabolism, and storage of nutrients in target tissues. A reduction in circulating nutrients follows, and β-cells respond by dampening the secretion of insulin. This negative feedback loop is important for preventing inappropriate insulin release and hypoglycaemia. In addition, several molecules can either potentiate or inhibit nutrient-induced insulin secretion, thus providing an additional layer of glycaemic regulation. Examples of modulators include neurotransmitters and neuropeptides, incretins such as GLP-1 and its pharmacological derivatives (Section 1.1.2.4), adipose tissue-derived peptides (adipokines), and other islet hormones (Jones & Persaud, 2017).

The intracellular mechanisms responsible for glucose-stimulated insulin secretion from the β-cell are illustrated in Figure 5. Glucose uptake into murine β-cells is mediated by the low affinity, high capacity glucose transporter, GLUT2 (Berger & Zdzieblo, 2020). Whilst GLUT2 is present at low levels, human β-cells predominantly rely on GLUT1 and GLUT3 transporters (Berger & Zdzieblo, 2020). Unlike GLUT2, these transporters have a high affinity for glucose (Km = 2-5mM), consequently aligning with the physiological glucose concentration range in humans (Litwack, 2018). Glucose transport into the β-cell activates glucokinase – an enzyme often referred to as the “glucose sensor” which mediates the coupling of insulin secretion and glucose levels (Fridlyand & Philipson, 2011). Glucose is phosphorylated by glucokinase, then metabolised further to pyruvate during glycolysis. Pyruvate is transported to the mitochondria where it enters the Krebs cycle and becomes oxidised to produce ATP. The subsequent change in the ATP/ADP ratio leads to the closure of K_{ATP} channels, decreased potassium efflux, and depolarisation of the β-cell membrane. This triggers the opening of voltage-gated Ca^{2+} channels and an influx of Ca^{2+} ions. The rise in cytoplasmic Ca^{2+} concentration ($[Ca^{2+}]_i$)

which follows causes the movement of insulin-containing granules to the membrane, and the exocytosis of insulin from the β-cell (Fridlyand & Philipson, 2011). Insulin is secreted in a pulsatile manner (Chou et al., 1991) and corresponds to oscillations in cytoplasmic Ca^{2+} concentrations (Bergsten et al., 1994). This pattern is synchronous in all β-cells across the islet and is crucial for a sharp and highly coordinated response to glucose (see Section 1.3 for further details).

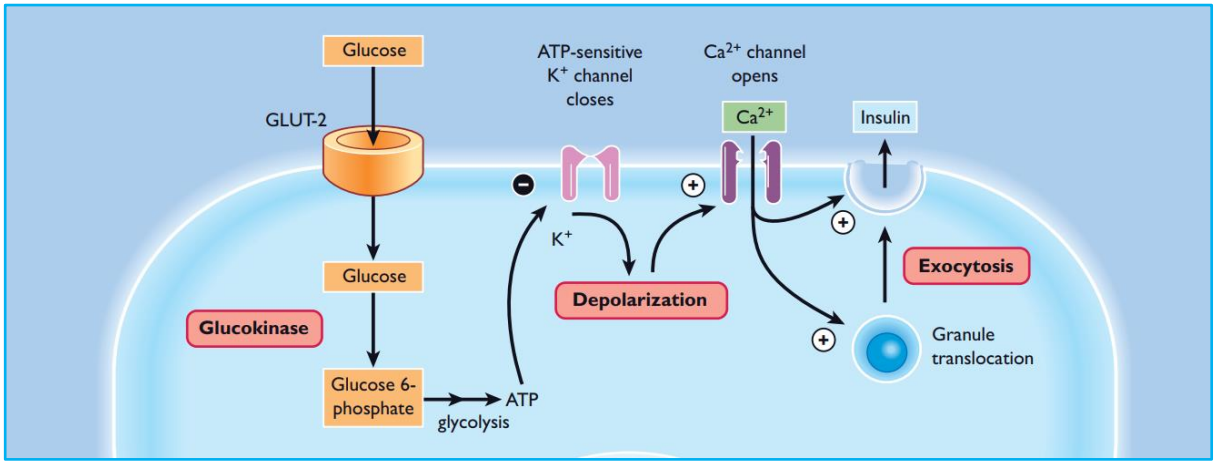

Figure 5. A schematic illustrating the intracellular mechanisms involved in the metabolism of glucose followed by the secretion of insulin from the β-cell. GLUT2-mediated glucose transport into the cytosol leads to glucose metabolism and the generation of ATP which closes K_{ATP} channels within the cell membrane. This inhibits the efflux of K^+ ions, causing membrane depolarisation and opening of voltage-gated Ca^{2+} channels. The subsequent influx of Ca^{2+} ions and increased cytosolic calcium initiates a cascade of molecular events leading to insulin exocytosis. (Jones & Persaud, 2017).

Glucose-stimulated insulin secretion is biphasic in nature (Figure 6). A rise in plasma glucose levels causes an initial rapid release of insulin. This is known as the “first phase” whereby insulin is exocytosed from readily releasable pools (RRPs) in a K_{ATP}-dependent manner (Bratanova-Tochkova et al., 2002). The acute first phase is followed by a prolonged and maintained “second phase” in which the insulin secretory response is amplified by a K_{ATP}-independent signal. Granule recruitment from a reserve pool (RP) supports the second phase which plateaus at 2-3 hours (Bratanova-Tochkova et al., 2002; Gerich, 2002). Exocytosis of insulin requires the fusion of insulin-containing vesicles to the β-cell plasma membrane. The process involves soluble N-ethylmaleimide-sensitive factor attachment protein receptor (SNARE) complex proteins (Goda, 1997). Complementary proteins, v-SNARE and t-SNARE, are embedded in the vesicle and target plasma membranes, respectively, and act as receptors to direct vesicle docking. Both SNARE proteins bind and consequently incorporate with a SNAP-NSF fusion complex to facilitate vesicle fusion and exocytosis (Goda, 1997).

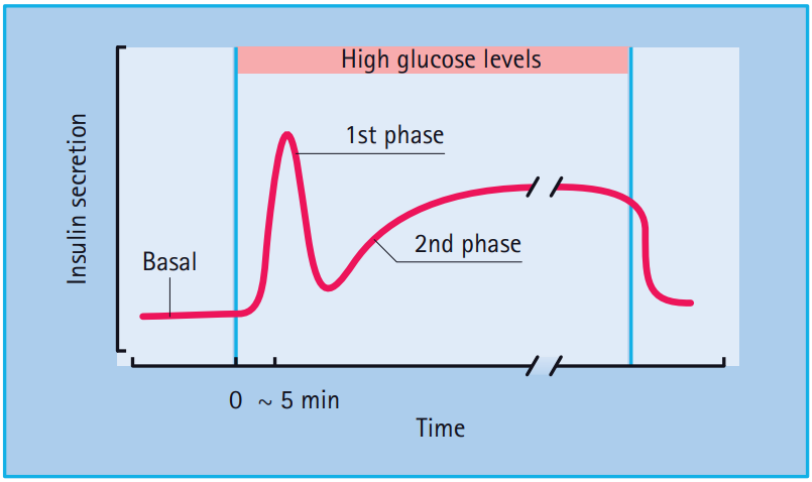

Figure 6. A schematic illustrating the biphasic insulin secretory response to increased circulating glucose concentration. A high glucose stimulus triggers an initial rapid release of insulin which lasts a few minutes. This is followed by a slowly-increasing second phase which is maintained until glucose levels normalise. (Jones & Persaud, 2017).

1.2.3.2 α-cells

As previously stated in Section 1.2.3.1, the β-cell suppresses the secretion of insulin when circulating nutrient levels decrease to prevent and correct detrimental hypoglycaemia. Additional defence mechanisms are executed by the α-cell through the synthesis and secretion of the glucose-mobilising hormone, glucagon. Low plasma glucose (<5mM) is a potent stimulus for glucagon release, whilst prolonged fasting (Flattem et al., 2001), exercise (Wasserman et al., 1989) and protein-rich meals (Claessens et al., 2008) can also be triggers. The cellular mechanisms responsible for hypoglycaemia-induced glucagon secretion from the α-cell are similar to those for hyperglycaemia-induced insulin secretion from the β-cell: changes to the intracellular ATP/ADP ratio as a result of low circulating glucose leads to the closure of K_{ATP} channels, membrane depolarisation, the opening of voltage-gated Ca^{2+} channels and an influx of Ca^{2+} ions triggering the exocytosis of glucagon from storage vesicles (Rorsman et al., 2012). In addition to the Ca^{2+} current, regulation of hormone secretion from α-cells relies heavily on voltage-dependent, tetrodotoxin-sensitive Na^{+} channels which drive the upstroke of action potentials (APs) when activated and contributes to AP termination when inactivated (Göpel et al., 2000; MacDonald et al., 2007). Once secreted, glucagon acts on highly selective glucagon receptors within the liver to promote glucose production from non-carbohydrate precursors (gluconeogenesis) and the breakdown of glycogen to glucose (glycogenolysis). In conjunction to this increase in hepatic glucose production, glucagon inhibits glycogen formation (glycogenesis) and glucose metabolism (glycolysis) to further enhance glucose availability. Supporting actions include a glucose-sparing mechanism whereby glucagon initiates a metabolic shift in fuel utilisation. Glucagon exhibits lipolytic effects as it is known to stimulate hormone-sensitive lipase (HSL) activity within adipocytes, leading to the release of FFAs into circulation (Perea et al., 1995). Bound to albumin, these FFAs are transported to the liver in which they are converted to ketone bodies to substitute glucose in a fasted state (Liljenquist et al., 1974). Together, the catabolic activity of glucagon raises blood glucose levels to defend against the potential damaging effects of hypoglycaemia. This defence mechanism is dysfunctional in uncontrolled T1D and T2D where there is persistent hyperglucagonaemia (Baron et al., 1987; Müller et al., 1973; Reaven et al., 1987;

Unger et al., 1970). The potential hypoglycaemic complications have severe consequences on cognitive function as glucose is the primary metabolic fuel of the brain. An inadequate glucose supply to the brain (neuroglycopenia) can lead to impaired neurological function, seizures, loss of consciousness, permanent brain damage, and ultimately death (Blaabjerg & Juhl, 2016).

The glucose-mobilising nature of glucagon opposes the glucose-depositing actions of insulin, making glucagon an important factor in glucose counterregulatory responses to hypoglycaemia. Both islet hormones contribute to feedback loops which maintain plasma glucose concentrations within the desired range (Figure 7) (Bosco et al., 2010).

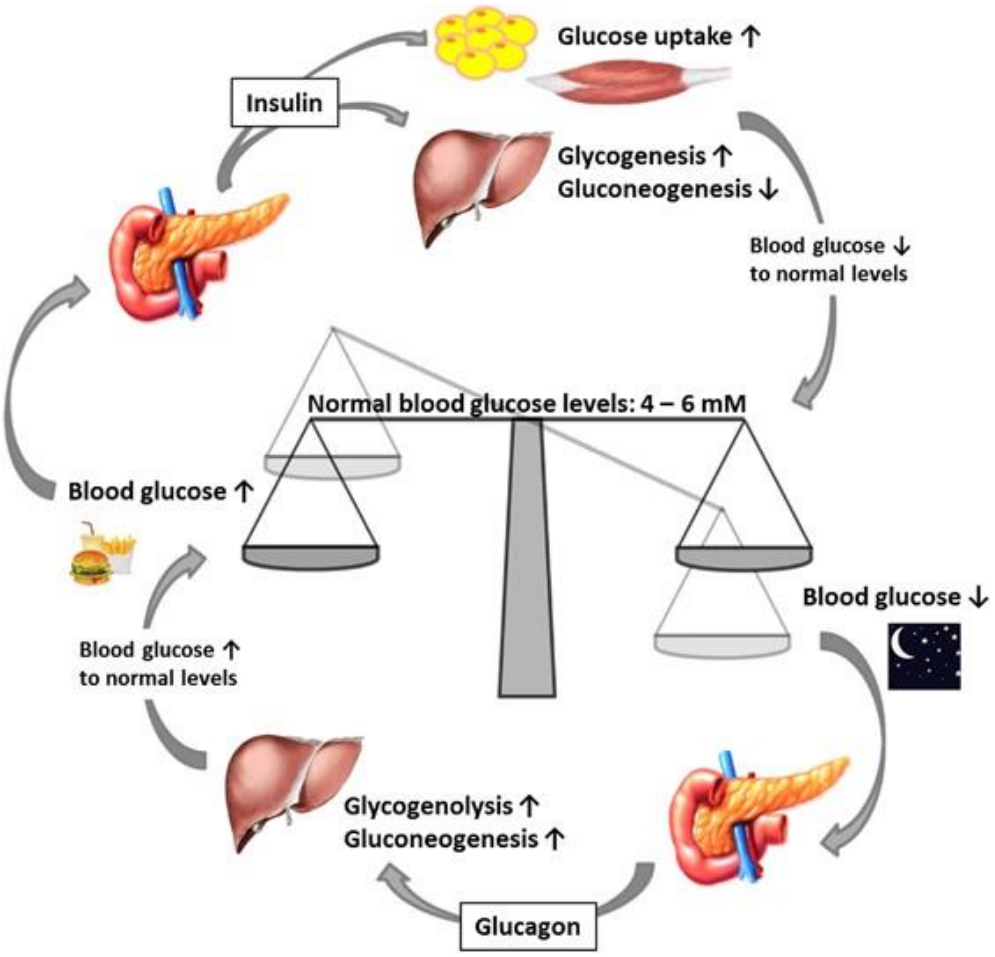

Figure 7. The counterregulatory actions of glucagon and insulin in the maintenance of normoglycaemia. Decreased blood glucose levels, e.g., during overnight fasting, stimulate glucagon secretion from α-cells, leading to several cellular responses to increase blood glucose to normal levels, including upregulated hepatic glycogenolysis and gluconeogenesis. Increased blood glucose levels following a meal triggers insulin secretion from β-cells to enhance glucose uptake into muscle and adipose tissue, and upregulate glycogenesis whilst diminishing gluconeogenesis in the liver. (Röder et al., 2016).

1.2.4 Intra-islet interactions

The three-dimensional (3D) islet architecture is crucial for the proper function of β-cells in response to physiological stimuli. Hetero- and homotypic contacts between cells create a signalling network that enables islet communication. The nature of these connections varies. Gap junctions are membrane channel proteins which electrically couple neighbouring cells. They serve to transport a range of intracellular ions, small metabolites and larger molecules, including inositol 1,4,5-triphosphate (IP_3) (Niessen et al., 2000), cyclic AMP (cAMP) (Bedner et al., 2006), RNA (Valiunas et al., 2005) and peptides (Neijssen et al., 2005). By facilitating the movement of Ca^{2+} ions throughout the islet, β-cells act as a single unit known as a "functional syncytium" (Nadal et al., 1999). As a result, insulin secretion is synchronised and highly coordinated (Bergsten et al., 1994). Gap junctions are composed of different connexin isoforms, the most abundant being connexin-36 (Cx36) in β-cells (Le Gurun et al., 2003). Loss of Cx36 from β-cells eliminates glucose-induced Ca^{2+} and insulin oscillations (Benninger et al., 2011; Ravier et al., 2005), translating to impaired insulin secretion (Le Gurun et al., 2003). Furthermore, the dysfunctional Ca^{2+} dynamics observed in islets of diabetic mouse models and patients can be ameliorated with Cx36 overexpression (Clair et al., 2023). This may not be sufficient, however, to overcome the disproportionate loss of β-cells and gain in α-cell fraction in diabetes (Kilimnik et al., 2011; Nir et al., 2007). Nevertheless, these studies demonstrate the dependence of Cx36-mediated signalling for proper β-cell function.

E-cadherin-mediated contacts provide an alternative route of communication between cells. Cadherins are calcium-dependent adhesion receptors that are necessary for maintaining the 3D islet structure, and for mediating signals involved in islet hormone secretion, proliferation and survival (Olaniru & Persaud, 2018). Indeed, interference of E-cadherin signalling in β-cells reduces glucose-stimulated insulin secretion (Jaques et al., 2008) and β-cell proliferation (Carvell et al., 2007).

Intra-islet autocrine and paracrine signalling confers an additional level of β-cell regulation. α- and δ-cells can secrete glucagon and somatostatin, respectively, to interact with neighbouring β-cells (paracrine). Glucagon is insulinotropic and maintains normoglycaemia in the post-prandial state by stimulating β-cell activity through the glucagon receptor, GCGR (Kieffer et al., 1996; Zhang et al., 2021). On the other hand, when chronically activated by glucagon, GCGR induces β-cell dedifferentiation (Wang et al., 2023) whereas GCGR antagonism can promote β-cell regeneration (Wei et al., 2023). Somatostatin is a ligand at multiple G protein-coupled somatostatin receptors and acts to suppress the release of several hormones, including insulin from the β-cell (Pace & Tarvin, 1981; Patel & Srikant, 1997). It does so by inhibiting glucose metabolism and oxidative respiration (Daunt et al., 2006). Furthermore, the dynamics of insulin exocytosis are disturbed by impeding Ca^{2+} influx (Daunt et al., 2006; Hsu et al., 1991; Pace & Tarvin, 1981).

Simultaneous to paracrine signalling, β-cells can secrete factors which bind to the same cell from which they were secreted to govern its own function (autocrine). The autocrine actions of insulin on β-cells are widely debated. Insulin receptors (IRs) and their downstream signalling elements are expressed in the β-cell (Harbeck et al., 1996; Muller et al., 2006; Velloso et al., 1995; Verspohl & Ammon, 1980; Xu & Rothenberg, 1998). IRs belong to the tyrosine kinase receptor superfamily. An IR is formed of two subunits and each subunit is comprised of an extracellular α-chain and a β-chain with transmembrane and intracellular domains

(Rachdaoui, 2020). The α-chain holds a site for ligand binding whilst the β-chain possesses tyrosine kinase activity which, when activated by insulin, autophosphorylates clusters of tyrosine residues. Effector proteins, such as insulin receptor substrates (IRS), and the phosphatidylinositol 3-kinase (PI3K)/AKT pathway are subsequently engaged. The two IR isoforms, IR-A and IR-B, have differing binding affinities and localisation patterns. IR-A has a higher affinity for insulin, but IR-B is predominantly expressed in adipose tissue, skeletal muscle, and liver, and mediates the majority of insulin's metabolic effects. IRs share high structural homology with the insulin-like growth factor 1 receptor (IGF-1R) and can therefore be bound and activated by insulin alongside its other ligands, IGF-1 and IGF-2. IGF-1R activity mediates potent insulin-induced mitogenic effects to promote protein synthesis, cellular growth and survival (Rachdaoui, 2020). There are opposing reports of negative and positive insulin action on β-cell function. Positive actions have been deduced from several knockout studies in which β-cell-specific depletion of insulin receptors or their downstream signalling components results in apoptosis, defective glucose-stimulated insulin secretion, and lack of compensatory islet growth to insulin resistance (Kubota et al., 2000; Kulkarni et al., 1999, 2002; Okada et al., 2007; Ren et al., 2014; Withers et al., 1998). Conversely, chronic exposure of β-cells to high insulin levels has shown to induce ER stress and promote β-cell death (Bucris et al., 2016; Guillen et al., 2008; Rachdaoui et al., 2019). Thus, a negative feedback loop where insulin limits its own secretion (Marchetti et al., 1995; Van Schravendijk et al., 1990) could provide a protective mechanism to maintain insulin levels at physiological level. Perturbed IR/IGF-1R signalling potentially occurs in a diabetogenic environment characterised by hyperinsulinaemia.

The importance of intra-islet connections for normal islet function is further emphasised by the divergent behaviours between intact and dissociated islets. Isolated β-cells fail to generate Ca^{2+} oscillations (Cabrera et al., 2006; Zhang et al., 2003), and the magnitude of the insulin secretory response from cells in suspension is markedly lower compared to that of intact islets (Benninger et al., 2011; Halban et al., 1982; Lernmark, 1974). Moreover, the level of insulin secretion from disrupted islets is comparable to that in $Cx36^{-/-}$ islets (Benninger et al., 2011). Insulin secretion from single β-cells can be partially rescued once cell-cell contacts are re-established (Wojtusciszyn et al., 2008). Additionally, the formation of pseudoislets, a 3D configuration of β-cells, improves glucose-stimulated insulin secretion and metabolic activity compared to monolayer cultures (Cornell et al., 2022; Hauge-Evans et al., 1999). Overall, there are remarkable differences in insulin secretory activity between intact and disrupted islets. This has profound implications on stem cell-derived β-cell and islet transplantation protocols for T1D therapy. Taking into account the islet architecture and spatial arrangement of different cell types is crucial for the functionality of islet grafts and favourable patient outcomes.

1.3 Regulation of insulin secretion

1.3.1 Regulation of insulin secretion by nutrients

Glucose is the primary nutrient which stimulates insulin secretion from β-cells. High circulating glucose levels are recognised by β-cells and induce facilitated transport of glucose into the cells via glucose transporters. The increase in intracellular glucose levels stimulates glucose metabolism and electrophysiological changes that ultimately result in Ca^{2+}-dependent translocation and exocytosis of insulin from secretory granules. In parallel to this pathway,

glucose can also amplify Ca^{2+}-induced insulin exocytosis by elevating cAMP formation (Shuai et al., 2021). It does so via activation of adenylate cyclase (AC), an enzyme that catalyses the generation of cAMP from ATP (Sharp et al., 1980; Tian et al., 2011). Indeed, the capacity of glucose to raise intracellular cAMP levels has been consistently observed in the MIN6 β-cell line and in primary islets (Dyachok et al., 2008; Grill & Cerasi, 1973; Hellman et al., 1974; Tian et al., 2011). Similar to $[Ca^{2+}]_i$, this occurs in a pulsatile fashion that mirrors oscillations in insulin secretion (Dyachok et al., 2008). The major effectors of cAMP are protein kinase A (PKA) and exchange proteins activated by cyclic AMP (EPACs) (Szaszák et al., 2008). PKA acts on several targets to elevate cytosolic Ca^{2+} and enhance glucose-stimulated insulin secretion: 1) PKA phosphorylates Ca^{2+} channels within the inhibitor of Ca^{2+}-dependent inactivation (ICDI) motif to increase their open probability and promote Ca^{2+} influx (Sang et al., 2016); 2) PKA phosphorylates the SUR1 subunits of K_{ATP} channels and induces their closure to trigger β-cell membrane depolarisation and Ca^{2+} entry through Ca^{2+} channels (Light et al., 2002); and 3) PKA phosphorylates IP_3 receptors to potentiate Ca^{2+} release from intracellular stores (Dyachok & Gylfe, 2004). In addition to increasing cytosolic Ca^{2+} levels, PKA is also thought to optimise insulin granule exocytosis by phosphorylating proteins associated with the mechanism (Kaihara et al., 2013). This is supported by observations of physical tethering between PKA pools and secretory compartments via A-kinase anchoring proteins (AKAPs) (Villalpando et al., 2016). This mobilisation of insulin granules can also be mediated by a PKA-independent mechanism involving cAMP-activated EPAC2. EPAC2 increases the density of insulin-containing secretory granules near the β-cell plasma membrane and potentiates fusion events during the first phase of glucose-stimulated insulin exocytosis (Shibasaki et al., 2007). Fusion events are significantly reduced in EPAC2-deficient mice, therefore demonstrating the importance of cAMP-induced regulation of insulin granule dynamics through EPAC2 (Shibasaki et al., 2007).

Insulin release can also be regulated by amino acids (Liu et al., 2008; McClenaghan et al., 1996). The majority require glucose and are therefore potentiators of insulin secretion, however, leucine, lysine and arginine are capable of initiating secretion alone (Jones & Persaud, 2017). There are three potential mechanisms for the stimulatory actions of amino acids in β-cells: 1) electrogenic transport and accumulation of cationic amino acids, such as arginine, depolarises the plasma membrane leading to increased $[Ca^{2+}]_i$ and insulin secretion (Smith et al., 1997); 2) co-transport with Na^+ ions elicits similar membrane depolarisation effects and potentiates glucose-dependent insulin secretion (McClenaghan et al., 1998); and 3) amino acid metabolism upregulates ATP generation and glucokinase expression to enhance glucose metabolism (Brennan et al., 2002; Yang et al., 2006). The insulinotropic effects of amino acids *in vitro* and *in vivo* have clinical applications for patients with type 2 diabetes as amino acid supplementation improves the insulin secretory response, post-prandial glucose disposal, and insulin sensitivity (Natarajan Sulochana et al., 2002; Tao et al., 2022; van Loon et al., 2003).

1.3.2 Regulation of insulin secretion by non-nutrients

β-cells respond to multiple non-nutrient potentiators of insulin secretion, such as islet and incretin hormones, adipokines, neurotransmitters and neuropeptides. The majority of these modulate β-cell function by binding and activating target membrane-bound receptors (Jones & Persaud, 2017). Key examples include GLP-1 and glucagon which amplify glucose-induced cAMP elevation in β-cells (Light et al., 2002; Shuai et al., 2021; Tian et al., 2011). Glucagon

is secreted from α-cells to act at GCGRs whilst GLP-1 is released from enteroendocrine L-cells to act at GLP-1Rs present in the β-cell plasma membrane. GCGR and GLP-1R are members of the G protein-coupled receptor (GPCR) family of receptors (see Section 1.6) and activate the AC signalling pathway (Figure 8, left). Neither can trigger insulin secretion alone, but glucagon and GLP-1 can potentiate insulin release in a glucose-dependent manner by activating PKA and EPAC2 (Light et al., 2002; Tian et al., 2011). Other ligands, such as FFAs, bind to GPCRs which activate phospholipase C (PLC)-dependent pathways (Figure 8, right) (Buteau et al., 2001). In addition to yielding IP_3 to trigger Ca^{2+} release from intracellular stores, PLC activity stimulates protein kinase C (PKC) through the generation of diacylglycerol (DAG), a membrane-bound protein which serves to recruit a range of peptides from the cytosol to the membrane. PKC phosphorylates intracellular proteins to further contribute to elevated cytosolic Ca^{2+}. However, studies which have examined the effect of PKC-dependent mechanisms on insulin secretion have yielded variable results (Fridolf & Ahrén, 1991; Gromada et al., 1995; Jacobo et al., 2009; Shigeto et al., 2015).

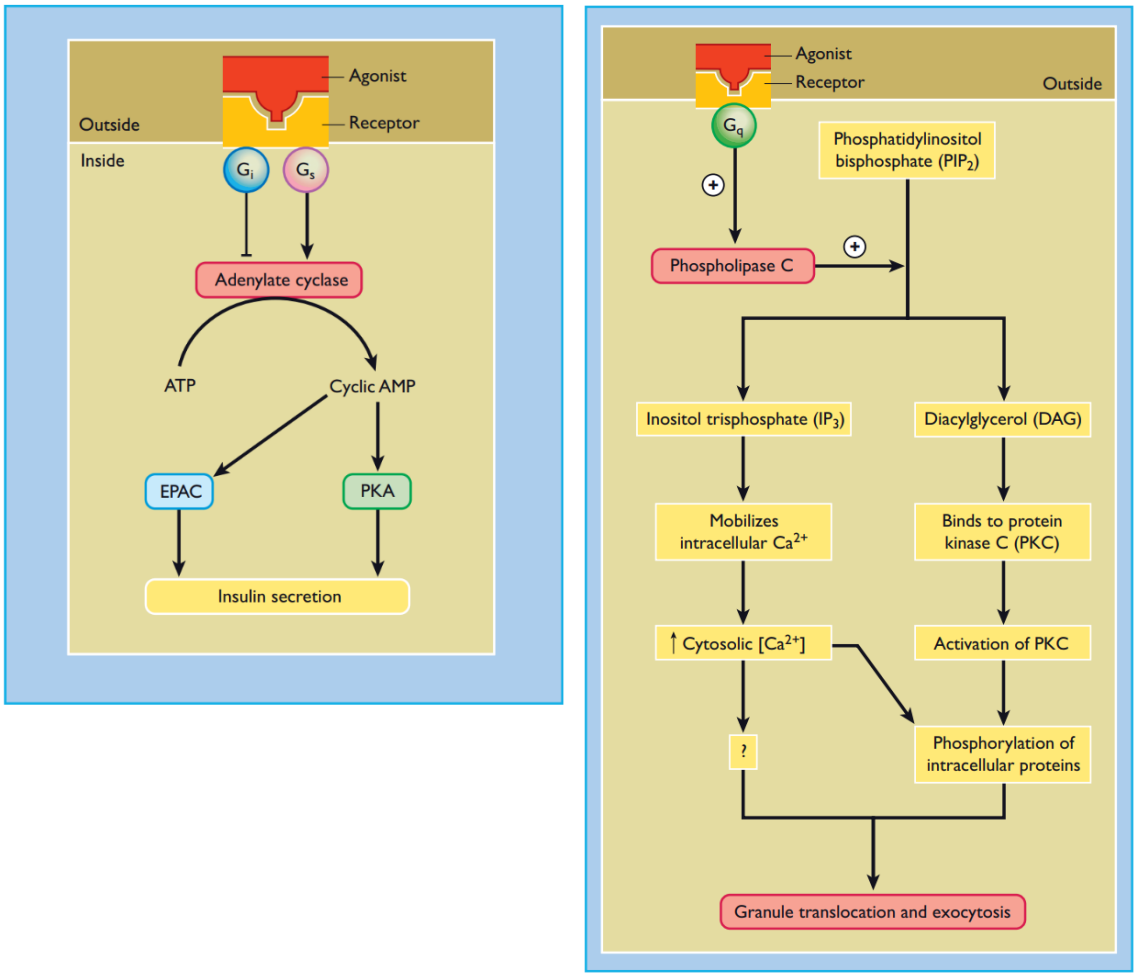

Figure 8. The regulation of insulin secretion by AC- (left) and PLC-mediated (right) signalling pathways. Several stimulatory agonists, such as GLP-1 and glucagon, bind to GPCRs coupled to $G\alpha_s$ proteins. Activation of this GPCR subclass induces AC activity and the production of cAMP from ATP. Subsequent stimulation of PKA and EPAC potentiates glucose-dependent insulin secretion. Some inhibitory agonists, such as somatostatin, inhibit AC-mediated signalling via $G\alpha_{i/o}$-coupled receptors to reduce AC activity and cAMP production. Other agonists, such as acetylcholine and cholecystokinin, activate $G\alpha_{q/11}$-coupled receptors associated with PLC activity leading to the hydrolysis of PIP_2. Liberated IP_3 mobilises Ca^{2+} from intracellular calcium stores whilst membrane-bound DAG recruits PKC to phosphorylate intracellular proteins. Thus, both effectors enhance glucose-stimulated insulin secretion. AC: adenylate cyclase; cAMP: cyclic AMP; PKA: protein kinase A; EPAC: exchange proteins activated by cyclic AMP; PLC: phospholipase C; PIP_2: phosphatidylinositol 4,5 bisphosphate; IP_3: inositol 1,4,5 trisphosphate; DAG: diacylglycerol; PKC: protein kinase C. (Jones & Persaud, 2017).

Alongside systemic and local factors, insulin secretion is also governed by the autonomic nervous system. The islets are innervated by parasympathetic (cholinergic), sympathetic (adrenergic) and sensory nerve fibres (Ahrén, 2012). Acetylcholine (ACh) is the main neurotransmitter of parasympathetic nerves and stimulates both insulin and glucagon release *in vitro* and *in vivo* (Boschero et al., 1995; Iismaa et al., 2000; Karlsson & Ahrén, 1993). ACh is released from the intra-islet nerves and diffuses to the islets cells where it predominantly binds to muscarinic M_3 receptors. Subsequent PLC-mediated generation of IP_3 and DAG leads to PKC activation and elevated cytosolic Ca^{2+}. Activation of muscarinic M_3 receptors is also associated with phospholipase A_2 (PLA_2) stimulation followed by elevated levels of arachidonic

acid (AA) (Konrad et al., 1992). AA is a well-known enhancer of glucose-induced insulin secretion and further contributes to the stimulatory effects of ACh (Konrad et al., 1992). ACh has been shown to mediate the cephalic insulin secretory response during the first minutes of feeding (Ahrén & Holst, 2001). It is also involved in the response to insulin-induced hypoglycaemia by stimulating glucagon release (Havel & Ahren, 1997).

Noradrenaline is the main neurotransmitter of sympathetic nerves. Noradrenaline can have both positive and negative effects on β-cell function as it targets stimulatory β_2-adrenoceptors (Ahrén & Lundquist, 1981) and inhibitory α_2-adrenoceptors (Hamamdzic et al., 1995). These receptors both target AC activity and cAMP production with β_2-adrenoceptor activity activating and α_2-adrenoceptors diminishing this pathway. Due to the receptor-dependent dual effect of noradrenaline, the relative expression of these receptor subtypes dictates its net action on hormone secretion (Jones & Persaud, 2017). Islet catecholamines (CAs), such as dopamine and adrenaline, also modulate insulin and glucagon release via α- and β-adrenoceptors (Aslanoglou et al., 2021; Borelli & Gagliardino, 2001).

1.4 Regulation of β-cell mass

To maintain plasma glucose levels within an optimal range, β-cells must have the capacity to produce, secrete, and store sufficient insulin to appropriately respond to changes in circulating glucose concentrations. To do so, several cellular mechanisms tightly regulate β-cell mass. β-cell proliferation (increased cell number), hypertrophy (increased cell size) and neogenesis (differentiation of precursor cells) expand β-cell mass, whereas β-cell apoptosis (cell death), atrophy (decreased cell size) and de/transdifferentiation reduce β-cell mass (Ackermann & Gannon, 2007). Islet cells exhibit a degree of functional and morphological plasticity under different metabolic conditions (Mezza et al., 2019). In pregnancy and obesity, insulin resistance causes an increase in β-cell proliferation and hypertrophy to enhance insulin secretion. In contrast, significant β-cell loss underlies the progression from insulin resistance to overt diabetes.

1.4.1 β-cell apoptosis

Whilst insulin resistance and increased insulin demand trigger an upregulation in β-cell mass, a 30-60% decline in β-cell mass occurs in patients with T2D (Cho et al., 2011). Interestingly, a 30% increase in average β-cell size is observed in these diabetic patients, suggesting that β-cell number decreases by 60% to reach the reported degree of β-cell mass reduction (Cho et al., 2011). β-cell loss is mediated by a process of programmed cell death, or apoptosis. Multiple physiological processes rely on apoptosis, including normal embryonic development, cell turnover, and functioning of the immune system (Elmore, 2007). However, both deficient and excessive apoptosis can contribute to disease progression: lack of apoptotic control can lead to the accumulation of mutations and cancer development (Pfeffer & Singh, 2018), whereas excessive apoptosis of neurons or β-cells can lead to neurogenerative diseases and diabetes, respectively (Barber & Nakamura, 2002).

There are two types of apoptotic pathways: the intrinsic and the extrinsic pathways (Figure 9). The intrinsic pathway is initiated by a range of lethal stimuli, such as DNA damage, ER stress, hypoxia, and metabolic stress (Lim et al., 2021). Mitochondria-associated Bcl-2 proteins, Bax and Bak, become activated and interact with the pro-apoptotic protein, Bid. Insertion of this

protein complex into the outer mitochondrial membrane triggers mitochondrial outer membrane permeabilisation (MOMP) and marks the commitment to apoptosis. Subsequent release of pro-apoptotic mitochondrial proteins, such as cytochrome c (Cyt c), into the cytoplasm results in the formation of a multimeric “apoptosome” consisting of Cyt c, APAF-1, dATP and pro-caspase-9 (Lim et al., 2021). This facilitates the activation of caspases – intracellular proteases which initiate and regulate apoptosis through cleavage of various proteins (Brentnall et al., 2013). The receptor-mediated extrinsic pathway involves binding of extracellular ligands (e.g. TNF-α, Fas) to their cognate death receptors (e.g. TNFR, FAS, TRAILR1 and TRAILR2) within the target cell membrane (Lim et al., 2021). Death-inducing signalling complexes (DISCs), comprising caspase-8 and FADD, are then recruited to not only activate additional caspases to drive apoptosis, but to also amplify the intrinsic apoptotic response (Lim et al., 2021).

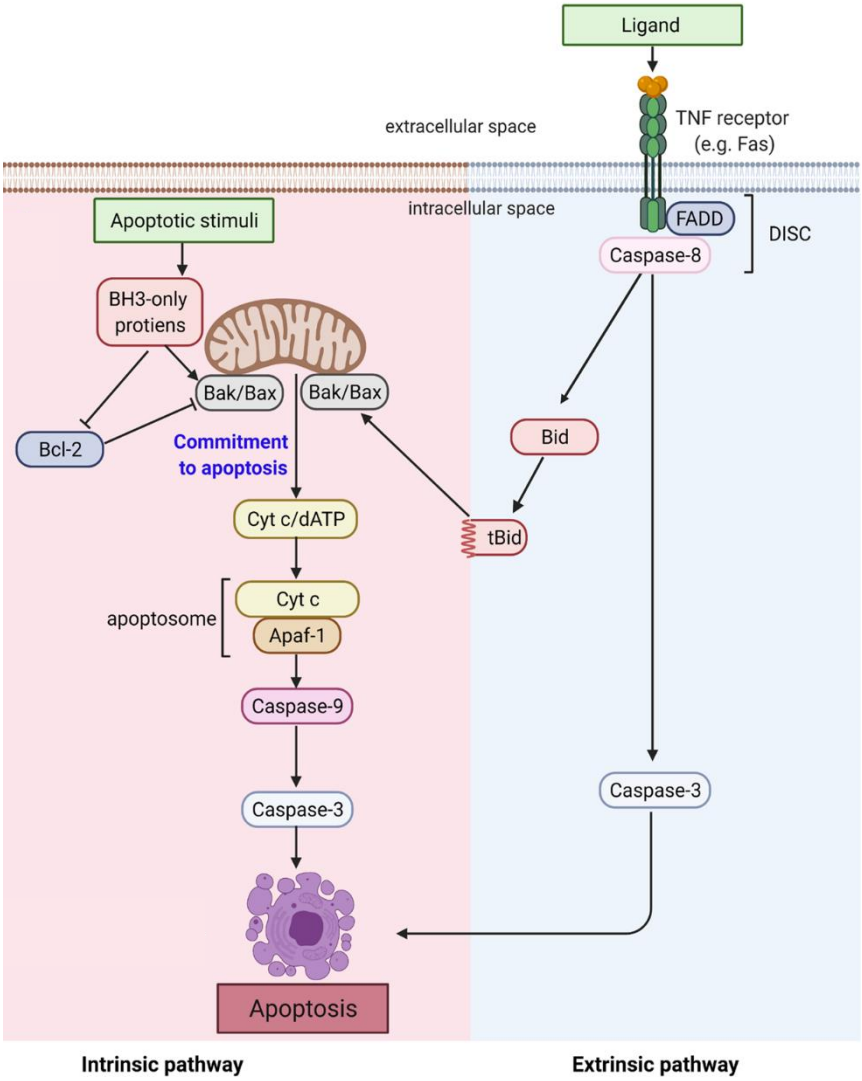

Figure 9. A schematic illustrating the cellular components of the intrinsic and extrinsic apoptotic pathways. The intrinsic pathway is initiated by a variety of cellular stress stimuli, such as DNA damage. Pro-apoptotic proteins, Bax, Bak and Bid, are activated and trigger permeabilisation of outer mitochondrial membranes. Subsequent release of the "apoptosome", consisting of Cyt c and APAF-1, initiates caspase-9 and -3-mediated apoptosis. The extrinsic pathway is initiated by the TNF family of receptors. Ligand binding recruits death-inducing signalling complexes to drive extrinsic apoptosis and exacerbate intrinsic apoptosis. Bcl-2: B-cell lymphoma-2; APAF-1: apoptotic protease-activating factor-1; dATP: deoxyadenosine triphosphate; FADD: FAS-associated death domain protein. (Lim et al., 2021).

In T1D, β-cell death is caused by a T-cell-mediated autoimmune attack. In T2D, a range of factors drive β-cell apoptosis: 1) glucose and lipid toxicity; 2) ectopic fat deposition; 3) chronic inflammation; 4) increased oxidative stress; 5) increased fibrosis; and 6) amyloidosis (cytotoxic amyloid deposition within the islets) (Cho et al., 2011). Parallel to changes at the β-cell level, new α-cell formation and expansion, either through neogenesis or replication, may exacerbate hyperglycaemia in diabetes (Cho et al., 2011). These pathological mechanisms feed into β-cell dysfunction and decline and are major contributors to T2D development. Consequently, β-cell apoptosis has become an important target for therapeutic approaches in the treatment of T2D.

1.4.1.1 Nutrient toxicity

Glucotoxicity refers to the detrimental effects of prolonged hyperglycaemia on β-cell function and insulin sensitivity (Kaiser et al., 2003). Exposure to high glucose causes deformities in mitochondrial morphology, increased production of reactive oxygen species (ROS), oxidative stress, and upregulated apoptosis in β-cells (Del Guerra et al., 2007). This corresponds to a significant reduction in insulin secretion (Del Guerra et al., 2007). Furthermore, β-cells from patients with T2D are more vulnerable to increased glucose levels than those from non-diabetic individuals, as several markers of ER stress are upregulated in diabetic islets (Marchetti et al., 2007).

Lipotoxicity refers to the pro-apoptotic effects on β-cells from chronic exposure to saturated FFAs, such as palmitate (Lupi et al., 2002; Wrede et al., 2002). Plasma FFA levels are significantly increased in obesity (Arner & Rydén, 2015) and this poses a risk for prediabetes in obese individuals due to its negative impact on insulin sensitivity and β-cell survival. Elevated circulating FFAs in obesity contributes to peripheral insulin resistance by inhibiting insulin-stimulated glucose uptake, glycogen synthesis and glucose oxidation (Boden et al., 1994). The compensatory hyperinsulinaemic response that follows contributes to β-cell fatigue and death. The direct pro-apoptotic effects of FFAs on β-cells are well-established with long-term treatment inducing marked increases in apoptosis in the pancreatic β-cell lines, INS-1 and MIN6 (Kristinsson et al., 2013; Ly et al., 2020; Rakatzi et al., 2004; Watson et al., 2011; Wrede et al., 2002; Wu et al., 2012; Xiong et al., 2016), and in human islets (Lupi et al., 2002). Interestingly, however, there is evidence that shows FFAs can also potentiate glucose-stimulated insulin secretion (Crespin et al., 1969; Warnotte et al., 1994). For example, acute stimulation of β-cells causes elevated insulin secretion via GPR40 activation (Doshi et al., 2009; Kebede et al., 2008). Nonetheless, this potentiation is insufficient to offset FFA-induced insulin resistance in obese individuals with a genetic predisposition towards T2D (Boden, 2001). The direction of insulin secretory effects by FFAs may be temporally controlled, as acute exposure to human islets potentiates glucose-stimulated insulin secretion and long-term exposure attenuates it (Kristinsson et al., 2013).

The combination of deleterious effects from elevated plasma FFAs and glucose levels on β-cell function is referred to as “glucolipotoxicity” (Roduit et al., 2000). Both insults involve the suppression of the Bcl-2 family of cell survival proteins (Lin et al., 2014) and overexpression of pro-apoptotic genes, including Bad, Bid and Bik (Federici et al., 2001), leading to enhanced β-cell death. The hypothesis behind glucolipotoxicity is that hyperglycaemia alone or hyperlipidaemia alone is non-toxic to islet cells, and synergy between the two is required to alter β-cell function to the point of T2D development (Prentki et al., 2002).

1.4.1.2 Chronic inflammation

As previously described, a range of pathological processes contribute to impaired β-cell function in obesity, such as nutrient toxicity, oxidative and ER stress, and ectopic fat deposition. All are associated with an inflammatory response. Excessive nutrient levels place considerable stress on the islets and on insulin-sensitive tissues, such as adipose tissue (Figure 10) (Donath & Shoelson, 2011). This leads to the local production and release of pro-inflammatory mediators from resident immune cells. Elevated immune cell numbers in both fat and islets occur in obesity and T2D; this results from a combination of existing cell proliferation

and increased cell infiltration into these tissues (Ehses et al., 2007; Xu et al., 2003). Macrophages are the dominant immune cell in T2D islet inflammation (Lundberg et al., 2017). Glucolipotoxicity enhances their production of pro-apoptotic cytokines, interleukin-1β (IL-1β) and TNF-α, which diminish insulin secretion and are pro-apoptotic towards β-cells with long-term exposure (Bendtzen et al., 1986; Ortis et al., 2006). The actions of IL-1β are transduced by IL-1 receptors (IL-1R) that are found highly expressed in β-cells (Scarim et al., 1997). Under healthy conditions, the IL-1R antagonist (IL-1RA) is abundantly expressed by β-cells to counterbalance IL-1β activity (Böni-Schnetzler et al., 2008). However, in T2D, this anti-inflammatory mechanism is defective and islet IL-1RA expression is significantly reduced (Böni-Schnetzler et al., 2018; Maedler et al., 2004). As a result, the islets are susceptible to IL-1β autostimulation, i.e. IL-1β induces the expression of itself (Böni-Schnetzler et al., 2008) and islet inflammation is exacerbated.

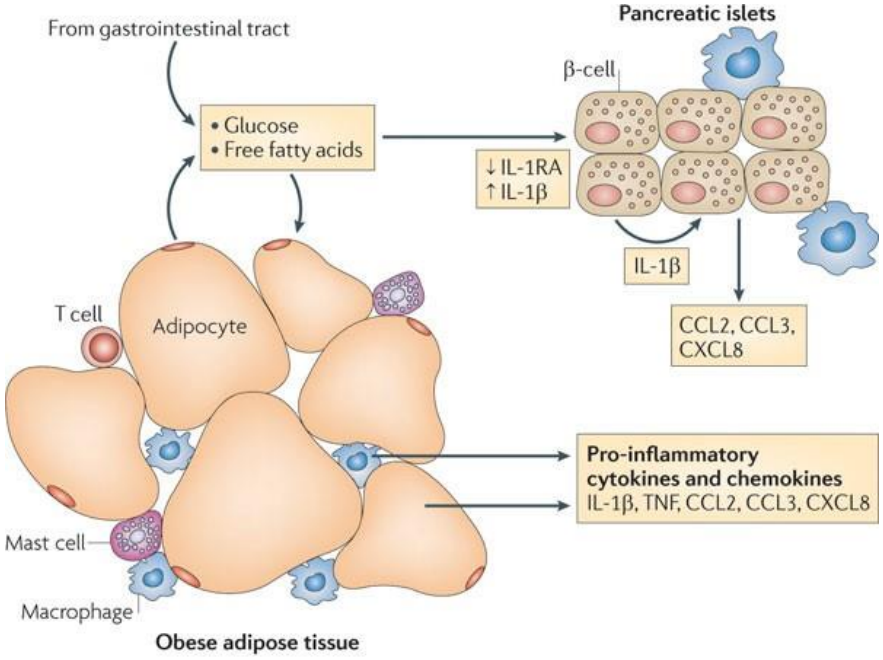

Figure 10. The development of inflammation within adipose tissue and the islets as a result of nutrient toxicity in obesity. Exposure of adipose tissue and β-cells to excessive levels of glucose and FFAs leads to the local production and secretion of pro-inflammatory chemokines and cytokines. Immune cell recruitment exacerbates tissue inflammation and release of factors, such as TNF-α and IL-1β, into the systemic circulation promotes inflammation in other tissues. (Donath & Shoelson, 2011).

In visceral adipose tissue, inflammation and macrophage-specific gene expression (e.g. MAC-1, CD68, MCP-1/CCL2, MIP-1α/CCL3) are significantly upregulated in genetic- and high-fat diet-induced obese mice (Xu et al., 2003). The gene and protein expression profiles of resident macrophages in obese adipose tissue are distinct from those in lean adipose tissue (Lumeng et al., 2007). Anti-inflammatory M2-type macrophages reside in fat depots from lean mice and secrete factors, such as IL-10, which resolve inflammation. However, the progression of obesity triggers a “phenotypic switch” to pro-inflammatory M1-type macrophages and promotes the production of TNF-α, IL-6 and IL-12 (Lumeng et al., 2007). These locally produced factors also advance to the circulation where they travel to skeletal muscle and the islets to aggravate inflammation. This is supported by a significant rise in circulating pro-

inflammatory cytokines and chemokines in obesity (Kim et al., 2006; Schmidt et al., 2015) and T2D (Bahgat & Ibrahim, 2020; King et al., 2003; Pan et al., 2021).

It is clear that the IL-1β pathway is a key mediator in the inflammatory response in obesity and T2D. The pathway is dependent on nuclear factor-κB (NF-κB) and JUN N-terminal kinase (JNK) activation (Toda et al., 2002), and can also be induced by TNF-α. The TNF family drives cell apoptosis by targeting the extrinsic caspase pathway, as previously mentioned in Section 1.4.1. TNF-α is capable of inducing caspase-mediated apoptotic death in β-cells (Stephens et al., 1999). TNF-α is also heavily implicated in tissue inflammation and impaired insulin sensitivity. Chronic exposure to TNF-α promoted resistance to insulin-induced GLUT4 translocation and glucose uptake in skeletal muscle (de Alvaro et al., 2004; Rosenzweig et al., 2002). In adipose tissue, TNF-α downregulates the expression of key genes involved in glucose and lipid uptake, leading to increased lipolysis and FFA release (Ruan et al., 2002). These detrimental effects on lipid and glucose homeostasis are worsened by the reduced mRNA expression of ACRP30, an adipocyte-exclusive protein which inhibits hepatic gluconeogenesis (Combs et al., 2001; Ruan et al., 2002). High plasma glucose and FFA levels, partly induced by the actions of TNF-α, accelerate β-cell failure and T2D progression.

1.4.2 β-cell dedifferentiation and transdifferentiation

The β- and α-cells are derived from a common endocrine progenitor and share multiple transcription factors and genes involved in glucose uptake, metabolism, and stimulus-induced hormone secretion (Meulen & Huising, 2015). These include pancreatic duodenal homeobox gene 1 (Pdx1) and neurogenin-3 (Neurog3), whose expression drives islet cell differentiation and regeneration. The induction of downstream β-cell-enriched transcription factors, paired box 4 (Pax4), V-maf musculoaponeurotic fibrosarcoma oncogene homolog A (Mafa) and forkhead box protein O1 (FoxO1) , among others, are required for subsequent β-cell differentiation and maturation. Due to their closely related lineage and function, conversion of insulin-expressing β-cells into glucagon-expressing α-cells via an intermediate dual-hormone positive cell type is thought to contribute to β-cell loss and dysfunction (Meulen & Huising, 2015; Papizan et al., 2011). This phenomenon, termed “transdifferentiation”, may also accompany dedifferentiation involving a complete regression of mature β-cells to precursor-like cells (Jonas et al., 1999). Both pathways are largely mediated by the downregulation of β-cell-specific genes, including insulin, glucokinase and the above mentioned transcription factors, and the upregulation of “disallowed” genes expressed by islet progenitor cells or mature α-cells which are otherwise suppressed in mature β-cells (Bensellam et al., 2018; Lemaire et al., 2017). Deficits in insulin synthesis, insulin granules and glucose-stimulated secretory function and subsequent hyperglycaemia result from this loss in β-cell identity. Increased α-cell mass and excessive glucagon production as part of β-to-α-cell reprogramming contribute further to dysregulated glycaemic control.

Evidence supporting β-cell dedifferentiation and transdifferentiation in T2D is growing. For example, markers of endocrine progenitor cells and disallowed genes, such as aldehyde dehydrogenase 1A3 (ALDH1A3) (Cinti et al., 2016), lactate dehydrogenase (LDHA) and phosphoenolpyruvate carboxykinase 1 (PCK1) (Marselli et al., 2014) were increased in diabetic human islets. In contrast, Pdx1 and Mafa protein levels were reduced in islets from diabetic mice and humans (Guo et al., 2013; Yang et al., 2012). Additionally, insulin-glucagon positive (polyhormonal) cells were observed within islets of diabetic mice (Brereton et al.,

2014), primates (Spijker et al., 2015) and patients (Cinti et al., 2016; Moin et al., 2016; Spijker et al., 2015). Deletion of Pdx1 (Kim-Muller et al., 2014) and FoxO1 (Talchai et al., 2012), also recapitulated diabetic features in mice, including reduced β-cell mass and insulin content, increased glucagon content and/or α-cell number, hypoinsulinaemia hyperglucagonaemia, and hyperglycaemia. Accordingly, glucolipotoxicity, oxidative and ER stress, inflammation, and hypoxia are T2D-related triggers of β-cell dedifferentiation and transdifferentiation (Bensellam et al., 2012; Brereton et al., 2014; Jonas et al., 1999; Kjørholt et al., 2005). Although the contribution of these mechanisms to overall β-cell loss in T2D is under debate, current evidence implicates β-cell plasticity and identity maintenance in diabetes pathophysiology.

1.4.3 β-cell proliferation

During postnatal development, β-cells have great replicative potential to facilitate significant mass expansion (Jacovetti et al., 2015). The rate of β-cell proliferation peaks during the first 2 years of life and β-cell mass remains relatively constant after the age of 5 (Jacovetti et al., 2015). In adults, the majority of β-cells are resistant to proliferation due to brakes upon the cell cycle, leaving only a small portion of replicating β-cells (Puri et al., 2018). This low proliferative capacity means β-cell expansion is severely limited (~0.2% of β-cells/24 hours) (Eguchi et al., 2022). Moreover, β-cells do not respond well to mitogens. Unfortunately, for diseases such as T2D where there is dramatic β-cell loss, this restricts the potential for developing therapies which stimulate the replication of the remaining β-cells (Eguchi et al., 2022). Whilst the rate of β-cell proliferation is very low in adults, under certain conditions where there is increased metabolic demand, β-cells can adapt to functionally compensate. This is the case in pregnancy (physiological) (Parsons et al., 1992) and obesity (pathophysiological) (Weir et al., 2001).

1.4.3.1 β-cell expansion in pregnancy

Maternal glucose metabolism gradually changes throughout gestation to ensure a continuous supply of nutrients that supports the growth and development of the fetus. Transport of glucose across the placenta is passive and relies on glucose transporters and a transplacental concentration gradient between the maternal and fetal circulations (Hay, 2006). During early gestation, glucose insensitivity and high basal insulin secretion in fetal β-cells maintains low glucose levels in the fetal circulation and thus, the concentration gradient. During late gestation, however, fetal hyperinsulineamia drives rapid glucose uptake, enhanced glucose utilisation, and growth of insulin-sensitive tissues. Maternal plasma glucose is subsequently lowered to a level that disrupts the transplacental concentration gradient. This process has been labelled the “feto-placental glucose steal phenomenon” and must be counteracted by increased maternal insulin resistance and hepatic glucose production (Nolan & Proietto, 1994). At this point in gestation, there is a risk of excessive nutrient shunting to the fetus and the development of harmful hyperglycaemia in both mother and offspring. To prevent this, the maternal islets undergo structural and functional changes to increase insulin secretion: 1) an augmented sensitivity to plasma glucose due to a decrease in the threshold value of glucose-induced insulin secretion (Green & Taylor, 1972; Parsons et al., 1992); 2) an enhanced insulin secretory capacity due to upregulated proinsulin biosynthesis, β-cell proliferation, and β-cell hypertrophy (Bone & Taylor, 1976; Xue et al., 2010); 3) an increase in gap-junctional coupling between β-cells to enhance electrical communication and activation in response to a rise in

plasma glucose (Parsons et al., 1992); and 4) greater glucose oxidation and cAMP concentrations within β-cells associated with the heightened glucose sensitivity and insulin secretion (Green et al., 1973).

Overall, the compensatory mechanisms observed in the islets are essential for meeting insulin demand and maintaining maternal normoglycaemia. Failure of these mechanisms leads to GD which is associated with multiple maternal and fetal complications (see Section 1.1.3). The potential severity of GD has led to investigations into the pathways responsible for the modifications of islet function seen in pregnancy. Indeed, the pregnancy-induced metabolic changes described above mirror fluctuations in several hormones and signalling molecules. Among them are two hormones which have been identified as key participants in regulating the islet adaptations to pregnancy: placental lactogen (PL) and prolactin (PRL) (Brelje et al., 1993; Parsons et al., 1992). Targeted overexpression of PL in cultured INS-1 β-cells (Fleenor et al., 2000) and in transgenic mice (Vasavada et al., 2000) increased both β-cell hyperplasia and hypertrophy. The subsequent growth of islet mass corresponded to elevated insulin content and plasma insulin concentrations (Vasavada et al., 2000). PRL treatment also significantly upregulated glucose-stimulated insulin secretion and GLUT2 mRNA expression in INS-1 β-cells (Arumugam et al., 2008). PL and PRL both act through the PRL receptor which, when deleted in mice, reduced β-cell mass, insulin mRNA and peptide content, and the insulin secretory response to glucose (Freemark et al., 2002). These observed effects in mouse and rat models translate into human islets which contain greater insulin content and secrete significantly more insulin when exposed to PL and PRL compared to control media (Brelje et al., 1993; Swenne et al., 1987).

Adipose tissue and its derived peptide, adiponectin, have been implicated in the underlying mechanisms which control PL-induced maternal β-cell expansion. Adiponectin is known for its insulin-sensitising function, and low plasma adiponectin levels (hypoadiponectinaemia) are observed in obesity (Arita et al., 1999; Hara et al., 2006), T2D (Hotta et al., 2000), and GD (Qiao et al., 2017). Knockout of the adiponectin gene (*Adipoq*$^{-/-}$) in pregnant mice models adiponectin deficiency in pregnancy. Several metabolic perturbations develop as a result of disturbed adiponectin signalling: greater rates of hepatic glucose and triglyceride production, and increased lipolysis in adipose tissue contribute to marked glucose intolerance and hyperlipidaemia in these mice; this is exacerbated by reduced β-cell mass and circulating insulin levels. Increased fetal body weight and blood glucose levels were also observed, highlighting the association between the maternal metabolome and newborn outcomes. Rescue of adiponectin deficiency by adenoviral vector-mediated *in vivo* transduction ameliorated the metabolic defects in pregnant mice and their offspring (Qiao et al., 2017). Adiponectin does not directly modulate β-cell proliferation during pregnancy (Qiao et al., 2021). Instead, adiponectin significantly raises PL mRNA and protein expression in the JEG3 placental cell line and in human placenta. PL injections administered to pregnant *Adipoq*$^{-/-}$ mice restored β-cell proliferation rates, β-cell mass, and maternal plasma insulin and glucose levels to those of wild-type pregnant mice (Qiao et al., 2021). These recent studies describe a fundamental regulatory role of adiponectin in pregnancy-induced β-cell adaptations via PL expression. The crosstalk between adipose tissue and the placenta therefore contributes to the maintenance of glucose homeostasis during pregnancy. In fact, adipose tissue expansion, driven by adipocyte hyperplasia and lipogenesis, is a physiological adaptation to a healthy pregnancy. However, maternal obesity is characterised by systemic, placental and fetal inflammation (Stewart et al., 2007) and may be partly attributed to pro-inflammatory

adipokines, such as leptin. Leptin regulates maternal glucose metabolism and, by increasing nutrient availability, supports fetal development in pregnancy (Misra & Trudeau, 2011). Whilst circulating concentrations do increase throughout normal gestation, its levels are significantly upregulated in serum of pregnant overweight/obese women compared to their lean counterparts (Misra & Trudeau, 2011). Leptin has been shown to promote the release of other inflammatory factors, e.g. IL-6 and nitric oxide, from human trophoblast cells which feeds into placental inflammation and oxidative stress (Parisi et al., 2021). Approximately 33% of obese mothers suffer from adverse pregnancy outcomes compared to 15% of lean mothers (Trivett et al., 2021). These are often linked to metabolic dysfunction with obesity-induced adipokine imbalance a possible component.

1.4.3.2 β-cell expansion in obesity

Growing adiposity correlates with increased insulin resistance and hyperglycaemia. The primary response is to expand β-cell mass via proliferation. Thus, obesity is characterised by a compensatory expansion in islet cell volume following increased insulin demand. This is a consistent event that occurs across obese mouse models and in human subjects with obesity (Bock et al., 2003; Butler et al., 2003; Cox et al., 2016). The mechanisms responsible for this expansion remain unclear. Multiple studies have deduced that obesity-induced β-cell expansion is not the result of neogenesis, but of self-duplication of pre-existing cells (Bock et al., 2003; Cox et al., 2016; Dor et al., 2004; Teta et al., 2007). Evidence implicates sub-threshold ER stress as a regulator of β-cell proliferation (Sharma et al., 2015; Szabat et al., 2016). The unfolded protein response (UPR) is thought to promote the expression of *Atf6*, a transcription factor, that, when inhibited, reduces β-cell proliferation and when overexpressed, induces it (Sharma et al., 2015). β-arrestin-1 (*barr1*) may also be required for β-cell expansion in obesity, as its deficiency reduces the expression of *Pdx1*, a β-cell-enriched transcription factor critical for proliferation and survival (Barella et al., 2021). Neuronal signals have also been shown to play an important role. The release of neurotransmitters from vagal nerves that supply the islets activates the foxhead box M1 (FoxM1) pathway in obese β-cells (Yamamoto et al., 2017). The pathway regulates several steps in the cell cycle, and the expression of FoxM1 and its target mitogenic genes were significantly upregulated in obesity (Yamamoto et al., 2017). Whilst the exact mechanisms have yet to be fully elucidated, the large body of data supports a clear linear correlation between body weight and β-cell mass (Montanya et al., 2000). However, if the rate of β-cell proliferation is insufficient to overcome chronic hyperglycaemia, overt T2D develops. The proliferative capacity of β-cells also declines with age (Puff et al., 2011) and contributes to the elevated age-related risk of T2D development. Yet, whilst proliferative dysfunction partly underpins the loss of β-cell volume in T2D, a great deal can be attributed to increased apoptotic frequency (Butler et al., 2003; Puff et al., 2011).

1.5 Adipose tissue

1.5.1 Morphology and function

Adipose tissue comprises a heterogenous population of cell types such as mature adipocytes, preadipocytes, and immune, nerve and endothelial cells surrounded by extracellular matrix (ECM) (Kershaw & Flier, 2004). Reports of the proportion of mature adipocytes within adipose tissue are highly variable in the literature. The percentage of mature adipocytes has been

reported to be as low as ~20% (Tsiloulis & Watt, 2015) and as high as ~60% (Bourgeois et al., 2019) of the total cell population. Although this value is under dispute, it is generally accepted that mature adipocytes represent ~80% adipose tissue volume due to the extensive storage of lipids within the cytoplasm (Bourgeois et al., 2019). To accommodate even further tissue expansion in the event of chronic energy intake, the volume of mature adipocytes must increase. Mature adipocytes can undergo cellular hypertrophy to facilitate adipose tissue growth, however, hypertrophic adipose tissue is highly dysfunctional. It is associated with diminished glucose uptake, elevated lipolysis and FFA release, hypoxia, fibrosis, and macrophage-mediated inflammation (Jernås et al., 2006). Large and small adipocytes can be separated by distinct genetic profiles with upregulated expression of several genes, such as serum amyloid A (SAA), in hypertrophic adipocytes potentially contributing to insulin resistance (Jernås et al., 2006). In contrast, adipose tissue hyperplasia is a protective mechanism in obesity. Mature adipocytes are terminally differentiated cells and therefore have no proliferative capacity (Song & Kuang, 2019). New cells are derived from multipotent mesenchymal stem cells which enter a determination stage and convert to pluripotent stem cells (Rosen & MacDougald, 2006). These cells then commit to the adipocyte lineage and transform into preadipocyte cells that rely on an adipogenic transcriptional cascade to terminally differentiate into mature adipocytes (Figure 11) (Rosen & MacDougald, 2006). Unlike their fibroblast-like precursor cells, mature adipocytes have a specialised lipid storage function and express adipocyte genes to support insulin sensitisation, and glucose and lipid metabolism. This differentiation process is termed “adipogenesis” and is heavily influenced by three classes of transcription factors: PPARγ, CCAAT/enhancer binding proteins (C/EBP), and adipocyte determination and differentiation-dependent factor 1 (ADD1 or SREBP1) (Drolet et al., 2008).

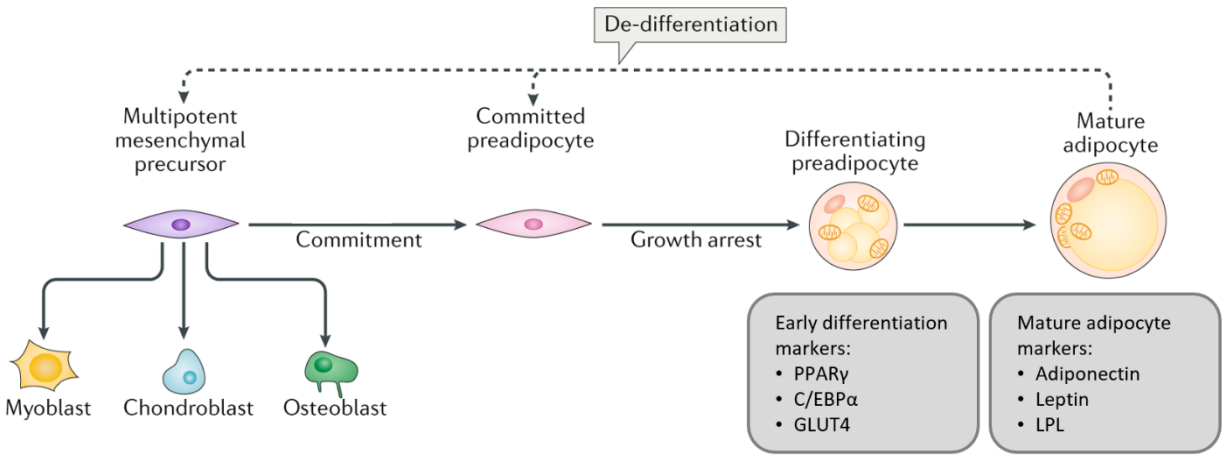

Figure 11. A schematic illustrating the molecular mechanisms of adipogenesis. Multipotent mesenchymal stem cells commit to a preadipocyte lineage. Committed preadipocyte cells are fibroblast-like, and once growth is arrested, master regulator of adipogenesis, PPARγ, and its transcription co-activator, C/EBPα, are activated. Early differentiation is characterised by lipid accumulation which drives the expression of early adipocyte markers, including GLUT4. Once fully differentiated, adipocytes express both early and mature adipocyte markers, such as adiponectin, leptin, and LPL. Adipocytes have the capacity to undergo de-differentiation back to fibroblast-like preadipocytes. LPL: lipoprotein lipase. Adapted from Ghaben & Scherer (2019).

PPARγ belongs to a nuclear receptor family of ligand-activated transcription factors and is essential for adipogenesis, the regulation of insulin sensitivity, lipogenesis, and overall adipocyte survival and function (Lefterova et al., 2014). It exists as two isoforms: PPARγ1 is expressed at low levels in a variety of non-adipose tissues, whereas PPARγ2 is adipocyte-specific (Tontonoz et al., 1994; Zhu et al., 1995). As previously noted in Section 1.1.2.4, PPARγ is a master regulator of adipocyte differentiation as its activity is both necessary and sufficient for the process to occur (Tontonoz et al., 1994). Upon ligand activation, PPARγ2 activates target gene promoters to induce transcription of several adipogenic genes, including lipoprotein lipase (LPL) and adipsin. Furthermore, PPARγ2 and C/EBPα mutually induce the expression of each other, and the two act synergistically to efficiently stimulate adipocyte differentiation. C/EBPα is involved in the later stages of adipogenesis by targeting genes involved in growth arrest and lipid accumulation (Tontonoz et al., 1994). C/EBPα cannot instigate adipogenesis in the absence of PPARγ2, but it is important in maintaining mature adipocytes in a differentiated state by reinforcing PPARγ2 expression as part of a positive feedback loop (Rosen et al., 2002). Similarly, ADD1/SREBP1 cannot initiate adipogenesis, however, it can augment the process by enhancing PPARγ-mediated expression of fatty acid synthase (FAS) and LPL, two genes which regulate fatty acid metabolism (Kim & Spiegelman, 1996).

The traditional view that adipose merely acts as a lipid storage compartment has long surpassed. It is now appreciated that mature adipocytes are highly active sources of secretory products which are expressed and released in response to various hormonal and central afferent signals (Kershaw & Flier, 2004). Adipose tissue-derived secretory products range from growth factors, cytokines, ECM proteins, factors associated with lipid metabolism, and adipose tissue-specific peptides (Gerst et al., 2019). The diversity of this secretome gives adipose tissue the ability to integrate and communicate with a plethora of organs (Kershaw & Flier, 2004). The integrative network that exists between adipose tissue and other systems facilitates the coordination of various physiological processes, including those concerning immunity, reproduction, neuroendocrine function, and energy homeostasis (Kershaw & Flier, 2004).

1.5.2 Adipokines and metabolic crosstalk

The secretory products from adipose tissue are plentiful. Several contribute to the maintenance of glucose homeostasis by establishing metabolic crosstalk with β-cells. Through receptor binding, these adipokines can regulate mechanisms involved in insulin secretion and/or gene expression. Examples include alterations to GLUT transporter transcription and glucose sensing, and effects on cell proliferation and apoptosis. Other adipokines act on peripheral tissues, such as liver and skeletal muscle, and/or partake in paracrine or autocrine signalling whereby factors act locally to alter the function of adipose tissue itself. By targeting nutrient metabolism, storage, and transport, these adipokines can modulate insulin sensitivity at the adipocyte level and throughout the periphery. Adiponectin and leptin are the most well-characterised adipose tissue-derived peptides that influence β-cell function and insulin sensitivity. Additional factors which have similar capabilities include chemerin, resistin, apelin and adipsin.

1.5.2.1 Adiponectin

Adiponectin is an adipocyte-exclusive peptide with roles in nutrient metabolism and insulin sensitisation. The full-length protein is composed of single-chain trimers and, due to its high structural homology, adiponectin is a member of the complement 1Q factor/TNF-related (CTRP) family of peptides (Scherer et al., 1995). Its monomers can assemble into trimers, hexamers, and multimers – also referred to as low-, middle- and high-molecular weight forms, respectively – which preferentially bind to target adiponectin receptors (Khoramipour et al., 2021). The actions of adiponectin are transduced by the receptors, AdipoR1, AdipoR2, and T-cadherin (Hug et al., 2004). The cadherin family of cell-surface proteins mediate calcium-dependent cell-cell adhesions and signal transduction, and are essential for cell migration, mammalian development and tissue morphogenesis (Aberle et al., 1996). Adiponectin was identified as a ligand for T-cadherin receptors expressed in vascular cells, such as smooth muscle cells (Tkachuk et al., 1998), endothelial cells (Wyder et al., 2000), and pericytes (Ivanov et al., 2001). Adiponectin/T-cadherin interactions are anti-atherogenic and thus, protective against vascular injury (Fujishima et al., 2017). T-cadherin expression is also thought to be a marker of preadipocyte plasticity and their capacity to terminally differentiate, which potentially reflects adipose tissue health, however, this hypothesis requires further investigation (Göddeke et al., 2018). AdipoR1 and AdipoR2 belong to the progestin and adipoQ family of receptors. Similar to GPCRs, both receptors contain seven transmembrane domains, however, there are several structural and functional differences which distinguish AdipoR1 and AdipoR2 from the GPCR family (Lee et al., 2008). For example, the N-terminus and C-terminus of the adiponectin receptors have an opposing orientation to that of GPCRs (Yamauchi et al., 2003). Moreover, GPCRs respond to ligand binding by activating associated G proteins which is not the case for AdipoR1 and AdipoR2. Further details on GPCR structure and function can be found in Section 1.6. Once bound to AdipoR1 and/or AdipoR2, the actions of adiponectin are primarily mediated by AMPK and PPARα signalling pathways within target tissues (Lee et al., 2008). AdipoR1 is most abundantly expressed in skeletal muscle, whereas AdipoR2 is mostly expressed in the liver (Yamauchi et al., 2003). This pattern of receptor localisation is significant for the insulin sensitising function of adiponectin.

The inverse relationship between BMI, insulin sensitivity and circulating adiponectin levels has been well established. Plasma concentration levels of adiponectin are significantly reduced in obese individuals (Arita et al., 1999; Hara et al., 2006) and patients with type 2 diabetes (Hotta et al., 2000). Furthermore, hypoadiponectinaemia is associated with elevated fasting plasma insulin levels (Weyer et al., 2001) and insulin resistance, as determined by the homeostasis model assessment for insulin resistance (HOMA-IR) (Hara et al., 2006; Weyer et al., 2001; Yatagai et al., 2003). High plasma adiponectin levels are linked to improvements in insulin sensitivity, as both genetic and pharmacological approaches to upregulate circulating adiponectin leads to enhanced glucose tolerance in insulin resistant, obese rodent models (Yamauchi et al., 2001; Combs et al., 2004). The mechanisms responsible for these effects on insulin sensitivity may involve adiponectin-mediated increases in fatty acid oxidation and reduced triglyceride content in skeletal muscle and liver (Yamauchi et al., 2001). Additionally, adiponectin treatment leads to the suppression of gluconeogenic gene expression in mouse hepatocytes, thus reducing hepatic glucose production (Miller et al., 2011). Insulin-induced phosphorylation of the insulin receptor, IRS-1 and AKT kinase in skeletal muscle is also amplified, indicating improved insulin signalling (Yamauchi et al., 2001). Increased GLUT4 translocation in skeletal muscle cells exposed to adiponectin contributes to greater glucose

uptake and the lowering of plasma glucose levels (Ceddia et al., 2005). Alongside its insulin sensitising effects, adiponectin also ameliorates cytokine- and palmitate-induced INS-1 β-cell apoptosis, as shown by reduced caspase-3 activity and DNA fragmentation (Holland et al., 2011; Rakatzi et al., 2004). Furthermore, adiponectin impedes the suppression of glucose-stimulated insulin secretion by mixed cytokines and palmitate in these cells (Rakatzi et al., 2004). This provides evidence to support a protective role of adiponectin against β-cell lipotoxicity, a pathophysiological component in T2D development. Interestingly, significant augmentation of glucose-stimulated but not basal insulin secretion was observed in adiponectin-treated islets isolated from high-fat diet-induced insulin resistant mice, suggesting a dichotomy in adiponectin action that is dependent on the glucose environment (Winzell et al., 2004).

1.5.2.2 Leptin

Leptin is an adipocyte-derived cytokine which acts centrally in the regulation of satiety and food intake, energy expenditure, and the onset of puberty. Leptin receptors, or LEP-Rs, are members of a class I cytokine receptor family. There are six isoforms (LEP-Ra to LEP-Rf) which are generated by alternative RNA splicing of the leptin receptor gene (*Lepr* or *db*). Each receptor isoform consists of an extracellular, intracellular, and transmembrane region, and the extracellular leptin binding domain is conserved across all six isoforms. The intracellular and transmembrane regions, however, slightly differ between them. LEP-Rb is the longest leptin receptor isoform and is the well-established primary mediator of all leptin signalling. Tyrosine residues located within the intracellular domain are sites for Janus kinase 2 (JAK2)-induced tyrosine phosphorylation. Binding of leptin to LEP-Rb recruits cytoplasmic JAK2 to the membrane and ultimately results in the phosphorylation of STAT proteins and altered gene expression. LEP-Rb is present in a range of immune cells, such as neutrophils, monocytes and lymphocytes, and modulates both adaptive and innate immune responses (Fernández-Riejos et al., 2010). However, LEP-Rb is mainly expressed in the hypothalamus, specifically the orexigenic NPY/AgRP neurons (appetite-stimulating) and the anorexigenic POMC/CART neurons (appetite-suppressing) (Schwartz et al., 2000). Both sets of neurons are found in the arcuate nucleus (ARC) and project onto melanocortin-4 receptor (MC4R)-expressing neurons located within the paraventricular hypothalamus (PVH), dorsomedial hypothalamus (DMH), and other hypothalamic sites which control feeding behaviour and energy expenditure (Sutton et al., 2016). Leptin dampens NPY/AgRP neuronal activity and inhibits the release of the MC4R antagonist, agouti-related peptide. In parallel, leptin activates POMC/CART neurons and stimulates the secretion of MC4R agonists, including α-melanocyte-stimulating hormone (α-MSH). The leptin-induced activation of pathways with opposing effects on energy balance collectively diminishes satiety and food intake (Schwartz et al., 2000). Due to the fundamental role of leptin signalling in the control of food intake, deficiencies in either leptin or the leptin receptor leads to monogenic forms of obesity. Monogenic obesity resulting from disturbed leptin signalling has been extensively studied in the *ob/ob* (Zhang et al., 1994) and *db/db* (Bahary et al., 1990) genetic mouse models of obesity, which lack leptin and the leptin receptor, respectively. Both defects are typically characterised by severe hyperphagia (excessive eating), endocrine abnormalities, such as hypogonadotropic hypogonadism, and high infection rates (Dubern & Clement, 2012). Leptin replacement therapy has proven to be an effective treatment in leptin-deficient patients with daily subcutaneous injections causing reduced food intake and weight loss, normalised puberty onset, and resolution of associated co-morbidities (Farooqi et al., 1999; Licinio et al., 2004). Unfortunately, this course of treatment

is ineffective in patients with leptin receptor deficiencies. However, a recent breakthrough has made the MC4R agonist, setmelanotide, available to leptin receptor-deficient individuals (Clément et al., 2018). MC4R agonism restores the function of the leptin-melanocortin signalling pathway to reduce hunger and promote profound weight loss (Clément et al., 2018).

Short isoforms, LEP-Ra, LEP-Rc, LEP-Rd and LEP-Rf, also bind JAK kinases, however, their capacity to activate signal transduction pathways is reduced compared to the long LEP-Rb isoform (Bjørbaek et al., 1997). LEP-Ra is the most common leptin receptor isoform found in various tissues, such as kidney, lungs and brain (Tartaglia et al., 1995). It is thought to mediate leptin internalisation and degradation, and ligand-induced receptor downregulation (Uotani et al., 1999). LEP-Re is the most distinctive isoform as it lacks intracellular and transmembrane domains. Instead, this soluble receptor is secreted into the circulation where it can bind to serum leptin (Huang et al., 2001). By acting as a leptin-binding protein, LEP-Re can inhibit leptin binding to cell membranes thereby blocking signal transduction in target tissues (Liu et al., 1997). On the other hand, by delaying leptin clearance from the circulation, this isoform may elevate the bioavailability of leptin (Huang et al., 2001).

The level of circulating leptin is directly proportional to adipose tissue mass and lipid content. In accordance, serum leptin concentrations are significantly augmented in obese vs normal weight individuals (Considine et al., 1996). This reflected a doubling of leptin mRNA expression in mature adipocytes of obese subjects (Considine et al., 1996). Moreover, fasting serum leptin levels are positively correlated with total body lipids in mice (Frederich et al., 1995), and with both BMI and body fat percentage in humans (Kennedy et al., 1997). In healthy humans, leptin has the ability to exert its anorexigenic effects to reduce appetite, food intake and body weight. In obesity, however, the effects of leptin are severely blunted. This impairment in leptin action is termed “leptin resistance” and there are several potential mechanisms which underlie its development (Gruzdeva et al., 2019). Examples include defective leptin receptor signalling and reduced leptin receptor expression in target tissues. Also, leptin resistance compounds diet-induced adipose tissue expansion which drives further increases in leptin production. Thus, leptin can play a significant role in the development of its resistance (Gruzdeva et al., 2019).

The pathological increase in circulating leptin levels observed in obesity can directly influence β-cell function. The expression of the full-length leptin receptor, LEP-Rb, has been reported in multiple β-cell lines, including βTC-3, MIN6 and INS-1 (Fehmann et al., 1997; Kieffer et al., 1996; Tanizawa et al., 1997), and in primary mouse, rat and human islets (Emilsson et al., 1997; Kieffer et al., 1996; Poitout et al., 1998; Seufert et al., 1999). An inhibitory action of leptin on glucose-stimulated insulin secretion is well-documented in these cells and tissues (Emilsson et al., 1997; Fehmann et al., 1997; Kulkarni et al., 1997; Poitout et al., 1998; Tanizawa et al., 1997). The translation into an *in vivo* setting reveals a subsequent rise in plasma glucose levels (Cases et al., 2001; Kulkarni et al., 1997).

1.5.2.3 Other adipokines of interest

Chemerin is an adipokine and a chemotactic agent. It activates GPCRs, ChemR23 and GPR1, both of which signal via mitogen-activated protein kinase (MAPK) and RhoA/ROCK cascades (Kennedy & Davenport, 2018). Patterns of chemerin expression and secretion in relation to obesity and diabetes are heterogeneous across multiple studies (Bozaoglu et al., 2007;

Hansen et al., 2014; Sell et al., 2009; Stelmanska et al., 2013; Takahashi et al., 2008). It is unclear whether changes in chemerin mRNA and plasma peptide levels are causative, compensatory, or simply correlative to an insulin-resistant/diabetic state. Similar discrepancies regarding chemerin action have been reported, with both negative and positive functional effects observed at the β-cell (Ernst et al., 2012; Rourke et al., 2014; Takahashi et al., 2011) and at insulin-responsive peripheral tissues (Ernst et al., 2010, 2012; Huang et al., 2021; Kralisch et al., 2009; Sell et al., 2009; Takahashi et al., 2008). Marked differences in study designs could explain the conflicting results. Mouse strain, animal age and gender, severity of the diabetic phenotype, the target receptor, experimental protocol, choice of diet-, pharmacologically or genetically induced animal models of obesity/diabetes, method of genetic manipulation, and duration of high-fat diet feeding are all factors that could influence study outcomes.

Adipsin protects against β-cell dedifferentiation and apoptosis in T2D by increasing complement peptide C3a levels (Gómez-Banoy et al., 2019), a ligand that improves islet function via the GPCR, C3aR (Atanes et al., 2018). Apelin is an agonist for the GPCR, APJ, which signals via $G\alpha_i$ to inhibit AC activity and reduce cAMP generation (Sörhede Winzell et al., 2005). The APJ receptor is expressed by islets and its activation inhibits glucose-stimulated insulin secretion *in vitro* and *in vivo* (Sörhede Winzell et al., 2005). Resistin exerts similar impairment of glucose-dependent insulin secretion in β-cells and contributes to resistin-induced insulin resistance and inflammation at the periphery (Nakata et al., 2007; Wen et al., 2017). The specific receptor(s) for resistin have not been conclusively identified, however, toll-like receptor 4 (TLR4) (Tarkowski et al., 2010), ROR1 (Sánchez-Solana et al., 2012), and CAP1 (Lee et al., 2014) are potential mediators of resistin action.

1.5.2.4 Paracrine and autocrine signalling in adipose tissue

Adipose tissue-derived peptides not only act systemically via endocrine pathways, but they can also engage in paracrine or autocrine signalling to modulate tissue function in a process of self-regulation. Leptin, for example, has been shown to suppress lipid synthesis and accumulation in preadipocytes (Bai et al., 1996; Singh et al., 2012). Leptin also blocked several metabolic actions of insulin on adipocytes, including glucose influx, lipogenesis, and protein synthesis (Müller et al., 1997). These effects are mediated by long and short leptin receptor isoforms expressed by adipose tissue (Kielar et al., 1998). In contrast to the above inhibitory effects on metabolism, leptin treatment stimulates the expression of PPARγ co-activator-1α (PGC-1α) whose activity is required for the activation of PPARα, a key regulator in adipogenesis and energy metabolism (Brun et al., 1996; Kakuma et al., 2000). A regulatory role in adipogenesis by leptin is further supported by increased preadipocyte differentiation and induced adipogenic markers in adipose tissue-derived stromal cells (ASCs) (Palhinha et al., 2019). Based on the above observations of both positive and negative effects on adipocyte function, leptin's role in autocrine signalling within adipose tissue remains unclear. The evidence implicating chemerin as a regulator of adipocyte differentiation and metabolism is more robust. The adipocyte expression of chemerin and its receptors, ChemR23 and GPR1, dramatically increases throughout adipogenesis (Dranse et al., 2016; Goralski et al., 2007; Roh et al., 2007; Sell et al., 2009; Takahashi et al., 2008). Loss of chemerin signalling impairs several morphological, transcriptional and functional features of differentiated adipocytes:

downregulated PPARγ, adiponectin, leptin and GLUT4 mRNA expression, reduced lipid storage as indicated by Oil Red O staining, and return to a fibroblast-like state (Goralski et al., 2007; Takahashi et al., 2011). Studies therefore highlight chemerin as having an important role in maintaining adipocyte identity.

Paracrine signalling between adipocytes and resident macrophages is an important component in obesity-induced inflammation and T2D. Indeed, co-culture of macrophages with 3T3-L1 adipocytes leads to a significant upregulation in pro-inflammatory TNF-α and a downregulation in anti-inflammatory adiponectin (Suganami et al., 2005). This mirrors the inflammatory response in adipocytes exposed to FFAs, a condition which mimics an obesogenic environment (Suganami et al., 2005). These effects are likely mediated by macrophage-expressed TLR4 and the NF-κB pathway: TLR4 mutation dampens FFA-induced TNF-α production whilst NF-κB inhibitors in the co-culture suppressed pro-inflammatory cytokine production and adipocyte lipolysis (Suganami et al., 2007). Further details of adipose tissue inflammation in obesity can be found below in Section 1.5.3.

1.5.2.5 Indirect adipose tissue–β-cell crosstalk

Alongside the direct communication between adipose tissue and β-cells outlined above, there is also evidence supporting more complex, indirect inter-organ crosstalk. For example, adipocyte-derived leptin and adiponectin directly act on the β-cell, however, these peptides also exert indirect effects through their participation in the adipocyte-brain-bone-β-cell axis (Tanabe et al., 2017). Both leptin and adiponectin regulate osteocalcin production and bioactivity within bone. They do so via actions on the hypothalamus and subsequent modulation of sympathetic tone that innervates osteoblast cells. Osteocalcin targets GPCR6A receptors within the β-cell membrane to enhance cell proliferation and insulin secretion, as evidenced by genetic studies in mice (Tanabe et al., 2017; Wei et al., 2014). The communication that exists between several organ systems and the multitude of signals which integrate and feed into the β-cell adds another layer of complexity when investigating how adipose tissue modulates β-cell function.

1.5.3 Adipose tissue dynamics in obesity and diabetes

The morphological and functional characteristics of adipose tissue are highly modifiable, dynamic, and dependent on metabolic status, specifically the presence of obesity and diabetes. Under lean or physiological conditions (Figure 12A), balanced production and secretion of pro- and anti-inflammatory factors limit the degree of adipose tissue inflammation (Chait & den Hartigh, 2020). This is supported by the presence of anti-inflammatory M2-type macrophages. A balanced redox environment also minimises ER and oxidative stress, thereby alleviating cellular dysfunction and death induced by misfolded proteins and ROS. Furthermore, mature adipocytes exhibit normal insulin sensitivity and metabolic activity, therefore, they can contribute to insulin-stimulated glucose uptake and the maintenance of optimal plasma glucose levels. Mature adipocytes also retain their morphological adaptability meaning they respond to changes in energy balance by increasing lipid storage capacity. This prevents ectopic fat deposition where lipids are deposited in other organs, such as the pancreas and liver, and subsequently, protects against cell death and metabolic dysfunction (Chait & den Hartigh, 2020).

Under conditions of chronic energy intake and obesity (Figure 12B), dysregulation in adipose tissue structure and function can occur. Alterations in adipokine production and secretion favour pro-diabetic, pro-inflammatory factors which negatively impact both adipose tissue and β-cell function. Examples of such factors include IL-6 and TNF-α which feed into chronic inflammation (Gerst et al., 2019). In parallel, levels of adipokines associated with improved insulin sensitivity and β-cell function, such as adiponectin, significantly diminish (Tanabe et al., 2017). The inflammatory environment is exacerbated further by increased macrophage infiltration and the predominance of pro-inflammatory M1-type macrophages (Xu et al., 2003). This is a common feature of dysfunctional hypertrophic adipose tissue observed in obesity. Hypertrophic fat depots release FFAs which bind to macrophage TLR4 receptors and activate NF-κB pathways leading to augmented TNF-α production (Jernås et al., 2006). Chronic ER and oxidative stress accompany this low-grade chronic inflammation. The resulting accumulation of cellular and DNA damage ultimately triggers apoptotic pathways and cell death. The remaining mature adipocytes become resistant to insulin action which places considerable pressure on β-cells to secrete more insulin to combat hyperglycaemia. Obesity is also characterised by increased collagen deposition and the generation of fibrotic tissue within adipose tissue itself, thus limiting adipose tissue plasticity (Pellegrinelli et al., 2016). Additionally, the expression of PPARγ2 and C/EBPα genes which maintain adipocyte maturity are also significantly reduced leading to adipocyte dedifferentiation and reduced lipid storage capacity (Nadler et al., 2000). Both phenomena contribute to ectopic fat deposition, or “lipid overspill” into other organs and cells, including the β-cells (Pellegrinelli et al., 2016). Infiltration of intrapancreatic fat is negatively associated with several parameters of β-cell function, such as glucose insensitivity, dedifferentiation, and loss of specialised function (Taylor, 2019). Overall, exposure to an obesogenic milieu alters adipose tissue physiology and underpins glucose dyshomeostasis in T2D development.

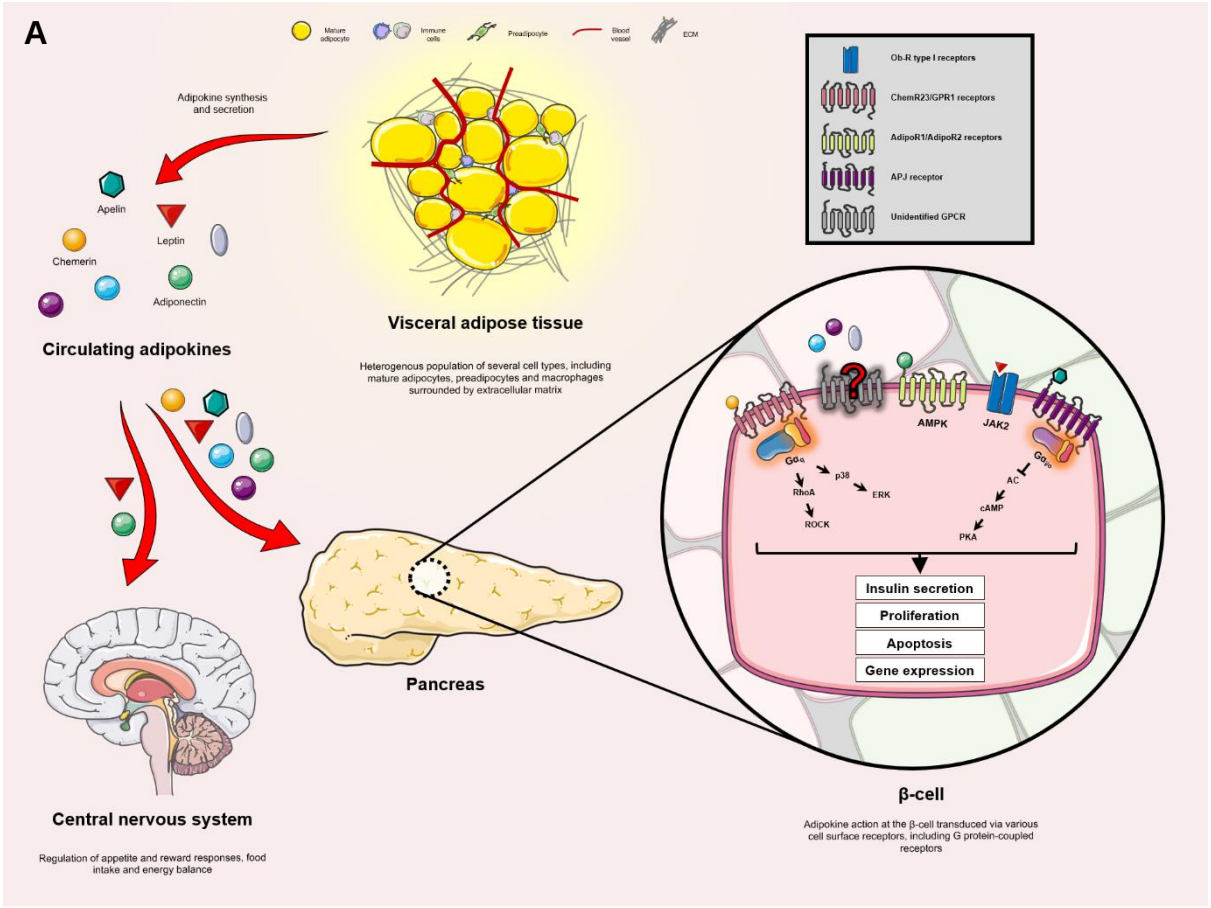
A
Mature adipocyte
Immune cells
Preadipocyte
Blood vessel
ECM
Adipokine synthesis and secretion
Apelin
Leptin
Chemerin
Adiponectin
Circulating adipokines
Visceral adipose tissue
Heterogenous population of several cell types, including mature adipocytes, preadipocytes and macrophages surrounded by extracellular matrix
Ob-R type I receptors
ChemR23/GPR1 receptors
AdipoR1/AdipoR2 receptors
APJ receptor
Unidentified GPCR
AMPK
JAK2
Gαi
Gαs
p38
ERK
RhoA
ROCK
AC
cAMP
PKA
Insulin secretion
Proliferation
Apoptosis
Gene expression
Pancreas
β-cell
Adipokine action at the β-cell transduced via various cell surface receptors, including G protein-coupled receptors
Central nervous system
Regulation of appetite and reward responses, food intake and energy balance

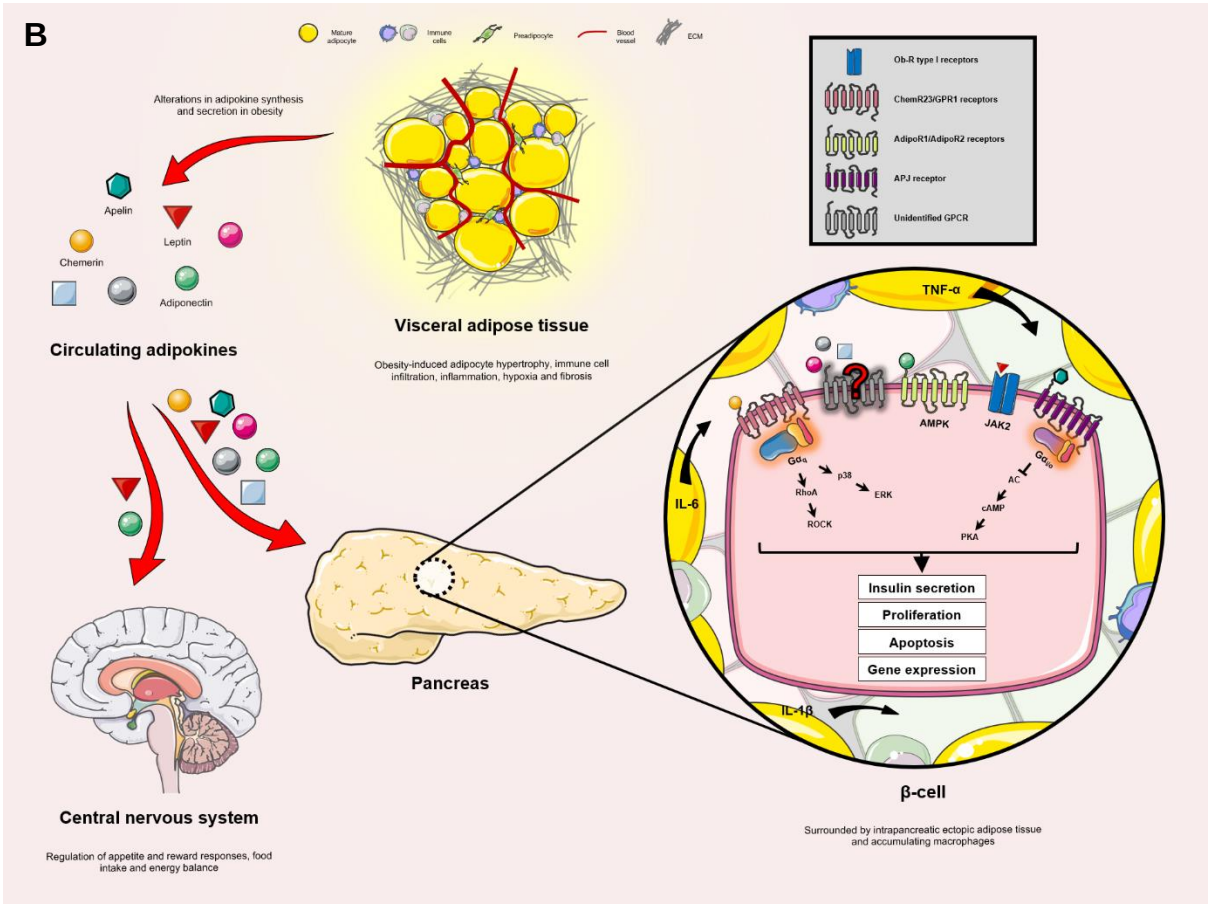
B
Mature adipocyte
Immune cells
Preadipocyte
Blood vessel
ECM
Alterations in adipokine synthesis and secretion in obesity
Apelin
Leptin
Chemerin
Adiponectin
Circulating adipokines
Visceral adipose tissue
Obesity-induced adipocyte hypertrophy, immune cell infiltration, inflammation, hypoxia and fibrosis
Ob-R type I receptors
ChemR23/GPR1 receptors
AdipoR1/AdipoR2 receptors
APJ receptor
Unidentified GPCR
TNF-α
AMPK
JAK2
Gαi
Gαs
p38
ERK
RhoA
ROCK
AC
cAMP
PKA
IL-6
Insulin secretion
Proliferation
Apoptosis
Gene expression
IL-1β
Pancreas
β-cell
Surrounded by intrapancreatic ectopic adipose tissue and accumulating macrophages
Central nervous system
Regulation of appetite and reward responses, food intake and energy balance

Figure 12. The dynamics of adipose tissue structure and function between lean (A) and obese (B) states. Obesity triggers structural and functional changes within adipose tissue that can contribute to hyperglycaemia and whole-body dysfunction: 1) upregulated expression of pro-diabetic, pro-inflammatory adipokines and downregulated expression of anti-diabetic, anti-inflammatory adipokines; 2) altered regulation of CNS-mediated satiety and food intake; 3) decline in insulin sensitivity of peripheral tissues, including adipose tissue; 4) chronic inflammation and accumulation of fibrotic tissue; 5) ER and oxidative stress causing DNA damage and cell death; and 6) intrapancreatic ectopic fat deposition leading to islet inflammation and β-cell dysfunction. Well-characterised adipokines, adiponectin and leptin, act on non-GPCRs in β-cells, whilst other adipokines, such as apelin and chemerin, act at islet GPCRs to modulate insulin secretion. It is likely that additional, as yet uncharacterised, adipokines also bind to islet GPCRs to regulate functional β-cell mass. Adapted from Atanes et al. (2021).

In conjunction to alterations in circulating adipokine levels in obesity, there is evidence to support changes in the expression of GPCRs through which some of them act. Furthermore, GPCR modulation is thought to be tissue-dependent following these obesity-induced changes in ligand levels. For example, more than a 2-fold increase in plasma chemerin levels has been reported in mice fed a high-fat diet, and this is accompanied by reduced *Gpr1* expression in skeletal muscle (Rourke et al., 2014). Serum levels of apelin are also increased in obesity (Hehir & Morrison, 2012), however, whilst the levels of its target receptor, APJ, are reduced in skeletal muscle (Ji et al., 2017), they are elevated in adipose tissue (Dray et al., 2010). Metabolic status therefore has the capacity to modify the crosstalk between adipose tissue and islets such that adipose expansion in obesity will lead to increased secretion of adipokines, and, for those that signal via GPCRs, this may be accompanied by changes in levels of the target GPCRs and modified responses to those ligands.

1.6 G protein-coupled receptors

The peptides mentioned above demonstrate the importance of adipose tissue in normal physiological function and metabolic homeostasis through the modulation of insulin secretion and insulin action. This lends the possibility of exploiting the adipose secretome in developing a new therapy for T2D. A promising avenue for future drug development is the regulation of islet GPCR activity. 293 GPCRs were identified as being expressed in human islets using quantitative polymerase chain reaction (qPCR), with 110 of these being the targets of peptide or protein ligands (Amisten et al., 2013). The effects of a majority of identified GPCRs on islet hormone secretion are, however, unknown. Adipose tissue-derived factors can influence β-cell function by binding to their target receptors, some of which are members of the GPCR family of receptors.

GPCRs contain seven transmembrane loops with an extracellular N-terminus for ligand binding and an intracellular C-terminus which is associated with a heterotrimeric G protein (Atanes & Persaud, 2020). Agonist binding leads to signal transduction from the extracellular to the intracellular compartment. Subsequent activation of the associated G protein triggers a cascade of intracellular signalling pathways that serve to recruit enzymes, remodel the cytoskeleton, alter insulin synthesis and secretion, and modulate gene expression (Atanes & Persaud, 2020). This mechanism of signal transduction involving a series of molecular effectors serves to propagate and amplify a single signal throughout a cell. The overall effect of a given GPCR is dependent on several factors: 1) the nature and availability of the

occupying GPCR ligand; 2) the associated G protein subclass ($G\alpha_s$, $G\alpha_{i/o}$, $G\alpha_{q/11}$ and $G\alpha_{12/13}$) which are coupled to distinct downstream modulators (Figure 13); 3) receptor, system or ligand bias that results in a preference for either G protein signalling or β-arrestin recruitment and GPCR desensitisation; and 4) the localisation of the expressed GPCR and its cell- or tissue-dependent pharmacological profiles (Atanes et al., 2021).

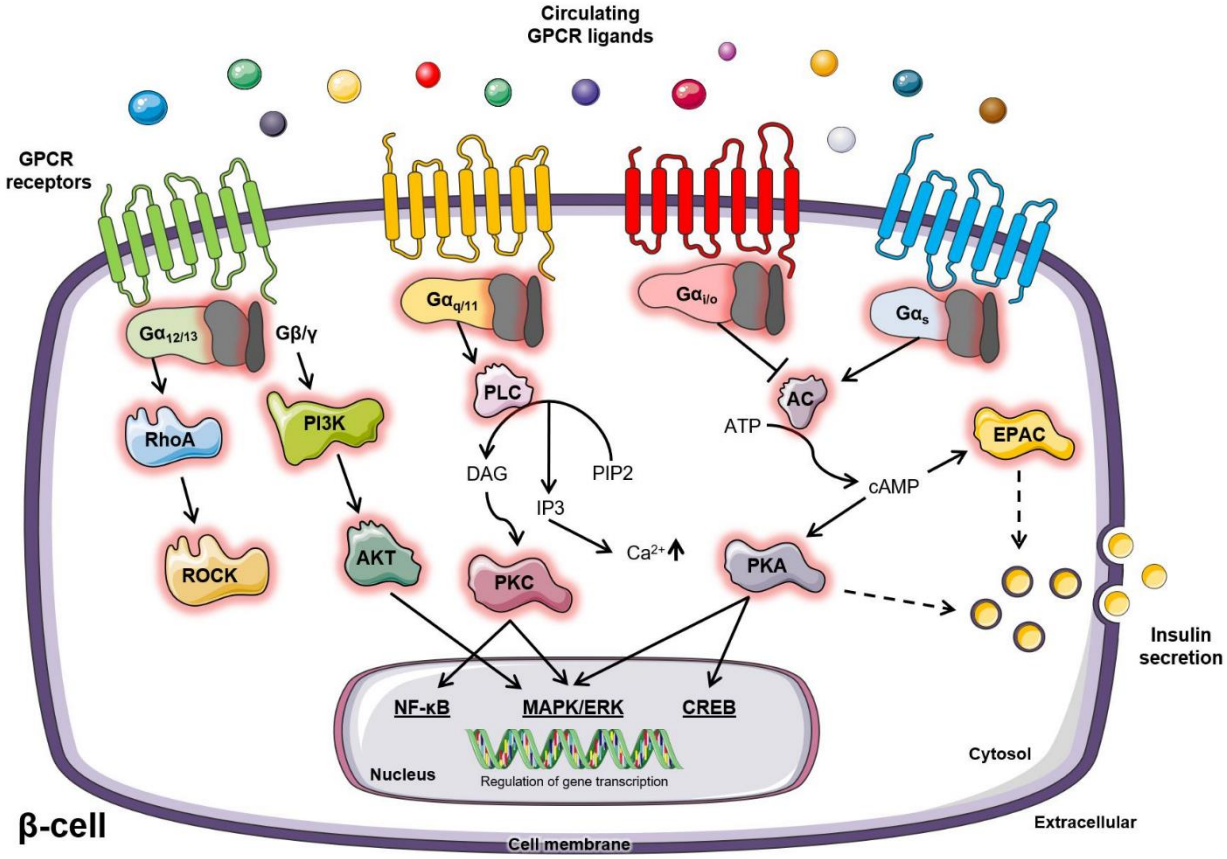

Figure 13. A schematic illustrating the downstream intracellular signalling pathways of GPCRs in the regulation of insulin secretion and overall β-cell function. All GPCRs undergo confirmation changes in response to ligand binding. This facilitates the exchange of GDP for GTP on the Gα subunit leading to its dissociation from the Gβγ dimer. GTP-bound Gα subunits can then modulate the activity of corresponding enzymes: AC is either activated ($G\alpha_s$) or inhibited ($G\alpha_{i/o}$) to regulate intracellular cAMP levels; PLC is activated ($G\alpha_{q/11}$) to hydrolyse PIP_2 and produce IP_3 and DAG. IP_3 mobilises Ca^{2+} from the ER to activate CaMKs, whilst cAMP and DAG activate PKA and PKC, respectively. Kinases phosphorylate intracellular proteins involved in insulin secretion (acute) and in gene expression (long term). Elevated cAMP also activates EPACs which mediate exocytosis of insulin-containing granules. The $G\alpha_{12/13}$ subunit is less relevant to the β-cell and more so to insulin-sensitive cells, as activation of PKB/AKT via PI3K stimulates the translocation of GLUT4 to the membranes in muscle and adipose tissue. Adapted from Atanes & Persaud (2020).

Whilst activation of GPCRs plays a vital role in normal cellular function and in a range of physiological processes, overstimulation can result in deleterious effects on both cellular and tissue level (Rajagopal & Shenoy, 2018). Therefore, GPCR activation is tightly regulated by the action of β-arrestins for which there are two isoforms: β-arrestin-1 and β-arrestin-2 (Jones et al., 2018). These adaptor proteins coordinate the acute desensitisation and long-term

downregulation of GPCRs (Rajagopal & Shenoy, 2018): desensitisation is initiated by receptor phosphorylation by GPCR kinases (GRKs) and subsequent β-arrestin recruitment, ultimately preventing interactions between the receptor C-terminus and G proteins (Ahmadzai et al., 2017); downregulation occurs following agonist exposure of hours or days, and encompasses receptor degradation within lysosomes following endocytic internalisation, and in some cases, diminished transcriptional activity (Jones et al., 2018; Rajagopal & Shenoy, 2018). Whilst the roles of β-arrestins extend beyond this, β-arrestin action is classically associated with reduced cellular responses, and contributions to tachyphylaxis and the undesired effects observed during chronic drug administration (Rajagopal & Shenoy, 2018).

1.6.1 Classes and functions

The portfolio of GPCR ligands is diverse: peptides and proteins, lipids, ions, hormones, neurotransmitters and small organic molecules can be capable of high-affinity binding and activation of GPCRs (Wacker et al., 2017). Binding of a ligand to its target GPCR results in a conformational change and the exchange of bound GDP for free cytosolic GTP on the Gα subunit (Atanes & Persaud, 2020). The GDP/GTP exchange triggers the dissociation of the Gα-GTP subunit from the Gβγ dimer and its subsequent activation. $G\alpha_{i/o}$ and $G\alpha_{s}$ subunits modulate AC activity, the production of cAMP and, in turn, the activation of PKA and EPAC2. The $G\alpha_{i/o}$ subclass inhibits this pathway whilst the $G\alpha_{s}$ subclass activates it. The $G\alpha_{q/11}$ subclass, on the other hand, is associated with a differing downstream pathway as activated $G\alpha_{q/11}$ triggers PLC-mediated production of DAG and IP_3 from the hydrolysis of phosphatidylinositol 4,5 bisphosphate (PIP_2). Free cytosolic IP_3 binds to its receptors within the membranes of storage organelles, including the ER, to mobilise Ca^{2+} ions. The increase in $[Ca^{2+}]_i$ activates Ca^{2+}/calmodulin-dependent protein (CaMK). Membrane-bound DAG facilitates the movement and activation of PKC at the plasma membrane.

CaMK, PKA and PKC phosphorylate serine and threonine residues on intracellular proteins to, in the short term, stimulate the secretion of insulin, or, in the longer term, regulate the expression of genes involved in β-cell function (Atanes & Persaud, 2020). Acute activation of EPAC2, for example, mobilises Ca^{2+} ions from intracellular calcium pools and, as previously described in Section 1.3.1, increases the density of insulin-containing granules near the β-cell plasma membrane to facilitate insulin secretion (Shibasaki et al., 2007). Longer term regulation of gene expression depends on cAMP-responsive element binding protein (CREB), MAPK or extracellular signal-regulated protein kinase (ERK), and NF-κB pathways. CREB is a nuclear transcription factor which, once phosphorylated on its serine-133 acceptor site, can recruit CREB-binding protein (CBP) (Chrivia et al., 1993). By associating with RNA polymerase II complexes and histone acetyltransferases, CREB/CBP drives the transcription of numerous genes (Kee et al., 1996; Korzus et al., 1998). CREB can be induced by a plethora of extracellular stimuli, such as growth factors and inflammatory signals, and is implicated in diverse cellular functions, including proliferation, differentiation, adaptation, metabolism, and survival (Mayr & Montminy, 2001). The MAPK/ERK signalling pathway has similar activators and functions within the β-cell. Conventional MAPKs, including the p38 and p42/44 families of protein kinases, have been shown, through inhibition and depletion studies, to exert mitogenic responses in healthy, obese and diabetic β-cells (Burns et al., 2000; Chen et al., 2011; Ikushima et al., 2021). As established in previous sections, the NF-κB pathway is a key component in modulating β-cell mass via apoptotic signals. Indeed, by blocking NF-κB-mediated expression of apoptotic genes (e.g. Fas, MCP-1/CCL2, and inducible nitric oxide

synthase (iNOS)), islets are protected against stress-induced dysfunction and death (Baker et al., 2001; Eldor et al., 2006; Kutlu et al., 2003; Ortis et al., 2006).

1.6.1.1 $G\alpha_s$ and $G\alpha_{i/o}$

$G\alpha_s$ and $G\alpha_{i/o}$ subclasses have opposing effects on the cAMP/PKA pathway. $G\alpha_s$ signalling promotes insulin secretion, β-cell differentiation and proliferation while protecting against apoptosis. Accordingly, $G\alpha_s$-coupled receptors have been the focus of β-cell-targeted drug development for T2D treatment. As previously discussed, GLP-1R signalling has been successfully utilised to produce several insulin secretagogues that are used clinically in the treatment of type 2 diabetes. The actions of other $G\alpha_s$-coupled receptors, such as GPR119 and GPR56, on β-cell function have also been explored, as described below.

GPR56, encoded by the ADGRG1 gene, is the most abundantly expressed GPCR within human islets (Dunér et al., 2016). As an adhesion receptor (aGPCR) with a long and "sticky" N-terminal domain, GPR56 mediates cell-cell and cell-matrix interactions (Olaniru et al., 2018). In addition to this structural role, the identification of its ligand, collagen III, indicates a potential signalling role. Collagen III is localised to the islet ECM and potentiation of glucose-stimulated insulin secretion and protection against cytokine-induced apoptosis implicates collagen/GPR56 interactions in normal islet function (Olaniru et al., 2018). Given that GPR56 expression is markedly reduced in islets from diabetic mice and patients (Dunér et al., 2016), this GPCR is of interest as a novel treatment for T2D. GPR119 is expressed by β-cells and enteroendocrine L- and K-cells (Chu et al., 2007, 2008). It is an example of a lipid-binding GPCR that is activated by oleoylethanolamide (OEA) and other oleic acid-containing lipids (Chu et al., 2010; Overton et al., 2006). Stimulation of GPR119 promotes cAMP generation and glucose-dependent insulin secretion from β-cells (Chu et al., 2007; Soga et al., 2005). GPR119 activation within enteroendocrine L- and K-cells triggers the release of their respective incretin hormones, GLP-1 and glucose-dependent insulinotropic peptide (GIP) (Chu et al., 2008; Lauffer et al., 2009). GPR119 as a pharmacological target attracted considerable interest because of its insulinotropic and anorectic effects both *in vitro* and *in vivo* (Chu et al., 2007, 2008; Lan et al., 2012). However, these benefits have failed to translate into humans with clinical testing of GPR119 agonists reporting unfavourable outcomes and adverse effects (Persaud, 2017; Ritter et al., 2016).

In terms of T2D drug development, an alternative to $G\alpha_s$-coupled receptor agonism is $G\alpha_{i/o}$-coupled receptor antagonism. Engagement of $G\alpha_{i/o}$ signalling pathways suppresses insulin release and acts as a physiological brake to prevent excessive insulin secretion and hypoglycaemia. This is the case for somatostatin released from δ-cells which mediates paracrine effects on the β-cell via $G\alpha_{i/o}$-coupled SSTR2 and SSTR5 receptors (Kailey et al., 2012). Furthermore, expression of these receptors in α-cells supports somatostatin-induced inhibition of glucagon release (Kailey et al., 2012). Elevated somatostatin signalling and reduced glucagon responsiveness to hypoglycaemia in diabetes represents dysfunction of counterregulatory mechanisms (Yue et al., 2012). Antagonising somatostatin GPCRs as an adjunct to insulin administration could provide a therapeutic approach for diabetes.

1.6.1.2 $G\alpha_{q/11}$

The $G\alpha_{q/11}$ subclass is associated with stimulatory pathways involving PLC-mediated elevations in cytosolic Ca^{2+} and activation of PKC. $G\alpha_{q/11}$-coupled receptors expressed within β-cell plasma membranes potentiate insulin secretion following activation by a variety of ligands, including FFAs (GPR40, GPR43 and GPR120) (Itoh et al., 2003), carbachol (Chm3/M3R) (Verspohl & Herrmann, 1996) and calcium (CaR) (Gray et al., 2006). Loss of $G\alpha_{q/11}$ signalling reduces the production of its downstream effectors, including IP_3 and Ca^{2+}, and subsequently impairs glucose-stimulated insulin secretion (Sassmann et al., 2010). GPR75, is a novel islet GPCR given its insulinotropic effects are activated by the chemokine (C-C motif) ligand 5 (CCL5) (Liu et al., 2013). Like many of the chemokines previously described here, CCL5 promotes the recruitment of immune cells to sites of inflammation. However, it also induces calcium entry into isolated islets via a PLC-dependent mechanism and improves glucose tolerance in lean and hyperglycaemic mice. Despite the fact that CCL5 contributes to islet inflammation in diabetes pathology, GPR75-specific agonism may be a promising therapeutic avenue (Liu et al., 2013).

Similar to the abovementioned GPCRs, islet GPR54 also potentiates glucose-stimulated insulin secretion when activated by its ligand, kisspeptin (Bowe et al., 2012; Kotani et al., 2001). Interestingly, some studies have reported an inhibitory effect of kisspeptin on insulin secretion (Silvestre et al., 2008; Vikman & Ahrén, 2009), however, when using a standardised perifusion protocol and peptides synonymous with endogenous kisspeptin, stimulatory observations mirror the $G\alpha_{q/11}$-coupled signalling associated with GPR54 (Bowe et al., 2012). Moreover, GPR54 signalling has been implicated in pregnancy-induced cellular adaptations, namely increased proliferation of several cells types, including mammary epithelial cells (Li et al., 2020) and β-cells (Bowe et al., 2019).

1.6.1.3 $G\alpha_{12/13}$

GPCRs coupled to $G\alpha_{12/13}$ proteins regulate the activity of Rho GTPases, a family of kinases with roles in cell migration, growth, shape, and differentiation. The classic members of this kinase family are RhoA, Rac1 and Cdc42; all regulate the translocation of GLUT4 vesicles between different cellular compartments through reorganisation of the actin cytoskeleton (Wennerberg & Der, 2004). Thus, $G\alpha_{12/13}$ signalling pathways are highly relevant to insulin-mediated glucose uptake into adipocytes and myocytes. In addition, lysophosphatidic acid (LPA) is a lipid mediator of several GPCRs, one of which is the adipocyte-expressing $G\alpha_{12/13}$-coupled LPAR4 (Yanagida et al., 2018). LPAR4 activity inhibits adipogenesis and reduces the expression of PPARγ ligands and an array of mitochondrial genes within adipose tissue, including adiponectin and the master regulator of mitochondrial biogenesis, PGC-1α. In accordance, LPAR4 ablation enhances adipose tissue expansion and protects against insulin resistance and hepatosteatosis (fatty liver) in obesity (Yanagida et al., 2018). Similar effects of $G\alpha_{12/13}$ signalling on mitochondrial biogenesis and energy metabolism are implicated in skeletal muscle. Myofibre-specific deletion of $G\alpha_{13}$ increased insulin sensitivity in diet-induced obese mouse model (Koo et al., 2017). A potential mechanism could be suppressed signalling of NFATc1, a RhoA-activated transcription factor which determines muscle fibre type in muscle regeneration (Shin et al., 2023). Overall, due to their crucial functions in insulin-responsive tissues, modulation of $G\alpha_{12/13}$ and its downstream effector could be of therapeutic interest.

1.6.2 GPCR-targeting diabetes therapies

It is clear that GPCRs have a significant role in islet function and insulin release and the capacity for GPCRs as druggable entities is considerable. Indeed, this large family of receptors represents ~35% of all current drug targets for treatment across a wide range of diseases (Sriram & Insel, 2018). However, there are only three direct GPCR-targeted pharmacotherapies for T2D and only one acts on an islet GPCR (Atanes & Persaud, 2020): 1) GLP-1RAs mimic the actions of endogenous GLP-1 to potentiate glucose-stimulated insulin secretion; 2) bromocriptine, an activator of dopamine D2 receptors, improves post-prandial plasma glucose levels by modulating dopamine levels (Grant, 2011); and 3) pramlintide, an amylin analogue, acts centrally at calcitonin receptor/receptor activity-modifying protein heterodimers to reduce food intake, slow gastric emptying and delay glucose absorption (Edelman et al., 2008).

GLP-1RAs, such as exenatide and liraglutide, are widely prescribed to patients with obesity and T2D. As described in Section 1.1.2.4, their effects on insulin secretion and gastric emptying are successful in lowering post-prandial plasma glucose levels and HbA1c without risk of hypoglycaemic events (Liu et al., 2015). GLP-1RAs also exhibit anorectic properties which, by penetrating into critical feeding brain centres, including POMC/CART appetite-controlling hypothalamic nuclei, contribute to improved glycaemic control (Secher et al., 2014). Furthermore, binding of GLP-1 analogues to GLP-1Rs expressed on islet α-cells suppresses glucagon secretion and mitigates the risks of detrimental hyperglucagonaemia that occurs in T2D. The recent introduction of oral GLP-1RA medication will likely improve the attractiveness of this class of drug (Pratley et al., 2021), since subcutaneous formulations are unappealing for some patients who are unable to self-administer or have needle phobia. However, there are still therapeutic limitations as commonly occurring gastrointestinal adverse effects, most notably dose-dependent nausea, often lead to discontinuation of treatment (Jones et al., 2018). Not only is refinement of existing pharmacotherapies necessary to improve patient quality of life, but further research and drug development are required to combat the ongoing deterioration of glycaemic control in T2D. Providing individuals who fail to maintain normoglycaemia with alternative therapeutic options is important for preventing long-term complications that arise from chronic hyperglycaemia. Based on cumulative evidence implicating visceral adipose tissue in diabetes pathophysiology, it would be sensible to direct attention towards possible adipose tissue-derived peptides which engage in β-cell crosstalk through GPCR activation, which is the subject of the experiments described in this thesis.

1.7 Aims and objectives

At present, the following key points regarding islet function, adipose tissue and GPCR signalling in the context of metabolic homeostasis are known to us:

1. Adipose tissue is a vital source of secretory peptides that regulate glucose homeostasis via actions either directly on β-cells, or on insulin-targeting tissues, including liver and skeletal muscle (Kershaw & Flier, 2004).

2. Alterations in the expression and secretion of adipose tissue-derived peptides occur between lean and obese states (Gerst et al., 2019).

3. GPCRs have substantial capacity as druggable entities, as high-affinity drug binding is facilitated by specialised interactions between the GPCR and its ligand(s) (Atanes & Persaud, 2020).

4. β-cell mass, viability and overall insulin secretory function are modulated by the activation of GPCRs and their associated downstream signalling pathways in β-cells (Winzell & Ahrén, 2007).

What is unknown to us, however, are the effects of a majority of the 293 identified islet GPCRs on islet morphology and function. In light of the above information, it is hypothesised that some adipose tissue-derived GPCR-activating peptide ligands may regulate insulin secretion and overall β-cell function, and that this may be modified under conditions of obesity. Identification of such peptides and their actions could translate into new pharmacotherapies for T2D treatment.

To investigate this, my PhD project was divided into three phases using the following approaches:

1. Identification of differentially expressed islet GPCR peptide ligand mRNAs derived from visceral adipose tissue between lean and obese states following optimisation of RNA extraction, reverse transcription, and quantitative PCR techniques for the analysis of high triglyceride, low RNA tissue samples.

2. Comparison of gene expression profiles of islet GPCR peptide ligand mRNAs between whole adipose tissue and isolated mature adipocytes from diet-induced mice, whole adipose tissue from genetically obese mice, and whole adipose tissue from human donors.

3. Selection of a candidate of interest and characterisation of its functional effects on target GPCR activation, apoptotic, proliferative and insulin secretory effects in an immortalised MIN6 β-cell line and primary mouse islets, and potential paracrine/autocrine signalling in adipocytes.

Chapter 2: Materials and Methods

2.1 Materials

Culture media and supplements, Histopaque, collagenase type I and XI, TRIzol® reagent, cDNA reverse transcription kit, glycogen, SYBR Red Safe Dye, TriTrack DNA Loading Dye, GeneRuler™ 50bp DNA ladder, Restore™ Western Blot Stripping Buffer, Trypan Blue solution, Cell Countess slides, Mr. Frosty™ Freezing Container, flasks and vials were supplied by Thermo Fisher Scientific (Loughborough, UK). RNase-free DNase set, RNA extraction kits, QuantiTect primers and QuantiFast SYBR Green PCR Kit were supplied by Qiagen Ltd. (Manchester, UK). Custom qPCR primers for AdipoQ, Pparγ and Hprt1 genes were supplied by Integrated DNA Technologies (Ontario, Canada). The Cell Proliferation ELISA Kit was supplied by Roche Diagnostics, whilst the Caspase-Glo® 3/7 Assay and Bright-Glo™ Luciferase Assay Systems were supplied by Promega (Southampton, UK). The PRESTO-Tango GPCR Kit was provided by the Roth Lab (University of North Carolina, USA) and Hanks' Balanced Salt Solution supplied by Santa Cruz Biotechnology (Middlesex, UK). Recombinant human and mouse Ccl4 peptides were supplied by BioLegend (London, UK). Chloroform was supplied by MP Biomedicals (Cambridge, UK), and IL-1β, TNF-α and IFN-γ cytokines were provided by PeproTech EC (London, UK). β-mercaptoethanol, Oil Red O powder, poly-L-lysine hydrobromide, dialysed fetal bovine serum, and the glucagon primary antibody were supplied by Sigma-Aldrich (Gillingham, UK). Insulin, somatostatin and Ki67 primary antibodies were supplied by Abcam PLC (Cambridge, UK). Alexa Fluor 488 secondary antibody was provided by Jackson ImmunoResearch (Suffolk, UK). DAPI, and Alexa Fluor 647 and 568 secondary antibodies were supplied by Invitrogen (Loughborough, UK), and DAPI-Fluoromount was supplied by Cambridge Bioscience (Cambridge, UK). Primary and secondary antibodies for Western blotting were supplied by Cell Signalling. Protein Assay Dye Reagent Concentrate, Laemmli Sample Buffer, Precision Plus Protein Dual Color Standards and Clarity Max Enhanced Chemiluminescence substrates were supplied by Bio-Rad Laboratories (Ontario, Canada). I-Block™ Protein-Based Blocking Reagent was provided by Applied Biosystems (Ontario, Canada).

Adipose tissue homogenisation was achieved using a TissueLyser II and stainless-steel beads also supplied by Qiagen Ltd. (Manchester, UK). The Countess Automated Cell Counter was supplied by Invitrogen (Loughborough, UK). The multifunctional microplate reader, PHERAstar FS®, was supplied by BMG Labtech (Aylesbury, UK). Using RNA isolated from MIN6 β-cells, mouse islets, mouse mature adipocytes, and whole adipose tissue retrieved from mouse models and human patients: the concentration and purity of RNA samples were measured using a Nanodrop™ 1000 spectrophotometer supplied by Thermo Fisher Scientific (Loughborough, UK); cDNA generation was performed in a T100™ thermal cycler from Bio-Rad Laboratories (Hertfordshire, UK); real-time qPCR was performed with a LightCycler® 480 or 96 supplied by Roche Diagnostics (Hertfordshire, UK). Using RNA isolated from the 3T3-L1 adipocyte cell line: the concentration and purity of RNA samples was measured using a NanoDrop™ One spectrophotometer supplied by Thermo Fisher Scientific (Ontario, Canada); reverse transcription was performed in a Mastercycler® Nexus GX2 from Eppendorf (Ontario, Canada); real-time qPCR was performed using the QuantStudio™ 6 Flex Real-Time PCR System from Applied Biosystems (Ontario, Canada). Confocal images were captured using a Nikon Eclipse Ti-E Inverted A1 inverted confocal microscope. Amplicon bands from mature adipocyte qPCRs were visualised using as a BioDoc-It™ Imaging System supplied by Analytik

Jena, formerly UVP (London, UK). For 3T3-L1 adipocyte experiments, absorbance was measured using a Wallac 1420 Victor2™ microplate reader and immunoreactive proteins generated during Western blotting were visualised and quantified using an iBright 1500 Imaging System supplied by Thermo Fisher Scientific (Ontario, Canada). The Mini-PROTEAN Tetra Vertical Electrophoresis Cell and Trans-Blot® Turbo™ Transfer System were supplied by Bio-Rad Laboratories (Ontario, Canada).

2.2 Specialised protocols for RNA isolation and quantification of islet GPCR peptide ligand mRNA expression in visceral adipose tissue

2.2.1 Background

The structure and function of mature adipocytes and whole adipose tissue are highly distinctive to those of any other tissue: a high triglyceride content, and relatively low cell numbers and RNA content have meant standard routine protocols are neither appropriate nor reliable for sample processing (Cirera, 2013). The challenges of isolating good quality RNA of sufficient yield from adipose tissue are well-documented (Cirera, 2013; Nandi Jui et al., 2022; Zhang et al., 2023). Poor RNA yield and failure to maintain RNA integrity due to partial degradation and/or contamination severely limit the success of downstream applications such as reverse transcription-quantitative polymerase chain reaction (RT-qPCR) – the gold standard approach for studying gene expression within cells (Guan & Yang, 2008). Low quality RNA that is generated using routine protocols translates into inaccurate and unreliable results. Consequently, many researchers have explored alternative approaches to optimise protocols for the study of adipose tissue (Cirera, 2013; Guan & Yang, 2008; Hemmrich et al., 2010; Méndez et al., 2011; Tan et al., 2018). As the experiments generated in this thesis relied on analysis of gene expression in mouse and human adipose tissue, reliable and effective protocols for the isolation of mature adipocytes and purification of RNA from both adipocytes and whole adipose tissue were initially established, as described below.

2.2.2 Mouse models (C57BL/6, *db/db*)

All animal procedures were performed in accordance with UK legislation under the Animals (Scientific Procedures) Act 1986 Amendment Regulations. For the isolation of mature adipocytes from adipose tissue of lean and diet-induced obese mice, 12-13-week-old C57BL/6 male mice had *ad libitum* access to water and either standard laboratory chow (10% fat) or high-fat diet (60% fat) for 16 weeks prior to culling at 28 weeks of age. For the processing of whole adipose tissue from lean and diet-induced obese mice, 6-week-old C57BL/6 male mice had *ad libitum* access to water and either standard laboratory chow (10% fat) or high-fat diet (60% fat) for a duration of 16 weeks prior to culling at 24 weeks of age. For the processing of whole adipose tissue from genetically induced obese mice, 10-week-old *db*/+ and *db/db* male mice had *ad libitum* access to water and standard laboratory chow diet (10% fat) for 14 weeks prior to culling at 24 weeks of age. All animals were housed at 21-25°C with a 12-hour light-dark cycle.

2.2.3 Human adipose tissue donors

With appropriate ethical approval (REC ref: 21/NW/0100; IRAS project ID: 293789) and in accordance with the Human Tissue Act 2004, omental visceral adipose tissue samples were

isolated from human donors undergoing elective laparotomies at Princess Grace Hospital, London. Details of each donor's gender, age and BMI are summarised in Table 1. Samples were stratified according to BMI (kg/m^2): lean: 18.5-24.9; overweight: 25.0-29.9; and obese: 30.0-39.9.

Table 1. Patient characteristics of omental adipose tissue donors.

Donor	Gender	Age (years)	BMI (kg/m^2)
Lean			
A	Male	57	23.8
B	Female	67	19.5
C	Male	62	20.3
D	Male	59	22.0
E	Female	48	21.1
Overweight			
F	Female	65	29.6
G	Female	58	25.9
H	Female	49	28.2
Obese			
I	Male	50	37.7
J	Male	82	38.5
K	Female	76	30.0
L	Male	53	30.0

2.2.4 Preparation of experimental buffers and media

A 10X Krebs-Ringer bicarbonate HEPES (KRBH) buffer stock was prepared (Table 2) and 15mL aliquots of stock were stored at –20°C. A 1X KRBH buffer solution was prepared by diluting 5mL of KRBH buffer stock in 45mL of distilled water (dH_2O). 100U/mL penicillin and 100mg/mL streptomycin were added to the 1X KRBH buffer solution, which was used for washing adipose tissue immediately following its retrieval from mice. A separate volume of 1X KRBH buffer solution was supplemented with 2mM $NaHCO_3$, 5.5mM glucose and 150µM of 1% bovine serum albumin (BSA) and used later in the protocol to dissolve collagenase type I. Before use, both buffer solutions were filtered under a sterilised laminar flow hood using a 200µm syringe filter.

Table 2. Preparation of 10X KRBH buffer stock.

Reagent	Volume (mL) or Mass (g)	Final Concentration (mM)
NaCl	14.60g	125.0
KCl	0.70g	4.8
NaH_2PO_4	0.12g	0.5
$MgSO_4$	0.58g	1.2
$CaCl_2$	0.76g	2.6
HEPES	11.90g	25.0
dH_2O	200mL	-

Sterilised Dulbecco's modified Eagle's medium (DMEM)/Ham's F12 (F12) was used as the basal medium to support the survival of whole adipose tissue and isolated mature adipocytes during processing. DMEM and F12 were present in a 1:1 ratio and provided a range of nutrients and vitamins to cells, including amino acids and glucose. DMEM/F12 was supplemented with 100U/mL penicillin and 100mg/mL streptomycin prior to use.

2.2.5 Optimisation of mature adipocyte isolation from mouse visceral adipose tissue

Visceral adipose tissue is a complex composition of mature adipocytes and the stromal vascular fraction (SVF). Several different cell populations are contained within this fraction, including preadipocytes, macrophages and stromovascular cells (Cat & Briones, 2017). Mature adipocytes are the specialised lipid-storing cell type within adipose tissue and are responsible for the production of multiple adipokines that contribute to the regulation of metabolic homeostasis (Kershaw & Flier, 2004). An optimised mature adipocyte isolation protocol was developed (Figure 14) to identify alterations in gene expression in obesity.

Male mice were euthanised by cervical dislocation. This was the preferred method in comparison to other forms of euthanasia (e.g. carbon dioxide and anaesthetic overdose) as cervical dislocation lowers the risk of tissue hypoxia and avoids the administration of exogenous chemicals that could interfere with or damage tissues (Overmyer et al., 2015). Both epididymal fat pads were retrieved from the abdominal cavity of each animal. Epididymal fat pads were selected as a source of visceral adipose tissue as they are the largest and most easily accessible visceral fat depot (Chusyd et al., 2016). Fat pads retrieved from two mice were pooled and processed together as a single sample so that there were sufficient adipocytes isolated for gene expression quantification. The tissue was washed with KRBH buffer, containing 100U/mL penicillin and 100mg/mL streptomycin, before transfer to a 50mL Falcon tube on ice containing 15mL of DMEM/F12 medium. Under a sterilised laminar flow hood, adipose tissue was visualised under a dissecting microscope and cleaned of blood vessels and fibrous tissue using forceps and scissors. The weight of each sample was then determined. Adipose tissue has a tendency to dry when exposed to the air, subsequently causing incorrect measurements of total weight (Tan et al., 2018). Therefore, towel drying to remove excess media, as described in the original protocol (Cat & Briones, 2017), was deemed unsuitable. In the protocol used in these studies, the weight of each adipose tissue sample was determined using a "balance" falcon tube containing 5mL of DMEM/F12 media. Samples were transferred to individual falcon tubes each containing 5mL of DMEM/F12

media, and the difference in weight between the balance and sample tubes was calculated. This allowed more accurate weighing whilst avoiding unnecessary tampering and potential contamination of the tissue. The weight of epididymal adipose tissue samples retrieved from lean C57BL/6 mice was ~750-850mg. Samples were placed into individual petri dishes and a volume of DMEM/F12 equal to the weight of the tissue was added. For example, an adipose tissue sample weighing 500mg would require 500µL of DMEM/F12 media.

For efficient enzymatic digestion, the tissue was minced into small pieces using sterile forceps and scissors. A volume of collagenase type I (2mg/mL) equal to the weight of the tissue was added. For example, 500mg of adipose tissue suspended in 500µL of DMEM/F12 would require 500µL of collagenase solution. Adipose tissue samples were transferred to individual 50mL Falcon tubes and digested at 37°C for 30 minutes with gentle and continuous shaking using a water bath. This timing was selected so that digestion was terminated before appearance of oil, which is indicative of cell death. The solution containing digested adipose tissue was then filtered through a sterile 200µm cell strainer into new 50mL Falcon tubes. The filter was washed with an additional 5mL of DMEM/F12 media to maximise the recovery of mature adipocytes.

Samples were centrifuged at 50xg, 20°C for 5 minutes. A white ring of mature adipocyte cells was observed floating on the upper portion of the solution, whilst the SVF formed a pellet found at the base of the Falcon tube. Additional centrifugation steps described in the original protocol (Cat & Briones, 2017) were eliminated to prevent the loss of mature adipocytes with each wash. The white ring was collected and transferred into individual Eppendorf tubes. It is important to note that during collection using a Gilson pipette, the mature adipocytes rise through the infranatant within the tip and float on the surface. Therefore, as much infranatant as possible was removed into waste and the remaining mature adipocytes were transferred into the Eppendorf tube. To maximise the recovery of adipocytes that may have attached within the Gilson tip, this was rinsed with 800µL of TRIzol® Reagent and subsequently added to the Eppendorf tube. After this, the samples were inverted by hand for ~5 seconds to ensure thorough mixing of adipocytes and TRIzol® Reagent before immediate freezing in liquid nitrogen.

Although it is generally considered that adipokines are synthesised and secreted by adipocytes, there is evidence that they may also be secreted from the non-adipocyte SVF fraction of adipose tissue (Fain et al., 2004). Therefore, the SVF pellet was also collected to assess the yield of RNA, the presence of mature adipocytes, if any and, if appropriate, the expression of islet GPCR peptide ligand mRNAs. To collect the SVF, the supernatant was removed, and the pellets were transferred into individual Eppendorf tubes. Similar to the steps described above for the collection of mature adipocytes, maximal recovery of the SVF was achieved by rinsing the Gilson tip with 800µL of TRIzol® Reagent before subsequently adding to the Eppendorf tubes. The SVF and TRIzol® Reagent were thoroughly mixed by manual inversion for ~5 seconds and immediately frozen in liquid nitrogen. Mature adipocyte and SVF samples can be processed immediately after isolation but freezing at –70°C for storage can be introduced to shorten the length of the protocol.

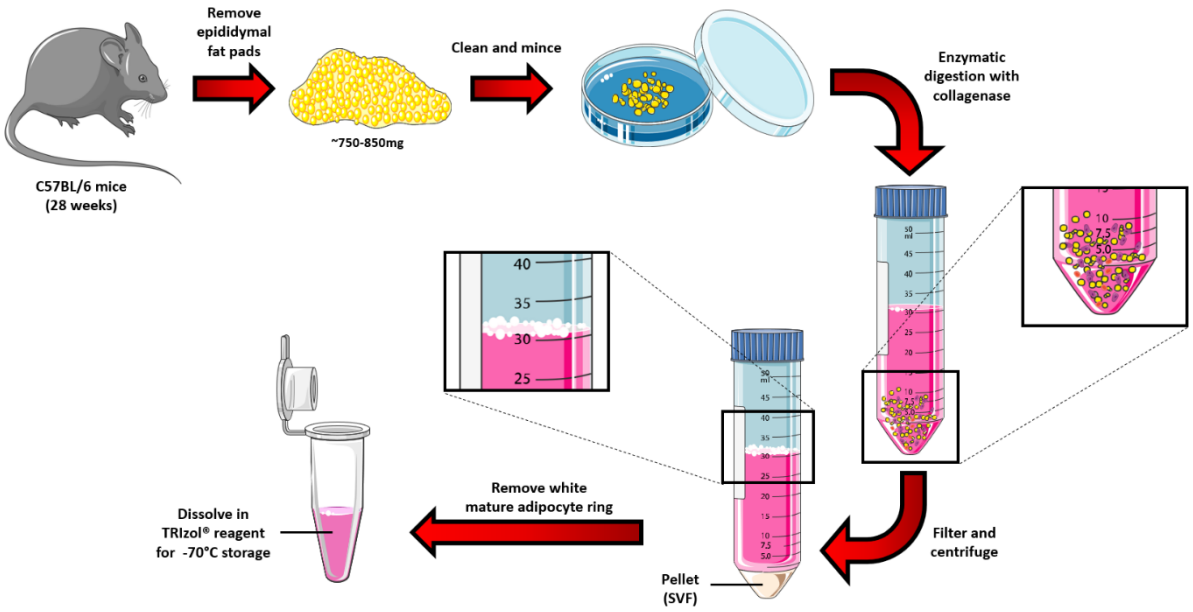

Figure 14. A step-by-step schematic illustrating the isolation of mature adipocytes from visceral epididymal adipose tissue retrieved from C57BL/6 mice. The optimised protocol was based on steps outlined in Cat & Briones (2017).

2.2.6 Optimisation of RNA extraction and purification from isolated mature mouse adipocytes

As described above, the generation of sufficient high-quality RNA is essential for the success of downstream processes, such as RT-qPCR (Guan & Yang, 2008). There are two main methods of RNA isolation and purification that can be adopted: 1) Use of commercial RNA extraction kits, such as the miRNeasy Mini Kit; or 2) Use of the more traditional TRIzol® Reagent method (Cirera, 2013). The advantages and disadvantages of each can be found in Table 3. Given the unique nature of adipose tissue, mainly because of its high triglyceride and low RNA content, the choice of method for RNA isolation is critical for its success (Tan et al., 2018). This is further emphasised by the small amount of fat mass available from lean rodent models for analysis. The downstream applications that follow RNA isolation are also key in determining which method is most appropriate (Tan et al., 2018).

Table 3. The advantages and disadvantages of the main methods for the isolation and purification of RNA. (Cirera, 2013; Tan et al., 2018).

	Advantages	**Disadvantages**
TRIzol® Reagent method	• Less RNA degradation • Ability to isolate RNA, DNA and proteins from a single sample • Less expensive	• Potential contamination by salts and solvents • Time-consuming and labour intensive • Use of harmful reagents
Commercial RNA extraction kits (e.g. miRNeasy Mini Kit)	• Greater RNA purity • Less time-consuming • Published success using adipose tissue	• Greater susceptibility of RNA degradation • Lower RNA yield • Expensive

The TRIzol® Reagent method is a phenol-based technique for RNA extraction involving several organic solvents, including chloroform and isopropanol. There is potential for these solvents to remain within the sample, and if this occurs, it reduces sample purity and causes interference with sample analysis. On the other hand, this method generates RNA of greater integrity compared to commercial extraction kits as the RNA is less prone to degradation (Cirera, 2013). As the experiments described in this thesis make use of a limited amount of starting material from rodent models, especially from lean mice, this approached was considered to be the most appropriate to maximise RNA yield. However, despite optimisation of the adipocyte isolation protocol and efforts to minimise contamination by DNA, proteins and environmental nucleases that contribute to RNA degradation, both the yield and purity of RNA achieved were unsatisfactory using the TRIzol® Reagent method. This was consistent with results reported in other studies using adipose tissue (Cirera, 2013). This confirmed the need to adapt routine protocols specifically for lipid-rich adipose that are otherwise successful in other tissues (Guan & Yang, 2008).

An alternative method for RNA extraction is the use of commercial RNA extraction kits. These employ spin columns to purify RNA from a wide range of tissues without the risk of salt or phenol carry-over (Cirera, 2013; Tan et al., 2018). Several different isolation kits are available, one of which is the miRNeasy Mini Kit. It is a relatively quick approach which generates high purity and quality RNA samples (Hemmrich et al., 2010). Furthermore, the use of commercial RNA extraction kits results in reduced contamination and greater RNA purity compared to the TRIzol® Reagent method (Cirera, 2013). However, the RNA yield achieved from obese samples with this method is generally inferior compared to the results with the phenol-based technique (Cirera, 2013).

Both approaches fail to achieve both high yield and high purity RNA when extracting from isolated mature adipocytes and whole adipose tissue. A protocol has been described that combined the advantages of the TRIzol® Reagent method and a commercial RNA extraction kit to generate good quality RNA of sufficient yield from isolated mature adipocytes and whole adipose tissue (Cirera, 2013). This was based on measurements of the yield, purity and integrity of RNA extracted from adipose tissue using the TRIzol® Reagent method alone, the miRNeasy Mini Kit alone, or the combination of the two. Given the lack of success with the

TRIzol® Reagent method alone, an optimised protocol was developed for RNA extraction from isolated mature adipocytes and whole adipose tissue that integrates the TRIzol® Reagent method with the miRNeasy Mini Kit.

Frozen samples of isolated mouse visceral mature adipocytes dissolved in TRIzol® were incubated at room temperature until thoroughly defrosted and to allow complete dissociation of nucleoprotein complexes. 200µL of chloroform were added and samples were vigorously shaken by hand for 15 seconds before being incubated for 2 minutes at room temperature. Samples were centrifuged at 12,000xg, 4°C for 15 minutes. Following centrifugation, three distinct phases were observed: 1) a lower, red organic phase containing proteins; 2) an interphase containing DNA; and 3) an upper, colourless aqueous phase containing RNA (Figure 15).

Approximately 600µL of upper aqueous phase was transferred to new Eppendorf tubes. 3-4mm of aqueous phase was left above the interphase to minimise the carryover of contaminating DNA. Subsequent steps utilised the miRNeasy Mini Kit following the manufacturer's instructions. The Eppendorf tubes containing the interphase and lower organic phase for each sample were frozen at –70°C so that the DNA and protein within these phases, respectively, could be analysed, if necessary, at a later date.

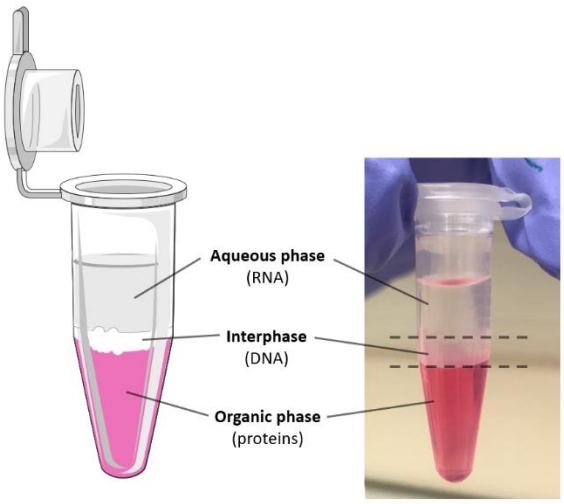

Figure 15. Three distinct phases observed following the initial centrifugation step during RNA isolation from isolated mature mouse adipocytes using TRIzol® reagent.

1.5 volumes of 100% molecular biology grade ethanol were added and thoroughly mixed with the RNA-containing aqueous phase by pipetting up and down with a Gilson pipette. The miRNeasy Mini spin columns have a maximum capacity of 700µL, so samples of a greater volume must be passed through in fractions. 700µL of a 1.2mL sample, for example, were transferred to a miRNeasy Mini spin column in a 2mL collection tube. Samples were centrifuged at 12,000xg, 20°C for 30 seconds. The flowthrough was discarded and, using the same collection tube, the previous step was repeated with the remainder of the sample. The flow-through was discarded, 350µL of RWT buffer were added and samples were centrifuged at 12,000xg, 20°C for 30 seconds. RWT, a stringent washing buffer, contains a high concentration of guanidine isothiocyanate to facilitate RNA binding to the spin column silica

membrane. The flow-through was discarded. Downstream processing included the conversion of isolated RNA into cDNA by RT. Genomic DNA present within RNA samples could also be amplified, thereby contaminating the results generated from RT-qPCR. Therefore, RNA samples were treated with 80µL DNase I and incubated at room temperature for 15 minutes to degrade any contaminating DNA. An additional 350µL of RWT buffer were added and samples were centrifuged at 12,000xg, 20°C for 30 seconds. The flow-through was discarded. 500µL of RPE buffer were added and samples were centrifuged at 12,000xg, 20°C for 30 seconds. The flow-through was discarded. An additional 500µL of RPE buffer were added and samples were centrifuged at 12,000xg, 20°C for 2 minutes. The purpose of using RPE, a mild washing buffer, is mainly to remove salt contamination from previous buffers used during RNA extraction. The flow-through was discarded and final centrifugation step in the absence of buffer was performed at 12,000xg, 20°C for 1 minute to eliminate carryover of buffer. The collection tube was discarded and the miRNeasy Mini spin column was placed into a new Eppendorf tube. 30-50µL DNase-RNase-free water was directly added onto the miRNeasy Mini spin column membrane and samples were centrifuged at 12,000xg, 20°C for 1 minute to elute the RNA. The elution was added onto the miRNeasy Mini spin column, and the centrifugation step was repeated to maximise the yield of RNA extracted from the samples.

2.2.7 Optimisation of RNA extraction and purification from whole visceral adipose tissue

The initial step for RNA isolation from whole adipose tissue was similar to that described in Tan et al. (2018) and Amisten (2016). C57BL/6, *db*/+ and *db/db* male mice were euthanised by cervical dislocation. Both epididymal fat pads were retrieved from the abdominal cavity and processed together as a single sample. Unlike the isolated mature adipocyte protocol, adipose tissue samples retrieved from animals were not pooled for whole adipose tissue analysis as there was sufficient material for quantification to be performed using two fat pads available from each mouse.

Mouse and human tissues were washed with KRBH containing 100U/mL penicillin and 100mg/mL streptomycin, stored in individual Eppendorf tubes and immediately snap frozen in liquid nitrogen. Samples were placed on dry ice to prevent defrosting and potential degradation of RNA. Using a scalpel and forceps, 100-500mg of adipose tissue of each sample were cut and transferred to an Eppendorf tube on dry ice. 1mL of TRIzol® was added to samples in addition to stainless-steel magnetic beads in preparation for rapid and efficient disruption of adipose tissue with a TissueLyser system II. Samples were homogenised using a TissueLyser II set at frequency 20/s for 2 minutes to fully dissolve adipose tissue in the TRIzol® Reagent. It is important to note that the choice of method for tissue homogenisation has proven critical for minimal carryover of lipids from the upper layer (Tan et al., 2018). Homogenisation using a mortar and pestle causes an abundance of fatty acids to remain within the sample, leading to a large lipid layer that is difficult to avoid following centrifugation. Use of the TissueLyser II, however, causes the fatty acids to “stick” to the sides of the Eppendorf tube, resulting in a smaller lipid layer that can be avoided more easily (Tan et al., 2018). Consequently, the TissueLyser II was used for RNA extraction from adipose tissue in the experiments described in this thesis. Following homogenisation, samples were centrifuged at 9,500xg, 4°C for 30 minutes. A red phenol phase containing RNA was observed below a yellow upper lipid layer. The RNA was transferred to a new Eppendorf tube. To prevent the carryover of lipids and the contamination of RNA, the upper lipid layer was pierced at the side and touching of the lipid-coated Gilson tip with the sides of the new Eppendorf tube was avoided. The volume of RNA-

containing phenol phase was topped up with TRIzol® Reagent to 1mL total volume. For example, 600µL of TRIzol® would be added to 400µL of RNA sample. The RNA isolation protocol continued, as described in Section 2.2.6, beginning with the addition of 200µL of chloroform.

2.2.8 Determination of RNA concentration and purity

The concentration and purity of whole adipose tissue- and mature adipocyte-derived RNA samples were measured using a Nanodrop™ 1000 spectrophotometer. The presence of proteins and DNA, which indicates sample contamination, dictates the level of RNA purity achieved. The amount of each is determined by 260/280 and 260/230 ratios, respectively, measured during spectrophotometric analysis. This is a highly favourable method as only 1µL of sample is required for analysis, thus preserving the large majority of RNA for downstream applications. A 260/280 ratio of ~1.8 is generally accepted as "pure" for DNA, whilst a ratio of ~2.0 is generally accepted as "pure" for RNA. For adipose tissue RNA samples, ratios of ≥1.8 are considered to be appropriate (Cirera, 2013). Improvements in adipocyte isolation and RNA extraction protocols are reflected in Table 4 which shows increased mean RNA yield and purity in mature adipocytes and whole adipose tissue during the optimisation process. Once measured, RNA samples were either stored at –70°C to await further processing or kept on ice for preparation of RT reactions.

Table 4. Comparisons of RNA concentration and purity obtained from mature adipocytes and whole adipose tissue of lean mice throughout the protocol optimisation process. 'Initial' data corresponds to mean values achieved during the first two sets of attempted mature adipocyte isolation experiments (n=6 each). 'Optimised' data corresponds to mean values from experiments using mature adipocytes (n=3 pooled samples from 6 mice) and whole adipose tissue (n=5) once protocol optimisation was established.

Starting material	Stage	Mouse strain	Age (weeks)	Pooled samples	Concentration (ng/µL)	Purity (260/280)
Mature adipocytes	Initial	CD1	8-10	No	25.2	1.65
	Optimised	C57BL/6	12-13	Yes	125.1	2.09
Whole adipose tissue	Optimised	C57BL/6	22	No	256.6	2.13

2.2.9 Reverse transcription for complementary DNA generation

The generation of complementary DNA (cDNA) involves the conversion of total RNA to single-stranded cDNA by reverse transcription (RT). The reaction is catalysed by reverse transcriptase, a DNA polymerase enzyme, which uses random primers to synthesise DNA that is complementary to an RNA template. RT reactions of 20µL (including 40ng of RNA per µL) were prepared from RNA stock samples by dilution with the required volume of DNase-RNase free water and MasterMix solution. The RNA stock was diluted in DNase-RNase free water to form a 10µL RNA solution (40ng/µL). 10µL of MasterMix were then added to each diluted RNA

sample to generate the total 20µL reaction volume. The MasterMix was prepared separately using components from the High-Capacity cDNA Reverse Transcription Kit (Table 5) that contains all reagents required for the synthesis of cDNA from the RNA template. This includes the reverse transcriptase enzyme and deoxynucleoside triphosphate (dNTP) substrates for DNA polymerisation. RT was performed in a T100™ thermal cycler set at the following programme: 10 minutes at 25°C for primer annealing and extension, 120 minutes at 37°C for DNA polymerisation, 5 minutes at 85°C for reverse transcriptase deactivation, then maintenance at 4°C. cDNA samples were either stored at –20°C to await further processing or kept on ice to perform qPCR.

Table 5. Preparation of MasterMix for cDNA generation.

Reagent	Volume/Reaction (µL)	Final concentration
10X RT buffer	2.0	1X
25X dNTP mix	0.8	4mM
10X RT random primers	2.0	1X
MultiScribe transcriptase	1.0	2.5U/µL
DNase-RNase-free water	4.2	-

2.2.10 Optimisation of quantitative polymerase chain reaction protocol using cDNA generated from isolated mature adipocyte and whole adipose tissue

The expression level of genes of interest was determined using a dye-based (SYBR Green) qPCR protocol. This is a reliable and sensitive technique which combines conventional real-time qPCR with a non-specific fluorescent dye that binds to double-stranded DNA. Real-time qPCR allows the quantification of PCR products as the reaction occurs (Guan & Yang, 2008). This method is superior to traditional PCR which quantifies the cumulative amount of PCR product at the reaction end-point. The main advantage of a dye-based PCR protocol is the ability to perform multiple assays for a range of mRNAs. There is no need for the synthesis of different probes which is a limitation of probe-based qPCR protocols (e.g. TaqMan probe). However, there is a risk of generating false-positive signals due to the non-specificity of the dye to any double-stranded DNA. Consequently, PCR specificity must be validated when performing dye-based qPCR. This can be done by analysis of melting curves and further confirmation can be achieved by sequencing of PCR products (Guan & Yang, 2008).

293 human islet GPCR mRNAs were previously identified, 110 of which were found to be peptide- or protein-activated (Amisten et al., 2017). As the primary aim of this thesis was to identify potential crosstalk between adipose-derived GPCR peptide ligands and islet GPCRs, qPCR was performed to identify expression in adipocytes and adipose tissue of 155 genes encoding peptide ligands that target these 110 islet GPCRs (Amisten et al., 2013). Mapping of the similarities and differences in GPCR mRNA expression between human and mouse islets demonstrated sufficient similarity to support the use of both mouse and human tissues with translation of possible findings to humans (Amisten et al., 2017). Positive control genes, that do not target GPCRs, were included in the analysis to confirm the presence of mature adipocyte cDNA. *Lep* and *AdipoQ*, encoding leptin and adiponectin, respectively, were chosen as positive control genes due to their almost exclusive expression in adipose tissue (Frühbeck

et al., 2018). Accurate analysis of gene expression by qPCR is reliant on the selection of a suitable reference gene whose expression is stable under alterations in experimental conditions (Perez et al., 2017). Multiple studies have assessed a range of potential candidates that are appropriate for mature adipocytes, including *Gapdh*, *Actb*, *18S rRNA*, *Hprt1*, *Tbp* and *Ubc* (Catalán et al., 2007; Mehta et al., 2010; Perez et al., 2017). This validation process is important as the expression of commonly used reference genes can vary between different tissues (Mehta et al., 2010). Initial qPCR experiments were therefore performed using *Gapdh*, *Actb* and *Tbp* to establish the most appropriate reference gene for isolated mature adipocytes. The expression of *Actb* proved to be the most stable compared to the other genes and it was selected as the reference for subsequent qPCR screenings.

A 1:8 dilution of cDNA samples was performed using DNase-RNase free water. A reaction mix per cDNA sample was prepared separately with SYBR Green, 1:8 diluted cDNA and DNase-RNase free water present in a 5:2:1 ratio. QuantiTect Primer Assays were used as forward and reverse primers for each mouse- and human-specific gene. Primers were bioinformatically validated by the manufacturer (primer sequences are unavailable). 5X working sub-stocks were prepared from 10X stocks by dilution in TE buffer. 8µL reaction mix and 2µL primers per well were loaded into a 96-well white plate (individual samples tested in duplicate). The plate was centrifuged at 150xg, 4°C for 1 minute to ensure collection of samples at the base of the well. qPCR was performed on a LightCycler® 480 or 96 following a standard programme: 1) a pre-incubation step for reaction activation; 2) an amplification step of 40 cycles of DNA denaturation and annealing; 3) the construction of a melting curve from the fluorescent intensity generated throughout the qPCR; and 4) a final cooling cycle whereby amplification has ceased (Table 6).

Table 6. Programme settings for qPCR.

Step	Temperature (ºC)	Time	Cycles
Pre-incubation	95	5 minutes	1
Amplification	95	10 seconds	40
	60	30 seconds	
Melting curve	95	5 seconds	1
	65	1 minute	
	97	-	
Cooling	40	30 seconds	1

2.2.11 Agarose gel electrophoresis

To determine the specificity of SYBR Green to target DNA sequences vs nonspecific DNA sequences during RT-qPCR, agarose gel electrophoresis was performed. Using a microwave, 1.5g of agarose was dissolved in 150mL of 1X bionic buffer to form a 1% agarose gel solution. 1.5µL of SYBR Red Safe Dye was added and the solution was poured into a pre-prepared cast. 2µL of 6X TriTrack DNA Loading Dye were added into each well of the 96-well white plate containing amplified qPCR product. To ensure the collection of PCR product and dye at the base of the well, the plate was centrifuged at 200xg, 4°C for 1 minute. 5µL of GeneRuler™ 50bp DNA ladder were loaded into the first well of the agarose gel. Subsequent wells were

loaded with 12µL of the PCR product/dye mix (individual samples tested in duplicate). The agarose gel was electrophoresed at 150V for 40 minutes. The gel was removed from the cast and PCR amplicon bands were visualised under ultraviolet (UV) light using a BioDoc-It™ Imaging System. The amplicon band lengths were compared to the predicted lengths provided by the manufacturer.

2.3 Measurement of circulating Ccl4 levels

2.3.1 Animals (C57BL/6)

For the extraction of plasma to assess circulating Ccl4 concentrations in lean and diet-induced obese mice, 6-week-old C57BL/6 male mice had *ad libitum* access to water and either standard laboratory chow (10% fat) or high-fat diet (60% fat) for a duration of 16 weeks prior to culling at 24 weeks of age. All animals were housed at 21-25°C with a 12-hour light-dark cycle.

2.3.2 Blood sampling and plasma extraction

Blood samples from lean and diet-induced obese mice were obtained by cardiac puncture. 1mL syringes, 23G needles and Eppendorf tubes were coated with the anti-coagulant, heparin (1000U/mL) prior to blood collection. Mice were euthanised by cervical dislocation. The thoracic cavity was opened by thoracotomy using dissecting scissors to cut through the diaphragm and expose the heart. A needle was inserted into the left ventricle and blood was drawn slowly to avoid collapsing the heart. Blood samples were transferred to 1.5mL Eppendorf tubes, stored on ice and then centrifuged at 16,000xg, 4°C for 10 minutes to separate blood cells from plasma. Following centrifugation, the resulting cell-free plasma supernatant was transferred to fresh Eppendorf tubes and stored at –70°C to await quantification of Ccl4 levels by an enzyme-linked immunosorbent assay (ELISA).

2.3.3 Quantification of plasma Ccl4 peptide concentration using ELISA

A Mouse MIP-1 beta/CCL4 ELISA Kit was used to quantify the concentration of Ccl4 peptide in plasma extracted from lean and diet-induced obese mice. The kit used a solid-phase sandwich type of ELISA. The wells of a 96-well plate act as a solid-phase to covalently immobilise specific antibodies that target an antigen of interest present within plasma. Once plasma samples are added to the wells and the antigen is bound to the solid-phase antibody, an enzyme-labelled antibody can then be added to form a “sandwich complex” (antibody-antigen-antibody). Any unbound antibody is washed away and an enzyme substrate is added. The product of the enzymatic reaction causes colour development which can be detected by spectrophotometry. The resulting absorbance is directly proportional to the amount of antigen within a sample. Using known concentrations of antigen, referred to as “standards”, the corresponding absorbance values can be used to generate a standard curve. The unknown concentrations of antigen within plasma samples can then be extrapolated using this standard curve.

A serial dilution of recombinant mouse Ccl4 stock using 1X assay diluent produced a range of Ccl4 concentrations (2.5-1000pg/mL). 100µL/well of each was added in duplicate to corresponding mouse Ccl4 antibody-coated wells of a clear 96-well plate. Mouse plasma

samples were diluted 1:2 with 1X assay diluent and 100µL/well of each was added to separate wells. The standards and plasma samples were incubated at room temperature for 2.5 hours. During this time, any Ccl4 peptide present within the samples became bound to immobilised solid-phase antibodies. After several washes with washing buffer to remove samples, 100µL/well of biotin-conjugated secondary antibody solution was added to all wells to interact with bound antigen-antibodies and form sandwich complexes. Following an incubation period of 1 hour at room temperature, wells were washed to remove any unbound antibody and 100µL/well of streptavidin-horseradish peroxidase (HRP) solution was incubated for 45 minutes at room temperature. Streptavidin has a high affinity for biotin molecules and therefore binds to the biotinylated secondary antibody. HRP acts as a reporter enzyme for the breakdown of a chemiluminescent substrate. Thus, after several washes with washing buffer, 100µL/well of tetramethylbenzidine (TMB) substrate was added to wells. During the 30-minute incubation period at room temperature, TMB reacts with HRP to produce a blue-coloured product. The reaction was stopped using 50µL/well of stop solution and the absorbance was quantified at a 450nm wavelength using the multifunctional microplate reader, PHERAstar FS®. The degree of colour development and the corresponding absorbance directly correlated with the concentration of Ccl4 peptide within mouse plasma.

2.4 MIN6 β-cell culture

Islet dysfunction is at the centre of diabetes pathophysiology and assessment of islet function *in vitro* can provide essential information on the mechanisms responsible for defective glucose-stimulated insulin secretion, and the loss of β-cell mass and function. However, there are several limitations of using primary islets, particularly those from human donors, including cellular heterogeneity, high cost, laborious pancreas and islet isolation protocols, and limited organ availability (Hart & Powers, 2019). A mouse insulinoma-derived cell line, known as the MIN6 β-cell line, was established from a transgenic mouse expressing the large T-antigen simian virus 40 (SV40) coupled to the insulin promoter within its β-cells (Miyazaki et al., 1990). The functional characteristics of MIN6 β-cells mimic those of primary mouse β-cells in many respects: glucose transport is mediated by the GLUT2 membrane transporter, glucose phosphorylation is mainly driven by glucokinase activity, and glucose-stimulated insulin secretion is maintained in the appropriate range (Miyazaki et al., 1990). These similarities in physiological characteristics make MIN6 β-cells an appropriate model for the study of β-cell function (Persaud et al., 2014) and both MIN6 β-cells and primary mouse islets were used for functional analyses.

However, when using immortalised cell lines, there are several caveats that should be considered. One of the most important considerations is the occurrence of additional mutations in the genome during subculturing causing deviation from the intended phenotype (Segeritz & Vallier, 2017). Indeed, MIN6 β-cells that are maintained in long-term culture lose their capacity to secrete insulin in response to glucose (Miyazaki et al., 2021). Evidence for this was observed in cells at a high passage number (60-70), whereby the first phase of glucose-stimulated insulin secretion was absent and the second phase was markedly impaired (Cheng et al., 2012). This was coupled with significant reductions in intracellular ATP generation, decreased glucose uptake and oxidation, and basal lipid oxidation. The frequency of insulin granules was also reduced, and cell morphology was altered with the rounded appearance of low passage cells (30-40) transforming into an irregular shape with cellular protrusions with increasing passage. Alongside these deficits in MIN6 β-cell function and

morphology were changes in the expression of genes implicated in β-cell identity, and glucose transport and metabolism, including glucokinase and Pdx1 (Cheng et al., 2012). Similar phenotypic changes between low and high passage MIN6 β-cells have been reported (Dowling et al., 2006; O'Driscoll et al., 2004, 2006; Yamato et al., 2013). Therefore, MIN6 β-cells of passage no greater than 40 were used for experiments described in this thesis.

2.4.1 Maintenance and subculture of MIN6 β-cells

MIN6 β-cells were kindly provided by Dr Catherine Arden (Newcastle University, United Kingdom). Cells were maintained in sterile-filtered DMEM containing 25mM glucose, 10% (v/v) fetal bovine serum (FBS), 100U/mL penicillin, 100µg/mL streptomycin, 2mM L-glutamine and 0.0005% (v/v) β-mercaptoethanol (β-ME). Cells were incubated at 37°C, 5% CO_2 and 95% humidity, and phenol red acted as a pH indicator to monitor cell culture pH changes that can occur from the accumulation of waste products, dying cells or bacterial contamination. Aseptic technique was used throughout cell and reagent handling to prevent contamination from pathogens.

MIN6 β-cells were grown as an adherent monolayer in 75cm^2 Nunc™-treated flasks containing 15mL DMEM with media changes every 3-4 days. Once 70-90% confluency was reached, MIN6 β-cells were sub-cultured, and a portion was used in experimental protocols. To do so, cell detachment from the flask surface and cell-cell separation were performed by trypsinisation using a mixture of trypsin (0.1%) and ethylenediaminetetraacetic acid (EDTA; 0.02%). Trypsin is an endopeptidase which cleaves lysine and arginine residues within and between proteins to detach cells from the flask floor. EDTA is a chelator which sequesters metallic ions, such as calcium and magnesium, at the cell surface to enhance trypsin activity and weaken cell-cell interactions. Following aspiration of DMEM and washing with Dulbecco′s Phosphate Buffered Saline (PBS), MIN6 β-cells were exposed to trypsin-EDTA at 37°C and monitored carefully for 3-5 minutes to prevent over-digestion and cell death. Flasks were tapped against the palm to assist cell detachment prior to the addition of serum-containing DMEM to inactivate trypsin. The cell suspension was centrifuged at 200xg, 20°C for 5 minutes, the supernatant was removed, and the cell pellet was resuspended in an appropriate volume of DMEM to enable cell counting.

2.4.2 Cell counting and viability

At the time of subculturing, the number of MIN6 β-cells was calculated to seed the required numbers of cells into plates for each experiment. Two methods of cell counting were used in this project: 1) manual cell counting using a haemocytometer; and 2) automated cell counting using a Countess Automated Cell Counter.

A haemocytometer is a specialised glass chamber laser-etched with 4 square grids, each of which consists of 12 smaller squares. A single grid has a surface area of 1mm^2 and a depth of 0.1mm, giving a defined volume of 0.1mm^3 or 10^{-4}mL. Using the known dimensions of the chamber, the density of cells within suspension can be quantified. The azo dye, Trypan blue, is commonly used for the visualisation and quantification of viable cells as the blue-coloured solution cannot penetrate into live cells with intact membranes and can only cross damaged membranes of dead cells. Therefore, Trypan blue-stained non-viable cells can be distinguished from healthy viable cells. Each MIN6 β-cell suspension was mixed with an equal

volume of Trypan blue (0.2% w/v) and, by placing the Gilson pipette between the chamber and coverglass, 10µL of cell suspension was drawn up by capillary action to fill the chamber. The grids were then visualised under a light microscope for manual counting of cells within the defined areas of known volume (Figure 16). Given each grid has a volume of 0.1mm^3 and considering the dilution of cells in Trypan blue, the following formula can be used to calculate total cell number per mL: mean cell number across 4 grids x 10,000 x 2. By following this Trypan blue exclusion protocol, cell viability can also be determined by calculating the proportions of viable and non-viable cells; dead cells are subsequently excluded from the final cell count.

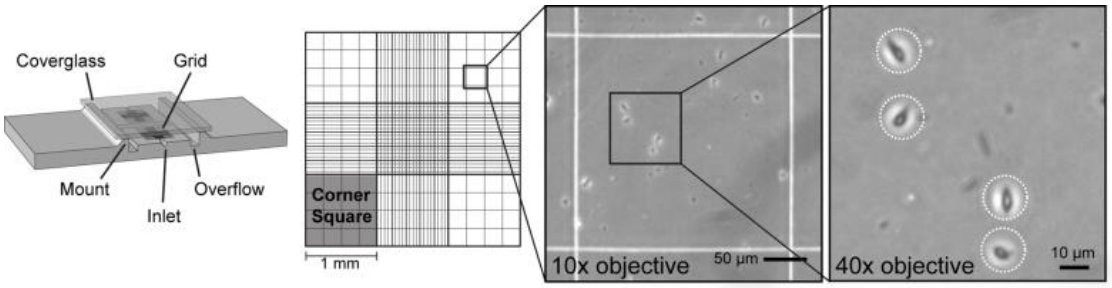

Figure 16. Counting cells with a haemocytometer and Trypan blue dye. (Zhang & Kuhn, 2018).

Whilst manual counting with a haemocytometer is a simple, rapid, and cheap technique for quantifying cell number and viability, there are several disadvantages. For example, counting error may occur due to inaccurate cell dilution, poor cell dispersion and improper chamber filling (Aslantürk, 2018). Furthermore, variations in human perception can lead to significant variability in cell number and viability calculations. An alternative to manual cell counting is using an automated method which provides greater precision and reproducibility by avoiding human interference. The Countess Automated Cell Counter was used for automated counting of cells in suspension. Like manual counting, equal volumes of cell suspension and Trypan blue dye were mixed, but in this case 10µL of mixture was transferred to a disposable counting chamber slide closely resembling a haemocytometer chamber. The slide was then inserted into the instrument to visualise cells and for automated counting of cell number and viability. These values were used to calculate the volume of cell suspension required to seed cells for experiment protocols. The following formula was used: desired cell number per well x (total required volume/cell concentration). A range of MIN6 β-cell densities were used, depending on the protocol, as indicated below: between 15,000-300,000 cells per well were seeded into 6-well or 96-well plates.

2.4.3 Cryopreservation and thawing of MIN6 β-cells from frozen storage

To maintain stocks of MIN6 β-cells for future experiments, healthy cells in the log growth phase must be frozen down for long-term storage and preservation. For this, MIN6 β-cells were trypsinised at 70-90% confluency and resuspended in fresh DMEM, as previously described in Section 2.4.1. To avoid cell damage and death caused by intracellular ice formation at low temperatures, the cells were resuspended in media containing 10% (v/v) dimethyl sulfoxide (DMSO), a cryoprotective agent, prior to freezing. Aliquots of 1mL cell suspension, containing 2-3 million cells, were transferred to Nunc™ cryogenic vials. The vials were placed into a Mr. Frosty™ Freezing Container which has 100% isopropanol filled within its outer compartment

to achieve an optimal cooling rate of -1°C/minute for cell preservation. The Mr. Frosty™ Freezing Container was kept at –70°C for 2 hours before the cell-containing vials were transferred to a liquid nitrogen vessel for long-term storage at –196°C.

When required, frozen cells were retrieved from liquid nitrogen storage and reconstituted by thawing. Whilst cell freezing must occur at a slow and controlled rate to avoid ice crystal formation, cell thawing must be performed quickly as the prolonged stress can significantly reduce cell recovery. A vial containing frozen MIN6 β-cells was rapidly thawed in a 37°C water bath for 1 minute. The contents of the vial were transferred to a 15mL Falcon tube containing 9mL of warmed DMEM. The MIN6 β-cells were centrifuged at 200xg, 20°C for 5 minutes and the cell pellet was resuspended in DMEM before transfer to a T25 flask. The cells were incubated overnight at 37°C, 5% CO_2 and 95% humidity and the medium was changed to remove any non-adherent cells. The cells were maintained in culture, as described in Section 2.4.1.

2.5 Mouse islet isolation

2.5.1 Mice

For the isolation and purification of mouse islets used for functional experiments, 8-12-week-old CD1 male mice (Charles River) had *ad libitum* access to standard laboratory chow and water. All animals were housed at 21-25°C with a 12-hour light-dark cycle.

2.5.2 Preparation of experimental buffers and media

For pancreas perfusion and digestion, collagenase solution (1mg/mL) was made up by dissolving collagenase type IX in non-supplemented, serum-free Minimum Essential Media (MEM). For islet isolation and purification, MEM was supplemented with 10% (v/v) newborn calf serum (NCS), 100U/mL penicillin, 100µg/mL streptomycin and 2mM L-glutamine. For islet culture, Roswell Park Memorial Institute (RPMI) cell culture medium containing 11mM glucose was supplemented with 10% (v/v) FBS, 100U/mL penicillin, 100µg/mL streptomycin and 2mM L-glutamine.

2.5.3 Pancreas perfusion and digestion

Mice were euthanised by cervical dislocation. The abdominal cavity was opened by laparotomy using dissecting scissors to cut through the peritoneal wall, firstly following the rib line before moving vertically. The ampulla of Vater, the small opening which connects the pancreatic and bile ducts to the duodenum (see Figure 3 in Section 1.2.1), was clamped and 2.5mL of collagenase solution was injected into the common bile duct using a 2.5mL syringe and 32G needle. The distended pancreas was dissected out from the abdominal cavity and placed on ice into a 50mL Falcon tube. Samples were incubated at 37°C in a water bath for 10 minutes to facilitate the enzymatic digestion of pancreatic exocrine tissue. To stop the reaction, ice cold 25mL supplemented MEM was added and the Falcon tubes were shaken vigorously by hand for 10 seconds. The samples were kept on ice for subsequent steps of the protocol.

2.5.4 Islet isolation, purification, and culture

Digested pancreas samples went through a series of wash steps beginning with centrifugation at 180xg, 10ºC for 1.5 minutes. The supernatant was decanted, fresh MEM was added to the pellets and the Falcon tubes were vortexed. This step was repeated a further two times. The resuspended pellet was passed through a sieve into new Falcon tubes to remove any undigested exocrine tissue. Samples were further purified by centrifugation at 210xg, 10ºC for 1.5 minutes. The supernatant was decanted and the Falcon tubes were thoroughly dried before the addition of 15mL Histopaque, a density gradient medium, which is used to optimise the separation and purification of mouse islets (McCall et al., 2011). Samples were vortexed and 10mL MEM was slowly added to the Falcon tubes to create gradient layers of media and Histopaque. Samples were centrifuged at 1170xg, 10ºC for 24 minutes. Floating islets at the MEM-Histopaque interface were collected and transferred to new Falcon tubes. A final series of washes were performed using a gravity separation technique: islets were suspended in 25mL MEM and, after 4-5 minutes, 10mL MEM was removed and replaced with fresh media; this step was repeated a further three times. Islets were hand-picked into Petri dishes containing supplemented RPMI and maintained in culture at 37°C, 5% CO_2 and 95% humidity.

2.6 Quantification of GPCR mRNA expression

2.6.1 Total RNA extraction from MIN6 β-cells and mouse islets

The extraction and purification of RNA from MIN6 β-cells was performed using the RNeasy Mini Kit and began with seeding of 250,000-300,000 cells/2mL/well into a 6-well plate. After 2-3 days of incubation at 37°C, 5% CO_2 and 95% humidity, MIN6 β-cells were washed with PBS, trypsinised and resuspended in DMEM then centrifuged at 200xg, 20°C for 5 minutes, as described in Section 2.4.1. DMEM was removed from each cell pellet followed by the addition of 700µL RLT, a lysis buffer which, like RWT buffer, contains a high concentration of guanidine isothiocycanate to support RNA binding to the spin column silica membrane. The RLT buffer was supplemented with 1% (v/v) of the reducing agent, β-ME, to inactivate RNases within the cell lysate. Samples were vortexed for 1 minute to disrupt the cell pellets and 1 volume of 70% molecular biology grade ethanol was thoroughly mixed with the homogenised lysates. Samples were transferred to RNeasy Mini spin columns and centrifuged at 12,000xg, 20°C for 30 seconds. The flow-through was discarded and 350µL RW1 buffer was added to each spin column followed by centrifugation at 12,000xg, 20°C for 30 seconds. The purpose of RW1, another stringent washing buffer, is to remove non-specifically bound biomolecules, such as fatty acids, proteins, etc., from the silica membrane. The flow-through was discarded and the spin columns were treated with 80µL DNase I for 15 minutes at room temperature to degrade any contaminating DNA. An additional 350µL of RW1 buffer was added and samples were centrifuged at 12,000xg, 20°C for 30 seconds. The flow-through was discarded. 500µL of RPE buffer were added and samples were centrifuged at 12,000xg, 20°C for 30 seconds. The flow-through was discarded. An additional 500µL of RPE buffer were added and samples were centrifuged at 12,000xg, 20°C for 2 minutes. The flow-through was discarded and a dry centrifuge performed at 12,000xg, 20°C for 1 minute to elute any residual ethanol-based buffers. The collection tube was discarded, and the RNeasy Mini spin columns were placed into new Eppendorf tubes. 30-50µL DNase-RNase-free water was directly added onto the RNeasy Mini spin column membrane and samples were centrifuged at 12,000xg, 20°C for 1

minute to elute the RNA. The elution was added onto the RNeasy Mini spin column and the centrifugation step was repeated to maximise the yield of RNA extracted from the samples.

The extraction and purification of RNA from mouse islets used a modified version of the TRIzol® Reagent method whereby total RNA was precipitated using isopropanol. Following isolation and overnight incubation, groups of 150-200 mouse islets were transferred to 1.5mL Eppendorf tubes and centrifuged at 200xg, 20°C for 5 minutes. Using a Gilson pipette, RPMI was carefully removed without disruption of the islet pellets and a series of washes with PBS were performed. After the final wash, PBS was replaced with 1mL of TRIzol® Reagent. 200µL of chloroform were added and samples were vigorously shaken by hand for 15 seconds before incubation at room temperature for 2 minutes. Samples were centrifuged at 12,000xg, 4°C for 15 minutes. Following centrifugation, the upper, colourless aqueous phase containing RNA was transferred to new 1.5mL Eppendorf tubes each containing 0.5µL of RNA grade glycogen (20µg/µL). Glycogen is a polysaccharide which is insoluble in ethanol and acts as an inert carrier during ethanol precipitation. When added to purified RNA or DNA, glycogen forms a precipitate which traps target nucleic acids present within a sample. Therefore, the addition of glycogen can increase the visibility of an RNA pellet and enhance recovery of nucleic acids. 500µL of cooled 100% isopropanol (–20°C) was added to each sample, stored at –70°C for 1 hour then samples were centrifuged at 12,000xg, 4°C for 15 minutes. Following centrifugation, all liquid was removed from the Eppendorf tubes with care taken to avoid disruption of RNA pellets. 1mL of 75% ethanol was added and samples were centrifuged at 7,500xg, 4°C for 10 minutes. All liquid was removed, and Eppendorf tubes were placed in a heat block at 37°C with the lids open until the RNA pellets dried. The RNA was then dissolved in 25µL of DNase-RNase-free water.

2.6.2 Determination of RNA concentration and purity

The concentration and purity of RNA extracted from MIN6 β-cells and mouse islets were quantified using a Nanodrop™ 1000 spectrophotometer, as previously described in Section 2.2.8. Once measured, RNA samples were either stored at –70°C to await further processing or kept on ice for preparation of RT reactions.

2.6.3 Reverse transcription for complementary DNA generation

RT reactions of 20µL (including 50ng of RNA per µL) were prepared from RNA stock samples by dilution with the required volume of DNase-RNase free water and MasterMix solution and processed in a T100™ thermal cycler set at the previously described programme (Section 2.2.9). cDNA samples were either stored at –20°C to await further processing or kept on ice to perform qPCR.

2.6.4 Quantitative polymerase chain reaction

The SYBR Green fluorescent dye-based qPCR protocol was performed to measure the expression level of GPCRs of interest in MIN6 β-cells and mouse islets. QuantiTect Primer Assays for Ccl4-activating receptors, *Ackr2*, *Ccr1*, *Ccr2*, *Ccr5*, *Ccr9*, *Cxcr1* and *Cxcr5* were used to determine whether islet cells express receptors through which Ccl4 signals. The housekeeping gene, β-actin (*Actb*), was used as an appropriate reference gene for qPCR using MIN6 β-cell and mouse islet cDNAs. A reaction mixture per cDNA sample was prepared

with SYBR Green, DNase-RNase free water and diluted cDNA sample (1:8) present in a 5:2:1 ratio. 8µL reaction mix and 2µL primers per well were loaded into a 96-well white plate (individual samples tested in duplicate). The plate was centrifuged at 150xg, 4°C for 1 minute to ensure collection of samples at the base of the well. qPCR was performed on a LightCycler® 96 following a standard programme outlined in Section 2.2.10.

2.7 PRESTO-Tango β-arrestin GPCR reporter assay

2.7.1 Background

To facilitate the interrogation of the human GPCR-ome, the Roth group developed a method, known as PRESTO-Tango, which combines Parallel Receptor-ome Expression and Screening via Transcriptional Output (PRESTO) and transcriptional activation following arrestin translocation (Tango) approaches (Kroeze et al., 2015). The method takes advantage of ligand-induced β-arrestin2 recruitment to measure GPCR activity following exposure to potential agonists. It uses a novel HEK293 cell line, known as HTLA, which stably expresses a tTA-dependent luciferase reporter and a β-arrestin2-TEV fusion gene (Figure 17A). The assay requires transfection of HTLA cells with a recombinant GPCR plasmid of interest. Each GPCR in this system is linked to an exogenous transcription factor via a peptide cleavage site at the C-terminus (Figure 17B). Ligand binding to HTLA cells transfected with recombinant GPCRs triggers receptor desensitisation, which is mediated by the recruitment of a protease-tagged β-arrestin that cleaves the linkage site, thereby liberating the transcription factor from the receptor. The transcription factor translocates to the nucleus where it drives expression of the β-lactamase reporter gene. The β-lactamase enzyme then catalyses cleavage of a substrate thus generating a luminescent signal that can be quantified. The resulting signal readouts correlate with the activity of the target GPCR when exposed to an experimental compound (Kroeze et al., 2015).

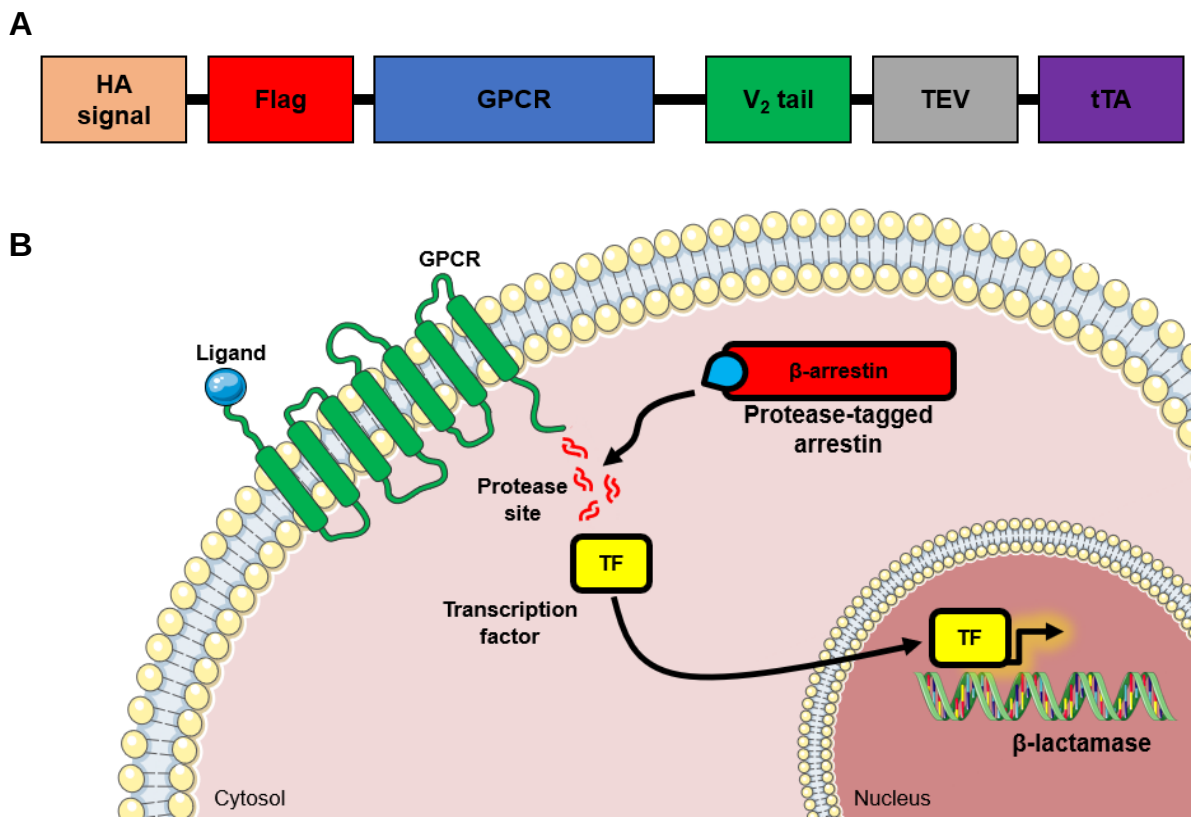

Figure 17. The design and principle of the PRESTO-Tango β-arrestin GPCR reporter assay. (A) The components of a GPCR gene construct for transfection into HTLA cells: a HA signal encoding a cleavage sequence for membrane localisation; a Flag epitope tag to enable identification and quantification of cell surface receptor expression by immunohistochemistry; a sequence for a specific GPCR of interest; a V_2 vasopressin receptor (V_2 tail) to promote β-arrestin recruitment; a Tobacco Etch Virus (TEV) nuclear inclusion endopeptidase; and a tetracycline transactivator (tTA) transcription factor. Adapted from Kroeze et al. (2015). (B) A schematic illustrating the recruitment of a protease-tagged β-arrestin to a specific GPCR upon ligand binding, followed by the liberation and translocation of the tTA transcription factor to the nucleus to drive β-lactamase expression. Adapted from Hanson et al. (2009).

2.7.2 Maintenance of HTLA cells

The PRESTO-Tango β-arrestin reporter assay used HTLA cells kindly provided by the Roth Lab (University of North Carolina, USA). Cells were maintained at 37°C, 5% CO_2 and 95% humidity in DMEM containing 25mM glucose, 10% (v/v) FBS, 2µg/mL puromycin, 100µg/mL hygromycin B, 100U/mL penicillin, and 100µg/mL streptomycin.

2.7.3 Ccl4-target GPCR screening using PRESTO-Tango technology

96-well white clear-bottom plates were aseptically coated with poly-L-lysine hydrobromide, rinsed with sterile water, and left to dry for 1 hour. HTLA cells were subcultured and a portion harvested for experimental use, as previously described for the MIN6 β-cell line in Section 2.4.1. Cells were plated at a density of 25,000 cells/100µL/well in DMEM supplemented with 10% (v/v) dialysed FBS and incubated overnight at 37°C, 5% CO_2 and 95% humidity. Medium was then replaced with fresh DMEM containing dialysed FBS and pre-prepared plasmids encoding Tango versions of Ackr2, Ccr1, Ccr2, Ccr5, Ccr9, Cxcr1, and positive control

plasmids A2ar and Chm3, were transfected individually into HTLA cells by the calcium phosphate precipitation method. Aiming for 200ng per well, DNAs were diluted in 1X Hanks' Balanced Salt Solution (HBSS) containing 2.5M $CaCl_2$. The documented Ccl4 targets, Ccr1 and Ccr9, were not included in the GPCR screening as Tango versions of these plasmids were not available. The plasmid solution was vortexed, incubated at room temperature for 15 minutes, and added dropwise to the corresponding wells. HTLA cells were then incubated overnight at 37°C, 5% CO_2 and 95% humidity.

After overnight incubation, transfected HTLA cells were incubated with FBS-free DMEM supplemented with 100U/mL penicillin, and 100µg/mL streptomycin for 1 hour. Subsequently, cells were incubated overnight (37°C, 5% CO_2 and 95% humidity) in assay buffer (1X HBSS containing 20mM HEPES) in the absence or presence of 100ng/mL Ccl4. Positive control agonists, clonidine and carbachol, were also used to activate their cognate target receptors, α_2-adrenoceptor, A2ar, and cholinergic receptor muscarinic 3 receptor, Chm3, respectively, to ensure that the reporter assay was operating appropriately. Agonists were then removed, and the cells were incubated for 15 minutes at room temperature with 70µL of Bright-Glo™ Reagent diluted 1:10 with assay buffer. The multifunctional microplate reader, PHERAstar FS®, was used to quantify luminescence which correlated to the degree of GPCR activation.

2.8 Measurement of insulin secretion

2.8.1 Insulin secretion

The quantification of secreted insulin from MIN6 β-cells and mouse islets is an important assessment of β-cell function. The effects of exogenous Ccl4 on insulin secretion from MIN6 β-cells and mouse islets were investigated using static incubation experiments in which supernatants were retrieved for the measurement of accumulated insulin content.

2.8.1.1 Insulin secretion from MIN6 β-cells

MIN6 β-cells (passage 25-40) were seeded into a 96-well plate at a density of 25,000 cells/100µL/well using sterile-filtered DMEM containing 25mM glucose, 10% (v/v) FBS, 100U/mL penicillin, 100µg/mL streptomycin, 2mM L-glutamine and 0.0005% (v/v) β-ME. Following overnight incubation at 37°C, 5% CO_2 and 95% humidity, MIN6 β-cells were washed with PBS and the medium was replaced with DMEM containing 2.5mM glucose for 16 hours. Cells were then pre-incubated for 2 hours with a bicarbonate-buffered physiological salt solution (Gey & Gey, 1936) supplemented with 2mM glucose, 2mM $CaCl_2$ and 0.5mg/mL BSA and pH was adjusted to 7.4 using carbon dioxide (Table 7 and 8). As the MIN6 β-cells used for these experiments did not show an appropriate glucose-stimulated insulin secretory response, insulin secretion was stimulated using α-ketoisocaproic acid (KIC), a metabolite of the amino acid, leucine, which has similar insulin-releasing potency to glucose (Panten et al., 2023). MIN6 β-cells were incubated for 1 hour with Gey and Gey buffer containing 2mM glucose with or without 10mM KIC, in the absence or presence of recombinant Ccl4 (100ng/mL) or the α_2-adrenoceptor agonist, clonidine (10µM) which was used as a $G\alpha_i$-coupled receptor control agonist. The supernatants were retrieved and stored at –20°C until measurement of insulin content by radioimmunoassay (see Section 2.8.2 below).

Table 7. Preparation of 2X Gey and Gey stock solution in distilled water.

Reagent	Mass (g/L)	Final Concentration (mM)
NaCl	13.00	111
KCl	0.74	5.00
$NaHCO_3$	4.54	27.0
$MgCl_2$-$6H_2O$	0.42	1.00
KH_2PO_4	0.06	0.22
$MgSO_4$-$7H_2O$	0.14	0.28

Table 8. Preparation of 1X Gey and Gey working solution containing 2mM glucose. To prepare 1X Gey and Gey working solution containing 20mM glucose, an additional 0.648g glucose was added to 200mL of 2mM glucose solution.

Reagent	Volume (mL) or Mass (g)	Final Concentration
2X Gey and Gey stock	200mL	1X
dH_2O	200mL	-
Glucose powder	0.14g	2mM
$CaCl_2$ solution	0.80mL	2mM
BSA powder	0.20g	0.05% (w/v)

2.8.1.2 Insulin secretion from mouse islets

Freshly isolated CD1 mouse islets (Section 2.5) were maintained in culture in RPMI 1640 overnight then washed and pre-incubated with Gey and Gey buffer (2mM glucose) for 1 hour at 37°C, 5% CO_2 and 95% humidity. Groups of 3 islets per replicate per condition were then transferred, on ice, to 1.5mL Eppendorf tubes containing 300µL buffer at 2mM or 20mM glucose in the absence or presence of recombinant mouse Ccl4 (5, 10, 50 and 100ng/mL). The muscarinic receptor agonist, carbachol (500µM), and the α_2-adrenoceptor agonist, clonidine (10µM), were used as positive and negative controls, respectively. After incubation at 37°C for 1 hour, islets were centrifuged at 200xg, 4°C for 1 minute and 100µL of supernatant was diluted in 400µL borate buffer, with care taken not to dislodge islets. Diluted supernatant was stored at –20°C prior to measurement of insulin content by radioimmunoassay.

2.8.2 Radioimmunoassay

The concentration of insulin secreted from MIN6 β-cells and mouse islets was quantified by radioimmunoassay, a highly sensitive immunoassay that is based on competition between unlabelled insulin (antigen, AG) and radiolabelled insulin (tracer, AG*) for a limited number of anti-insulin antibody (AB) binding sites. The following equation summarises the equilibrium achieved when these three components react:

$$\mathbf{AB + AG + AG^* \leftrightarrow AB{:}AG + AB{:}AG^* + AG + AG^*}$$

Whilst the concentrations of unlabelled AG are variable, the concentrations of AB and radiolabelled AG* remain fixed. As the concentration of AG increases, the number of AB:AG* complexes decline due to greater competition and the displacement of radiolabelled AG*. Using known concentrations of insulin ("standards"), the corresponding radioactivity AG* values can be used to generate a standard curve. The unknown concentrations of insulin within samples can then be extrapolated using this standard curve.

Exogenous insulin was labelled with the most commonly used radioisotope: iodine-125 (I^{125}) (Sharma et al., 2014). The I^{125} radioisotope has a half-life of 60 days and emits low energy γ radiation that is easily and efficiently detected by a crystal scintillation counter, thus making this a popular radiolabel for proteins of interest (Fitch et al., 1962). The iodination of insulin involves oxidation of I^- ions using a strong oxidising agent, iodogen (1,3,4,6-tetrachloro-3α,6α-diphenyl glycoluril), at a neutral pH to produce reactive I^+ ions. The reactive I^+ ions then covalently bind to tyrosine residues within the insulin protein. The iodinated insulin was purified from unincorporated I^+ ions using Sephadex gel filtration chromatography. The radiolabelled insulin is recognised by the anti-insulin antibody, which was raised in-house in guinea pig. This host species was chosen due to the structural differences between guinea pig insulin and that of other mammalian species, therefore allowing for the generation of antibodies in guinea pigs following injection of bovine insulin.

Borate-buffered saline (pH 8.0) was used in the radioimmunoassay protocol to dilute reagents and to maintain optimal pH for insulin-antibody binding to occur (Table 9). The anti-insulin antibody was diluted 1:60,000 and the iodinated insulin tracer was diluted to produce approximately 12,000 counts per minute (CPM)/100µL (the degree of dilution was dependent on the level of radioisotope decay). The stock of insulin standard (10ng/mL) was serially diluted to produce a range of insulin concentrations (0.08-10ng/mL) in triplicate. Reference tubes, also in triplicate, were prepared to measure non-specific antigen binding (NSB), maximum binding (MB) of iodinated insulin to the antibody and total γ-emission (Table 10). Following the addition of insulin tracer and anti-insulin antibody, where applicable, the sample, standard and reference tubes were incubated at 4°C for 48 hours for the binding to equilibrate. Subsequently, the antibody-antigen complexes were separated from free antigen by precipitation using γ-globulins (Table 11). Precipitant was added to all tubes, except for the Totals, and centrifuged at 2000xg, 4°C for 15 minutes. Following centrifugation, the free antigen in solution was aspirated and the pellet containing antibody-antigen complexes were placed into a Packard Cobra II γ counter to measure γ emissions. Insulin content within samples was determined by extrapolating sample CPM counts from standard curve CPM counts.

Table 9. Preparation of borate-buffered saline using distilled water and adjusted to pH8 using 12N HCl.

Reagent	Mass (g/L)	Final Concentration (mM)
Boric acid	8.25	133.4
NaOH	2.70	7.5
EDTA	3.70	12.7

Table 10. Preparation of insulin standards, reference tubes and samples. Totals (T): to determine the amount of radioactivity of iodinated insulin tracer; Non-specific binding (NSB): to determine background antigen binding in the absence of antibody; Maximum binding (MB): to determine radiolabelled tracer binding to antibody in the absence of unlabelled insulin. *Borate buffer is not added to the 10ng/mL insulin standard. †The 1:5 sample dilution in borate buffer is performed during the radioimmunoassay with MIN6 β-cell supernatant only; The 1:5 sample dilution of mouse islet supernatant is performed immediately after the insulin secretion experiment.

	Volume (µL)			
Reagent	**Borate Buffer**	**Insulin Antibody**	**Insulin Tracer**	**Sample**
Non-specific binding (NSB)	200	-	100	-
Maximum binding (MB)	100	100	100	-
Totals (T)	-	-	100	-
Insulin standards	100*	100	100	-
Samples	80†	100	100	20†

Table 11. Preparation of precipitant for the separation of antibody-complexes and free antigen.

Reagent	Volume/Mass (per L)	Final Concentration
30% PEG	500mL	50% (v/v)
γ-globulins	1000mg	1% (w/v)
Tween	500µL	-
PBS	500mL	-

2.9 Islet cell apoptosis

β-cell mass is dynamic, and it is regulated through a fine balance of cell proliferation, cell apoptosis, and islet neogenesis from pancreatic progenitor cells. Apoptosis, or programmed cell death, is coordinated by a family of cysteine proteases, known as caspases. In response to a variety of pro-apoptotic intrinsic and extrinsic stimuli, such as exposure to cytokines or saturated fatty acids, DNA damage or hypoxia, “initiator” caspases (caspase-2, -8, -9 and -10) become activated (Tomita, 2016). This triggers a chain of proteolytic cleavage and activation of downstream caspases (caspase-3, -6 and -7). These “effector” caspases degrade a range of protein substrates leading to typical morphological features of apoptosis, including cell shrinkage, nuclear fragmentation and eventual phagocytosis into neighbouring cells (Saraste & Pulkki, 2000; Tomita, 2016). As caspase-3 and -7 are integral mediators of cell apoptosis, commonly used *in vitro* functional assays measure caspase-3/7 activity as a marker for cell apoptosis.

2.9.1 Caspase-Glo 3/7 assay

Islet and MIN6 β-cell apoptosis was detected using the Caspase-Glo® 3/7 Assay System. The kit contains a Caspase-Glo® Reagent consisting of a proluminescent DEVD-aminoluciferin substrate and the luciferase enzyme, Ultra-Glo™ rLuciferase. Addition of the Caspase-Glo® Reagent to cells results in cell lysis and cleavage of the substrate by active caspase-3/7 enzymes. The luciferase catalyses a light-producing reaction with liberated aminoluciferin. The resulting luminescent signal is proportionate to caspase-3/7 activity within apoptotic cells.

2.9.2 Cytokine-induced and palmitate-induced islet cell apoptosis

Apoptosis of MIN6 β-cells and mouse islets was induced by either the saturated fatty acid, palmitate (500µM, Table 12), or a cocktail of pro-apoptotic cytokines: IL-1β (0.05U/µL), TNF-α (1U/µL) and IFN-γ (1U/µL). MIN6 β-cells were seeded into an opaque-walled 96-well plate at a density of 20,000 cells/100µL/well in DMEM containing 25mM glucose, 10% (v/v) FBS, 100U/mL penicillin, 100µg/mL streptomycin, 2mM L-glutamine and 0.0005% (v/v) β-ME. Following overnight incubation, MIN6 β-cells were treated with fresh DMEM supplemented with 2% (v/v) FBS and in the presence or absence of an apoptotic inducer and/or peptide(s) of interest. MIN6 β-cells were incubated for 20 hours at 37°C, 5% CO_2 and 95% humidity. For experiments with mouse islets, groups of 90 islets isolated from CD1 mice were incubated overnight with or without peptide(s) of interest diluted in RPMI containing 5.5mM glucose, 10% (v/v) FBS, 100U/mL penicillin, 100µg/mL streptomycin and 2mM L-glutamine. Thereafter, mouse islets were seeded into an opaque-walled 96-well plate at a density of 5 islets/40µL/well (6 wells per treatment group) in fresh RPMI supplemented with 2% (v/v) FBS and in the presence or absence of an apoptotic inducer and/or peptide(s) of interest. Mouse islets were further incubated for 20 hours at 37°C, 5% CO_2 and 95% humidity.

An equal volume of Caspase-Glo® 3/7 assay reagent, consisting of luciferase substrate and lysis buffer, was added to wells containing MIN6 β-cells or mouse islets and incubated for 1 hour at room temperature. A Turner Biosystems Veritas Microplate Luminometer was used to detect and quantify relative luminescence units (RLUs), a measure of bioluminescence that correlated to the degree of apoptosis.

Table 12. Preparation of palmitate working solution to treat islet cells for the Caspase-Glo® 3/7 assay. 13.9mg/mL sodium palmitate was dissolved in EtOH:dH_2O (1:1) at 70°C for 10 minutes and diluted in medium containing 2% FBS and 10% fatty acid-free BSA. For control groups, EtOH:dH_2O (1:1) was prepared without palmitate. Following a 1-hour incubation at 37°C, control or palmitate-containing medium was further diluted in DMEM (MIN6 β-cells; 25mM glucose) or RPMI (mouse islets; 11mM glucose) supplemented with 2% (v/v) FBS prior to the addition of peptide(s) of interest.

Palmitate Concentration	Palmitate	Palmitate Control
50mM	13.9mg/mL palmitate + 1:1 EtOH:dH_2O Heat at 70°C for 10 minutes	1:1 EtOH:dH_2O only
5mM	Dilute 1:10 in sterile-filtered media supplemented with 2% FBS and 10% fatty acid-free BSA	
	Incubate at 37°C for 1 hour	
500µM	Dilute 1:10 in media supplemented with 2% FBS	
	Add peptide(s) of interest and treat islet cells	

2.10 Islet cell proliferation

As previously mentioned in Section 1.4, cell proliferation is a regulator of β-cell mass together with cell apoptosis and islet neogenesis. Given that β-cell damage and death are hallmarks of severe T2D progression, identification of agents that stimulate β-cell proliferation could lead to enhanced insulin secretion capacity to compensate for impaired β-cell function in diabetes.

2.10.1 Proliferation of MIN6 β-cells

MIN6 β-cell proliferation was assessed using a Cell Proliferation ELISA Kit. This is a colorimetric immunoassay which quantifies cell proliferation by measuring the incorporation of a synthetic thymidine analogue, 5-bromo-2′-deoxyuridine (BrdU), during DNA synthesis. MIN6 β-cells were seeded into a 96-well plate at a density of 15,000 cells/100µL/well using DMEM containing 25mM glucose, 10% (v/v) FBS, 100U/mL penicillin, 100µg/mL streptomycin, 2mM L-glutamine and 0.0005% (v/v) β-ME. Following an overnight incubation, MIN6 β-cells were washed with PBS and replaced with FBS-free DMEM containing 5.5mM glucose. The overnight incubation with this ‘starving medium’ was to ensure that cells reached a quiescent state whereby cell growth was inhibited. MIN6 β-cells were then treated with DMEM containing either 2% or 10% FBS in the absence or presence of peptide(s) of interest for 48 hours. The supplementation of 10% FBS promotes cell survival and growth due to the presence of growth factors, and therefore this served as a positive control condition for the assessment of MIN6 β-cell proliferation. After 48 hours, MIN6 β-cells were labelled with 100µM BrdU reagent and incubated for 2 hours at 37°C, 5% CO_2 and 95% humidity. During this time, BrdU replaces endogenous thymidine and becomes incorporated into newly synthesised DNA within proliferating cells. Subsequently, MIN6 β-cells were fixed, and DNA was denatured with

FixDenat solution for 30 minutes at room temperature to improve the accessibility the anti-BrdU antibody for detection of incorporated BrdU. Removal of the FixDenat solution was followed by incubation of MIN6 β-cells with the anti-BrdU-phosphodiesterase solution for 90 minutes at room temperature. After several washes with washing buffer to remove the anti-BrdU antibody solution, MIN6 β-cells were treated with TMB substrate solution for 10 minutes at room temperature to initiate a reaction for the detection of immune complexes. The reaction was stopped using 1M H_2SO_4 stopping solution and the absorbance was quantified at a 450nm wavelength using the multifunctional microplate reader, PHERAstar FS®. The degree of colour development and the corresponding absorbance directly correlated with the level of DNA synthesis and thus, the number of proliferating MIN6 β-cells.

2.10.2 Immunofluorescence *ex-vivo* of whole mouse islets

Primary islets have a very low proliferative capacity, so the BrdU ELISA is not appropriate for quantifying DNA replication, as it is for MIN6 cells. Therefore, mouse islets were subjected to immunofluorescence staining to identify and measure proliferating β-cells. Groups of 5-10 mouse islets were transferred into wells of a 96-well plate and maintained in RPMI containing 5.5mM glucose, 10% (v/v) FBS, 100U/mL penicillin, 100µg/mL streptomycin and 2mM L-glutamine and in the absence or presence of Ccl4 (100ng/mL). Following a 72-hour incubation period at 37°C, 5% CO_2 and 95% humidity, islets were fixed in 4% paraformaldehyde (PFA) for 45 minutes at room temperature. After washing three times in PBS, islets were permeabilised for 2 hours at room temperature on a plate shaker with 0.2% v/v Triton X-100 in PBS supplemented with 0.8% FBS and 1% BSA. Islets were then incubated overnight with primary antibodies targeting insulin, glucagon, somatostatin, and the nuclear proliferation marker, Ki67 (Table 13) at room temperature on a plate shaker. Once primary antibody solutions were removed, islets were washed three times with PBS and subsequently treated with DAPI (1:500 dilution) and the corresponding secondary antibodies (Table 14). Incubation for 2 hours at room temperature on a plate shaker was followed by three washes with PBS. Islets were mounted on superfrost glass slides with DAPI-Fluoromount and topped with a coverslip. Slides were dried overnight at room temperature and either stored at 4°C for short-term storage or at –20°C for long-term storage. Images were captured using a Nikon Eclipse Ti-E Inverted A1 inverted confocal microscope and analysed using ImageJ and Cell Profiler software.

Table 13. List of primary antibodies used for immunofluorescence staining of mouse islets.

Hormone/Protein	Primary Antibody	Dilution	Supplier
Insulin	Guinea pig polyclonal anti-insulin	1:200	Abcam ab7842
Glucagon	Mouse monoclonal anti-glucagon	1:1000	Sigma Aldrich G2654
Somatostatin	Rat monoclonal anti-somatostatin	1:65	Abcam ab30788
Ki67	Rabbit polyclonal anti-Ki67	1:200	Abcam ab15580

Table 14. List of secondary antibodies used for immunofluorescence staining of mouse islets.

Secondary Antibody	Dilution	Supplier/Catalogue Number
Donkey anti-guinea pig Alexa Fluor 488	1:200	Jackson ImmunoResearch 706-545-148
Donkey anti-mouse Alexa Fluor 647	1:500	Invitrogen A31571
Donkey anti-rat Alexa Fluor 647	1:500	Invitrogen A78947
Donkey anti-rabbit Alexa Fluor 568	1:500	Invitrogen A10042

2.11 Differentiation of 3T3-L1 preadipocyte cells

The following work was carried out during a 3-month research stay at Le Centre de recherche du CHUM under the supervision of Dr Gareth Lim and funded by the Mitacs Globalinks Research Award in partnership with UK Research and Innovation (UKRI).

2.11.1 Maintenance and subculture of 3T3-L1 preadipocyte cells

Due to its capacity to differentiate into adipocytes, the established murine preadipocyte cell line, 3T3-L1, was used as a model of adipogenesis. Similar to endogenous preadipocytes, immortalised 3T3-L1 cells have a fibroblast-like morphology with few stored lipids (Cowherd et al., 1999). Exposure to a hormonal differentiation cocktail activates an adipogenic program which involves the expression and coordination of multiple cell cycle regulators and adipocyte-specific transcription factors and genes at various stages. As triglyceride synthesis and lipid droplet accumulation increases, cells transform into a rounded morphology. Once terminally differentiated, 3T3-L1 adipocyte cells exhibit characteristics which resemble those of adipocytes found *in vivo*. This includes the expression of adipocyte genes, such as PPARγ, adipsin and leptin (Cowherd et al., 1999).

3T3-L1 preadipocyte cells were grown as an adherent monolayer in 125cm^2 flasks and maintained in sterile-filtered DMEM containing 25mM glucose, 10% (v/v) NCS, 100U/mL penicillin, 100µg/mL streptomycin and 2mM L-glutamine. Once 70-80% confluency was reached, cells were sub-cultured, and a portion were harvested for use in experimental protocols as previously described for MIN6 β-cells in Section 2.4.1. Care was taken to avoid 100% confluency as 3T3-L1 preadipocyte cells lose their capacity to differentiate when they are overconfluent. Cells were maintained in culture at 37°C, 5% CO_2 and 95% humidity.

2.11.2 Induction of differentiation of 3T3-L1 preadipocyte cells

Differentiation of 3T3-L1 preadipocyte cells to mature adipocytes was induced by a differentiation cocktail, referred to as MDi: DMEM containing 25mM glucose, 10% (v/v) FBS, 100U/mL penicillin, 100µg/mL streptomycin, 2mM L-glutamine, 500µM 3-isobutyl-1-methylxanthine (IBMX), 500nM dexamethasone (DEX) and 172nM insulin. Addition of MDi commits preadipocyte cells to adipogenesis by promoting the expression of adipogenic genes

(Stone & Bernlohr, 1990). 3T3-L1 preadipocyte cells (passage 8-16) were seeded into a 12-well plate at a density of 90,000 cells/2mL/well in maintenance DMEM. Following a 48-hour incubation, cells were treated for a further 48 hours with DMEM or MDi in the absence or presence of recombinant mouse Ccl4 (100ng/mL). Cells were then washed with PBS and maintained in DMEM with 172nM insulin (committed cells) or without insulin (non-committed cells). Medium was replaced every 48 hours for a period of 6 days when differentiation of 3T3-L1 cells was complete and ready for experimental protocols, as indicated below.

2.11.3 RNA extraction and RT-qPCR in differentiated 3T3-L1 cells

The extraction and purification of RNA from differentiated and non-differentiated 3T3-L1 cells were performed using the RNeasy Mini Kit, as described in Section 2.6.1, and RNA yield and purity were measured using a NanoDrop™ One spectrophotometer (Section 2.2.8). The synthesis of cDNA from the RNA template was performed using the High-Capacity cDNA Reverse Transcription Kit, as described in Section 2.2.9, and a Mastercycler® Nexus GX2. Expression of mRNAs encoding two key adipocyte proteins, PPARγ and adiponectin, was quantified using the SYBR Green-based qPCR protocol (Section 2.2.10), custom primers from Integrated DNA Technologies, and a QuantStudio™ 6 Flex Real-Time PCR System. Adiponectin expression significantly increases during adipogenesis (Trujillo & Scherer, 2005) which is induced by the master regulator, PPARγ (Yang et al., 2018), thus the expression of these two genes was used to determine adipocyte differentiation and maturity. The housekeeping gene, hypoxanthine phosphoribosyltransferase 1 (*Hprt1*), was used as an appropriate reference gene for 3T3-L1 adipocyte cells.

2.11.4 Oil Red O staining and quantification

Oil Red O (ORO) is a fat-soluble, hydrophobic diazo dye which stains lipids, fatty acids, and triglycerides with an orange-red tint (Du et al., 2023). As lipid droplet accumulation dramatically increases during adipocyte differentiation, visualisation and quantification of ORO incorporation into 3T3-L1 cells can be performed to assess adipogenesis. 0.7g ORO powder was dissolved overnight at room temperature in 100% isopropanol to generate a 0.7% (w/v) ORO stock solution. The solution was filtered through a 0.22µm membrane filter and stored at 4°C.

At the end of the differentiation protocol (Section 1.5.1), 3T3-L1 cells were washed twice with PBS followed by exposure to 60% isopropanol for 10 minutes. All isopropanol was then removed to allow the cells to dry. ORO stock solution was diluted with dH_2O (3:2 dilution), incubated at room temperature for 20 minutes, then filtered through a 0.22µm membrane filter. Cells were incubated with the ORO working solution at room temperature for 15 minutes, then washed four times with dH_2O. During the final wash, images were captured using a light microscope to visualise ORO-stained stored lipid droplets within 3T3-L1 cells. The dH_2O was removed, ORO was eluted from the cells by the addition of 100% isopropanol for 10 minutes at room temperature, then each sample was transferred, in duplicate, to a 96-well plate. Wells containing 100% isopropanol alone were used as a blank control. Absorbance was measured at a wavelength of 490-520nm using a Wallac 1420 Victor2™ microplate reader to quantify lipid content.

2.11.5 Western blotting

Western blotting, also known as protein immunoblotting, is a widely used technique that involves antigen-antibody interactions to detect and identify specific proteins within a sample of tissue homogenate. The first step of the Western blot protocol is to separate proteins based on molecular weight using polyacrylamide gel electrophoresis. The separated proteins are then transferred to a membrane which is immunostained with primary and secondary antibodies to identify antigens of interest. In this thesis, Western blot experiments were performed using proteins extracted from 3T3-L1 cells to investigate the phosphorylation of key enzymes involved in insulin signalling and lipolysis. As described in Section 1.2.4, insulin action at IRs within the adipose tissue membrane stimulates the intracellular PI3K/AKT pathway. PI3K phosphorylates and activates AKT, a serine/threonine-specific protein kinase which mediates downstream insulin signalling. Consequently, the quantification of AKT phosphorylation is used as a measure of insulin transduction and sensitivity. As outlined in Section 1.2.3.2, stimulation of the HSL enzyme leads to FFA release from adipose tissue into the circulation. This is the result of its lipolytic action on stored triglycerides. HSL becomes activated when phosphorylated by PKA and is subsequently translocated to intracellular lipid droplets where it catalyses the first rate-limiting step in lipolysis (Anthonsen et al., 1998). Accordingly, the level of HSL phosphorylation can be quantified by western blotting to assess lipolysis within adipocyte cells.

Western blot experiments began with the treatment of 3T3-L1 preadipocyte cells with either DMEM or MDi in the absence or presence of Ccl4 (100ng/mL), as described in Section 2.11.2. For the measurement of total AKT (t-AKT) and phosphorylated AKT (p-AKT), cells were incubated with 10nM or 100nM insulin for 15 minutes at 37°C, 5% CO_2 and 95% humidity. For the measurement of total HSL (t-HSL) and phosphorylated HSL (p-HSL), cells were first incubated with starvation buffer consisting of KRBH and further supplemented with 5mM glucose and 0.2% BSA (pH 7.4 adjusted) for 2 hours at 37°C, 5% CO_2 and 95% humidity. This was followed by a second incubation for an additional 2 hours with or without isoprenaline (1µM; also known as isoproterenol), a potent stimulator of lipolysis through activation of β-adrenergic receptors (Anthonsen et al., 1998). Proteins were extracted from 3T3-L1 cells using radioimmunoprecipitation assay (RIPA) lysis buffer supplemented with phosphatase and protease inhibitors (Table 15). The buffer enables rapid and efficient lysis of cells for the extraction of whole-cell, membrane-bound and nuclear proteins (Jain et al., 2021), whilst phosphatase and protease inhibitors maintain protein phosphorylation and prevent proteolysis, respectively. Once 3T3-L1 cells were washed with PBS, 150µL/well of RIPA buffer was added and cells were incubated on ice for 15 minutes. A cell scraper was used to lift and transfer cell lysates into 1.5mL Eppendorf tubes for centrifugation at 18,500xg 4°C for 20 minutes. The supernatants were collected, and protein concentration was determined using the Bradford method (Bradford, 1976).

Table 15. Preparation of RIPA lysis buffer for the extraction of proteins from 3T3-L1 cells.

Reagent	Volume/Mass (per L)	Final Concentration
β-glycerophosphate	10.8g	50mM
HEPES	2.4g	10mM
Triton X-100	10mL	1% (v/v)
NaCl	4.1g	70mM
Phosphatase inhibitors		
EGTA	20mL	2mM
Na_3VO_4	5mL	1mM
NaF	20mL	1mM
Protease inhibitor cocktail		
Aprotinin	10mL	25µg/mL
Leupeptin		10µg/mL

The Bradford method is a protein determination method that uses Coomassie brilliant blue dye, which contains bicinchoninic acid (BCA). When exposed to cupric (Cu^{2+}) ions within the reagent, sample proteins reduce these ions to cuprous (Cu^{+}) ions to generate a blue protein-dye complex that absorbs at a wavelength of 595nm (Bradford, 1976). The intensity of the blue colour is directly proportional to the protein content within a sample. The reagent used for the Western blot experiments described in this thesis was the Protein Assay Dye Reagent Concentrate. A standard curve was generated by performing a serial dilution of BSA using dH_2O: 1.5, 3.0, 6.0 and 12.0µg/µL. 160µL of each standard concentration was transferred into a clear 96-well plate in duplicate with dH_2O alone acting as a blank. Also in duplicate, by pipetting directly into the plate, 1µL of each supernatant sample containing unknown concentrations of protein was diluted in 159µL dH_2O. Thereafter, 40µL/well of Protein Assay Dye Reagent Concentrate was mixed thoroughly with standard and sample volumes, and absorbance was measured at a wavelength of 595nm using a Wallac 1420 Victor2™ microplate reader.

Once protein concentrations had been determined, 28µL of each sample were prepared: 7µL of a 1:10 mixture of 4X Laemmli Sample Buffer and β-ME were added to 60µg of protein supernatants and the remaining volume made up with RIPA lysis buffer. Samples were transferred to a heat block to denature proteins at 95°C for 15 minutes. 25µL of each denatured protein sample (2µg/µL) and 5µL of Precision Plus Protein Dual Color Standards were then loaded into previously prepared gels (Table 16) and subjected to sodium dodecyl-sulphate polyacrylamide gel electrophoresis (SDS-PAGE) using running buffer (Table 17) in a Mini-PROTEAN Tetra Vertical Electrophoresis Cell. The gel was run at 90V for 30 minutes immediately followed by 120V for 1-1.5 hours. Once proteins from 3T3-L1 cell lysates were separated by their molecular masses, the proteins were transferred onto a polyvinylidene fluoride (PDVF) membrane which was briefly submerged into 100% methanol. The gel, the membrane and stacking paper that was immersed in transfer buffer (Table 18) were locked

into a cassette and inserted into the Trans-Blot® Turbo™ Transfer System to run at 25V for 7 minutes.

Table 16. Preparation of resolving gel (10%) and stacking gel (4%) for the separation of proteins by sodium dodecyl-sulphate polyacrylamide gel electrophoresis (SDS-PAGE). SDS: sodium dodecyl-sulphate; AP: Ammonium persulphate; TEMED: Tetramethylethylenediamine.

	Resolving Gel		Stacking Gel	
Reagent	**Volume (mL per 10mL)**		**Volume (mL per 10mL)**	**Final Concentration**
dH_2O	7.2	-	5.84	-
Acrylamide	4.9	20% (v/v)	0.96	4% (v/v)
Bis solution	2.7	0.5% (v/v)	0.52	0.1% (v/v)
Tris (pH 8.8)	5.0	750mM	-	-
Tris (pH 6.8)	-	-	2.50	125mM
SDS	0.2	0.2% (v/v)	0.10	0.1% (v/v)
AP	0.1	0.1% (v/v)	0.05	0.05% (v/v)
TEMED	0.01	0.01% (v/v)	0.01	0.01% (v/v)

Table 17. Preparation of 1X running buffer for the separation of proteins by sodium dodecyl-sulphate polyacrylamide gel electrophoresis (SDS-PAGE). SDS: sodium dodecyl-sulphate; DTT: dithiothreitol.

Reagent	**Volume/Mass (per 1L)**	**Final Concentration**
Tris-HCL	100mL	0.1M
SDS	20.0g	2% (w/v)
Glycerol	100mL	10% (v/v)
DTT	7.7g	50mM

Table 18. Preparation of 1X transfer buffer.

Reagent	**Volume (per 100mL)**	**Final Concentration**
H_2O	60mL	-
EtOH	20mL	20% (v/v)
Trans-Blot Turbo buffer	20mL	20% (v/v)

The membrane was immediately washed with 1X PBS/Tween for 5 minutes then incubated in I-Block™ Protein-Based Blocking Reagent at room temperature for 1 hour to prevent non-specific binding of primary and secondary antibodies. Thereafter, the membrane was incubated overnight at 4°C with the appropriate primary antibody (Table 19). The membrane was then washed five times with 1X PBS/Tween for 5 minutes each, followed by an incubation at room temperature for 1 hour with the corresponding horseradish HRP-conjugated

secondary antibody (Table 20). Once washed three times with 1X PBS/Tween for 5 minutes each, the membrane was exposed to a 1:1 mixture of Clarity Max Enhanced Chemiluminescence substrates which consisted of peroxide and luminol solutions. Immunoreactive proteins were then visualised and quantified using an iBright 1500 Imaging System. To immunostain with additional antibodies, the membrane was immersed in Restore™ Western Blot Stripping Buffer at room temperature for 15 minutes to remove primary and secondary antibodies. Following a wash with 1X PBS/Tween for 5 minutes and an hour incubation with I-Block™, the membrane was ready for re-probing.

Table 19. List of primary antibodies used for Western blot experiments using proteins extracted from 3T3-L1 cells. Antibodies were prepared using I-Block™ as a diluent.

Protein	Primary Antibody	Dilution	Supplier
p-AKT(Ser473)	Rabbit monoclonal anti-phospho-AKT	1:1000	Cell Signalling 4060
t-AKT	Mouse monoclonal anti-AKT	1:1000	Cell Signalling 2920
p-HSL(Ser660)	Rabbit polyclonal anti-phospho-HSL	1:1000	Cell Signalling 4126
t-HSL	Rabbit polyclonal anti-HSL	1:1000	Cell Signalling 4107

Table 20. List of HRP-conjugated secondary antibodies used for Western blot experiments using proteins extracted from 3T3-L1 cells. Antibodies were prepared using I-Block™ as a diluent.

Secondary Antibody	Dilution	Supplier/Catalogue Number
HRP-conjugated anti-mouse	1:5000	Cell Signalling 7076
HRP-conjugated anti-rabbit	1:2000	Cell Signalling 7074

2.12 Statistical analysis

Numerical data are expressed as mean ± standard error of the mean (S.E.M). The number of biological replicates is indicated by the n-number (n). Statistical analyses were performed in GraphPad Prism 9 using an unpaired two-tailed t-test, an unpaired multiple t-test or a one-, two- or three-way ANOVA with the recommended multiple comparisons tests (Tukey's or Holm-Šídák multiple comparisons tests) to determine the following significance levels for indicated comparisons: *p<0.05, **p<0.01, ***p<0.001, ****p<0.0001.

Immunohistochemistry images were analysed using Cell Profiler (4.2.4) and ImageJ software. Melting profiles of PCR products were evaluated using LightCycler® software. Gene expression was relative to internal reference genes and was calculated using the ΔΔCt method (Pfaffl, 2001), where E = primer efficiency value; gioCt = Ct value of the gene of interest; hCt = Ct value of the housekeeping gene.

Chapter 3: Quantification of changes in isolated mature mouse adipocytes of islet GPCR peptide ligand mRNA expression with high-fat feeding

3.1 Introduction

Adipokines are secreted signalling peptides that have roles in a wide range of biological functions, including systemic lipid and glucose metabolism, local inflammation, and adipocyte differentiation and metabolism. The degree of adiposity profoundly affects the level of expression and secretion of multiple adipokines. In a healthy individual, tight regulation exists to maintain a balance between the release of anti-inflammatory, anti-diabetic adipokines and pro-inflammatory, pro-diabetic adipokines. The expansion of adipose tissue stores in obesity, particularly visceral adipose tissue, leads to an imbalance of these opposing groups of peptides, such that the level of pro-inflammatory and pro-diabetic adipokines, such as TNF-α and MCP-1/CCL2, supersedes (Gerst et al., 2019). It is unlikely that a single adipokine is responsible for the metabolic perturbations that accompany obesity, but multiple adipokines can operate cooperatively and/or synergistically to induce dysglycaemia. Not all adipokines are detrimental, however: adiponectin is an insulin-sensitising peptide that also increases insulin output (Gu et al., 2006), and adipsin also improves glucose homeostasis through stimulation of insulin secretion (Lo et al., 2014). It is readily accepted that enteroendocrine cells of the gastrointestinal tract secrete incretin peptides, such as GLP-1, that potentiate insulin secretion (Müller et al., 2019), but the concept of adipose tissue-islet crosstalk is not well-established. Given that GPCRs are a large receptor family that represent ~35% of all current drug targets for treatment across a wide range of diseases (Sriram & Insel, 2018), islets express mRNAs encoding nearly 300 GPCRs (Amisten et al., 2013) and adipose tissue is a source of signalling peptides (Khan & Joseph, 2014), it is hypothesised that adipokines crosstalk with islets, via GPCRs, and provide a mechanism through which functional β-cell mass is regulated in obesity. Therefore, the following chapters aimed to profile mRNA expression of adipokines that have been identified as ligands for islet GPCRs in visceral adipose tissue and to determine whether there were changes in expression with growing adiposity.

Adipokines are secreted from mature adipocytes and from non-adipocyte cells, such as macrophages, that are found within the SVF of adipose tissue. To begin deciphering the contribution of adipocytes to overall adipokine secretion and their transcriptional dynamics in obesity, in this chapter, the expression levels of islet GPCR peptide ligand mRNAs were measured in mature adipocytes isolated from epididymal fat pads in lean and diet-induced obese mice. Previous comparisons between mouse and human islets revealed 189 GPCR mRNAs were shared between the two species (Amisten et al., 2017). The similarity in their expression profiles of GPCR mRNAs was deemed sufficient for results obtained using mouse tissue to be translated to humans (Amisten et al., 2017). Subsequently, the experiments described in this chapter screened a total of 155 peptide ligand mRNAs that target the 110 peptide/protein-activated human islet GPCRs originally described by Amisten et al. (2013).

3.2 Methods

3.2.1 Mature adipocyte isolation from mice

Following rigorous troubleshooting and protocol optimisation, mature adipocytes were isolated from visceral epididymal adipose tissue retrieved from control diet-fed (10% fat) and high-fat diet-induced (60% fat) obese mice as described in Section 2.2. Due to a limited volume of adipose tissue in lean mice, epididymal fat pads from two mice were pooled to generate a single sample. Larger volumes of visceral adipose tissue present in diet-induced obese mice allowed sufficient adipocyte numbers to be isolated and processed per animal without the need for pooling. Isolated mature adipocytes were dissolved in TRIzol® Reagent, snap frozen in liquid nitrogen and stored at –70°C to await downstream processing.

3.2.2 RNA extraction from mouse mature adipocytes

The analysis of RNA quality and yield using differing methods of RNA extraction revealed a combination of the traditional TRIzol® Reagent method and the use of the commercial miRNeasy Mini Kit was superior in isolating sufficient high-quality RNA from isolated mature adipocytes (Section 2.2.6). The addition of chloroform and the separation of aqueous, interphase and organic phases were followed by several centrifugation cycles using spin columns and ethanol-based buffers. As outlined in Section 2.2.8, total RNA concentration and RNA purity, measured by 260/280 and 260/230 ratios, were assessed using the Nanodrop™ 1000 spectrophotometer. Thereafter, RNA samples were either stored at –70°C or immediately processed for cDNA generation.

3.2.3 RT-qPCR

The High-Capacity cDNA Reverse Transcription Kit contained the necessary components for the conversion of mature adipocyte RNA to cDNA (40ng/µL) using a T100™ thermal cycler, as described in Section 2.2.9. Generated cDNA samples were subsequently used for the qPCR screening of 155 mRNAs encoding islet GPCR peptide ligands and positive control adipokine genes, adiponectin (*AdipoQ*) and leptin (*Lep*). The amplification of cDNA and quantification of mRNA expression followed a SYBR Green-based protocol and use of the LightCycler® 480 (Section 2.2.10).

3.2.4 Agarose gel electrophoresis

PCR products were subjected to validation by agarose gel electrophoresis to confirm that amplicons were of the predicted sizes and to determine the presence of adipocyte-exclusive genes following the isolation of mature adipocytes using newly optimised protocols. Section 2.2.11 outlines the use of a GeneRuler™ 50bp DNA ladder as reference for products representing the positive control adipokine genes, *AdipoQ* and *Lep*, and islet GPCR peptide ligand genes. Amplicons were run using agarose gel electrophoresis and visualisation under UV light revealed investigative genes were expressed at varied levels in mature adipocytes.

3.3 Results

3.3.1 Mouse characteristics and expression of islet GPCR peptide ligand mRNAs in mature adipocytes isolated from lean and diet-induced obese mice

Mice fed a control diet of 10% fat had a mean terminal weight of 30.1±0.50g and a mean terminal non-fasting plasma glucose level of 8.9±0.47mM (Figure 18), indicating they were lean and had normoglycaemia at the time of tissue retrieval. On the other hand, mice fed a high-fat diet of 60% fat for 16 weeks were obese (45.6g±1.68g; p<0.0001) and hyperglycaemic (14.3±1.33mM glucose; p<0.001).

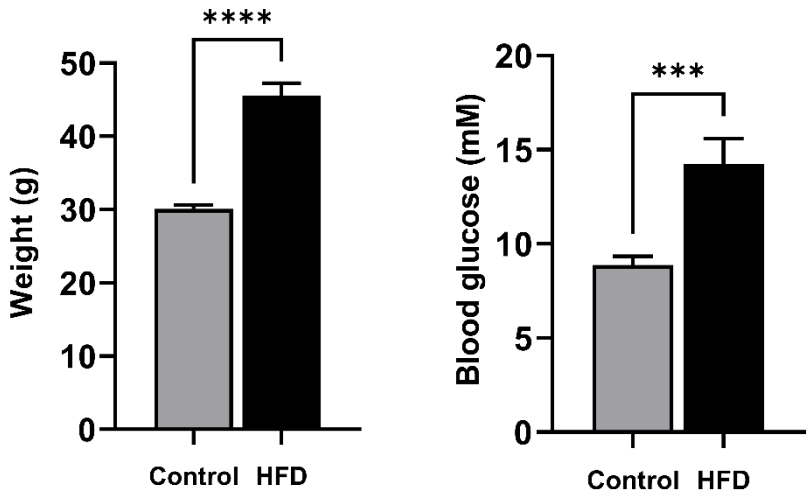

Figure 18. Terminal weight (left) and non-fasting plasma glucose (right) measurements in C57BL/6 mice fed a control or high-fat diet for 16 weeks. Data are expressed as the mean ± S.E.M. Unpaired two-tailed t-test; n=4-8; ***p<0.001, ****p<0.0001 vs control.

RT-qPCR was performed using RNA purified from isolated mature adipocytes from visceral epididymal adipose tissue retrieved from control-fed, lean mice and high-fat diet-fed, obese mice. Gene expression analysis showed 45 and 42 islet GPCR peptide ligand mRNAs were expressed in isolated mature adipocytes retrieved from lean and diet-induced obese mice, respectively (Figure 19). The remaining genes were either expressed at trace level (0.0001% to 0.001% relative to *Actb* expression) or absent (<0.0001% of *Actb*). Positive control genes, *Lep* and *AdipoQ*, confirmed amplification of PCR products from mature adipocyte cDNA. The Venn diagrams in Figure 19 illustrate these three categories of GPCR peptide ligand mRNA expression in isolated mature adipocytes from lean (blue) and obese (orange) mice with pink intersections representing the overlap in mRNA expression between lean and obese groups. Thus, 38 of the expressed genes were common to mature adipocytes isolated from both lean and diet-induced obese mice. Furthermore, of the 155 mRNAs quantified, 18 and 92 were expressed at trace levels or absent in lean mice, while 21 and 92 were trace or absent in obese mice, with overlaps of 12 and 89 mRNAs in these categories.

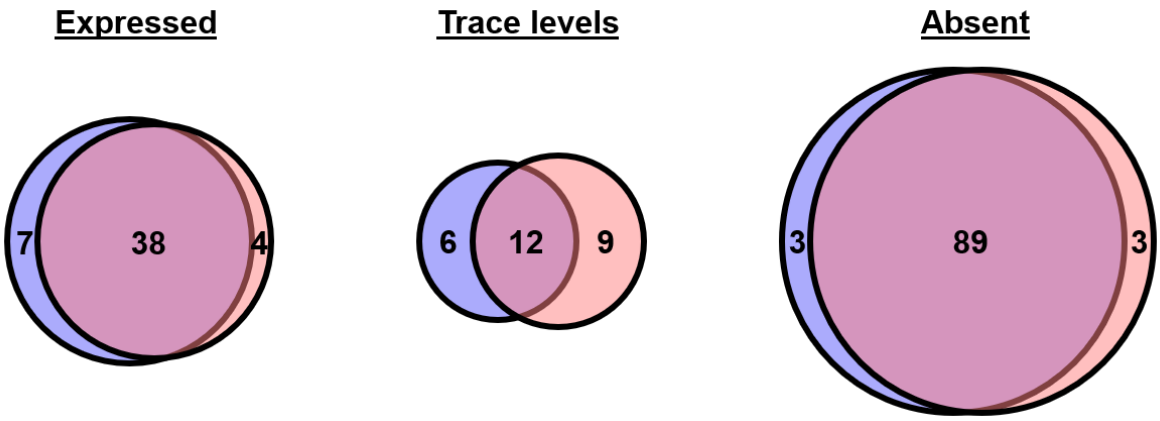

Figure 19. Proportions of islet GPCR peptide ligand mRNAs classified as being expressed, at trace level, or absent in mature adipocytes isolated from visceral adipose tissue retrieved from lean and obese mice. Data were obtained by RT-qPCR quantifications of RNA isolated from 4 pooled samples from 8 lean mice (blue) and 4 samples from diet-induced obese mice (orange). Genes common to both lean and obese mice are shown by the pink intersections. Expressed >0.001% relative to *Actb*; trace = 0.0001% to 0.001% relative to *Actb*; absent < 0.0001% relative to *Actb*.

3.3.2 Expression of islet GPCR peptide ligand mRNAs in mature adipocytes isolated from visceral adipose tissue retrieved from lean mice

Of the 45 islet GPCR peptide ligand mRNAs expressed in isolated mature adipocytes retrieved from lean mice, *Anxa1*, encoding annexin A1, displayed the greatest level of mRNA expression (0.541±0.0618 relative to *Actb*) (Figure 20). There was also high expression of mRNAs encoding the complement peptide, *C4a* (0.373±0.0878 relative to *Actb*) and collagen type IV α-1 chain, *Col4a1* (0.245±0.0351 relative to *Actb*). In contrast, mRNAs encoding neuropeptide Y, *Npy* (0.001±0.0002 relative to *Actb*), collagen type IV α-5 chain, *Col4a5* (0.001±0.0001 relative to *Actb*), and chemokine, *Cxcl11* (0.001±0.0001 relative to *Actb*), were expressed at low levels in isolated mature adipocytes from lean mice.

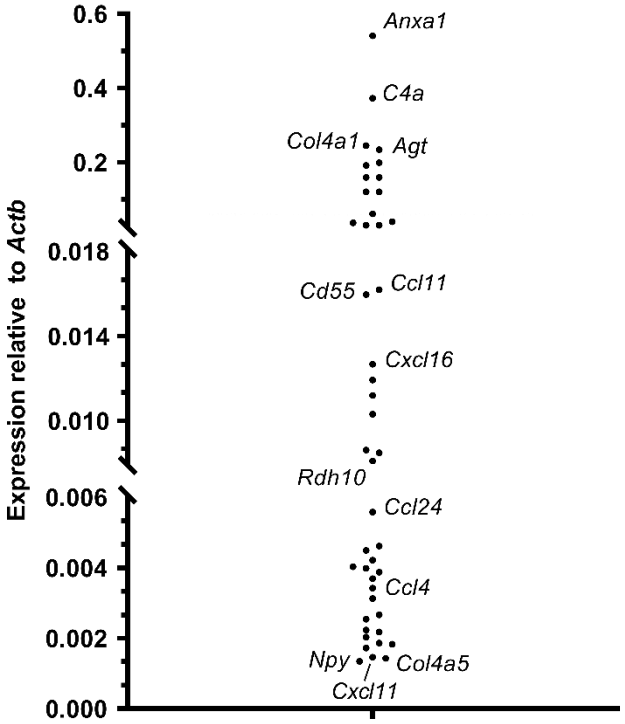

Figure 20. Islet GPCR peptide ligand mRNA expression in mature adipocytes isolated from visceral adipose tissue retrieved from lean mice. Data were generated by RT-qPCR and are displayed relative to expression of the housekeeping gene, *Actb* (n=4 pooled samples from 8 lean mice).

3.3.3 Expression of islet GPCR peptide ligand mRNAs in mature adipocytes isolated from visceral adipose tissue retrieved from diet-induced obese mice

The quantification of islet GPCR peptide ligand mRNAs in mature adipocytes isolated from visceral adipose tissue retrieved from diet-induced obese mice revealed a similar profile of expression with *Anxa1* (0.557±0.067 relative to *Actb*), *Col4a1* (0.315±0.0563 relative to *Actb*), and *C4a* (0.300±0.0785 relative to *Actb*), also being the most abundant mRNAs quantified (Figure 21). mRNAs encoding *Cxcl14* (0.002±0.0003 relative to *Actb*), *Apln* (0.001±0.0003 relative to *Actb*) and *Wnt5b* (0.001±0.0003 relative to *Actb*) were expressed at low levels in isolated mature adipocytes from diet-induced obese mice.

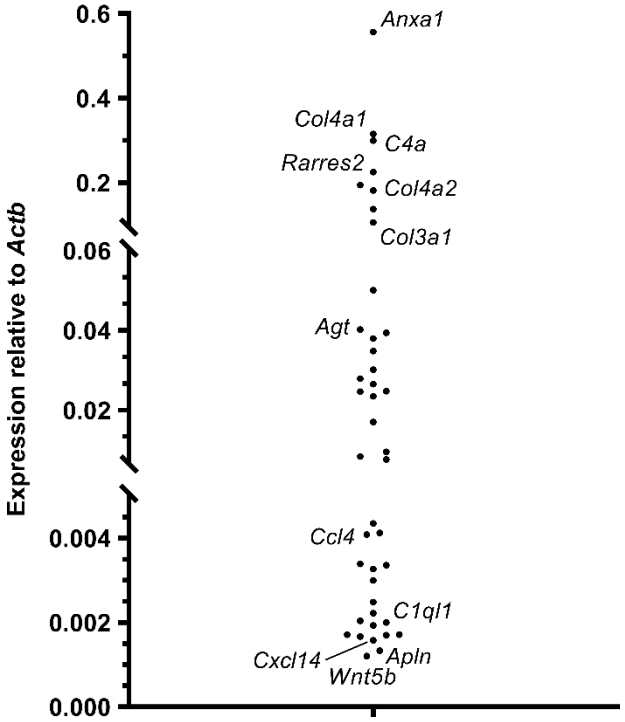

Figure 21. Islet GPCR peptide ligand mRNA expression in mature adipocytes isolated from visceral adipose tissue retrieved from diet-induced obese mice. Data were generated by RT-qPCR and are displayed relative to expression of the housekeeping gene, *Actb* (n=4).

3.3.4 Comparative analysis of islet GPCR peptide ligand mRNA expression in isolated mature adipocytes between lean and diet-induced obese mice

The mRNA expression of islet GPCR peptide ligands in mature visceral adipocytes was significantly altered as a result of high-fat feeding. Figure 22 illustrates key adipokine genes whose expression is either upregulated or downregulated in obesity, with a focus on those mRNAs whose expression was above trace level in mature adipocytes isolated from lean and/or diet-induced obese mice. It can be seen that *Ghrh* and *Ccl19* mRNAs exhibit the most marked upregulation with high-fat feeding (6810±1833.4% and 884±254.4% of control diet expression, respectively) which proved significant when data from mature adipocyte samples were compared between lean and diet-induced obese mice (Supplementary Table 21). In contrast, mRNAs encoding *Cxcl3* and *Agt* were markedly decreased in expression with high-fat feeding, however, only reduction in *Agt* mRNA was statistically significant (17.2±2.9% of control diet expression) (Supplementary Table 21). A cluster of adipokines showed no significant changes in their mRNA expression with high-fat feeding, including *Anxa1* (103±12.4% of control diet expression), *Ccl4* (119±30.6% of control diet expression) and *Calca* (96.9±8.8% of control diet expression).

Adiponectin and leptin were used as positive control genes based on their exclusive production and secretion from adipose tissue which changes in magnitude with growing adiposity (Arita et al., 1999; Considine et al., 1996). As expected, *Lep* and *AdipoQ* mRNAs were readily detectable in mature adipocytes isolated from visceral fat depots, with a significant increase in *Lep* (457±112.3% of control diet expression) and a decrease in *AdipoQ* (53.8±6.0% of control diet expression) in obesity (Supplementary Table 21). Supplementary

Table 21 also indicates that some GPCR peptide ligand mRNAs that were considered to be absent, because they were expressed at <0.0001% relative to *Actb*, or expressed at trace levels (0.0001% to 0.001% relative to *Actb* expression) in adipose tissue from lean mice were significantly downregulated in obesity: *Qrfp* (92.3±3.7% decrease), *Rln1* (92.1±4.8% decrease), *Rspo3* (88.6±8.3% decrease), *Wnt4* (84.8±8.8% decrease), *Col4a6* (59.6±14.6% decrease), *Wnt10b* (54.8±16.2% decrease), and *Ppbp* (42.9±8.5% decrease).

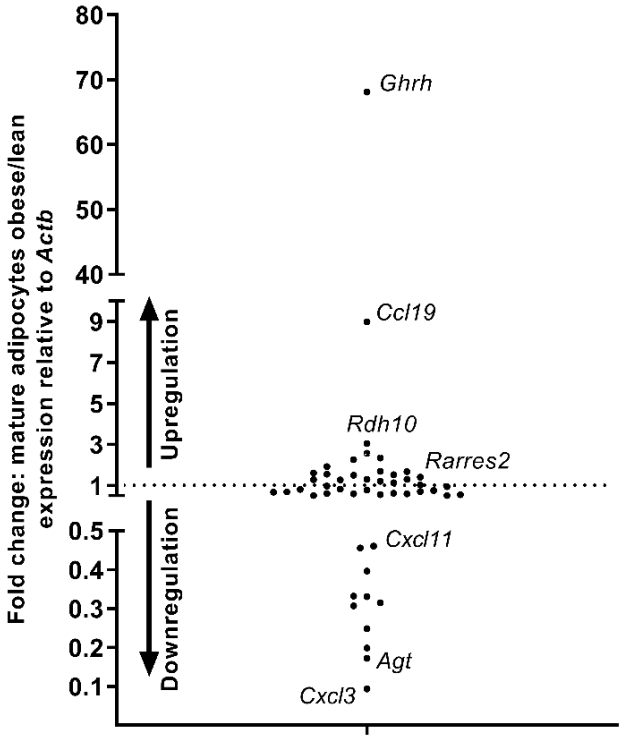

Figure 22. Upregulated and downregulated islet GPCR peptide ligand mRNAs in mature adipocytes isolated from visceral adipose tissue from lean and diet-induced obese mice. Data were generated by RT-qPCR and are displayed as fold change of mean expression values in obese vs lean mice (upregulated: >1; downregulated: <1), relative to the housekeeping gene, *Actb* (n=4 per group).

3.3.5 Confirmation of amplicons from isolated mature adipocyte qPCR screening

The amplification of target DNA sequences during qPCR screenings was validated by agarose gel electrophoresis. Figure 23 shows a representative agarose gel whereby PCR products from isolated mature adipocytes were run. Following RT-qPCR experiments, *Lep*, *AdipoQ* and *Anxa1* were found to be highly expressed, whilst *Aldh1a2* and *Aldh1a3* were expressed at trace level. This was reflected in the greater intensity of representative bands for *Lep* (134 bp), *AdipoQ* (135 bp) and *Anxa1* (170 bp) genes compared to bands representing *Aldh1a2* (86 bp) and *Aldh1a3* (72 bp). *Adcyap1* (92 bp) was identified as absent within isolated mature adipocytes; this was supported by the absence of amplicon bands in the agarose gel. Based on expected amplicon sizes, the amplification of target DNA sequences from isolated mature adipocytes was successfully validated.

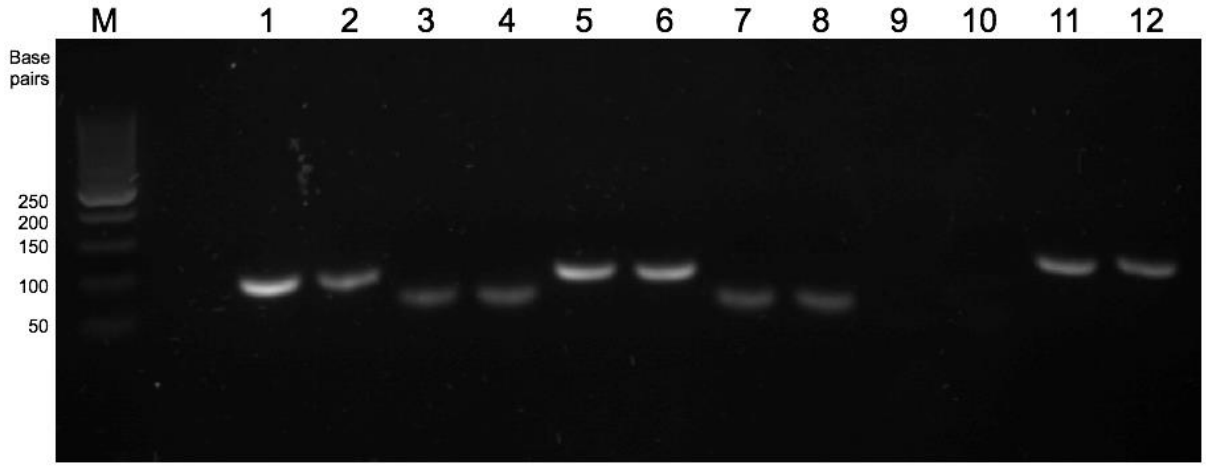

Figure 23. Agarose gel electrophoresis (1% agarose) of amplified PCR products from isolated mature adipocytes. Lanes: (1-2) *Lep*; (3-4) *Aldh1a2*; (5-6) *AdipoQ*; (7-8) *Aldh1a3*; (9-10) *Adcyap1*; (11-12) *Anxa1*. Lane M: GeneRuler 50bp DNA ladder.

3.4 Discussion

The present chapter described quantification of islet GPCR peptide ligand genes in cDNAs from high triglyceride-containing mature adipocytes. The success of the adipocyte isolation protocol and RNA isolation was measured by both RNA yield and purity (see Section 2.2.8), and later confirmed by the presence and quantification of the adipocyte-exclusive genes, adiponectin and leptin, by qPCR and gel electrophoresis. Protocol optimisation facilitated the generation of sufficient, high-quality RNA to characterise the mRNA profiles of 155 islet GPCR peptide ligands in epididymal fat depots retrieved from mice fed a control diet (10% fat) or a high-fat diet (60%). A deeper understanding of the genotypic changes within visceral adipocytes under normal and abhorrent metabolic states was subsequently gained.

In lean and obese mice, *Anxa1*, which encodes the phospholipid-binding protein annexin A1, was the most highly expressed islet GPCR ligand mRNA in mature adipocytes and its expression was not significantly changed with high-fat feeding. This is inconsistent with a recent high throughput screening study of alterations in mouse adipocyte transcriptional profiles which identified *Anxa1* expression in epididymal adipocytes isolated from mice maintained on a 60% fat diet for 12 weeks was 364±26.4% of that quantified in adipocytes of mice fed a 10% fat diet (*GEO Accession Viewer*, 2022; Zapata et al., 2022). When comparing with the experimental design described here, this study used C57BL/6 mice that were 6-7 weeks younger at the time of adipocyte isolation, and the duration of high-fat feeding was 4 weeks shorter. Thus, the differences in methodology may explain the discrepancy between the data presented here and the recent study that reported upregulation of adipocyte *Anxa1* mRNA expression in obesity. Annexin A1 is known to have beneficial effects in islets by potentiating glucose-stimulated insulin release and protecting against apoptosis via binding to the formylpeptide receptor, FPR2 (Kreutter et al., 2017; Rackham et al., 2018).

In addition to the *Anxa1* gene, *C4a* and *Col4a1* mRNAs encoding complement factor 4A and collagen type IV α-1 chain, respectively, are shared in lean and obese mature adipocytes as the most abundantly expressed adipokines which target islet GPCRs.

C4a is an integral protein in the complement system with a role in immune surveillance and defence, but its role in glucose homeostasis is not well-defined. C3AR1, C5AR1 and C5AR2 receptors are thought to be activated by C4a, and while these receptors are expressed by human islets, the effect of C4a on islet hormone secretion is unknown (Amisten et al., 2013). Similarly, little is known about its effects on peripheral insulin sensitivity although loose associations between C4a and glucose regulation in T1D and T2D have been reported (Kingery et al., 2012). Higher gene copy-number and plasma protein levels of C4a appear to correlate with higher C-peptide levels and the preservation of residual β-cell function in new-onset T1D (Kingery et al., 2012). Circulating C4 levels are also associated with an occurrence of metabolic syndrome and several risk factors for cardiovascular disease, including BMI, waist circumference, fasting plasma glucose levels and insulin resistance (Bratti et al., 2017; Nilsson et al., 2014). Serum C4 concentrations are significantly greater in obese individuals than lean subjects (Bratti et al., 2017). However, given *C4a* mRNA expression is unchanged in isolated mature adipocytes with high-fat feeding, it is unlikely that the increased circulating C4 observed in obesity originates from adipocytes.

Positive effects of collagen type IV α1 (*Col4a1*) and its associated gene, *Col4a2*, encoding collagen type IV α2, on insulin secretion have been reported. Both Col4a1 and Col4a2 form collagen type IV heterotrimers (α1α1α2) which polymerise into protein complexes that are the main component of basement membranes (Kuo et al., 2012). Accordingly, the two peptides are abundantly expressed in almost all tissues. Collagen type IV is also an agonist for the GPCR, GPR126, expressed within mouse and human islet membranes (Olaniru et al., 2015). Short-term treatment with collagen type IV augmented basal and glucose-stimulated insulin secretion and enhanced viability of MIN6 β-cells (Olaniru et al., 2015). In contrast, long-term treatment significantly reduced insulin mRNA expression and insulin content within human β-cells (Kaido et al., 2006), indicating that collagen IV peptides are not a suitable treatment for chronic human diseases like T2D.

The mRNA expression of several islet GPCR peptide ligands in mature adipocytes were altered in obesity and the most upregulated was *Ghrh* encoding growth hormone-releasing hormone. This is consistent with findings of upregulated *Ghrh* mRNA in mature adipocytes isolated from morbidly obese humans (Rodríguez-Pacheco et al., 2017). GHRH is secreted from a variety of tissues, and it binds to the $G\alpha_s$-coupled receptor, GHRH-R, to stimulate the release of growth hormone (GH) from the anterior pituitary. GH targets adipocytes to induce lipolysis whilst inhibiting lipogenesis to dampen adipose tissue growth. In obesity, however, a reduction in GH secretion is consistently observed (Ghigo et al., 1992; Iranmanesh et al., 1991; Riedel et al., 1995; Veldhuis et al., 1991) which promotes further visceral fat accumulation, thereby feeding into a vicious cycle. Increased *Ghrh* expression in isolated mature adipocytes may be compensatory for impaired responses to GH in obese patients (Williams et al., 1984). GHRH-R has also been detected in the INS-1 cell line, and in rat and human islets (Amisten et al., 2013; Atanes et al., 2021; Ludwig et al., 2010), and when stimulated, leads to increased islet cell proliferation and glucose-stimulated insulin secretion, and decreased apoptosis (Ludwig et al., 2010). The metabolic actions of GHRH and GH have motivated the development of tesamorelin, a GHRH analogue (Makimura et al., 2012; Stanley, Chen, et al., 2011; Stanley et al., 2012, 2014; Stanley, Falutz, et al., 2011). Visceral fat mass and circulating triglycerides are significantly diminished in tesamorelin-treated individuals with excessive adiposity and it is currently prescribed for human immunodeficiency virus (HIV)-associated lipodystrophy. The translation to improved glucose regulation, however, has been

inconsistent as indicated by reports of unchanged, negative and positive effects on fasting and 2-hour plasma glucose, HbA1c and insulin sensitivity measures (Falutz et al., 2010; Makimura et al., 2012; Stanley et al., 2012, 2014).

Downregulated mRNAs within obese mouse mature adipocytes include *Cxcl3* which encodes chemokine (C-X-C motif) ligand 3 and this mRNA showed the largest reduction in expression with high-fat feeding. Cxcl3 is a chemotaxis peptide that promotes the movement of neutrophils to sites of inflammation and injury. It is one of many ligands that target Cxcr2, a GPCR whose expression in islet membranes is negatively associated with transplanted islet survival due to immune cell recruitment (Citro et al., 2012). In addition, the expression of *Cxcl3* mRNA within adipocytes is stimulated during adipogenesis and Cxcl3 is thought to be a promoting factor of the process (Kusuyama et al., 2016). Therefore, reduced Cxcl3 mRNA may contribute to severe impairment in adipocyte differentiation in obesity (Sánchez-Ceinos et al., 2021).

In summary, the optimisation of adipocyte isolation protocols led to the quantification of mRNAs encoding islet GPCR peptide ligand mRNAs in mature adipocytes from lean and obese mice. Significant alterations in expression of some genes were revealed in obesity. This study alone cannot determine the contribution of mature adipocytes to the overall secretome of adipose tissue. Parallel quantification of obesity-induced changes in mRNA expression in whole adipose tissue will shine a light on the source of upregulated or downregulated adipokines, i.e. from mature adipocytes or from cells within the non-adipocyte SVF fraction. This was examined in Chapter 4.

Chapter 4: Quantification of changes in whole mouse adipose tissue of islet GPCR peptide ligand mRNA expression with high-fat feeding

4.1 Introduction

The previous chapter, which determined the expression level of islet GPCR peptide ligand mRNAs in isolated mature adipocytes from lean and diet-induced obese mice, emphasises the dynamics of the adipocyte secretome and its dependence on metabolic conditions. However, as previously described in Section 1.5.1, adipose tissue consists of mature adipocytes and several other peptide-secreting cell types present in inconsistently reported proportions. If mature adipocytes are present in a minority proportion, their contribution of expressed and secreted islet GPCR peptide ligands and/or their influence on islet function may be marginal compared to the contributions from other cell types within the tissue. In consequence, the use of isolated mature adipocytes may not be appropriate to assess changes in the expression of adipose tissue-derived islet GPCR peptide ligand mRNAs between lean and obese states.

The current chapter reports a parallel qPCR screening using whole visceral adipose tissue which allowed the comparison of mRNA expression profiles between isolated mature adipocytes and whole adipose tissue. This provided insight into the contribution of mature adipocyte cells to adipokine production in adipose tissue. The comparison also assisted in deciding whether isolated mature adipocytes or whole adipose tissue was the optimal starting material for future experiments using additional models of obesity. It is important to note the requirement to age-match mouse models when making comparisons at whole organ-level and at the cellular level due to potential changes in mRNA expression of islet GPCR peptide ligands with increasing age. Ageing accompanies a change in the gene expression profiles of all tissues and can cause alterations in adipose tissue function and composition (Mancuso & Bouchard, 2019). Moreover, with age comes a redistribution of lipids from subcutaneous to visceral adipose tissue compartments and the deposition of ectopic fat into non-adipose tissue organs. This is, in part, the result of reductions in hormone levels, particularly sex hormones, and in the cellularity and function of subcutaneous fat depots. In turn, the expression and secretion of adipokines become altered, and the physiological processes within fat and other tissues which they regulate become affected. Such processes include inflammation (Mancuso & Bouchard, 2019) with current evidence showing elevated pro-inflammatory markers and chronic inflammation in ageing, a phenomenon known as “inflammageing” (Ferrucci & Fabbri, 2018). These age-associated changes are supported by an analysis of gene expression within subcutaneous adipose tissue retrieved from 856 female twins aged 39-85 years (Glass et al., 2013). Use of a linear mixed model revealed 188 genes were differentially expressed within adipose tissue with increasing age. Of these 188 age-related genes, 50.8% declined in their level of expression (Glass et al., 2013).

Consequently, in this chapter, a qPCR screening of islet GPCR peptide ligand mRNAs was performed in whole epididymal adipose tissue retrieved from lean and diet-induced obese mice of similar age to those used for the analysis of isolated epididymal mature adipocytes to rule out any influence of ageing on the level of mRNA expression. Identical methodology concerning mouse strain, diet composition, duration of feeding and data analysis was also adopted. Furthermore, consistent with the qPCR screening of mature adipocytes, the same

155 peptide ligand mRNAs that target the 110 peptide/protein-activated human islet GPCRs originally described by Amisten et al. (2013) were quantified in whole adipose tissue.

4.2 Methods

4.2.1 Total RNA extraction from mouse epididymal adipose tissue

Total RNA was isolated from whole epididymal adipose tissue retrieved from control diet-fed (10% fat) and high-fat diet-fed (60% fat) obese mice using the optimised standardised protocol outlined in Section 2.2. Fat pads were homogenised in TRIzol® using a TissueLyser II and stainless-steel beads prior to centrifugation and the retrieval of the RNA-containing phenol phase. Once the phenol phase was topped up with TRIzol® Reagent to 1mL total volume, the remaining steps followed the RNA isolation protocol outlined in Section 2.2.6 at the point of chloroform addition. The aqueous, interphase and organic phases were separated, and total RNA was extracted and purified by several centrifugation cycles using spin columns and ethanol-based buffers. RNA yield and purity were measured by the NanoDrop™ 1000 spectrophotometer. Samples were either stored at –70°C or immediately processed for the generation of cDNA.

There were several advantages of using whole adipose tissue without the separation of the mature adipocyte and non-adipocyte fractions: 1) an entire step of mature adipocyte isolation was bypassed making the protocol far less labour intensive and complex; 2) the pooling of fat pads from two animals is only necessary to increase the yield of mature adipocytes during their isolation, therefore, fewer mice were required when processing whole adipose tissue; and 3) the use of fewer animals, reagents and equipment rendered the analysis of whole adipose tissue less expensive overall, and thus fits with 3Rs requirements.

4.2.2 RT-qPCR

The generation of cDNA and the screening of islet GPCR peptide ligand mRNAs by qPCR in whole fat followed identical protocols to those performed in isolated mature adipocytes. Conversion of adipose RNA to cDNA (40ng/µL) used components of the High-Capacity cDNA Reverse Transcription Kit and a T100™ thermal cycler, as described in Section 2.2.8. The expression of 155 islet GPCR peptide ligand mRNAs were quantified using a SYBR Green-based qPCR protocol and the LightCycler® 480. Again, the adipokines, *AdipoQ* and *Lep*, were included in the screen as positive control genes (Section 2.2.10).

4.2.3 Ccl4 ELISA using mouse plasma

Blood samples were collected from control diet-fed (10% fat) and high-fat diet-fed (60% fat) obese mice by cardiac puncture at the end of the diet interventions (Sections 2.3.1 and 2.3.2). Samples were then processed to extract cell-free plasma and colorimetric quantification of Ccl4 concentrations was determined using a Mouse MIP-1 beta/CCL4 ELISA Kit, as described in Section 2.3.3.

4.3 Results

4.3.1 Mouse characteristics and expression of islet GPCR peptide ligand mRNAs in visceral whole adipose tissue from lean and diet-induced obese mice

The five mice fed on the 10% fat diet had a mean weight of 29.8±0.15g at the time of tissue retrieval, while those maintained on the 60% fat diet weighed 51.1±0.59g ($p<0.0001$) and the fasting blood glucose levels were 5.3±0.77mM and 8.3±0.47mM ($p<0.05$), respectively (Figure 24).

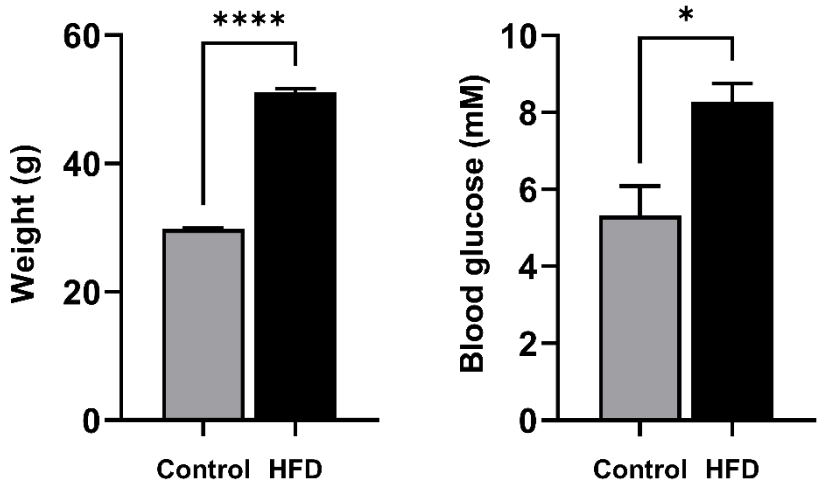

Figure 24. Terminal weight (left) and fasting plasma glucose (right) measurements in C57BL/6 mice fed a control or high-fat diet for 16 weeks. Data are expressed as the mean ± S.E.M. Unpaired two-tailed t-test; n=5 per group; *p<0.05, ****p<0.0001 vs control.

RT-qPCR screening of islet GPCR peptide ligands indicated that 45 and 40 mRNAs were expressed in visceral adipose tissue retrieved from control diet-fed (lean) and high fat diet-fed (obese) mice, respectively (Figure 25) following the RT-qPCR screening of 155 genes that encode ligands for islet GPCRs. The remaining mRNAs were either expressed at trace level (0.0001% to 0.001% relative to *Actb* expression) or absent (<0.0001% of *Actb*). The Venn diagrams in Figure 25 show these three categories of GPCR peptide ligand mRNA expression in adipose tissue from lean (blue) and obese (orange) mice and the overlap in expression of mRNAs is shown in the pink intersection. Thus, 35 of the expressed genes were common to the adipose tissue from both lean and obese mice. In addition, of the 155 mRNAs quantified 28 and 82 were expressed at trace levels or absent or in lean mice, while 25 and 90 were trace or absent in obese mice, with overlaps of 12 and 75 mRNAs in these categories (Figure 25).

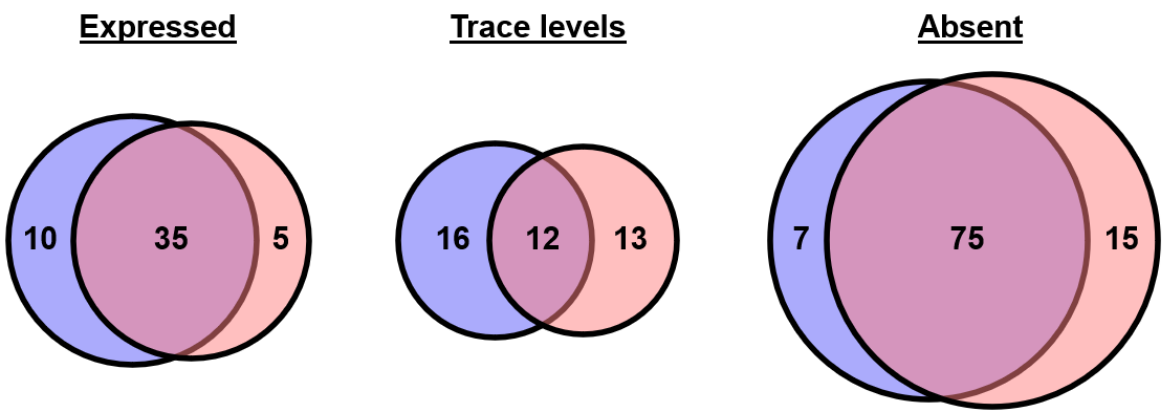

Figure 25. Proportions of islet GPCR peptide ligand mRNAs classified as being expressed, at trace level, or absent in visceral adipose tissue retrieved from lean and diet-induced obese mice. Data were obtained by RT-qPCR quantifications of RNA isolated from 5 lean (blue) and 5 obese (orange) mice. Genes common to both lean and obese mice are shown by the pink intersections. Expressed >0.001% relative to *Actb*; trace = 0.0001% to 0.001% relative to *Actb*; absent < 0.0001% relative to *Actb*.

4.3.2 Expression of islet GPCR peptide ligand mRNAs in whole adipose tissue retrieved from lean mice

Of the 45 islet GPCR peptide ligand mRNAs expressed in whole adipose tissue retrieved from lean mice, *Agt*, encoding angiotensinogen, displayed the greatest level of mRNA expression (0.254±0.0620 relative to *Actb*) (Figure 26). There was also high expression of mRNAs encoding the complement peptide, *C3* (0.238± 0.0715 relative to *Actb*) and for collagen type III α-1 chain, *Col3a1* (0.205±0.1095 relative to *Actb*). In contrast, mRNAs encoding calcitonin-related polypeptide α, *Calca* (0.001±0.0002 relative to *Actb*), the Wnt ligand, *Wnt9a* (0.001±0.0002 relative to *Actb*), and osteocalcin, *Bglap* (0.001± 0.0011 relative to *Actb*) were expressed at low levels in whole adipose tissue from lean mice.

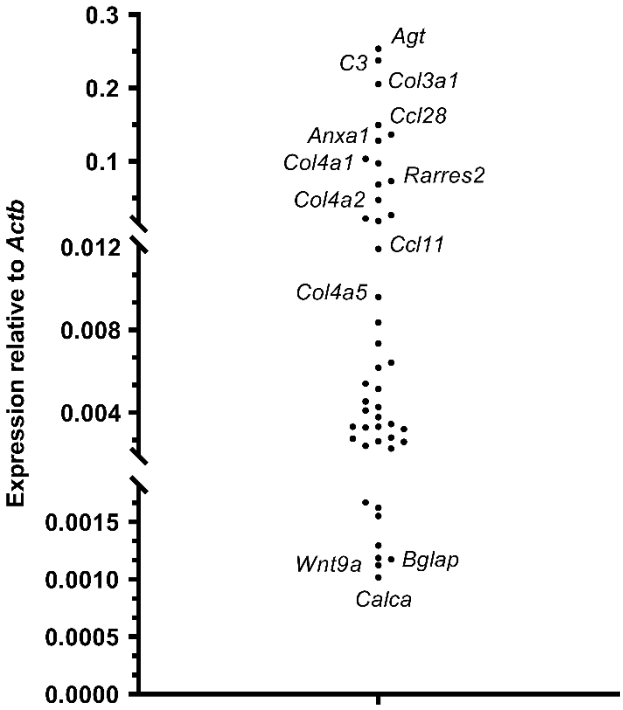

Figure 26. Islet GPCR peptide ligand mRNA expression in visceral adipose tissue retrieved from lean mice. Data were generated by RT-qPCR and are displayed relative to expression of the housekeeping gene, *Actb* (n=5).

4.3.3 Expression of islet GPCR peptide ligand mRNAs in whole adipose tissue retrieved from diet-induced obese mice

The quantification of islet GPCR peptide ligand mRNAs in whole adipose tissue from diet-induced obese mice revealed *Anxa1* (0.423±0.0688 relative to *Actb*), *C3* (0.145± 0.0287 relative to *Actb*), and *Col4a1* (0.126± 0.0215 relative to *Actb*) were the most abundant mRNAs quantified while mRNAs encoding *Col4a6* (0.001±0.0006 relative to *Actb*), *Npy* (0.001±0.0003 relative to *Actb*) and *Rdh10* (0.001±0.0002 relative to *Actb*) were expressed at low levels in whole adipose tissue from diet-induced obese mice (Figure 27).

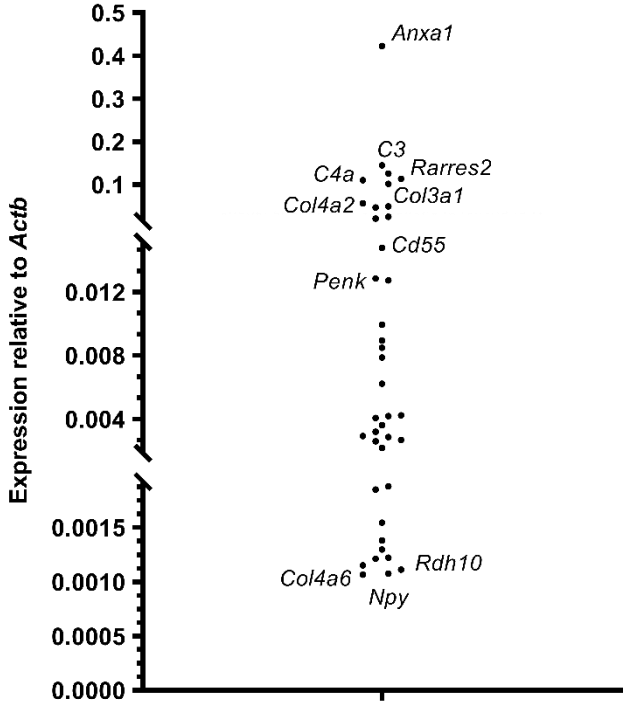

Figure 27. Islet GPCR peptide ligand mRNA expression in visceral adipose tissue retrieved from diet-induced obese mice. Data were generated by RT-qPCR and are displayed relative to expression of the housekeeping gene, *Actb* (n=5).

4.3.4 Comparative analysis of islet GPCR peptide ligand mRNA expression in whole adipose tissue between lean and diet-induced obese mice

The dynamics of visceral adipose tissue mRNA expression between lean and obese conditions can be clearly shown by Figure 28 in which islet GPCR peptide ligand mRNAs were upregulated or downregulated in whole fat depots with high-fat feeding. It can be seen that *Npy*, *Ccl4*, *Ccl3*, *Ccl5* and *Anxa1* mRNAs exhibit the most marked upregulation with high-fat feeding (2502±610%, 1112±167%, 820±200%, 342±130% and 329±54% of control diet expression, respectively) and all of these, except *Ccl5*, showed significant upregulation when data from the five lean and five obese adipose tissue samples were compared (Supplementary Table 22). Figure 28 also shows that mRNAs encoding *Agt* (96.9±0.8% decrease), *Ccl17* (96.3±0.8% decrease) and *Ccl24* (87.9±0.5% decrease) were markedly downregulated with high-fat feeding, although of these, only changes in *Agt* were statistically significant (Supplementary Table 22).

As expected, *Lep* and *AdipoQ* were readily detectable in epididymal adipose tissue and there was a significant increase in *Lep* (286±33% of control diet expression) and a decrease *in AdipoQ* (37.7±7.3% of control diet expression) in obesity (Supplementary Table 22). Like data retrieved from isolated mature adipocytes, several islet GPCR peptide ligand mRNAs considered to be absent (<0.0001% of *Actb*) or expressed at trace levels (0.0001% to 0.001% relative to *Actb* expression) in adipose tissue from lean mice were significantly upregulated or downregulated as a result of high-fat feeding. Thus, *Ghrh*, *Cck*, *C5* and *Ccl2* were upregulated (1759±618%, 1408±314%, 1119±370% and 955±104% of control diet expression, respectively) in epididymal adipose tissue isolated from obese mice, whereas there were

significant reductions in several non-abundant mRNAs including *Cxcl3* (94.7±3.0% decrease) *Wnt4* (94.5±1.3% decrease), *Wnt7b* 84.6±3.4% decrease) and *Col4a4* (81.5±5.0% decrease) (Supplementary Table 22).

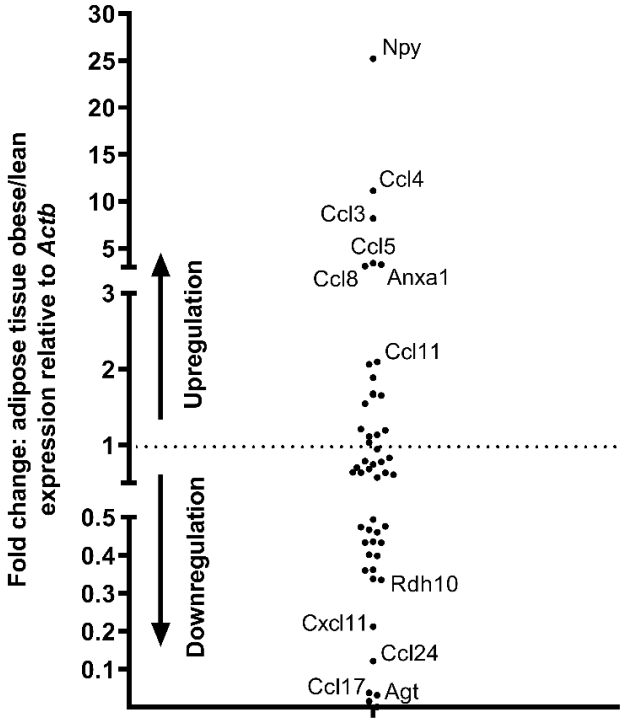

Figure 28. Upregulated and downregulated islet GPCR peptide ligand mRNAs in visceral adipose tissue retrieved from lean and obese mice. Data were generated by RT-qPCR and are displayed as fold change of mean expression values in obese vs lean mice (upregulated: >1; downregulated: <1), relative to the housekeeping gene, *Actb* (n=5 samples per group).

4.3.5 Quantification of plasma Ccl4 levels in lean and diet-induced obese mice

There have been several studies investigating the effects of NPY, the product of the most upregulated mRNA in adipose tissue in obesity, on islet function (Bennet et al., 1996; Franklin et al., 2018; Imai et al., 2007; Yang et al., 2022), but nothing is known about the chemokine Ccl4, encoded by the second most highly upregulated mRNA, *Ccl4*. For *Ccl4* to have functional effects on islets, it must be translated and secreted from adipose tissue. Therefore, to determine whether the alterations in *Ccl4* mRNA expression in visceral adipose tissue were accompanied by alterations in circulating peptide levels, plasma samples were extracted from control diet-fed (10% fat) and high-fat diet-fed (60% fat) mice and circulating Ccl4 levels were quantified using a solid-phase sandwich ELISA. Lean mice had a mean plasma Ccl4 concentration of 5.6±1.0pg/mL whereas circulating Ccl4 levels in diet-induced obese mice were markedly higher at 11.2±2.1pg/mL (p=0.054) (Figure 29).

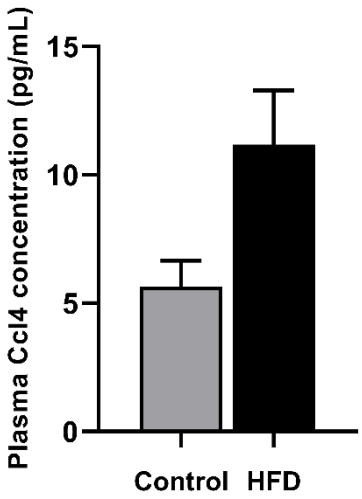

Figure 29. Terminal plasma Ccl4 levels in C57BL/6 mice fed a control or high-fat diet for 16-weeks. Data are expressed as the mean ± S.E.M. Unpaired two-tailed t-test; n=5-6 per group.

4.4 Discussion

Experiments described in the present chapter characterised the mRNA profiles of islet GPCR peptide ligands in whole visceral adipose tissue from lean and diet-induced obese mice, and subsequently provided insight into the dynamics of adipokine mRNAs under healthy and abnormal metabolic states. The most abundant islet GPCR peptide ligand mRNA in adipose tissue isolated from lean mice was angiotensinogen, encoded by *Agt*, and its expression was significantly downregulated over 32-fold in obese mice. Angiotensinogen is a precursor for all angiotensin peptides, the most prominent being angiotensin II – a major regulator of water, sodium, and blood pressure within the renin-angiotensin system (RAS) (Lu et al., 2016). Although islets express AT1 receptors and exogenous angiotensin stimulates insulin secretion (Ramracheya et al., 2006), the systemic hypertensive effects of angiotensin preclude its use therapeutically in diabetes. In fat pads retrieved from obese mice, *Anxa1* was the most highly expressed ligand mRNA. As discussed in the previous chapter in which *Anxa1* was identified as being the most abundant islet GPCR peptide ligand mRNA in lean and obese mature adipocytes, annexin A1 has been shown to improve islet function by enhancing glucose-stimulated insulin secretion and protecting against β-cell apoptosis via FPR2 binding (Kreutter et al., 2017; Rackham et al., 2018).

Neuropeptide Y, encoded by *Npy*, was upregulated over 25-fold in adipose tissue from obese mice and previous studies have detected elevated plasma Npy levels in obese mice (Kuo et al., 2007), and humans (Baranowska et al., 1997). Interestingly, the increase in circulating Npy in obese humans coincided with a pronounced upregulation in Npy expression within subcutaneous fat depots, suggestive of an adipose tissue source (Baranowska et al., 1997). Furthermore, Npy has autocrine effects to stimulate preadipocyte proliferation and adipogenesis, leading to significant adipose tissue expansion and enhanced Npy secretion (Kuo et al., 2007). Npy inhibits glucose-stimulated insulin secretion (Bennet et al., 1996) and islet-specific Npy deletion in mice enhanced basal and glucose-stimulated insulin secretion, which was attributed to a significantly greater islet area compared to their wild-type littermates (Imai et al., 2007). However, despite its negative regulation of insulin secretory function, there

is evidence of Npy promoting β-cell proliferation and protecting against cytokine- and streptozotocin-induced islet apoptosis (Franklin et al., 2018).

While Npy has established effects on islet function, the >11-fold upregulation of mRNA encoding chemokine (C-C motif) ligand 4 (Ccl4), identifies this as a candidate of interest for investigations into a potential role in regulating insulin secretion and functional β-cell mass. Ccl4, also known as macrophage inflammatory protein-1β (MIP-1β), is a chemoattractant protein produced by endothelial and epithelial cells, fibroblasts, neutrophils, monocytes and lymphocytes, and it has an established role in promoting leukocyte activation and recruitment to sites of inflammation (Estevao et al., 2021). The observations here of significant upregulation of *Ccl4* mRNA epididymal adipose tissue from diet-induced obese mice are consistent with an earlier report of a significant rise in *Ccl4* mRNA expression in epididymal fat depots from mice fed a high-fat diet for 10 weeks (Kitade et al., 2012), therefore suggesting the involvement of adipose-derived Ccl4 from the early stages of obesity. Upregulated Ccl4 has been recently implicated in obesity-induced metabolic dysfunction, as Ccl4 inhibition in high-fat diet-fed mice was associated with improved insulin sensitivity, delayed hyperglycaemia progression, and reduced serum triglycerides and systemic inflammation (Chang et al., 2021; Chang & Chen, 2021). In terms of islet function, microscopic imaging showed enlarged pancreatic volume and insulin-positive areas with Ccl4 inhibition, although, these data were not quantified. One study also characterised anti-apoptotic effects of Ccl4 antibodies in NIT-1 β-cells (Chang et al., 2021), however, this insulinoma cell line is derived from a non-obese diabetic (NOD)/Lt mouse model (Hamaguchi et al., 1991) and cells were treated with the β-cell-specific cytotoxin, streptozotocin (STZ), to induce rapid β-cell loss resembling T1D pathology. Thus, measures of β-cell function following Ccl4 treatment and/or inhibition in the context obesity and metabolic syndrome remain undetermined.

Quantification of plasma Ccl4 indicated that upregulated *Ccl4* mRNA in visceral fat depots was accompanied by increased circulating Ccl4 peptide levels in obese mice compared to their lean counterparts. It is possible that Ccl4 is one of the many chemokines that are secreted into the circulation from adipose tissue and travel to the islets where the β-cell is a target of inflammatory responses in diabetes and obesity. Indeed, a meta-analysis revealed CCL4 levels are significantly higher in patients with T2D, while no differences were observed between healthy controls and patients with prediabetes, suggesting an association between CCL4 levels and diabetes progression (Pan et al., 2021). Similar elevations are observed in patients with T1D (Maier et al., 2008) and islet autoantibody-positive individuals at high risk of developing of T1D (Hanifi-Moghaddam et al., 2006; Rydén & Faresjö, 2013), indicating a common participation of Ccl4 in different diabetes types.

The qPCR screening data presented in this chapter allowed comparisons between mature adipocytes and whole adipose tissue regarding the adipokines secreted from each and the magnitude of their contributions (Supplementary Figure 61 & Supplementary Table 26). For example, whilst the expression of *Ccl4* mRNA is elevated in whole adipose tissue, quantification of islet GPCR peptide ligand mRNAs in isolated mature adipocytes revealed no significant change in the expression of *Ccl4* mRNA. This indicates that the majority of increased *Ccl4* mRNA in obesity was sourced from the non-adipocyte SVF which is consistent with the production of Ccl4 from the above mentioned cell types, including immune cells which accumulate within obesogenic adipose tissue and contribute to local inflammation (Weisberg et al., 2003). Removal of the heterogeneous SVF allows a focused molecular analysis of

specialised adipocyte cells without interference from other cell types that can also be found in other tissues. However, much like β-cells within an islet, adipocyte cells do not function alone. Instead, they interact with non-adipocyte cells to alter the metabolic and immune properties of adipose tissue (Zhao & Saltiel, 2020). Additionally, the composition of the SVF is dependent on several factors, including metabolic status (Cousin et al., 2006; Silva et al., 2015). Therefore, eliminating the SVF from investigations into adipokine dynamics in obesity is likely to hide important information and key factors with therapeutic potential. Furthermore, there are practical and economic benefits of using whole adipose tissue vs isolated mature adipocytes, as described in Section 4.2.1. Based on these arguments, it was decided that future qPCR screenings in additional obese models used whole adipose tissue as the starting material.

In summary, quantification of mRNAs encoding islet GPCR peptide ligand mRNAs in adipose tissue from lean and obese mice revealed significant alterations in gene expression in obesity. The data generated in this chapter pointed to ligands of interest for future research on adipose-islet crosstalk via secreted ligands acting at islet GPCRs. The chemokine, Ccl4, could be a potential novel candidate for functional characterisation in islet cells given the correlation between its mRNA expression, circulating peptide levels, and growing adiposity, as well as the relatively limited availability of data investigating its action on β-cells. The experiments described in Chapters 5 and 6 investigated whether the same upregulation in adipose tissue-derived *Ccl4* mRNA observed in high-fat diet-fed mice is recapitulated in a genetic mouse model of obesity (*db/db*) and in visceral adipose tissue from obese humans, which would suggest a consistent trend of increased Ccl4 mRNA expression in obesity.

Chapter 5: Quantification of changes in the expression of islet GPCR peptide ligand mRNAs in whole adipose tissue from the *db/db* obese mouse model

5.1 Introduction

The previous chapters characterised the mRNA expression profiles of islet GPCR peptide ligands in whole adipose tissue and mature adipocytes harvested from the commonly used diet-induced obese mouse model. The high-fat diet mimics a human Western diet on a C57BL/6 background which is susceptible to weight gain and insulin resistance. Since obesity and T2D have a polygenic nature in humans, the diet-induced obese mouse model is a suitable representative of the human disease progression. Alternatively, mice carrying a mutation in the leptin receptor (*db*) also serve as an effective and reliable mouse model of obesity and T2D. The mutation, in what was initially referred to as the "diabetes" gene, was first identified in an inbred C57BL/Ks mouse strain which displayed abnormal fat deposition from 3 weeks of age shortly followed by hyperglycaemia, polyuria and glycosuria (Coleman & Hummel, 1967; Hummel et al., 1966). The mutated gene responsible for this severe obese phenotype was later discovered to encode the leptin receptor (Chen et al., 1996; Tartaglia et al., 1995) and was found to be present in patients experiencing hyperphagia and other complications associated with leptin's role in puberty and immunity (Farooqi et al., 2007). The monogenic *db/db* model exhibits comparable weight gain, adaptative islet growth, elevated serum insulin levels, and adipose tissue inflammation to their diet-induced obese equivalents (Burke et al., 2017). Indeed, several features of obesity in the *db/db* mouse resemble those in human obesity: morphological islet adaptations to compensate for increased insulin demand occur during the early stages, but fail at the late stage resulting in insulin resistance, insulin secretory defects and hyperglycaemia (Coleman & Hummel, 1967; Hummel et al., 1966). Furthermore, certain features of human T2D, such as hyperglucagonaemia, are observed in the *db/db* model that are not observed in weight-matched mice fed a Western-style diet (Burke et al., 2017). For these reasons, the *db/db* mouse model is widely utilised in research studies and, when included alongside diet-induced obese models, can enhance the understanding and the development of treatments for obesity and T2D.

Consequently, in this chapter, a qPCR screening of islet GPCR peptide ligand mRNAs was performed in whole epididymal adipose tissue retrieved from *db*/+ and *db/db* mice. Whilst severe obesity and hyperglycaemia is caused by complete leptin receptor deficiency in *db/db* mice, their heterozygous counterparts (*db*/+) carry a normal functional leptin receptor allele and therefore have normal body weights and do not develop T2D. Age-related differences were avoided by using mice of a similar age to those used for the analysis of isolated mature adipocytes and whole adipose tissue from lean and diet-induced obese mice, the results of which were described in Chapters 3 and 4. Moreover, consistent with these previous qPCR screenings, the same 155 peptide ligand mRNAs that target the 110 peptide/protein-activated human islet GPCRs originally described by Amisten et al. (2013) were quantified here.

5.2 Methods

5.2.1 Total RNA extraction from mouse epididymal adipose tissue

The method for isolating and purifying RNA from whole epididymal adipose tissue retrieved from lean *db*/+ and obese *db/db* mice was identical to that performed using fat pads from control and high-fat diet-fed mice. As described in Section 2.2.7, whole adipose tissue was dissolved in TRIzol®, then homogenised using a TissueLyser II and stainless-steel beads. Thereafter, a centrifuge cycle allowed separation of lipids from the RNA-containing phenol phase which was transferred to a fresh Eppendorf tube and topped up to 1mL total volume with TRIzol®. The addition of chloroform marked the continuation of the RNA isolation protocol described in Section 2.2.6 which used spin columns and ethanol-based buffers from an miRNeasy Kit. Once the yield and purity of isolated RNA was determined using a NanoDrop™ 1000 spectrophotometer, samples were stored at –70°C or immediately converted to cDNA.

5.2.2 RT-qPCR

The High-Capacity cDNA Reverse Transcription Kit and a T100™ thermal cycler were used to generate cDNA (40ng/µL) from adipose RNA sample templates, as described in Section 2.2.9. The expression of 155 islet GPCR peptide ligand mRNAs, and positive control adipokine genes, *AdipoQ* and *Lep*, were quantified using a SYBR Green-based qPCR protocol and the LightCycler® 96 (Section 2.2.10).

5.3 Results

5.3.1 Mouse characteristics and expression of islet GPCR peptide ligand mRNAs in visceral whole adipose tissue from lean *db*/+ and obese *db/db* mice

Lean *db*/+ mice, each of which possessed one functioning allele encoding the leptin receptor, had a mean weight of 31.5±1.06g at the time of tissue retrieval whilst obese *db/db* mice that lacked leptin receptors weighed 55.5±2.97g ($p<0.001$) and the fasting blood glucose levels were 7.8±0.32mM and 32.6±0.37mM ($p<0.0001$), respectively (Figure 30).

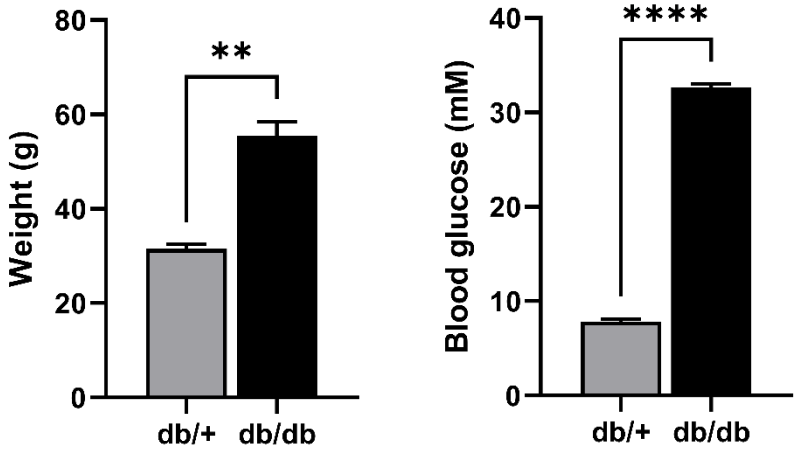

Figure 30. Terminal weight (left) and fasting plasma glucose (right) measurements in *db*/+ and *db/db* mice. Data are expressed as the mean ± S.E.M. Unpaired two-tailed t-test; n=3 per group; **p<0.01, ****p<0.0001 vs *db*/+ control.

The RT-qPCR screening of 155 genes that encode ligands for islet GPCRs revealed 49 and 38 were expressed in visceral adipose tissue retrieved from lean *db*/+ and obese *db/db* mice, respectively (Figure 31). The remaining mRNAs were either expressed at trace level (0.0001% to 0.001% relative to *Actb* expression) or absent (<0.0001% of *Actb*). The Venn diagrams in Figure 31 show these three categories of GPCR peptide ligand mRNA expression in adipose tissue from lean *db*/+ (blue) and obese *db/db* (orange) mice and the overlap in expression of mRNAs is shown in the pink intersection. Thus, 36 of the expressed genes were common to the adipose tissue from both lean and obese mice. In addition, of the 155 mRNAs quantified 33 and 73 were expressed at trace levels or absent in lean mice, while 33 and 84 were trace or absent in obese mice, with overlaps of 18 and 70 mRNAs in these categories (Figure 31).

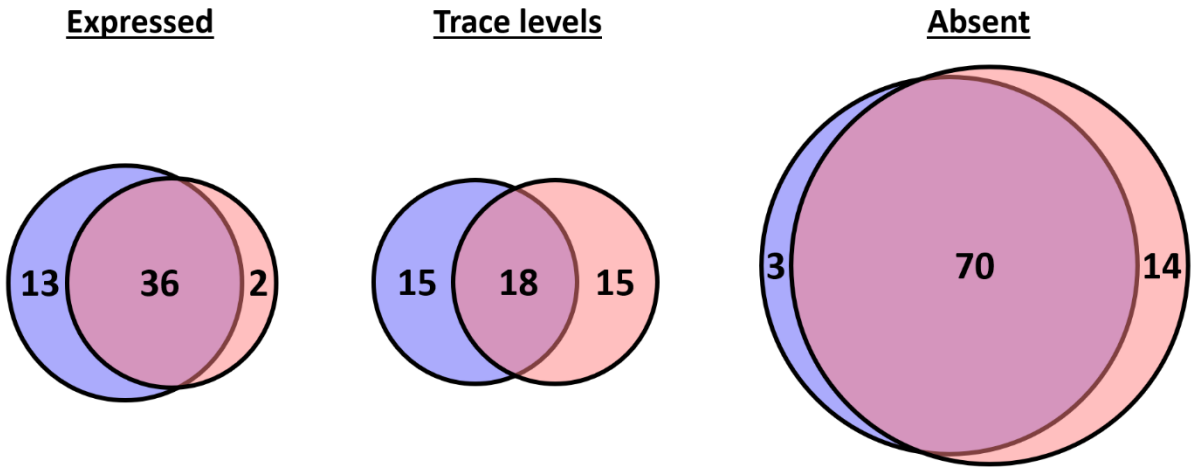

Figure 31. Proportions of islet GPCR peptide ligand mRNAs classified as being expressed, at trace level, or absent in visceral adipose tissue retrieved from lean *db*/+ and obese *db/db* mice. Data were obtained by RT-qPCR quantifications of RNA isolated from 3 lean *db*/+ (blue) and 3 *db/db* obese (orange) mice. Genes common to both lean and obese mice are shown by the pink intersections. Expressed >0.001% relative to *Actb*; trace = 0.0001% to 0.001% relative to *Actb*; absent < 0.0001% relative to *Actb*.

5.3.2 Expression of islet GPCR peptide ligand mRNAs in whole adipose tissue retrieved from lean *db*/+ mice

Of the 49 islet GPCR peptide ligand mRNAs expressed in whole adipose tissue retrieved from lean *db*/+ mice, *Col3a1*, encoding the collagen type III α-1 chain, displayed the greatest level of mRNA expression (0.335±0.0339 relative to *Actb*) (Figure 32). There was also high expression of mRNAs encoding the complement peptide, *C4a* (0.257±0.0357 relative to *Actb*) and collagen type IV α-1 chain, *Col4a1* (0.245±0.0254 relative to *Actb*). In contrast, mRNAs encoding chemokines, *Ccl28* (0.001±0.0001 relative to *Actb*), *Cx3cl1* (0.001±0.0001 relative to *Actb*), and *Cxcl1* (0.001± 0.0004 relative to *Actb*) were expressed at low levels in whole adipose tissue from lean *db*/+ mice.

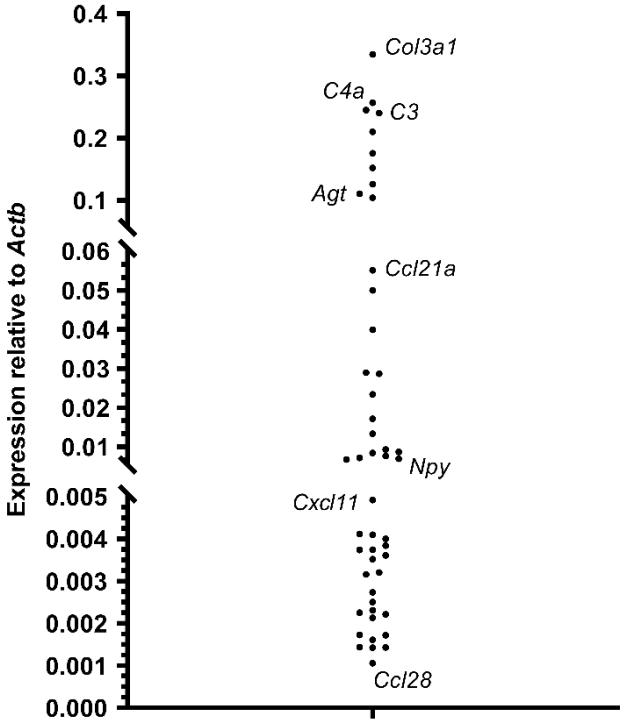

Figure 32. Islet GPCR peptide ligand mRNA expression in visceral adipose tissue retrieved from lean *db*/+ mice. Data were generated by RT-qPCR and are displayed relative to expression of the housekeeping gene, *Actb* (n=3).

5.3.3 Expression of islet GPCR peptide ligand mRNAs in whole adipose tissue retrieved from obese *db/db* mice

The quantification of islet GPCR peptide ligand mRNAs in whole adipose tissue from obese *db/db* mice revealed similar expression profiles to those from lean *db*/+ mice, with *Col3a1* (0.473±0.0241 relative to *Actb*) being the most abundant mRNA quantified, following by *Anxa1* (0.194±0.0271 relative to *Actb*) and *Col4a1* (0.170±0.0184 relative to *Actb*) (Figure 33). Conversely, mRNAs encoding *Ccl5* (0.001±0.0002 relative to *Actb*), *Wnt11* (0.001±0.0003 relative to *Actb*) and *Npff* (0.001±0.0002 relative to *Actb*) were expressed at low levels in whole adipose tissue from obese *db/db* mice.

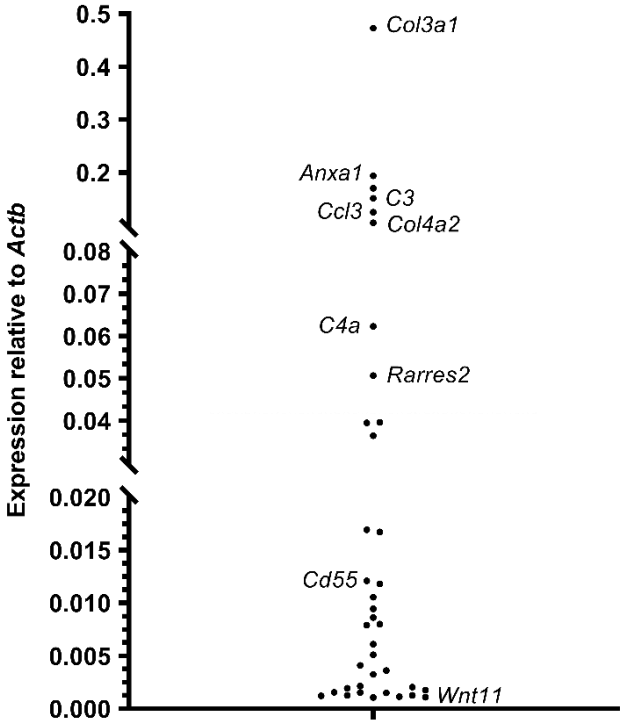

Figure 33. Islet GPCR peptide ligand mRNA expression in visceral adipose tissue retrieved from obese *db/db* mice. Data were generated by RT-qPCR and are displayed relative to expression of the housekeeping gene, *Actb* (n=3).

5.3.4 Comparative analysis of islet GPCR peptide ligand mRNA expression in whole adipose tissue between *db*/+ and *db/db* mice

Excessive adiposity caused by disrupted leptin signalling resulted in alterations in the expression of key adipokines which target islet GPCRs (Figure 34). With a focus on those mRNAs whose expression was above trace level in adipose tissue from lean *db*/+ and/or obese *db/db* mice, several genes were upregulated or downregulated in obesity. It can be seen that *Ccl2*, *Ccl4*, *Ccl7*, *Cxcl14* and *Col3a1* mRNAs exhibit the most marked and significant upregulation (1191±111%, 674±137%, 316±15%, 230±16% and 141±7% of lean expression, respectively) when data from the three lean *db*/+ and three obese *db/db* adipose tissue samples were compared (Supplementary Table 23). In contrast, deletion of leptin receptors was associated with significant downregulation in the expression of mRNAs encoding *Ccl28* (95.9±4.1% decrease), *Cxcl11* (94.9±1.4% decrease) and *Agt* (92.8±1.1% decrease) (Figure 34 & Supplementary Table 23).

As expected, *Lep* and *AdipoQ* were readily detectable in visceral adipose tissue and their mRNA expression levels were upregulated and downregulated, respectively in obesity (Supplementary Table 23). However, whilst the observed reduction in *AdipoQ* mRNA expression level was significant following leptin receptor deletion (86.3±3.4% decrease, $p<0.001$), the increased in *Lep* mRNA expression was not statistically significant (158±53% of lean expression, $p=0.334$). Disturbed leptin signalling also altered the expression of multiple adipose tissue-derived GPCR peptide ligand mRNAs that were considered absent (<0.0001% of *Actb*) or expressed at trace levels (0.0001% to 0.001% relative to *Actb* expression). Thus,

C5, *Kng*, *Cxcl3*, and *Ndp* were upregulated (4399±111%, 3237±137%, 1882±15% and 470±7% of lean expression, respectively) in epididymal adipose tissue isolated from obese *db/db* mice, whereas there were significant reductions in several non-abundant mRNAs including *Rspo2* (96.0±2.4% decrease), *Rln1* (94.7±5.3% decrease), *Col4a4* (93.2±1.1% decrease) and *Lhb* (90.7±5.1% decrease) (Supplementary Table 23).

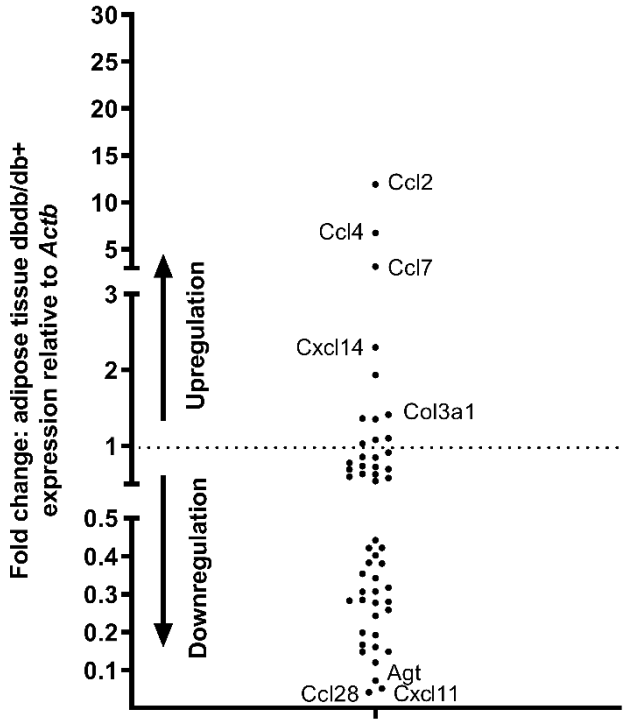

Figure 34. Upregulated and downregulated islet GPCR peptide ligand mRNAs in visceral adipose tissue retrieved from lean *db*/+ and obese *db/db* mice. Data were generated by RT-qPCR and are displayed as fold change of mean expression values in lean *db*/+ vs obese *db/db* mice (upregulated: >1; downregulated: <1), relative to the housekeeping gene, *Actb* (n=3 samples per group).

5.4 Discussion

The present chapter determined the differential expression of adipose tissue-derived islet GPCR peptide ligand mRNAs between lean *db*/+ and obese *db/db* mice. This monogenic model of obesity – the product of a leptin receptor-deficiency – provided an alternative to the diet-induced obese model. Gene candidates both distinct and common to environmental and genetic forms of obesity could therefore be identified (Supplementary Figure 62 & Supplementary Table 27).

Collagen type III α1, encoded by *Col3a1*, was the most highly expressed islet GPCR ligand mRNA in lean and genetically obese epididymal fat pads. Furthermore, *Col3a1* mRNA expression was significantly elevated in obese *db/db* mice compared to their lean equivalents which retained leptin receptor activity (141±7% of lean expression). *In vivo* collagen type III α1 peptide chains aggregate in triplicate to generate collage type III homotrimers which, due to their fibrillar structure and tensile strength, are abundant in the ECM of hollow organs that undergo significant stretch, such as large vessels, the uterus and bowel (see Section 1.6.1.1) (Kuivaniemi & Tromp, 2019). Accordingly, collagen III is a structural component of the

interstitial matrix within adipose tissue (Marcelin et al., 2017). It is also secreted from mesenchymal cell types (Casey & MacDonald, 1996) and acts as a ligand at GPR56, the most abundantly expressed GPCR in human islets (Dunér et al., 2016). Anti-apoptotic and potentiating insulin secretory properties of collagen III treatment have been observed in islet cells (Olaniru et al., 2018), and the significant rise in adipose *Col3a1* mRNA in the *db/db* genetic obese model may indicate compensation for reduced islet GPR56 expression seen in diabetic mice and patients (Dunér et al., 2016). Significant upregulated expression of other collagen types, including collagen I, V and VI, in epididymal fat depots from *db/db* mice indicates a widespread increase in ECM components that could contribute to adipose tissue fibrosis in obesity (Khan et al., 2009). The rise in *Col3a1* mRNA is also comparable to a recent publication in which 12 weeks of high-fat feeding in male mice induced significant upregulation in epididymal *Col3a1* expression and other fibrotic markers (Marcelin et al., 2017), indicating obesity-induced fibrogenesis regardless of the obesogenic driver. However, elevated collagen III expression seen here and in previous publications are in contrast to the data generated in Chapter 4 whereby *Col3a1* mRNA expression decreased in whole epididymal adipose tissue following 16 weeks of high-fat feeding (49±14.0% of lean expression). Quantitative proteomic studies of differentiating adipocytes (Ojima et al., 2016) and the small interfering RNA (siRNA)-mediated reduction in *Col3a1* mRNA in 3T3-L1 adipocyte cells (Al Hasan et al., 2021) have shown collagen III is required for adipogenesis. Thus, impaired adipocyte differentiation may predominate in a diet-induced obese model with a more severe phenotype, although, the expression of *Col3a1* mRNA is more concentrated in the SVF vs the adipocyte fraction (Divoux et al., 2010) suggesting that additional mechanisms account for the ~50% reduction in adipose *Col3a1* mRNA with high-fat feeding. As collagen III is localised to perivascular adipose tissue, it is possible that the discrepancies may be due to a variation in blood vessel supply within fat pad samples as opposed to changes in mRNA expression. It is also unclear as to whether observations of collagen III expression in the data presented here and in the above mentioned studies represent the deposition of insoluble fibrous collagen or the secretion of the soluble form into the circulation where it can travel and interact with the GPR56 receptor in peripheral tissues.

The most significantly upregulated islet GPCR peptide ligand mRNA in *db/db* fat pads was the chemokine, *Ccl2*, and was closely followed by *Ccl4* and *Ccl7* mRNAs. Similar increases in *Ccl2* mRNA in epididymal adipose tissue expansion have been reported for diet-induced obese mice (Chen et al., 2005), as well as *db/db* and *ob/ob* obese mice (Kanda et al., 2006; Xu et al., 2003) which, due to leptin deficiency, are also characterised by defective leptin signalling pathways. This coincided with elevated expression of the GPCR, Ccr5, and the macrophage markers, Cd68, CD11b, CD45 and F4/80, within the SVF of *db/db*, *ob/ob* and diet-induced obese mice (Kanda et al., 2006; Kitade et al., 2012; Xu et al., 2003). Furthermore, CCL2, also known as monocyte chemoattractant protein-1 (MCP-1), and CD68 mRNAs are upregulated in human adipose tissue (Christiansen et al., 2005; Di Gregorio et al., 2005). Together, these observations support a common pathology of chemokine-mediated migration and infiltration of macrophages into adipose tissue across several models of obesity.

As for the observations made in visceral adipose tissue of diet-induced obese mice reported in Chapter 4, the expression of *Ccl4* mRNA was significantly upregulated in obese murine adipose tissue with leptin receptor deficiency being the driving force for excessive weight gain instead of an environmental cue. The beneficial outcomes of Ccl4 inhibition initially described in high-fat diet-fed mice (Chang et al., 2021) have been replicated in *Lepr^{db}/JNarl* (*db/db*)

diabetic mice: administration of anti-Ccl4 antibodies delayed hyperglycaemia progression by improving hepatic and muscle insulin sensitivity, as evidenced by decreased serine phosphorylation of IRS-1 (Chang et al., 2021). Reduced serum TNF-α and IL-6 levels were also indicative of dampened systemic inflammation with Ccl4 inhibition. As for diet-induced obese mice, microscopic images showed an increased in insulin-positive areas within the pancreas of Ccl4-treated mice, but these observations were not quantified (Chang et al., 2021). Thus, the current data indicate mutual involvement of adipose tissue-derived Ccl4 in environmental and genetic obesity that is supported by previous publications (Kanda et al., 2006; Xu et al., 2003). Ccl4 antagonism may be beneficial for improved glucose regulation in obesity and diabetes, however, there is no published information on the contribution of Ccl4 to overall β-cell function.

Of the above chemokines, Ccl2 has been studied the most extensively in relation to obesity, insulin resistance, inflammation, and insulitis. Adipocyte-specific overexpression of Ccl2 caused significant macrophage infiltration into adipose tissue depots, insulin resistance and glucose intolerance accompanied by increased hepatic glucose production and triglyceride content (Kanda et al., 2006). In contrast, both Ccr2-knockout mice (Boring et al., 1997), Ccr5-knockout mice (Kitade et al., 2012), and Ccl2-deficient mice (Kanda et al., 2006; Lu et al., 1998) display blunted monocyte/macrophage recruitment and immune responses. Ccl2-deficient mice are also protected against high-fat diet-induced metabolic disturbances (Kanda et al., 2006). Ccr2 blockade has also been associated with improvements in T2D-related renal complications, as oral administration of a Ccr2 antagonist to *db/db* mice reduced glomerulosclerosis and improved glomerular filtration rate (Sayyed et al., 2011). The negative implications of elevated Ccl2 levels are also seen within the islets, as evidenced by the spontaneous development of diabetes resulting from insulitis (Martin et al., 2008). Furthermore, high levels of secreted islet *CCL2* are associated with islet graft loss and poor clinical outcomes for human islet transplantations (Melzi et al., 2010; Piemonti et al., 2002). Abrogation of islet macrophage accumulation following CCR2 deletion supports a role for the CCL2/CCR2 axis in T1D (Martin et al., 2008). β-cells produce and secrete Ccl2, but it does not directly modulate basal and glucose-stimulated insulin secretion, nor does it induce elevations in intracellular calcium from β-cells (Piemonti et al., 2002). This lack of effect of Ccl2 on β-cell function is not surprising given that *CCR2* mRNA is not expressed by human islets (Amisten et al., 2013).

In summary, quantification of mRNAs encoding islet GPCR peptide ligand mRNAs in adipose tissue from lean *db*/+ and obese *db/db* mice revealed significant alterations in gene expression. mRNA encoding the chemokine, Ccl4, was significantly upregulated in monogenic obesity, an observation also made in polygenic, diet-induced obesity described in the previous chapter. Whether Ccl4 expansion within visceral fat depots also occurs in human obesity was investigated in Chapter 6. Additionally, whilst previous publications which studied Ccl4 antagonism in various diabetes mouse models have shed some light on the activity of this chemokine *in vivo*, details of its direct functional effects on β-cells are largely undetermined. Therefore, if data in murine obesity are translated in humans, Ccl4 could be a potential novel candidate for functional characterisation in islet cells.

Chapter 6: Quantification of changes in the expression of islet GPCR peptide ligand mRNAs in whole adipose tissue from lean and obese human donors

6.1 Introduction

Thus far, the experiments described in this thesis on differential expression of adipose tissue-derived islet GPCR peptide ligand mRNAs between lean and obese states were investigated in mouse models only. The use of mice as animal models is considered an essential tool in biomedical research, and there are several advantages of doing so. The anatomy and physiology of mice and humans are comparable with genome sequencing revealing similarities between the two species (Chinwalla et al., 2002). Consequently, knowledge gained from mouse studies, such as the identification and characterisation of genes involved in physiological function and disease pathology, can be extrapolated and applied to humans. There are also economic benefits to using rodent models in research: mice are relatively inexpensive to maintain compared to other animal models as they require less space and fewer resources; short gestation and postnatal development periods facilitate a rapid generation of animals for studies; and large numbers of offspring broadens the availability of mice and tissue samples to assure adequate power for statistical analysis. Overall, the translation of physiological functions and pathological processes from mice to humans forms the fundamental basis of biomedical research and comparative medicine. However, there are challenges and limitations when using animal models of human disease. Whilst similarities do exist, mice do not fully recapitulate the physiology, disease progression and symptoms, and responses to clinical interventions seen in humans. In consequence, results obtained from mouse experiments cannot always be replicated in human trials. Variation between different mouse strains, models, and laboratory techniques can also influence outcomes in animal experiments. This can create difficulties in interpretating data and how they relate to humans. Although the use of mouse models is valuable and often necessary, for these reasons, it is important to perform investigations using human tissue, where possible, to ensure relevance to human systems.

Accordingly, in this chapter, qPCR screening of islet GPCR peptide ligand mRNAs was performed in visceral omental adipose tissue retrieved from lean, overweight, and obese patients who underwent elective surgeries at Princess Grace Hospital, London. Some murine genes screened in the previous chapters of this thesis have human orthologs or homologs: human CCL21 is orthologous to murine Ccl21a and Ccl21b; human CCL27 is orthologous to murine Ccl27a and Ccl27b; and human TAC3 is homologous to murine Tac2. Thus, a total of 154 peptide ligand mRNAs that target the 110 peptide/protein-activated human islet GPCRs originally described by Amisten et al. (2013) were quantified.

6.2 Methods

6.2.1 Total RNA extraction from human omental adipose tissue

The experiments in this chapter were carried out with appropriate ethical approval (REC ref: 21/NW/0100; IRAS project ID: 293789) that allowed the acquisition, handling, and processing of omental adipose tissue samples from lean, overweight, and obese human donors in accordance with the Human Tissue Act 2004. Patient samples were stratified according to

BMI (kg/m^2): lean: 18.5-24.9; overweight: 25.0-29.9; and obese: 30.0-39.9, as described in Section 2.2.3. As for the processing of samples from obese mouse models, human fat pads were dissolved in TRIzol® Reagent, efficiently disrupted with a TissueLyser system II and stainless-steel magnetic beads, and then centrifuged (Section 2.2.7). The red phenol phase containing RNA was removed from the upper lipid layer and topped up to 1mL total volume with TRIzol® Reagent. The remaining steps followed the RNA isolation protocol described in Section 2.2.6 which began with the addition of chloroform, and the separation of aqueous, interphase and organic phases. Several centrifugation cycles using spin columns and ethanol-based buffers led to the isolation and purification of RNA from human omental fat depots, the yield and purity of which was assessed by the NanoDrop™ 1000 spectrophotometer. Samples that were not immediately stored at –70°C were converted to cDNA for downstream processing.

6.2.2 RT-qPCR

The generation of cDNA from RNA (40ng/µL) used reagents from the High-Capacity cDNA Reverse Transcription Kit and a T100™ thermal cycler (Section 2.2.9). The same positive control adipokine genes, *ADIPOQ* and *LEP*, that were included in qPCR screenings using mouse cDNA were also used in the human qPCR screening. However, due to slight differences between mouse and human peptide isoforms, the expression of 154, not 155, islet GPCR peptide ligand mRNAs were quantified using human adipose cDNA and followed the SYBR Green-based qPCR protocol described in Section 2.2.10.

6.3 Results

6.3.1 Patient characteristics and expression of islet GPCR peptide ligand mRNAs in adipose tissue from lean and obese human donors

As described in Section 2.2.3, samples from human donors were stratified according to BMI, with mean BMI of lean, overweight, and obese patients being 21.4±0.74kg/m^2, 27.9±1.08kg/m^2 and 34.1±2.34 kg/m^2, respectively (Figure 35).

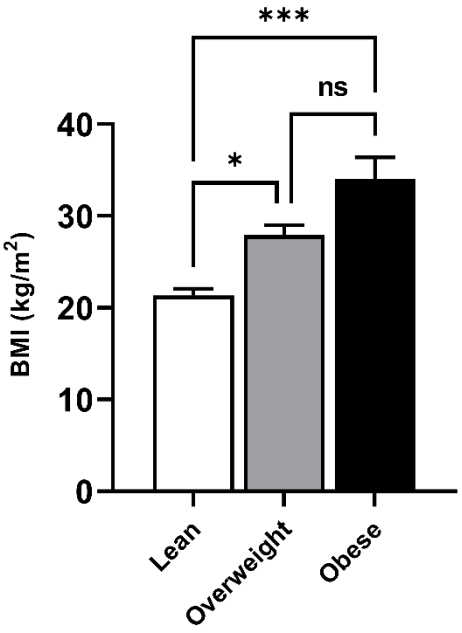

Figure 35. BMI measurements of lean, overweight, and obese human adipose tissue donors. Data are expressed as the mean ± S.E.M. One-way ANOVA; n=3-5 samples per group; *p<0.05, ***p<0.001, ns: non-significant vs overweight.

45 and 38 islet GPCR peptide ligand mRNAs were expressed in omental adipose tissue retrieved from lean and obese human donors, respectively (Figure 36) following an RT-qPCR screening of 154 candidate genes. The remaining mRNAs were either expressed at trace level (0.0001% to 0.001% relative to *ACTB* expression) or absent (<0.0001% of *ACTB*). The Venn diagrams in Figure 36 show these three categories of islet GPCR peptide ligand mRNA expression in adipose tissue from lean (blue) and obese (orange) patients and the overlap in expression of mRNAs is shown in the pink intersection. Thus, 35 of the expressed genes were common to the adipose tissue from both lean and obese humans. In addition, of the 154 mRNAs quantified, 29 and 32 were expressed at trace levels in lean and obese individuals with an overlap of 22 mRNAs, whereas almost all absent mRNAs were shared between the two patient groups with only 4 genes exclusive in obesity (Figure 36).

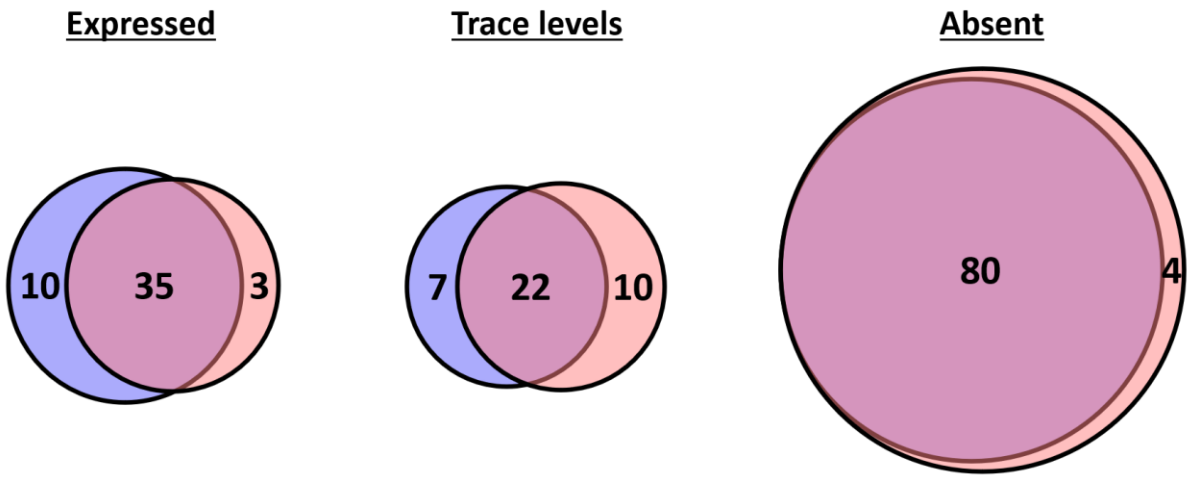

Figure 36. Proportions of islet GPCR peptide ligand mRNAs classified as being expressed, at trace level, or absent in visceral adipose tissue retrieved from lean and obese human patients. Data were obtained by RT-qPCR quantifications of RNA isolated from 5 lean (blue) and 5 obese (orange) donors. Genes common to both lean and obese donors are shown by the pink intersections. Expressed >0.001% relative to *ACTB*; trace = 0.0001% to 0.001% relative to *ACTB*; absent < 0.0001% relative to *ACTB*.

6.3.2 Expression of islet GPCR peptide ligand mRNAs in whole adipose tissue retrieved from lean human donors

Of the 45 islet GPCR peptide ligand mRNAs expressed in whole visceral adipose tissue retrieved from lean human subjects, *C3*, displayed the greatest level of mRNA expression (0.646±0.1603 relative to *ACTB*) (Figure 37). There was also high expression of mRNAs encoding for collagen type III α-1 chain, *COL3A1* (0.191±0.0260 relative to *ACTB*), for chemerin, *RARRES2* (0.164±0.0283 relative to *ACTB*), for annexin A1, *ANXA1* (0.136±0.0166 relative to *Actb*) and for the chemokine, *CXCL12* (0.127±0.0229 relative to *ACTB*). In contrast, mRNAs encoding *BGLAP* (0.001±0.0002 relative to *ACTB*), *PTHLH* (0.001±0.0003 relative to *ACTB*), *COL4A5* (0.001± 0.0003 relative to *ACTB*) and *WNT10A* (0.001± 0.0004 relative to *ACTB*) were expressed at low levels in whole adipose tissue from lean individuals.

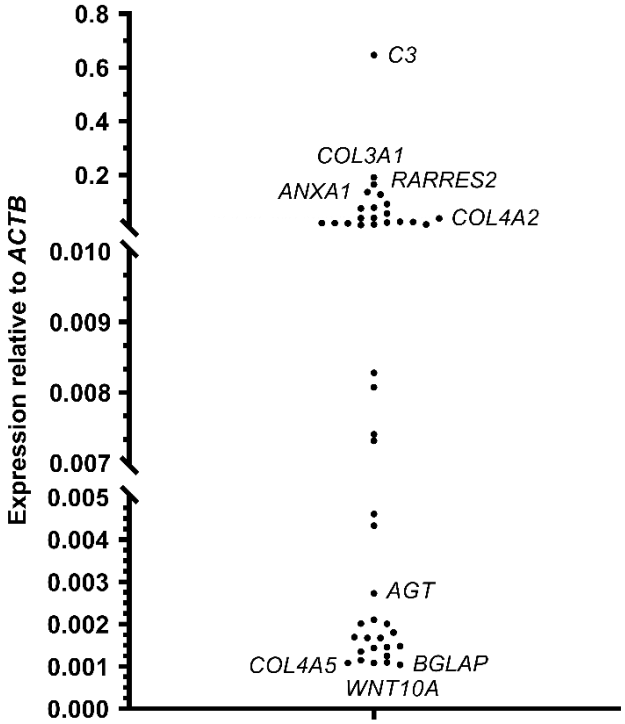

Figure 37. Islet GPCR peptide ligand mRNA expression in visceral adipose tissue retrieved from lean human donors. Data were generated by RT-qPCR and are displayed relative to expression of the housekeeping gene, *ACTB* (n=5).

6.3.3 Expression of islet GPCR peptide ligand mRNAs in whole adipose tissue retrieved from overweight human donors

The expression profile of islet GPCR peptide ligand mRNAs in whole adipose tissue from overweight human donors was markedly similar to the expression profile in lean individuals (Figure 38). *C3* (0.704±0.3228 relative to *ACTB*), *ANXA1* (0.179±0.0565 relative to *ACTB*), *COL3A1* (0.131±0.0275 relative to *ACTB*), *RARRES2* (0.119±0.0083 relative to *ACTB*) and *CXCL12* (0.103±0.0334 relative to *ACTB*) were also the most abundant mRNAs quantified. Adipose tissue-derived mRNAs which were expressed at low levels in overweight patients included those encoding *PTHLH* (0.001±0.0004 relative to *ACTB*), *CXCL9* (0.001±0.0006 relative to *ACTB*), *CCL19* (0.001±0.0006 relative to *ACTB*) and *RSPO1* (0.001±0.0006 relative to *ACTB*).

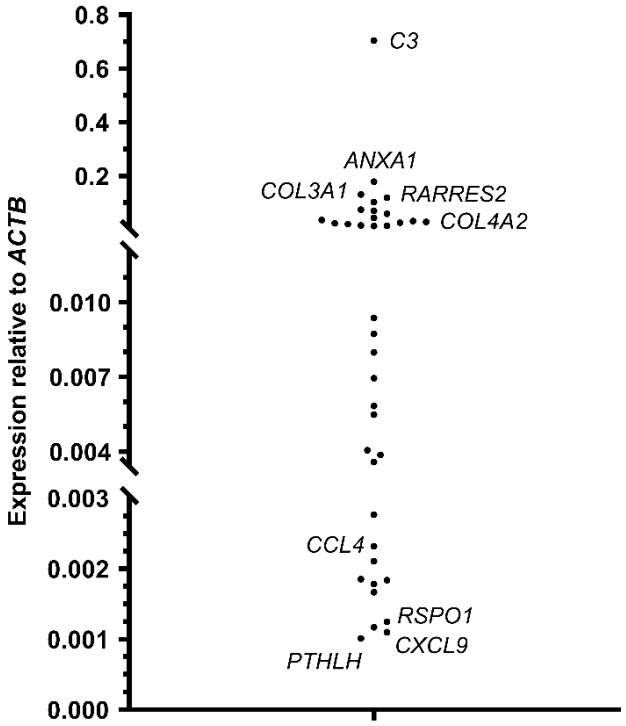

Figure 38. Islet GPCR peptide ligand mRNA expression in visceral adipose tissue retrieved from overweight human donors. Data were generated by RT-qPCR and are displayed relative to expression of the housekeeping gene, *ACTB* (n=3).

6.3.4 Expression of islet GPCR peptide ligand mRNAs in whole adipose tissue retrieved from obese human donors

Similarities can also be observed in the expression of islet GPCR peptide ligand mRNAs in whole adipose tissue when comparing obese donors to lean and overweight patient categories (Figure 39). Once again, the most highly expressed mRNAs in obese fat depots were *C3* (0.512±0.1305 relative to *ACTB*), *ANXA1* (0.203±0.0296 relative to *ACTB*), *COL3A1* (0.190±0.0255 relative to *ACTB*) and *RARRES2* (0.100±0.0168 relative to *ACTB*), but the aldehyde dehydrogenase enzyme, *ALDH1A1*, was also highly abundant (0.083±0.0040 relative to *ACTB*). Similar to adipose tissue retrieved from overweight patients, mRNAs encoding the parathyroid hormone like hormone, *PTHLH* (0.001±0.0002 relative to *ACTB*) and the R-spondin peptide, *RSPO1* (0.001±0.0004 relative to *ACTB*) were expressed at low levels in obese patients in addition to the prokineticin protein, *PROK2* (0.001±0.0004 relative to *ACTB*).

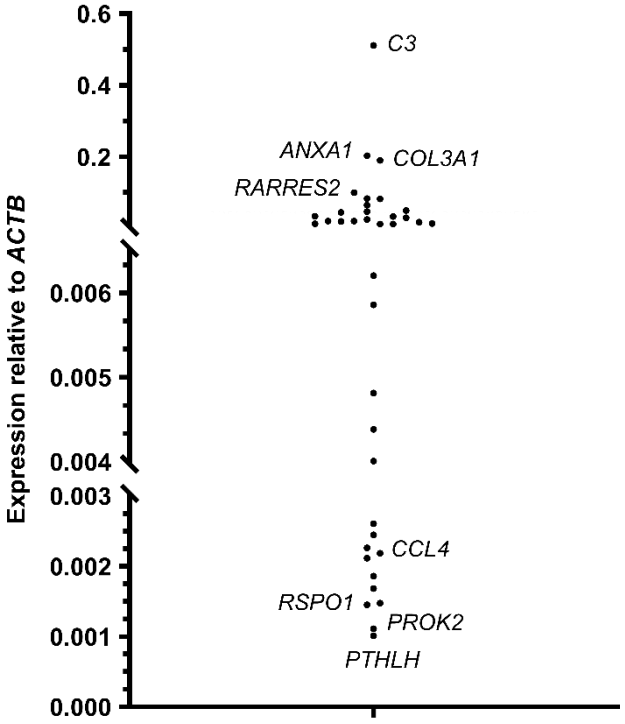

Figure 39. Islet GPCR peptide ligand mRNA expression in visceral adipose tissue retrieved from obese human donors. Data were generated by RT-qPCR and are displayed relative to expression of the housekeeping gene, *ACTB* (n=4).

6.3.5 Comparative analysis of islet GPCR peptide ligand mRNA expression in in whole adipose tissue between lean and obese human donors

The mRNA expression of islet GPCR peptide ligands in omental adipose tissue was significantly altered in obesity. Figure 40 illustrates key adipokine genes whose expression is either upregulated or downregulated as a result of excessive adiposity, with a focus on those mRNAs whose expression was above trace level in adipose tissue isolated from lean and obese human donors. It can be seen that *CCL3* and *PROK2* mRNAs exhibit the most marked upregulation in obesity (482±120.3% and 430±160.0% of lean expression, respectively), but only changes in *CCL3* mRNA expression were significant ($p<0.05$). (Supplementary Table 24). Similarly, the expression of *CXCL1* and *CCL4* mRNAs were also upregulated (262±104.6% and 260±28.2% of lean expression, respectively) and the increased *CCL4* mRNA expression was statistically significant ($p<0.05$) when data in omental adipose tissue were compared between lean and obese individuals. mRNAs which were markedly decreased in obesity include *CCL11* (69.7±10.1% decrease), *CCL21* (67.2±7.6% decrease) and *C5* (58.4±7.1% decrease), but only reductions in *C5* mRNA were statistically significant ($p<0.05$) (Supplementary Table 24).

In line with the previously described qPCR screenings in chapters 3-5, which used mouse models of obesity, the adipose tissue-exclusive genes, adiponectin and leptin, were used as positive controls for qPCR screenings using human omental fat. *LEP* and *ADIPOQ* mRNAs were readily detectable in visceral adipose tissue, and both displayed the expected trend of expression in obesity, with an increase in *LEP* (294±86.8% of lean expression) and a decrease

in *ADIPOQ* (66.4± 8.2% of lean expression) (Supplementary Table 24). However, due to variation in mRNA expression between individuals in each BMI group, these changes failed to achieve statistical significance. Supplementary Table 24 also indicates the expression of islet GPCR peptide ligand mRNAs, *ADCYAP1* and *C1QL4*, which were considered to be absent (<0.0001% relative to *ACTB*) or expressed at trace levels (0.0001% to 0.001% relative to *ACTB* expression) in adipose tissue, were significantly altered in obesity (411±104.9% and 41.0±12.4% of lean expression, respectively).

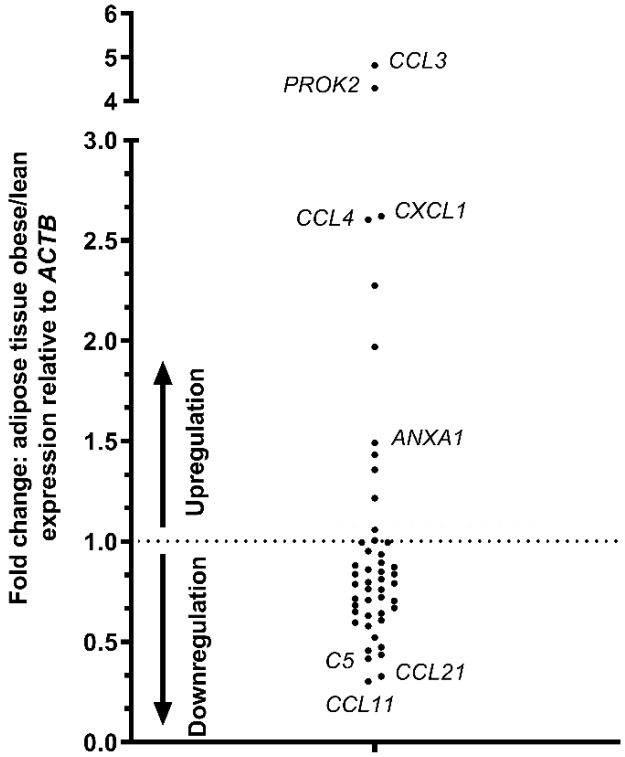

Figure 40. Upregulated and downregulated islet GPCR peptide ligand mRNAs in visceral adipose tissue retrieved from lean and obese human donors. Data were generated by RT-qPCR and are displayed as fold change of mean expression values in lean vs obese human patients (upregulated: >1; downregulated: <1), relative to the housekeeping gene, *ACTB* (n=4-5 samples per group).

6.4 Discussion

The present chapter established the expression of islet GPCR peptide ligand mRNAs in omental adipose tissue donated by lean, overweight and obese patients. Subsequently, differentially expressed adipokine mRNAs were identified in individuals with obesity and in lean individuals with a normal metabolic profile. Furthermore, together with qPCR screenings outlined in previous chapters, comparisons of the adipose tissue secretome between human and murine models of obesity were made possible (Supplementary Figure 63 & Supplementary Table 28). Of the 154 mRNAs quantified, the following adipokines were consistently identified as the top four most abundantly expressed in visceral adipose tissue across all BMI categories: complement component 3 (*C3*), annexin A1 (*ANXA1*), chemerin (*RARRES2)* and collagen type III α1 (*COL3A1*). Annexin A1 and chemerin are well-known to be expressed by adipose tissue, and their actions, as well as that of collagen III, at islet cells have been discussed in previous chapters. C3 is a key player in the complement cascade, a

vital pathway for the detection and defence against pathogens and foreign material (Copenhaver et al., 2020). Its peptide fragment, C3a, is the product of catalytic conversion by the adipokine, adipsin. Both C3 and C3a peptides are implicated in lipid metabolism and glucose regulation with documented positive correlations with circulating triglycerides, insulin resistance and diabetes incidence (Engström et al., 2005; Koistinen et al., 2001; Muscari et al., 2007). Several studies have detected *C3* mRNA in visceral and subcutaneous adipose tissue, but the contribution of adipose tissue to C3 plasma levels in obesity remains unclear (Clemente-Postigo et al., 2011; Dusserre et al., 2000; Koistinen et al., 2001; MacLaren et al., 2010). There have been reports of significantly greater serum C3 levels in obese subjects compared to lean individuals (Bratti et al., 2017), with BMI rather than metabolic status playing a more relevant role in changes in circulating C3 levels as both lean and obese patients with T2D display similar significant increases compared to non-diabetic controls (Yang et al., 2006). Treatment of mouse (Atanes et al., 2018; Lo et al., 2014) and human islets (Atanes et al., 2018) with C3/C3a stimulated the activity of its target GPCRs, C3AR1 and C5AR1, and led to the potentiation of glucose-stimulated insulin secretion. This was linked to anti-apoptotic effects, and elevated ATP generation and intracellular calcium. Similar observations in islets were made following treatment with the C3AR1/C5AR1 ligand, complement component 5 (C5) (Atanes et al., 2018). Despite the downregulation of multiple islet GPCR peptide ligand mRNAs in obese omental adipose tissue, only *C5* mRNA was significantly decreased. This is in contrast to *C3*, its related complement peptide, whose expression is not significantly altered between lean and obese states (79±20.2% of lean expression). The above mentioned improvements in β-cell function following C3AR1/C5AR1 stimulation are observed in islets from lean, non-diabetic mice and humans. The activity of C3/C5 target GPCRs may have detrimental effects in an obesogenic environment, as receptor antagonism abrogated insulin and glucose intolerance, visceral fat accumulation and inflammation caused by a high-carbohydrate, high-fat diet (Lim et al., 2013). This is further supported by data obtained with $C3aR^{-/-}$ and $C5aR^{-/-}$ mice, which were protected against high-fat diet-induced insulin resistance (Mamane et al., 2009; Phieler et al., 2013). β-cell mass was unaltered in these mice (Phieler et al., 2013), and the mechanisms by which C5 and its receptors influence islet function in obesity requires further investigation.

Comparative analysis of islet GPCR peptide ligand mRNAs in adipose tissue retrieved from lean and obese individuals revealed significant upregulation of only two genes: *CCL3* (MIP-1α) and *CCL4* (MIP-1β). The increase in *CCL3* mRNA expression observed here corroborated similar studies which measured the same elevation in *CCL3* in omental adipose tissue from obese subjects compared to lean individuals (Huber et al., 2008; Keophiphath et al., 2010). It has been reported that its expression is more concentrated in macrophages compared to other cell types of adipose tissue, which is consistent with the production and secretion of chemokines from immune cells. Furthermore, *CCL3* mRNA expression was positively correlated with several inflammatory markers in visceral fat depots, including TNF-α, and was linked to macrophage recruitment and survival (Chan et al., 2022; Keophiphath et al., 2010). The GPCRs CCR1, CCR3, CCR5 and GPR75 are targets of CCL3 action (Ignatov et al., 2006; Sarvaiya et al., 2013); CCR1 and GPR75 are expressed in human islets, and only *CCR1* mRNA expression was significantly increased in obesity, although this observation may be derived from CCR1-expressing immune cell infiltration rather than upregulation within endocrine cells (Atanes et al., 2021). CCR1 and CCR5 are mutual target receptors of both CCL3 and CCL4. In addition to existing as monomeric peptides, mass spectrometry of cell contents and supernatants from human monocytes and lymphocytes indicated that CCL3 and

CCL4 also aggregate with each other and are secreted as heterodimers (Guan et al., 2001). CCL3/CCL4 aggregation may protect against protease-mediated degradation and clearance to enhance chemokine activity, although changes in configuration and high molecular weight may have implications on ligand-receptor binding (Liang et al., 2015; Ren et al., 2010). Potential interactions between the two chemokines are further indicated by an association between the intrapancreatic CCL3:CCL4 ratio and inflammatory processes in T1D: an increased ratio correlated with Th1-cell infiltration, the progression of destructive insulitis and diabetes development in the NOD mouse model; in contrast, a reduced ratio was observed in non-obese diabetes-resistant (NOR) mice and was associated with a Th2-cell-like profile of cytokine production, such as the anti-inflammatory IL-4 (Bergerot et al., 1999; Cameron et al., 2000). Since circulating CCL3 is correlated with circulating CCL4 throughout early T1D progression (Pfleger et al., 2008), the increase in CCL4 may represent a counter mechanism against the inflammatory processes induced by CCL3. More robust data implicating the negative impact of CCL3 in T1D comes from a reduction of destructive insulitis in NOD.CCL3$^{-/-}$ (Cameron et al., 2000). Additionally, co-administration of diabetogenic T-cells and an anti-CCL3 monoclonal antibody into NOD.*Scid* mice, which do not harbour functional T- or B-cells, delayed the onset of diabetes (Cameron et al., 2000). CCL4, on the other hand, is associated with reduced β-cell stress and dampened islet inflammatory responses in mouse models and patients with T1D (Meagher et al., 2007, 2010; Pfleger et al., 2008). Despite sharing some target receptors, evidence points towards CCL3 as a contributor of T1D development whereas CCL4 may confer protection.

Several limitations should be considered in the interpretation of these data. The first caveat of this human study was the unavailability of plasma glucose data which prevented further characterisation of metabolic status beyond BMI. Certain adipokines may be differently expressed in a hyperglycaemic vs normoglycaemic environment regardless of the presence of obesity, thus, this information would be valuable. In addition, due to a limited supply of adipose tissue samples, it was not possible to match patient characteristics between categories. Several factors influence genetic profiles, such as age, gender, race, current medications, comorbidities, and medical history. These variables could not be controlled and therefore contributed to significant variability when adipokine mRNA expression in lean and obese individuals was compared. A greater number of samples are required to reduce variation and increase the chance of finding significant differences in mRNA expression.

In summary, the mRNA expression of a handful of islet GPCR peptide ligands within omental adipose tissue were significantly altered in human obesity. *CCL4* mRNA was significantly upregulated, an observation consistent with those in environmental and genetic mouse models of obesity. Whether the previously published protection of CCL4 seen in T1D extends to obesity and T2D pathophysiology remains unclear. Therefore, the aim of the following chapters was to characterise the effects of Ccl4 on islet cell and adipocyte function to help define its role in obesity.

Chapter 7: Investigating the direct functional effects of Ccl4 on MIN6 β-cells

7.1 Introduction

A dramatic decline in β-cell function and survival fuels diabetes progression, yet there is a deficit in islet-targeting pharmacotherapies which aim to expand β-cell mass or recover the activity of existing β-cells. Despite the availability of numerous diabetes medications (see Section 1.1.2.4), a significant proportion of patients still fail to achieve adequate glycaemic control. Thus, there is a growing need to develop more effective therapies which improve β-cell function and/or promote β-cell mass expansion. The β-cell is the target of adipokine action leading to acute changes to insulin secretion and/or longer-term regulation of the expression of genes that maintain overall β-cell function. Some of these adipokines mediate their effects via GPCRs which are highly druggable entities. The identification of an adipose tissue-derived islet GPCR peptide ligand which has favourable actions at the β-cell has the potential to meet the above therapeutic demand.

The previous chapters in this thesis described qPCR screens of islet GPCR peptide ligand mRNAs in visceral adipose tissue retrieved from multiple models of obesity. Several mRNAs were differentially expressed between lean and obese states, and of these, the expression of *Ccl4* mRNA was significantly upregulated in all models of obesity. There is limited data regarding the effects of Ccl4 on β-cell function with the available publications investigating the role of Ccl4 in T1D pathology (Hanifi-Moghaddam et al., 2006; Meagher et al., 2007, 2010; Pfleger et al., 2008; Rydén & Faresjö, 2013; Thorsen et al., 2014).

Therefore, Ccl4 was selected for islet cell experiments which aimed to functionally characterise this adipokine. Previous publications which assessed the migration of several cell types exposed to Ccl4, which acts as a chemotaxis peptide, used a range of concentrations from 1ng/mL to 1000ng/mL (Grindstaff & Baer, 2020; Hannan et al., 2006; Lee et al., 2018; Lien et al., 2018; Quandt & Dorovini-Zis, 2004; Reinart et al., 2013). The biological activity of recombinant Ccl4 was shown to be 20-100ng/mL as determined by chemotaxis bioassays using immune cells. Based on these reports, concentrations between 5-100ng/mL of recombinant Ccl4 peptide were used in the functional experiments described in this chapter.

The MIN6 β-cell line provides a preliminary model to assess the effects, if any, of peptides of interest on β-cell function prior to the use of primary mouse islets which require time-consuming protocols using animal models. This is possible due to functional similarities between MIN6 β-cells and mouse islets, such as GLUT2 expression, glucokinase activity and insulin secretory capacity (Miyazaki et al., 1990; Persaud et al., 2014). Therefore, in the current chapter, experiments were performed using MIN6 β-cells to investigate the influence of Ccl4 treatment on multiple cellular functions, including apoptosis, proliferation, and insulin secretion. Potential GPCRs which mediate the actions of Ccl4 were also interrogated and their mRNAs were quantified in MIN6 β-cells.

7.2 Methods

7.2.1 Cell viability

The viability of MIN6 β-cells treated with Ccl4 was assessed using the Trypan blue exclusion test. Unlike the intact membranes of viable cells, the Trypan blue azo dye can penetrate through the damaged membranes of dying and dead cells. Thus, Trypan blue-stained non-viable cells can be identified, and the viability of a cell suspension can be measured. MIN6 β-cells were seeded into 6-well plates at a density of 250,000-300,000 cells/2mL/well and incubated at 37°C, 5% CO_2 and 95% humidity in DMEM containing 25mM glucose, 10% (v/v) FBS, 100U/mL penicillin, 100µg/mL streptomycin, 2mM L-glutamine and 0.0005% (v/v) β-ME in the absence or presence of recombinant mouse Ccl4 (5-100ng/mL). Following a 48-hour exposure to Ccl4, Trypan blue uptake into MIN6 β-cells was assessed by their incubation in Trypan blue (0.2% w/v) for 15 minutes. Trypan blue-stained non-viable cells and non-stained healthy cells were visualised by light microscopy.

7.2.2 Cytokine- and palmitate-induced apoptosis

Apoptosis of MIN6 β-cells was detected using the Caspase-Glo® 3/7 Assay. MIN6 β-cells were seeded into 96-well plates at a density of 20,000 cells/100µL/well and incubated overnight at 37°C, 5% CO_2 and 95% humidity in DMEM containing 25mM glucose, 10% (v/v) FBS, 100U/mL penicillin, 100µg/mL streptomycin, 2mM L-glutamine and 0.0005% (v/v) β-ME. Cells were exposed to either medium supplemented with 500µM palmitate or a cocktail of pro-apoptotic cytokines (0.05U/µL IL-1β, 1U/µL TNF-α and 1U/µL IFN-γ) in the presence or absence of Ccl4 (5-100ng/mL) for 20 hours. Incubation with Caspase-Glo® Reagent for 1 hour was followed by the measurement of luminescence, as described in Sections 2.9.1 and 2.9.2, which correlated with caspase-3/7 activity.

7.2.3 BrdU ELISA proliferation

Proliferation of MIN6 β-cells was measured using the Cell Proliferation ELISA Kit which allows quantification of BrdU incorporation into the DNA of replicating. MIN6 β-cells were seeded into 96-well plates at a density of 15,000 cells/100µL/well and incubated overnight at 37°C, 5% CO_2 and 95% humidity in DMEM containing 25mM glucose, 10% (v/v) FBS, 100U/mL penicillin, 100µg/mL streptomycin, 2mM L-glutamine and 0.0005% (v/v) β-ME. Following a 24-hour starvation period in 0% (v/v) DMEM, cells were exposed to DMEM containing either 2% or 10% (v/v) FBS in the absence or presence of recombinant mouse Ccl4 (5-100ng/mL) for 48 hours. Thereafter, β-cells were labelled with 100µM BrdU reagent for 2 hours at 37°C, 5% CO_2 and 95% humidity, and proliferation was determined by colorimetric quantification of Brdu incorporation into newly synthesised DNA, as described in Section 2.10.1.

7.2.4 Insulin secretion

Static incubation experiments were performed to assess insulin secretion from Ccl4-treated MIN6 β-cells that were stimulated by the amino acid metabolite, KIC (Section 2.8.1.1). Cells were seeded into a 96-well plate at a density of 25,000 cells/100µL/well using sterile-filtered DMEM containing 25mM glucose, 10% (v/v) FBS, 100U/mL penicillin, 100µg/mL streptomycin, 2mM L-glutamine and 0.0005% (v/v) β-ME. Following overnight incubation at 37°C, 5% CO_2

and 95% humidity, medium was replaced with DMEM containing 2.5mM glucose. After 16 hours, MIN6 β-cells were incubated for 1 hour with Gey and Gey buffer containing 2mM glucose with or without 10mM KIC, in the absence or presence of recombinant Ccl4 (100ng/mL). The α_2-adrenoceptor agonist, clonidine (10μM), was used as a $G\alpha_i$-coupled receptor control agonist. The supernatants were retrieved and stored at –20°C until measurement of insulin content by radioimmunoassay (Section 2.8.2).

7.2.5 PRESTO-Tango β-arrestin reporter assays

The PRESTO-Tango β-arrestin reporter assay measures the activation of target GPCRs by a ligand of interest (see Section 2.7.1). Thus, the assay was performed to determine which GPCRs are the target of CCL4 action. HTLA cells were seeded into a 96-well plate at a density of 25,000 cells/100μL/well and incubated overnight at 37°C, 5% CO_2 and 95% humidity in DMEM containing 10% (v/v) dialysed FBS. Individual plasmids encoding Tango versions of ACKR2, CCR1, CCR2, CCR5, CCR9, CXCR1, and positive control plasmids A2AR and CHM3, were transfected into HTLA cells. Due to a limited selection of GPCR-expressing plasmids, the documented CCL4 targets, CCR1 and CCR9, could not be included in the GPCR screening. Cells were incubated in assay buffer with or without 100ng/mL recombinant human CCL4 for 1 hour at 37°C. Positive control GPCRs, α_2-adrenoceptor, A2AR, and cholinergic receptor muscarinic 3 receptor, CHM3, were also activated by agonists, clonidine and carbachol, respectively. Bright-Glo™ Reagent was added to wells for 15 minutes and luminescence was measured as described in Section 2.7.3.

7.2.6 Ccl4-targeted GPCR qPCR screening

Standardised RNA extraction and RT-qPCR protocols were performed to quantify the expression of Ccl4-targeted GPCR mRNAs in MIN6 β-cells. The RNeasy Mini Kit was used to extract and purify RNA from MIN6 β-cells. Cells were seeded into 6-well plates at a density of 250,000-300,000 cells/2mL/well and incubated in DMEM containing 25mM glucose, 10% (v/v) FBS, 100U/mL penicillin, 100μg/mL streptomycin, 2mM L-glutamine and 0.0005% (v/v) β-ME for 2-3 days at 37°C, 5% CO_2 and 95% humidity. MIN6 β-cells were washed with PBS, trypsinised and pelleted by centrifugation. Samples were then processed using ethanol-based buffers, spin columns and multiple centrifuge steps to isolate high-quality RNA, as described in Section 2.6.1. A Nanodrop™ 1000 spectrophotometer was used to measure the concentration and purity of RNA extracted from MIN6 β-cells. RT reactions (50ng/μL) were prepared using the High-Capacity cDNA Reverse Transcription Kit and RT was performed in a T100™ thermal cycler (Section 2.2.9). The mRNA expression of Ccl4-activating receptors, *Ackr2*, *Ccr1*, *Ccr2*, *Ccr5*, *Ccr9*, *Cxcr1* and *Cxcr5*, were then quantified in MIN6 β-cells using a SYBR Green fluorescent dye-based qPCR protocol and a LightCycler® 96 (Section 2.2.10).

7.3 Results

7.3.1 The effects of Ccl4 on MIN6 β-cell viability

To determine whether exposure to Ccl4 affects viability, MIN6 β-cells were treated with 5-100ng/mL Ccl4 for 48 hours and cell viability was measured by assessing the extent of Trypan blue uptake. Whilst no significant changes in MIN6 β-cell viability were observed following treatment with Ccl4 at all concentrations compared to control media (% relative to control:

control: 100.0±1.21; +5ng/mL: 99.3±1.39; +10ng/mL: 93.1±3.85; +50ng/mL: 91.4±6.29; +100ng/mL: 87.7±6.18; n=4; ns vs control) (Figure 41), there appears to be a concentration-dependent downward trend.

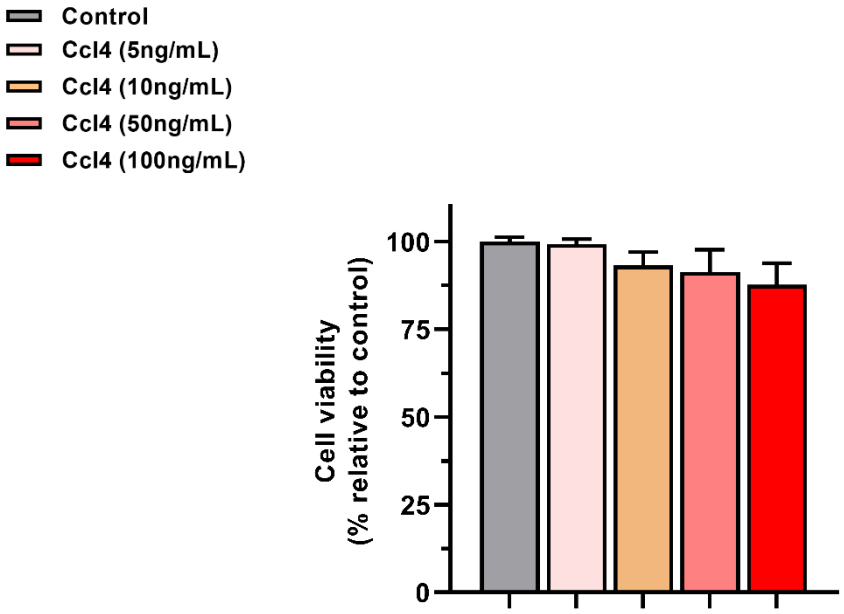

Figure 41. The effect of 48-hour treatment with Ccl4 on MIN6 β-cell viability. Data are expressed as the mean ± S.E.M. One-way ANOVA; n=4.

7.3.2 The effects of Ccl4 on cytokine- and palmitate-induced MIN6 β-cell apoptosis

To determine whether Ccl4 affects apoptosis, MIN6 β-cells were treated with 5-100ng/mL Ccl4 for 24 hours in the presence or absence of either mixed cytokines or the saturated fatty acid, palmitate. Caspase 3/7 activity, representative of the degree of cell apoptosis, was quantified using a proluminescent assay.

A mixed cytokine cocktail of IL-1β, TNF-α and IFN-γ induced a significant increase in MIN6 β-cell apoptosis (% relative to control: 595.2±37.02 vs 100.0±7.88; n=3 independent experiments; $p<0.0001$) (Figure 42, left). The addition of 100ng/mL Ccl4 significantly reduced the apoptotic effect of mixed cytokines (% relative to control: +100ng/mL: 469.1±24.54; $p<0.01$ vs control), but lower concentrations of Ccl4 had no affect (% relative to control: +5ng/mL: 532.8±25.02; +10ng/mL: 502.8±18.06; +50ng/mL: 497.8±19.54; ns vs control).

Similar to mixed cytokines, the saturated fatty acid, palmitate, significantly upregulated MIN6 β-cell apoptosis compared to control media (% relative to control: 291.5±14.25 vs 100.0±6.24; n=3 independent experiments; $p<0.0001$) (Figure 42, right). All concentrations of Ccl4 significantly protected against palmitate-induced MIN6 β-cell apoptosis in a concentration dependent manner (% relative to control: +5ng/mL: 232.2±17.74; +10ng/mL: 222.7±13.59; +50ng/mL: 197.5±12.65; +100ng/mL: 195.1±9.69; $p<0.0001$ vs control).

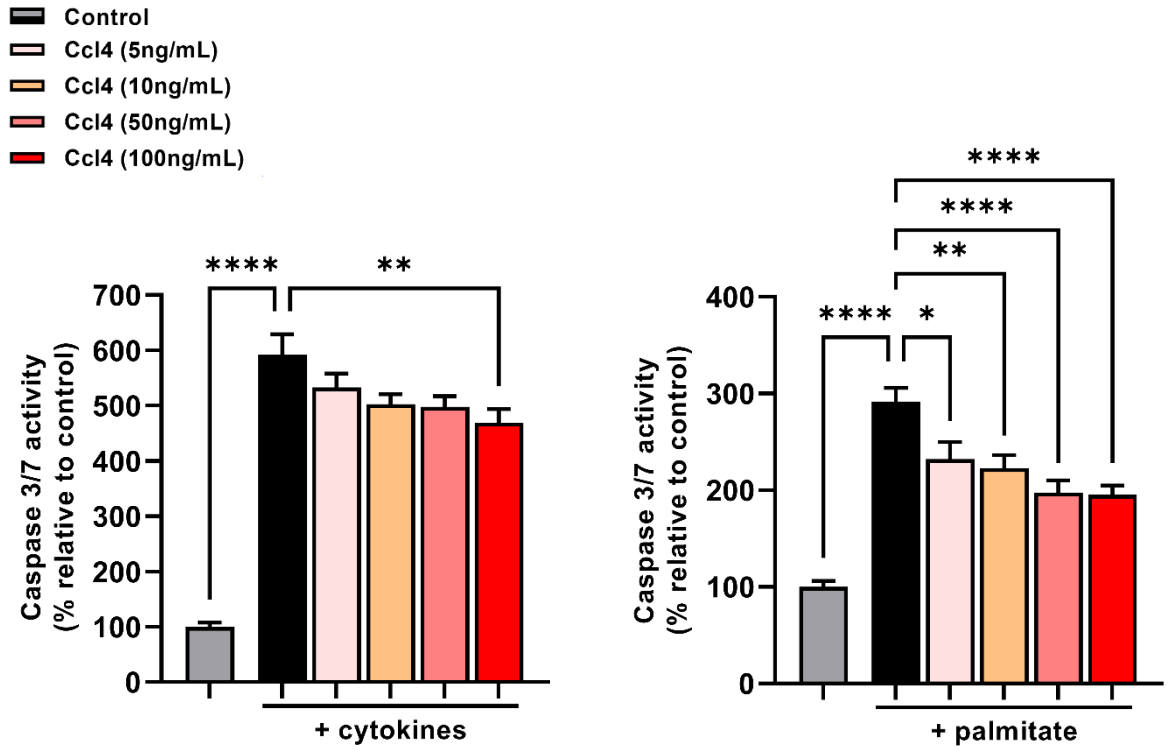

Figure 42. The effect of 24-hour treatment with Ccl4 on cytokine-induced (left) and palmitate-induced (right) apoptosis in MIN6 β-cells. Data are expressed as the mean ± S.E.M relative to control without cytokines or without palmitate. One-way ANOVA; n=3 independent experiments; *p<0.05, **p<0.01, ***p<0.001, ****p<0.0001 vs control.

7.3.3 The effects of Ccl4 on MIN6 β-cell proliferation

To determine whether Ccl4 affects proliferation, MIN6 β-cells were exposed to 5-100ng/mL Ccl4 for 48 hours and BrdU incorporation was quantified by ELISA. 10% FBS significantly increased MIN6 β-cell proliferation compared to 2% FBS (% BrdU incorporation relative to 2% FBS control: 176.1±6.49 vs 100.0±4.90; n=3 independent experiments; p<0.0001) (Figure 43). 100ng/mL Ccl4 significantly attenuated serum-stimulated MIN6 β-cell proliferation (% BrdU incorporation relative to 2% FBS control: +100ng/mL: 129.8±5.32; p<0.001 vs control) whilst no differences were observed with 5, 10 and 50ng/mL Ccl4 (% BrdU incorporation relative to 2% FBS control: +5ng/mL: 169.2±7.99; +10ng/mL: 162.0±7.89; +50ng/mL: 156.7±9,51; ns vs control).

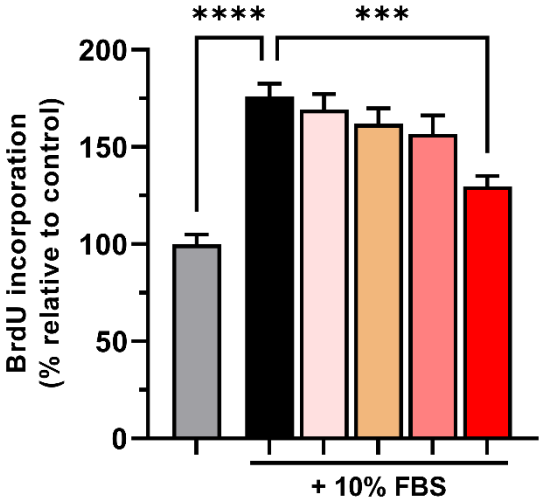

Figure 43. The effect of 48-hour treatment with Ccl4 on MIN6 β-cell proliferation. Data are expressed as the mean ± S.E.M relative to 2% FBS control. One-way ANOVA; n=3 independent experiments; ***p<0.001, ****p<0.0001 vs control.

7.3.4 The effects of Ccl4 on insulin secretion from MIN6 β-cells

The MIN6 β-cells used in the functional experiments described in this chapter were relatively late passage and did not show reproducible elevations in insulin secretion in response to elevation in glucose concentration. Therefore, to determine whether Ccl4 affects nutrient-stimulated insulin secretion, MIN6 β-cells were exposed to Ccl4 (100ng/mL) in the presence of the leucine metabolite, KIC (10mM), and insulin levels in harvested supernatant were quantified using radioimmunoassay. Incubation with KIC significantly increased insulin secretion vs control buffer (% relative to control: 225.8±43.71 vs 100.0±12.57; n=3 independent experiments; p<0.01 vs control buffer) (Figure 44). Treatment with 100ng/mL Ccl4 failed to induce any significant changes in KIC-stimulated insulin secretion (% relative to control: +100ng/mL: 189.1±24.29; ns vs KIC-treated control). As expected, clonidine significantly attenuated KIC-induced insulin secretion due to its action at the inhibitory $G\alpha_i$-coupled α_2-adrenoceptor (% relative to control: +10μM clonidine: 19.9±4.69; p<0.0001 vs KIC-treated control).

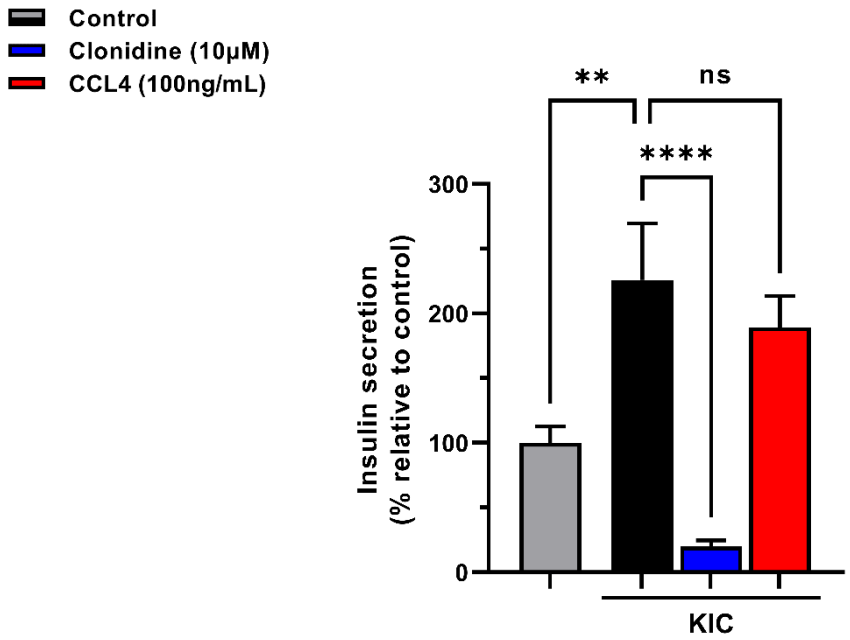

Figure 44. The effect of 1-hour treatment with Ccl4 on KIC-induced insulin secretion from MIN6 β-cells. Clonidine acted as a negative control to inhibit KIC-stimulated insulin secretion. Data are expressed as the mean ± S.E.M. relative to 2mM glucose control (grey bar). One-way ANOVA; n=3 independent experiments; **p<0.01, ****p<0.0001, ns: non-significant vs control.

7.3.5 Identification of Ccl4-activated GPCRs using PRESTO-Tango β-arrestin reporter assay technology

17 chemokine GPCRs were screened to interrogate potential receptors activated by CCL4. Of these, CCL4 (100ng/mL) significantly activated CXCR1 (relative luminescence units: control: 5953±876.1; +100ng/mL CCL4: 9223±697.0; n=3 independent experiments; p<0.05 vs control assay buffer) and CXCR5 (relative luminescence units: control: 33700±389.6; +100ng/mL CCL4: 53556±5328.0; p<0.05 vs control) (Figure 45). The remaining receptors displayed no significant increase or decrease in activity with treatment of CCL4. As expected, the positive controls, clonidine and carbachol, significantly activated their respective target GPCRs, A2AR (relative luminescence units: control: 19033±6662.0; +10μM clonidine: 1897537±203463; p<0.0001 vs control) and CHM3 (relative luminescence units: control: 29627±3410; + 500μM carbachol: 3487811±123380; p<0.0001 vs control).

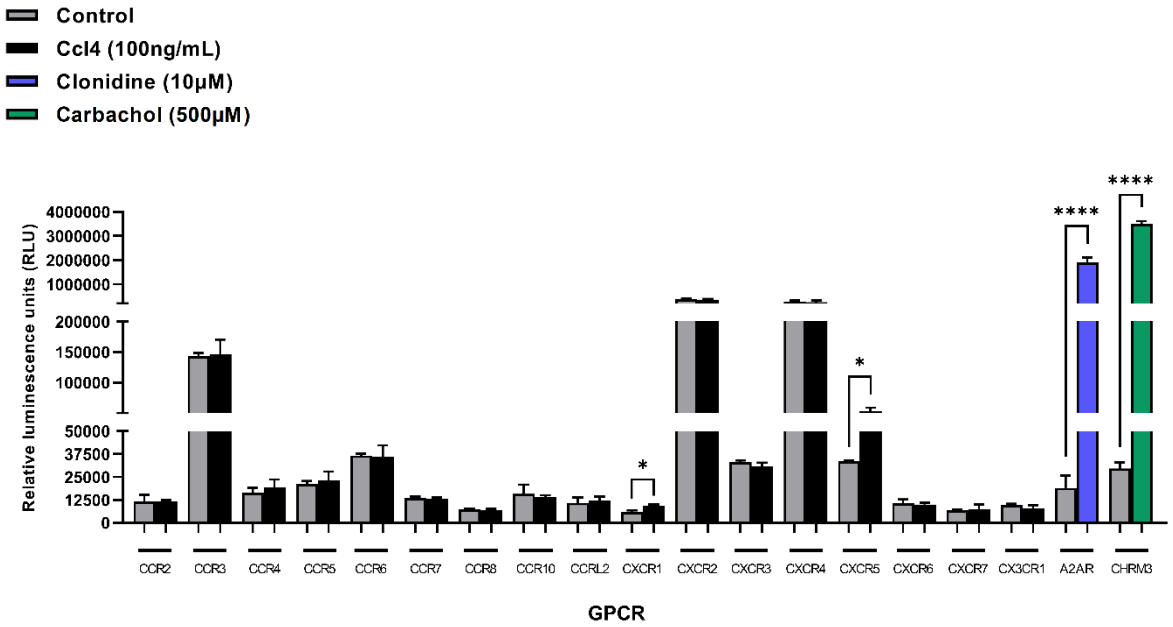

Figure 45. Quantification of GPCR activity in transfected HTLA cells using the PRESTO-Tango β-arrestin reporter assay. Relative luminescence corresponds to the activation level of GPCRs of interest. Clonidine and carbachol acted as positive controls acting at $G\alpha_i$- and $G\alpha_{q/11}$-coupled GPCRs, respectively. Data are expressed as the mean ± S.E.M. Multiple unpaired two-tailed t-tests; n=3 independent experiments; *p<0.05, ****p<0.0001 vs control.

7.3.6 Expression of Ccl4-targeted GPCR mRNAs in MIN6 β-cells

Results from the PRESTO-Tango β-arrestin reporter experiments revealed CXCR1 and CXCR5 are activated by CCL4. Due to the limited availability of plasmids expressing potential chemokine-activated GPCRs of interest, additional Ccl4-targeted GPCRs, if any, were searched for in the literature, which indicated that Acrk2, Ccr1, Ccr2, Ccr5 and Ccr9 are Ccl4-activated (Bonecchi et al., 2004; Civatte et al., 2005; Guan et al., 2002; Nibbs et al., 1997). To determine the target GPCR(s) which mediated the functional effects of Ccl4 on MIN6 β-cells, a qPCR screening was performed to quantify the mRNA expression levels of *Acrk2*, *Ccr1*, *Ccr2*, *Ccr5*, *Ccr9*, *Cxcr1* and *Cxcr5* in MIN6 β-cells relative to the housekeeping gene, *Actb*. Although most mRNAs encoding putative Ccl4 receptors were quantifiable, the expression levels of all mRNAs were extremely low (<0.0001% of *Actb*) (Figure 46, Supplementary Table 25).

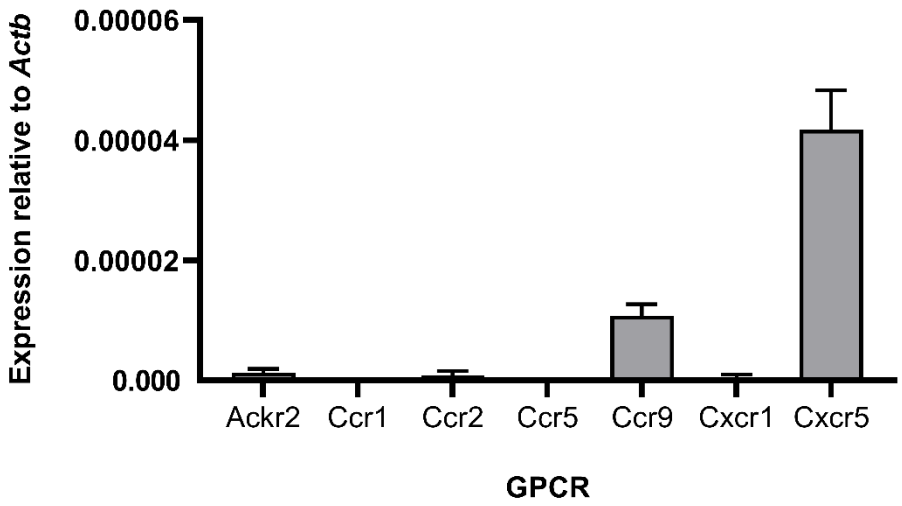

Figure 46. The expression of Ccl4-target GPCR mRNAs in MIN6 β-cells. Data are expressed as the mean ± S.E.M. n=4.

7.4 Discussion

The present chapter investigated a potential endocrine function for Ccl4 at β-cells. Experiments measured the effects of recombinant mouse Ccl4 on MIN6 β-cell viability, apoptosis, proliferation, and insulin secretion, and aimed to identify potential Ccl4-target GPCRs which mediated these effects.

Ccl4 over the range of 5-100ng/mL was well-tolerated by MIN6 β-cells, so this concentration range was used in functional experiments, although it is important to consider the downward trend in MIN6 β-cell viability and the possibility that the lack of significance was due to low power (n=4) and type 2 error. This is particularly relevant when interpreting Ccl4-mediated protective effects of MIN6 β-cells against apoptosis induced by both a mixed cytokine cocktail and the saturated fatty acid, palmitate. No significant changes to basal MIN6 β-cell apoptosis in the presence of Ccl4 (not shown) supported observations made during Trypan Blue exclusion testing, therefore indicating that cell loss did not contribute to reduced caspase-3/7 activity readouts. Nevertheless, increases in n-number and subsequent power, as well as performance of additional cell viability and cytotoxicity assays, e.g. tetrazolium reduction and lactate dehydrogenase release assays, should be implemented to confirm tolerance of Ccl4 by β-cells. Although there is limited data on the effects of Ccl4 on β-cell apoptosis, there are a handful of *in vitro* and *in vivo* studies suggesting an anti-apoptotic function of Ccl4 in other cell types. For example, incubation of preosteoclast cells with 10ng/mL Ccl4 decreased expression of the pro-apoptotic regulator, Bax, and protected against apoptosis induced by hydrogen peroxide (Lee et al., 2018). Neutralising Ccl4 antibodies increased apoptosis in lymphoblastoid cell lines (Tsai et al., 2013) and short hairpin RNA (shRNA) against CCL4 expression raised cell apoptosis in HEC-1B and AN3CA cells (Hua & Tian, 2017). Similarly, siRNA-induced silencing of Ccl4 enhanced chondrocyte apoptosis and led to a significant reduction in chondrocyte viability (Yang et al., 2019). In the latter study, Ccl4 was identified as a target gene of the microRNA, miR-495, whose activity decreased Ccl4 expression. Interestingly, miR-495 also regulates the expression of TP53INP1, a β-cell apoptotic factor which is upregulated in T2D islets (Kameswaran et al., 2014; Okamura et al., 2001). A role for

miR-125b in regulating CCL4 expression in human immune cells has also been reported, as shRNA-induced knockdown increased CCL4 protein production in monocytes and naïve CD8 T-cells, whereas overexpression reduced CCL4 mRNA and protein expression (Cheng et al., 2015). Thus, microRNAs may be involved in modulating Ccl4 levels within stressed islets through epigenetic mechanisms *in vivo*. Previous publications which have investigated inflammatory mediators in T1D showed IL-4-induced protection against insulitis in NOD mice was associated with a 6-fold increase in intrapancreatic Ccl4 (Cameron et al., 1997, 2000). A later investigation on the influence of Ccl4 action showed intradermal delivery of Ccl4-expressing plasmids suppressed the recruitment of CD8+ T-cells and preserved insulin expression within islets (Meagher et al., 2007). Moreover, islet T-cells retrieved from Ccl4-administered mice displayed a greater anti-inflammatory secretory profile than control-treated mice, as indicated by diminished IFN-γ but augmented IL-4 and IL-10 production (Meagher et al., 2007). Further antagonism of pro-inflammatory pathways is shown by Ccl4-mediated blockage of CD4/IL-16 interactions at the surface of human T-cells to decrease their migration (Mashikian et al., 1999). Overall, Ccl4 appears to hinder the recruitment of diabetogenic immune cells into the islets whilst simultaneously promoting anti-inflammatory mediators. The apoptotic phase and the presence of pro-apoptotic factors can also affect chemokine signalling by regulating cell-surface receptor expression. TNF-α, for example, reduced CCR5 expression in late apoptotic human polymorphonuclear (PMN) cells whereas anti-inflammatory mediators, such as lipoxin A_4, increased it (Ariel et al., 2006). The observation that Ccl4 expression is induced by TNF-α in human neutrophils (Glennon-Alty et al., 2021) but repressed by IFN-γ in mouse macrophages (Rapisarda et al., 2002) highlights the complexity of chemokine dynamics in immune cell responses to inflammatory signals. Interestingly, CCR5 receptors present on late apoptotic cells were reported to have significantly greater affinity for CCL4 compared to receptors on early apoptotic and live cells, as evidenced by elevated CCR5/CCL4 binding (Ariel et al., 2006). Treatment with zVAD-fmk, a general caspase inhibitor which prevents apoptosis, abrogated CCR5/CCL4 binding, indicating a caspase-dependent regulation of chemokine signalling (Ariel et al., 2006).

In contrast to the earlier studies described above and the observations here that Ccl4-induced protection of MIN6 β-cells against pro-inflammatory stimuli, other studies have suggested that Ccl4 promotes inflammation. For example, Ccl4 was co-secreted with IFN-γ from natural killer (NK) cells and CD8+ T-cells, and acted synergistically to stimulate the release of TNF-α, IL-12 and nitric oxide from macrophages (Dorner et al., 2002). In support, Ccl4 treatment was also shown to increase the cytotoxicity of CD56+ NK cells (Maghazachi et al., 1996). In β-cells, Ccl4 blockade has been linked to a reduction in Ccl4-induced inflammation as the expression of inflammatory cytokines, IL-6 and TNF-α, was reduced in the NIT-1 β-cell line by siRNA-mediated knockdown of Ccr2 and Ccr5, GPCRs for which Ccl4 is a reported ligand (Chang et al., 2021). Many studies, such as those described above, focus largely on the well-characterised GPCR, CCR5. This is particularly due to the role of CCR5 as a co-receptor for HIV-1 infection with CCL4 acting as a suppressive factor (Petkov et al., 2022). The data in this chapter described qPCR experiments which quantified the full range of proposed Ccl4 GCPRs (Ackr2, Ccr1, Ccr2, Ccr5, Ccr9, Cxcr1 and Cxcr5) and deemed all receptors absent (<0.0001% of *Actb* expression) in unstressed MIN6 β-cells. Other studies have also reported undetectable levels of *Ccr1*, *Ccr2* and *Ccr5* mRNAs in MIN6 β-cells (Cai et al., 2011; Liu et al., 2013). It is important to note that the thresholds for expressed, trace and absent categories for gene expression are arbitrary. Furthermore, GPCR mRNA expression does not always correlate

with protein expression at the cell surface (Michel et al., 2009). Some receptor mRNAs, especially that encoding Cxcr5, were quantifiable in this current chapter, therefore, translation to functional proteins cannot be completely ruled out. GPCR expression is also dynamically regulated and receptor density is influenced by various physiological conditions and pharmacological treatments (Insel et al., 2007). Ariel et al. (2006) provide an example of how chemokine receptor expression and activity become altered by the presence of pro-inflammatory factors. It would be interesting to see whether the expression of Ccl4-target GPCR mRNAs are altered in MIN6 β-cells exposed to Ccl4 and/or apoptotic stimuli, and how receptor-ligand binding kinetics may be affected. Conversely, while some receptor mRNAs were quantifiable in MIN6 β-cells, Ccl4 action is potentially mediated through one or more unknown receptor(s) present within MIN6 β-cell membranes. To investigate this possibility, future PRESTO-Tango β-arrestin reporter experiments will require the generation of Tango plasmids expressing additional chemokine receptor targets. Unexpectedly, data generated from the PRESTO-Tango experiments disputed CCR2 and CCR5 as established CCL4 targets, as 100ng/mL CCL4 did not significantly activate these receptors in HTLA cells. Human CCL4 exists in two forms – full length and truncated – and each exhibits differential receptor specificity. Both forms induce CCR5 signalling, but, unlike full length CCL4, truncated CCL4, which lacks two N-terminal amino acids, is reported to also activate CCR1 and CCR2B (Guan et al., 2001, 2002). Full length recombinant human CCL4 peptide was used for the PRESTO-Tango β-arrestin reporter assays and therefore this may explain the lack of observed CCR2 activation. The reason for the absence in CCR5 activation by CCL4 is unclear and would prompt using fresh CCR5 plasmids and positive control ligands such as CCL3 in future repeat experiments. CCL4 treatment significantly activated CXCR1 and CXCR5 which have not been previously reported as receptors for CCL4. They therefore represent potential new CCL4 targets for further investigation. Studies of CXCR5 and its established ligand, CXCL13, in T1D development were initiated in transgenic mice whereby Cxcl13-expressing islets attracted Cxcr5-expressing B-cells (Luther et al., 2000), although subsequent studies have yielded equivocal results. CXCR1/2 inhibitors are currently undergoing clinical trials in patients with T1D and islet transplant recipients following the successful suppression of IL-8-induced neutrophil recruitment into islets and improved glycaemic control in diabetic NOD mice (Citro et al., 2012; Maffi et al., 2020; Piemonti et al., 2022; Witkowski et al., 2021). These benefits, however, were not the result of improved insulin secretion from β-cells (Maffi et al., 2020).

Ccl4 had no effect on KIC-induced insulin secretion from MIN6 β-cells. As explained in Section 1.2.3.1, insulin secretion is a Ca^{2+}-dependent process. Ccl4-target chemokine receptors are $G\alpha_{i/o}$-coupled receptor, therefore, ligand binding and subsequent activation of the $G\alpha_{i/o}$ subunit suppresses AC activity, cAMP production, and PKA and EPAC activity (Section 1.6.1.1). Whilst this pathway in isolation decreases intracellular calcium levels, chemokine action is largely mediated through Gβγ subunits leading to PLC activation, PIP_2 hydrolysis and IP_3 generation, and increased cytosolic Ca^{2+} (Mueller et al., 2002; Oppermann, 2004; Upadhyaya et al., 2020). Accordingly, CCL4 has previously increased intracellular calcium concentrations in human smooth muscle cells in a CCR5-dependent manner (Schecter et al., 2000), in human NK cells (Loetscher et al., 1996), and in Ccr5-transfected Chinese hamster ovary (CHO) cells (Mueller et al., 2002). Thus, the lack of Ca^{2+}-dependent insulin secretory effects may reflect that it does not induce Gβγ signalling in MIN6 β-cells and the absence of an inhibitory effect on insulin release also indicates an absence of $G\alpha_{i/o}$ coupling. The anti-proliferative effects of Ccl4 observed here in MIN6 β-cells are consistent with observations that treatment of STZ-induced diabetic mice with anti-Ccl4 antibodies increased islet cell proliferation and serum

insulin levels, leading to improved plasma glucose control (Chang et al., 2021). It is important to note the caveat in the Ccl4 treatment periods between insulin secretion (1 hour) and proliferation (48 hours) experiments described here. Future experiments in which insulin secretion is measured from MIN6 β-cells exposed to Ccl4 for 48 hours will help determine whether the reduction in β-cell proliferation translates to a decrease in insulin secretory capacity. Unlike the enhanced islet cell proliferation following Ccl4 inhibition seen in Chang et al. (2021), other studies have shown that Ccl4 promotes cell proliferation: 10ng/mL Ccl4 increased the proliferation of NK cells (Maghazachi et al., 1996); neutralising Ccl4 antibodies diminished cell proliferation in lymphoblastoid cell lines (Tsai et al., 2013); silencing of CCL4 gene expression using shRNA significantly impaired human endometrial cancer (EC) cell growth (Hua & Tian, 2017). This proliferative role may be mediated via CCR5 whose additional PI3K pathway has been linked to cell survival, growth and proliferation (Upadhyaya et al., 2020), and this receptor is absent in MIN6 β-cells.

In summary, Ccl4 has anti-apoptotic and anti-proliferative effects on MIN6 β-cells that are potentially mediated through unidentified receptor(s), while acute treatment of MIN6 β-cells with Ccl4 had no effect on insulin secretion. PRESTO-Tango β-arrestin reporter assays have identified two previously unknown GPCR targets of CCL4 whose roles in β-cell function have yet to be determined. There is much disparity between published studies regarding Ccl4 function, and data in β-cells and/or islets are extremely limited. The effects of Ccl4 observed in MIN6 β-cells will need to be investigated in primary islets to determine whether they are of physiological relevance, and this was carried out in the following chapter.

Chapter 8: Investigating the direct functional effects of Ccl4 on primary mouse islets

8.1 Introduction

Immortalised insulin-secreting cell lines provide a valuable tool for obtaining preliminary data regarding the functional effects of candidate peptides on β-cell function. Indeed, the previous chapter in which MIN6 β-cells were treated with recombinant Ccl4 revealed anti-apoptotic and anti-proliferative actions without effects on insulin secretory capacity. The similarities in physiological functions to primary β-cells allow predictions to be made from MIN6 β-cell experiments. However, there are no guarantees that results will be replicated as the characteristics of cell lines can deviate from those of the original tissue. With serial passaging, cell lines also tend to undergo genotypic and phenotypic changes that lead to further variation. Moreover, cell lines do not mimic an *in vivo* environment as MIN6 β-cells are maintained as a 2-dimensional (2D) monolayer in the absence of other islet cells; this differs greatly from the 3D islet structure in which hetero- and homotypic contacts between cell types support the proper functioning of β-cells in islets. Taken together, it is possible that findings in MIN6 β-cells may not be replicated in primary islets.

Consequently, in this chapter, the functional effects of Ccl4 were investigated in mouse islets. Based on previously reported experimental Ccl4 concentrations and the biological activity of recombinant Ccl4 being 20-100ng/mL, concentrations of 5-100ng/mL of recombinant mouse Ccl4 peptide were used in the functional experiments described in this chapter. As for experiments conducted in MIN6 β-cells, apoptotic, proliferative and insulin secretory effects in mouse islets were assessed, and the expression of previously identified Ccl4-target GPCR mRNAs were measured.

8.2 Methods

8.2.1 Cytokine- and palmitate-induced apoptosis

Apoptosis of primary mouse islets induced by either 500μM palmitate or a cocktail of pro-apoptotic cytokines (0.05U/μL IL-1β, 1U/μL TNF-α and 1U/μL IFN-γ) was detected using the Caspase-Glo® 3/7 Assay. Isolated islets were incubated overnight with or without Ccl4 (5-100ng/mL) in RPMI containing 5.5mM glucose, 10% (v/v) FBS, 100U/mL penicillin, 100μg/mL streptomycin and 2mM L-glutamine. Thereafter, 5 islets/40μL/well (6 wells per treatment group) were incubated in fresh RPMI supplemented with 2% (v/v) FBS and in the presence or absence of an apoptotic inducer and/or Ccl4 (5-100ng/mL) for 20 hours. Incubation with Caspase-Glo® Reagent for 1 hour was followed by the measurement of luminescence, as described in Sections 2.9.1 and 2.9.2, which correlated with caspase-3/7 activity.

8.2.2 Proliferation of mouse islets

Immunofluorescence staining of *ex vivo* mouse islets was performed to assess islet cell number and β-cell proliferation. Groups of 5-10 mouse islets were maintained in RPMI containing 5.5mM glucose, 10% (v/v) FBS, 100U/mL penicillin, 100μg/mL streptomycin and 2mM L-glutamine and in the absence or presence of 100ng/mL Ccl4. Following a 72-hour

incubation period at 37°C, 5% CO_2 and 95% humidity, islets were fixed in 4% PFA for 45 minutes at room temperature. After washing three times in PBS, islets were then permeabilised for 2 hours at room temperature with 0.2% v/v Triton X-100 in PBS, 0.8% FBS and 1% BSA. Subsequently, islets were treated with primary antibodies targeting insulin, glucagon, somatostatin, and the nuclear proliferation marker, Ki67 (Section 2.10.2). After an overnight incubation at room temperature, islets were treated with DAPI and the corresponding secondary antibodies for 2 hours at room temperature. Once islets were mounted onto coverslips, images were captured using a Nikon Eclipse Ti-E Inverted A1 inverted confocal microscope and analysed using ImageJ and Cell Profiler software.

8.2.3 Insulin secretion

Static incubation experiments were performed to assess the effect of Ccl4 on glucose-stimulated insulin secretion from mouse islets. Groups of 3 islets per replicate per condition were incubated for 1 hour with Gey and Gey buffer containing 2mM or 20mM glucose with or without recombinant Ccl4 (5-100ng/mL) as described in Section 2.8.1.2. The muscarinic receptor agonist, carbachol (500µM), and the α_2-adrenoceptor agonist, clonidine (10µM), were used as positive and negative controls, respectively. The supernatants were retrieved, pre-diluted in borate buffer, and stored at –20°C until measurement of insulin content by radioimmunoassay (Section 2.8.2).

8.3.4 Expression of Ccl4-targeted GPCR mRNAs in mouse islets

Standardised RNA extraction and RT-qPCR protocols were performed to quantify the expression of Ccl4-targeted GPCR mRNAs in islets isolated from CD1 mice. Following isolation and overnight incubation, groups of 150-200 mouse islets were dissolved in TRIzol® Reagent. The addition of chloroform and a subsequent centrifugation cycle led to the separation of an upper aqueous phase containing RNA which was transferred to a mixture of cooled 100% isopropanol and glycogen (Section 2.6.1). After a 1-hour incubation at –70°C, samples were centrifuged to form RNA pellets. Isopropanol was replaced with 75% ethanol, samples underwent a final centrifuge step, and all ethanol was removed to facilitate the drying of RNA pellets at 37°C. Once reconstituted in DNase-RNase-free water, the yield and purity of RNA was determined by a Nanodrop™ 1000 spectrophotometer. RT reactions (50ng/µL) were prepared using the High-Capacity cDNA Reverse Transcription Kit and RT was performed in a T100™ thermal cycler (Section 2.2.9). The mRNA expression of Ccl4-activating receptors, *Ackr2*, *Ccr1*, *Ccr2*, *Ccr5*, *Ccr9*, *Cxcr1* and *Cxcr5*, were then quantified in mouse islets using a SYBR Green fluorescent dye-based qPCR protocol and a LightCycler® 96 as described in Section 2.2.10.

8.3 Results

8.3.1 The effects of Ccl4 on cytokine- and palmitate-induced apoptosis in mouse islets

To determine whether Ccl4 affects apoptosis in primary tissue, mouse islets were treated with 5-100ng/mL Ccl4 for 48 hours and exposed to either Ccl4 alone, mixed cytokines or palmitate in the final 20 hours. Similar to experiments using MIN6 β-cells, Caspase 3/7 activity was quantified using a proluminescent assay to measure the degree of apoptosis.

A mixed cytokine cocktail of IL-1β, TNF-α and IFN-γ induced a significant increase in mouse islet apoptosis (% relative to control: 210.0±21.72 vs 100.0±11.07; n=3 independent experiments; p<0.001) (Figure 47, left). The addition of Ccl4 at all concentrations resulted in no changes to the apoptotic effect of mixed cytokines (% relative to control: +5ng/mL: 231.3±20.07; +10ng/mL: 278.3±21.23; +50ng/mL: 231.3±19.07; +100ng/mL: 242.9±15.88; ns vs control).

As for mixed cytokines, the saturated fatty acid, palmitate, significantly increased mouse islet apoptosis compared to control media (% relative to control: 126.9±10.01 vs 100.0±6.23; n=5 independent experiments; p<0.05) (Figure 47, right). No significant differences in mouse islet apoptosis were observed with treatment of Ccl4 at all concentrations (% relative to control: +5ng/mL: 101.5±4.92; +10ng/mL: 110.1±4.27; +50ng/mL: 116.6±6.38; +100ng/mL:105.7±4.90; ns vs control).

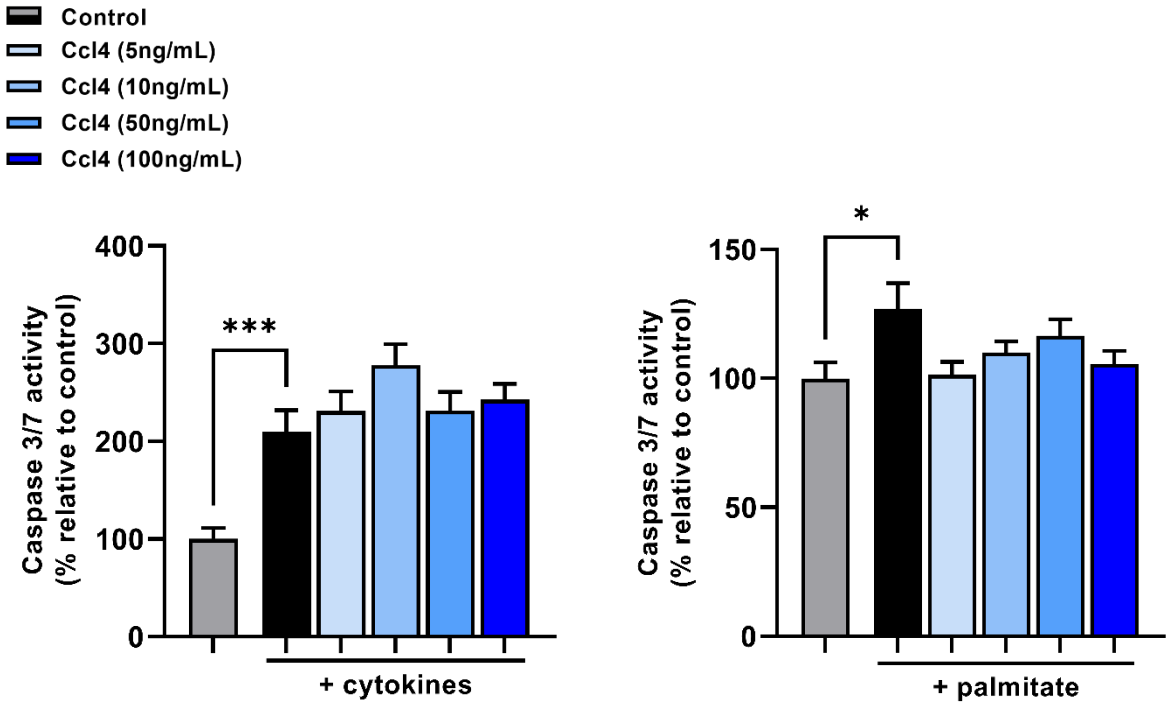

Figure 47. The effect of 48-hour treatment with Ccl4 on cytokine-induced (left) and palmitate-induced (right) apoptosis in mouse islets. Data are expressed as the mean ± S.E.M relative to control without cytokines or without palmitate. One-way ANOVA; n=3-5 independent experiments; *p<0.05, ***p<0.001 vs control.

8.3.2 The effects of Ccl4 on β-cell proliferation in mouse islets

To determine whether Ccl4 treatment affects islet cell proliferation and number, mouse islets were treated with 100ng/mL Ccl4 for 72 hours and co-stained with DAPI, a blue-fluorescent DNA stain, and either antibodies directed against Ki67, insulin, glucagon, or somatostatin. β-cells were identified by DAPI-positive, insulin-positive cells; α-cells were identified by DAPI-positive, glucagon-positive cells; and δ-cells were identified by DAPI-positive, somatostatin-positive cells (Figure 48). The percentage proportions of β-, α- and δ-cells within individual mouse islets were unchanged by exposure to 100ng/mL Ccl4 (% DAPI-positive cells: control vs +100ng/mL: insulin: 69.2±2.70 vs 66.4±2.03; glucagon: 16.9±3.15 vs 8.6±1.97;

somatostatin: 10.7±0.82 vs 13.4±3.05; n=14-18 single mouse islets; ns vs control) (Figure 49A). The number of β-cells (% relative to control: control: 100.0±3.89; +100ng/mL: 95.7±2.93; ns vs control) and δ-cells (% relative to control: control: 100.0±7.67; +100ng/mL: 124.9±28.57; ns vs control) were also not significantly different between mouse islets treated with control media and 100ng/mL Ccl4 (Figure 49B, D), but the number of α-cells was significantly reduced when islets were treated with 100ng/mL Ccl4 (% relative to control: control: 100.0±18.60; Ccl4: +100ng/mL: 50.8±11.60) (Figure 49C).

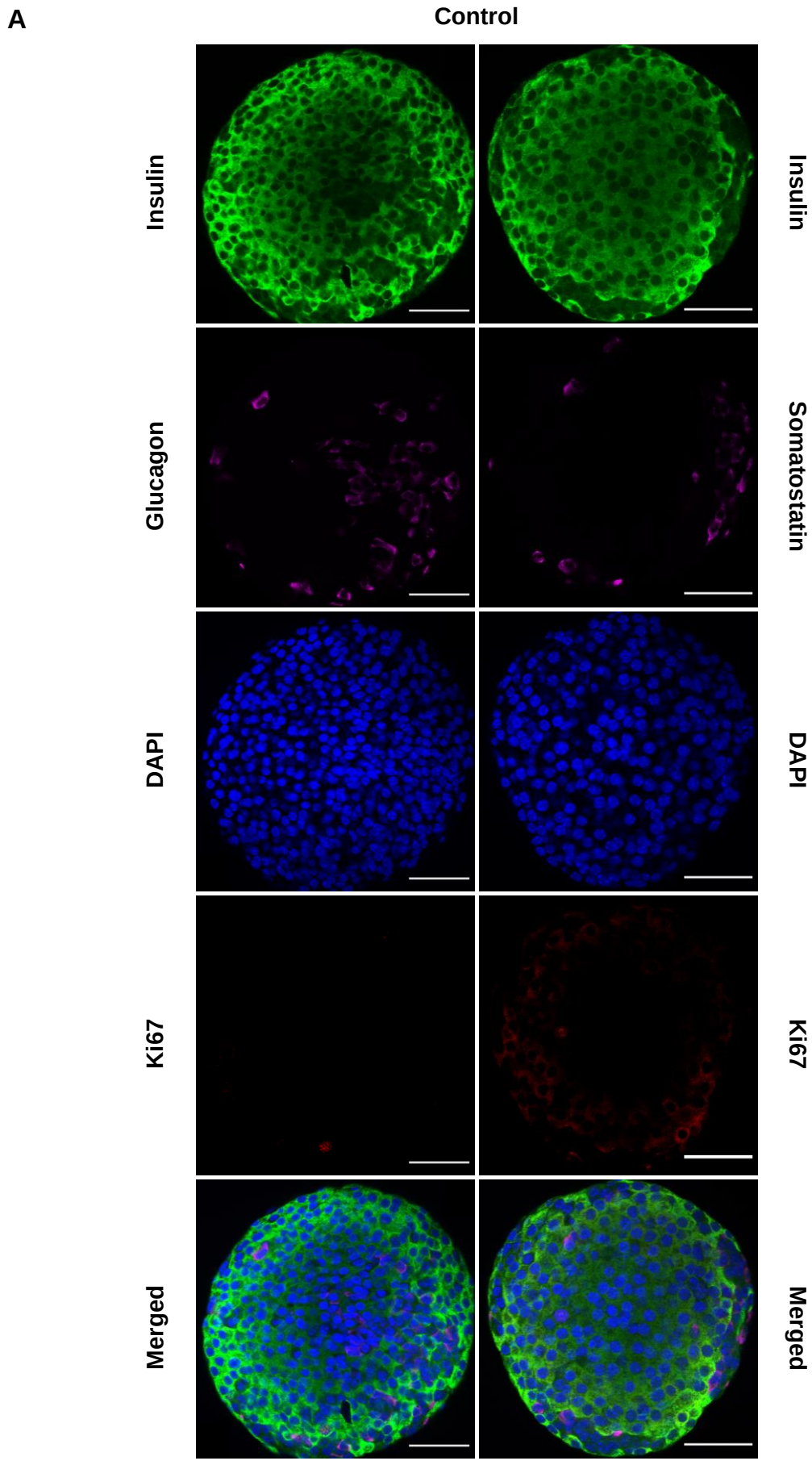
A
Control
Insulin
Glucagon
DAPI
Ki67
Merged
Insulin
Somatostatin
DAPI
Ki67
Merged

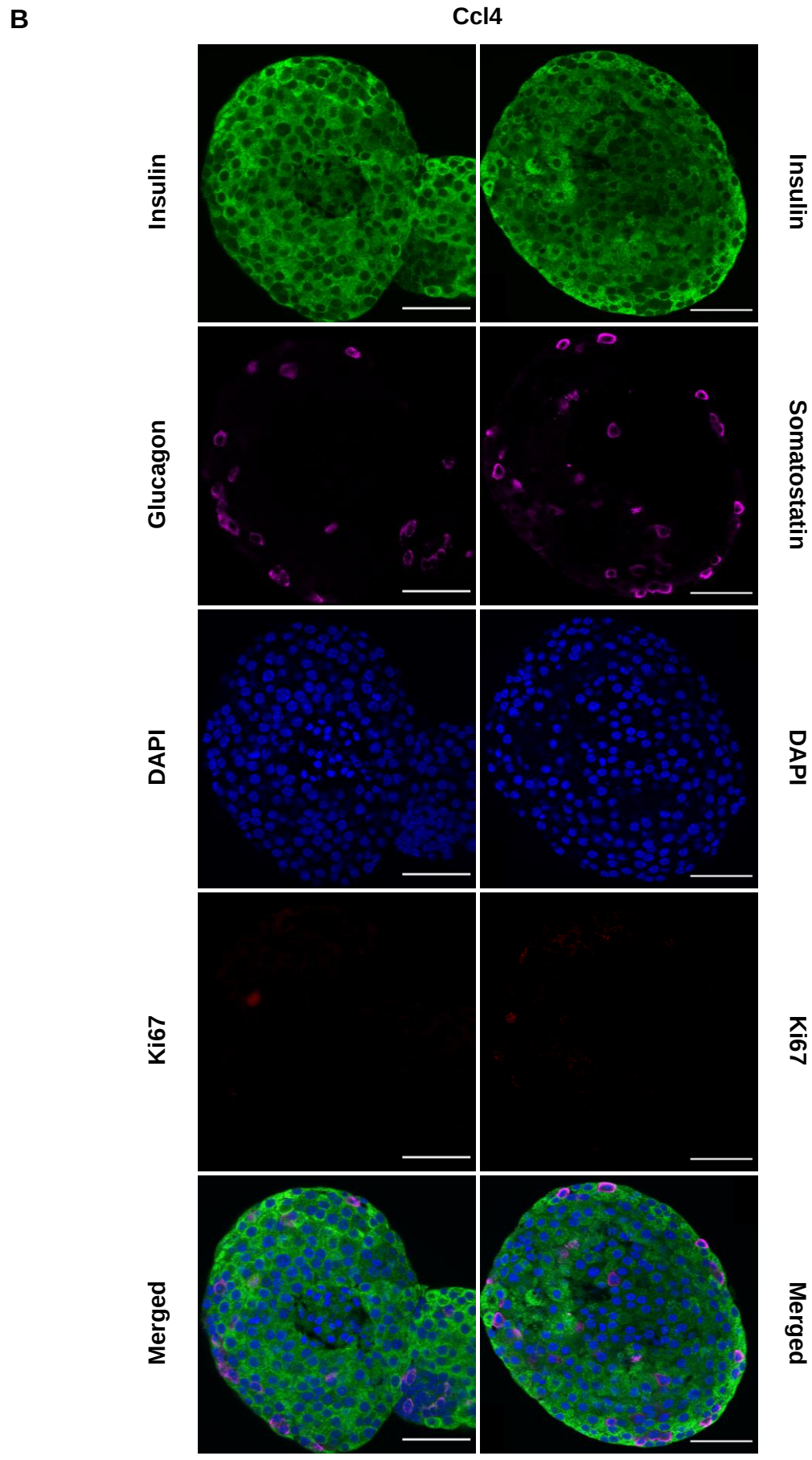
B
Ccl4
Insulin
Glucagon
DAPI
Ki67
Merged
Insulin
Somatostatin
DAPI
Ki67
Merged

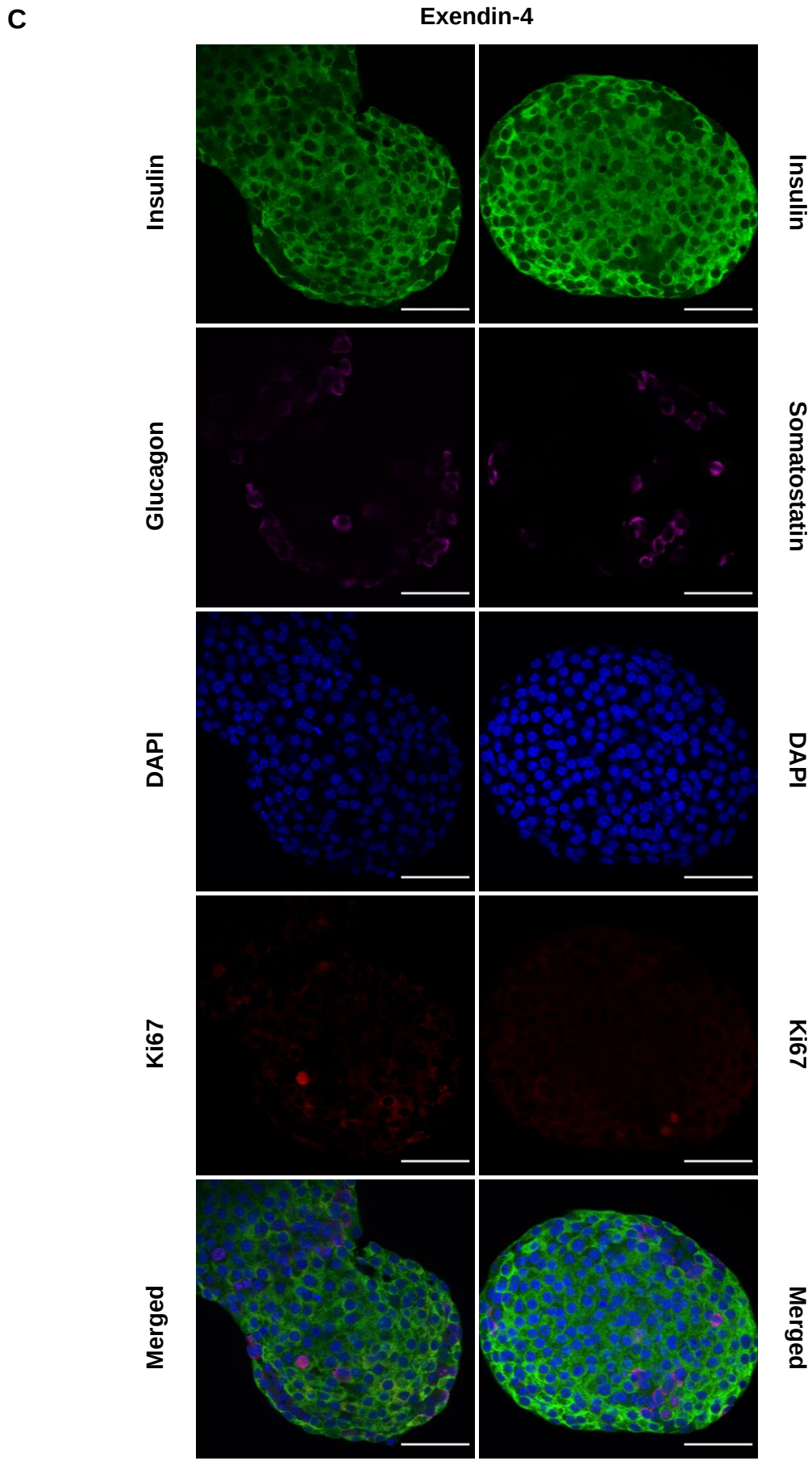
C
Exendin-4
Insulin
Glucagon
DAPI
Ki67
Merged
Insulin
Somatostatin
DAPI
Ki67
Merged

Figure 48. Representative confocal images of immunostained *ex vivo* mouse islets. Mouse islets were treated with either control media (A), Ccl4 (100ng/mL; B) or the positive control, Ex4 (20nM; C) prior to immunofluorescence staining. Proliferating β-cells were identified by the co-localisation of the nuclear stain, DAPI (blue), and the nuclear proliferation marker, Ki67 (red) within the nucleus of insulin-containing (green) cells. α-cells and δ-cells were identified by glucagon and somatostatin (magenta) staining. Scale bar = 50µm.

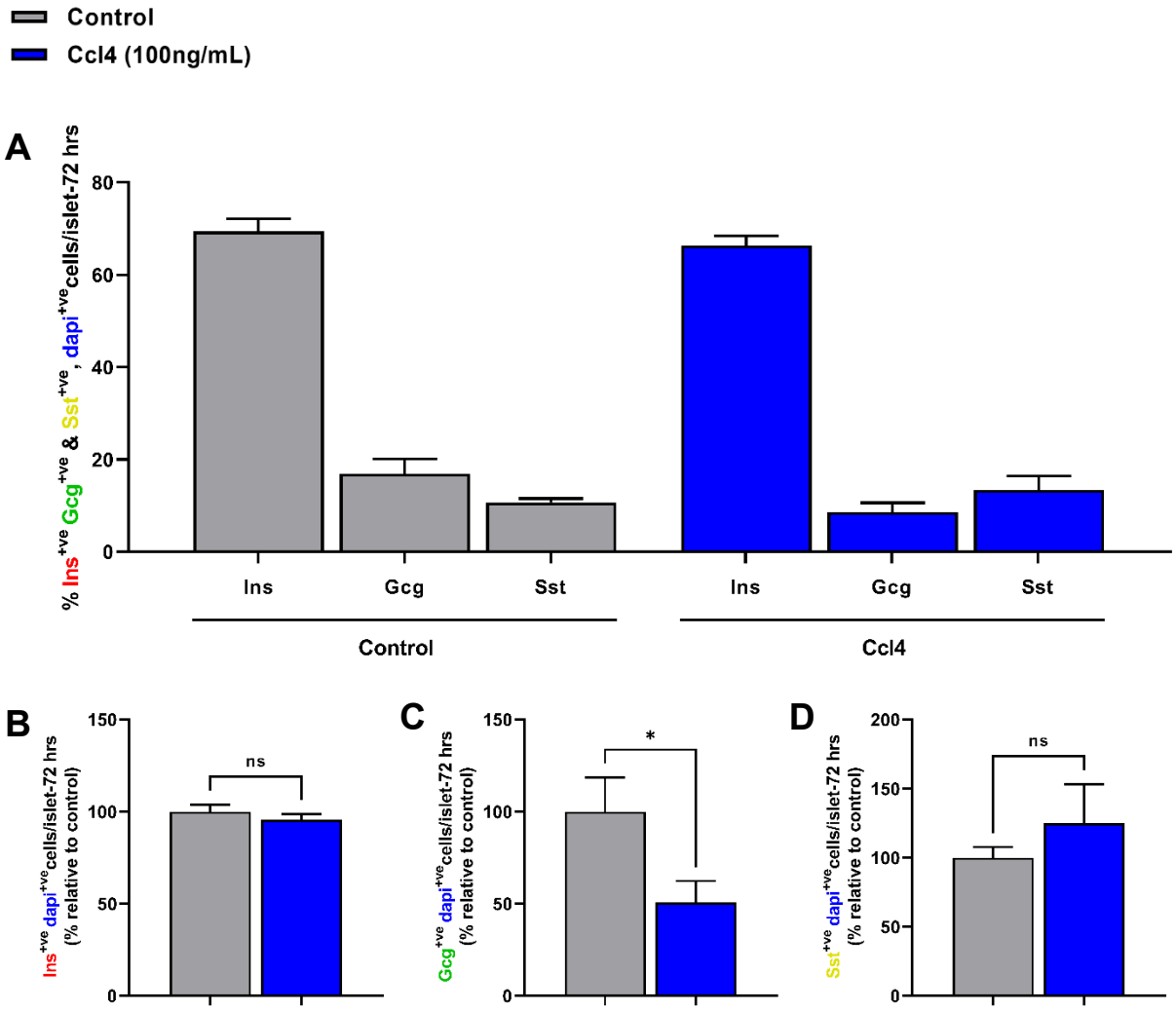

Figure 49. The effect of 72-hour treatment with Ccl4 on mouse islet cell number. β-cells, α-cells and δ-cells were identified by the co-localisation of DAPI and either insulin, glucagon, or somatostatin, respectively. (A) Quantification of the relative proportion of insulin-, glucagon- and somatostatin-positive cells in control and 100ng/mL Ccl4-treated islets. Data are expressed as mean ± S.E.M. One-way ANOVA; n=14-18 single mouse islets; ns vs control. (B-D) Quantification of β-cell, α-cell, and δ-cell number. Data are expressed as the mean ± S.E.M relative to control media. Unpaired two-tailed t-test; n=14-18 single mouse islets; *p<0.05, ns: non-significant vs control.

The level of β-cell proliferation was quantified through the identification of Ki67-, an endogenous cell proliferation marker localised to the nucleus, and insulin-positive staining (Figure 48). The GLP-1 receptor agonist analogue, Ex4, was used as a positive control due to its reported effects as a stimulator of β-cell proliferation (Xu et al., 1999). Single mouse islets

treated with 100ng/mL Ccl4 showed no changes in β-cell proliferation (% relative to control: control: 100.0±29.51; +100ng/mL Ccl4: 70.4±22.90; ns vs control) but, as expected, 20nM Ex4 induced a significant increase in β-cell proliferation (% relative to control: 374.4±40.84; p<0.0001 vs control) (Figure 50).

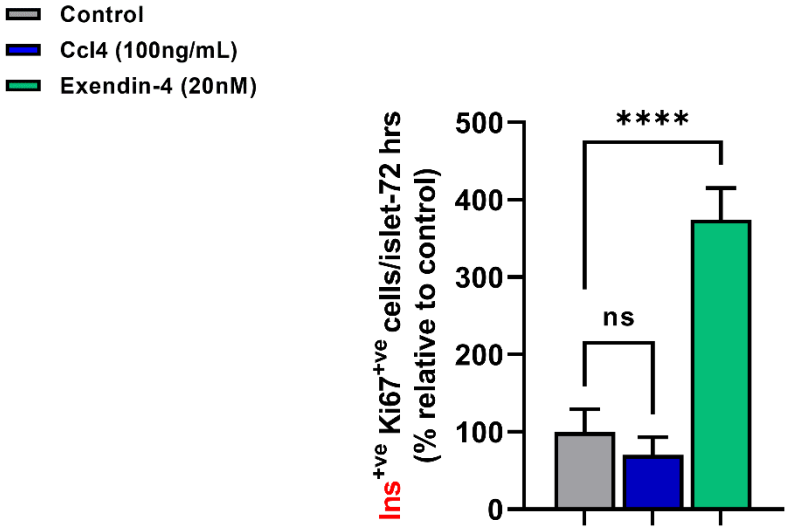

Figure 50. The effect of 72-hour treatment with Ccl4 on β-cell proliferation. Proliferating β-cells were identified by the co-localisation of Ki67 and insulin. Ex4 treatment was used as positive control. Data are expressed as the mean ± S.E.M relative to control media. One-way ANOVA; n=14-18 single mouse islets; ****p<0.0001, ns: non-significant vs control.

8.3.3 The effects of Ccl4 on insulin secretion from mouse islets

To determine whether Ccl4 affects glucose-stimulated insulin secretion in primary tissue, mouse islets were exposed to 5-100ng/mL Ccl4 in the presence of 20mM glucose and insulin levels in harvested supernatant were quantified using radioimmunoassay. Incubation with 20mM glucose significantly increased insulin secretion vs 2mM glucose (% relative to control: 337.7±34.64 vs 100.0±14.91; n=5 independent experiments; p<0.0001 vs control) (Figure 51). All concentrations of Ccl4 failed to potentiate or attenuate glucose-stimulated insulin secretion (% relative to control: +5ng/mL: 315.1±32.19; +10ng/mL: 308.8±27.08; +50ng/mL: 338.6±28.02; +100ng/mL: 365.3±29.79; ns vs control).

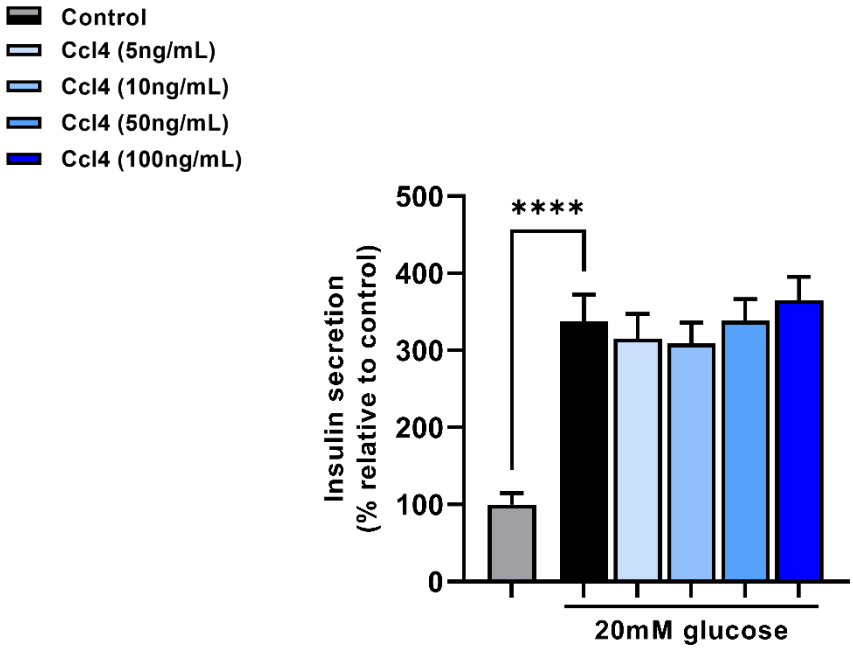

Figure 51. The effect of treatment with Ccl4 (5-100ng/mL) on glucose-stimulated insulin secretion from mouse islets. Data are expressed as the mean ± S.E.M relative to 2mM glucose control (grey bar). One-way ANOVA; n=5 independent experiments; ****p<0.0001 vs control.

8.3.4 Expression of Ccl4-targeted GPCR mRNAs in mouse islets

Results from the PRESTO-Tango β-arrestin reporter experiments revealed CXCR1 and CXCR5 are the targets of CCL4 action (Section 7.3.5). Acrk2, Ccr1, Ccr2, Ccr5 and Ccr9 are also reported to be Ccl4-activated (Bonecchi et al., 2004; Civatte et al., 2005; Guan et al., 2002; Nibbs et al., 1997). To gain better understanding of the lack of observed functional effects of Ccl4 in mouse islets, a qPCR screening was performed to quantify the mRNA expression levels of *Acrk2*, *Ccr1*, *Ccr2*, *Ccr5*, *Ccr9*, *Cxcr1* and *Cxcr5* in mouse islets relative to the housekeeping gene, *Actb*. *Cxcr5* mRNA was expressed in mouse islets (0.0017±0.0003 relative to *Actb*) (Figure 52) thereby confirming the presence of a Ccl4-activating GPCR. The remaining putative Ccl4 receptors were absent (<0.0001% of *Actb*) or present at trace level (0.0001% to 0.001% relative to *Actb* expression) (Supplementary Table 25).

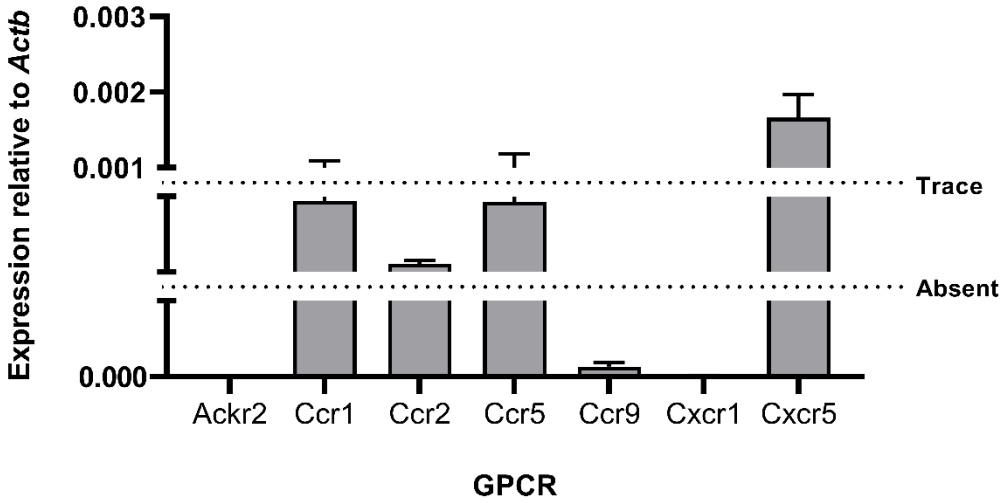

Figure 52. The expression of Ccl4-target GPCR mRNAs in mouse islets. Data are expressed as the mean ± S.E.M. n=4.

8.4 Discussion

The present chapter investigated a potential function for Ccl4 at primary mouse islets. To assess whether observations in MIN6 β-cells were recapitulated in primary tissue, similar experiments measured the effects of recombinant mouse Ccl4 on islet apoptosis, proliferation, and insulin secretion, and aimed to identify GPCRs through which Ccl4 potentially acts.

In accordance with data obtained using MIN6 β-cells, glucose-stimulated insulin secretion from islet β-cells was unchanged following incubation with Ccl4. However, unlike the anti-proliferative and anti-apoptotic effects seen in MIN6 β-cells, Ccl4 treatment did not alter cytokine- or palmitate-induced islet apoptosis, nor did it affect β-cell proliferation within islets. Despite a lack of effect at the β-cell, immunofluorescence staining revealed a significant 50% reduction in the number of glucagon-producing α-cells when islets were exposed to Ccl4 for 72 hours. Together with β-cells, α-cells have a key role in regulating glycaemia, yet they have been less extensively studied. A recent paper compared α-cell vs β-cell expressomes in diabetic NOD mice and T1D patients and found that α-cells were subjected to a higher rate of inflammatory stress (Nigi et al., 2020). These data suggest that α-cells may be more vulnerable to environmental stressors than β-cells. On the other hand, a study which retrieved α-cells and β-cells from humans and rats revealed α-cells, but not β-cells, were resistant to palmitate-induced apoptosis (Marroqui et al., 2015). These findings fit with a report in which α-cell mass was similar in non-diabetic humans and T2D subjects, whilst β-cell was decreased in T2D (Henquin & Rahier, 2011). Several publications have also documented increases in the absolute number and proportion of α-cells relative to β-cells. For example, increased α-cell but reduced β-cell volume led to an imbalanced α/β-cell ratio in baboons with hyperglycaemic and islet amyloidosis (Guardado-Mendoza et al., 2009). Similar increases in the proportion of α-cells to β-cells was observed in cadaveric pancreas samples from patients with T2D compared to non-diabetic individuals (Henquin & Rahier, 2011; Kilimnik et al., 2011). Taken together, α-cell defence mechanisms may differ between T1D (immunological) and T2D (metabolic).

Interestingly, the substantial decrease in α-cell number with Ccl4 treatment was not evident in results from islet apoptosis experiments. The disagreement between apoptotic levels and α-cell loss may be due to differences in Ccl4 incubation times (48 vs 72 hours). Increasing the treatment period in apoptosis experiments to match that in immunofluorescence experiments may resolve this. A more likely explanation could be that α-cells are a minority cell type, therefore, the magnitude of α-cell loss was insufficient to alter overall apoptotic levels within the whole islet. Another explanation could be the fact that assays which quantify caspase-3/7 activity, like the assay used here, only detect apoptosis and not necrosis or necroptosis. These alternate mechanisms of cell death, which involve separate regulators from apoptosis, could be occurring within the α-cells, especially in the event of prolonged apoptosis which leads to secondary necrosis (Butterick et al., 2014). Other techniques, such as cytofluorometry which detects morphological modifications, or luminometry which quantifies intracellular energy stores, could help discriminate apoptotic cells from necrotic ones (Galluzzi et al., 2009). The depletion of α-cells may have been mediated through the activation of Cxcr5, the only Ccl4-target GPCR mRNA found expressed within mouse islets and triggering potential NF-κB pathways. Unfortunately, qPCR experiments alone cannot distinguish *Cxcr5* mRNA expression between the different islet cell populations. *Cxcr5* mRNA expression in specific islet cells from control- and high-fat diet-fed mice could not be determined from a recently published single cell RNA sequencing (scRNAseq) dataset (*GEO Accession Viewer*, 2022; Rubio-Navarro et al., 2023), although, filtering of low-expressed genes which improves the detection of differentially expressed genes means detectable *Cxcr5* mRNA expression may have been removed. Compared to bulk RNAseq and qPCR techniques, scRNAseq generates more variable data with greater technical noise that requires several quality control steps to eliminate (Chen et al., 2019). As a result, true signals representing low expressed genes may be removed, making scRNAseq a less reliable approach for identifying such genes, including those that encode GPCRs. Additional immunofluorescence staining experiments could be performed to detect receptor expression by specific islet cells, but there is insufficient antibody selectivity against GPCRs, rendering this technique unreliable and inaccurate (Michel et al., 2009). Use of cell sorting techniques, such as fluorescence-activated cell sorting (FACS), prior to qPCR screening could help clarify GPCR expression patterns within specific endocrine cell subtypes. The mRNA expression profile of Ccl4-target GPCRs was established here in islets isolated from outbred CD1 mice; this differs from the expression profile in islets from CD1 mice (referred to as ICR) previously published by our group (Amisten et al., 2017). *Cxcr5* mRNA was expressed in CD1 islets, but in the earlier report, this receptor was expressed only at trace level in ICR islets. Although a handful of CD1 islet samples expressed *Ccr1* and *Ccr5* mRNAs, sample variation meant their mean mRNA expression levels were considered present only at trace level. The same was observed by Amisten et al. regarding *Ccr1* mRNA, however, *Ccr5* mRNA was expressed in ICR islets. The remaining receptors were similarly absent or expressed at trace level in both qPCR screenings (Amisten et al., 2017). It is unclear why the data reported by Amisten et al. were not reproduced here, especially given experimental protocols are standardised within our group, although GPCR dynamics, age differences between mouse cohorts, and variation in individual investigator practice may have been contributing factors.

In summary, the experiments in this current chapter have shown that Ccl4 does not have the same functional effects in primary β-cells as it does in the immortalised MIN6 β-cell line. Genomic content, key morphological features, and overall phenotype can all deviate away from those of the original tissue from which cell lines are derived. Thus, the observed

discrepancies are not unexpected given cell lines have relatively low physiological relevance to primary tissues. In contrast, Ccl4 may negatively impact α-cell function. Such dysfunction could disrupt the counterregulatory mechanisms that exist between α-cells and β-cells to maintain normoglycaemia *in vivo*. Further investigation is required to confirm this potential regulatory role on α-cell function by Ccl4.

Chapter 9: Investigating the paracrine/autocrine effects of visceral adipose tissue-derived Ccl4 on 3T3-L1 preadipocyte cell differentiation and function

9.1 Introduction

Based on the results from functional experiments in primary mouse islets, it is unlikely that upregulated Ccl4 in obese adipose tissue participates in crosstalk with β-cells to alter their function. The upregulation of *Ccl4* mRNA in whole adipose tissue and not mature adipocytes from diet-induced obese mice supports increased chemokine expression within the SVF in obesity, most likely from the expansion of the immune cell population. As previously described in Section 1.5.2.4, a paracrine loop between adipocytes and resident macrophages has been established whereby soluble factors, such as adipocyte-derived FFAs and macrophage-derived TNF-α, induce functional changes within their neighbouring cell types (Suganami et al., 2005, 2007). Therefore, instead of mediating endocrine actions, locally produced Ccl4 may modulate adipocyte cell function through paracrine signalling in obesity.

The experiments described so far in this thesis have identified several differentially expressed islet GPCR peptide ligand mRNAs in obese models, some of which have known paracrine/autocrine interactions with adipose tissue. An example is Cxcl3 whose mRNA expression was downregulated in mature adipocytes isolated from high-fat diet-induced obese mice (see Section 3.3.4). It has been reported that recombinant Cxcl3 treatment promoted lipid accumulation and expression of adipogenic markers, *Pparg2*, *Fabp4* and *C/ebpa*, during differentiation of the preadipocyte cell line, 3T3-L1 (Kusuyama et al., 2016). This was inhibited by siRNA-induced gene knockdown of Cxcl3 or its target GPCR, Cxcr2. The involvement of Cxcr2 signalling in adipocyte differentiation is supported further by reduced Fabp4 copy number and adipocyte cell size in $Cxcr2^{-/-}$ mice (Dyer et al., 2019). An additional example of an adipocyte-derived islet GPCR ligand which acts locally within adipose tissue is Npy. High-fat feeding and obesity resulted in elevated *Npy* mRNA expression in visceral mature adipocytes from mice (Section 4.3.4). The obese state can be exacerbated further by associated increases in Npy levels, as Npy stimulated preadipocyte proliferation and white adipose tissue adipogenesis (Kuo et al., 2007) and inhibited brown adipose tissue thermogenesis via downregulated uncoupling protein 1 (UCP1) expression (Shi et al., 2013). Moreover, delivery of exogenous Npy to lean and obese mice resulted in a 50% expansion of adipose tissue weight and volume (Kuo et al., 2007). Treatment of 3T3-L1 adipocytes with exogenous Npy inhibited insulin-stimulated glucose uptake via diminished GLUT4 translocation, an effect that was abolished by a Y1-specific receptor antagonist, suggesting involvement of this Npy target GPCR in glucose tolerance (Gericke et al., 2012).

CCL4 and its target GPCRs, CXCR1, CCR1, CCR2 and CCR5 are all present within human mature adipocytes and preadipocytes (Gerhardt et al., 2001). The expression of these receptors and its other chemokine ligands, CCL2, CCL3 and IL-8, vary across different stages of adipogenesis. Given all three chemokines significantly inhibit lipid accumulation and the expression of major adipogenic transcription factors, Pparγ and C/ebpα, chemokine signalling may be involved in regulating adipocyte differentiation, maturity and function (Gerhardt et al., 2001). This is likely true under both normal and obese conditions. Indeed, significant elevations in the expression of chemokine ligands and receptors were observed within adipose tissue from mice and humans with obesity (Huber et al., 2008; Kanda et al., 2006; Kim et al.,

2014; Kitade et al., 2012). This includes Ccl4 and its target receptors, Ccr2 and Ccr5, in epididymal fat pads from diet-induced obese and leptin-deficient, *ob/ob*, mice (Kitade et al., 2012). Furthermore, pharmacological and genetic manipulations of receptor/ligand expression or activity, either globally, within adipocytes or adipose tissue-derived immune cells, have implicated the chemokine system in insulin resistance (Chavey et al., 2009; Huh et al., 2018; Inouye et al., 2007; Kamei et al., 2006, 2006; Kanda et al., 2006; Kim et al., 2014; Kirk et al., 2008; Kitade et al., 2012; Weisberg et al., 2006).

Consequently, the aim of this chapter was to assess the influence of Ccl4 action on adipocyte differentiation, lipolysis, and insulin sensitivity. The established murine preadipocyte cell line, 3T3-L1, was used as a model of adipogenesis based on its capacity to differentiate and its possession of adipogenic characteristics which mimic *in vivo* adipocytes. The following experiments investigated a potential role for the obesity-induced upregulated Ccl4 within adipose tissue to alter adipocyte function through a paracrine/autocrine-mediated mechanism.

9.2 Methods

9.2.1 Differentiation of 3T3-L1 preadipocyte cells

The 3T3-L1 preadipocyte cell line was used to assess the effects of Ccl4 treatment on adipogenesis which was induced by a differentiation cocktail, also referred to as MDi (Section 2.11.2). This adipogenic cocktail contains IBMX, DEX, and insulin which are necessary promoters for efficient differentiation of 3T3-L1 cells (Zhao et al., 2019). Cells were seeded into a 12-well plate at a density of 90,000 cells/2mL/well and maintained at 37°C, 5% CO_2 and 95% humidity in sterile-filtered DMEM containing 25mM glucose, 10% (v/v) NCS, 100U/mL penicillin, 100µg/mL streptomycin and 2mM L-glutamine. 3T3-L1 preadipocyte cells were incubated for 48 hours with DMEM or MDi in the absence or presence of recombinant 100ng/mL Ccl4. Thereafter, medium was replaced every 48 hours for a period of 6 days when differentiation of 3T3-L1 cells was complete and ready for experimental protocols, as indicated below.

9.2.2 Oil Red O staining and quantification

Increasing lipid accumulation occurs within maturing adipocytes during adipogenesis, therefore, intracellular lipid content can be quantified to evaluate differentiation (Section 2.11.4). Once the differentiation protocol was completed, 3T3-L1 adipocyte cells were stained an orange-red tint by the fat-soluble, hydrophobic diazo ORO dye. Images were captured using a light microscope to visualise ORO-stained stored lipid droplets within 3T3-L1 cells. ORO was subsequently eluted by the addition of 100% isopropanol and absorbance was measured at a wavelength of 490-520nm using a Wallac 1420 Victor2™ microplate reader to quantify lipid content.

9.2.3 qPCR screening of adipocyte differentiation genes

The expression of the adipogenic gene markers, PPARγ and adiponectin, was quantified in 3T3-L1 cells to assess the effect of Ccl4 treatment on adipocyte differentiation and maturity. The extraction and purification of RNA from differentiated and non-differentiated 3T3-L1 cells were performed using the RNeasy Mini Kit, as described in Section 2.6.1. Once RNA yield

and purity were determined by a NanoDrop™ One spectrophotometer, RT reactions (50ng/µL) were prepared using the High-Capacity cDNA Reverse Transcription Kit and performed in a Mastercycler® Nexus GX2. Expression of *Pparγ* and *AdipoQ* mRNAs relative to the housekeeping gene, *Hprt1*, were quantified using the SYBR Green-based qPCR protocol (Section 2.2.10) and a QuantStudio™ 6 Flex Real-Time PCR System.

9.2.4 Western blotting

The phosphorylation of AKT and HSL proteins were measured to assess the effect of Ccl4 treatment on insulin signalling and lipolysis, respectively, within adipocytes. Proteins were extracted from undifferentiated and differentiated 3T3-L1 cells and quantified using the Bradford method (Section 2.11.5). This involved the addition of RIPA lysis buffer supplemented with phosphatase/protease inhibitors to cells and the collection of protein supernatants following centrifugation. Samples and standards of unknown and known protein concentrations, respectively, were mixed with Protein Assay Dye Reagent Concentrate containing BCA to generate a blue protein-dye complex. Absorbance was measured at a wavelength of 595nm using a Wallac 1420 Victor2™ microplate reader and was directly proportional to protein content. Thereafter, immunoreactive total and phosphorylated forms of AKT and HSL were detected by Western Blotting as described in Section 2.11.5. The protocol began with the dilution of 60µg of each protein sample in 7µL Laemmli Buffer/β-ME mixture and the volume topped up to 28µL with RIPA lysis buffer. Proteins were then denatured at 95°C for 15 minutes. 25µL of each samples (2µg/µL) and Precision Plus Protein Dual Color Standards were loaded into a prepared gel and subjected to SDS-PAGE at 90V for 30 minutes followed by 120V for 1-1.5 hours in a Mini-PROTEAN Tetra Vertical Electrophoresis Cell. Subsequently, using a Trans-Blot® Turbo™ Transfer System set at 25V for 7 minutes, proteins were transferred to a PDVF membrane which was immunostained with primary and secondary antibodies targeting peptides of interest.

9.3 Results

9.3.1 The effects of Ccl4 on lipid accumulation during the differentiation of 3T3-L1 preadipocyte cells

To determine whether Ccl4 participates in paracrine/autocrine signalling to influence adipocyte differentiation, 3T3-L1 preadipocytes were treated with control DMEM or the differentiation cocktail, MDi, in the absence or presence of 100ng/mL Ccl4 and subsequently stained with ORO to visualise and quantify lipid accumulation during adipogenesis. The low lipid content and fibroblast-like morphology of undifferentiated 3T3-L1 preadipocyte cells was highly distinct from the marked accumulation of ORO-stained lipids within rounded differentiated cells (Figure 53). These observations were confirmed by the elution and quantification of ORO staining as MDi-induced differentiation of 3T3-L1 preadipocytes led to an increase in intracellular lipid content, however, due to a low n-number of 2, the degree of significance could not be determined (% relative to non-differentiated control: 195.0±24.03 vs 100.0±15.50; n=2 independent experiments) (Figure 54). Although statistical analysis could not be performed, little difference in lipid accumulation between non-differentiated 3T3L-1 cells (% relative to non-differentiated control: +100ng/mL: 100.5±14.66) and differentiated 3T3L-1 cells (% relative to non-differentiated control: +100ng/mL: 192.0±24.49) with 100ng/mL Ccl4 treatment suggests a lack of effect.

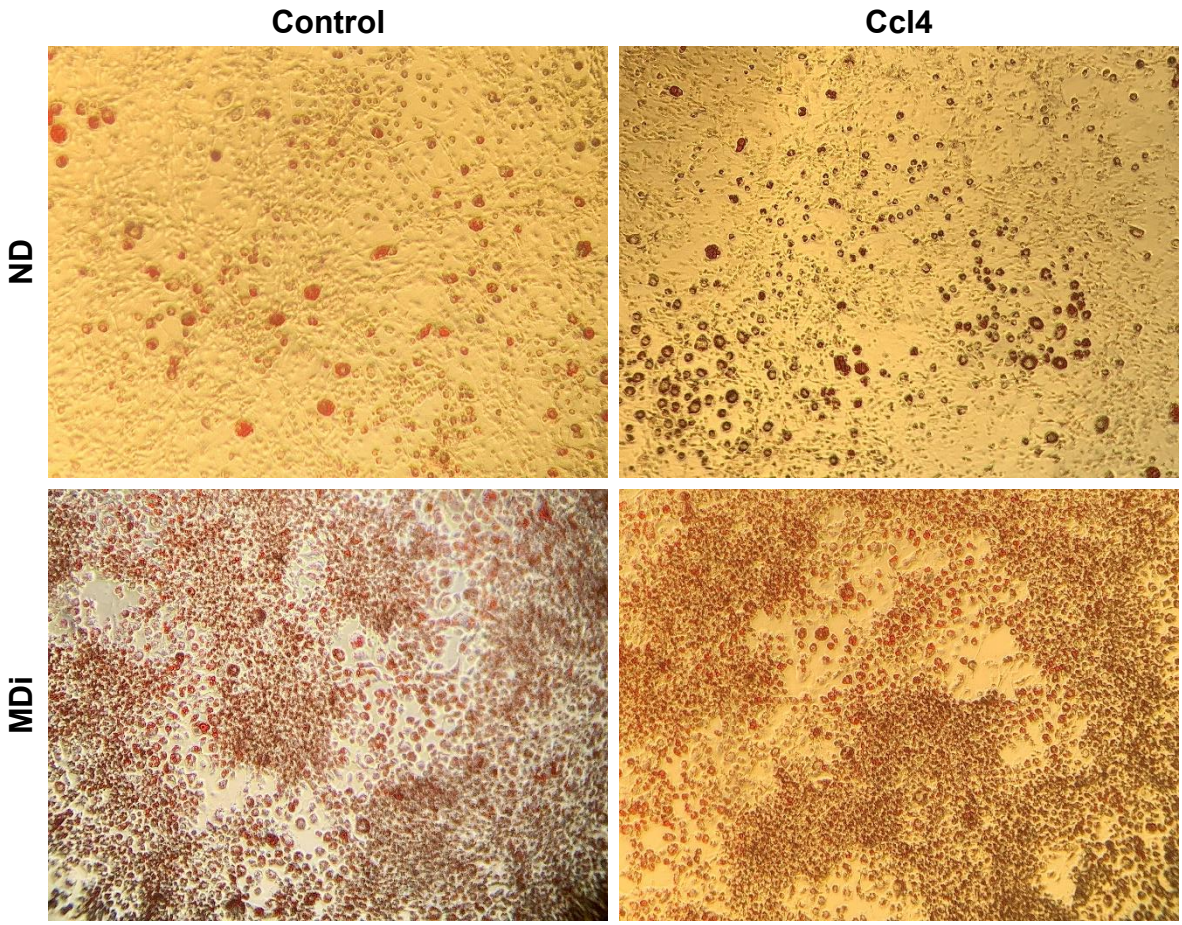

Figure 53. Representative light microscopic images of ORO-stained intracellular lipid droplets within 3T3-L1 cells. Cells were treated with either control media or the differentiation cocktail, MDi, in the absence or presence of Ccl4 (100ng/mL) prior to staining with the fat-soluble, hydrophobic ORO dye. 10X magnification. ND: non-differentiated; MDi: differentiated.

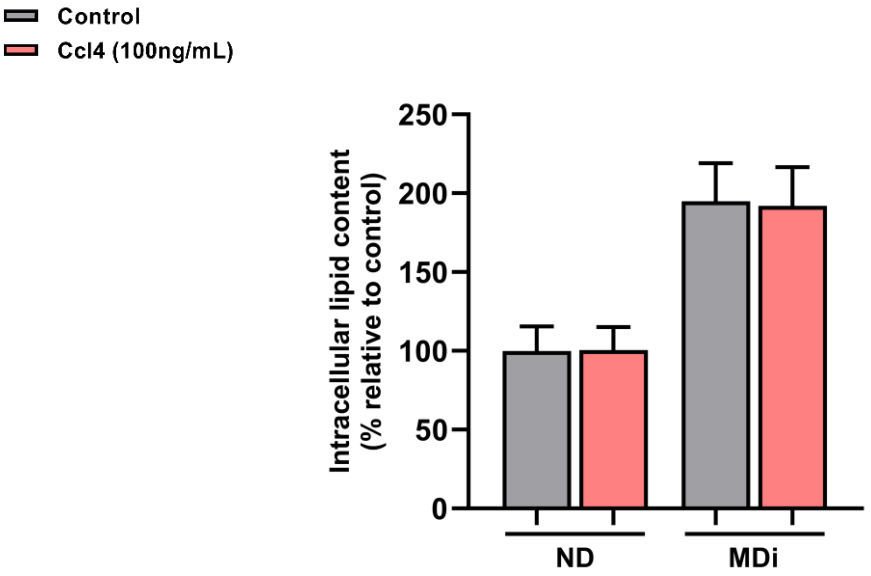

Figure 54. The effect of 48-hour treatment of Ccl4 on lipid accumulation in the 3T3-L1 adipocyte cell line. Data are expressed as the mean ± range relative to control-treated non-differentiated cells. n=2 independent experiments. ND: non-differentiated; MDi: differentiated.

9.3.2 The effects of Ccl4 on the expression of maturity gene markers during the differentiation of 3T3-L1 preadipocyte cells

To extend the investigation into Ccl4-mediated paracrine/autocrine effects on adipocyte differentiation, the mRNA expression of adipogenic gene markers, PPARγ and adiponectin, was quantified in 3T3-L1 cells that were treated with control DMEM or the differentiation cocktail, MDi, in the absence or presence of 100ng/mL Ccl4. As expected, the expression of *Pparγ* mRNA was significantly elevated following differentiation of 3T3-L1 preadipocyte cells (% relative to non-differentiated control: 257.7±4.94 vs 100.0±3.84; n=3 independent experiments; p<0.0001 vs control) (Figure 55). The addition of 100ng/mL Ccl4 did not alter *Pparγ* mRNA expression in non-differentiated 3T3L-1 cells (% relative to non-differentiated control: +100ng/mL: 94.6±3.00; ns vs control) and differentiated 3T3L-1 cells (% relative to non-differentiated control: +100ng/mL: 246.7±4.02; ns vs control). Differentiation of 3T3-L1 cells also significantly increased the expression of mRNA encoding *AdipoQ* (381.4±23.36 vs 100.0±15.39; n=3 independent experiments; p<0.0001 vs control) (Figure 55). Whilst no differences in *AdipoQ* mRNA expression were observed in non-differentiated 3T3-L1 cells treated with Ccl4 compared to control media (% relative to non-differentiated control: +100ng/mL: 77.2±11.00; ns vs control), *AdipoQ* mRNA levels were significantly reduced in Ccl4-treated differentiated cells (% relative to non-differentiated control: +100ng/mL: 246.4±10.21; p<0.0001 vs control).

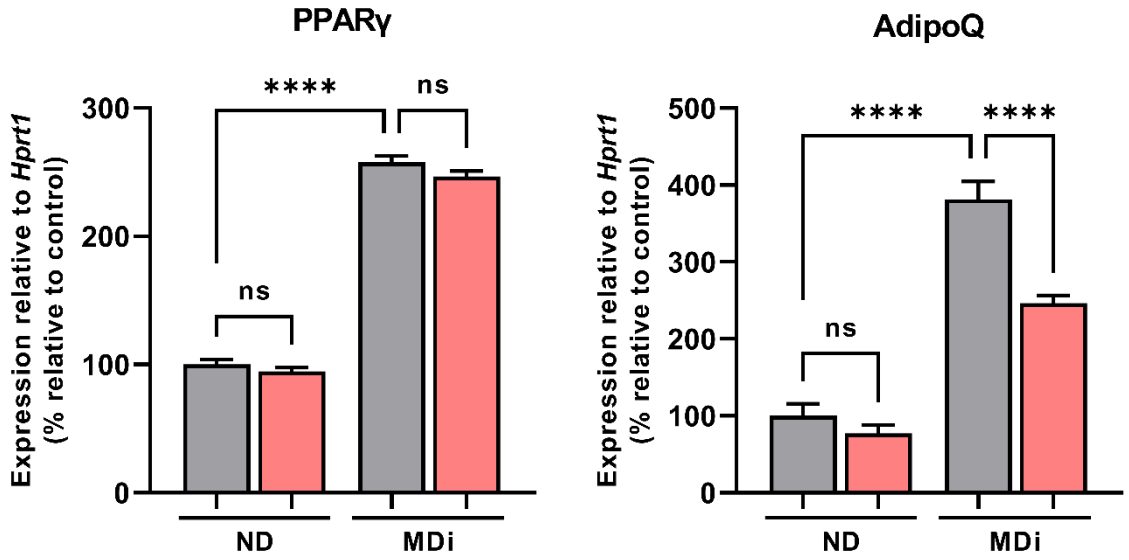

Figure 55. The effect of 48-hour treatment with Ccl4 on gene markers for adipocyte differentiation and maturity. Data are expressed as the mean ± S.E.M relative to control-treated non-differentiated cells. One-way ANOVA; n=3 independent experiments; ****p<0.0001, ns: non-significant vs control. ND: non-differentiated; MDi: differentiated.

9.3.3 The effects of Ccl4 on insulin signalling during the differentiation of 3T3-L1 preadipocyte cells

To determine whether the reductions in the mRNA expression of the adipogenic marker, *AdipoQ*, translated to changes in insulin signalling, Western blot experiments were performed to detect immunoreactive p-AKT(Ser473) and t-AKT proteins extracted from 3T3-L1 cells treated with control DMEM or the differentiation cocktail, MDi, with or without 100ng/mL Ccl4 and 10nM and 100nM insulin. As expected, in the absence of insulin, AKT was unphosphorylated in all cells regardless of differentiation status or the presence of Ccl4 (Figure 56 and 57) (p-AKT/t-AKT: 0nM insulin: non-differentiated control: 0.001±0.0001; +100ng/mL Ccl4: 0.001±0.0001; differentiated control: 0.002±0.0019; +100ng/mL Ccl4: 0.003±0.0010).

When exposed to 10nM insulin, AKT phosphorylation displayed an upward trend following differentiation of 3T3-L1 preadipocyte cells (p-AKT/t-AKT: 10nM insulin: non-differentiated control: 0.734±0.0211; differentiated control: 3.040±1.4915; n=2 independent experiments). The addition of Ccl4 resulted in little change to AKT phosphorylation in non-differentiated (p-AKT/t-AKT: 10nM insulin: +100ng/mL: 0.802±0.3273) but an increase was measured in differentiated 3T3-L1 cells (p-AKT/t-AKT: 10nM insulin: +100ng/mL: 4.204±0.8491) (Figure 56 and 57). Increasing the concentration of insulin to 100nM elevated AKT phosphorylation in both non-differentiated and differentiated 3T3-L1 cells (p-AKT/t-AKT: 100nM insulin: non-differentiated control: 1.591±0.0232; differentiated control: 3.703±0.9577). In the presence of Ccl4, a trend of increased AKT phosphorylation was observed in both non-differentiated (p-AKT/t-AKT: 100nM insulin: +100ng/mL: 1.270±0.1799) and differentiated 3T3-L1 cells (p-AKT/t-AKT: 100nM insulin: +100ng/mL: 5.693±0.5532) (Figure 56 and 57). Like experiments assessing lipid content in Section 9.3.1., an n=2 experiments to investigate the effect of Ccl4 on insulin sensitivity rendered statistical analysis inappropriate.

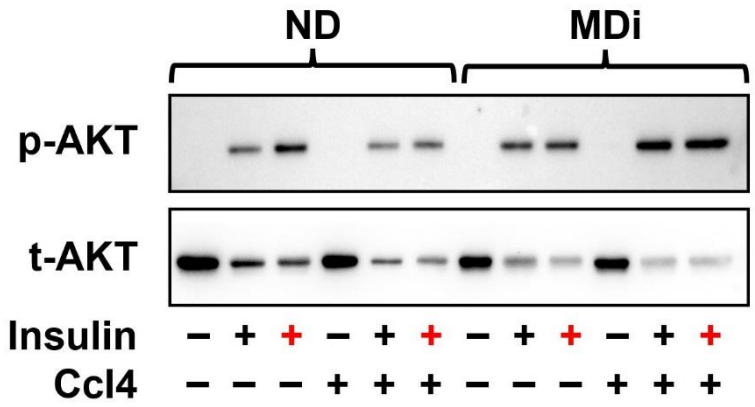

Figure 56. Representative bands for phospho-AKT and total-AKT from Western Blot experiments using 3T3-L1 cells. Cells were treated with either control medium or the differentiation cocktail, MDi, in the absence or presence of Ccl4 (100ng/mL). Prior to protein extraction and immunoblotting, cells were treated with media containing no insulin (–), 10nM insulin (+) or 100nM insulin (+). Immunoreactive proteins each of 60kDa represent p-AKT(Ser473) and t-AKT. ND: non-differentiated; MDi: differentiated.

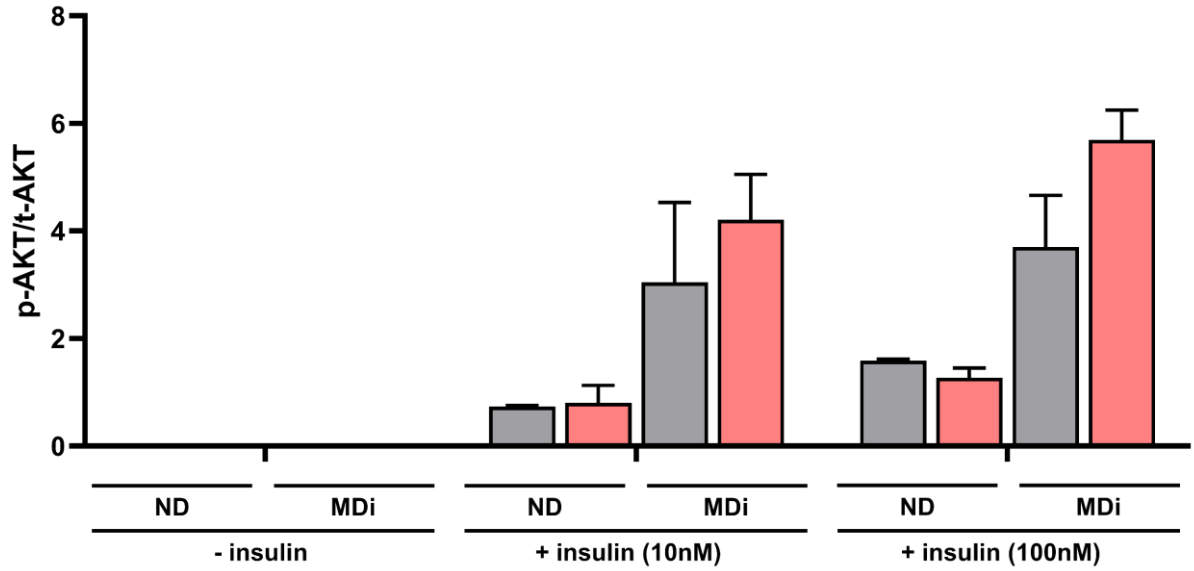

Figure 57. The effect of 48-hour treatment with Ccl4 on Akt phosphorylation in the 3T3-L1 adipocyte cell line. Data are expressed as the mean p-Akt/t-Akt ratio ± range. n=2 independent experiments. ND: non-differentiated; MDi: differentiated.

9.3.4 The effects of Ccl4 on lipolysis during the differentiation of 3T3-L1 preadipocyte cells

To determine whether the reductions in *AdipoQ* mRNA expression during adipogenesis translated to changes in lipolysis, Western blot experiments were performed to detect immunoreactive p-HSL(Ser660) and t-HSL proteins extracted from 3T3-L1 cells treated with control DMEM or the differentiation cocktail, MDi, with or without 100ng/mL Ccl4 and 1µM isoprenaline. In the absence of the lipolytic inducer, isoprenaline, Ccl4 did not appear to alter HSL phosphorylation in both non-differentiated (p-HSL/t-HSL: control: 0.177±0.0209; +100ng/mL: 0.191±0.0859; n=2 independent experiments) and differentiated 3T3-L1 cells (p-

HSL/t-HSL: control: 0.193±0.0523; +100ng/mL: 0.198±0.0180 ; n=2 independent experiments) (Figure 58 and 59). Treatment with isoprenaline increased HSL phosphorylation in non-differentiated (p-HSL/t-HSL: +1µM: 0.377±0.0624) and differentiated 3T3-L1 cells (p-HSL/t-HSL: +1µM: 0.611±0.1878). The lipolytic actions of isoprenaline showed a downward trend following the addition of Ccl4 in non-differentiated 3T3-L1 cells (p-HSL/t-HSL: non-differentiated control: +100ng/mL: 0.271±0.1153) whereas little change was observed in differentiated cells (p-HSL/t-HSL: differentiated control: +100ng/mL: 0.602±0.0215) (Figure 58 and 59). Once again, statistical analysis could not be performed on an n=2, therefore, the significance level of treatment effects on lipolysis could not be deduced.

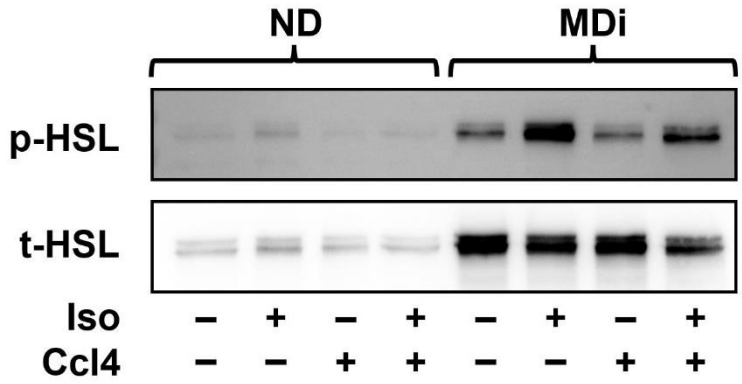

Figure 58. Representative bands for phospho-HSL and total-HSL from Western Blot experiments using 3T3-L1 cells. Cells were treated with either control media or the differentiation cocktail, MDi, in the absence or presence of Ccl4 (100ng/mL). Prior to protein extraction and immunoblotting, cells were treated with medium in the absence of isoprenaline (–) or containing 1µM isoprenaline (Iso) (+). Immunoreactive proteins each of 81/83kDa represent p-HSL(Ser660) and t-HSL. ND: non-differentiated; MDi: differentiated.

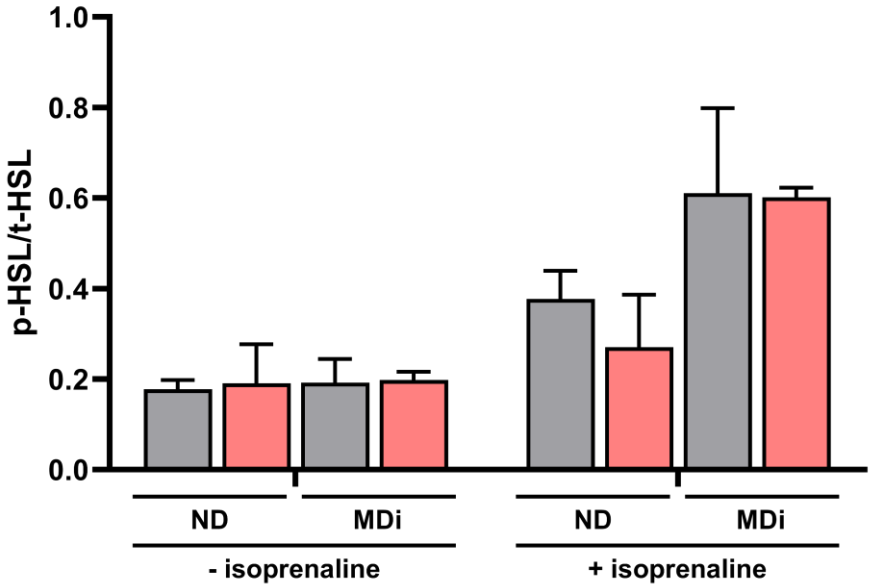

Figure 59. The effect of 48-hour treatment with Ccl4 on lipolysis in the 3T3-L1 adipocyte cell line. Data are expressed as the mean p-HSL/t-HSL ratio ± range. n=2 independent experiments. ND: non-differentiated; MDi: differentiated.

9.4 Discussion

The present chapter evaluated the effects of Ccl4 on some adipogenic functions using the 3T3-L1 preadipocyte cell line which expresses at least one Ccl4-targeted GPCR (Ccr5) (de Mello Coelho et al., 2009). These preliminary data have provided initial insight into the paracrine/autocrine actions of Ccl4 at adipocyte cells.

Undifferentiated or differentiated 3T3-L1 cells displayed signs of unaltered triglyceride synthesis and accumulation following Ccl4 treatment, as evidenced by the quantification of ORO-stained lipid droplets. Measurement of key adipogenic mRNAs by RT-qPCR also showed no significant changes in the expression of the master regulator of adipogenesis, *Pparγ*, with Ccl4 treatment. This contradicts a previous publication which observed increased protein expression of Pparγ2 and an additional adipogenic differentiation marker, aP2, in Ccl4-treated 3T3-L1 preadipocyte cells (de Mello Coelho et al., 2009). These conclusions, however, were made from visualising Western blot bands without any quantification. Furthermore, the differentiation of 3T3-L1 cells was not induced by an MDi cocktail, as is routine, but instead was allowed to spontaneously occur at a significantly slower rate. Thus, microscopic images of control- and Ccl4-treated 3T3-L1 cells indicated lack of confluency and inefficient adipocyte differentiation, as evidenced by scarce cell numbers and limited lipid accumulation (de Mello Coelho et al., 2009). Therefore, these data may be unreliable to compare against the results presented in this current chapter. Despite *Pparγ* mRNA expression being unaltered by Ccl4 treatment, the expression of the adipocyte-specific gene, *AdipoQ*, was significantly downregulated in Ccl4-treated adipocyte cells. This was an interesting observation as *AdipoQ* is a downstream target of Pparγ action. The same expression patterns have been identified by Kim et al. (2015) in adipocytes isolated from high-fat diet-fed obese mice. Subsequently, authors aimed to identify Pparγ-independent pathways, other than transcriptional failure, that were responsible for the obesity-induced reduction in adiponectin expression. They

discovered DNA hypermethylation of the adiponectin promoter impeded adiponectin expression in 3T3-L1 cells, a process promoted by a variety of inflammatory cytokines (Kim et al., 2015). These findings may provide a possible mechanism for Ccl4-induced suppression of *AdipoQ* mRNA expression in the absence of *Pparγ* mRNA changes: as adipose tissue *Ccl4* mRNA is significantly upregulated in obesity, exposure to 3T3-L1 cells in the current chapter partially mimics an obesogenic environment, thereby contributing to epigenetic modifications at the adiponectin promoter. Given the insulin-sensitising properties of adiponectin, reduced *AdipoQ* mRNA expression indicated disturbed insulin sensitivity. However, trends of AKT phosphorylation levels gathered from Western blot experiments suggests a possible absence of Ccl4-induced perturbations to insulin action in 3T3-L1 adipocyte cells, although, there was an upward trend observed in Ccl4-treated differentiated adipocyte cells. Ccl4 treatment may not affect basal lipolysis, whereas a pattern of diminished isoprenaline-stimulated lipolysis in the presence of Ccl4 points towards potential disruption. Only two independent Western blot experiments were conducted for measures of lipid content, lipolysis and insulin sensitivity; an n=3 is the minimum requirement to perform statistical analysis on comparisons between treatment groups, therefore, definitive conclusions regarding the regulatory role of Ccl4 on adipocyte function cannot be made without further repetition.

Ccl4 has been previously implicated in peripheral insulin resistance. Western blot experiments revealed significant improvements in insulin signalling within epididymal adipocytes isolated from diet-induced obese mice administered with a dual Ccr2/Ccr5 antagonist (Huh et al., 2018). This coincided with attenuated weight gain and beneficial morphological changes, as Ccr2/Ccr5 antagonism caused a substantial shift from dysfunctional hypertrophic adipocytes, which are characteristic of metabolic stress, to smaller adipocytes with improved adiponectin secretion. Huh et al. (2018) attributed the improvements in insulin sensitivity to suppressed Ccl2-/Ccl4-induced migration of macrophages and reduced inflammation *in vivo*. This is supported by *in vitro* studies in which adipocyte Ccl2 overexpression induced insulin resistance and macrophage infiltration into adipose tissue of transgenic mice (Kanda et al., 2006). Unfortunately, the direct effect of Ccr2/Ccr5 antagonism on adipocyte function was not fully established. Furthermore, the redundancy of the chemokine system, whereby more than one chemokine can bind and activate a given receptor, means the effect of Ccl4 alone cannot be deduced from antagonising target receptors of multiple chemokines. Ccl4-specific inhibition in diet-induced obese mice was achieved using monoclonal antibodies, which led to improved hepatic and muscle insulin sensitivity, and significantly ameliorated glucose clearance, although adipocyte function was not assessed (Chang et al., 2021). Additional studies have concluded that Ccl4 is a pro-inflammatory adipokine which is associated with perturbed adipocyte function. For example, the endocannabinoid (eCB) system has been shown to modulate adiponectin and Ccl4 expression within adipose tissue. The eCB system comprises of lipid-derived ligands which act at the cannabinoid type 1 receptor (CB1R) to modulate adipocyte differentiation and lipolysis, adipose tissue inflammation, and central adiposity (Ge et al., 2013; Muccioli et al., 2010). Obesity and T2D is characterised by a dysregulation in eCB system tone (Ge et al., 2013). The decrease in adiponectin expression typically observed in obesity was attenuated by CB1R blockade, whereas the mRNA levels of CCL4 and other pro-inflammatory markers were diminished in adipose tissue explants retrieved from obese patients (Ge et al., 2013). Lipopolysaccharide (LPS), which augments eCB tone in adipose tissue, increased the production of Ccl4, TNF-α, IL-6 and IL-10 in 3T3-L1 adipocyte cells, and significantly impaired adipogenesis and lipogenesis (Chirumbolo et al., 2014; Muccioli et al., 2010). Together, these studies suggest Ccl4 is one of several pro-inflammatory chemotactic

mediators which play a deleterious role in modulating adipose tissue function in obesity. Whether this involves direct action at the adipocyte level via chemokine receptor binding remains uncertain.

In summary, the preliminary data presented in this chapter are the first to investigate direct paracrine/autocrine action of Ccl4 on adipocyte differentiation, lipolysis, and insulin sensitivity. Ccl4-induced reductions in *AdipoQ* mRNA may represent a mechanism by which Ccl4 impairs insulin sensitivity. Due to limited time available to carry out additional replicate experiments, the consequence of this reduction in *AdipoQ* on lipolysis and insulin sensitivity could not be confirmed. Further study is required to validate the observed effects of obesity-induced upregulated adipose tissue-derived Ccl4 on adipocyte function.

Chapter 10: General discussion

T2D is a complex, multifactorial disease whose pathology is rooted in the failure of β-cell compensatory mechanisms to overcome peripheral insulin resistance. Subsequent impairment in glucose homeostasis leads to persistent hyperglycaemia, the development of severe complications, and a reduced quality of life for the millions of patients affected worldwide. Inter-organ and inter-cellular communication, particularly in and between adipose tissue and the islets of Langerhans, is a growing topic of extensive research as its dysfunction is a hallmark in insulin resistance and β-cell failure. Various factors produced by adipose tissue cells mediate these communications, including adipokines (peptides), lipokines (lipids), and extracellular vesicles (EVs), to alter islet cell or adipocyte function. The importance of this network is emphasised by changes in the production of secretory products causing significant disruption to normal cellular function and contributing to metabolic dysfunction. These changes typically occur in obesity, a critical risk factor for T2D. Several secretory mediators derived from adipose tissue have already been identified as major regulators of β-cell function. Key examples include leptin, whose pharmacological elevation reverses obesity induced by leptin deficiency, and adiponectin, whose circulating levels are increased by administration of TZDs. The actions of most adipokines, including those that target islet GPCRs, have yet to be characterised and exploited as a pharmacotherapy for T2D. Current pharmacological treatments largely target insulin secretion (e.g. GLP-1RAs) or insulin action (e.g. metformin), but a lack of glycaemic control in most patients fuels the development of new therapies for T2D. Given that GPCRs have considerable druggable capacity, identification of one or more adipokines with functional roles at islet GPCRs in obesity could present a valuable drug candidate for T2D treatment. Consequently, this thesis focused on gaining a greater understanding of the interactions between islet GPCRs and endogenous adipokines in obesity to determine whether candidate(s) could be identified that were appropriate, in the longer term, for new T2D pharmacotherapy development.

Initial experiments screened for islet GPCR peptide ligand mRNAs which were differentially expressed within adipose tissue under lean and obese conditions in several models of obesity. Data were collected from epididymal mature adipocytes and whole epididymal adipose tissue from high-fat diet-induced obese mice, whole epididymal adipose tissue from genetically obese *db/db* mice, and whole omental adipose tissue from obese patients. Several adipokines exhibited significant changes in mRNA expression in obesity. Some notable adipokines, such as Npy and chemerin, have already been extensively researched with respect to their effects on islet function, whilst others, such as angiotensin, are not appropriate candidates for future drug development due to their roles in other organ systems. The chemokine, Ccl4, was selected for further characterisation for three main reasons: 1) Ccl4 mRNA levels were consistently, significantly upregulated in visceral adipose tissue across all obese models suggesting common involvement regardless of aetiology and species; 2) in line with adipose tissue mRNA levels, plasma Ccl4 concentrations were also elevated in obesity indicating potential secretion into the circulation to mediate systemic biological effects; and 3) there is very little published research examining the actions of Ccl4 at islet cells with particular focus on insulin secretion and β-cell mass. Taken together, Ccl4 was flagged as a peptide of interest and functional studies were performed in the MIN6 β-cell line and primary mouse islets to decipher potential modulation of β-cell function. The award of a UKRI/Mitacs grant allowed me to go to Montreal, to the lab of Dr. Gareth Lim, to conduct research on Ccl4-mediated

paracrine/autocrine signalling for the regulation of adipocyte function. These studies present novel findings describing a role for Ccl4 in metabolic metabolism.

10.1 The functional effects of Ccl4 on metabolic tissues

10.1.1 Does Ccl4 have direct effects on islet cells?

Functional experiments which assessed Ccl4-mediated effects in MIN6 β-cells and primary mouse islets revealed inconsistent findings. Although MIN6 β-cell viability and insulin secretion were unaffected, Ccl4 treatment showed initial promise of providing protection to MIN6 β-cells against metabolic stressors observed in obesity. Chemokines are typically associated with deleterious pro-inflammatory effects as their chemotaxis properties regulate the migration of immune cells. On the other hand, some chemokines have been shown to promote cell survival by inhibiting apoptosis. For example, Cxcl12 attenuated apoptosis induced by mixed cytokines, thapsigargin, and glucotoxicity in the INS-1 β-cell line (Liu et al., 2011; Liu & Habener, 2009). Inhibition of its target receptor, Cxcr4, reduced the expression of pro-survival Bcl-2 protein and increased ROS production in MIN6 β-cells, translating to elevated cell death as evidenced by increased numbers of TUNEL+ cells (Yano et al., 2007). Similar observations have been made in other cell types: activation of CXCR4 and CCR7 by their respective ligands, CXCL12 and CCL21, altered the ratio of anti- and pro-apoptotic Bcl proteins to favour the survival of human breast cancer cells (Kochetkova et al., 2009). An inhibition of cytochrome c release suggested interference with the mitochondrial-dependent apoptotic pathway within these cells. Furthermore, the ability of CXCL12 and CCL21 to improve cell viability was prevented by shRNA-induced knockdown of CXCR4 and CCR7, further implicating these receptors in survival mechanisms (Kochetkova et al., 2009). CXCL12 has also promoted the survival of B-chronic lymphocytic leukemia (B-CLL) cells (Ticchioni et al., 2007), human lung adenocarcinoma cells (Wang et al., 2017), CD4+ T-cells (Suzuki et al., 2001), and hematopoietic progenitor cells (Hodohara et al., 2000; Lataillade et al., 2002; Lee et al., 2002). Other chemokines which have enhanced cell survival include CCL19, CCL27 and CXCL13 (Murakami et al., 2003; Ticchioni et al., 2007). Many are linked to the activation of protein kinase B (PKB)/AKT and MAPK/ERK pathways which regulate apoptotic, proliferative, and growth responses. Collectively, the above mentioned studies support the novel anti-apoptotic action of Ccl4. As Ccl4 inhibited MIN6 β-cell proliferation, it is unlikely to have an overall positive effect on β-cell mass despite its ability to promote the survival of β-cells. Factors which confer resistance to apoptosis whilst being anti-proliferative are uncommon. However, astaxanthin (AST), a naturally occurring carotenoid is reported to have anti-apoptotic, anti-proliferative properties in retinal epithelial cells derived from models of diabetic retinopathy (Küçüködük et al., 2019). AST improves cell survival by suppressing mitochondrial production of oxygen radicals, stabilising mitochondrial morphology and activity, and protecting against apoptosis and necroptosis related to mitochondrial and oxidative stress (Dong et al., 2013; Li et al., 2013). On the other hand, AST inhibits proliferation, most likely by reducing the production of vascular endothelial growth factor (VEGF) (Sun et al., 2011). Taking these data into account, Ccl4 may regulate a variety of signalling pathways which converge on the observed phenotype in MIN6 β-cells. However, known Ccl4-target GPCR mRNAs could not be detected in MIN6 β-cells, making it difficult to deduce the specific downstream pathways.

In contrast, when using primary mouse islets, Ccl4 did not alter islet cell apoptosis, and it had no effect on β-cell proliferation or glucose-stimulated insulin secretion. Altogether, the observations seen in MIN6 β-cells failed to translate into primary tissue. It is important to note that many documented chemokine-mediated anti-apoptotic effects were observed in cancerous cells and have implicated chemokines in tumour growth and metastasis. It is possible, therefore, that the actions of the chemokine system are partly dependent on cell or tissue type whereby effects are pronounced in pathological cells which exhibit excessive cell proliferation. This may provide an explanation for why Ccl4 treatment alters the function of an immortal insulinoma β-cell line, but not primary β-cells. Cell-specificity of chemokine action is further supported by the observations here of Ccl4-induced significant loss of islet α-cells but not β- or δ-cells. Cxcl12 provides another example, as its activation of Cxcr4 did not alter proliferation of INS-1 β-cells (Liu & Habener, 2009), but did stimulate the proliferation of alphaTC1-9 cells, an adenoma α-cell line (Liu et al., 2011). There are several factors which dictate the overall effect of GPCR activation, as described in Section 1.6, including distinct pharmacological profiles between differing cell types which may account for Ccl4-mediated α-cell-specific depletion. Alternatively, the only identified Ccl4-target islet GPCR, Cxcr5, may be expressed within α-cells exclusively. It is also possible that islet cell function in response to Ccl4 treatment is influenced by signalling from other endocrine subtypes present within the islet network. It is well-established that β-cells and α-cells communicate, particularly in the event of islet cell injury, and chemokine signalling is a potential method of such communication. For example, it has been hypothesised that Cxcl12/Cxcr4 signalling between β- and α-cells promotes β-cell survival via AKT activation in STZ-damaged islets of Cxcl12 transgenic mice (Yano et al., 2007). It is likely, however, that several chemokines regulate islet cell mass as part of a complex signalling network within the islets. In lieu of cell-specific responses, Ccl4-mediated α-cell loss may be simply a consequence of islet morphology and accessibility, with α-cells located at the periphery being more vulnerable to chemokine toxicity than β-cells localised at the core. However, δ-cell numbers were not affected by Ccl4 treatment despite also being localised in the islet mantle, so accessibility may not account for these differences.

Overall, the data suggest that Ccl4 does not directly act on primary β-cells. Indirect effects via immune cell recruitment to islets *in vivo* is, however, a possibility and this has been demonstrated in published studies. In contrast, Ccl4 reduced the number of islet α-cells, potentially identifying an islet cell that is particularly vulnerable to chemokine action. A resulting decrease in glucagon production would diminish glucoregulatory responses to hypoglycaemia and consequently increase the risk of detrimental hypoglycaemic events.

10.1.2 Does Ccl4 participate in paracrine/autocrine signalling within adipose tissue?

The experiments described here in primary mouse islets indicate that β-cells are not targets of Ccl4 action. However, experiments in an adipocyte cell line have provided preliminary observations of Ccl4-mediated autocrine/paracrine signalling within adipose tissue. Despite there being no change in *Pparγ* mRNA levels, Ccl4 markedly decreased *AdipoQ* mRNA expression in mature adipocytes. Epigenetic modifications were previously discussed in Section 9.4 as being a potential mechanism involved in altered adiponectin expression independent of PPARγ-mediated regulation. Key epigenetic processes are DNA methylation, post-translational histone modifications, chromatin remodelling, and non-coding RNA interactions (Retis-Resendiz et al., 2021); one or more of these could be implicated in this

expression pattern. Given that adiponectin is a crucial adipogenic peptide required for normal adipocyte activity, it was interesting to begin exploring the potential effects of significant *AdipoQ* mRNA reductions on lipid accumulation, lipolysis, and insulin sensitivity in 3T3-L1 cells. Only trends could be established from the interpretation of these data, although some measurements imply the maintenance of some adipocyte function. Changes at the mRNA level do not necessarily correlate with their corresponding protein products. Transcription modifications caused by environmental manipulation can be altered or overridden by translational regulation of which there are multiple levels (Koussounadis et al., 2015). Indeed, studies have observed discordance between mRNA and protein expression in a range of cell types as a result of post-transcriptional and post-translational regulatory mechanisms (de Godoy et al., 2008; Fessler et al., 2002; Huber et al., 2004; Jayapal et al., 2008; Tian et al., 2004). On the other hand, Koussounadis et al. (2015) have studied the relationship between mRNA and protein expression using a xenograft model system exposed to differing environmental conditions and provided details on why mRNA data can be confidently interpreted. For example, mRNAs that are differentially expressed by an environmental condition are more likely to show concordant protein expression compared to mRNAs whose expression does not change by the same condition. Additionally, the rate of protein production can be increased or decreased to align with transcriptional flux (Koussounadis et al., 2015). Follow-up investigations to assess adiponectin protein levels in Ccl4-treated adipocytes will help determine whether divergence from *AdipoQ* mRNA expression contributed to trends in lipolytic and insulin sensitivity effects (see Section 10.2 for future studies).

In parallel with direct action, an indirect influence on adipocyte/adipose tissue function by Ccl4 cannot be ruled out. This would be expected given its chemotactic properties which mediate immune cell migration and inflammatory responses. *In vivo* and *in vitro* experiments, previously mentioned in Section 9.4, have shown the impact of blocking Ccl4-target GPCRs on immunity and inflammation in obesity caused by a high-fat diet (Huh et al., 2018). Reduced adipose tissue macrophage number, a shift from a pro-inflammatory M1 phenotype to an anti-inflammatory M2 phenotype, and diminished CD8+ T-cells within epididymal adipose tissue resulted in attenuated insulin resistance, followed by a global improvement in glucose tolerance and insulin sensitivity (Huh et al., 2018). Ccl4 likely operates in conjunction with other chemokines, such as adipocyte-derived Cxcl12 which, despite displaying beneficial anti-apoptotic properties in β-cell lines, promotes inflammation and insulin resistance in obese adipose tissue by mediating macrophage chemotaxis (Kim et al., 2014). The same can be said for Ccl2 whose suppression and overexpression have supported its involvement in these obesity-related processes (Kanda et al., 2006). Consequently, when progressing towards clinical utility, the immune system must be considered in its entirety. Considerations of chemokine-based therapies are discussed below in Section 10.1.4.

Overall, it is difficult to deduce direct Ccl4-mediated effects on adipocyte function from the data presented here. However, as for the hypothesis described above regarding islet function, Ccl4's chemotactic activity could provide an indirect mechanism to alter adipocyte/adipose tissue function via immune cell/inflammatory regulation.

10.1.3 What are the potential signalling pathways for Ccl4-mediated effects?

Chemokine receptors are GPCRs typically coupled to $G\alpha_{i/o}$ subunits which, upon ligand binding and activation, suppress AC activation, cAMP production and subsequent PKA and

EPAC activity. Simultaneously, as mentioned above in Section 7.4, a large portion of chemokine signalling is conducted through the Gβγ subunits, thereby promoting PLC and PI3K activation. PLC-mediated PIP_2 cleavage generates IP_3, which triggers calcium mobilisation, and DAG, a membrane-bound PKC activator. 3-phosphoinositides are the product of PI3K activity and they serve as anchors for proteins containing pleckstrin homology domains (e.g. PKB/AKT). These signalling pathways are shared amongst Ccl4-target GPCRs, Ccr1, Ccr2, Ccr5, Ccr9, Cxcr1, and Cxcr5. In a recent publication, CCL4 not only significantly activated $G\alpha_i$ and $G\alpha_o$ subunits, but also activated $G\alpha_{12}$ subunits in HEK293T cells expressing CCR5 (Corbisier et al., 2015). As previously described in Section 1.6.1.3, $G\alpha_{12/13}$ proteins play roles in cell migration, growth, shape, and differentiation by regulating Rho GTPase activity and the organisation of the actin cytoskeleton. Moreover, GPCRs coupled to $G\alpha_{12/13}$ subunits at the surface of metabolic tissues (liver, muscle, and adipose tissue) modulate glucose uptake, metabolism, mitochondrial function, and adipocyte differentiation. Abnormal activation, migration, and proliferation of immune cells, including T-cells and lymphocytes, have also been observed following manipulation of $G\alpha_{12}$ signalling (Galandrini et al., 1997; Girkontaite et al., 2001; Herroeder et al., 2009; Rieken et al., 2006). Ccr5 is expressed by 3T3-L1 cells, primary adipocytes, and immune cells within adipose tissue (de Mello Coelho et al., 2009; Hazan et al., 2002), so both $G\alpha_{i/o}$ and $G\alpha_{12}$ signalling pathways may mediate the suppressive effects of Ccl4 on adiponectin expression and/or other undefined actions.

In addition to different associated G protein subclasses, signal bias is a factor which may be affecting the outcome of chemokine receptor stimulation, as GPCRs can signal through multiple downstream signalling pathways with different efficacies. This phenomenon, also termed “biased agonism”, can take the form of ligand, receptor, or tissue bias. The majority of GPCR ligands were once viewed as exhibiting balanced activation of the receptor, i.e. equal activation of G protein signalling and β-arrestin signalling in an “unbiased” response (Wang et al., 2017). However, the concept of biased agonism arose following the identification of ligands which have the capacity to preferentially engage with one pathway over the other (Jones et al., 2018). Similarly, a receptor will signal primarily through a particular pathway (receptor bias), or differential expression of a ligand/receptor complex can induce biased responses (tissue bias). The bidirectional promiscuity of the chemokine family, i.e. several chemokines can activate the same receptor and a single chemokine can activate multiple receptors, was thought to impart functional redundancy. Consequently, differential spatial and temporal expression would determine the function of chemokines and chemokine receptors (Rajagopal et al., 2013). However, biased agonism within the chemokine system has emerged as a mechanism for diverse signalling. For example, Ccr5 is a target for Ccl4, Ccl3 and Ccl5, but assays assessing Ca^{2+} responses, GTPγS binding and receptor internalisation revealed Ccl5 induced signalling with greater potency than Ccl3 and Ccl4 (Corbisier et al., 2015; Mueller et al., 2002; Oppermann et al., 1999). As well as this observed ligand bias, subpopulations of CCR5 possessing distinct conformations were detected within human T-cells, monocytes, and macrophages (Berro et al., 2011; Fox et al., 2015). The subpopulations displayed differences in receptor internalisation induced by Ccl5 analogues in monocyte and macrophage cells, but not T-cells. One such subpopulation acted as a HIV-1 co-receptor but was refractory to chemokine-induced receptor downregulation, so targeting this receptor may prove less effective at inhibiting HIV-1 entry (Fox et al., 2015). Treatment of CCR5-expressing HEK293T cells with CCL4, CCL3 and CCL5 showed no significant differences between G protein and β-arrestin-2 signalling, indicating an absence of signal bias (Corbisier et al., 2015). Interestingly, CCL4 action at CCR5 revealed significant bias towards intracellular calcium mobilisation

relative to cAMP inhibition (Corbisier et al., 2015). This observation supports the favouring of Gβγ- vs Gα-mediated Ccl4 signalling. It is unclear whether Cxcr5, the only Ccl4-activating GPCR expressed in mouse islets, exhibits signal bias and whether this accounts for α-cell-specific responses to Ccl4 treatment.

Ccl4 also targets the atypical chemokine receptor, ACKR2, formerly known as D6. This receptor interacts with most chemokines but is non-signalling and instead functions predominantly as a scavenger receptor through constant cell surface expression, and continuous chemokine internalisation and lysosomal degradation (Galliera et al., 2004). Consequently, ACKR2 is considered a biased receptor as it relies on a G protein-independent, β-arrestin-dependent pathway. Although the receptor was not expressed in MIN6 β-cells or primary islets and likely has no role in signalling pathway activation, by promoting the uptake and removal of chemokines, the presence of ACKR2 on immune cell membranes could regulate the levels of Ccl4 *in vivo*.

Signalling pathways responsible for triggering Ccl4 expression and secretion in obesity may involve TLR4, its associated adaptor protein, myeloid differentiation factor-88 (MyD88), and the subsequent activation of stress-activated protein kinases (SAPKs), JNK activity, and MAPK/NF-κB pathways (Ahmad et al., 2019; Sindhu et al., 2019). This cascade is based on experiments using human monocyte and macrophage cells which were stimulated with TNF-α and palmitate to mimic elevated inflammatory cytokines and FFAs, a hallmark of obesity. Both TNF-α and palmitate augmented CCL4 expression and secretion, and pharmacological or genetic suppression of the TLR4-MyD88 axis, TNF receptors, SAPK/JNK or MAPK/NF-κB pathways abrogated this response (Ahmad et al., 2019; Sindhu et al., 2019).

10.1.4 Could Ccl4 have a novel use in treating type 2 diabetes?

Chemokine-based therapies are already in clinical use, the most established being the CCR5 antagonists which serve as potent anti-viral agents against HIV infection. Abnormal fat distribution, characterised by subcutaneous fat loss (lipoatrophy) and central fat accumulation (lipohypertrophy), is frequently seen in HIV-positive patients (Rodwell et al., 2000). Older generation antiretroviral drugs have been linked to these fat alterations, a phenomenon termed “lipodystrophy” (Koethe et al., 2020). The metabolic effects of clinically approved CCR5 antagonists, such as maraviroc, have been recently investigated in animal models of obesity. Maraviroc inhibits CCL4 as well as CCL3 and CCL5 binding to CCR5 in transfected HEK293 cells, and prevents ligand-stimulated GDP-GTP exchange (Dorr et al., 2005). Maraviroc treatment ameliorated high-fat diet-induced obesity, glucose intolerance (Chan et al., 2021), macrophage accumulation in epididymal fat depots (Pérez-Matute et al., 2017), improved hepatic triglyceride content (Pérez-Martínez et al., 2014, 2018) and modified gut microbiota composition (Pérez-Matute et al., 2015) in mice. The effects of pharmacological Ccr5 antagonism mirrored genetic Ccr5 knockout in high-fat diet-fed mice, whose weight gain, glucose intolerance, insulin resistance and pancreatic inflammation were all improved following Ccr5 depletion (Chan et al., 2021). In support of these animal studies, the expression and release of pro-inflammatory factors, such as IL-6, IL-8 and CCL2, were significantly reduced in maraviroc-treated human adipocytes (Díaz-Delfín et al., 2013). The effects of maraviroc therapy have also been evaluated in obese, insulin-resistant subjects as part of a small Phase I clinical trial, but study outcomes relating to plasma triglycerides and cardiometabolic effects have yet to be published (Washington University School of Medicine,

2013). Altogether, there is a growing body of evidence to support the repurposing of maraviroc to treat metabolic disorders. However, as CCR5 mRNA is not expressed by human islets (Atanes et al., 2021) it is unlikely that CCR5 antagonists will influence β-cell mass and function in human obesity and T2D but their use as a conjunctive may provide a successful therapeutic strategy to address peripheral perturbations.

Previously described publications have shown anti-Ccl4 antibodies improved obesity-induced dysfunction *in vivo* (Chang et al., 2021; Chang & Chen, 2021). Ameliorated insulin resistance, delayed hyperglycaemia progression, and reduced serum triglycerides and systemic inflammation were key improvements (Chang et al., 2021; Chang & Chen, 2021). These early studies indicate the potential for a Ccl4-directed therapy using neutralising antibodies. Figure 60 illustrates the hypothetical pathways through which Ccl4 may mediate its metabolic effects and the potential targets of such a therapy. Instead of functioning at the β-cell, Ccl4 appears to reduce primary α-cell number. Not only would this promote hypoglycaemia due to insufficient glucagon production but would also cause disturbed islet cell-cell communication that is vital for normal islet function. Ccl4-specific antagonism could potentially correct obesity-induced glucose dyshomeostasis by re-establishing the α-cell population, global islet cell connectivity and counterregulatory mechanisms between β-cells and α-cells. Furthermore, blockade of Ccl4-mediated autocrine/paracrine signalling may diminish infiltration of pro-inflammatory mediators and immune cells into adipose tissue and restore adiponectin mRNA expression. These mechanisms would improve adipocyte/adipose tissue function and alleviate insulin resistance, hyperlipidaemia, and systemic inflammation associated with obesity.

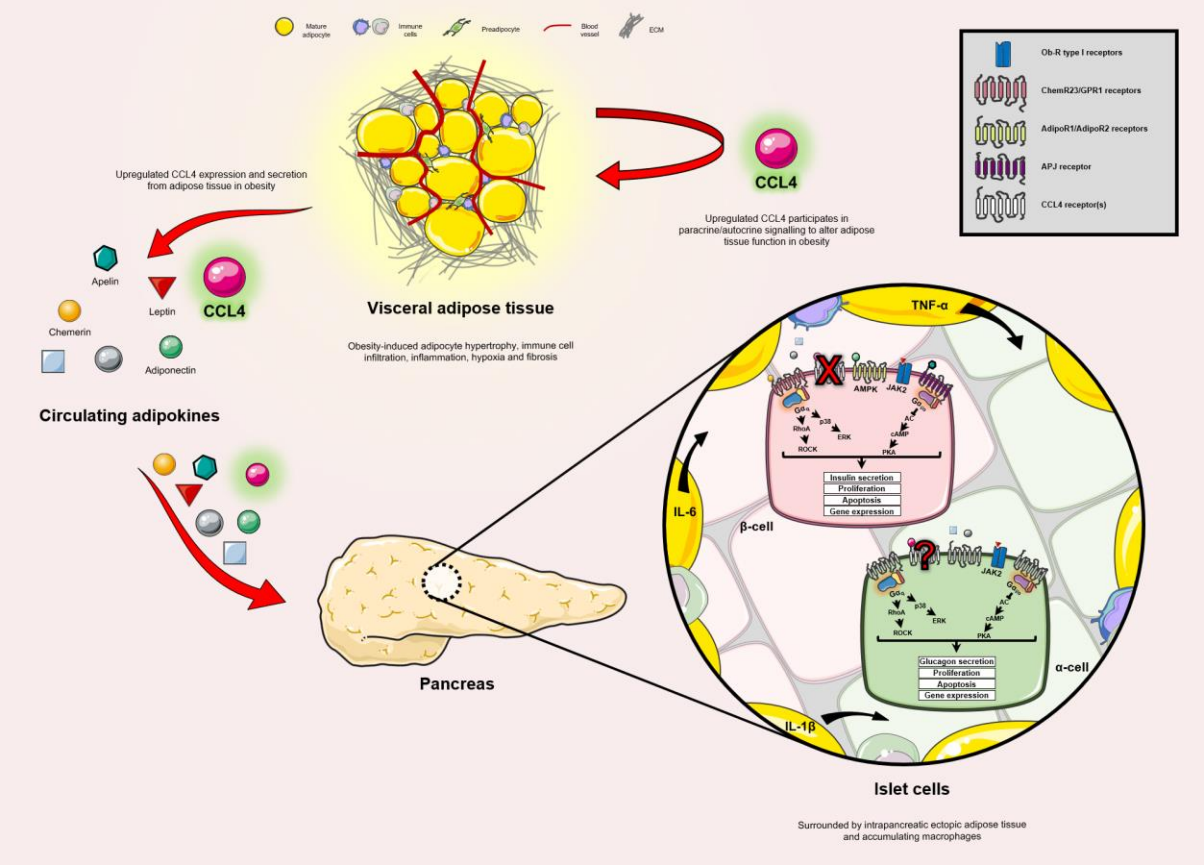

Figure 60. A schematic illustrating the proposed actions of upregulated adipose tissue-derived Ccl4 on islet cells and adipocytes in obesity. There is increased Ccl4 expression within obese adipose tissue which may be the source of increased plasma Ccl4 levels. Circulating adipose tissue-derived Ccl4 may target islet α-cells, but not β-cells, by binding to unknown target GPCR(s) and triggering downstream signalling pathways that lead to α-cell loss. It is possible that Ccl4 influences other α-cell functions, such as glucagon secretion and cell proliferation: these have yet to be determined. Upregulated Ccl4 may also act locally within adipose tissue to directly alter mature adipocyte function and/or indirectly by mediating macrophage recruitment and contributing to inflammatory responses in obesity. Adapted from Atanes et al. (2021).

In summary, CCR5 antagonists and other emerging chemokine-based therapies, such as anti-cancer vaccines (Mizumoto et al., 2020), emphasise the ability of exploiting chemokine signalling in drug development. Ccl4 appears to have a detrimental role in islet and adipose tissue function and represents a potential target for pharmaceutical inhibition for obesity and T2D treatment. There are several considerations, however, that need to be addressed when developing therapies based on chemokine action. Due to the promiscuity of the chemokine system and their involvement in a variety of cellular functions, including global immune cell migration and inflammatory responses, off-target effects pose a significant obstacle. Choosing the appropriate target for modulating Ccl4 signalling is therefore vital. An additional challenge, as with all drugs, is pharmacokinetic interactions which could greatly impact efficacy and toxicity of a chemokine-based therapy. These concerns are particularly relevant to higher-risk patients who are susceptible to or suffer from other comorbidities, such as immunological disorders and cardiovascular disease, which require additional medication. Determining correct dosing and timing of drug administration will help overcome such barriers. Collectively, these challenges will need to be thoroughly assessed in animal models and, if safe and efficacious, translated to human clinical trials.

10.2 Study limitations and future work

The experiments described in this thesis work towards establishing a potential role for Ccl4 in regulating islet and adipocyte function in obesity. The investigation would benefit from additional *in vitro* and *in vivo* studies to further expand our understanding of Ccl4 action. Furthermore, there are several limitations to consider, some of which were caused by laboratory closures and restrictions imposed by the coronavirus pandemic (March to September 2020). Firstly, it was not possible to perform glucose and insulin tolerance testing in high-fat diet-induced obese mice from which whole adipose tissue samples were retrieved. This was due to animal unit closures and limited accessibility which allowed only a handful of researchers to carry out necessary, high priority procedures. Data relating to insulin and glucose tolerance also could not be retrieved from high-fat diet-induced obese mice and *db/db* mice for the isolation of mature adipocytes and the retrieval of whole fat depots, respectively. All mice were kindly shared by colleagues in the Department of Diabetes and additional experiments outside of sample collection could not be carried out. When using animal models of obesity, glucose and insulin tolerance testing is usually performed to ensure they present the expected phenotype, i.e. hyperglycaemia, hyperinsulinaemia and insulin resistance. Although it was not possible to do so in these studies, a 16-week high-fat diet is standard protocol in our department and consistently causes glucose intolerance and overt insulin resistance in mice. Furthermore, the C57BL/6 strain has a greater susceptibility to diet-induced obesity and associated impairment in glucose homeostasis compared to other mouse strains. The diabetic *db/db* mouse model also reliably exhibits the typical metabolic features of obesity. Therefore, despite lacking glucose/insulin tolerance data, there is a high level of confidence that the obese mice were glucose intolerant and insulin resistant. Recordings of significantly elevated plasma glucose levels prior to culling (Figures 18, 24 & 30) also provided good indication of poor glycaemic control in these mice. Plasma glucose and insulin sensitivity data from human donors of omental adipose tissue samples were not available. Individuals were stratified according to BMI, a metric that does not consider multiple factors, such as fat distribution, differentiation between muscle and fat mass, and ethnicities beyond the Caucasian population. Thus, BMI is not an accurate measure of metabolic health in humans and requires supplementation of other clinical measures to better stratify individuals. In addition, patient characteristics could not be matched between BMI categories due to limited sample availability, as described in Section 6.4. Consequently, factors other than excessive visceral adiposity could have influenced mRNA expression profiles of islet GPCR peptide ligand mRNAs in adipose tissue, including age, gender, race, current medications, comorbidities, and medical history. The retrieval of more samples in the future would permit patient matching to control for these variables.

An additional limitation was an incomplete library of chemokine receptor-expressing Tango plasmids, which hindered the identification of all CCL4-activating GPCRs by PRESTO-Tango β-arrestin reporter assays. Until additional plasmids become available, alternative GPCR signalling assays may be used to interrogate the remaining chemokine receptors. For example, the TriCEPS protocol identifies ligand-receptor interactions in living cells by conjugating a biotin-tagged TriCEPS reagent to free amino groups on a peptide ligand and to the glycostructure of its receptor (Frei et al., 2013). Subsequent purification of captured ligand-receptor pairs and analysis by mass spectrometry could establish Ccl4-target receptors (Frei et al., 2013). Other assays based on fluorescence resonance energy transfer (FRET) or bioluminescence resonance energy transfer (BRET) can measure cAMP production or

GTPase activity. These results would aid investigations into the molecular mechanisms of Ccl4 action. A wide variety of approaches could be used to establish signalling partners (e.g. use of enzyme inhibitors, immunohistochemistry to label target proteins, calcium microfluorimetry) and protein-protein interactions (e.g. Western blot/immunoprecipitation, glutathione S-transferase (GST) binding) within β-cells exposed to Ccl4 (Svoboda & Reenstra, 2002).

Future experiments would also include perifusion experiments to supplement static incubation techniques that were performed here. Static incubation experiments involved incubating MIN6 β-cells or primary mouse islets with nutrients and varying Ccl4 concentrations and measuring insulin secretion after a specific time interval. Whilst this is a standard and simple method for assessing insulin secretion without the need for specialised equipment, it has its limitations: the static nature of this technique differs significantly from the dynamics of an *in vivo* environment, and only provides a snapshot of what is occurring within the islet; moreover, depending on the interval length, an accumulation of insulin and additional hormones from the β-cell and other islet cells may influence insulin secretion (Gomez et al., 2020). Islet perifusion experiments, on the other hand, can monitor physiologically relevant dynamic insulin secretion, including first-phase, second-phase, and pulsations of insulin secretion. The method involves the use of perifusion chambers in which groups of islets are exposed to a constant flow of physiological salt solution (Gey & Gey buffer) containing glucose and compounds of interest. The entire experiment is performed at 37ºC, in a temperature-controlled chamber or room, thereby simulating the physiological environment within the pancreas *in vivo*. Perifusate fractions can then be collected at regular intervals (usually every one or two minutes) for later quantification of hormone secretion by radioimmunoassay or ELISA. It would be interesting to see whether the magnitude and pulsation of insulin secretion is influenced by the treatment of islets with Ccl4 during perifusion experiments, which is not visible over the one-hour static incubation protocol. Given that Ccl4 caused significant loss of α-cells within primary mouse islets, glucagon secretion could also be quantified in perifusate fractions to determine a potential reduction that mirrors this loss or whether there is a compensatory increase in glucagon secretory capacity in the remaining α-cells. Moreover, alterations in islet cell-cell communication because of Ccl4-induced α-cell loss may affect β-cell function, therefore, perifusion experiments may provide some insight into coordinated secretion between the two endocrine subtypes when Ccl4 becomes elevated.

Insulin secretion and other functional experiments used islets isolated from lean mice. Assessing insulin secretion, apoptosis, proliferation and GPCR expression in islets isolated from obese mouse models may be more relevant to Ccl4 action since its expression and secretion are upregulated in obesity. Using metabolically stressed islet cells may reveal effects that could not be observed in healthy islets. The same approach could be applied to paracrine/autocrine signalling experiments using adipocytes: 3T3-L1 cells would be exposed to an obesogenic milieu (mixed cytokines or palmitate) and primary adipocytes would be isolated from obese mice. First and foremost, however, Western blot experiments to assess insulin sensitivity and lipolysis in Ccl4-treated 3T3-L1 cells will need to be repeated given that it was not possible to perform statistical evaluation due to insufficient n-number. This will generate more reliable data to either support or oppose functional consequences of reduced adiponectin mRNA expression following Ccl4 treatment. Future adipocyte studies would also quantify adiponectin protein levels to determine whether these mirror adiponectin mRNA levels. This investigation would also benefit from establishing the full expression profile of

Ccl4-target receptors in adipocyte cells and adipose tissue to help determine the signalling pathways involved.

In conjunction with experiments using islets or adipocytes retrieved from obese animal models, it is important to perform parallel studies using human tissues to establish potential species differences in the functional effects of CCL4. If CCL4-mediated effects are not observed in human islets or adipose tissue, future experiments could be carried out using another adipokine of interest from the original qPCR screenings of adipose tissue-derived peptide ligand mRNAs. Peptides involved in crosstalk between islets and adipose tissue/mature adipocytes could also be investigated using a transwell cell culture system. Transwells consist of a lower and upper chamber separated by a permeable small-pored membrane insert through which nutrients, oxygen and secretory peptides can diffuse (Harms et al., 2019). Mature adipocytes that are cultured using this method, termed “mature adipocyte aggregate cultures” (MAAC), retain functionality due to reduced hypoxic stress, are resistant to dedifferentiation, and better maintain adipogenic gene expression compared to other methods, such as ceiling or *ex vivo* cultures (Harms et al., 2019). The secretion of islet GPCR peptide ligands could be measured in supernatants from the long-term culture of mature adipocytes isolated from lean and obese animal models and human subjects; these data would complement mRNA expression data as translation from mRNA expression to peptide secretion from adipose tissue could be deduced. Additionally, the transwell system facilitates communication between mature adipocytes in the lower compartment and different cell types housed in the upper compartment. By exploiting species differences between mouse and humans, future studies would aim to characterise responses of adipocyte/macrophage co-cultures to Ccl4 treatment by analysing culture medium.

10.3 Conclusion

The mRNA expression of the chemokine Ccl4 in visceral adipose tissue is significantly upregulated in murine and human obesity. Whilst Ccl4 has anti-apoptotic and anti-proliferative effects in MIN6 β-cells, it does not act directly on primary β-cells. Ccl4 does, however, cause significant α-cell depletion that may have implications on dynamic islet function. Ccl4 treatment also reduces adiponectin mRNA expression in mature adipocytes pointing towards a paracrine/autocrine function within adipose tissue. Further study in healthy and/or obesogenic α-cells and mature adipocytes will help expand our understanding of how Ccl4 signalling impacts metabolic function in obesity. The GPCR(s) and associated downstream pathways responsible for the observed functional effects of Ccl4 remain undetermined. Nevertheless, the qPCR screenings described here have made available a range of obesity-induced differentially expressed adipose tissue-derived islet GPCR peptide ligand mRNAs for future selection and characterisation. These data contribute to efforts in identifying therapeutically relevant adipokines for the development of new drugs to treat obesity and T2D.

Supplementary Data

Table 21. Significantly upregulated and downregulated islet GPCR peptide ligand mRNAs in isolated mature adipocytes retrieved from control-fat diet and high-fat diet-fed mice. *p<0.05, **p<0.01, ***p<0.001, ****p<0.0001 vs control.

Gene	Fold Change (% Control)	SEM	p-value	Significance
Downregulated genes				
Aldh1a3	67.3	1.44	0.0229	*
Col3a1	55.2	13.73	0.0350	*
Ccl27a	50.6	10.92	0.0330	*
Adm	39.6	7.04	0.0022	***
Nmb	33.0	8.10	0.0094	**
Cxcl1	31.5	3.73	0.0008	***
Penk	19.9	4.97	0.0007	***
Agt	17.2	2.89	0.0162	*
Upregulated genes				
Ghrh	6809.8	1833.39	0.0271	*
Ccl19	883.7	254.40	0.0025	**
Wnt11	225.1	46.68	0.0474	*
Cd55	155.3	19.72	0.0450	*
Col4a2	149.8	10.78	0.0162	*
Cxcl11	46.7	8.66	0.0073	**
Positive controls				
AdipoQ	53.8	6.02	0.0197	*
Lep	457.3	112.29	0.0133	*
Significant trace/absent genes				
Ppbp	57.1	8.46	0.0250	*
Wnt10b	45.2	16.18	0.0351	*
Col4a6	40.4	14.59	0.0458	*
Wnt4	15.2	8.77	0.0083	**
Rspo3	11.4	8.32	0.0019	***
Rln1	7.9	4.83	0.0363	*
Qrfp	7.7	3.76	0.0334	*

Table 22. Significantly upregulated and downregulated islet GPCR peptide ligand mRNAs in whole adipose tissue retrieved from control-fat diet and high-fat diet-fed mice. *p<0.05, **p<0.01, ***p<0.001, ****p<0.0001, ns: non-significant vs control.

Gene	Fold Change (% Control)	SEM	p-value	Significance
Downregulated genes				
Aldh1a2	46.7	7.18	0.0094	**
Wnt9a	46.0	6.67	0.0316	*
Edn1	43.3	8.08	0.0465	*
Wnt2b	40.1	7.63	0.0119	*
Rspo1	39.8	4.57	0.0488	*
Calca	36.2	10.13	0.0245	*
Rdh10	33.5	5.02	0.0206	*
Agt	3.1	0.77	0.0042	****
Upregulated genes				
Npy	2502.3	610.37	0.0107	*
Ccl4	1112.4	166.88	0.0003	****
Ccl3	819.5	200.32	0.0075	**
Anxa1	328.8	53.56	0.0047	***
Ccl8	310.3	58.12	0.0114	*
Ccl11	209.5	44.62	0.0403	*
Ccl7	206.3	31.51	0.0342	*
Wnt11	166.1	18.93	0.0295	*
Positive controls				
AdipoQ	37.7	7.34	0.0759	**NS**
Lep	285.5	32.95	0.0089	***
Significant trace/absent genes				
Ghrh	1759.1	617.81	0.0257	*
Cck	1408.0	313.41	0.0033	***
C5	1118.8	369.56	0.0259	*
Ccl2	955.4	104.26	0.0000	****
Ctsg	494.6	94.52	0.0042	***
Xcl1	169.0	14.99	0.0090	**
Prok2	25.0	12.53	0.0016	*
Wnt10b	22.7	3.61	0.0322	*
Col4a4	18.5	4.95	0.0125	*
Wnt7b	15.4	3.38	0.0459	*
Wnt4	5.5	1.30	0.0494	*
Cxcl3	5.3	3.00	0.0039	***

Table 23. Significantly upregulated and downregulated islet GPCR peptide ligand mRNAs in whole adipose tissue retrieved from lean *db/+* and obese *db/db* mice. *p<0.05, **p<0.01, ***p<0.001, ****p<0.0001, ns: non-significant vs control.

Gene	Fold Change (% Control)	SEM	p-value	Significance
Downregulated genes				
Insl3	77.6	2.77	0.0377	*
C3	62.8	12.92	0.0470	*
Ccl3	59.5	3.18	0.0332	*
Adm	53.7	5.13	0.0016	**
Edn1	44.2	6.93	0.0016	**
Cd55	42.2	9.06	0.0053	**
Rarres2	40.2	9.97	0.0073	**
Rdh10	38.3	5.55	0.0006	***
Aldh1a1	38.0	10.28	0.0064	**
Ppbp	35.3	5.38	0.0023	**
Aldh1a2	34.2	10.37	0.0042	**
Rspo1	31.7	8.38	0.0014	**
Wnt5a	30.7	5.88	0.0012	**
Wnt9a	30.6	8.49	0.0033	**
Npff	28.4	5.21	0.0048	**
Wnt2b	28.0	9.17	0.0031	*
Col4a6	27.7	4.08	0.0008	***
Ccl5	25.8	5.51	0.0293	*
C4a	24.3	3.19	0.0060	**
Ccl21a	19.2	9.22	0.0058	**
Ccl24	16.6	2.54	0.0000	****
Penk	16.0	3.45	0.0001	****
Ccl27b	14.9	1.12	0.0031	**
Ccl27a	14.7	1.94	0.0037	**
Cxcl9	12.0	2.90	0.0099	**
Agt	7.2	1.13	0.0057	**
Cxcl11	5.1	1.44	0.0373	*
Ccl28	4.1	4.05	0.0005	***
Upregulated genes				
Ccl2	1191.2	111.23	0.0006	***
Ccl4	673.6	136.96	0.0147	*
Ccl7	316.2	15.25	0.0003	***
Cxcl14	229.6	16.40	0.0033	**
Col3a1	141.2	7.19	0.0295	*

Positive controls				
AdipoQ	13.7	3.39	0.0009	***
Lep	158.0	52.50	0.3337	**NS**
Significant trace/absent genes				
C5	4398.8	111.23	0.0307	*
Kng	3237.3	136.96	0.0408	*
Cxcl3	1882.0	15.25	0.0337	*
Ndp	470.4	7.19	0.0362	*
Ctsg	459.6	16.40	0.0005	***
Cxcl2	387.9	29.14	0.0027	*
Npw	236.3	16.17	0.0028	**
Trh	67.7	1.80	0.0408	*
C1ql1	63.6	8.54	0.0256	*
Ccl25	53.8	4.56	0.0057	**
Ccl1	44.9	11.99	0.0259	*
Ccl19	37.7	3.85	0.0168	*
C1ql3	34.9	6.86	0.0015	**
Wnt2b	28.0	9.17	0.0031	**
Xcl1	27.8	1.92	0.0369	*
Rspo3	27.2	4.84	0.0049	**
Ghrl	27.1	14.79	0.0272	*
Insl5	26.5	11.84	0.0214	*
Wnt6	25.8	5.85	0.0044	**
Ccl17	25.8	6.04	0.0269	*
Wnt9b	24.2	8.90	0.0494	*
Sct	23.7	5.72	0.0006	***
Vip	22.1	12.17	0.0260	*
Wnt10b	16.5	6.69	0.0023	**
Wnt10a	14.6	10.64	0.0062	**
Wnt5b	12.5	1.86	0.0000	****
C1ql4	12.3	5.54	0.0021	**
Col4a3	11.5	2.58	0.0018	**
Wnt3a	9.9	9.88	0.0148	*
Lhb	9.3	5.05	0.0044	**
Col4a4	6.8	1.07	0.0002	***
Rln1	5.3	5.33	0.0029	**
Rspo2	4.0	2.35	0.0001	****

Table 24. Significantly upregulated and downregulated islet GPCR peptide ligand mRNAs in whole adipose tissue retrieved from lean and obese human patients. *p<0.05, **p<0.01, ns: non-significant vs control.

Gene	Fold Change (% Control)	SEM	p-value	Significance
Downregulated genes				
C5	41.6	7.13	0.0306	*
Upregulated genes				
CCL3	481.9	120.33	0.0157	*
CCL4	260.5	28.21	0.0144	*
Positive controls				
ADIPOQ	66.4	8.23	0.3585	NS
LEP	293.6	86.76	0.1148	NS
Significant trace/absent genes				
ADCYAP1	410.6	104.86	0.0326	*
C1QL4	41.0	12.43	0.0031	**

Table 25. Expression levels of mRNAs encoding Ccl4-targeting GPCRs in MIN6 β-cells and mouse islets. mRNAs were classified as being expressed (>0.001% relative to *Actb*), at trace level (0.0001% to 0.001% relative to *Actb* expression) or absent (< 0.0001% relative to *Actb*) (n=4 per group).

		Level of mRNA expression			
		MIN6 β-cells		Mouse islets	
		Mean	SEM	Mean	SEM
GPCR	***Ackr2***	0.0000013	0.0000006	0.0000000	0.0000000
	Ccr1	0.0000000	0.0000000	0.0009480	0.0001416
	Ccr2	0.0000008	0.0000008	0.0002000	0.0000389
	Ccr5	0.0000000	0.0000000	0.0009375	0.0002484
	Ccr9	0.0000108	0.0000019	0.0000133	0.0000054
	Cxcr1	0.0000005	0.0000005	0.0000008	0.0000008
	Cxcr5	0.0000418	0.0000065	0.0016630	0.0003068

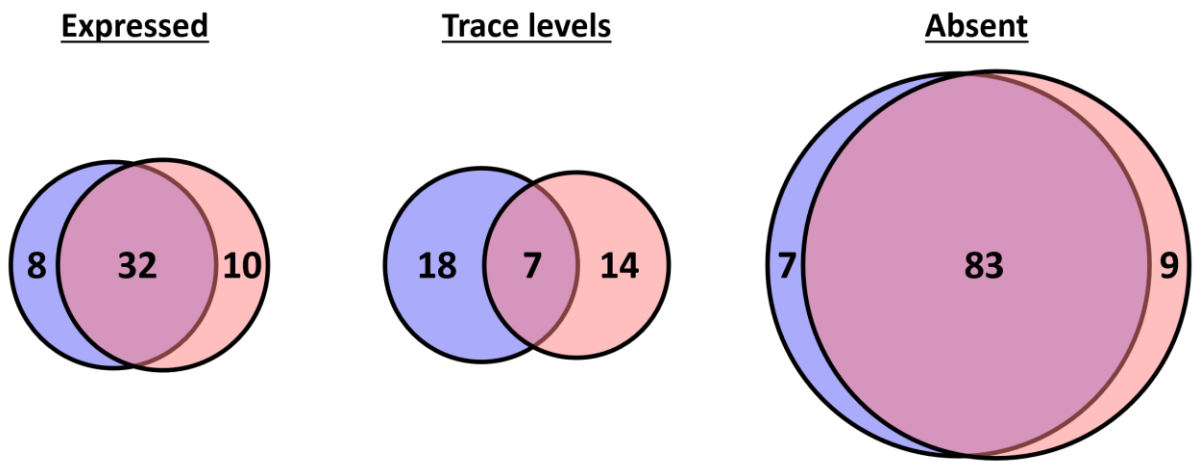

Figure 61. Proportions of islet GPCR peptide ligand mRNAs classified as being expressed, at trace level, or absent in whole adipose tissue (blue) and isolated mature adipocytes (orange) retrieved from high-fat diet-induced obese mice. Data were obtained by RT-qPCR quantifications of RNA isolated from 5 whole fat samples and 4 pooled adipocyte samples. Genes common to both whole adipose tissue and isolated mature adipocytes are shown by the pink intersections. Expressed >0.001% relative to *Actb*; trace = 0.0001% to 0.001% relative to *Actb*; absent < 0.0001% relative to *Actb*.

Table 26. Unique (white) and common (red) mRNAs encoding islet GPCR peptide ligands found expressed, at trace level, or absent in whole adipose tissue and isolated mature adipocytes (adipo) retrieved from high-fat diet-induced obese mice.

Whole Adipose Tissue vs Isolated Mature Adipocytes (Mouse)					
Expressed		**Trace**		**Absent**	
Whole	**Adipo**	**Whole**	**Adipo**	**Whole**	**Adipo**
Col4a5	*Apln*	*Apln*	*C1ql3*	*C1ql1*	*C5*
Col4a6	*C1ql1*	*C5*	*Ccl17*	*C1ql3*	*Cck*
Cxcl13	*Calca*	*Calca*	*Ccl21a*	*Ccl17*	*Ctsg*
Edn1	*Ccl2*	*Cck*	*Col4a5*	*Ccl21a*	*F2*
Nmb	*Ccl24*	*Ccl2*	*Col4a6*	*Cxcl3*	*Gnhr1*
Npff	*Ccl27b*	*Ccl24*	*Cxcl13*	*Wnt8b*	*Kng1*
Npy	*Cxcl10*	*Ccl27b*	*Cxcl3*	*Xcl1*	*Pthlh*
Wnt2b	*Cxcl2*	*Ctsg*	*Edn1*	*Adcyap1*	*Rspo3*
Adm	*Ghrh*	*Cxcl10*	*Nmb*	*Adm2*	*Wnt2*
Agt	*Wnt5b*	*Cxcl2*	*Npff*	*Avp*	*Adcyap1*
Aldh1a1	*Adm*	*F2*	*Npy*	*Bglap*	*Adm2*
Aldh1a2	*Agt*	*Ghrh*	*Wnt2b*	*C1ql2*	*Avp*
Aldh1a3	*Aldh1a1*	*Gnhr1*	*Wnt8b*	*C1ql4*	*Bglap*
Anxa1	*Aldh1a2*	*Kng1*	*Xcl1*	*Calcb*	*C1ql2*

C3	Aldh1a3	Pthlh	Ccl22	Cartpt	C1ql4
C4a	Anxa1	Rspo3	Ccl25	Ccl1	Calcb
Ccl11	C3	Wnt2	Cx3cl1	Ccl20	Cartpt
Ccl19	C4a	Wnt5b	Cxcl11	Ccl26	Ccl1
Ccl27a	Ccl11	Ccl22	Ppbp	Ccl28	Ccl20
Ccl3	Ccl19	Ccl25	Rspo1	Cga	Ccl26
Ccl4	Ccl27a	Cx3cl1	Wnt9a	Col4a3	Ccl28
Ccl5	Ccl3	Cxcl11		Col4a4	Cga
Ccl7	Ccl4	Ppbp		Cort	Col4a3
Ccl8	Ccl5	Rspo1		Crh	Col4a4
Cd55	Ccl7	Wnt9a		Cxcl17	Cort
Col3a1	Ccl8			Cxcl5	Crh
Col4a1	Cd55			Edn2	Cxcl17
Col4a2	Col3a1			Edn3	Cxcl5
Cxcl1	Col4a1			Fshb	Edn2
Cxcl12	Col4a2			Gal	Edn3
Cxcl14	Cxcl1			Galp	Fshb
Cxcl16	Cxcl12			Gast	Gal
Cxcl4	Cxcl14			Gcg	Galp
Cxcl9	Cxcl16			Ghrl	Gast
Insl3	Cxcl4			Gip	Gcg
Penk	Cxcl9			Grp	Ghrl
Rarres2	Insl3			Hcrt	Gip
Rdh10	Penk			Iapp	Grp
Wnt11	Rarres2			Insl5	Hcrt
Wnt5a	Rdh10			Kiss1	Iapp
	Wnt11			Lhb	Insl5
	Wnt5a			Ndp	Kiss1
				Nms	Lhb
				Nmu	Ndp
				Nps	Nms
				Npvf	Nmu
				Npw	Nps
				Nts	Npvf
				Oxt	Npw
				Pdny	Nts
				Pmch	Oxt
				Pnoc	Pdny
				Pomc	Pmch
				Ppy	Pnoc
				Prlh	Pomc
				Prok1	Ppy
				Prok2	Prlh
				Prss1	Prok1
				Pth	Prok2
				Pth2	Prss1

				Pyy	*Pth*
				Qrfp	*Pth2*
				Rln1	*Pyy*
				Rln3	*Qrfp*
				Rspo2	*Rln1*
				Rspo4	*Rln3*
				Sct	*Rspo2*
				Sst	*Rspo4*
				Tac1	*Sct*
				Tac2	*Sst*
				Thy1	*Tac1*
				Trh	*Tac2*
				Tshb	*Thy1*
				Ucn	*Trh*
				Ucn2	*Tshb*
				Ucn3	*Ucn*
				Uts2	*Ucn2*
				Vip	*Ucn3*
				Wnt1	*Uts2*
				Wnt10a	*Vip*
				Wnt10b	*Wnt1*
				Wnt16	*Wnt10a*
				Wnt3	*Wnt10b*
				Wnt3a	*Wnt16*
				Wnt4	*Wnt3*
				Wnt6	*Wnt3a*
				Wnt7a	*Wnt4*
				Wnt7b	*Wnt6*
				Wnt8a	*Wnt7a*
				Wnt9b	*Wnt7b*
					Wnt8a
					Wnt9b

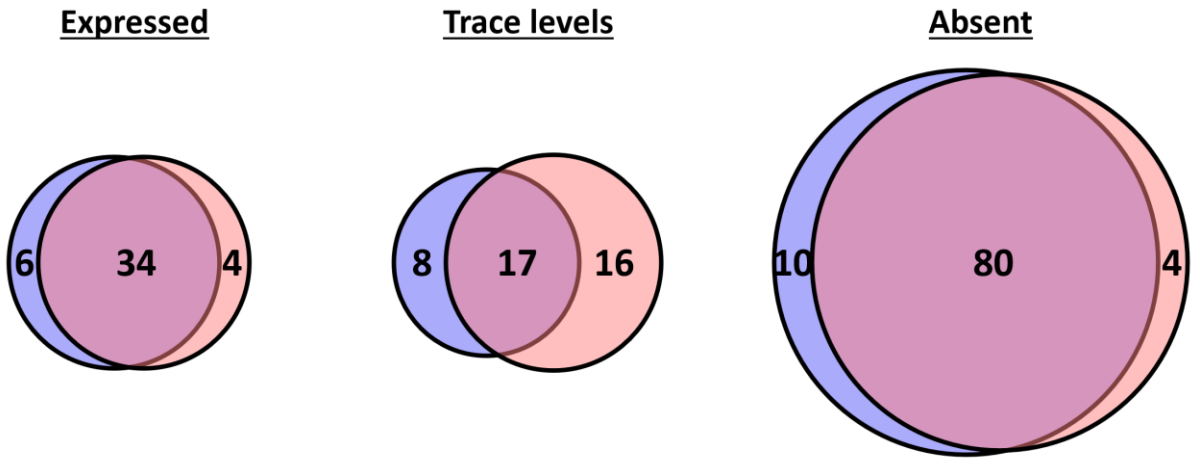

Figure 62. Proportions of islet GPCR peptide ligand mRNAs classified as being expressed, at trace level, or absent in whole visceral adipose tissue retrieved from high-fat diet-induced obese mice (blue) and *db/db* obese mice (orange). Data were obtained by RT-qPCR quantifications of RNA isolated from 5 diet-induced obese mice and 3 *db/db* obese mice. Genes common to both environmental and genetic mouse models are shown by the pink intersections. Expressed >0.001% relative to *Actb*; trace = 0.0001% to 0.001% relative to *Actb*; absent < 0.0001% relative to *Actb*.

Table 27. Unique (white) and common (red) mRNAs encoding islet GPCR peptide ligands found expressed, at trace level, or absent in whole adipose tissue retrieved from obese mice fed a high-fat diet (HFD) and obese *db/db* mice.

Environmental vs Genetic Obesity (Mouse)					
Expressed		**Trace**		**Absent**	
HFD	***db/db***	**HFD**	***db/db***	**HFD**	***db/db***
Ccl19	*Ccl2*	*Cck*	*C1ql1*	*C1ql1*	*Cck*
Ccl27a	*Ccl21a*	*Ccl2*	*Calcb*	*Calcb*	*F2*
Col4a6	*Ccl24*	*Ccl24*	*Ccl17*	*Ccl17*	*Kng1*
Cxcl13	*Cx3cl1*	*Cx3cl1*	*Ccl19*	*Ccl21a*	*Wnt5b*
Edn1	*Adm*	*F2*	*Ccl27a*	*Cxcl3*	*Adcyap1*
Nmb	*Agt*	*Gnhr1*	*Col4a6*	*Cxcl5*	*Adm2*
Adm	*Aldh1a1*	*Kng1*	*Cxcl13*	*Npw*	*Avp*
Agt	*Aldh1a2*	*Wnt5b*	*Cxcl3*	*Thy1*	*Bglap*
Aldh1a1	*Aldh1a3*	*Apln*	*Cxcl5*	*Wnt10b*	*C1ql2*
Aldh1a2	*Anxa1*	*C5*	*Edn1*	*Wnt4*	*C1ql3*
Aldh1a3	*C3*	*Calca*	*Gnrh1*	*Adcyap1*	*C1ql4*
Anxa1	*C4a*	*Ccl22*	*Nmb*	*Adm2*	*Cartpt*
C3	*Ccl11*	*Ccl25*	*Npw*	*Avp*	*Ccl1*
C4a	*Ccl3*	*Ccl27b*	*Thy1*	*Bglap*	*Ccl20*

Ccl11	Ccl4	Ctsg	Wnt10b	C1ql2	Ccl26
Ccl3	Ccl5	Cxcl10	Wnt4	C1ql3	Ccl28
Ccl4	Ccl7	Cxcl11	Apln	C1ql4	Cga
Ccl5	Ccl8	Cxcl2	C5	Cartpt	Col4a3
Ccl7	Cd55	Ghrh	Calca	Ccl1	Col4a4
Ccl8	Col3a1	Ppbp	Ccl22	Ccl20	Cort
Cd55	Col4a1	Pthlh	Ccl25	Ccl26	Crh
Col3a1	Col4a2	Rspo1	Ccl27b	Ccl28	Cxcl17
Col4a1	Col4a5	Rspo3	Ctsg	Cga	Edn2
Col4a2	Cxcl1	Wnt2	Cxcl10	Col4a3	Edn3
Col4a5	Cxcl12	Wnt9a	Cxcl11	Col4a4	Fshb
Cxcl1	Cxcl14		Cxcl2	Cort	Gal
Cxcl12	Cxcl16		Ghrh	Crh	Galp
Cxcl14	Cxcl4		Ppbp	Cxcl17	Gast
Cxcl16	Cxcl9		Pthlh	Edn2	Gcg
Cxcl4	Insl3		Rspo1	Edn3	Ghrl
Cxcl9	Npff		Rspo3	Fshb	Gip
Insl3	Npy		Wnt2	Gal	Grp
Npff	Penk		Wnt9a	Galp	Hcrt
Npy	Rarres2			Gast	Iapp
Penk	Rdh10			Gcg	Insl5
Rarres2	Wnt11			Ghrl	Kiss1
Rdh10	Wnt2b			Gip	Lhb
Wnt11	Wnt5a			Grp	Ndp
Wnt2b				Hcrt	Nms
Wnt5a				Iapp	Nmu
				Insl5	Nps
				Kiss1	Npvf
				Lhb	Nts
				Ndp	Oxt
				Nms	Pdny
				Nmu	Pmch
				Nps	Pnoc
				Npvf	Pomc
				Nts	Ppy
				Oxt	Prlh
				Pdny	Prok1
				Pmch	Prok2
				Pnoc	Prss1
				Pomc	Pth
				Ppy	Pth2
				Prlh	Pyy
				Prok1	Qrfp
				Prok2	Rln1
				Prss1	Rln3
				Pth	Rspo2

				Pth2	*Rspo4*
				Pyy	*Sct*
				Qrfp	*Sst*
				Rln1	*Tac1*
				Rln3	*Tac2*
				Rspo2	*Trh*
				Rspo4	*Tshb*
				Sct	*Ucn*
				Sst	*Ucn2*
				Tac1	*Ucn3*
				Tac2	*Uts2*
				Trh	*Vip*
				Tshb	*Wnt1*
				Ucn	*Wnt10a*
				Ucn2	*Wnt16*
				Ucn3	*Wnt3*
				Uts2	*Wnt3a*
				Vip	*Wnt6*
				Wnt1	*Wnt7a*
				Wnt10a	*Wnt7b*
				Wnt16	*Wnt8a*
				Wnt3	*Wnt8b*
				Wnt3a	*Wnt9b*
				Wnt6	*Xcl1*
				Wnt7a	
				Wnt7b	
				Wnt8a	
				Wnt8b	
				Wnt9b	
				Xcl1	

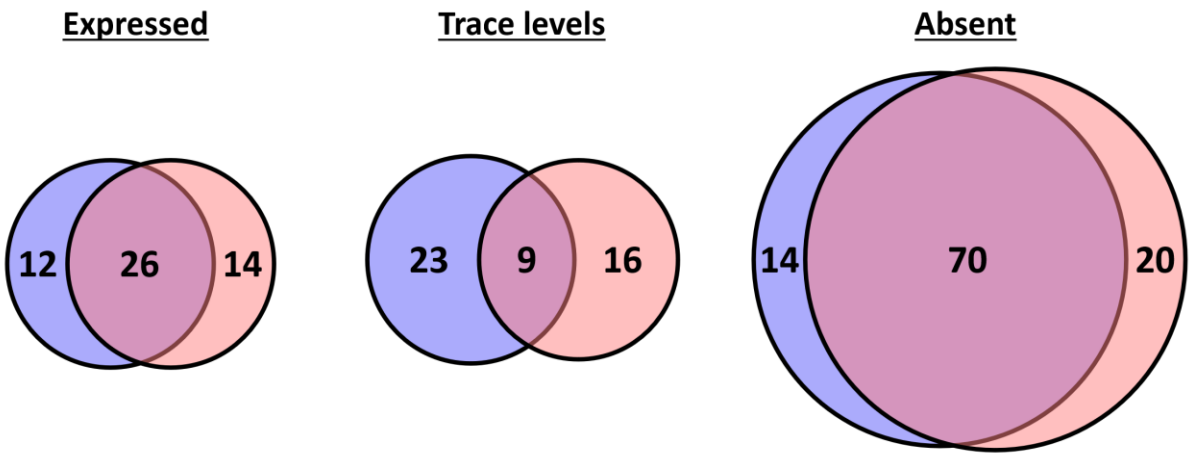

Figure 63. Proportions of islet GPCR peptide ligand mRNAs classified as being expressed, at trace level, or absent in whole visceral adipose tissue retrieved from obese human donors (blue) and high-fat diet-induced obese mice (orange). Data were obtained by RT-qPCR quantifications of RNA isolated from 5 mice and 4 human donors. Genes common to both mice and humans are shown by the pink intersections. Expressed >0.001% relative to *ACTB*; trace = 0.0001% to 0.001% relative to *ACTB*; absent < 0.0001% relative to *ACTB*.

Table 28. Unique (white) and common (red) mRNAs encoding islet GPCR peptide ligands found expressed, at trace level, or absent in whole adipose tissue retrieved from obese human subjects and high-fat diet-induced obese mice.

Human vs Mouse					
Expressed		**Trace**		**Absent**	
Human	**Mouse**	**Human**	**Mouse**	**Human**	**Mouse**
CCL2	*Ccl11*	*ADCYAP1*	*Calca*	*CALCA*	*Adcyap1*
CCL21	*Ccl19*	*BGLAP*	*Cck*	*CCK*	*Bglap*
CCL24	*Ccl27a*	*C1QL1*	*Ccl2*	*CCL25*	*C1ql1*
CTSG	*Ccl7*	*C1QL3*	*Ccl24*	*CCL27*	*C1ql3*
CX3CL1	*Ccl8*	*CCL11*	*Ccl25*	*CCL7*	*Ccl20*
CXCL2	*Col4a5*	*CCL19*	*Ccl27b*	*CCL8*	*Ccl21a*
CXCL3	*Col4a6*	*CCL20*	*Ctsg*	*CXCL11*	*Ccl26*
PROK2	*Cxcl13*	*CCL26*	*Cx3cl1*	*CXCL13*	*Cxcl3*
PTHLH	*Cxcl4*	*COL4A5*	*Cxcl11*	*F2*	*Npw*
RSPO1	*Cxcl9*	*COL4A6*	*Cxcl2*	*GHRH*	*Nts*
RSPO3	*Insl3*	*CXCL4*	*F2*	*INSL3*	*Prok1*
THY1	*Npff*	*CXCL9*	*Ghrh*	*KNG1*	*Prok2*
ADM	*Npy*	*NPFF*	*Kng1*	*NPY*	*Qrfp*
AGT	*Wnt2b*	*NPW*	*Pthlh*	*TAC3*	*Tac2*
ALDH1A1	*Adm*	*NTS*	*Rspo1*	*ADM2*	*Thy1*
ALDH1A2	*Agt*	*PROK1*	*Rspo3*	*AVP*	*Ucn*

ALDH1A3	Aldh1a1	QRFP	Apln	C1QL2	Vip
ANXA1	Aldh1a2	UCN	C5	C1QL4	Wnt10a
C3	Aldh1a3	VIP	Ccl22	CALCB	Wnt3
C4A	Anxa1	WNT10A	Cxcl10	CARTPT	Wnt4
CCL3	C3	WNT2B	Gnhr1	CCL1	Adm2
CCL4	C4a	WNT3	Ppbp	CCL17	Avp
CCL5	Ccl3	WNT4	Wnt2	CCL28	C1ql2
CD55	Ccl4	APLN	Wnt5b	CGA	C1ql4
COL3A1	Ccl5	C5	Wnt9a	COL4A3	Calcb
COL4A1	Cd55	CCL22		COL4A4	Cartpt
COL4A2	Col3a1	CXCL10		CORT	Ccl1
CXCL1	Col4a1	GNHR1		CRH	Ccl17
CXCL12	Col4a2	PPBP		CXCL17	Ccl28
CXCL14	Cxcl1	WNT2		CXCL5	Cga
CXCL16	Cxcl12	WNT5B		EDN2	Col4a3
EDN1	Cxcl14	WNT9A		EDN3	Col4a4
NMB	Cxcl16			FSHB	Cort
PENK	Edn1			GAL	Crh
RARRES2	Nmb			GALP	Cxcl17
RDH10	Penk			GAST	Cxcl5
WNT11	Rarres2			GCG	Edn2
WNT5A	Rdh10			GHRL	Edn3
	Wnt11			GIP	Fshb
	Wnt5a			GRP	Gal
				HCRT	Galp
				IAPP	Gast
				INSL5	Gcg
				KISS1	Ghrl
				LHB	Gip
				NDP	Grp
				NMS	Hcrt
				NMU	Iapp
				NPS	Insl5
				NPVF	Kiss1
				OXT	Lhb
				PDNY	Ndp
				PMCH	Nms
				PNOC	Nmu
				POMC	Nps
				PPY	Npvf
				PRLH	Oxt
				PRSS1	Pdny
				PTH	Pmch
				PTH2	Pnoc
				PYY	Pomc
				RLN1	Ppy

				RLN3	Prlh
				RSPO2	Prss1
				RSPO4	Pth
				SCT	Pth2
				SST	Pyy
				TAC1	Rln1
				TRH	Rln3
				TSHB	Rspo2
				UCN2	Rspo4
				UCN3	Sct
				UTS2	Sst
				WNT1	Tac1
				WNT10B	Trh
				WNT16	Tshb
				WNT3A	Ucn2
				WNT6	Ucn3
				WNT7A	Uts2
				WNT7B	Wnt1
				WNT8A	Wnt10b
				WNT8B	Wnt16
				WNT9B	Wnt3a
				XCL1	Wnt6
					Wnt7a
					Wnt7b
					Wnt8a
					Wnt8b
					Wnt9b
					Xcl1

References

Aberle, H., Schwartz, H., & Kemler, R. (1996). Cadherin-catenin complex: Protein interactions and their implications for cadherin function. *Journal of Cellular Biochemistry*, *61*(4), 514–523. https://doi.org/10.1002/(SICI)1097-4644(19960616)61:4%3C514::AID-JCB4%3E3.0.CO;2-R

Ackermann, A. M., & Gannon, M. (2007). Molecular regulation of pancreatic beta-cell mass development, maintenance, and expansion. *Journal of Molecular Endocrinology*, *38*(1–2), 193–206. https://doi.org/10.1677/JME-06-0053

Adams, T. D., Davidson, L. E., Litwin, S. E., Kim, J., Kolotkin, R. L., Nanjee, M. N., Gutierrez, J. M., Frogley, S. J., Ibele, A. R., Brinton, E. A., Hopkins, P. N., McKinlay, R., Simper, S. C., & Hunt, S. C. (2017). Weight and Metabolic Outcomes 12 Years after Gastric Bypass. *The New England Journal of Medicine*, *377*(12), 1143–1155. https://doi.org/10.1056/NEJMoa1700459

Ahmad, R., Kochumon, S., Chandy, B., Shenouda, S., Koshy, M., Hasan, A., Arefanian, H., Al-Mulla, F., & Sindhu, S. (2019). TNF-α Drives the CCL4 Expression in Human Monocytic Cells: Involvement of the SAPK/JNK and NF-κB Signaling Pathways. *Cellular Physiology and Biochemistry: International Journal of Experimental Cellular Physiology, Biochemistry, and Pharmacology*, *52*(4), 908–921. https://doi.org/10.33594/000000063

Ahmadzai, M. M., Broadbent, D., Occhiuto, C., Yang, C., Das, R., & Subramanian, H. (2017). Canonical and Noncanonical Signaling Roles of β-Arrestins in Inflammation and Immunity. *Advances in Immunology*, *136*, 279–313. https://doi.org/10.1016/bs.ai.2017.05.004

Ahrén, B. (2012). Islet nerves in focus—Defining their neurobiological and clinical role. *Diabetologia*, *55*(12), 3152–3154. https://doi.org/10.1007/s00125-012-2727-6

Ahrén, B., & Holst, J. J. (2001). The cephalic insulin response to meal ingestion in humans is dependent on both cholinergic and noncholinergic mechanisms and is important for postprandial glycemia. *Diabetes*, *50*(5), 1030–1038. https://doi.org/10.2337/diabetes.50.5.1030

Ahrén, B., & Lundquist, I. (1981). Effects of selective and non-selective beta-adrenergic agents on insulin secretion in vivo. *European Journal of Pharmacology*, *71*(1), 93–104. https://doi.org/10.1016/0014-2999(81)90390-3

Al Hasan, M., Martin, P. E., Shu, X., Patterson, S., & Bartholomew, C. (2021). Type III Collagen is Required for Adipogenesis and Actin Stress Fibre Formation in 3T3-L1 Preadipocytes. *Biomolecules*, *11*(2), 156. https://doi.org/10.3390/biom11020156

Alarcon, C., Wicksteed, B., & Rhodes, C. J. (2006). Exendin 4 controls insulin production in rat islet beta cells predominantly by potentiation of glucose-stimulated proinsulin biosynthesis at the translational level. *Diabetologia*, *49*(12), 2920–2929. https://doi.org/10.1007/s00125-006-0433-y

Amisten, S. (2016). Quantification of the mRNA expression of G protein-coupled receptors in human adipose tissue. *Methods in Cell Biology*, *132*, 73–105. https://doi.org/10.1016/bs.mcb.2015.10.004

Amisten, S., Atanes, P., Hawkes, R., Ruz-Maldonado, I., Liu, B., Parandeh, F., Zhao, M., Huang, G. C., Salehi, A., & Persaud, S. J. (2017). A comparative analysis of human and mouse islet G-protein coupled receptor expression. *Scientific Reports*, *7*, 46600. https://doi.org/10.1038/srep46600

Amisten, S., Salehi, A., Rorsman, P., Jones, P. M., & Persaud, S. J. (2013). An atlas and functional analysis of G-protein coupled receptors in human islets of Langerhans. *Pharmacology & Therapeutics*, *139*(3), 359–391. https://doi.org/10.1016/j.pharmthera.2013.05.004

Andersen, A., Lund, A., Knop, F. K., & Vilsbøll, T. (2018). Glucagon-like peptide 1 in health and disease. *Nature Reviews Endocrinology*, *14*(7), Article 7. https://doi.org/10.1038/s41574-018-0016-2

Anthonsen, M. W., Rönnstrand, L., Wernstedt, C., Degerman, E., & Holm, C. (1998). Identification of Novel Phosphorylation Sites in Hormone-sensitive Lipase That Are Phosphorylated in

Response to Isoproterenol and Govern Activation Properties in Vitro *. *Journal of Biological Chemistry*, *273*(1), 215–221. https://doi.org/10.1074/jbc.273.1.215

Ariel, A., Fredman, G., Sun, Y.-P., Kantarci, A., Van Dyke, T. E., Luster, A. D., & Serhan, C. N. (2006). Apoptotic neutrophils and T cells sequester chemokines during immune response resolution through modulation of CCR5 expression. *Nature Immunology*, *7*(11), 1209–1216. https://doi.org/10.1038/ni1392

Arita, Y., Kihara, S., Ouchi, N., Takahashi, M., Maeda, K., Miyagawa, J., Hotta, K., Shimomura, I., Nakamura, T., Miyaoka, K., Kuriyama, H., Nishida, M., Yamashita, S., Okubo, K., Matsubara, K., Muraguchi, M., Ohmoto, Y., Funahashi, T., & Matsuzawa, Y. (1999). Paradoxical decrease of an adipose-specific protein, adiponectin, in obesity. *Biochemical and Biophysical Research Communications*, *257*(1), 79–83. https://doi.org/10.1006/bbrc.1999.0255

Armoni, M., Kritz, N., Harel, C., Bar-Yoseph, F., Chen, H., Quon, M. J., & Karnieli, E. (2003). Peroxisome proliferator-activated receptor-gamma represses GLUT4 promoter activity in primary adipocytes, and rosiglitazone alleviates this effect. *The Journal of Biological Chemistry*, *278*(33), 30614–30623. https://doi.org/10.1074/jbc.M304654200

Arner, P., & Rydén, M. (2015). Fatty Acids, Obesity and Insulin Resistance. *Obesity Facts*, *8*(2), 147–155. https://doi.org/10.1159/000381224

Arumugam, R., Horowitz, E., Lu, D., Collier, J. J., Ronnebaum, S., Fleenor, D., & Freemark, M. (2008). The Interplay of Prolactin and the Glucocorticoids in the Regulation of β-Cell Gene Expression, Fatty Acid Oxidation, and Glucose-Stimulated Insulin Secretion: Implications for Carbohydrate Metabolism in Pregnancy. *Endocrinology*, *149*(11), 5401–5414. https://doi.org/10.1210/en.2008-0051

Aslanoglou, D., Bertera, S., Sánchez-Soto, M., Benjamin Free, R., Lee, J., Zong, W., Xue, X., Shrestha, S., Brissova, M., Logan, R. W., Wollheim, C. B., Trucco, M., Yechoor, V. K., Sibley, D. R., Bottino, R., & Freyberg, Z. (2021). Dopamine regulates pancreatic glucagon and insulin

secretion via adrenergic and dopaminergic receptors. *Translational Psychiatry*, *11*(1), Article 1. https://doi.org/10.1038/s41398-020-01171-z

Aslantürk, Ö. S. (2018). In Vitro Cytotoxicity and Cell Viability Assays: Principles, Advantages, and Disadvantages. In M. L. Larramendy & S. Soloneski (Eds.), *Genotoxicity—A Predictable Risk to Our Actual World*. InTech. https://doi.org/10.5772/intechopen.71923

Atanes, P., Ashik, T., & Persaud, S. J. (2021). Obesity-induced changes in human islet G protein-coupled receptor expression: Implications for metabolic regulation. *Pharmacology & Therapeutics*, *228*, 107928. https://doi.org/10.1016/j.pharmthera.2021.107928

Atanes, P., & Persaud, S. J. (2020). Chapter 18—GPCR targets in type 2 diabetes. In B. Jastrzebska & P. S.-H. Park (Eds.), *GPCRs* (pp. 367–391). Academic Press. https://doi.org/10.1016/B978-0-12-816228-6.00018-0

Atanes, P., Ruz-Maldonado, I., Pingitore, A., Hawkes, R., Liu, B., Zhao, M., Huang, G. C., Persaud, S. J., & Amisten, S. (2018). C3aR and C5aR1 act as key regulators of human and mouse β-cell function. *Cellular and Molecular Life Sciences*, *75*(4), 715–726. https://doi.org/10.1007/s00018-017-2655-1

Atkinson, M. A., Campbell-Thompson, M., Kusmartseva, I., & Kaestner, K. H. (2020). Organisation of the human pancreas in health and in diabetes. *Diabetologia*, *63*(10), 1966–1973. https://doi.org/10.1007/s00125-020-05203-7

Avgerinos, I., Michailidis, T., Liakos, A., Karagiannis, T., Matthews, D. R., Tsapas, A., & Bekiari, E. (2020). Oral semaglutide for type 2 diabetes: A systematic review and meta-analysis. *Diabetes, Obesity and Metabolism*, *22*(3), 335–345. https://doi.org/10.1111/dom.13899

Bahary, N., Leibel, R. L., Joseph, L., & Friedman, J. M. (1990). Molecular mapping of the mouse db mutation. *Proceedings of the National Academy of Sciences of the United States of America*, *87*(21), 8642–8646. https://doi.org/10.1073/pnas.87.21.8642

Bahgat, M. M., & Ibrahim, D. R. (2020). Proinflammatory cytokine polarization in type 2 diabetes. *Central-European Journal of Immunology*, *45*(2), 170–175. https://doi.org/10.5114/ceji.2020.97904

Bai, Y., Zhang, S., Kim, K.-S., Lee, J.-K., & Kim, K.-H. (1996). Obese Gene Expression Alters the Ability of 30A5 Preadipocytes to Respond to Lipogenic Hormones. *Journal of Biological Chemistry*, *271*(24), 13939–13942. https://doi.org/10.1074/jbc.271.24.13939

Baker, M. S., Chen, X., Cao, X. C., & Kaufman, D. B. (2001). Expression of a dominant negative inhibitor of NF-kappaB protects MIN6 beta-cells from cytokine-induced apoptosis. *The Journal of Surgical Research*, *97*(2), 117–122. https://doi.org/10.1006/jsre.2001.6121

Banday, M. Z., Sameer, A. S., & Nissar, S. (2020). Pathophysiology of diabetes: An overview. *Avicenna Journal of Medicine*, *10*(4), 174–188. https://doi.org/10.4103/ajm.ajm_53_20

Baranowska, B., Wasilewska-Dziubińska, E., Radzikowska, M., Płonowski, A., & Roguski, K. (1997). Neuropeptide Y, galanin, and leptin release in obese women and in women with anorexia nervosa. *Metabolism: Clinical and Experimental*, *46*(12), 1384–1389. https://doi.org/10.1016/s0026-0495(97)90136-0

Barber, A. J., & Nakamura, M. (2002). Apoptosis and Neurodegeneration in Diabetes: Lessons from the Retina. In E. A. Friedman & F. A. L'Esperance (Eds.), *Diabetic Renal-Retinal Syndrome: Pathogenesis and Management Update 2002* (pp. 35–45). Springer Netherlands. https://doi.org/10.1007/978-94-010-0614-9_4

Barella, L. F., Rossi, M., Pydi, S. P., Meister, J., Jain, S., Cui, Y., Gavrilova, O., Fulgenzi, G., Tessarollo, L., & Wess, J. (2021). β-Arrestin-1 is required for adaptive β-cell mass expansion during obesity. *Nature Communications*, *12*(1), Article 1. https://doi.org/10.1038/s41467-021-23656-1

Baron, A. D., Schaeffer, L., Shragg, P., & Kolterman, O. G. (1987). Role of hyperglucagonemia in maintenance of increased rates of hepatic glucose output in type II diabetics. *Diabetes*, *36*(3), 274–283. https://doi.org/10.2337/diab.36.3.274

Bedner, P., Niessen, H., Odermatt, B., Kretz, M., Willecke, K., & Harz, H. (2006). Selective permeability of different connexin channels to the second messenger cyclic AMP. *The Journal of Biological Chemistry*, *281*(10), 6673–6681. https://doi.org/10.1074/jbc.M511235200

Ben Nasr, M., D'Addio, F., Montefusco, L., Usuelli, V., Loretelli, C., Rossi, A., Pastore, I., Abdelsalam, A., Maestroni, A., Dell'Acqua, M., Ippolito, E., Assi, E., Seelam, A. J., Fiorina, R. M., Chebat, E., Morpurgo, P., Lunati, M. E., Bolla, A. M., Abdi, R., … Fiorina, P. (2022). Indirect and Direct Effects of SARS-CoV-2 on Human Pancreatic Islets. *Diabetes*, *71*(7), 1579–1590. https://doi.org/10.2337/db21-0926

Benalcazar, D. A., & Cascella, M. (2023). Obesity Surgery Pre-Op Assessment And Preparation. In *StatPearls*. StatPearls Publishing. http://www.ncbi.nlm.nih.gov/books/NBK546667/

Bender, C., Christen, S., Scholich, K., Bayer, M., Pfeilschifter, J. M., Hintermann, E., & Christen, U. (2017). Islet-Expressed CXCL10 Promotes Autoimmune Destruction of Islet Isografts in Mice With Type 1 Diabetes. *Diabetes*, *66*(1), 113–126. https://doi.org/10.2337/db16-0547

Bendtzen, K., Mandrup-Poulsen, T., Nerup, J., Nielsen, J. H., Dinarello, C. A., & Svenson, M. (1986). Cytotoxicity of human pI 7 interleukin-1 for pancreatic islets of Langerhans. *Science (New York, N.Y.)*, *232*(4757), 1545–1547. https://doi.org/10.1126/science.3086977

Bener, A., Alsaied, A., Al-Ali, M., Al-Kubaisi, A., Basha, B., Abraham, A., Guiter, G., & Mian, M. (2009). High prevalence of vitamin D deficiency in type 1 diabetes mellitus and healthy children. *Acta Diabetologica*, *46*(3), 183–189. https://doi.org/10.1007/s00592-008-0071-6

Bennet, W. M., Wang, Z. L., Jones, P. M., Wang, R. M., James, R. F., London, N. J., Ghatei, M. A., & Bloom, S. R. (1996). Presence of neuropeptide Y and its messenger ribonucleic acid in human islets: Evidence for a possible paracrine role. *The Journal of Clinical Endocrinology and Metabolism*, *81*(6), 2117–2120. https://doi.org/10.1210/jcem.81.6.8964837

Benninger, R. K. P., Head, W. S., Zhang, M., Satin, L. S., & Piston, D. W. (2011). Gap junctions and other mechanisms of cell–cell communication regulate basal insulin secretion in the

pancreatic islet. *The Journal of Physiology*, *589*(Pt 22), 5453–5466. https://doi.org/10.1113/jphysiol.2011.218909

Bensellam, M., Duvillié, B., Rybachuk, G., Laybutt, D. R., Magnan, C., Guiot, Y., Pouysségur, J., & Jonas, J.-C. (2012). Glucose-induced O_2 consumption activates hypoxia inducible factors 1 and 2 in rat insulin-secreting pancreatic beta-cells. *PloS One*, *7*(1), e29807. https://doi.org/10.1371/journal.pone.0029807

Bensellam, M., Jonas, J.-C., & Laybutt, D. R. (2018). Mechanisms of β-cell dedifferentiation in diabetes: Recent findings and future research directions. *Journal of Endocrinology*, *236*(2), R109–R143. https://doi.org/10.1530/JOE-17-0516

Berger, C., & Zdzieblo, D. (2020). Glucose transporters in pancreatic islets. *Pflugers Archiv*, *472*(9), 1249–1272. https://doi.org/10.1007/s00424-020-02383-4

Bergerot, I., Arreaza, G. A., Cameron, M. J., Burdick, M. D., Strieter, R. M., Chensue, S. W., Chakrabarti, S., & Delovitch, T. L. (1999). Insulin B-chain reactive CD4+ regulatory T-cells induced by oral insulin treatment protect from type 1 diabetes by blocking the cytokine secretion and pancreatic infiltration of diabetogenic effector T-cells. *Diabetes*, *48*(9), 1720–1729. https://doi.org/10.2337/diabetes.48.9.1720

Bergsten, P., Grapengiesser, E., Gylfe, E., Tengholm, A., & Hellman, B. (1994). Synchronous oscillations of cytoplasmic Ca2+ and insulin release in glucose-stimulated pancreatic islets. *Journal of Biological Chemistry*, *269*(12), 8749–8753. https://doi.org/10.1016/S0021-9258(17)37032-1

Berro, R., Klasse, P. J., Lascano, D., Flegler, A., Nagashima, K. A., Sanders, R. W., Sakmar, T. P., Hope, T. J., & Moore, J. P. (2011). Multiple CCR5 conformations on the cell surface are used differentially by human immunodeficiency viruses resistant or sensitive to CCR5 inhibitors. *Journal of Virology*, *85*(16), 8227–8240. https://doi.org/10.1128/JVI.00767-11

Bjørbaek, C., Uotani, S., da Silva, B., & Flier, J. S. (1997). Divergent signaling capacities of the long and short isoforms of the leptin receptor. *The Journal of Biological Chemistry*, *272*(51), 32686–32695. https://doi.org/10.1074/jbc.272.51.32686

Blaabjerg, L., & Juhl, C. B. (2016). Hypoglycemia-Induced Changes in the Electroencephalogram: An Overview. *Journal of Diabetes Science and Technology*, *10*(6), 1259–1267. https://doi.org/10.1177/1932296816659744

Bock, T., Pakkenberg, B., & Buschard, K. (2003). Increased islet volume but unchanged islet number in ob/ob mice. *Diabetes*, *52*(7), 1716–1722. https://doi.org/10.2337/diabetes.52.7.1716

Boden, G. (2001). Free Fatty Acids—The Link Between Obesity and Insulin Resistance. *Endocrine Practice*, *7*(1), 44–51. https://doi.org/10.4158/EP.7.1.44

Boden, G., Chen, X., Ruiz, J., White, J. V., & Rossetti, L. (1994). Mechanisms of fatty acid-induced inhibition of glucose uptake. *Journal of Clinical Investigation*, *93*(6), 2438–2446.

Bone, A. J., & Taylor, K. W. (1976). Metabolic adaptation to pregnancy shown by increased biosynthesis of insulin in islets of Langerhans isolated from pregnant rats. *Nature*, *262*(5568), Article 5568. https://doi.org/10.1038/262501a0

Bonecchi, R., Locati, M., Galliera, E., Vulcano, M., Sironi, M., Fra, A. M., Gobbi, M., Vecchi, A., Sozzani, S., Haribabu, B., Van Damme, J., & Mantovani, A. (2004). Differential Recognition and Scavenging of Native and Truncated Macrophage-Derived Chemokine (Macrophage-Derived Chemokine/CC Chemokine Ligand 22) by the D6 Decoy Receptor1. *The Journal of Immunology*, *172*(8), 4972–4976. https://doi.org/10.4049/jimmunol.172.8.4972

Böni-Schnetzler, M., Häuselmann, S. P., Dalmas, E., Meier, D. T., Thienel, C., Traub, S., Schulze, F., Steiger, L., Dror, E., Martin, P., Herrera, P. L., Gabay, C., & Donath, M. Y. (2018). β Cell-Specific Deletion of the IL-1 Receptor Antagonist Impairs β Cell Proliferation and Insulin Secretion. *Cell Reports*, *22*(7), 1774–1786. https://doi.org/10.1016/j.celrep.2018.01.063

Böni-Schnetzler, M., Thorne, J., Parnaud, G., Marselli, L., Ehses, J. A., Kerr-Conte, J., Pattou, F., Halban, P. A., Weir, G. C., & Donath, M. Y. (2008). Increased interleukin (IL)-1beta messenger

ribonucleic acid expression in beta -cells of individuals with type 2 diabetes and regulation of IL-1beta in human islets by glucose and autostimulation. *The Journal of Clinical Endocrinology and Metabolism*, *93*(10), 4065–4074. https://doi.org/10.1210/jc.2008-0396

Borelli, M. I., & Gagliardino, J. J. (2001). Possible modulatory effect of endogenous islet catecholamines on insulin secretion. *BMC Endocrine Disorders*, *1*(1), 1. https://doi.org/10.1186/1472-6823-1-1

Boring, L., Gosling, J., Chensue, S. W., Kunkel, S. L., Farese, R. V., Broxmeyer, H. E., & Charo, I. F. (1997). Impaired monocyte migration and reduced type 1 (Th1) cytokine responses in C-C chemokine receptor 2 knockout mice. *Journal of Clinical Investigation*, *100*(10), 2552–2561.

Boschero, A. C., Szpak-Glasman, M., Carneiro, E. M., Bordin, S., Paul, I., Rojas, E., & Atwater, I. (1995). Oxotremorine-m potentiation of glucose-induced insulin release from rat islets involves M3 muscarinic receptors. *The American Journal of Physiology*, *268*(2 Pt 1), E336-342. https://doi.org/10.1152/ajpendo.1995.268.2.E336

Bosco, D., Armanet, M., Morel, P., Niclauss, N., Sgroi, A., Muller, Y. D., Giovannoni, L., Parnaud, G., & Berney, T. (2010). Unique arrangement of alpha- and beta-cells in human islets of Langerhans. *Diabetes*, *59*(5), 1202–1210. https://doi.org/10.2337/db09-1177

Bourgeois, C., Gorwood, J., Barrail-Tran, A., Lagathu, C., Capeau, J., Desjardins, D., Le Grand, R., Damouche, A., Béréziat, V., & Lambotte, O. (2019). Specific Biological Features of Adipose Tissue, and Their Impact on HIV Persistence. *Frontiers in Microbiology*, *10*, 2837. https://doi.org/10.3389/fmicb.2019.02837

Bowe, J. E., Foot, V. L., Amiel, S. A., Huang, G. C., Lamb, M., Lakey, J., Jones, P. M., & Persaud, S. J. (2012). GPR54 peptide agonists stimulate insulin secretion from murine, porcine and human islets. *Islets*, *4*(1), 20–23. https://doi.org/10.4161/isl.18261

Bowe, J. E., Hill, T. G., Hunt, K. F., Smith, L. I., Simpson, S. J., Amiel, S. A., & Jones, P. M. (2019). A role for placental kisspeptin in β cell adaptation to pregnancy. *JCI Insight*, *4*(20), e124540, 124540. https://doi.org/10.1172/jci.insight.124540

Bowker, S. L., Yasui, Y., Veugelers, P., & Johnson, J. A. (2010). Glucose-lowering agents and cancer mortality rates in type 2 diabetes: Assessing effects of time-varying exposure. *Diabetologia*, *53*(8), 1631–1637. https://doi.org/10.1007/s00125-010-1750-8

Bozaoglu, K., Bolton, K., McMillan, J., Zimmet, P., Jowett, J., Collier, G., Walder, K., & Segal, D. (2007). Chemerin is a novel adipokine associated with obesity and metabolic syndrome. *Endocrinology*, *148*(10), 4687–4694. https://doi.org/10.1210/en.2007-0175

Bradford, M. M. (1976). A rapid and sensitive method for the quantitation of microgram quantities of protein utilizing the principle of protein-dye binding. *Analytical Biochemistry*, *72*(1), 248–254. https://doi.org/10.1016/0003-2697(76)90527-3

Bratanova-Tochkova, T. K., Cheng, H., Daniel, S., Gunawardana, S., Liu, Y.-J., Mulvaney-Musa, J., Schermerhorn, T., Straub, S. G., Yajima, H., & Sharp, G. W. G. (2002). Triggering and augmentation mechanisms, granule pools, and biphasic insulin secretion. *Diabetes*, *51 Suppl 1*, S83-90. https://doi.org/10.2337/diabetes.51.2007.s83

Bratti, L. de O. S., do Carmo, Í. A. R., Vilela, T. F., Wopereis, S., de Moraes, A. C. R., Borba, B. G. M., Souza, L. C., & Filippin-Monteiro, F. B. (2017). Complement component 3 (C3) as a biomarker for insulin resistance after bariatric surgery. *Clinical Biochemistry*, *50*(9), 529–532. https://doi.org/10.1016/j.clinbiochem.2017.02.006

Brelje, T. C., Scharp, D. W., Lacy, P. E., Ogren, L., Talamantes, F., Robertson, M., Friesen, H. G., & Sorenson, R. L. (1993). Effect of homologous placental lactogens, prolactins, and growth hormones on islet B-cell division and insulin secretion in rat, mouse, and human islets: Implication for placental lactogen regulation of islet function during pregnancy. *Endocrinology*, *132*(2), 879–887. https://doi.org/10.1210/en.132.2.879

Brennan, L., Shine, A., Hewage, C., Malthouse, J. P. G., Brindle, K. M., McClenaghan, N., Flatt, P. R., & Newsholme, P. (2002). A nuclear magnetic resonance-based demonstration of substantial oxidative L-alanine metabolism and L-alanine-enhanced glucose metabolism in a clonal

pancreatic beta-cell line: Metabolism of L-alanine is important to the regulation of insulin secretion. *Diabetes*, *51*(6), 1714–1721. https://doi.org/10.2337/diabetes.51.6.1714

Brentnall, M., Rodriguez-Menocal, L., De Guevara, R. L., Cepero, E., & Boise, L. H. (2013). Caspase-9, caspase-3 and caspase-7 have distinct roles during intrinsic apoptosis. *BMC Cell Biology*, *14*(1), 32. https://doi.org/10.1186/1471-2121-14-32

Brereton, M. F., Iberl, M., Shimomura, K., Zhang, Q., Adriaenssens, A. E., Proks, P., Spiliotis, I. I., Dace, W., Mattis, K. K., Ramracheya, R., Gribble, F. M., Reimann, F., Clark, A., Rorsman, P., & Ashcroft, F. M. (2014). Reversible changes in pancreatic islet structure and function produced by elevated blood glucose. *Nature Communications*, *5*, 4639. https://doi.org/10.1038/ncomms5639

Brun, R. P., Tontonoz, P., Forman, B. M., Ellis, R., Chen, J., Evans, R. M., & Spiegelman, B. M. (1996). Differential activation of adipogenesis by multiple PPAR isoforms. *Genes & Development*, *10*(8), 974–984. https://doi.org/10.1101/gad.10.8.974

Bucris, E., Beck, A., Boura-Halfon, S., Isaac, R., Vinik, Y., Rosenzweig, T., Sampson, S. R., & Zick, Y. (2016). Prolonged insulin treatment sensitizes apoptosis pathways in pancreatic β cells. *The Journal of Endocrinology*, *230*(3), 291–307. https://doi.org/10.1530/JOE-15-0505

Burke, S. J., Batdorf, H. M., Burk, D. H., Noland, R. C., Eder, A. E., Boulos, M. S., Karlstad, M. D., & Collier, J. J. (2017). Db/db Mice Exhibit Features of Human Type 2 Diabetes That Are Not Present in Weight-Matched C57BL/6J Mice Fed a Western Diet. *Journal of Diabetes Research*, *2017*, 8503754. https://doi.org/10.1155/2017/8503754

Burns, C. J., Squires, P. E., & Persaud, S. J. (2000). Signaling through the p38 and p42/44 Mitogen-Activated Families of Protein Kinases in Pancreatic β-Cell Proliferation. *Biochemical and Biophysical Research Communications*, *268*(2), 541–546. https://doi.org/10.1006/bbrc.2000.2179

Burrack, A. L., Martinov, T., & Fife, B. T. (2017). T Cell-Mediated Beta Cell Destruction: Autoimmunity and Alloimmunity in the Context of Type 1 Diabetes. *Frontiers in Endocrinology*, *8*, 343. https://doi.org/10.3389/fendo.2017.00343

Buteau, J., Foisy, S., Rhodes, C. J., Carpenter, L., Biden, T. J., & Prentki, M. (2001). Protein kinase Czeta activation mediates glucagon-like peptide-1-induced pancreatic beta-cell proliferation. *Diabetes*, *50*(10), 2237–2243. https://doi.org/10.2337/diabetes.50.10.2237

Butler, A. E., Janson, J., Bonner-Weir, S., Ritzel, R., Rizza, R. A., & Butler, P. C. (2003). Beta-cell deficit and increased beta-cell apoptosis in humans with type 2 diabetes. *Diabetes*, *52*(1), 102–110. https://doi.org/10.2337/diabetes.52.1.102

Butterick, T. A., Duffy, C. M., Lee, R. E., Billington, C. J., Kotz, C. M., & Nixon, J. P. (2014). Use of a Caspase Multiplexing Assay to Determine Apoptosis in a Hypothalamic Cell Model. *Journal of Visualized Experiments : JoVE*, *86*, 51305. https://doi.org/10.3791/51305

Cabrera, O., Berman, D. M., Kenyon, N. S., Ricordi, C., Berggren, P.-O., & Caicedo, A. (2006). The unique cytoarchitecture of human pancreatic islets has implications for islet cell function. *Proceedings of the National Academy of Sciences of the United States of America*, *103*(7), 2334–2339. https://doi.org/10.1073/pnas.0510790103

Cai, K., Qi, D., Hou, X., Wang, O., Chen, J., Deng, B., Qian, L., Liu, X., & Le, Y. (2011). MCP-1 Upregulates Amylin Expression in Murine Pancreatic β Cells through ERK/JNK-AP1 and NF-κB Related Signaling Pathways Independent of CCR2. *PLoS ONE*, *6*(5), e19559. https://doi.org/10.1371/journal.pone.0019559

Calderon, B., Suri, A., Pan, X. O., Mills, J. C., & Unanue, E. R. (2008). IFN-gamma-dependent regulatory circuits in immune inflammation highlighted in diabetes. *Journal of Immunology (Baltimore, Md.: 1950)*, *181*(10), 6964–6974. https://doi.org/10.4049/jimmunol.181.10.6964

Cameron, M. J., Arreaza, G. A., Grattan, M., Meagher, C., Sharif, S., Burdick, M. D., Strieter, R. M., Cook, D. N., & Delovitch, T. L. (2000). Differential Expression of CC Chemokines and the CCR5

Receptor in the Pancreas Is Associated with Progression to Type I Diabetes1. *The Journal of Immunology*, *165*(2), 1102–1110. https://doi.org/10.4049/jimmunol.165.2.1102

Cameron, M. J., Arreaza, G. A., Zucker, P., Chensue, S. W., Strieter, R. M., Chakrabarti, S., & Delovitch, T. L. (1997). IL-4 prevents insulitis and insulin-dependent diabetes mellitus in nonobese diabetic mice by potentiation of regulatory T helper-2 cell function. *Journal of Immunology (Baltimore, Md.: 1950)*, *159*(10), 4686–4692.

Carvell, M. J., Marsh, P. J., Persaud, S. J., & Jones, P. M. (2007). E-cadherin interactions regulate beta-cell proliferation in islet-like structures. *Cellular Physiology and Biochemistry: International Journal of Experimental Cellular Physiology, Biochemistry, and Pharmacology*, *20*(5), 617–626. https://doi.org/10.1159/000107545

Cases, J. A., Gabriely, I., Ma, X. H., Yang, X. M., Michaeli, T., Fleischer, N., Rossetti, L., & Barzilai, N. (2001). Physiological increase in plasma leptin markedly inhibits insulin secretion in vivo. *Diabetes*, *50*(2), 348–352. https://doi.org/10.2337/diabetes.50.2.348

Casey, M. L., & MacDonald, P. C. (1996). Interstitial collagen synthesis and processing in human amnion: A property of the mesenchymal cells. *Biology of Reproduction*, *55*(6), 1253–1260. https://doi.org/10.1095/biolreprod55.6.1253

Cat, A. N. D., & Briones, A. M. (2017). Isolation of Mature Adipocytes from White Adipose Tissue and Gene Expression Studies by Real-Time Quantitative RT-PCR. *Methods in Molecular Biology (Clifton, N.J.)*, *1527*, 283–295. https://doi.org/10.1007/978-1-4939-6625-7_22

Catalán, V., Gómez-Ambrosi, J., Rotellar, F., Silva, C., Rodríguez, A., Salvador, J., Gil, M. J., Cienfuegos, J. A., & Frühbeck, G. (2007). Validation of endogenous control genes in human adipose tissue: Relevance to obesity and obesity-associated type 2 diabetes mellitus. *Hormone and Metabolic Research = Hormon- Und Stoffwechselforschung = Hormones Et Metabolisme*, *39*(7), 495–500. https://doi.org/10.1055/s-2007-982502

Ceddia, R. B., Somwar, R., Maida, A., Fang, X., Bikopoulos, G., & Sweeney, G. (2005). Globular adiponectin increases GLUT4 translocation and glucose uptake but reduces glycogen

synthesis in rat skeletal muscle cells. *Diabetologia*, *48*(1), 132–139. https://doi.org/10.1007/s00125-004-1609-y

Chait, A., & den Hartigh, L. J. (2020). Adipose Tissue Distribution, Inflammation and Its Metabolic Consequences, Including Diabetes and Cardiovascular Disease. *Frontiers in Cardiovascular Medicine*, *7*, 22. https://doi.org/10.3389/fcvm.2020.00022

Chan, P.-C., Liao, M.-T., Lu, C.-H., Tian, Y.-F., & Hsieh, P.-S. (2021). Targeting inhibition of CCR5 on improving obesity-associated insulin resistance and impairment of pancreatic insulin secretion in high fat-fed rodent models. *European Journal of Pharmacology*, *891*, 173703. https://doi.org/10.1016/j.ejphar.2020.173703

Chan, P.-C., Lu, C.-H., Chien, H.-C., Tian, Y.-F., & Hsieh, P.-S. (2022). Adipose Tissue-Derived CCL5 Enhances Local Pro-Inflammatory Monocytic MDSCs Accumulation and Inflammation via CCR5 Receptor in High-Fat Diet-Fed Mice. *International Journal of Molecular Sciences*, *23*(22), Article 22. https://doi.org/10.3390/ijms232214226

Chang, T.-T., & Chen, J.-W. (2021). Direct CCL4 Inhibition Modulates Gut Microbiota, Reduces Circulating Trimethylamine N-Oxide, and Improves Glucose and Lipid Metabolism in High-Fat-Diet-Induced Diabetes Mellitus. *Journal of Inflammation Research*, *14*, 6237–6250. https://doi.org/10.2147/JIR.S343491

Chang, T.-T., Lin, L.-Y., & Chen, J.-W. (2021). A Novel Resolution of Diabetes: C-C Chemokine Motif Ligand 4 Is a Common Target in Different Types of Diabetes by Protecting Pancreatic Islet Cell and Modulating Inflammation. *Frontiers in Immunology*, *12*, 650626. https://doi.org/10.3389/fimmu.2021.650626

Chaudhury, A., Duvoor, C., Reddy Dendi, V. S., Kraleti, S., Chada, A., Ravilla, R., Marco, A., Shekhawat, N. S., Montales, M. T., Kuriakose, K., Sasapu, A., Beebe, A., Patil, N., Musham, C. K., Lohani, G. P., & Mirza, W. (2017). Clinical Review of Antidiabetic Drugs: Implications for Type 2 Diabetes Mellitus Management. *Frontiers in Endocrinology*, *8*, 6. https://doi.org/10.3389/fendo.2017.00006

Chavey, C., Lazennec, G., Lagarrigue, S., Clapé, C., Iankova, I., Teyssier, J., Annicotte, J.-S., Schmidt, J., Mataki, C., Yamamoto, H., Sanches, R., Guma, A., Stich, V., Vitkova, M., Jardin-Watelet, B., Renard, E., Strieter, R., Tuthill, A., Hotamisligil, G. S., … Fajas, L. (2009). CXC ligand 5 is an adipose-tissue derived factor that links obesity to insulin resistance. *Cell Metabolism*, *9*(4), 339–349. https://doi.org/10.1016/j.cmet.2009.03.002

Chen, A., Mumick, S., Zhang, C., Lamb, J., Dai, H., Weingarth, D., Mudgett, J., Chen, H., MacNeil, D. J., Reitman, M. L., & Qian, S. (2005). Diet Induction of Monocyte Chemoattractant Protein-1 and its Impact on Obesity. *Obesity Research*, *13*(8), 1311–1320. https://doi.org/10.1038/oby.2005.159

Chen, G., Ning, B., & Shi, T. (2019). Single-Cell RNA-Seq Technologies and Related Computational Data Analysis. *Frontiers in Genetics*, *10*, 317. https://doi.org/10.3389/fgene.2019.00317

Chen, H., Charlat, O., Tartaglia, L. A., Woolf, E. A., Weng, X., Ellis, S. J., Lakey, N. D., Culpepper, J., Moore, K. J., Breitbart, R. E., Duyk, G. M., Tepper, R. I., & Morgenstern, J. P. (1996). Evidence that the diabetes gene encodes the leptin receptor: Identification of a mutation in the leptin receptor gene in db/db mice. *Cell*, *84*(3), 491–495. https://doi.org/10.1016/s0092-8674(00)81294-5

Chen, H., Gu, X., Liu, Y., Wang, J., Wirt, S. E., Bottino, R., Schorle, H., Sage, J., & Kim, S. K. (2011). PDGF signalling controls age-dependent proliferation in pancreatic β-cells. *Nature*, *478*(7369), Article 7369. https://doi.org/10.1038/nature10502

Cheng, K., Delghingaro-Augusto, V., Nolan, C. J., Turner, N., Hallahan, N., Andrikopoulos, S., & Gunton, J. E. (2012). High passage MIN6 cells have impaired insulin secretion with impaired glucose and lipid oxidation. *PloS One*, *7*(7), e40868. https://doi.org/10.1371/journal.pone.0040868

Cheng, N.-L., Chen, X., Kim, J., Shi, A. H., Nguyen, C., Wersto, R., & Weng, N. (2015). MicroRNA-125b modulates inflammatory chemokine CCL4 expression in immune cells and its reduction causes CCL4 increase with age. *Aging Cell*, *14*(2), 200. https://doi.org/10.1111/acel.12294

Chilcott, J., Tappenden, P., Jones, M. L., & Wight, J. P. (2001). A systematic review of the clinical effectiveness of pioglitazone in the treatment of type 2 diabetes mellitus. *Clinical Therapeutics*, *23*(11), 1792–1823; discussion 1791. https://doi.org/10.1016/s0149-2918(00)80078-8

Chinwalla, A. T., Cook, L. L., Delehaunty, K. D., Fewell, G. A., Fulton, L. A., Fulton, R. S., Graves, T. A., Hillier, L. W., Mardis, E. R., McPherson, J. D., Miner, T. L., Nash, W. E., Nelson, J. O., Nhan, M. N., Pepin, K. H., Pohl, C. S., Ponce, T. C., Schultz, B., Thompson, J., … Members of the Mouse Genome Analysis Group. (2002). Initial sequencing and comparative analysis of the mouse genome. *Nature*, *420*(6915), Article 6915. https://doi.org/10.1038/nature01262

Chirumbolo, S., Franceschetti, G., Zoico, E., Bambace, C., Cominacini, L., & Zamboni, M. (2014). LPS response pattern of inflammatory adipokines in an in vitro 3T3-L1 murine adipocyte model. *Inflammation Research*, *63*(6), 495–507. https://doi.org/10.1007/s00011-014-0721-9

Cho, J., Kim, J., Shin, J., Shin, J., & Yoon, K. (2011). B-cell mass in people with type 2 diabetes. *Journal of Diabetes Investigation*, *2*(1), 6–17. https://doi.org/10.1111/j.2040-1124.2010.00072.x

Choo, S. Y. (2007). The HLA System: Genetics, Immunology, Clinical Testing, and Clinical Implications. *Yonsei Medical Journal*, *48*(1), 11–23. https://doi.org/10.3349/ymj.2007.48.1.11

Chou, H.-F., Ipp, E., Bowsher, R. R., Berman, N., Ezrin, C., & Griffiths, S. (1991). *Sustained Pulsatile Insulin Secretion From Adenomatous Human p-Cells*. *40*.

Christiansen, T., Richelsen, B., & Bruun, J. M. (2005). Monocyte chemoattractant protein-1 is produced in isolated adipocytes, associated with adiposity and reduced after weight loss in morbid obese subjects. *International Journal of Obesity (2005)*, *29*(1), 146–150. https://doi.org/10.1038/sj.ijo.0802839

Chrivia, J. C., Kwok, R. P., Lamb, N., Hagiwara, M., Montminy, M. R., & Goodman, R. H. (1993). Phosphorylated CREB binds specifically to the nuclear protein CBP. *Nature*, *365*(6449), 855–859. https://doi.org/10.1038/365855a0

Chu, Z.-L., Carroll, C., Alfonso, J., Gutierrez, V., He, H., Lucman, A., Pedraza, M., Mondala, H., Gao, H., Bagnol, D., Chen, R., Jones, R. M., Behan, D. P., & Leonard, J. (2008). A Role for Intestinal Endocrine Cell-Expressed G Protein-Coupled Receptor 119 in Glycemic Control by Enhancing Glucagon-Like Peptide-1 and Glucose-Dependent Insulinotropic Peptide Release. *Endocrinology*, *149*(5), 2038–2047. https://doi.org/10.1210/en.2007-0966

Chu, Z.-L., Carroll, C., Chen, R., Alfonso, J., Gutierrez, V., He, H., Lucman, A., Xing, C., Sebring, K., Zhou, J., Wagner, B., Unett, D., Jones, R. M., Behan, D. P., & Leonard, J. (2010). N-oleoyldopamine enhances glucose homeostasis through the activation of GPR119. *Molecular Endocrinology (Baltimore, Md.)*, *24*(1), 161–170. https://doi.org/10.1210/me.2009-0239

Chu, Z.-L., Jones, R. M., He, H., Carroll, C., Gutierrez, V., Lucman, A., Moloney, M., Gao, H., Mondala, H., Bagnol, D., Unett, D., Liang, Y., Demarest, K., Semple, G., Behan, D. P., & Leonard, J. (2007). A Role for β-Cell-Expressed G Protein-Coupled Receptor 119 in Glycemic Control by Enhancing Glucose-Dependent Insulin Release. *Endocrinology*, *148*(6), 2601–2609. https://doi.org/10.1210/en.2006-1608

Chukir, T., Shukla, A. P., Saunders, K. H., & Aronne, L. J. (2018). Pharmacotherapy for obesity in individuals with type 2 diabetes. *Expert Opinion on Pharmacotherapy*, *19*(3), 223–231. https://doi.org/10.1080/14656566.2018.1428558

Chun, J. H., & Butts, A. (2020). Long-acting GLP-1RAs: An overview of efficacy, safety, and their role in type 2 diabetes management. *JAAPA: Official Journal of the American Academy of Physician Assistants*, *33*(8), 3–18. https://doi.org/10.1097/01.JAA.0000669456.13763.bd

Chusyd, D. E., Wang, D., Huffman, D. M., & Nagy, T. R. (2016). Relationships between Rodent White Adipose Fat Pads and Human White Adipose Fat Depots. *Frontiers in Nutrition*, *3*, 10. https://doi.org/10.3389/fnut.2016.00010

Cinti, F., Bouchi, R., Kim-Muller, J. Y., Ohmura, Y., Sandoval, P. R., Masini, M., Marselli, L., Suleiman, M., Ratner, L. E., Marchetti, P., & Accili, D. (2016). Evidence of β-Cell Dedifferentiation in

Human Type 2 Diabetes. *The Journal of Clinical Endocrinology and Metabolism*, *101*(3), 1044–1054. https://doi.org/10.1210/jc.2015-2860

Cirera, S. (2013). Highly efficient method for isolation of total RNA from adipose tissue. *BMC Research Notes*, *6*, 472. https://doi.org/10.1186/1756-0500-6-472

Citro, A., Cantarelli, E., Maffi, P., Nano, R., Melzi, R., Mercalli, A., Dugnani, E., Sordi, V., Magistretti, P., Daffonchio, L., Ruffini, P. A., Allegretti, M., Secchi, A., Bonifacio, E., & Piemonti, L. (2012). CXCR1/2 inhibition enhances pancreatic islet survival after transplantation. *The Journal of Clinical Investigation*, *122*(10), 3647–3651. https://doi.org/10.1172/JCI63089

Civatte, M., Bartoli, C., Schleinitz, N., Chetaille, B., Pellissier, J. F., & Figarella-Branger, D. (2005). Expression of the beta chemokines CCL3, CCL4, CCL5 and their receptors in idiopathic inflammatory myopathies. *Neuropathology and Applied Neurobiology*, *31*(1), 70–79. https://doi.org/10.1111/j.1365-2990.2004.00591.x

Claessens, M., Saris, W. H. M., & van Baak, M. A. (2008). Glucagon and insulin responses after ingestion of different amounts of intact and hydrolysed proteins. *The British Journal of Nutrition*, *100*(1), 61–69. https://doi.org/10.1017/S0007114507886314

Clair, J. R. S., Westacott, M. J., Miranda, J., Farnsworth, N. L., Kravets, V., Schleicher, W. E., Dwulet, J. M., Levitt, C. H., Heintz, A., Ludin, N. W., & Benninger, R. K. (2023). *Restoring Connexin-36 Function in Diabetogenic Environments Precludes Mouse and Human Islet Dysfunction* (p. 2020.11.03.366179). bioRxiv. https://doi.org/10.1101/2020.11.03.366179

Clément, K., Biebermann, H., Farooqi, I. S., Van der Ploeg, L., Wolters, B., Poitou, C., Puder, L., Fiedorek, F., Gottesdiener, K., Kleinau, G., Heyder, N., Scheerer, P., Blume-Peytavi, U., Jahnke, I., Sharma, S., Mokrosinski, J., Wiegand, S., Müller, A., Weiß, K., … Kühnen, P. (2018). MC4R agonism promotes durable weight loss in patients with leptin receptor deficiency. *Nature Medicine*, *24*(5), Article 5. https://doi.org/10.1038/s41591-018-0015-9

Clemente-Postigo, M., Queipo-Ortuño, M. I., Fernandez-Garcia, D., Gomez-Huelgas, R., Tinahones, F. J., & Cardona, F. (2011). Adipose Tissue Gene Expression of Factors Related to Lipid

Processing in Obesity. *PLoS ONE*, *6*(9), e24783. https://doi.org/10.1371/journal.pone.0024783

Cnop, M., Welsh, N., Jonas, J.-C., Jörns, A., Lenzen, S., & Eizirik, D. L. (2005). Mechanisms of Pancreatic β-Cell Death in Type 1 and Type 2 Diabetes: Many Differences, Few Similarities. *Diabetes*, *54*(suppl_2), S97–S107. https://doi.org/10.2337/diabetes.54.suppl_2.S97

Colclough, K., Bellanne-Chantelot, C., Saint-Martin, C., Flanagan, S. E., & Ellard, S. (2013). Mutations in the Genes Encoding the Transcription Factors Hepatocyte Nuclear Factor 1 Alpha and 4 Alpha in Maturity-Onset Diabetes of the Young and Hyperinsulinemic Hypoglycemia. *Human Mutation*, *34*(5), 669–685. https://doi.org/10.1002/humu.22279

Colclough, K., Ellard, S., Hattersley, A., & Patel, K. (2022). Syndromic monogenic diabetes genes should be tested in patients with a clinical suspicion of MODY. *Diabetes*, *71*(3), 530. https://doi.org/10.2337/db21-0517

Coleman, D. L., & Hummel, K. P. (1967). Studies with the mutation, diabetes, in the mouse. *Diabetologia*, *3*(2), 238–248. https://doi.org/10.1007/BF01222201

Combs, T. P., Berg, A. H., Obici, S., Scherer, P. E., & Rossetti, L. (2001). Endogenous glucose production is inhibited by the adipose-derived protein Acrp30. *The Journal of Clinical Investigation*, *108*(12), 1875–1881. https://doi.org/10.1172/JCI14120

Considine, R. V., Sinha, M. K., Heiman, M. L., Kriauciunas, A., Stephens, T. W., Nyce, M. R., Ohannesian, J. P., Marco, C. C., McKee, L. J., & Bauer, T. L. (1996). Serum immunoreactive-leptin concentrations in normal-weight and obese humans. *The New England Journal of Medicine*, *334*(5), 292–295. https://doi.org/10.1056/NEJM199602013340503

Copenhaver, M. M., Yu, C.-Y., Zhou, D., & Hoffman, R. P. (2020). Relationships of Complement Components C3 and C4 and their Genetics to Cardiometabolic Risk in Healthy, Non-Hispanic White Adolescents. *Pediatric Research*, *87*(1), 88–94. https://doi.org/10.1038/s41390-019-0534-1

Corbisier, J., Galès, C., Huszagh, A., Parmentier, M., & Springael, J.-Y. (2015). Biased Signaling at Chemokine Receptors. *The Journal of Biological Chemistry*, *290*(15), 9542–9554. https://doi.org/10.1074/jbc.M114.596098

Cornell, D., Miwa, S., Georgiou, M., Anderson, S. J., Honkanen-Scott, M., Shaw, J. A. M., & Arden, C. (2022). Pseudoislet Aggregation of Pancreatic β-Cells Improves Glucose Stimulated Insulin Secretion by Altering Glucose Metabolism and Increasing ATP Production. *Cells*, *11*(15), 2330. https://doi.org/10.3390/cells11152330

Costello, R. A., Nicolas, S., & Shivkumar, A. (2023). Sulfonylureas. In *StatPearls*. StatPearls Publishing. http://www.ncbi.nlm.nih.gov/books/NBK513225/

Cousin, B., Caspar-Bauguil, S., Planat-Bénard, V., Laharrague, P., Pénicaud, L., & Casteilla, L. (2006). [Adipose tissue: A subtle and complex cell system]. *Journal De La Societe De Biologie*, *200*(1), 51–57. https://doi.org/10.1051/jbio:2006007

Cowherd, R. M., Lyle, R. E., & McGehee, R. E. (1999). Molecular regulation of adipocyte differentiation. *Seminars in Cell & Developmental Biology*, *10*(1), 3–10. https://doi.org/10.1006/scdb.1998.0276

Cox, A. R., Lam, C. J., Rankin, M. M., King, K. A., Chen, P., Martinez, R., Li, C., & Kushner, J. A. (2016). Extreme obesity induces massive beta cell expansion in mice through self-renewal and does not alter the beta cell lineage. *Diabetologia*, *59*(6), 1231–1241. https://doi.org/10.1007/s00125-016-3922-7

Crespin, S. R., Greenough, W. B., & Steinberg, D. (1969). Stimulation of insulin secretion by infusion of free fatty acids. *The Journal of Clinical Investigation*, *48*(10), 1934–1943. https://doi.org/10.1172/JCI106160

Currie, C. J., Poole, C. D., Jenkins-Jones, S., Gale, E. A. M., Johnson, J. A., & Morgan, C. L. (2012). Mortality after incident cancer in people with and without type 2 diabetes: Impact of metformin on survival. *Diabetes Care*, *35*(2), 299–304. https://doi.org/10.2337/dc11-1313

Daunt, M., Dale, O., & Smith, P. A. (2006). Somatostatin inhibits oxidative respiration in pancreatic beta-cells. *Endocrinology*, *147*(3), 1527–1535. https://doi.org/10.1210/en.2005-0873

de Alvaro, C., Teruel, T., Hernandez, R., & Lorenzo, M. (2004). Tumor necrosis factor alpha produces insulin resistance in skeletal muscle by activation of inhibitor kappaB kinase in a p38 MAPK-dependent manner. *The Journal of Biological Chemistry*, *279*(17), 17070–17078. https://doi.org/10.1074/jbc.M312021200

De Franco, E., Flanagan, S. E., Houghton, J. A. L., Lango Allen, H., Mackay, D. J. G., Temple, I. K., Ellard, S., & Hattersley, A. T. (2015). The effect of early, comprehensive genomic testing on clinical care in neonatal diabetes: An international cohort study. *Lancet (London, England)*, *386*(9997), 957–963. https://doi.org/10.1016/S0140-6736(15)60098-8

De Franco, E., Saint-Martin, C., Brusgaard, K., Knight Johnson, A. E., Aguilar-Bryan, L., Bowman, P., Arnoux, J.-B., Larsen, A. R., Sanyoura, M., Greeley, S. A. W., Calzada-León, R., Harman, B., Houghton, J. A. L., Nishimura-Meguro, E., Laver, T. W., Ellard, S., del Gaudio, D., Christesen, H. T., Bellanné-Chantelot, C., & Flanagan, S. E. (2020). Update of variants identified in the pancreatic β-cell KATP channel genes KCNJ11 and ABCC8 in individuals with congenital hyperinsulinism and diabetes. *Human Mutation*, *41*(5), 884–905. https://doi.org/10.1002/humu.23995

de Godoy, L. M. F., Olsen, J. V., Cox, J., Nielsen, M. L., Hubner, N. C., Fröhlich, F., Walther, T. C., & Mann, M. (2008). Comprehensive mass-spectrometry-based proteome quantification of haploid versus diploid yeast. *Nature*, *455*(7217), Article 7217. https://doi.org/10.1038/nature07341

de Mello Coelho, V., Bunbury, A., Rangel, L. B., Giri, B., Weeraratna, A., Morin, P. J., Bernier, M., & Taub, D. D. (2009). Fat-Storing Multilocular Cells Expressing CCR5 Increase in the Thymus with Advancing Age: Potential Role for CCR5 Ligands on the Differentiation and Migration of Preadipocytes. *International Journal of Medical Sciences*, *7*(1), 1–14.

DeFronzo, R. A. (2009). From the Triumvirate to the Ominous Octet: A New Paradigm for the Treatment of Type 2 Diabetes Mellitus. *Diabetes*, *58*(4), 773–795. https://doi.org/10.2337/db09-9028

Del Guerra, S., Grupillo, M., Masini, M., Lupi, R., Bugliani, M., Torri, S., Boggi, U., Del Chiaro, M., Vistoli, F., Mosca, F., Del Prato, S., & Marchetti, P. (2007). Gliclazide protects human islet beta-cells from apoptosis induced by intermittent high glucose. *Diabetes/Metabolism Research and Reviews*, *23*(3), 234–238. https://doi.org/10.1002/dmrr.680

Deshpande, A. D., Harris-Hayes, M., & Schootman, M. (2008). Epidemiology of Diabetes and Diabetes-Related Complications. *Physical Therapy*, *88*(11), 1254–1264. https://doi.org/10.2522/ptj.20080020

Di Gregorio, G. B., Yao-Borengasser, A., Rasouli, N., Varma, V., Lu, T., Miles, L. M., Ranganathan, G., Peterson, C. A., McGehee, R. E., & Kern, P. A. (2005). Expression of CD68 and Macrophage Chemoattractant Protein-1 Genes in Human Adipose and Muscle Tissues: Association With Cytokine Expression, Insulin Resistance, and Reduction by Pioglitazone. *Diabetes*, *54*(8), 2305–2313. https://doi.org/10.2337/diabetes.54.8.2305

Diamanti-Kandarakis, E., Kouli, C., Tsianateli, T., & Bergiele, A. (1998). Therapeutic effects of metformin on insulin resistance and hyperandrogenism in polycystic ovary syndrome. *European Journal of Endocrinology*, *138*(3), 269–274. https://doi.org/10.1530/eje.0.1380269

Díaz-Delfín, J., Domingo, P., Giralt, M., & Villarroya, F. (2013). Maraviroc reduces cytokine expression and secretion in human adipose cells without altering adipogenic differentiation. *Cytokine*, *61*(3), 808–815. https://doi.org/10.1016/j.cyto.2012.12.013

Divoux, A., Tordjman, J., Lacasa, D., Veyrie, N., Hugol, D., Aissat, A., Basdevant, A., Guerre-Millo, M., Poitou, C., Zucker, J.-D., Bedossa, P., & Clément, K. (2010). Fibrosis in Human Adipose Tissue: Composition, Distribution, and Link With Lipid Metabolism and Fat Mass Loss. *Diabetes*, *59*(11), 2817–2825. https://doi.org/10.2337/db10-0585

Dolenšek, J., Rupnik, M. S., & Stožer, A. (2015). Structural similarities and differences between the human and the mouse pancreas. *Islets*, *7*(1), e1024405. https://doi.org/10.1080/19382014.2015.1024405

Donath, M. Y., & Shoelson, S. E. (2011). Type 2 diabetes as an inflammatory disease. *Nature Reviews Immunology*, *11*(2), Article 2. https://doi.org/10.1038/nri2925

Dong, L.-Y., Jin, J., Lu, G., & Kang, X.-L. (2013). Astaxanthin Attenuates the Apoptosis of Retinal Ganglion Cells in db/db Mice by Inhibition of Oxidative Stress. *Marine Drugs*, *11*(3), Article 3. https://doi.org/10.3390/md11030960

Dor, Y., Brown, J., Martinez, O. I., & Melton, D. A. (2004). Adult pancreatic beta-cells are formed by self-duplication rather than stem-cell differentiation. *Nature*, *429*(6987), 41–46. https://doi.org/10.1038/nature02520

Dorner, B. G., Scheffold, A., Rolph, M. S., Hüser, M. B., Kaufmann, S. H. E., Radbruch, A., Flesch, I. E. A., & Kroczek, R. A. (2002). MIP-1α, MIP-1β, RANTES, and ATAC/lymphotactin function together with IFN-γ as type 1 cytokines. *Proceedings of the National Academy of Sciences*, *99*(9), 6181–6186. https://doi.org/10.1073/pnas.092141999

Dorr, P., Westby, M., Dobbs, S., Griffin, P., Irvine, B., Macartney, M., Mori, J., Rickett, G., Smith-Burchnell, C., Napier, C., Webster, R., Armour, D., Price, D., Stammen, B., Wood, A., & Perros, M. (2005). Maraviroc (UK-427,857), a Potent, Orally Bioavailable, and Selective Small-Molecule Inhibitor of Chemokine Receptor CCR5 with Broad-Spectrum Anti-Human Immunodeficiency Virus Type 1 Activity. *Antimicrobial Agents and Chemotherapy*, *49*(11), 4721–4732. https://doi.org/10.1128/aac.49.11.4721-4732.2005

Doshi, L. S., Brahma, M. K., Sayyed, S. G., Dixit, A. V., Chandak, P. G., Pamidiboina, V., Motiwala, H. F., Sharma, S. D., & Nemmani, K. V. S. (2009). Acute administration of GPR40 receptor agonist potentiates glucose-stimulated insulin secretion in vivo in the rat. *Metabolism*, *58*(3), 333–343. https://doi.org/10.1016/j.metabol.2008.10.005

Dowling, L. (2021). Effective management of type 1 diabetes in children and young people. *Nursing Children and Young People*, *33*(4), 26–33. https://doi.org/10.7748/ncyp.2021.e1310

Dowling, P., O'Driscoll, L., O'Sullivan, F., Dowd, A., Henry, M., Jeppesen, P. B., Meleady, P., & Clynes, M. (2006). Proteomic screening of glucose-responsive and glucose non-responsive MIN-6 beta cells reveals differential expression of proteins involved in protein folding, secretion and oxidative stress. *Proteomics*, *6*(24), 6578–6587. https://doi.org/10.1002/pmic.200600298

Dranse, H. J., Muruganandan, S., Fawcett, J. P., & Sinal, C. J. (2016). Adipocyte-secreted chemerin is processed to a variety of isoforms and influences MMP3 and chemokine secretion through an NFkB-dependent mechanism. *Molecular and Cellular Endocrinology*, *436*, 114–129. https://doi.org/10.1016/j.mce.2016.07.017

Dray, C., Debard, C., Jager, J., Disse, E., Daviaud, D., Martin, P., Attané, C., Wanecq, E., Guigné, C., Bost, F., Tanti, J.-F., Laville, M., Vidal, H., Valet, P., & Castan-Laurell, I. (2010). Apelin and APJ regulation in adipose tissue and skeletal muscle of type 2 diabetic mice and humans. *American Journal of Physiology. Endocrinology and Metabolism*, *298*(6), E1161-1169. https://doi.org/10.1152/ajpendo.00598.2009

Drolet, R., Richard, C., Sniderman, A. D., Mailloux, J., Fortier, M., Huot, C., Rhéaume, C., & Tchernof, A. (2008). Hypertrophy and hyperplasia of abdominal adipose tissues in women. *International Journal of Obesity*, *32*(2), Article 2. https://doi.org/10.1038/sj.ijo.0803708

Drucker, D. J., & Nauck, M. A. (2006). The incretin system: Glucagon-like peptide-1 receptor agonists and dipeptidyl peptidase-4 inhibitors in type 2 diabetes. *Lancet (London, England)*, *368*(9548), 1696–1705. https://doi.org/10.1016/S0140-6736(06)69705-5

Drucker, D. J., Philippe, J., Mojsov, S., Chick, W. L., & Habener, J. F. (1987). Glucagon-like peptide I stimulates insulin gene expression and increases cyclic AMP levels in a rat islet cell line. *Proceedings of the National Academy of Sciences of the United States of America*, *84*(10), 3434–3438.

Du, J., Zhao, L., Kang, Q., He, Y., & Bi, Y. (2023). An optimized method for Oil Red O staining with the salicylic acid ethanol solution. *Adipocyte*, *12*(1), 2179334. https://doi.org/10.1080/21623945.2023.2179334

Dubern, B., & Clement, K. (2012). Leptin and leptin receptor-related monogenic obesity. *Biochimie*, *94*(10), 2111–2115. https://doi.org/10.1016/j.biochi.2012.05.010

Dunér, P., Al-Amily, I. M., Soni, A., Asplund, O., Safi, F., Storm, P., Groop, L., Amisten, S., & Salehi, A. (2016). Adhesion G Protein-Coupled Receptor G1 (ADGRG1/GPR56) and Pancreatic β-Cell Function. *The Journal of Clinical Endocrinology & Metabolism*, *101*(12), 4637–4645. https://doi.org/10.1210/jc.2016-1884

Dusserre, E., Moulin, P., & Vidal, H. (2000). Differences in mRNA expression of the proteins secreted by the adipocytes in human subcutaneous and visceral adipose tissues. *Biochimica Et Biophysica Acta*, *1500*(1), 88–96. https://doi.org/10.1016/s0925-4439(99)00091-5

Dyachok, O., & Gylfe, E. (2004). Ca(2+)-induced Ca(2+) release via inositol 1,4,5-trisphosphate receptors is amplified by protein kinase A and triggers exocytosis in pancreatic beta-cells. *The Journal of Biological Chemistry*, *279*(44), 45455–45461. https://doi.org/10.1074/jbc.M407673200

Dyachok, O., Idevall-Hagren, O., Sågetorp, J., Tian, G., Wuttke, A., Arrieumerlou, C., Akusjärvi, G., Gylfe, E., & Tengholm, A. (2008). Glucose-induced cyclic AMP oscillations regulate pulsatile insulin secretion. *Cell Metabolism*, *8*(1), 26–37. https://doi.org/10.1016/j.cmet.2008.06.003

Dyer, D. P., Nebot, J. B., Kelly, C. J., Medina-Ruiz, L., Schuette, F., & Graham, G. J. (2019). The chemokine receptor CXCR2 contributes to murine adipocyte development. *Journal of Leukocyte Biology*, *105*(3), 497–506. https://doi.org/10.1002/JLB.1A0618-216RR

Edelman, S., Maier, H., & Wilhelm, K. (2008). Pramlintide in the treatment of diabetes mellitus. *BioDrugs: Clinical Immunotherapeutics, Biopharmaceuticals and Gene Therapy*, *22*(6), 375–386. https://doi.org/10.2165/0063030-200822060-00004

Eggleton, J. S., & Jialal, I. (2023). Thiazolidinediones. In *StatPearls*. StatPearls Publishing. http://www.ncbi.nlm.nih.gov/books/NBK551656/

Eguchi, N., Toribio, A. J., Alexander, M., Xu, I., Whaley, D. L., Hernandez, L. F., Dafoe, D., & Ichii, H. (2022). Dysregulation of β-Cell Proliferation in Diabetes: Possibilities of Combination Therapy in the Development of a Comprehensive Treatment. *Biomedicines*, *10*(2), 472. https://doi.org/10.3390/biomedicines10020472

Ehses, J. A., Perren, A., Eppler, E., Ribaux, P., Pospisilik, J. A., Maor-Cahn, R., Gueripel, X., Ellingsgaard, H., Schneider, M. K. J., Biollaz, G., Fontana, A., Reinecke, M., Homo-Delarche, F., & Donath, M. Y. (2007). Increased Number of Islet-Associated Macrophages in Type 2 Diabetes. *Diabetes*, *56*(9), 2356–2370. https://doi.org/10.2337/db06-1650

Eldor, R., Yeffet, A., Baum, K., Doviner, V., Amar, D., Ben-Neriah, Y., Christofori, G., Peled, A., Carel, J. C., Boitard, C., Klein, T., Serup, P., Eizirik, D. L., & Melloul, D. (2006). Conditional and specific NF-kappaB blockade protects pancreatic beta cells from diabetogenic agents. *Proceedings of the National Academy of Sciences of the United States of America*, *103*(13), 5072–5077. https://doi.org/10.1073/pnas.0508166103

Elmore, S. (2007). Apoptosis: A review of programmed cell death. *Toxicologic Pathology*, *35*(4), 495–516. https://doi.org/10.1080/01926230701320337

Elten, M., Donelle, J., Lima, I., Burnett, R. T., Weichenthal, S., Stieb, D. M., Hystad, P., van Donkelaar, A., Chen, H., Paul, L. A., Crighton, E., Martin, R. V., Decou, M. L., Luo, W., & Lavigne, É. (2020). Ambient air pollution and incidence of early-onset paediatric type 1 diabetes: A retrospective population-based cohort study. *Environmental Research*, *184*, 109291. https://doi.org/10.1016/j.envres.2020.109291

Emilsson, V., Liu, Y. L., Cawthorne, M. A., Morton, N. M., & Davenport, M. (1997). Expression of the functional leptin receptor mRNA in pancreatic islets and direct inhibitory action of leptin on insulin secretion. *Diabetes*, *46*(2), 313–316. https://doi.org/10.2337/diab.46.2.313

Engström, G., Hedblad, B., Eriksson, K.-F., Janzon, L., & Lindgärde, F. (2005). Complement C3 is a risk factor for the development of diabetes: A population-based cohort study. *Diabetes*, *54*(2), 570–575. https://doi.org/10.2337/diabetes.54.2.570

Ernst, M. C., Haidl, I. D., Zúñiga, L. A., Dranse, H. J., Rourke, J. L., Zabel, B. A., Butcher, E. C., & Sinal, C. J. (2012). Disruption of the Chemokine-Like Receptor-1 (CMKLR1) Gene Is Associated with Reduced Adiposity and Glucose Intolerance. *Endocrinology*, *153*(2), 672–682. https://doi.org/10.1210/en.2011-1490

Ernst, M. C., Issa, M., Goralski, K. B., & Sinal, C. J. (2010). Chemerin exacerbates glucose intolerance in mouse models of obesity and diabetes. *Endocrinology*, *151*(5), 1998–2007. https://doi.org/10.1210/en.2009-1098

Estevao, C., Bowers, C. E., Luo, D., Sarker, M., Hoeh, A. E., Frudd, K., Turowski, P., & Greenwood, J. (2021). CCL4 induces inflammatory signalling and barrier disruption in the neurovascular endothelium. *Brain, Behavior, & Immunity - Health*, *18*, 100370. https://doi.org/10.1016/j.bbih.2021.100370

Fain, J. N., Madan, A. K., Hiler, M. L., Cheema, P., & Bahouth, S. W. (2004). Comparison of the release of adipokines by adipose tissue, adipose tissue matrix, and adipocytes from visceral and subcutaneous abdominal adipose tissues of obese humans. *Endocrinology*, *145*(5), 2273–2282. https://doi.org/10.1210/en.2003-1336

Falutz, J., Mamputu, J.-C., Potvin, D., Moyle, G., Soulban, G., Loughrey, H., Marsolais, C., Turner, R., & Grinspoon, S. (2010). Effects of tesamorelin (TH9507), a growth hormone-releasing factor analog, in human immunodeficiency virus-infected patients with excess abdominal fat: A pooled analysis of two multicenter, double-blind placebo-controlled phase 3 trials with safety extension data. *The Journal of Clinical Endocrinology and Metabolism*, *95*(9), 4291–4304. https://doi.org/10.1210/jc.2010-0490

Farooqi, I. S., Jebb, S. A., Langmack, G., Lawrence, E., Cheetham, C. H., Prentice, A. M., Hughes, I. A., McCamish, M. A., & O'Rahilly, S. (1999). Effects of Recombinant Leptin Therapy in a Child

with Congenital Leptin Deficiency. *New England Journal of Medicine*, *341*(12), 879–884. https://doi.org/10.1056/NEJM199909163411204

Farooqi, I. S., Wangensteen, T., Collins, S., Kimber, W., Matarese, G., Keogh, J. M., Lank, E., Bottomley, B., Lopez-Fernandez, J., Ferraz-Amaro, I., Dattani, M. T., Ercan, O., Myhre, A. G., Retterstol, L., Stanhope, R., Edge, J. A., McKenzie, S., Lessan, N., Ghodsi, M., … O'Rahilly, S. (2007). Clinical and molecular genetic spectrum of congenital deficiency of the leptin receptor. *The New England Journal of Medicine*, *356*(3), 237–247. https://doi.org/10.1056/NEJMoa063988

Federici, M., Hribal, M., Perego, L., Ranalli, M., Caradonna, Z., Perego, C., Usellini, L., Nano, R., Bonini, P., Bertuzzi, F., Marlier, L. N., Davalli, A. M., Carandente, O., Pontiroli, A. E., Melino, G., Marchetti, P., Lauro, R., Sesti, G., & Folli, F. (2001). High glucose causes apoptosis in cultured human pancreatic islets of Langerhans: A potential role for regulation of specific Bcl family genes toward an apoptotic cell death program. *Diabetes*, *50*(6), 1290–1301. https://doi.org/10.2337/diabetes.50.6.1290

Fehmann, H.-C., Peiser, C., Bode, H.-P., Stamm, M., Staats, P., Hedetoft, C., Lang, R. E., & Göke, B. (1997). Leptin: A Potent Inhibitor of Insulin Secretion. *Peptides*, *18*(8), 1267–1273. https://doi.org/10.1016/S0196-9781(97)00135-6

Fehse, F., Trautmann, M., Holst, J. J., Halseth, A. E., Nanayakkara, N., Nielsen, L. L., Fineman, M. S., Kim, D. D., & Nauck, M. A. (2005). Exenatide augments first- and second-phase insulin secretion in response to intravenous glucose in subjects with type 2 diabetes. *The Journal of Clinical Endocrinology and Metabolism*, *90*(11), 5991–5997. https://doi.org/10.1210/jc.2005-1093

Fernández-Riejos, P., Najib, S., Santos-Alvarez, J., Martín-Romero, C., Pérez-Pérez, A., González-Yanes, C., & Sánchez-Margalet, V. (2010). Role of Leptin in the Activation of Immune Cells. *Mediators of Inflammation*, *2010*, 568343. https://doi.org/10.1155/2010/568343

Ferrucci, L., & Fabbri, E. (2018). Inflammageing: Chronic inflammation in ageing, cardiovascular disease, and frailty. *Nature Reviews. Cardiology*, *15*(9), 505–522. https://doi.org/10.1038/s41569-018-0064-2

Fessler, M. B., Malcolm, K. C., Duncan, M. W., & Worthen, G. S. (2002). A Genomic and Proteomic Analysis of Activation of the Human Neutrophil by Lipopolysaccharide and Its Mediation by p38 Mitogen-activated Protein Kinase *. *Journal of Biological Chemistry*, *277*(35), 31291–31302. https://doi.org/10.1074/jbc.M200755200

Fitch, F. W., Winebright, J., & Harper, P. V. (1962). Iodine-125 as a protein label in immunology. *Science (New York, N.Y.)*, *135*(3508), 1068–1069. https://doi.org/10.1126/science.135.3508.1068

Flattem, N., Igawa, K., Shiota, M., Emshwiller, M. G., Neal, D. W., & Cherrington, A. D. (2001). Alpha- and beta-cell responses to small changes in plasma glucose in the conscious dog. *Diabetes*, *50*(2), 367–375. https://doi.org/10.2337/diabetes.50.2.367

Fleenor, D., Petryk, A., Driscoll, P., & Freemark, M. (2000). Constitutive Expression of Placental Lactogen in Pancreatic β Cells: Effects on Cell Morphology, Growth, and Gene Expression. *Pediatric Research*, *47*(1), Article 1. https://doi.org/10.1203/00006450-200001000-00023

Flint, A., Raben, A., Astrup, A., & Holst, J. J. (1998). Glucagon-like peptide 1 promotes satiety and suppresses energy intake in humans. *The Journal of Clinical Investigation*, *101*(3), 515–520. https://doi.org/10.1172/JCI990

Fonseca, V. A. (2009). Defining and Characterizing the Progression of Type 2 Diabetes. *Diabetes Care*, *32*(Suppl 2), S151–S156. https://doi.org/10.2337/dc09-S301

Fox, J. M., Kasprowicz, R., Hartley, O., & Signoret, N. (2015). CCR5 susceptibility to ligand-mediated down-modulation differs between human T lymphocytes and myeloid cells. *Journal of Leukocyte Biology*, *98*(1), 59–71. https://doi.org/10.1189/jlb.2A0414-193RR

Franciosi, M., Lucisano, G., Lapice, E., Strippoli, G. F. M., Pellegrini, F., & Nicolucci, A. (2013). Metformin therapy and risk of cancer in patients with type 2 diabetes: Systematic review. *PloS One*, *8*(8), e71583. https://doi.org/10.1371/journal.pone.0071583

Franklin, Z. J., Tsakmaki, A., Fonseca Pedro, P., King, A. J., Huang, G. C., Amjad, S., Persaud, S. J., & Bewick, G. A. (2018). Islet neuropeptide Y receptors are functionally conserved and novel targets for the preservation of beta-cell mass. *Diabetes, Obesity & Metabolism*, *20*(3), 599–609. https://doi.org/10.1111/dom.13119

Frederich, R. C., Hamann, A., Anderson, S., Löllmann, B., Lowell, B. B., & Flier, J. S. (1995). Leptin levels reflect body lipid content in mice: Evidence for diet-induced resistance to leptin action. *Nature Medicine*, *1*(12), 1311–1314. https://doi.org/10.1038/nm1295-1311

Freemark, M. (2010). Placental hormones and the control of fetal growth. *The Journal of Clinical Endocrinology and Metabolism*, *95*(5), 2054–2057. https://doi.org/10.1210/jc.2010-0517

Freemark, M., Avril, I., Fleenor, D., Driscoll, P., Petro, A., Opara, E., Kendall, W., Oden, J., Bridges, S., Binart, N., Breant, B., & Kelly, P. A. (2002). Targeted Deletion of the PRL Receptor: Effects on Islet Development, Insulin Production, and Glucose Tolerance. *Endocrinology*, *143*(4), 1378–1385. https://doi.org/10.1210/endo.143.4.8722

Frei, A. P., Moest, H., Novy, K., & Wollscheid, B. (2013). Ligand-based receptor identification on living cells and tissues using TRICEPS. *Nature Protocols*, *8*(7), Article 7. https://doi.org/10.1038/nprot.2013.072

Fridlyand, L. E., & Philipson, L. H. (2011). Mechanisms of glucose sensing in the pancreatic β-cell. *Islets*, *3*(5), 224–230. https://doi.org/10.4161/isl.3.5.16409

Fridolf, T., & Ahrén, B. (1991). GLP-1(7-36) amide stimulates insulin secretion in rat islets: Studies on the mode of action. *Diabetes Research (Edinburgh, Scotland)*, *16*(4), 185–191.

Frühbeck, G., Catalán, V., Rodríguez, A., & Gómez-Ambrosi, J. (2018). Adiponectin-leptin ratio: A promising index to estimate adipose tissue dysfunction. Relation with obesity-associated

cardiometabolic risk. *Adipocyte*, *7*(1), 57–62. https://doi.org/10.1080/21623945.2017.1402151

Fuchsberger, C., Flannick, J., Teslovich, T. M., Mahajan, A., Agarwala, V., Gaulton, K. J., Ma, C., Fontanillas, P., Moutsianas, L., McCarthy, D. J., Rivas, M. A., Perry, J. R. B., Sim, X., Blackwell, T. W., Robertson, N. R., Rayner, N. W., Cingolani, P., Locke, A. E., Tajes, J. F., … McCarthy, M. I. (2016). The genetic architecture of type 2 diabetes. *Nature*, *536*(7614), Article 7614. https://doi.org/10.1038/nature18642

Fujishima, Y., Maeda, N., Matsuda, K., Masuda, S., Mori, T., Fukuda, S., Sekimoto, R., Yamaoka, M., Obata, Y., Kita, S., Nishizawa, H., Funahashi, T., Ranscht, B., & Shimomura, I. (2017). Adiponectin association with T-cadherin protects against neointima proliferation and atherosclerosis. *FASEB Journal: Official Publication of the Federation of American Societies for Experimental Biology*, *31*(4), 1571–1583. https://doi.org/10.1096/fj.201601064R

Galandrini, R., Henning, S. W., & Cantrell, D. A. (1997). Different functions of the GTPase Rho in prothymocytes and late pre-T cells. *Immunity*, *7*(1), 163–174. https://doi.org/10.1016/s1074-7613(00)80519-1

Galliera, E., Jala, V. R., Trent, J. O., Bonecchi, R., Signorelli, P., Lefkowitz, R. J., Mantovani, A., Locati, M., & Haribabu, B. (2004). Beta-Arrestin-dependent constitutive internalization of the human chemokine decoy receptor D6. *The Journal of Biological Chemistry*, *279*(24), 25590–25597. https://doi.org/10.1074/jbc.M400363200

Galluzzi, L., Aaronson, S. A., Abrams, J., Alnemri, E. S., Andrews, D. W., Baehrecke, E. H., Bazan, N. G., Blagosklonny, M. V., Blomgren, K., Borner, C., Bredesen, D. E., Brenner, C., Castedo, M., Cidlowski, J. A., Ciechanover, A., Cohen, G. M., De Laurenzi, V., De Maria, R., Deshmukh, M., … Kroemer, G. (2009). Guidelines for the use and interpretation of assays for monitoring cell death in higher eukaryotes. *Cell Death & Differentiation*, *16*(8), Article 8. https://doi.org/10.1038/cdd.2009.44

Garcia-Vargas, L., Addison, S. S., Nistala, R., Kurukulasuriya, D., & Sowers, J. R. (2012). Gestational Diabetes and the Offspring: Implications in the Development of the Cardiorenal Metabolic Syndrome in Offspring. *Cardiorenal Medicine*, *2*(2), 134–142. https://doi.org/10.1159/000337734

Ge, Q., Maury, E., Rycken, L., Gérard, J., Noël, L., Detry, R., Navez, B., & Brichard, S. M. (2013). Endocannabinoids regulate adipokine production and the immune balance of omental adipose tissue in human obesity. *International Journal of Obesity (2005)*, *37*(6), 874–880. https://doi.org/10.1038/ijo.2012.123

Gęca, T., Wojtowicz, K., Guzik, P., & Góra, T. (2022). Increased Risk of COVID-19 in Patients with Diabetes Mellitus—Current Challenges in Pathophysiology, Treatment and Prevention. *International Journal of Environmental Research and Public Health*, *19*(11), 6555. https://doi.org/10.3390/ijerph19116555

GEO Accession viewer. (2022). https://www.ncbi.nlm.nih.gov/geo/query/acc.cgi?acc=GSE210014

Gerhardt, C. C., Romero, I. A., Cancello, R., Camoin, L., & Strosberg, A. D. (2001). Chemokines control fat accumulation and leptin secretion by cultured human adipocytes. *Molecular and Cellular Endocrinology*, *175*(1), 81–92. https://doi.org/10.1016/S0303-7207(01)00394-X

Gerich, J. E. (2002). Is Reduced First-Phase Insulin Release the Earliest Detectable Abnormality in Individuals Destined to Develop Type 2 Diabetes? *Diabetes*, *51*(suppl_1), S117–S121. https://doi.org/10.2337/diabetes.51.2007.S117

Gericke, M. T., Schröder, T., Kosacka, J., Nowicki, M., Klöting, N., & Spanel-Borowski, K. (2012). Neuropeptide Y impairs insulin-stimulated translocation of glucose transporter 4 in 3T3-L1 adipocytes through the Y1 receptor. *Molecular and Cellular Endocrinology*, *348*(1), 27–32. https://doi.org/10.1016/j.mce.2011.07.028

Gerst, F., Wagner, R., Oquendo, M. B., Siegel-Axel, D., Fritsche, A., Heni, M., Staiger, H., Häring, H.-U., & Ullrich, S. (2019). What role do fat cells play in pancreatic tissue? *Molecular Metabolism*, *25*, 1–10. https://doi.org/10.1016/j.molmet.2019.05.001

Gey, G. O., & Gey, M. K. (1936). The Maintenance of Human Normal Cells and Tumor Cells in Continuous Culture: I. Preliminary Report: Cultivation of Mesoblastic Tumors and Normal Tissue and Notes on Methods of Cultivation1. *The American Journal of Cancer*, *27*(1), 45–76. https://doi.org/10.1158/ajc.1936.45

Ghaben, A. L., & Scherer, P. E. (2019). Adipogenesis and metabolic health. *Nature Reviews. Molecular Cell Biology*, *20*(4), 242–258. https://doi.org/10.1038/s41580-018-0093-z

Ghigo, E., Procopio, M., Boffano, G. M., Arvat, E., Valente, F., Maccario, M., Mazza, E., & Camanni, F. (1992). Arginine potentiates but does not restore the blunted growth hormone response to growth hormone-releasing hormone in obesity. *Metabolism: Clinical and Experimental*, *41*(5), 560–563. https://doi.org/10.1016/0026-0495(92)90220-5

Girkontaite, I., Missy, K., Sakk, V., Harenberg, A., Tedford, K., Pötzel, T., Pfeffer, K., & Fischer, K. D. (2001). Lsc is required for marginal zone B cells, regulation of lymphocyte motility and immune responses. *Nature Immunology*, *2*(9), 855–862. https://doi.org/10.1038/ni0901-855

Giwa, A. M., Ahmed, R., Omidian, Z., Majety, N., Karakus, K. E., Omer, S. M., Donner, T., & Hamad, A. R. A. (2020). Current understandings of the pathogenesis of type 1 diabetes: Genetics to environment. *World Journal of Diabetes*, *11*(1), 13–25. https://doi.org/10.4239/wjd.v11.i1.13

Glass, D., Viñuela, A., Davies, M. N., Ramasamy, A., Parts, L., Knowles, D., Brown, A. A., Hedman, A. K., Small, K. S., Buil, A., Grundberg, E., Nica, A. C., Di Meglio, P., Nestle, F. O., Ryten, M., UK Brain Expression consortium, MuTHER consortium, Durbin, R., McCarthy, M. I., … Spector, T. D. (2013). Gene expression changes with age in skin, adipose tissue, blood and brain. *Genome Biology*, *14*(7), R75. https://doi.org/10.1186/gb-2013-14-7-r75

Glennon-Alty, L., Moots, R. J., Edwards, S. W., & Wright, H. L. (2021). Type I interferon regulates cytokine-delayed neutrophil apoptosis, reactive oxygen species production and chemokine expression. *Clinical and Experimental Immunology*, *203*(2), 151–159. https://doi.org/10.1111/cei.13525

Goda, Y. (1997). SNAREs and regulated vesicle exocytosis. *Proceedings of the National Academy of Sciences of the United States of America*, *94*(3), 769–772.

Göddeke, S., Knebel, B., Fahlbusch, P., Hörbelt, T., Poschmann, G., van de Velde, F., Benninghoff, T., Al-Hasani, H., Jacob, S., Van Nieuwenhove, Y., Lapauw, B., Lehr, S., Ouwens, D. M., & Kotzka, J. (2018). CDH13 abundance interferes with adipocyte differentiation and is a novel biomarker for adipose tissue health. *International Journal of Obesity (2005)*, *42*(5), 1039–1050. https://doi.org/10.1038/s41366-018-0022-4

Gomber, A., Ward, Z. J., Ross, C., Owais, M., Mita, C., Yeh, J. M., Reddy, C. L., & Atun, R. (2022). Variation in the incidence of type 1 diabetes mellitus in children and adolescents by world region and country income group: A scoping review. *PLOS Global Public Health*, *2*(11), e0001099. https://doi.org/10.1371/journal.pgph.0001099

Gomez, Y., Navarro-Tableros, V., Tetta, C., Camussi, G., & Brizzi, M. F. (2020). A Versatile Model of Microfluidic Perifusion System for the Evaluation of C-Peptide Secretion Profiles: Comparison Between Human Pancreatic Islets and HLSC-Derived Islet-Like Structures. *Biomedicines*, *8*(2), 26. https://doi.org/10.3390/biomedicines8020026

Gómez-Banoy, N., Guseh, J. S., Li, G., Rubio-Navarro, A., Chen, T., Poirier, B., Putzel, G., Rosselot, C., Pabón, M. A., Camporez, J. P., Bhambhani, V., Hwang, S.-J., Yao, C., Perry, R. J., Mukherjee, S., Larson, M. G., Levy, D., Dow, L. E., Shulman, G. I., … Lo, J. C. (2019). Adipsin preserves beta cells in diabetic mice and associates with protection from type 2 diabetes in humans. *Nature Medicine*, *25*(11), 1739–1747. https://doi.org/10.1038/s41591-019-0610-4

Göpel, S. O., Kanno, T., Barg, S., Weng, X.-G., Gromada, J., & Rorsman, P. (2000). Regulation of glucagon release in mouse α-cells by KATP channels and inactivation of TTX-sensitive Na+ channels. *The Journal of Physiology*, *528*(Pt 3), 509–520. https://doi.org/10.1111/j.1469-7793.2000.00509.x

Goralski, K. B., McCarthy, T. C., Hanniman, E. A., Zabel, B. A., Butcher, E. C., Parlee, S. D., Muruganandan, S., & Sinal, C. J. (2007). Chemerin, a novel adipokine that regulates

adipogenesis and adipocyte metabolism. *The Journal of Biological Chemistry*, *282*(38), 28175–28188. https://doi.org/10.1074/jbc.M700793200

Grant, B., Sandelson, M., Agyemang-Prempeh, B., & Zalin, A. (2021). Managing obesity in people with type 2 diabetes. *Clinical Medicine*, *21*(4), e327–e231. https://doi.org/10.7861/clinmed.2021-0370

Grant, P. (2011). Bromocriptine. *Practical Diabetes International*, *28*(6), 276–277a. https://doi.org/10.1002/pdi.1614

Gray, E., Muller, D., Squires, P. E., Asare-Anane, H., Huang, G.-C., Amiel, S., Persaud, S. J., & Jones, P. M. (2006). Activation of the extracellular calcium-sensing receptor initiates insulin secretion from human islets of Langerhans: Involvement of protein kinases. *The Journal of Endocrinology*, *190*(3), 703–710. https://doi.org/10.1677/joe.1.06891

Green, I. C., Howell, S. L., Montague, W., & Taylor, K. W. (1973). Regulation of insulin release from isolated islets of Langerhans of the rat in pregnancy. The role of adenosine 3’:5’-cyclic monophosphate. *The Biochemical Journal*, *134*(2), 481–487. https://doi.org/10.1042/bj1340481

Green, I. C., & Taylor, K. W. (1972). Effects of pregnancy in the rat on the size and insulin secretory response of the islets of Langerhans. *The Journal of Endocrinology*, *54*(2), 317–325. https://doi.org/10.1677/joe.0.0540317

Gregory, G. A., Robinson, T. I. G., Linklater, S. E., Wang, F., Colagiuri, S., de Beaufort, C., Donaghue, K. C., International Diabetes Federation Diabetes Atlas Type 1 Diabetes in Adults Special Interest Group, Magliano, D. J., Maniam, J., Orchard, T. J., Rai, P., & Ogle, G. D. (2022). Global incidence, prevalence, and mortality of type 1 diabetes in 2021 with projection to 2040: A modelling study. *The Lancet. Diabetes & Endocrinology*, *10*(10), 741–760. https://doi.org/10.1016/S2213-8587(22)00218-2

Gregory, J. M., Slaughter, J. C., Duffus, S. H., Smith, T. J., LeStourgeon, L. M., Jaser, S. S., McCoy, A. B., Luther, J. M., Giovannetti, E. R., Boeder, S., Pettus, J. H., & Moore, D. J. (2021). COVID-19

Severity Is Tripled in the Diabetes Community: A Prospective Analysis of the Pandemic's Impact in Type 1 and Type 2 Diabetes. *Diabetes Care*, *44*(2), 526–532. https://doi.org/10.2337/dc20-2260

Grill, V., & Cerasi, E. (1973). Activation by glucose of adenyl cyclase in pancreatic islets of the rat. *FEBS Letters*, *33*(3), 311–314. https://doi.org/10.1016/0014-5793(73)80218-2

Grindstaff, A. S., & Baer, R. W. (2020). Expression and Activity of CCR5 on THP-1 Monocytes and Monocyte-Derived Macrophages. *The FASEB Journal*, *34*(S1), 1–1. https://doi.org/10.1096/fasebj.2020.34.s1.06646

Gromada, J., Dissing, S., Bokvist, K., Renström, E., Frøkjær-Jensen, J., Wulff, B. S., & Rorsman, P. (1995). Glucagon-Like Peptide I Increases Cytoplasmic Calcium in Insulin-Secreting βTC3-Cells by Enhancement of Intracellular Calcium Mobilization. *Diabetes*, *44*(7), 767–774. https://doi.org/10.2337/diab.44.7.767

Gruzdeva, O., Borodkina, D., Uchasova, E., Dyleva, Y., & Barbarash, O. (2019). Leptin resistance: Underlying mechanisms and diagnosis. *Diabetes, Metabolic Syndrome and Obesity: Targets and Therapy*, *12*, 191–198. https://doi.org/10.2147/DMSO.S182406

Gu, W., Li, X., Liu, C., Yang, J., Ye, L., Tang, J., Gu, Y., Yang, Y., Hong, J., Zhang, Y., Chen, M., & Ning, G. (2006). Globular adiponectin augments insulin secretion from pancreatic islet beta cells at high glucose concentrations. *Endocrine*, *30*(2), 217–221. https://doi.org/10.1385/ENDO:30:2:217

Guan, E., Wang, J., & Norcross, M. A. (2001). Identification of human macrophage inflammatory proteins 1alpha and 1beta as a native secreted heterodimer. *The Journal of Biological Chemistry*, *276*(15), 12404–12409. https://doi.org/10.1074/jbc.M006327200

Guan, E., Wang, J., Roderiquez, G., & Norcross, M. A. (2002). Natural truncation of the chemokine MIP-1 beta /CCL4 affects receptor specificity but not anti-HIV-1 activity. *The Journal of Biological Chemistry*, *277*(35), 32348–32352. https://doi.org/10.1074/jbc.M203077200

Guan, H., & Yang, K. (2008). RNA isolation and real-time quantitative RT-PCR. *Methods in Molecular Biology (Clifton, N.J.)*, *456*, 259–270. https://doi.org/10.1007/978-1-59745-245-8_19

Guardado-Mendoza, R., Davalli, A. M., Chavez, A. O., Hubbard, G. B., Dick, E. J., Majluf-Cruz, A., Tene-Perez, C. E., Goldschmidt, L., Hart, J., Perego, C., Comuzzie, A. G., Tejero, M. E., Finzi, G., Placidi, C., La Rosa, S., Capella, C., Halff, G., Gastaldelli, A., DeFronzo, R. A., & Folli, F. (2009). Pancreatic islet amyloidosis, β-cell apoptosis, and α-cell proliferation are determinants of islet remodeling in type-2 diabetic baboons. *Proceedings of the National Academy of Sciences of the United States of America*, *106*(33), 13992–13997. https://doi.org/10.1073/pnas.0906471106

Guillen, C., Bartolomé, A., Nevado, C., & Benito, M. (2008). Biphasic effect of insulin on beta cell apoptosis depending on glucose deprivation. *FEBS Letters*, *582*(28), 3855–3860. https://doi.org/10.1016/j.febslet.2008.10.020

Gunton, J. E., Delhanty, P. J. D., Takahashi, S.-I., & Baxter, R. C. (2003). Metformin rapidly increases insulin receptor activation in human liver and signals preferentially through insulin-receptor substrate-2. *The Journal of Clinical Endocrinology and Metabolism*, *88*(3), 1323–1332. https://doi.org/10.1210/jc.2002-021394

Guo, S., Dai, C., Guo, M., Taylor, B., Harmon, J. S., Sander, M., Robertson, R. P., Powers, A. C., & Stein, R. (2013). Inactivation of specific β cell transcription factors in type 2 diabetes. *The Journal of Clinical Investigation*, *123*(8), 3305–3316. https://doi.org/10.1172/JCI65390

Hackett, E., Gallagher, A., & Jacques, N. (2013, March 26). *Type 1 diabetes: Pathophysiology and diagnosis*. The Pharmaceutical Journal. https://pharmaceutical-journal.com/article/ld/type-1-diabetes-pathophysiology-and-diagnosis

Halban, P. A., Wollheim, C. B., Blondel, B., Meda, P., Niesor, E. N., & Mintz, D. H. (1982). The possible importance of contact between pancreatic islet cells for the control of insulin release. *Endocrinology*, *111*(1), 86–94. https://doi.org/10.1210/endo-111-1-86

Haliyur, R., Tong, X., Sanyoura, M., Shrestha, S., Lindner, J., Saunders, D. C., Aramandla, R., Poffenberger, G., Redick, S. D., Bottino, R., Prasad, N., Levy, S. E., Blind, R. D., Harlan, D. M., Philipson, L. H., Stein, R. W., Brissova, M., & Powers, A. C. (2019). Human islets expressing *HNF1A* variant have defective **β** cell transcriptional regulatory networks. *The Journal of Clinical Investigation*, *129*(1), 246–251. https://doi.org/10.1172/JCI121994

Hamaguchi, K., Gaskins, H. R., & Leiter, E. H. (1991). NIT-1, a pancreatic beta-cell line established from a transgenic NOD/Lt mouse. *Diabetes*, *40*(7), 842–849. https://doi.org/10.2337/diab.40.7.842

Hamamdzic, D., Duzic, E., Sherlock, J. D., & Lanier, S. M. (1995). Regulation of alpha 2-adrenergic receptor expression and signaling in pancreatic beta-cells. *The American Journal of Physiology*, *269*(1 Pt 1), E162-171. https://doi.org/10.1152/ajpendo.1995.269.1.E162

Han, Y., Xie, H., Liu, Y., Gao, P., Yang, X., & Shen, Z. (2019). Effect of metformin on all-cause and cardiovascular mortality in patients with coronary artery diseases: A systematic review and an updated meta-analysis. *Cardiovascular Diabetology*, *18*(1), 96. https://doi.org/10.1186/s12933-019-0900-7

Hanifi-Moghaddam, P., Kappler, S., Seissler, J., Müller-Scholze, S., Martin, S., Roep, B. O., Strassburger, K., Kolb, H., & Schloot, N. C. (2006). Altered chemokine levels in individuals at risk of Type 1 diabetes mellitus. *Diabetic Medicine: A Journal of the British Diabetic Association*, *23*(2), 156–163. https://doi.org/10.1111/j.1464-5491.2005.01743.x

Hannan, N. J., Jones, R. L., White, C. A., & Salamonsen, L. A. (2006). The chemokines, CX3CL1, CCL14, and CCL4, promote human trophoblast migration at the feto-maternal interface. *Biology of Reproduction*, *74*(5), 896–904. https://doi.org/10.1095/biolreprod.105.045518

Hansen, I. R., Jansson, K. M., Cannon, B., & Nedergaard, J. (2014). Contrasting effects of cold acclimation versus obesogenic diets on chemerin gene expression in brown and brite adipose tissues. *Biochimica et Biophysica Acta (BBA) - Molecular and Cell Biology of Lipids*, *1841*(12), 1691–1699. https://doi.org/10.1016/j.bbalip.2014.09.003

Hanson, B. J., Wetter, J., Bercher, M. R., Kopp, L., Fuerstenau-Sharp, M., Vedvik, K. L., Zielinski, T., Doucette, C., Whitney, P. J., & Revankar, C. (2009). A homogeneous fluorescent live-cell assay for measuring 7-transmembrane receptor activity and agonist functional selectivity through beta-arrestin recruitment. *Journal of Biomolecular Screening*, *14*(7), 798–810. https://doi.org/10.1177/1087057109335260

Hara, K., Horikoshi, M., Yamauchi, T., Yago, H., Miyazaki, O., Ebinuma, H., Imai, Y., Nagai, R., & Kadowaki, T. (2006). Measurement of the high-molecular weight form of adiponectin in plasma is useful for the prediction of insulin resistance and metabolic syndrome. *Diabetes Care*, *29*(6), 1357–1362. https://doi.org/10.2337/dc05-1801

Harbeck, M. C., Louie, D. C., Howland, J., Wolf, B. A., & Rothenberg, P. L. (1996). Expression of Insulin Receptor mRNA and Insulin Receptor Substrate 1 in Pancreatic Islet β-Cells. *Diabetes*, *45*(6), 711–717. https://doi.org/10.2337/diab.45.6.711

Harding, J. L., Pavkov, M. E., Magliano, D. J., Shaw, J. E., & Gregg, E. W. (2019). Global trends in diabetes complications: A review of current evidence. *Diabetologia*, *62*(1), 3–16. https://doi.org/10.1007/s00125-018-4711-2

Harms, M. J., Li, Q., Lee, S., Zhang, C., Kull, B., Hallen, S., Thorell, A., Alexandersson, I., Hagberg, C. E., Peng, X.-R., Mardinoglu, A., Spalding, K. L., & Boucher, J. (2019). Mature Human White Adipocytes Cultured under Membranes Maintain Identity, Function, and Can Transdifferentiate into Brown-like Adipocytes. *Cell Reports*, *27*(1), 213-225.e5. https://doi.org/10.1016/j.celrep.2019.03.026

Hart, N. J., & Powers, A. C. (2019). Use of human islets to understand islet biology and diabetes: Progress, challenges and suggestions. *Diabetologia*, *62*(2), 212–222. https://doi.org/10.1007/s00125-018-4772-2

Hathout, E. H., Beeson, W. L., Ischander, M., Rao, R., & Mace, J. W. (2006). Air pollution and type 1 diabetes in children. *Pediatric Diabetes*, *7*(2), 81–87. https://doi.org/10.1111/j.1399-543X.2006.00150.x

Hauge-Evans, A. C., Squires, P. E., Persaud, S. J., & Jones, P. M. (1999). Pancreatic beta-cell-to-beta-cell interactions are required for integrated responses to nutrient stimuli: Enhanced Ca2+ and insulin secretory responses of MIN6 pseudoislets. *Diabetes*, *48*(7), 1402–1408. https://doi.org/10.2337/diabetes.48.7.1402

Havel, P. J., & Ahren, B. (1997). Activation of autonomic nerves and the adrenal medulla contributes to increased glucagon secretion during moderate insulin-induced hypoglycemia in women. *Diabetes*, *46*(5), 801–807. https://doi.org/10.2337/diab.46.5.801

Hay, W. W. (2006). Placental-fetal glucose exchange and fetal glucose metabolism. *Transactions of the American Clinical and Climatological Association*, *117*, 321–339; discussion 339-340.

Hazan, U., Romero, I. A., Cancello, R., Valente, S., Perrin, V., Mariot, V., Dumonceaux, J., Gerhardt, C. C., Strosberg, A. D., Couraud, P.-O., & Pietri-Rouxel, F. (2002). Human adipose cells express CD4, CXCR4, and CCR5 [corrected] receptors: A new target cell type for the immunodeficiency virus-1? *FASEB Journal: Official Publication of the Federation of American Societies for Experimental Biology*, *16*(10), 1254–1256. https://doi.org/10.1096/fj.01-0947fje

Hehir, M. P., & Morrison, J. J. (2012). The adipokine apelin and human uterine contractility. *American Journal of Obstetrics and Gynecology*, *206*(4), 359.e1-5. https://doi.org/10.1016/j.ajog.2012.01.032

Hellman, B., Idahl, L.-Å., Lernmark, Å., & Täljedal, I.-B. (1974). The Pancreatic β-Cell Recognition of Insulin Secretagogues: Does Cyclic AMP Mediate the Effect of Glucose? *Proceedings of the National Academy of Sciences of the United States of America*, *71*(9), 3405–3409.

Hemmrich, K., Denecke, B., Paul, N. E., Hoffmeister, D., & Pallua, N. (2010). RNA Isolation from Adipose Tissue: An Optimized Procedure for High RNA Yield and Integrity. *Laboratory Medicine*, *41*(2), 104–106. https://doi.org/10.1309/LMFSBPUOA19MH5BV

Henquin, J. C., & Rahier, J. (2011). Pancreatic alpha cell mass in European subjects with type 2 diabetes. *Diabetologia*, *54*(7), 1720–1725. https://doi.org/10.1007/s00125-011-2118-4

Herold, K. C., Gitelman, S. E., Gottlieb, P. A., Knecht, L. A., Raymond, R., & Ramos, E. L. (2023). Teplizumab: A Disease-Modifying Therapy for Type 1 Diabetes That Preserves β-Cell Function. *Diabetes Care*, *46*(10), 1848–1856. https://doi.org/10.2337/dc23-0675

Herroeder, S., Reichardt, P., Sassmann, A., Zimmermann, B., Jaeneke, D., Hoeckner, J., Hollmann, M. W., Fischer, K.-D., Vogt, S., Grosse, R., Hogg, N., Gunzer, M., Offermanns, S., & Wettschureck, N. (2009). Guanine nucleotide-binding proteins of the G12 family shape immune functions by controlling CD4+ T cell adhesiveness and motility. *Immunity*, *30*(5), 708–720. https://doi.org/10.1016/j.immuni.2009.02.010

Hillier, T. A., & Pedula, K. L. (2003). Complications in young adults with early-onset type 2 diabetes: Losing the relative protection of youth. *Diabetes Care*, *26*(11), 2999–3005. https://doi.org/10.2337/diacare.26.11.2999

Hod, M., Merlob, P., Friedman, S., Schoenfeld, A., & Ovadia, J. (1991). Gestational diabetes mellitus. A survey of perinatal complications in the 1980s. *Diabetes*, *40 Suppl 2*, 74–78. https://doi.org/10.2337/diab.40.2.s74

Hodohara, K., Fujii, N., Yamamoto, N., & Kaushansky, K. (2000). Stromal cell-derived factor-1 (SDF-1) acts together with thrombopoietin to enhance the development of megakaryocytic progenitor cells (CFU-MK). *Blood*, *95*(3), 769–775.

Holland, W. L., Miller, R. A., Wang, Z. V., Sun, K., Barth, B. M., Bui, H. H., Davis, K. E., Bikman, B. T., Halberg, N., Rutkowski, J. M., Wade, M. R., Tenorio, V. M., Kuo, M.-S., Brozinick, J. T., Zhang, B. B., Birnbaum, M. J., Summers, S. A., & Scherer, P. E. (2011). Receptor-mediated activation of ceramidase activity initiates the pleiotropic actions of adiponectin. *Nature Medicine*, *17*(1), Article 1. https://doi.org/10.1038/nm.2277

Hopkins, P. N., & Polukoff, G. I. (2003). Risk of valvular heart disease associated with use of fenfluramine. *BMC Cardiovascular Disorders*, *3*, 5. https://doi.org/10.1186/1471-2261-3-5

Horowitz, M., Aroda, V. R., Han, J., Hardy, E., & Rayner, C. K. (2017). Upper and/or lower gastrointestinal adverse events with glucagon-like peptide-1 receptor agonists: Incidence

and consequences. *Diabetes, Obesity & Metabolism*, *19*(5), 672–681. https://doi.org/10.1111/dom.12872

Hotta, K., Funahashi, T., Arita, Y., Takahashi, M., Matsuda, M., Okamoto, Y., Iwahashi, H., Kuriyama, H., Ouchi, N., Maeda, K., Nishida, M., Kihara, S., Sakai, N., Nakajima, T., Hasegawa, K., Muraguchi, M., Ohmoto, Y., Nakamura, T., Yamashita, S., … Matsuzawa, Y. (2000). Plasma concentrations of a novel, adipose-specific protein, adiponectin, in type 2 diabetic patients. *Arteriosclerosis, Thrombosis, and Vascular Biology*, *20*(6), 1595–1599. https://doi.org/10.1161/01.atv.20.6.1595

Hsu, W. H., Xiang, H. D., Rajan, A. S., Kunze, D. L., & Boyd, A. E. (1991). Somatostatin inhibits insulin secretion by a G-protein-mediated decrease in Ca2+ entry through voltage-dependent Ca2+ channels in the beta cell. *Journal of Biological Chemistry*, *266*(2), 837–843. https://doi.org/10.1016/S0021-9258(17)35249-3

Hua, F., & Tian, Y. (2017). CCL4 promotes the cell proliferation, invasion and migration of endometrial carcinoma by targeting the VEGF-A signal pathway. *International Journal of Clinical and Experimental Pathology*, *10*(11), 11288–11299.

Huang, C.-L., Xiao, L.-L., Xu, M., Li, J., Li, S.-F., Zhu, C.-S., Lin, Y.-L., He, R., & Li, X. (2021). Chemerin deficiency regulates adipogenesis is depot different through TIMP1. *Genes & Diseases*, *8*(5), 698–708. https://doi.org/10.1016/j.gendis.2020.04.003

Huang, L., Wang, Z., & Li, C. (2001). Modulation of circulating leptin levels by its soluble receptor. *The Journal of Biological Chemistry*, *276*(9), 6343–6349. https://doi.org/10.1074/jbc.M009795200

Huber, J., Kiefer, F. W., Zeyda, M., Ludvik, B., Silberhumer, G. R., Prager, G., Zlabinger, G. J., & Stulnig, T. M. (2008). CC Chemokine and CC Chemokine Receptor Profiles in Visceral and Subcutaneous Adipose Tissue Are Altered in Human Obesity. *The Journal of Clinical Endocrinology & Metabolism*, *93*(8), 3215–3221. https://doi.org/10.1210/jc.2007-2630

Huber, M., Bahr, I., Krätzschmar, J. R., Becker, A., Müller, E.-C., Donner, P., Pohlenz, H.-D., Schneider, M. R., & Sommer, A. (2004). Comparison of Proteomic and Genomic Analyses of the Human Breast Cancer Cell Line T47D and the Antiestrogen-resistant Derivative T47D-r *. *Molecular & Cellular Proteomics*, *3*(1), 43–55. https://doi.org/10.1074/mcp.M300047-MCP200

Hug, C., Wang, J., Ahmad, N. S., Bogan, J. S., Tsao, T.-S., & Lodish, H. F. (2004). T-cadherin is a receptor for hexameric and high-molecular-weight forms of Acrp30/adiponectin. *Proceedings of the National Academy of Sciences of the United States of America*, *101*(28), 10308–10313. https://doi.org/10.1073/pnas.0403382101

Huh, J. H., Kim, H. M., Lee, E. S., Kwon, M. H., Lee, B. R., Ko, H.-J., & Chung, C. H. (2018). Dual CCR2/5 Antagonist Attenuates Obesity-Induced Insulin Resistance by Regulating Macrophage Recruitment and M1/M2 Status. *Obesity*, *26*(2), 378–386. https://doi.org/10.1002/oby.22103

Hummel, K. P., Dickie, M. M., & Coleman, D. L. (1966). Diabetes, a new mutation in the mouse. *Science (New York, N.Y.)*, *153*(3740), 1127–1128. https://doi.org/10.1126/science.153.3740.1127

Iafusco, D., Massa, O., Pasquino, B., Colombo, C., Iughetti, L., Bizzarri, C., Mammì, C., Lo Presti, D., Suprani, T., Schiaffini, R., Nichols, C. G., Russo, L., Grasso, V., Meschi, F., Bonfanti, R., Brescianini, S., Barbetti, F., & Early Diabetes Study Group of ISPED. (2012). Minimal incidence of neonatal/infancy onset diabetes in Italy is 1:90,000 live births. *Acta Diabetologica*, *49*(5), 405–408. https://doi.org/10.1007/s00592-011-0331-8

Ignatov, A., Robert, J., Gregory-Evans, C., & Schaller, H. C. (2006). RANTES stimulates Ca2+ mobilization and inositol trisphosphate (IP3) formation in cells transfected with G protein-coupled receptor 75. *British Journal of Pharmacology*, *149*(5), 490–497. https://doi.org/10.1038/sj.bjp.0706909

Iismaa, T. P., Kerr, E. A., Wilson, J. R., Carpenter, L., Sims, N., & Biden, T. J. (2000). Quantitative and functional characterization of muscarinic receptor subtypes in insulin-secreting cell lines and rat pancreatic islets. *Diabetes*, *49*(3), 392–398. https://doi.org/10.2337/diabetes.49.3.392

Ikushima, Y. M., Awazawa, M., Kobayashi, N., Osonoi, S., Takemiya, S., Kobayashi, H., Suwanai, H., Morimoto, Y., Soeda, K., Adachi, J., Muratani, M., Charron, J., Mizukami, H., Takahashi, N., & Ueki, K. (2021). MEK/ERK Signaling in β-Cells Bifunctionally Regulates β-Cell Mass and Glucose-Stimulated Insulin Secretion Response to Maintain Glucose Homeostasis. *Diabetes*, *70*(7), 1519–1535. https://doi.org/10.2337/db20-1295

Imai, Y., Patel, H. R., Hawkins, E. J., Doliba, N. M., Matschinsky, F. M., & Ahima, R. S. (2007). Insulin secretion is increased in pancreatic islets of neuropeptide Y-deficient mice. *Endocrinology*, *148*(12), 5716–5723. https://doi.org/10.1210/en.2007-0404

Inoue, R., Nishiyama, K., Li, J., Miyashita, D., Ono, M., Terauchi, Y., & Shirakawa, J. (2021). The Feasibility and Applicability of Stem Cell Therapy for the Cure of Type 1 Diabetes. *Cells*, *10*(7), 1589. https://doi.org/10.3390/cells10071589

Inouye, K. E., Shi, H., Howard, J. K., Daly, C. H., Lord, G. M., Rollins, B. J., & Flier, J. S. (2007). Absence of CC chemokine ligand 2 does not limit obesity-associated infiltration of macrophages into adipose tissue. *Diabetes*, *56*(9), 2242–2250. https://doi.org/10.2337/db07-0425

Insel, P. A., Tang, C.-M., Hahntow, I., & Michel, M. C. (2007). Impact of GPCRs in clinical medicine: Monogenic diseases, genetic variants and drug targets. *Biochimica Et Biophysica Acta*, *1768*(4), 994–1005. https://doi.org/10.1016/j.bbamem.2006.09.029

Iranmanesh, A., Lizarralde, G., & Veldhuis, J. D. (1991). Age and relative adiposity are specific negative determinants of the frequency and amplitude of growth hormone (GH) secretory bursts and the half-life of endogenous GH in healthy men. *The Journal of Clinical Endocrinology and Metabolism*, *73*(5), 1081–1088. https://doi.org/10.1210/jcem-73-5-1081

Itoh, Y., Kawamata, Y., Harada, M., Kobayashi, M., Fujii, R., Fukusumi, S., Ogi, K., Hosoya, M., Tanaka, Y., Uejima, H., Tanaka, H., Maruyama, M., Satoh, R., Okubo, S., Kizawa, H., Komatsu, H.,

Matsumura, F., Noguchi, Y., Shinohara, T., … Fujino, M. (2003). Free fatty acids regulate insulin secretion from pancreatic beta cells through GPR40. *Nature*, *422*(6928), 173–176. https://doi.org/10.1038/nature01478

Ivanov, D., Philippova, M., Antropova, J., Gubaeva, F., Iljinskaya, O., Tararak, E., Bochkov, V., Erne, P., Resink, T., & Tkachuk, V. (2001). Expression of cell adhesion molecule T-cadherin in the human vasculature. *Histochemistry and Cell Biology*, *115*(3), 231–242. https://doi.org/10.1007/s004180100252

Jacobo, S. M. P., Guerra, M. L., & Hockerman, G. H. (2009). Cav1.2 and Cav1.3 Are Differentially Coupled to Glucagon-Like Peptide-1 Potentiation of Glucose-Stimulated Insulin Secretion in the Pancreatic β-Cell Line INS-1. *Journal of Pharmacology and Experimental Therapeutics*, *331*(2), 724–732. https://doi.org/10.1124/jpet.109.158519

Jacovetti, C., Matkovich, S. J., Rodriguez-Trejo, A., Guay, C., & Regazzi, R. (2015). Postnatal β-cell maturation is associated with islet-specific microRNA changes induced by nutrient shifts at weaning. *Nature Communications*, *6*, 8084. https://doi.org/10.1038/ncomms9084

Jain, B. P., Goswami, S. K., & Pandey, S. (2021). Chapter 4—Protein. In B. P. Jain, S. K. Goswami, & S. Pandey (Eds.), *Protocols in Biochemistry and Clinical Biochemistry* (pp. 31–48). Academic Press. https://doi.org/10.1016/B978-0-12-822007-8.00008-8

Jain, S. S., Ramanand, S. J., Ramanand, J. B., Akat, P. B., Patwardhan, M. H., & Joshi, S. R. (2011). Evaluation of efficacy and safety of orlistat in obese patients. *Indian Journal of Endocrinology and Metabolism*, *15*(2), 99–104. https://doi.org/10.4103/2230-8210.81938

Jaques, F., Jousset, H., Tomas, A., Prost, A.-L., Wollheim, C. B., Irminger, J.-C., Demaurex, N., & Halban, P. A. (2008). Dual effect of cell-cell contact disruption on cytosolic calcium and insulin secretion. *Endocrinology*, *149*(5), 2494–2505. https://doi.org/10.1210/en.2007-0974

Jayapal, K. P., Philp, R. J., Kok, Y.-J., Yap, M. G. S., Sherman, D. H., Griffin, T. J., & Hu, W.-S. (2008). Uncovering Genes with Divergent mRNA-Protein Dynamics in Streptomyces coelicolor. *PLOS ONE*, *3*(5), e2097. https://doi.org/10.1371/journal.pone.0002097

Jernås, M., Palming, J., Sjöholm, K., Jennische, E., Svensson, P.-A., Gabrielsson, B. G., Levin, M., Sjögren, A., Rudemo, M., Lystig, T. C., Carlsson, B., Carlsson, L. M. S., & Lönn, M. (2006). Separation of human adipocytes by size: Hypertrophic fat cells display distinct gene expression. *FASEB Journal: Official Publication of the Federation of American Societies for Experimental Biology*, *20*(9), 1540–1542. https://doi.org/10.1096/fj.05-5678fje

Ji, W., Gong, L., Wang, J., He, H., & Zhang, Y. (2017). Hypoxic Exercise Training Promotes apelin/APJ Expression in Skeletal Muscles of High Fat Diet-Induced Obese Mice. *Protein and Peptide Letters*, *24*(1), 64–70. https://doi.org/10.2174/0929866524666161111111726

Jonas, J. C., Sharma, A., Hasenkamp, W., Ilkova, H., Patanè, G., Laybutt, R., Bonner-Weir, S., & Weir, G. C. (1999). Chronic hyperglycemia triggers loss of pancreatic beta cell differentiation in an animal model of diabetes. *The Journal of Biological Chemistry*, *274*(20), 14112–14121. https://doi.org/10.1074/jbc.274.20.14112

Jones, B., Buenaventura, T., Kanda, N., Chabosseau, P., Owen, B. M., Scott, R., Goldin, R., Angkathunyakul, N., Corrêa, I. R., Bosco, D., Johnson, P. R., Piemonti, L., Marchetti, P., Shapiro, A. M. J., Cochran, B. J., Hanyaloglu, A. C., Inoue, A., Tan, T., Rutter, G. A., … Bloom, S. R. (2018). Targeting GLP-1 receptor trafficking to improve agonist efficacy. *Nature Communications*, *9*(1), 1602. https://doi.org/10.1038/s41467-018-03941-2

Jones, P. M., & Persaud, S. J. (2017). Islet Function and Insulin Secretion. In *Textbook of Diabetes* (pp. 87–102). John Wiley & Sons, Ltd. https://doi.org/10.1002/9781118924853.ch6

Kahanovitz, L., Sluss, P. M., & Russell, S. J. (2017). Type 1 Diabetes – A Clinical Perspective. *Point of Care*, *16*(1), 37. https://doi.org/10.1097/POC.0000000000000125

Kaido, T., Yebra, M., Cirulli, V., Rhodes, C., Diaferia, G., & Montgomery, A. M. (2006). Impact of Defined Matrix Interactions on Insulin Production by Cultured Human β-Cells: Effect on Insulin Content, Secretion, and Gene Transcription. *Diabetes*, *55*(10), 2723–2729. https://doi.org/10.2337/db06-0120

Kaihara, K. A., Dickson, L. M., Jacobson, D. A., Tamarina, N., Roe, M. W., Philipson, L. H., & Wicksteed, B. (2013). β-Cell–Specific Protein Kinase A Activation Enhances the Efficiency of Glucose Control by Increasing Acute-Phase Insulin Secretion. *Diabetes*, *62*(5), 1527–1536. https://doi.org/10.2337/db12-1013

Kailey, B., van de Bunt, M., Cheley, S., Johnson, P. R., MacDonald, P. E., Gloyn, A. L., Rorsman, P., & Braun, M. (2012). SSTR2 is the functionally dominant somatostatin receptor in human pancreatic β- and α-cells. *American Journal of Physiology - Endocrinology and Metabolism*, *303*(9), E1107–E1116. https://doi.org/10.1152/ajpendo.00207.2012

Kaiser, N., Leibowitz, G., & Nesher, R. (2003). Glucotoxicity and beta-cell failure in type 2 diabetes mellitus. *Journal of Pediatric Endocrinology & Metabolism: JPEM*, *16*(1), 5–22. https://doi.org/10.1515/jpem.2003.16.1.5

Kakuma, T., Wang, Z. W., Pan, W., Unger, R. H., & Zhou, Y. T. (2000). Role of leptin in peroxisome proliferator-activated receptor gamma coactivator-1 expression. *Endocrinology*, *141*(12), 4576–4582. https://doi.org/10.1210/endo.141.12.7804

Kamei, N., Tobe, K., Suzuki, R., Ohsugi, M., Watanabe, T., Kubota, N., Ohtsuka-Kowatari, N., Kumagai, K., Sakamoto, K., Kobayashi, M., Yamauchi, T., Ueki, K., Oishi, Y., Nishimura, S., Manabe, I., Hashimoto, H., Ohnishi, Y., Ogata, H., Tokuyama, K., … Kadowaki, T. (2006). Overexpression of monocyte chemoattractant protein-1 in adipose tissues causes macrophage recruitment and insulin resistance. *The Journal of Biological Chemistry*, *281*(36), 26602–26614. https://doi.org/10.1074/jbc.M601284200

Kameswaran, V., Bramswig, N. C., McKenna, L. B., Penn, M., Schug, J., Hand, N. J., Chen, Y., Choi, I., Vourekas, A., Won, K.-J., Liu, C., Vivek, K., Naji, A., Friedman, J. R., & Kaestner, K. H. (2014). Epigenetic regulation of the MEG3-DLK1 microRNA cluster in human Type 2 diabetic islets. *Cell Metabolism*, *19*(1), 135–145. https://doi.org/10.1016/j.cmet.2013.11.016

Kanda, H., Tateya, S., Tamori, Y., Kotani, K., Hiasa, K., Kitazawa, R., Kitazawa, S., Miyachi, H., Maeda, S., Egashira, K., & Kasuga, M. (2006). MCP-1 contributes to macrophage infiltration into

adipose tissue, insulin resistance, and hepatic steatosis in obesity. *Journal of Clinical Investigation*, *116*(6), 1494–1505. https://doi.org/10.1172/JCI26498

Karlsson, S., & Ahrén, B. (1993). Muscarinic receptor subtypes in carbachol-stimulated insulin and glucagon secretion in the mouse. *Journal of Autonomic Pharmacology*, *13*(6), 439–446. https://doi.org/10.1111/j.1474-8673.1993.tb00291.x

Kebede, M., Alquier, T., Latour, M. G., Semache, M., Tremblay, C., & Poitout, V. (2008). The Fatty Acid Receptor GPR40 Plays a Role in Insulin Secretion In Vivo After High-Fat Feeding. *Diabetes*, *57*(9), 2432–2437. https://doi.org/10.2337/db08-0553

Kee, B. L., Arias, J., & Montminy, M. R. (1996). Adaptor-mediated recruitment of RNA polymerase II to a signal-dependent activator. *The Journal of Biological Chemistry*, *271*(5), 2373–2375. https://doi.org/10.1074/jbc.271.5.2373

Kennedy, A., Gettys, T. W., Watson, P., Wallace, P., Ganaway, E., Pan, Q., & Garvey, W. T. (1997). The metabolic significance of leptin in humans: Gender-based differences in relationship to adiposity, insulin sensitivity, and energy expenditure. *The Journal of Clinical Endocrinology and Metabolism*, *82*(4), 1293–1300. https://doi.org/10.1210/jcem.82.4.3859

Kennedy, A. J., & Davenport, A. P. (2018). International Union of Basic and Clinical Pharmacology CIII: Chemerin Receptors CMKLR1 (Chemerin1) and GPR1 (Chemerin2) Nomenclature, Pharmacology, and Function. *Pharmacological Reviews*, *70*(1), 174–196. https://doi.org/10.1124/pr.116.013177

Keophiphath, M., Rouault, C., Divoux, A., Clément, K., & Lacasa, D. (2010). CCL5 Promotes Macrophage Recruitment and Survival in Human Adipose Tissue. *Arteriosclerosis, Thrombosis, and Vascular Biology*, *30*(1), 39–45. https://doi.org/10.1161/ATVBAHA.109.197442

Kershaw, E. E., & Flier, J. S. (2004). Adipose tissue as an endocrine organ. *The Journal of Clinical Endocrinology and Metabolism*, *89*(6), 2548–2556. https://doi.org/10.1210/jc.2004-0395

Khan, M. A. B., Hashim, M. J., King, J. K., Govender, R. D., Mustafa, H., & Al Kaabi, J. (2020). Epidemiology of Type 2 Diabetes – Global Burden of Disease and Forecasted Trends. *Journal of Epidemiology and Global Health*, *10*(1), 107–111. https://doi.org/10.2991/jegh.k.191028.001

Khan, M., & Joseph, F. (2014). Adipose tissue and adipokines: The association with and application of adipokines in obesity. *Scientifica*, *2014*, 328592. https://doi.org/10.1155/2014/328592

Khan, T., Muise, E. S., Iyengar, P., Wang, Z. V., Chandalia, M., Abate, N., Zhang, B. B., Bonaldo, P., Chua, S., & Scherer, P. E. (2009). Metabolic Dysregulation and Adipose Tissue Fibrosis: Role of Collagen VI. *Molecular and Cellular Biology*, *29*(6), 1575–1591. https://doi.org/10.1128/MCB.01300-08

Khoramipour, K., Chamari, K., Hekmatikar, A. A., Ziyaiyan, A., Taherkhani, S., Elguindy, N. M., & Bragazzi, N. L. (2021). Adiponectin: Structure, Physiological Functions, Role in Diseases, and Effects of Nutrition. *Nutrients*, *13*(4), 1180. https://doi.org/10.3390/nu13041180

Kieffer, T. J., Heller, R. S., & Habener, J. F. (1996). Leptin Receptors Expressed on Pancreatic β-Cells. *Biochemical and Biophysical Research Communications*, *224*(2), 522–527. https://doi.org/10.1006/bbrc.1996.1059

Kieffer, T. J., Heller, R. S., Unson, C. G., Weir, G. C., & Habener, J. F. (1996). Distribution of glucagon receptors on hormone-specific endocrine cells of rat pancreatic islets. *Endocrinology*, *137*(11), 5119–5125. https://doi.org/10.1210/endo.137.11.8895386

Kielar, D., Clark, J. S., Ciechanowicz, A., Kurzawski, G., Sulikowski, T., & Naruszewicz, M. (1998). Leptin receptor isoforms expressed in human adipose tissue. *Metabolism: Clinical and Experimental*, *47*(7), 844–847. https://doi.org/10.1016/s0026-0495(98)90124-x

Kilimnik, G., Zhao, B., Jo, J., Periwal, V., Witkowski, P., Misawa, R., & Hara, M. (2011). Altered Islet Composition and Disproportionate Loss of Large Islets in Patients with Type 2 Diabetes. *PLoS ONE*, *6*(11). https://doi.org/10.1371/journal.pone.0027445

Kim, A. Y., Park, Y. J., Pan, X., Shin, K. C., Kwak, S.-H., Bassas, A. F., Sallam, R. M., Park, K. S., Alfadda, A. A., Xu, A., & Kim, J. B. (2015). Obesity-induced DNA hypermethylation of the adiponectin gene mediates insulin resistance. *Nature Communications*, *6*(1), Article 1. https://doi.org/10.1038/ncomms8585

Kim, C.-S., Park, H.-S., Kawada, T., Kim, J.-H., Lim, D., Hubbard, N. E., Kwon, B.-S., Erickson, K. L., & Yu, R. (2006). Circulating levels of MCP-1 and IL-8 are elevated in human obese subjects and associated with obesity-related parameters. *International Journal of Obesity (2005)*, *30*(9), 1347–1355. https://doi.org/10.1038/sj.ijo.0803259

Kim, D., Kim, J., Yoon, J. H., Ghim, J., Yea, K., Song, P., Park, S., Lee, A., Hong, C.-P., Jang, M. S., Kwon, Y., Park, S., Jang, M. H., Berggren, P.-O., Suh, P.-G., & Ryu, S. H. (2014). CXCL12 secreted from adipose tissue recruits macrophages and induces insulin resistance in mice. *Diabetologia*, *57*(7), 1456–1465. https://doi.org/10.1007/s00125-014-3237-5

Kim, J. B., & Spiegelman, B. M. (1996). ADD1/SREBP1 promotes adipocyte differentiation and gene expression linked to fatty acid metabolism. *Genes & Development*, *10*(9), 1096–1107. https://doi.org/10.1101/gad.10.9.1096

Kim-Muller, J. Y., Zhao, S., Srivastava, S., Mugabo, Y., Noh, H.-L., Kim, Y. R., Madiraju, S. R. M., Ferrante, A. W., Skolnik, E. Y., Prentki, M., & Accili, D. (2014). Metabolic inflexibility impairs insulin secretion and results in MODY-like diabetes in triple FoxO-deficient mice. *Cell Metabolism*, *20*(4), 593–602. https://doi.org/10.1016/j.cmet.2014.08.012

King, D. E., Mainous, A. G., Buchanan, T. A., & Pearson, W. S. (2003). C-reactive protein and glycemic control in adults with diabetes. *Diabetes Care*, *26*(5), 1535–1539. https://doi.org/10.2337/diacare.26.5.1535

Kingery, S. E., Wu, Y. L., Zhou, B., Hoffman, R. P., & Yu, C. Y. (2012). Gene Copy-Number Variations (CNVs) and Protein Levels of Complement C4A and C4B as Novel Biomarkers for Partial Disease Remissions in New-Onset Type 1 Diabetes Patients. *Pediatric Diabetes*, *13*(5), 408–418. https://doi.org/10.1111/j.1399-5448.2011.00836.x

Kirk, E. A., Sagawa, Z. K., McDonald, T. O., O'Brien, K. D., & Heinecke, J. W. (2008). Monocyte Chemoattractant Protein-1 Deficiency Fails to Restrain Macrophage Infiltration Into Adipose Tissue. *Diabetes*, *57*(5), 1254–1261. https://doi.org/10.2337/db07-1061

Kitade, H., Sawamoto, K., Nagashimada, M., Inoue, H., Yamamoto, Y., Sai, Y., Takamura, T., Yamamoto, H., Miyamoto, K., Ginsberg, H. N., Mukaida, N., Kaneko, S., & Ota, T. (2012). CCR5 Plays a Critical Role in Obesity-Induced Adipose Tissue Inflammation and Insulin Resistance by Regulating Both Macrophage Recruitment and M1/M2 Status. *Diabetes*, *61*(7), 1680–1690. https://doi.org/10.2337/db11-1506

Kjørholt, C., Akerfeldt, M. C., Biden, T. J., & Laybutt, D. R. (2005). Chronic hyperglycemia, independent of plasma lipid levels, is sufficient for the loss of beta-cell differentiation and secretory function in the db/db mouse model of diabetes. *Diabetes*, *54*(9), 2755–2763. https://doi.org/10.2337/diabetes.54.9.2755

Kochetkova, M., Kumar, S., & McColl, S. R. (2009). Chemokine receptors CXCR4 and CCR7 promote metastasis by preventing anoikis in cancer cells. *Cell Death & Differentiation*, *16*(5), Article 5. https://doi.org/10.1038/cdd.2008.190

Koethe, J. R., Lagathu, C., Lake, J. E., Domingo, P., Calmy, A., Falutz, J., Brown, T. T., & Capeau, J. (2020). HIV and antiretroviral therapy-related fat alterations. *Nature Reviews Disease Primers*, *6*(1), Article 1. https://doi.org/10.1038/s41572-020-0181-1

Koistinen, H. A., Vidal, H., Karonen, S. L., Dusserre, E., Vallier, P., Koivisto, V. A., & Ebeling, P. (2001). Plasma acylation stimulating protein concentration and subcutaneous adipose tissue C3 mRNA expression in nondiabetic and type 2 diabetic men. *Arteriosclerosis, Thrombosis, and Vascular Biology*, *21*(6), 1034–1039. https://doi.org/10.1161/01.atv.21.6.1034

Kolterman, O. G., Buse, J. B., Fineman, M. S., Gaines, E., Heintz, S., Bicsak, T. A., Taylor, K., Kim, D., Aisporna, M., Wang, Y., & Baron, A. D. (2003). Synthetic exendin-4 (exenatide) significantly reduces postprandial and fasting plasma glucose in subjects with type 2 diabetes. *The*

Journal of Clinical Endocrinology and Metabolism, *88*(7), 3082–3089. https://doi.org/10.1210/jc.2002-021545

Kolterman, O. G., Kim, D. D., Shen, L., Ruggles, J. A., Nielsen, L. L., Fineman, M. S., & Baron, A. D. (2005). Pharmacokinetics, pharmacodynamics, and safety of exenatide in patients with type 2 diabetes mellitus. *American Journal of Health-System Pharmacy: AJHP: Official Journal of the American Society of Health-System Pharmacists*, *62*(2), 173–181. https://doi.org/10.1093/ajhp/62.2.173

Konrad, R. J., Jolly, Y. C., Major, C., & Wolf, B. A. (1992). Inhibition of phospholipase A2 and insulin secretion in pancreatic islets. *Biochimica Et Biophysica Acta*, *1135*(2), 215–220. https://doi.org/10.1016/0167-4889(92)90139-3

Koo, J. H., Kim, T. H., Park, S.-Y., Joo, M. S., Han, C. Y., Choi, C. S., & Kim, S. G. (2017). Gα13 ablation reprograms myofibers to oxidative phenotype and enhances whole-body metabolism. *The Journal of Clinical Investigation*, *127*(10), 3845–3860. https://doi.org/10.1172/JCI92067

Korzus, E., Torchia, J., Rose, D. W., Xu, L., Kurokawa, R., McInerney, E. M., Mullen, T. M., Glass, C. K., & Rosenfeld, M. G. (1998). Transcription factor-specific requirements for coactivators and their acetyltransferase functions. *Science (New York, N.Y.)*, *279*(5351), 703–707. https://doi.org/10.1126/science.279.5351.703

Kotani, M., Detheux, M., Vandenbogaerde, A., Communi, D., Vanderwinden, J. M., Le Poul, E., Brézillon, S., Tyldesley, R., Suarez-Huerta, N., Vandeput, F., Blanpain, C., Schiffmann, S. N., Vassart, G., & Parmentier, M. (2001). The metastasis suppressor gene KiSS-1 encodes kisspeptins, the natural ligands of the orphan G protein-coupled receptor GPR54. *The Journal of Biological Chemistry*, *276*(37), 34631–34636. https://doi.org/10.1074/jbc.M104847200

Koussounadis, A., Langdon, S. P., Um, I. H., Harrison, D. J., & Smith, V. A. (2015). Relationship between differentially expressed mRNA and mRNA-protein correlations in a xenograft model system. *Scientific Reports*, *5*(1), Article 1. https://doi.org/10.1038/srep10775

Kralisch, S., Weise, S., Sommer, G., Lipfert, J., Lossner, U., Bluher, M., Stumvoll, M., & Fasshauer, M. (2009). Interleukin-1beta induces the novel adipokine chemerin in adipocytes in vitro. *Regulatory Peptides*, *154*(1–3), 102–106. https://doi.org/10.1016/j.regpep.2009.02.010

Kreutter, G., Kassem, M., El Habhab, A., Baltzinger, P., Abbas, M., Boisrame-Helms, J., Amoura, L., Peluso, J., Yver, B., Fatiha, Z., Ubeaud-Sequier, G., Kessler, L., & Toti, F. (2017). Endothelial microparticles released by activated protein C protect beta cells through EPCR/PAR1 and annexin A1/FPR2 pathways in islets. *Journal of Cellular and Molecular Medicine*, *21*(11), 2759–2772. https://doi.org/10.1111/jcmm.13191

Kristinsson, H., Smith, D. M., Bergsten, P., & Sargsyan, E. (2013). FFAR1 is involved in both the acute and chronic effects of palmitate on insulin secretion. *Endocrinology*, *154*(11), 4078–4088. https://doi.org/10.1210/en.2013-1352

Kroeze, W. K., Sassano, M. F., Huang, X.-P., Lansu, K., McCorvy, J. D., Giguère, P. M., Sciaky, N., & Roth, B. L. (2015). PRESTO-Tango as an open-source resource for interrogation of the druggable human GPCRome. *Nature Structural & Molecular Biology*, *22*(5), Article 5. https://doi.org/10.1038/nsmb.3014

Kubota, N., Terauchi, Y., Kubota, T., Kumagai, H., Itoh, S., Satoh, H., Yano, W., Ogata, H., Tokuyama, K., Takamoto, I., Mineyama, T., Ishikawa, M., Moroi, M., Sugi, K., Yamauchi, T., Ueki, K., Tobe, K., Noda, T., Nagai, R., & Kadowaki, T. (2006). Pioglitazone ameliorates insulin resistance and diabetes by both adiponectin-dependent and -independent pathways. *The Journal of Biological Chemistry*, *281*(13), 8748–8755. https://doi.org/10.1074/jbc.M505649200

Kubota, N., Tobe, K., Terauchi, Y., Eto, K., Yamauchi, T., Suzuki, R., Tsubamoto, Y., Komeda, K., Nakano, R., Miki, H., Satoh, S., Sekihara, H., Sciacchitano, S., Lesniak, M., Aizawa, S., Nagai, R., Kimura, S., Akanuma, Y., Taylor, S. I., & Kadowaki, T. (2000). Disruption of insulin receptor substrate 2 causes type 2 diabetes because of liver insulin resistance and lack of

compensatory beta-cell hyperplasia. *Diabetes*, *49*(11), 1880–1889. https://doi.org/10.2337/diabetes.49.11.1880

Küçüködük, A., Helvacioglu, F., Haberal, N., Dagdeviren, A., Bacanli, D., Yilmaz, G., & Akkoyun, I. (2019). Antiproliferative and anti-apoptotic effect of astaxanthin in an oxygen-induced retinopathy mouse model. *Canadian Journal of Ophthalmology*, *54*(1), 65–74. https://doi.org/10.1016/j.jcjo.2018.02.017

Kuivaniemi, H., & Tromp, G. (2019). Type III collagen (COL3A1): Gene and protein structure, tissue distribution, and associated diseases. *Gene*, *707*, 151–171. https://doi.org/10.1016/j.gene.2019.05.003

Kulkarni, R. N., Brüning, J. C., Winnay, J. N., Postic, C., Magnuson, M. A., & Kahn, C. R. (1999). Tissue-Specific Knockout of the Insulin Receptor in Pancreatic β Cells Creates an Insulin Secretory Defect Similar to that in Type 2 Diabetes. *Cell*, *96*(3), 329–339. https://doi.org/10.1016/S0092-8674(00)80546-2

Kulkarni, R. N., Holzenberger, M., Shih, D. Q., Ozcan, U., Stoffel, M., Magnuson, M. A., & Kahn, C. R. (2002). Beta-cell-specific deletion of the Igf1 receptor leads to hyperinsulinemia and glucose intolerance but does not alter beta-cell mass. *Nature Genetics*, *31*(1), 111–115. https://doi.org/10.1038/ng872

Kulkarni, R. N., Wang, Z. L., Wang, R. M., Hurley, J. D., Smith, D. M., Ghatei, M. A., Withers, D. J., Gardiner, J. V., Bailey, C. J., & Bloom, S. R. (1997). Leptin rapidly suppresses insulin release from insulinoma cells, rat and human islets and, in vivo, in mice. *The Journal of Clinical Investigation*, *100*(11), 2729–2736. https://doi.org/10.1172/JCI119818

Kumar, A., Gangwar, R., Ahmad Zargar, A., Kumar, R., & Sharma, A. (2023). Prevalence of diabetes in India: A review of IDF Diabetes Atlas 10th edition. *Current Diabetes Reviews*. https://doi.org/10.2174/1573399819666230413094200

Kuo, D. S., Labelle-Dumais, C., & Gould, D. B. (2012). COL4A1 and COL4A2 mutations and disease: Insights into pathogenic mechanisms and potential therapeutic targets. *Human Molecular Genetics*, *21*(R1), R97–R110. https://doi.org/10.1093/hmg/dds346

Kuo, L. E., Kitlinska, J. B., Tilan, J. U., Li, L., Baker, S. B., Johnson, M. D., Lee, E. W., Burnett, M. S., Fricke, S. T., Kvetnansky, R., Herzog, H., & Zukowska, Z. (2007). Neuropeptide Y acts directly in the periphery on fat tissue and mediates stress-induced obesity and metabolic syndrome. *Nature Medicine*, *13*(7), 803–811. https://doi.org/10.1038/nm1611

Kusuyama, J., Komorizono, A., Bandow, K., Ohnishi, T., & Matsuguchi, T. (2016). CXCL3 positively regulates adipogenic differentiation. *Journal of Lipid Research*, *57*(10), 1806–1820. https://doi.org/10.1194/jlr.M067207

Kutlu, B., Cardozo, A. K., Darville, M. I., Kruhøffer, M., Magnusson, N., Ørntoft, T., & Eizirik, D. L. (2003). Discovery of gene networks regulating cytokine-induced dysfunction and apoptosis in insulin-producing INS-1 cells. *Diabetes*, *52*(11), 2701–2719. https://doi.org/10.2337/diabetes.52.11.2701

Laferrère, B., Swerdlow, N., Bawa, B., Arias, S., Bose, M., Oliván, B., Teixeira, J., McGinty, J., & Rother, K. I. (2010). Rise of oxyntomodulin in response to oral glucose after gastric bypass surgery in patients with type 2 diabetes. *The Journal of Clinical Endocrinology and Metabolism*, *95*(8), 4072–4076. https://doi.org/10.1210/jc.2009-2767

Lampousi, A.-M., Carlsson, S., & Löfvenborg, J. E. (2021). Dietary factors and risk of islet autoimmunity and type 1 diabetes: A systematic review and meta-analysis. *EBioMedicine*, *72*, 103633. https://doi.org/10.1016/j.ebiom.2021.103633

Lan, H., Lin, H. V., Wang, C. F., Wright, M. J., Xu, S., Kang, L., Juhl, K., Hedrick, J. A., & Kowalski, T. J. (2012). Agonists at GPR119 mediate secretion of GLP-1 from mouse enteroendocrine cells through glucose-independent pathways. *British Journal of Pharmacology*, *165*(8), 2799–2807. https://doi.org/10.1111/j.1476-5381.2011.01754.x

Lataillade, J.-J., Clay, D., Bourin, P., Hérodin, F., Dupuy, C., Jasmin, C., & Le Bousse-Kerdilès, M.-C. (2002). Stromal cell-derived factor 1 regulates primitive hematopoiesis by suppressing apoptosis and by promoting G(0)/G(1) transition in CD34(+) cells: Evidence for an autocrine/paracrine mechanism. *Blood*, *99*(4), 1117–1129. https://doi.org/10.1182/blood.v99.4.1117

Lauffer, L. M., Iakoubov, R., & Brubaker, P. L. (2009). GPR119 is essential for oleoylethanolamide-induced glucagon-like peptide-1 secretion from the intestinal enteroendocrine L-cell. *Diabetes*, *58*(5), 1058–1066. https://doi.org/10.2337/db08-1237

Le Gurun, S., Martin, D., Formenton, A., Maechler, P., Caille, D., Waeber, G., Meda, P., & Haefliger, J.-A. (2003). Connexin-36 contributes to control function of insulin-producing cells. *The Journal of Biological Chemistry*, *278*(39), 37690–37697. https://doi.org/10.1074/jbc.M212382200

Lean, M. E., Leslie, W. S., Barnes, A. C., Brosnahan, N., Thom, G., McCombie, L., Peters, C., Zhyzhneuskaya, S., Al-Mrabeh, A., Hollingsworth, K. G., Rodrigues, A. M., Rehackova, L., Adamson, A. J., Sniehotta, F. F., Mathers, J. C., Ross, H. M., McIlvenna, Y., Stefanetti, R., Trenell, M., … Taylor, R. (2018). Primary care-led weight management for remission of type 2 diabetes (DiRECT): An open-label, cluster-randomised trial. *The Lancet*, *391*(10120), 541–551. https://doi.org/10.1016/S0140-6736(17)33102-1

Lebovitz, H. E., Dole, J. F., Patwardhan, R., Rappaport, E. B., Freed, M. I., & Rosiglitazone Clinical Trials Study Group. (2001). Rosiglitazone monotherapy is effective in patients with type 2 diabetes. *The Journal of Clinical Endocrinology and Metabolism*, *86*(1), 280–288. https://doi.org/10.1210/jcem.86.1.7157

Lee, D., Shin, K.-J., Kim, D. W., Yoon, K.-A., Choi, Y.-J., Lee, B. N. R., & Cho, J.-Y. (2018). CCL4 enhances preosteoclast migration and its receptor CCR5 downregulation by RANKL promotes osteoclastogenesis. *Cell Death & Disease*, *9*(5), 495. https://doi.org/10.1038/s41419-018-0562-5

Lee, M.-H., Klein, R. L., El-Shewy, H. M., Luttrell, D. K., & Luttrell, L. M. (2008). The adiponectin receptors AdipoR1 and AdipoR2 activate ERK1/2 through a Src/Ras-dependent pathway and stimulate cell growth. *Biochemistry*, *47*(44), 11682–11692. https://doi.org/10.1021/bi801451f

Lee, S., Lee, H.-C., Kwon, Y.-W., Lee, S. E., Cho, Y., Kim, J., Lee, S., Kim, J.-Y., Lee, J., Yang, H.-M., Mook-Jung, I., Nam, K.-Y., Chung, J., Lazar, M. A., & Kim, H.-S. (2014). Adenylyl Cyclase-Associated Protein 1(CAP1) is a Receptor for Human Resistin and Mediates Inflammatory Actions of Human Monocytes. *Cell Metabolism*, *19*(3), 484–497. https://doi.org/10.1016/j.cmet.2014.01.013

Lee, Y., Gotoh, A., Kwon, H.-J., You, M., Kohli, L., Mantel, C., Cooper, S., Hangoc, G., Miyazawa, K., Ohyashiki, K., & Broxmeyer, H. E. (2002). Enhancement of intracellular signaling associated with hematopoietic progenitor cell survival in response to SDF-1/CXCL12 in synergy with other cytokines. *Blood*, *99*(12), 4307–4317. https://doi.org/10.1182/blood.v99.12.4307

Lefterova, M. I., Haakonsson, A. K., Lazar, M. A., & Mandrup, S. (2014). PPARγ and the Global Map of Adipogenesis and Beyond. *Trends in Endocrinology and Metabolism: TEM*, *25*(6), 293–302. https://doi.org/10.1016/j.tem.2014.04.001

Legøy, T. A., Mathisen, A. F., Salim, Z., Vethe, H., Bjørlykke, Y., Abadpour, S., Paulo, J. A., Scholz, H., Ræder, H., Ghila, L., & Chera, S. (2020). In vivo Environment Swiftly Restricts Human Pancreatic Progenitors Toward Mono-Hormonal Identity via a HNF1A/HNF4A Mechanism. *Frontiers in Cell and Developmental Biology*, *8*. https://www.frontiersin.org/articles/10.3389/fcell.2020.00109

Lemaire, K., Granvik, M., Schraenen, A., Goyvaerts, L., Van Lommel, L., Gómez-Ruiz, A., in 't Veld, P., Gilon, P., & Schuit, F. (2017). How stable is repression of disallowed genes in pancreatic islets in response to metabolic stress? *PLoS ONE*, *12*(8), e0181651. https://doi.org/10.1371/journal.pone.0181651

Lernmark, Å. (1974). The preparation of, and studies on, free cell suspensions from mouse pancreatic islets. *Diabetologia*, *10*(5), 431–438. https://doi.org/10.1007/BF01221634

Li, Y., Cao, Y., Wang, J., Fu, S., Cheng, J., Ma, L., Zhang, Q., Guo, W., Kan, X., & Liu, J. (2020). Kp-10 promotes bovine mammary epithelial cell proliferation by activating GPR54 and its downstream signaling pathways. *Journal of Cellular Physiology*, *235*(5), 4481–4493. https://doi.org/10.1002/jcp.29325

Li, Z., Dong, X., Liu, H., Chen, X., Shi, H., Fan, Y., Hou, D., & Zhang, X. (2013). Astaxanthin protects ARPE-19 cells from oxidative stress via upregulation of Nrf2-regulated phase II enzymes through activation of PI3K/Akt. *Molecular Vision*, *19*, 1656–1666.

Liang, W. G., Ren, M., Zhao, F., & Tang, W.-J. (2015). Structures of human CCL18, CCL3, and CCL4 reveal molecular determinants for quaternary structures and sensitivity to insulin degrading enzyme. *Journal of Molecular Biology*, *427*(6 0 0), 1345–1358. https://doi.org/10.1016/j.jmb.2015.01.012

Licinio, J., Caglayan, S., Ozata, M., Yildiz, B. O., de Miranda, P. B., O'Kirwan, F., Whitby, R., Liang, L., Cohen, P., Bhasin, S., Krauss, R. M., Veldhuis, J. D., Wagner, A. J., DePaoli, A. M., McCann, S. M., & Wong, M.-L. (2004). Phenotypic effects of leptin replacement on morbid obesity, diabetes mellitus, hypogonadism, and behavior in leptin-deficient adults. *Proceedings of the National Academy of Sciences of the United States of America*, *101*(13), 4531–4536. https://doi.org/10.1073/pnas.0308767101

Lien, M.-Y., Tsai, H.-C., Chang, A.-C., Tsai, M.-H., Hua, C.-H., Wang, S.-W., & Tang, C.-H. (2018). Chemokine CCL4 Induces Vascular Endothelial Growth Factor C Expression and Lymphangiogenesis by miR-195-3p in Oral Squamous Cell Carcinoma. *Frontiers in Immunology*, *9*, 412. https://doi.org/10.3389/fimmu.2018.00412

Light, P. E., Manning Fox, J. E., Riedel, M. J., & Wheeler, M. B. (2002). Glucagon-Like Peptide-1 Inhibits Pancreatic ATP-Sensitive Potassium Channels via a Protein Kinase A- and ADP-

Dependent Mechanism. *Molecular Endocrinology*, *16*(9), 2135–2144. https://doi.org/10.1210/me.2002-0084

Liljenquist, J. E., Bomboy, J. D., Lewis, S. B., Sinclair-Smith, B. C., Felts, P. W., Lacy, W. W., Crofford, O. B., & Liddle, G. W. (1974). Effects of glucagon on lipolysis and ketogenesis in normal and diabetic men. *The Journal of Clinical Investigation*, *53*(1), 190–197. https://doi.org/10.1172/JCI107537

Lim, J., Iyer, A., Suen, J. Y., Seow, V., Reid, R. C., Brown, L., & Fairlie, D. P. (2013). C5aR and C3aR antagonists each inhibit diet-induced obesity, metabolic dysfunction, and adipocyte and macrophage signaling. *FASEB Journal: Official Publication of the Federation of American Societies for Experimental Biology*, *27*(2), 822–831. https://doi.org/10.1096/fj.12-220582

Lim, Y., Dorstyn, L., & Kumar, S. (2021). The p53-caspase-2 axis in the cell cycle and DNA damage response. *Experimental & Molecular Medicine*, *53*(4), Article 4. https://doi.org/10.1038/s12276-021-00590-2

Lin, X., Guan, H., Huang, Z., Liu, J., Li, H., Wei, G., Cao, X., & Li, Y. (2014). Downregulation of Bcl-2 Expression by miR-34a Mediates Palmitate-Induced Min6 Cells Apoptosis. *Journal of Diabetes Research*, *2014*, e258695. https://doi.org/10.1155/2014/258695

Litwack, G. (2018). Chapter 8—Glycolysis and Gluconeogenesis. In G. Litwack (Ed.), *Human Biochemistry* (pp. 183–198). Academic Press. https://doi.org/10.1016/B978-0-12-383864-3.00008-9

Liu, B., Hassan, Z., Amisten, S., King, A. J., Bowe, J. E., Huang, G. C., Jones, P. M., & Persaud, S. J. (2013). The novel chemokine receptor, G-protein-coupled receptor 75, is expressed by islets and is coupled to stimulation of insulin secretion and improved glucose homeostasis. *Diabetologia*, *56*(11), 2467–2476. https://doi.org/10.1007/s00125-013-3022-x

Liu, B., Shao, Y., & Fu, R. (2021). Current research status of HLA in immune-related diseases. *Immunity, Inflammation and Disease*, *9*(2), 340–350. https://doi.org/10.1002/iid3.416

Liu, C., Liu, X. J., Barry, G., Ling, N., Maki, R. A., & De Souza, E. B. (1997). Expression and characterization of a putative high affinity human soluble leptin receptor. *Endocrinology*, *138*(8), 3548–3554. https://doi.org/10.1210/endo.138.8.5343

Liu, F., Dong, J., Yang, Q., Xue, X., Ren, Z., Gan, Y., & Liao, L. (2015). Glucagon-like peptide 1 receptor agonist therapy is more efficacious than insulin glargine for poorly controlled type 2 diabetes: A systematic review and meta-analysis. *Journal of Diabetes*, *7*(3), 322–328. https://doi.org/10.1111/1753-0407.12200

Liu, J., Bai, R., Chai, Z., Cooper, M. E., Zimmet, P. Z., & Zhang, L. (2022). Low- and middle-income countries demonstrate rapid growth of type 2 diabetes: An analysis based on Global Burden of Disease 1990–2019 data. *Diabetologia*, *65*(8), 1339–1352. https://doi.org/10.1007/s00125-022-05713-6

Liu, Z., & Habener, J. F. (2009). Stromal cell-derived factor-1 promotes survival of pancreatic beta cells by the stabilisation of beta-catenin and activation of transcription factor 7-like 2 (TCF7L2). *Diabetologia*, *52*(8), 1589–1598. https://doi.org/10.1007/s00125-009-1384-x

Liu, Z., Jeppesen, P. B., Gregersen, S., Chen, X., & Hermansen, K. (2008). Dose- and Glucose-Dependent Effects of Amino Acids on Insulin Secretion from Isolated Mouse Islets and Clonal INS-1E Beta-Cells. *The Review of Diabetic Studies: RDS*, *5*(4), 232–244. https://doi.org/10.1900/RDS.2008.5.232

Liu, Z., Stanojevic, V., Avadhani, S., Yano, T., & Habener, J. F. (2011). Stromal cell-derived factor-1 (SDF-1)/chemokine (C-X-C motif) receptor 4 (CXCR4) axis activation induces intra-islet glucagon-like peptide-1 (GLP-1) production and enhances beta cell survival. *Diabetologia*, *54*(8), 2067–2076. https://doi.org/10.1007/s00125-011-2181-x

Lo, J. C., Ljubicic, S., Leibiger, B., Kern, M., Leibiger, I. B., Moede, T., Kelly, M. E., Chatterjee Bhowmick, D., Murano, I., Cohen, P., Banks, A. S., Khandekar, M. J., Dietrich, A., Flier, J. S., Cinti, S., Blüher, M., Danial, N. N., Berggren, P.-O., & Spiegelman, B. M. (2014). Adipsin is an

adipokine that improves β cell function in diabetes. *Cell*, *158*(1), 41–53. https://doi.org/10.1016/j.cell.2014.06.005

Loetscher, P., Seitz, M., Clark-Lewis, I., Baggiolini, M., & Moser, B. (1996). Activation of NK cells by CC chemokines. Chemotaxis, Ca2+ mobilization, and enzyme release. *Journal of Immunology (Baltimore, Md.: 1950)*, *156*(1), 322–327.

Lu, B., Rutledge, B. J., Gu, L., Fiorillo, J., Lukacs, N. W., Kunkel, S. L., North, R., Gerard, C., & Rollins, B. J. (1998). Abnormalities in Monocyte Recruitment and Cytokine Expression in Monocyte Chemoattractant Protein 1–deficient Mice. *The Journal of Experimental Medicine*, *187*(4), 601–608.

Lu, H., Cassis, L. A., Kooi, C. W. V., & Daugherty, A. (2016). Structure and functions of angiotensinogen. *Hypertension Research*, *39*(7), Article 7. https://doi.org/10.1038/hr.2016.17

Ludwig, B., Ziegler, C. G., Schally, A. V., Richter, C., Steffen, A., Jabs, N., Funk, R. H., Brendel, M. D., Block, N. L., Ehrhart-Bornstein, M., & Bornstein, S. R. (2010). Agonist of growth hormone-releasing hormone as a potential effector for survival and proliferation of pancreatic islets. *Proceedings of the National Academy of Sciences*, *107*(28), 12623–12628. https://doi.org/10.1073/pnas.1005098107

Lumeng, C. N., Bodzin, J. L., & Saltiel, A. R. (2007). Obesity induces a phenotypic switch in adipose tissue macrophage polarization. *The Journal of Clinical Investigation*, *117*(1), 175–184. https://doi.org/10.1172/JCI29881

Lundberg, M., Seiron, P., Ingvast, S., Korsgren, O., & Skog, O. (2017). Insulitis in human diabetes: A histological evaluation of donor pancreases. *Diabetologia*, *60*(2), 346–353. https://doi.org/10.1007/s00125-016-4140-z

Lupi, R., Dotta, F., Marselli, L., Del Guerra, S., Masini, M., Santangelo, C., Patané, G., Boggi, U., Piro, S., Anello, M., Bergamini, E., Mosca, F., Di Mario, U., Del Prato, S., & Marchetti, P. (2002). Prolonged exposure to free fatty acids has cytostatic and pro-apoptotic effects on human

pancreatic islets: Evidence that beta-cell death is caspase mediated, partially dependent on ceramide pathway, and Bcl-2 regulated. *Diabetes*, *51*(5), 1437–1442. https://doi.org/10.2337/diabetes.51.5.1437

Luther, S. A., Lopez, T., Bai, W., Hanahan, D., & Cyster, J. G. (2000). BLC expression in pancreatic islets causes B cell recruitment and lymphotoxin-dependent lymphoid neogenesis. *Immunity*, *12*(5), 471–481. https://doi.org/10.1016/s1074-7613(00)80199-5

Ly, L. D., Ly, D. D., Nguyen, N. T., Kim, J.-H., Yoo, H., Chung, J., Lee, M.-S., Cha, S.-K., & Park, K.-S. (2020). Mitochondrial Ca2+ Uptake Relieves Palmitate-Induced Cytosolic Ca2+ Overload in MIN6 Cells. *Molecules and Cells*, *43*(1), 66–75. https://doi.org/10.14348/molcells.2019.0223

MacDonald, P. E., Marinis, Y. Z. D., Ramracheya, R., Salehi, A., Ma, X., Johnson, P. R. V., Cox, R., Eliasson, L., & Rorsman, P. (2007). A KATP Channel-Dependent Pathway within α Cells Regulates Glucagon Release from Both Rodent and Human Islets of Langerhans. *PLoS Biology*, *5*(6), e143. https://doi.org/10.1371/journal.pbio.0050143

MacLaren, R. E., Cui, W., Lu, H., Simard, S., & Cianflone, K. (2010). Association of adipocyte genes with ASP expression: A microarray analysis of subcutaneous and omental adipose tissue in morbidly obese subjects. *BMC Medical Genomics*, *3*, 3. https://doi.org/10.1186/1755-8794-3-3

Maedler, K., Sergeev, P., Ehses, J. A., Mathe, Z., Bosco, D., Berney, T., Dayer, J.-M., Reinecke, M., Halban, P. A., & Donath, M. Y. (2004). Leptin modulates β cell expression of IL-1 receptor antagonist and release of IL-1β in human islets. *Proceedings of the National Academy of Sciences of the United States of America*, *101*(21), 8138. https://doi.org/10.1073/pnas.0305683101

Maffi, P., Lundgren, T., Tufveson, G., Rafael, E., Shaw, J. A. M., Liew, A., Saudek, F., Witkowski, P., Golab, K., Bertuzzi, F., Gustafsson, B., Daffonchio, L., Ruffini, P. A., Piemonti, L., & REP0211 Study Group. (2020). Targeting CXCR1/2 Does Not Improve Insulin Secretion After Pancreatic

Islet Transplantation: A Phase 3, Double-Blind, Randomized, Placebo-Controlled Trial in Type 1 Diabetes. *Diabetes Care*, *43*(4), 710–718. https://doi.org/10.2337/dc19-1480

Maghazachi, A. A., Al-Aoukaty, A., & Schall, T. J. (1996). CC chemokines induce the generation of killer cells from CD56+ cells. *European Journal of Immunology*, *26*(2), 315–319. https://doi.org/10.1002/eji.1830260207

Maier, R., Weger, M., Haller-Schober, E.-M., El-Shabrawi, Y., Wedrich, A., Theisl, A., Aigner, R., Barth, A., & Haas, A. (2008). Multiplex bead analysis of vitreous and serum concentrations of inflammatory and proangiogenic factors in diabetic patients. *Molecular Vision*, *14*, 637.

Makimura, H., Feldpausch, M. N., Rope, A. M., Hemphill, L. C., Torriani, M., Lee, H., & Grinspoon, S. K. (2012). Metabolic Effects of a Growth Hormone-Releasing Factor in Obese Subjects with Reduced Growth Hormone Secretion: A Randomized Controlled Trial. *The Journal of Clinical Endocrinology & Metabolism*, *97*(12), 4769–4779. https://doi.org/10.1210/jc.2012-2794

Malmqvist, E., Larsson, H. E., Jönsson, I., Rignell-Hydbom, A., Ivarsson, S.-A., Tinnerberg, H., Stroh, E., Rittner, R., Jakobsson, K., Swietlicki, E., & Rylander, L. (2015). Maternal exposure to air pollution and type 1 diabetes—Accounting for genetic factors. *Environmental Research*, *140*, 268–274. https://doi.org/10.1016/j.envres.2015.03.024

Mamane, Y., Chung Chan, C., Lavallee, G., Morin, N., Xu, L.-J., Huang, J., Gordon, R., Thomas, W., Lamb, J., Schadt, E. E., Kennedy, B. P., & Mancini, J. A. (2009). The C3a Anaphylatoxin Receptor Is a Key Mediator of Insulin Resistance and Functions by Modulating Adipose Tissue Macrophage Infiltration and Activation. *Diabetes*, *58*(9), 2006–2017. https://doi.org/10.2337/db09-0323

Mancuso, P., & Bouchard, B. (2019). The Impact of Aging on Adipose Function and Adipokine Synthesis. *Frontiers in Endocrinology*, *10*, 137. https://doi.org/10.3389/fendo.2019.00137

Marcelin, G., Ferreira, A., Liu, Y., Atlan, M., Aron-Wisnewsky, J., Pelloux, V., Botbol, Y., Ambrosini, M., Fradet, M., Rouault, C., Hénégar, C., Hulot, J.-S., Poitou, C., Torcivia, A., Nail-Barthelemy, R., Bichet, J.-C., Gautier, E. L., & Clément, K. (2017). A PDGFRα-Mediated Switch toward

CD9high Adipocyte Progenitors Controls Obesity-Induced Adipose Tissue Fibrosis. *Cell Metabolism*, *25*(3), 673–685. https://doi.org/10.1016/j.cmet.2017.01.010

Marchetti, P., Bugliani, M., Lupi, R., Marselli, L., Masini, M., Boggi, U., Filipponi, F., Weir, G. C., Eizirik, D. L., & Cnop, M. (2007). The endoplasmic reticulum in pancreatic beta cells of type 2 diabetes patients. *Diabetologia*, *50*(12), 2486–2494. https://doi.org/10.1007/s00125-007-0816-8

Marchetti, P., Scharp, D. W., McLear, M., Finke, E. H., Olack, B., Swanson, C., Giannarelli, R., Navalesi, R., & Lacy, P. E. (1995). Insulin inhibits its own secretion from isolated, perifused human pancreatic islets. *Acta Diabetologica*, *32*(2), 75–77. https://doi.org/10.1007/BF00569560

Marroqui, L., Masini, M., Merino, B., Grieco, F. A., Millard, I., Dubois, C., Quesada, I., Marchetti, P., Cnop, M., & Eizirik, D. L. (2015). Pancreatic α Cells are Resistant to Metabolic Stress-induced Apoptosis in Type 2 Diabetes. *EBioMedicine*, *2*(5), 378–385. https://doi.org/10.1016/j.ebiom.2015.03.012

Marselli, L., Suleiman, M., Masini, M., Campani, D., Bugliani, M., Syed, F., Martino, L., Focosi, D., Scatena, F., Olimpico, F., Filipponi, F., Masiello, P., Boggi, U., & Marchetti, P. (2014). Are we overestimating the loss of beta cells in type 2 diabetes? *Diabetologia*, *57*(2), 362–365. https://doi.org/10.1007/s00125-013-3098-3

Martin, A. P., Rankin, S., Pitchford, S., Charo, I. F., Furtado, G. C., & Lira, S. A. (2008). Increased Expression of CCL2 in Insulin-Producing Cells of Transgenic Mice Promotes Mobilization of Myeloid Cells From the Bone Marrow, Marked Insulitis, and Diabetes. *Diabetes*, *57*(11), 3025–3033. https://doi.org/10.2337/db08-0625

Mashikian, M. V., Ryan, T. C., Seman, A., Brazer, W., Center, D. M., & Cruikshank, W. W. (1999). Reciprocal Desensitization of CCR5 and CD4 Is Mediated by IL-16 and Macrophage-Inflammatory Protein-1β, Respectively1. *The Journal of Immunology*, *163*(6), 3123–3130. https://doi.org/10.4049/jimmunol.163.6.3123

Mayr, B., & Montminy, M. (2001). Transcriptional regulation by the phosphorylation-dependent factor CREB. *Nature Reviews Molecular Cell Biology*, *2*(8), Article 8. https://doi.org/10.1038/35085068

McCall, M. D., Maciver, A. H., Pawlick, R., Edgar, R., & Shapiro, A. M. J. (2011). Histopaque provides optimal mouse islet purification kinetics: Comparison study with Ficoll, iodixanol and dextran. *Islets*, *3*(4), 144–149. https://doi.org/10.4161/isl.3.4.15729

McClenaghan, N. H., Barnett, C. R., & Flatt, P. R. (1998). Na+ cotransport by metabolizable and nonmetabolizable amino acids stimulates a glucose-regulated insulin-secretory response. *Biochemical and Biophysical Research Communications*, *249*(2), 299–303. https://doi.org/10.1006/bbrc.1998.9136

McClenaghan, N. H., Barnett, C. R., O'Harte, F. P., & Flatt, P. R. (1996). Mechanisms of amino acid-induced insulin secretion from the glucose-responsive BRIN-BD11 pancreatic B-cell line. *The Journal of Endocrinology*, *151*(3), 349–357. https://doi.org/10.1677/joe.0.1510349

McLaughlin, T., Lamendola, C., Liu, A., & Abbasi, F. (2011). Preferential fat deposition in subcutaneous versus visceral depots is associated with insulin sensitivity. *The Journal of Clinical Endocrinology and Metabolism*, *96*(11), E1756-1760. https://doi.org/10.1210/jc.2011-0615

Md Moin, A. S., Dhawan, S., Cory, M., Butler, P. C., Rizza, R. A., & Butler, A. E. (2016). Increased Frequency of Hormone Negative and Polyhormonal Endocrine Cells in Lean Individuals With Type 2 Diabetes. *The Journal of Clinical Endocrinology and Metabolism*, *101*(10), 3628–3636. https://doi.org/10.1210/jc.2016-2496

Meagher, C., Arreaza, G., Peters, A., Strathdee, C. A., Gilbert, P. A., Mi, Q.-S., Santamaria, P., Dekaban, G. A., & Delovitch, T. L. (2007). CCL4 Protects From Type 1 Diabetes by Altering Islet β-Cell–Targeted Inflammatory Responses. *Diabetes*, *56*(3), 809–817. https://doi.org/10.2337/db06-0619

Meagher, C., Beilke, J., Arreaza, G., Mi, Q.-S., Chen, W., Salojin, K., Horst, N., Cruikshank, W. W., & Delovitch, T. L. (2010). Neutralization of Interleukin-16 Protects Nonobese Diabetic Mice From Autoimmune Type 1 Diabetes by a CCL4-Dependent Mechanism. *Diabetes*, *59*(11), 2862–2871. https://doi.org/10.2337/db09-0131

Mehta, R., Birerdinc, A., Hossain, N., Afendy, A., Chandhoke, V., Younossi, Z., & Baranova, A. (2010). Validation of endogenous reference genes for qRT-PCR analysis of human visceral adipose samples. *BMC Molecular Biology*, *11*, 39. https://doi.org/10.1186/1471-2199-11-39

Melzi, R., Mercalli, A., Sordi, V., Cantarelli, E., Nano, R., Maffi, P., Sitia, G., Guidotti, L. G., Secchi, A., Bonifacio, E., & Piemonti, L. (2010). Role of CCL2/MCP-1 in Islet Transplantation. *Cell Transplantation*, *19*(8), 1031–1046. https://doi.org/10.3727/096368910X514639

Méndez, V., Avelar, E., Morales, A., Cervantes, M., Araiza, A., & González, D. (2011). A rapid protocol for purification of total RNA for tissues collected from pigs at a slaughterhouse. *Genetics and Molecular Research: GMR*, *10*(4), 3251–3255. https://doi.org/10.4238/2011.December.22.3

Meulen, T. van der, & Huising, M. O. (2015). Role of transcription factors in the transdifferentiation of pancreatic islet cells. *Journal of Molecular Endocrinology*, *54*(2), R103–R117. https://doi.org/10.1530/JME-14-0290

Mezza, T., Cinti, F., Cefalo, C. M. A., Pontecorvi, A., Kulkarni, R. N., & Giaccari, A. (2019). β-Cell Fate in Human Insulin Resistance and Type 2 Diabetes: A Perspective on Islet Plasticity. *Diabetes*, *68*(6), 1121–1129. https://doi.org/10.2337/db18-0856

Michel, M. C., Wieland, T., & Tsujimoto, G. (2009). How reliable are G-protein-coupled receptor antibodies? *Naunyn-Schmiedeberg's Archives of Pharmacology*, *379*(4), 385–388. https://doi.org/10.1007/s00210-009-0395-y

Miller, R. A., Chu, Q., Le Lay, J., Scherer, P. E., Ahima, R. S., Kaestner, K. H., Foretz, M., Viollet, B., & Birnbaum, M. J. (2011). Adiponectin suppresses gluconeogenic gene expression in mouse hepatocytes independent of LKB1-AMPK signaling. *The Journal of Clinical Investigation*, *121*(6), 2518–2528. https://doi.org/10.1172/JCI45942

Misra, V. K., & Trudeau, S. (2011). The influence of overweight and obesity on longitudinal trends in maternal serum leptin levels during pregnancy. *Obesity (Silver Spring, Md.)*, *19*(2), 416–421. https://doi.org/10.1038/oby.2010.172

Miyachi, Y., Miyazawa, T., & Ogawa, Y. (2022). HNF1A Mutations and Beta Cell Dysfunction in Diabetes. *International Journal of Molecular Sciences*, *23*(6), 3222. https://doi.org/10.3390/ijms23063222

Miyazaki, J., Araki, K., Yamato, E., Ikegami, H., Asano, T., Shibasaki, Y., Oka, Y., & Yamamura, K. (1990). Establishment of a pancreatic beta cell line that retains glucose-inducible insulin secretion: Special reference to expression of glucose transporter isoforms. *Endocrinology*, *127*(1), 126–132. https://doi.org/10.1210/endo-127-1-126

Miyazaki, S., Tashiro, F., Tsuchiya, T., Sasaki, K., & Miyazaki, J. (2021). Establishment of a long-term stable β-cell line and its application to analyze the effect of Gcg expression on insulin secretion. *Scientific Reports*, *11*(1), Article 1. https://doi.org/10.1038/s41598-020-79992-7

Mizumoto, Y., Hemmi, H., Katsuda, M., Miyazawa, M., Kitahata, Y., Miyamoto, A., Nakamori, M., Ojima, T., Matsuda, K., Nakamura, M., Hayata, K., Fukuda-Ohta, Y., Sugiyama, M., Ohta, T., Orimo, T., Okura, S., Sasaki, I., Tamada, K., Yamaue, H., & Kaisho, T. (2020). Anticancer effects of chemokine-directed antigen delivery to a cross-presenting dendritic cell subset with immune checkpoint blockade. *British Journal of Cancer*, *122*(8), Article 8. https://doi.org/10.1038/s41416-020-0757-2

Moltchanova, E. V., Schreier, N., Lammi, N., & Karvonen, M. (2009). Seasonal variation of diagnosis of Type 1 diabetes mellitus in children worldwide. *Diabetic Medicine: A Journal of the British Diabetic Association*, *26*(7), 673–678. https://doi.org/10.1111/j.1464-5491.2009.02743.x

Monami, M., Cremasco, F., Lamanna, C., Marchionni, N., & Mannucci, E. (2011). Predictors of response to dipeptidyl peptidase-4 inhibitors: Evidence from randomized clinical trials. *Diabetes/Metabolism Research and Reviews*, *27*(4), 362–372. https://doi.org/10.1002/dmrr.1184

Montanya, E., Nacher, V., Biarnés, M., & Soler, J. (2000). *Linear Correlation Between -Cell Mass and Body Weight Throughout the Lifespan in Lewis Rats*. *49*.

Moses, A., Bronson, S. C., & V., S. (2017). *Pharmacotherapy for management of Prediabetes* (pp. 375–377).

Muccioli, G. G., Naslain, D., Bäckhed, F., Reigstad, C. S., Lambert, D. M., Delzenne, N. M., & Cani, P. D. (2010). The endocannabinoid system links gut microbiota to adipogenesis. *Molecular Systems Biology*, *6*(1), 392. https://doi.org/10.1038/msb.2010.46

Mueller, A., Mahmoud, N. G., Goedecke, M. C., McKeating, J. A., & Strange, P. G. (2002). Pharmacological characterization of the chemokine receptor, CCR5. *British Journal of Pharmacology*, *135*(4), 1033–1043. https://doi.org/10.1038/sj.bjp.0704540

Muller, D., Huang, G. C., Amiel, S., Jones, P. M., & Persaud, S. J. (2006). Identification of Insulin Signaling Elements in Human β-Cells: Autocrine Regulation of Insulin Gene Expression. *Diabetes*, *55*(10), 2835–2842. https://doi.org/10.2337/db06-0532

Müller, G., Ertl, J., Gerl, M., & Preibisch, G. (1997). Leptin Impairs Metabolic Actions of Insulin in Isolated Rat Adipocytes. *Journal of Biological Chemistry*, *272*(16), 10585–10593. https://doi.org/10.1074/jbc.272.16.10585

Müller, J. A., Groß, R., Conzelmann, C., Krüger, J., Merle, U., Steinhart, J., Weil, T., Koepke, L., Bozzo, C. P., Read, C., Fois, G., Eiseler, T., Gehrmann, J., van Vuuren, J., Wessbecher, I. M., Frick, M., Costa, I. G., Breunig, M., Grüner, B., … Kleger, A. (2021). SARS-CoV-2 infects and replicates in cells of the human endocrine and exocrine pancreas. *Nature Metabolism*, *3*(2), 149–165. https://doi.org/10.1038/s42255-021-00347-1

Müller, T. D., Finan, B., Bloom, S. R., D'Alessio, D., Drucker, D. J., Flatt, P. R., Fritsche, A., Gribble, F., Grill, H. J., Habener, J. F., Holst, J. J., Langhans, W., Meier, J. J., Nauck, M. A., Perez-Tilve, D., Pocai, A., Reimann, F., Sandoval, D. A., Schwartz, T. W., … Tschöp, M. H. (2019). Glucagon-like peptide 1 (GLP-1). *Molecular Metabolism*, *30*, 72–130. https://doi.org/10.1016/j.molmet.2019.09.010

Müller, W. A., Faloona, G. R., & Unger, R. H. (1973). Hyperglucagonemia in diabetic ketoacidosis. Its prevalence and significance. *The American Journal of Medicine*, *54*(1), 52–57. https://doi.org/10.1016/0002-9343(73)90083-1

Muñoz, C., Floreen, A., Garey, C., Karlya, T., Jelley, D., Alonso, G. T., & McAuliffe-Fogarty, A. (2019). Misdiagnosis and Diabetic Ketoacidosis at Diagnosis of Type 1 Diabetes: Patient and Caregiver Perspectives. *Clinical Diabetes : A Publication of the American Diabetes Association*, *37*(3), 276–281. https://doi.org/10.2337/cd18-0088

Murakami, T., Cardones, A. R., Finkelstein, S. E., Restifo, N. P., Klaunberg, B. A., Nestle, F. O., Castillo, S. S., Dennis, P. A., & Hwang, S. T. (2003). Immune Evasion by Murine Melanoma Mediated through CC Chemokine Receptor-10. *Journal of Experimental Medicine*, *198*(9), 1337–1347. https://doi.org/10.1084/jem.20030593

Muscari, A., Antonelli, S., Bianchi, G., Cavrini, G., Dapporto, S., Ligabue, A., Ludovico, C., Magalotti, D., Poggiopollini, G., Zoli, M., & Pianoro Study Group. (2007). Serum C3 is a stronger inflammatory marker of insulin resistance than C-reactive protein, leukocyte count, and erythrocyte sedimentation rate: Comparison study in an elderly population. *Diabetes Care*, *30*(9), 2362–2368. https://doi.org/10.2337/dc07-0637

Nadal, A., Quesada, I., & Soria, B. (1999). Homologous and heterologous asynchronicity between identified α-, β- and δ-cells within intact islets of Langerhans in the mouse. *The Journal of Physiology*, *517*(Pt 1), 85–93. https://doi.org/10.1111/j.1469-7793.1999.0085z.x

Nadler, S. T., Stoehr, J. P., Schueler, K. L., Tanimoto, G., Yandell, B. S., & Attie, A. D. (2000). The expression of adipogenic genes is decreased in obesity and diabetes mellitus. *Proceedings of the National Academy of Sciences of the United States of America*, *97*(21), 11371–11376.

Nakata, M., Okada, T., Ozawa, K., & Yada, T. (2007). Resistin induces insulin resistance in pancreatic islets to impair glucose-induced insulin release. *Biochemical and Biophysical Research Communications*, *353*(4), 1046–1051. https://doi.org/10.1016/j.bbrc.2006.12.134

Nandi Jui, B., Sarsenbayeva, A., Jernow, H., Hetty, S., & Pereira, M. J. (2022). Evaluation of RNA Isolation Methods in Human Adipose Tissue. *Laboratory Medicine*, *53*(5), e129–e133. https://doi.org/10.1093/labmed/lmab126

Natarajan Sulochana, K., Lakshmi, S., Punitham, R., Arokiasamy, T., Sukumar, B., & Ramakrishnan, S. (2002). Effect of oral supplementation of free amino acids in type 2 diabetic patients—A pilot clinical trial. *Medical Science Monitor: International Medical Journal of Experimental and Clinical Research*, *8*(3), CR131-137.

Nathan, D. M., Turgeon, H., & Regan, S. (2007). Relationship between glycated haemoglobin levels and mean glucose levels over time. *Diabetologia*, *50*(11), 2239–2244. https://doi.org/10.1007/s00125-007-0803-0

Neijssen, J., Herberts, C., Drijfhout, J. W., Reits, E., Janssen, L., & Neefjes, J. (2005). Cross-presentation by intercellular peptide transfer through gap junctions. *Nature*, *434*(7029), 83–88. https://doi.org/10.1038/nature03290

Nellaiappan, K., Preeti, K., Khatri, D. K., & Singh, S. B. (2022). Diabetic Complications: An Update on Pathobiology and Therapeutic Strategies. *Current Diabetes Reviews*, *18*(1), e030821192146. https://doi.org/10.2174/1573399817666210309104203

Nestler, J. E., Jakubowicz, D. J., Evans, W. S., & Pasquali, R. (1998). Effects of metformin on spontaneous and clomiphene-induced ovulation in the polycystic ovary syndrome. *The New England Journal of Medicine*, *338*(26), 1876–1880. https://doi.org/10.1056/NEJM199806253382603

Nibbs, R. J., Wylie, S. M., Yang, J., Landau, N. R., & Graham, G. J. (1997). Cloning and characterization of a novel promiscuous human beta-chemokine receptor D6. *The Journal of Biological Chemistry*, *272*(51), 32078–32083. https://doi.org/10.1074/jbc.272.51.32078

Niessen, H., Harz, H., Bedner, P., Krämer, K., & Willecke, K. (2000). Selective permeability of different connexin channels to the second messenger inositol 1,4,5-trisphosphate. *Journal of Cell Science*, *113 (Pt 8)*, 1365–1372. https://doi.org/10.1242/jcs.113.8.1365

Nigi, L., Brusco, N., Grieco, G. E., Licata, G., Krogvold, L., Marselli, L., Gysemans, C., Overbergh, L., Marchetti, P., Mathieu, C., Dahl Jørgensen, K., Sebastiani, G., & Dotta, F. (2020). Pancreatic Alpha-Cells Contribute Together With Beta-Cells to CXCL10 Expression in Type 1 Diabetes. *Frontiers in Endocrinology*, *11*, 630. https://doi.org/10.3389/fendo.2020.00630

Nilsson, B., Hamad, O. A., Ahlström, H., Kullberg, J., Johansson, L., Lindhagen, L., Haenni, A., Ekdahl, K. N., & Lind, L. (2014). C3 and C4 are strongly related to adipose tissue variables and cardiovascular risk factors. *European Journal of Clinical Investigation*, *44*(6), 587–596. https://doi.org/10.1111/eci.12275

Nir, T., Melton, D. A., & Dor, Y. (2007). Recovery from diabetes in mice by β cell regeneration. *The Journal of Clinical Investigation*, *117*(9), 2553. https://doi.org/10.1172/JCI32959

Nolan, C. J., & Proietto, J. (1994). The feto-placental glucose steal phenomenon is a major cause of maternal metabolic adaptation during late pregnancy in the rat. *Diabetologia*, *37*(10), 976–984. https://doi.org/10.1007/BF00400460

Nomiyama, T., & Yanase, T. (2015). [Secondary diabetes]. *Nihon Rinsho. Japanese Journal of Clinical Medicine*, *73*(12), 2008–2012.

Norris, J. M., Yin, X., Lamb, M. M., Barriga, K., Seifert, J., Hoffman, M., Orton, H. D., Barón, A. E., Clare-Salzler, M., Chase, H. P., Szabo, N. J., Erlich, H., Eisenbarth, G. S., & Rewers, M. (2007). Omega-3 polyunsaturated fatty acid intake and islet autoimmunity in children at increased risk for type 1 diabetes. *JAMA*, *298*(12), 1420–1428. https://doi.org/10.1001/jama.298.12.1420

Nyman, L. R., Wells, K. S., Head, W. S., McCaughey, M., Ford, E., Brissova, M., Piston, D. W., & Powers, A. C. (2008). Real-time, multidimensional in vivo imaging used to investigate blood flow in mouse pancreatic islets. *The Journal of Clinical Investigation*, *118*(11), 3790–3797. https://doi.org/10.1172/JCI36209

O'Driscoll, L., Gammell, P., & Clynes, M. (2004). Mechanisms associated with loss of glucose responsiveness in beta cells. *Transplantation Proceedings*, *36*(4), 1159–1162. https://doi.org/10.1016/j.transproceed.2004.04.011

O'Driscoll, L., Gammell, P., McKiernan, E., Ryan, E., Jeppesen, P. B., Rani, S., & Clynes, M. (2006). Phenotypic and global gene expression profile changes between low passage and high passage MIN-6 cells. *The Journal of Endocrinology*, *191*(3), 665–676. https://doi.org/10.1677/joe.1.06894

Ojima, K., Oe, M., Nakajima, I., Muroya, S., & Nishimura, T. (2016). Dynamics of protein secretion during adipocyte differentiation. *FEBS Open Bio*, *6*(8), 816–826. https://doi.org/10.1002/2211-5463.12091

Ojo, O., Wang, X.-H., Ojo, O. O., & Ibe, J. (2018). The Effects of Substance Abuse on Blood Glucose Parameters in Patients with Diabetes: A Systematic Review and Meta-Analysis. *International Journal of Environmental Research and Public Health*, *15*(12), 2691. https://doi.org/10.3390/ijerph15122691

Okada, T., Liew, C. W., Hu, J., Hinault, C., Michael, M. D., Kŕtzfeldt, J., Yin, C., Holzenberger, M., Stoffel, M., & Kulkarni, R. N. (2007). Insulin receptors in β-cells are critical for islet compensatory growth response to insulin resistance. *Proceedings of the National Academy of Sciences*, *104*(21), 8977–8982. https://doi.org/10.1073/pnas.0608703104

Okamura, S., Arakawa, H., Tanaka, T., Nakanishi, H., Ng, C. C., Taya, Y., Monden, M., & Nakamura, Y. (2001). P53DINP1, a p53-inducible gene, regulates p53-dependent apoptosis. *Molecular Cell*, *8*(1), 85–94. https://doi.org/10.1016/s1097-2765(01)00284-2

Olaniru, O. E., Jones, P. M., & Persaud, S. J. (2015). Basic and clinical science posters. *Diabetic Medicine*, *32*(S1), 48. https://doi.org/10.1111/dme.12668

Olaniru, O. E., & Persaud, S. J. (2018). Identifying novel therapeutic targets for diabetes through improved understanding of islet adhesion receptors. *Current Opinion in Pharmacology*, *43*, 27–33. https://doi.org/10.1016/j.coph.2018.07.009

Olaniru, O. E., Pingitore, A., Giera, S., Piao, X., Castañera González, R., Jones, P. M., & Persaud, S. J. (2018). The adhesion receptor GPR56 is activated by extracellular matrix collagen III to improve β-cell function. *Cellular and Molecular Life Sciences*, *75*(21), 4007–4019. https://doi.org/10.1007/s00018-018-2846-4

Oppermann, M. (2004). Chemokine receptor CCR5: Insights into structure, function, and regulation. *Cellular Signalling*, *16*(11), 1201–1210. https://doi.org/10.1016/j.cellsig.2004.04.007

Oppermann, M., Mack, M., Proudfoot, A. E., & Olbrich, H. (1999). Differential effects of CC chemokines on CC chemokine receptor 5 (CCR5) phosphorylation and identification of phosphorylation sites on the CCR5 carboxyl terminus. *The Journal of Biological Chemistry*, *274*(13), 8875–8885. https://doi.org/10.1074/jbc.274.13.8875

Ortis, F., Cardozo, A. K., Crispim, D., Störling, J., Mandrup-Poulsen, T., & Eizirik, D. L. (2006). Cytokine-induced proapoptotic gene expression in insulin-producing cells is related to rapid, sustained, and nonoscillatory nuclear factor-kappaB activation. *Molecular Endocrinology (Baltimore, Md.)*, *20*(8), 1867–1879. https://doi.org/10.1210/me.2005-0268

Overmyer, K. A., Thonusin, C., Qi, N. R., Burant, C. F., & Evans, C. R. (2015). Impact of anesthesia and euthanasia on metabolomics of mammalian tissues: Studies in a C57BL/6J mouse model. *PloS One*, *10*(2), e0117232. https://doi.org/10.1371/journal.pone.0117232

Overton, H. A., Babbs, A. J., Doel, S. M., Fyfe, M. C. T., Gardner, L. S., Griffin, G., Jackson, H. C., Procter, M. J., Rasamison, C. M., Tang-Christensen, M., Widdowson, P. S., Williams, G. M., & Reynet, C. (2006). Deorphanization of a G protein-coupled receptor for oleoylethanolamide and its use in the discovery of small-molecule hypophagic agents. *Cell Metabolism*, *3*(3), 167–175. https://doi.org/10.1016/j.cmet.2006.02.004

Pace, C. S., & Tarvin, J. T. (1981). Somatostatin: Mechanism of action in pancreatic islet beta-cells. *Diabetes*, *30*(10), 836–842. https://doi.org/10.2337/diab.30.10.836

Packer, M. (2018). Do DPP-4 Inhibitors Cause Heart Failure Events by Promoting Adrenergically Mediated Cardiotoxicity? Clues From Laboratory Models and Clinical Trials. *Circulation Research*, *122*(7), 928–932. https://doi.org/10.1161/CIRCRESAHA.118.312673

Palhinha, L., Liechocki, S., Hottz, E. D., Pereira, J. A. da S., de Almeida, C. J., Moraes-Vieira, P. M. M., Bozza, P. T., & Maya-Monteiro, C. M. (2019). Leptin Induces Proadipogenic and Proinflammatory Signaling in Adipocytes. *Frontiers in Endocrinology*, *10*, 841. https://doi.org/10.3389/fendo.2019.00841

Pan, X., Kaminga, A. C., Wen, S. W., & Liu, A. (2021). Chemokines in Prediabetes and Type 2 Diabetes: A Meta-Analysis. *Frontiers in Immunology*, *12*, 622438. https://doi.org/10.3389/fimmu.2021.622438

Panten, U., Brüning, D., & Rustenbeck, I. (2023). Regulation of insulin secretion in mouse islets: Metabolic amplification by alpha-ketoisocaproate coincides with rapid and sustained increase in acetyl-CoA content. *Naunyn-Schmiedeberg's Archives of Pharmacology*, *396*(2), 353–364. https://doi.org/10.1007/s00210-022-02290-8

Papizan, J. B., Singer, R. A., Tschen, S.-I., Dhawan, S., Friel, J. M., Hipkens, S. B., Magnuson, M. A., Bhushan, A., & Sussel, L. (2011). Nkx2.2 repressor complex regulates islet β-cell specification and prevents β-to-α-cell reprogramming. *Genes & Development*, *25*(21), 2291–2305. https://doi.org/10.1101/gad.173039.111

Parisi, F., Milazzo, R., Savasi, V. M., & Cetin, I. (2021). Maternal Low-Grade Chronic Inflammation and Intrauterine Programming of Health and Disease. *International Journal of Molecular Sciences*, *22*(4), 1732. https://doi.org/10.3390/ijms22041732

Parsons, J. A., Brelje, T. C., & Sorenson, R. L. (1992). Adaptation of islets of Langerhans to pregnancy: Increased islet cell proliferation and insulin secretion correlates with the onset of placental lactogen secretion. *Endocrinology*, *130*(3), 1459–1466. https://doi.org/10.1210/endo.130.3.1537300

Patel, Y. C., & Srikant, C. B. (1997). Somatostatin receptors. *Trends in Endocrinology and Metabolism: TEM*, *8*(10), 398–405. https://doi.org/10.1016/s1043-2760(97)00168-9

Pathak, V., Pathak, N. M., O'Neill, C. L., Guduric-Fuchs, J., & Medina, R. J. (2019). Therapies for Type 1 Diabetes: Current Scenario and Future Perspectives. *Clinical Medicine Insights. Endocrinology and Diabetes*, *12*, 1179551419844521. https://doi.org/10.1177/1179551419844521

Pellegrinelli, V., Carobbio, S., & Vidal-Puig, A. (2016). Adipose tissue plasticity: How fat depots respond differently to pathophysiological cues. *Diabetologia*, *59*, 1075–1088. https://doi.org/10.1007/s00125-016-3933-4

Perea, A., Clemente, F., Martinell, J., Villanueva-Peñacarrillo, M. L., & Valverde, I. (1995). Physiological effect of glucagon in human isolated adipocytes. *Hormone and Metabolic Research = Hormon- Und Stoffwechselforschung = Hormones Et Metabolisme*, *27*(8), 372–375. https://doi.org/10.1055/s-2007-979981

Perez, L. J., Rios, L., Trivedi, P., D'Souza, K., Cowie, A., Nzirorera, C., Webster, D., Brunt, K., Legare, J.-F., Hassan, A., Kienesberger, P. C., & Pulinilkunnil, T. (2017). Validation of optimal reference genes for quantitative real time PCR in muscle and adipose tissue for obesity and diabetes research. *Scientific Reports*, *7*(1), 3612. https://doi.org/10.1038/s41598-017-03730-9

Pérez-Martínez, L., Ochoa-Callejero, L., Rubio-Mediavilla, S., Narro, J., Bernardo, I., Oteo, J.-A., & Blanco, J.-R. (2018). Maraviroc improves hepatic triglyceride content but not inflammation in a murine nonalcoholic fatty liver disease model induced by a chronic exposure to high-fat diet. *Translational Research*, *196*, 17–30. https://doi.org/10.1016/j.trsl.2018.01.004

Pérez-Martínez, L., Pérez-Matute, P., Aguilera-Lizarraga, J., Rubio-Mediavilla, S., Narro, J., Recio, E., Ochoa-Callejero, L., Oteo, J.-A., & Blanco, J.-R. (2014). Maraviroc, a CCR5 antagonist, ameliorates the development of hepatic steatosis in a mouse model of non-alcoholic fatty liver disease (NAFLD). *The Journal of Antimicrobial Chemotherapy*, *69*(7), 1903–1910. https://doi.org/10.1093/jac/dku071

Pérez-Matute, P., Pérez-Martínez, L., Aguilera-Lizarraga, J., Blanco, J. R., & Oteo, J. A. (2015). Maraviroc modifies gut microbiota composition in a mouse model of obesity: A plausible therapeutic option to prevent metabolic disorders in HIV-infected patients. *Revista Espanola De Quimioterapia: Publicacion Oficial De La Sociedad Espanola De Quimioterapia*, *28*(4), 200–206.

Pérez-Matute, P., Pichel, J. G., Iñiguez, M., Recio-Fernández, E., Pérez-Martínez, L., Torrens, R., Blanco, J. R., & Oteo, J. A. (2017). Maraviroc Ameliorates the Increased Adipose Tissue Macrophage Recruitment Induced by a High-Fat Diet in a Mouse Model of Obesity. *Antiviral Therapy*, *22*(2), 163–168. https://doi.org/10.3851/IMP3099

Pernicova, I., & Korbonits, M. (2014). Metformin—Mode of action and clinical implications for diabetes and cancer. *Nature Reviews Endocrinology*, *10*(3), Article 3. https://doi.org/10.1038/nrendo.2013.256

Persaud, S. J. (2017). Islet G-protein coupled receptors: Therapeutic potential for diabetes. *Current Opinion in Pharmacology*, *37*, 24–28. https://doi.org/10.1016/j.coph.2017.08.001

Persaud, S. J., Hauge-Evans, A. C., & Jones, P. M. (2014). Chapter 15 - Insulin-Secreting Cell Lines: Potential for Research and Diabetes Therapy. In A. Ulloa-Aguirre & P. M. Conn (Eds.), *Cellular Endocrinology in Health and Disease* (pp. 239–256). Academic Press. https://doi.org/10.1016/B978-0-12-408134-5.00015-9

Petkov, S., Herrera, C., Else, L., Mugaba, S., Namubiru, P., Odoch, G., Opoka, D., Pillay, A.-D. A. P., Seiphetlo, T. B., Serwanga, J., Ssemata, A. S., Kaleebu, P., Webb, E. L., Khoo, S., Lebina, L., Gray, C. M., Martinson, N., Fox, J., & Chiodi, F. (2022). Mobilization of systemic CCL4 following HIV pre-exposure prophylaxis in young men in Africa. *Frontiers in Immunology*, *13*, 965214. https://doi.org/10.3389/fimmu.2022.965214

Pfaffl, M. W. (2001). A new mathematical model for relative quantification in real-time RT-PCR. *Nucleic Acids Research*, *29*(9), e45. https://doi.org/10.1093/nar/29.9.e45

Pfeffer, C. M., & Singh, A. T. K. (2018). Apoptosis: A Target for Anticancer Therapy. *International Journal of Molecular Sciences*, *19*(2), 448. https://doi.org/10.3390/ijms19020448

Pfleger, C., Kaas, A., Hansen, L., Alizadeh, B., Hougaard, P., Holl, R., Kolb, H., Roep, B. O., Mortensen, H. B., & Schloot, N. C. (2008). Relation of circulating concentrations of chemokine receptor CCR5 ligands to C-peptide, proinsulin and HbA1c and disease progression in type 1 diabetes. *Clinical Immunology*, *128*(1), 57–65. https://doi.org/10.1016/j.clim.2008.03.458

Phieler, J., Chung, K.-J., Chatzigeorgiou, A., Klotzsche-von Ameln, A., Garcia-Martin, R., Sprott, D., Moisidou, M., Tzanavari, T., Ludwig, B., Baraban, E., Ehrhart-Bornstein, M., Bornstein, S. R., Mziaut, H., Solimena, M., Karalis, K. P., Economopoulou, M., Lambris, J. D., & Chavakis, T. (2013). The Complement Anaphylatoxin C5a Receptor Contributes to Obese Adipose Tissue Inflammation and Insulin Resistance. *The Journal of Immunology*, *191*(8), 4367–4374. https://doi.org/10.4049/jimmunol.1300038

Piemonti, L., Keymeulen, B., Gillard, P., Linn, T., Bosi, E., Rose, L., Pozzilli, P., Giorgino, F., Cossu, E., Daffonchio, L., Goisis, G., Ruffini, P. A., Maurizi, A. R., Mantelli, F., & Allegretti, M. (2022). Ladarixin, an inhibitor of the interleukin-8 receptors CXCR1 and CXCR2, in new-onset type 1 diabetes: A multicentre, randomized, double-blind, placebo-controlled trial. *Diabetes, Obesity and Metabolism*, *24*(9), 1840–1849. https://doi.org/10.1111/dom.14770

Piemonti, L., Leone, B. E., Nano, R., Saccani, A., Monti, P., Maffi, P., Bianchi, G., Sica, A., Peri, G., Melzi, R., Aldrighetti, L., Secchi, A., Di Carlo, V., Allavena, P., & Bertuzzi, F. (2002). Human pancreatic islets produce and secrete MCP-1/CCL2: Relevance in human islet transplantation. *Diabetes*, *51*(1), 55–65. https://doi.org/10.2337/diabetes.51.1.55

Poitout, V., Rouault, C., Guerre-Millo, M., Briaud, I., & Reach, G. (1998). Inhibition of Insulin Secretion by Leptin in Normal Rodent Islets of Langerhans. *Endocrinology*, *139*(3), 822–826. https://doi.org/10.1210/endo.139.3.5812

Pratley, R. E., Catarig, A.-M., Lingvay, I., Viljoen, A., Paine, A., Lawson, J., Chubb, B., Gorst-Rasmussen, A., & Miresashvili, N. (2021). An indirect treatment comparison of the efficacy of

semaglutide 1.0 mg versus dulaglutide 3.0 and 4.5 mg. *Diabetes, Obesity & Metabolism*, *23*(11), 2513–2520. https://doi.org/10.1111/dom.14497

Prentki, M., Joly, E., El-Assaad, W., & Roduit, R. (2002). Malonyl-CoA Signaling, Lipid Partitioning, and Glucolipotoxicity: Role in β-Cell Adaptation and Failure in the Etiology of Diabetes. *Diabetes*, *51*(suppl_3), S405–S413. https://doi.org/10.2337/diabetes.51.2007.S405

Priya, G., & Kalra, S. (2018). A Review of Insulin Resistance in Type 1 Diabetes: Is There a Place for Adjunctive Metformin? *Diabetes Therapy*, *9*(1), 349–361. https://doi.org/10.1007/s13300-017-0333-9

Puff, R., Dames, P., Weise, M., Göke, B., Seissler, J., Parhofer, K. G., & Lechner, A. (2011). Reduced proliferation and a high apoptotic frequency of pancreatic beta cells contribute to genetically-determined diabetes susceptibility of db/db BKS mice. *Hormone and Metabolic Research = Hormon- Und Stoffwechselforschung = Hormones Et Metabolisme*, *43*(5), 306–311. https://doi.org/10.1055/s-0031-1271817

Puri, S., Roy, N., Russ, H. A., Leonhardt, L., French, E. K., Roy, R., Bengtsson, H., Scott, D. K., Stewart, A. F., & Hebrok, M. (2018). Replication confers β cell immaturity. *Nature Communications*, *9*(1), 485. https://doi.org/10.1038/s41467-018-02939-0

Qiao, L., Saget, S., Lu, C., Hay, W. W., Karsenty, G., & Shao, J. (2021). Adiponectin Promotes Maternal β-Cell Expansion Through Placental Lactogen Expression. *Diabetes*, *70*(1), 132–142. https://doi.org/10.2337/db20-0471

Qiao, L., Wattez, J.-S., Lee, S., Nguyen, A., Schaack, J., Hay, W. W., & Shao, J. (2017). Adiponectin Deficiency Impairs Maternal Metabolic Adaptation to Pregnancy in Mice. *Diabetes*, *66*(5), 1126–1135. https://doi.org/10.2337/db16-1096

Quandt, J., & Dorovini-Zis, K. (2004). The beta chemokines CCL4 and CCL5 enhance adhesion of specific CD4+ T cell subsets to human brain endothelial cells. *Journal of Neuropathology and Experimental Neurology*, *63*(4), 350–362. https://doi.org/10.1093/jnen/63.4.350

Quddusi, S., Vahl, T. P., Hanson, K., Prigeon, R. L., & D'Alessio, D. A. (2003). Differential effects of acute and extended infusions of glucagon-like peptide-1 on first- and second-phase insulin secretion in diabetic and nondiabetic humans. *Diabetes Care*, *26*(3), 791–798. https://doi.org/10.2337/diacare.26.3.791

Rachdaoui, N. (2020). Insulin: The Friend and the Foe in the Development of Type 2 Diabetes Mellitus. *International Journal of Molecular Sciences*, *21*(5), Article 5. https://doi.org/10.3390/ijms21051770

Rachdaoui, N., Polo-Parada, L., & Ismail-Beigi, F. (2019). Prolonged Exposure to Insulin Inactivates Akt and Erk1/2 and Increases Pancreatic Islet and INS1E β-Cell Apoptosis. *Journal of the Endocrine Society*, *3*(1), 69–90. https://doi.org/10.1210/js.2018-00140

Rackham, C. L., Amisten, S., Persaud, S. J., King, A. J. F., & Jones, P. M. (2018). Mesenchymal stromal cell secretory factors induce sustained improvements in islet function pre- and post-transplantation. *Cytotherapy*, *20*(12), 1427–1436. https://doi.org/10.1016/j.jcyt.2018.07.007

Rahmati, M., Keshvari, M., Mirnasuri, S., Yon, D. K., Lee, S. W., Il Shin, J., & Smith, L. (2022). The global impact of COVID-19 pandemic on the incidence of pediatric new-onset type 1 diabetes and ketoacidosis: A systematic review and meta-analysis. *Journal of Medical Virology*, *94*(11), 5112–5127. https://doi.org/10.1002/jmv.27996

Rajagopal, S., Bassoni, D. L., Campbell, J. J., Gerard, N. P., Gerard, C., & Wehrman, T. S. (2013). Biased Agonism as a Mechanism for Differential Signaling by Chemokine Receptors. *The Journal of Biological Chemistry*, *288*(49), 35039–35048. https://doi.org/10.1074/jbc.M113.479113

Rajagopal, S., & Shenoy, S. K. (2018). GPCR desensitization: Acute and prolonged phases. *Cellular Signalling*, *41*, 9–16. https://doi.org/10.1016/j.cellsig.2017.01.024

Rakatzi, I., Mueller, H., Ritzeler, O., Tennagels, N., & Eckel, J. (2004). Adiponectin counteracts cytokine- and fatty acid-induced apoptosis in the pancreatic beta-cell line INS-1. *Diabetologia*, *47*(2), 249–258. https://doi.org/10.1007/s00125-003-1293-3

Ramracheya, R. D., Muller, D. S., Wu, Y., Whitehouse, B. J., Huang, G. C., Amiel, S. A., Karalliedde, J., Viberti, G., Jones, P. M., & Persaud, S. J. (2006). Direct regulation of insulin secretion by angiotensin II in human islets of Langerhans. *Diabetologia*, *49*(2), 321–331. https://doi.org/10.1007/s00125-005-0101-7

Rapisarda, A., Pastorino, S., Massazza, S., Varesio, L., & Bosco, M. C. (2002). Antagonistic effect of picolinic acid and interferon-gamma on macrophage inflammatory protein-1alpha/beta production. *Cellular Immunology*, *220*(1), 70–80. https://doi.org/10.1016/s0008-8749(03)00008-x

Ravier, M. A., Güldenagel, M., Charollais, A., Gjinovci, A., Caille, D., Söhl, G., Wollheim, C. B., Willecke, K., Henquin, J.-C., & Meda, P. (2005). Loss of Connexin36 Channels Alters β-Cell Coupling, Islet Synchronization of Glucose-Induced Ca2+ and Insulin Oscillations, and Basal Insulin Release. *Diabetes*, *54*(6), 1798–1807. https://doi.org/10.2337/diabetes.54.6.1798

Reaven, G. M., Chen, Y. D., Golay, A., Swislocki, A. L., & Jaspan, J. B. (1987). Documentation of hyperglucagonemia throughout the day in nonobese and obese patients with noninsulin-dependent diabetes mellitus. *The Journal of Clinical Endocrinology and Metabolism*, *64*(1), 106–110. https://doi.org/10.1210/jcem-64-1-106

Rehman, M. B., Tudrej, B. V., Soustre, J., Buisson, M., Archambault, P., Pouchain, D., Vaillant-Roussel, H., Gueyffier, F., Faillie, J.-L., Perault-Pochat, M.-C., Cornu, C., & Boussageon, R. (2017). Efficacy and safety of DPP-4 inhibitors in patients with type 2 diabetes: Meta-analysis of placebo-controlled randomized clinical trials. *Diabetes & Metabolism*, *43*(1), 48–58. https://doi.org/10.1016/j.diabet.2016.09.005

Reinart, N., Nguyen, P.-H., Boucas, J., Rosen, N., Kvasnicka, H.-M., Heukamp, L., Rudolph, C., Ristovska, V., Velmans, T., Mueller, C., Reiners, K. S., von Strandmann, E. P., Krause, G., Montesinos-Rongen, M., Schlegelberger, B., Herling, M., Hallek, M., & Fingerle-Rowson, G. (2013). Delayed development of chronic lymphocytic leukemia in the absence of

macrophage migration inhibitory factor. *Blood*, *121*(5), 812–821. https://doi.org/10.1182/blood-2012-05-431452

Ren, D., Sun, J., Mao, L., Ye, H., & Polonsky, K. S. (2014). BH3-Only Molecule Bim Mediates β-Cell Death in IRS2 Deficiency. *Diabetes*, *63*(10), 3378–3387. https://doi.org/10.2337/db13-1814

Ren, M., Guo, Q., Guo, L., Lenz, M., Qian, F., Koenen, R. R., Xu, H., Schilling, A. B., Weber, C., Ye, R. D., Dinner, A. R., & Tang, W.-J. (2010). Polymerization of MIP-1 chemokine (CCL3 and CCL4) and clearance of MIP-1 by insulin-degrading enzyme. *The EMBO Journal*, *29*(23), 3952–3966. https://doi.org/10.1038/emboj.2010.256

Retis-Resendiz, A. M., González-García, I. N., León-Juárez, M., Camacho-Arroyo, I., Cerbón, M., & Vázquez-Martínez, E. R. (2021). The role of epigenetic mechanisms in the regulation of gene expression in the cyclical endometrium. *Clinical Epigenetics*, *13*(1), 116. https://doi.org/10.1186/s13148-021-01103-8

Riddle, M. C., Henry, R. R., Poon, T. H., Zhang, B., Mac, S. M., Holcombe, J. H., Kim, D. D., & Maggs, D. G. (2006). Exenatide elicits sustained glycaemic control and progressive reduction of body weight in patients with type 2 diabetes inadequately controlled by sulphonylureas with or without metformin. *Diabetes/Metabolism Research and Reviews*, *22*(6), 483–491. https://doi.org/10.1002/dmrr.646

Riedel, M., Hoeft, B., Blum, W. F., von zur Mühlen, A., & Brabant, G. (1995). Pulsatile growth hormone secretion in normal-weight and obese men: Differential metabolic regulation during energy restriction. *Metabolism: Clinical and Experimental*, *44*(5), 605–610. https://doi.org/10.1016/0026-0495(95)90117-5

Rieken, S., Sassmann, A., Herroeder, S., Wallenwein, B., Moers, A., Offermanns, S., & Wettschureck, N. (2006). G12/G13 family G proteins regulate marginal zone B cell maturation, migration, and polarization. *Journal of Immunology (Baltimore, Md.: 1950)*, *177*(5), 2985–2993. https://doi.org/10.4049/jimmunol.177.5.2985

Ritter, K., Buning, C., Halland, N., Pöverlein, C., & Schwink, L. (2016). G Protein-Coupled Receptor 119 (GPR119) Agonists for the Treatment of Diabetes: Recent Progress and Prevailing Challenges. *Journal of Medicinal Chemistry*, *59*(8), 3579–3592. https://doi.org/10.1021/acs.jmedchem.5b01198

Röder, P. V., Wu, B., Liu, Y., & Han, W. (2016). Pancreatic regulation of glucose homeostasis. *Experimental & Molecular Medicine*, *48*(3), Article 3. https://doi.org/10.1038/emm.2016.6

Rodríguez-Pacheco, F., Gutierrez-Repiso, C., García-Serrano, S., Ho-Plagaro, A., Gómez-Zumaquero, J. M., Valdes, S., Gonzalo, M., Rivas-Becerra, J., Montiel-Casado, C., Rojo-Martínez, G., García-Escobar, E., & García-Fuentes, E. (2017). Growth hormone-releasing hormone is produced by adipocytes and regulates lipolysis through growth hormone receptor. *International Journal of Obesity (2005)*, *41*(10), 1547–1555. https://doi.org/10.1038/ijo.2017.145

Roduit, R., Morin, J., Massé, F., Segall, L., Roche, E., Newgard, C. B., Assimacopoulos-Jeannet, F., & Prentki, M. (2000). Glucose down-regulates the expression of the peroxisome proliferator-activated receptor-alpha gene in the pancreatic beta -cell. *The Journal of Biological Chemistry*, *275*(46), 35799–35806. https://doi.org/10.1074/jbc.M006001200

Rodwell, G. E. J., Maurer, T. A., & Berger, T. G. (2000). Fat redistribution in HIV disease. *Journal of the American Academy of Dermatology*, *42*(5, Part 1), 727–730. https://doi.org/10.1067/mjd.2000.104791

Roh, S., Song, S.-H., Choi, K.-C., Katoh, K., Wittamer, V., Parmentier, M., & Sasaki, S. (2007). Chemerin—A new adipokine that modulates adipogenesis via its own receptor. *Biochemical and Biophysical Research Communications*, *362*(4), 1013–1018. https://doi.org/10.1016/j.bbrc.2007.08.104

Rorsman, P., Braun, M., & Zhang, Q. (2012). Regulation of calcium in pancreatic α- and β-cells in health and disease. *Cell Calcium*, *51*(3–4), 300–308. https://doi.org/10.1016/j.ceca.2011.11.006

Rosen, E. D., Hsu, C.-H., Wang, X., Sakai, S., Freeman, M. W., Gonzalez, F. J., & Spiegelman, B. M. (2002). C/EBPalpha induces adipogenesis through PPARgamma: A unified pathway. *Genes & Development*, *16*(1), 22–26. https://doi.org/10.1101/gad.948702

Rosen, E. D., & MacDougald, O. A. (2006). Adipocyte differentiation from the inside out. *Nature Reviews Molecular Cell Biology*, *7*(12), Article 12. https://doi.org/10.1038/nrm2066

Rosenzweig, T., Braiman, L., Bak, A., Alt, A., Kuroki, T., & Sampson, S. R. (2002). Differential effects of tumor necrosis factor-alpha on protein kinase C isoforms alpha and delta mediate inhibition of insulin receptor signaling. *Diabetes*, *51*(6), 1921–1930. https://doi.org/10.2337/diabetes.51.6.1921

Rourke, J. L., Muruganandan, S., Dranse, H. J., McMullen, N. M., & Sinal, C. J. (2014). Gpr1 is an active chemerin receptor influencing glucose homeostasis in obese mice. *The Journal of Endocrinology*, *222*(2), 201–215. https://doi.org/10.1530/JOE-14-0069

Ruan, H., Miles, P. D. G., Ladd, C. M., Ross, K., Golub, T. R., Olefsky, J. M., & Lodish, H. F. (2002). Profiling Gene Transcription In Vivo Reveals Adipose Tissue as an Immediate Target of Tumor Necrosis Factor-α: Implications for Insulin Resistance. *Diabetes*, *51*(11), 3176–3188. https://doi.org/10.2337/diabetes.51.11.3176

Rubio-Cabezas, O., Klupa, T., Malecki, M. T., & CEED3 Consortium. (2011). Permanent neonatal diabetes mellitus—The importance of diabetes differential diagnosis in neonates and infants. *European Journal of Clinical Investigation*, *41*(3), 323–333. https://doi.org/10.1111/j.1365-2362.2010.02409.x

Rubio-Navarro, A., Gómez-Banoy, N., Stoll, L., Dündar, F., Mawla, A. M., Ma, L., Cortada, E., Zumbo, P., Li, A., Reiterer, M., Montoya-Oviedo, N., Homan, E. A., Imai, N., Gilani, A., Liu, C., Naji, A., Yang, B., Chong, A. C. N., Cohen, D. E., … Lo, J. C. (2023). A beta cell subset with enhanced insulin secretion and glucose metabolism is reduced in type 2 diabetes. *Nature Cell Biology*, *25*(4), 565–578. https://doi.org/10.1038/s41556-023-01103-1

Rydén, A., & Faresjö, M. (2013). Altered immune profile from pre-diabetes to manifestation of type 1 diabetes. *Diabetes Research and Clinical Practice*, *100*(1), 74–84. https://doi.org/10.1016/j.diabres.2013.01.014

Salehi, M., Prigeon, R. L., & D'Alessio, D. A. (2011). Gastric bypass surgery enhances glucagon-like peptide 1-stimulated postprandial insulin secretion in humans. *Diabetes*, *60*(9), 2308–2314. https://doi.org/10.2337/db11-0203

Salpeter, S. R., Buckley, N. S., Kahn, J. A., & Salpeter, E. E. (2008). Meta-analysis: Metformin treatment in persons at risk for diabetes mellitus. *The American Journal of Medicine*, *121*(2), 149-157.e2. https://doi.org/10.1016/j.amjmed.2007.09.016

Sanchez Caballero, L., Gorgogietas, V., Arroyo, M. N., & Igoillo-Esteve, M. (2021). Molecular mechanisms of β-cell dysfunction and death in monogenic forms of diabetes. *International Review of Cell and Molecular Biology*, *359*, 139–256. https://doi.org/10.1016/bs.ircmb.2021.02.005

Sánchez-Ceinos, J., Guzmán-Ruiz, R., Rangel-Zúñiga, O. A., López-Alcalá, J., Moreno-Caño, E., Del Río-Moreno, M., Romero-Cabrera, J. L., Pérez-Martínez, P., Maymo-Masip, E., Vendrell, J., Fernández-Veledo, S., Fernández-Real, J. M., Laurencikiene, J., Rydén, M., Membrives, A., Luque, R. M., López-Miranda, J., & Malagón, M. M. (2021). Impaired mRNA splicing and proteostasis in preadipocytes in obesity-related metabolic disease. *ELife*, *10*, e65996. https://doi.org/10.7554/eLife.65996

Sánchez-Solana, B., Laborda, J., & Baladrón, V. (2012). Mouse resistin modulates adipogenesis and glucose uptake in 3T3-L1 preadipocytes through the ROR1 receptor. *Molecular Endocrinology (Baltimore, Md.)*, *26*(1), 110–127. https://doi.org/10.1210/me.2011-1027

Sang, L., Dick, I. E., & Yue, D. T. (2016). Protein kinase A modulation of CaV1.4 calcium channels. *Nature Communications*, *7*, 12239. https://doi.org/10.1038/ncomms12239

Saraste, A., & Pulkki, K. (2000). Morphologic and biochemical hallmarks of apoptosis. *Cardiovascular Research*, *45*(3), 528–537. https://doi.org/10.1016/s0008-6363(99)00384-3

Sarvaiya, P. J., Guo, D., Ulasov, I. V., Gabikian, P., & Lesniak, M. S. (2013). Chemokines in tumor progression and metastasis. *Oncotarget*, *4*(12), 2171–2185. https://doi.org/10.18632/oncotarget.1426

Sassmann, A., Gier, B., Gröne, H.-J., Drews, G., Offermanns, S., & Wettschureck, N. (2010). The Gq/G11-mediated signaling pathway is critical for autocrine potentiation of insulin secretion in mice. *The Journal of Clinical Investigation*, *120*(6), 2184–2193. https://doi.org/10.1172/JCI41541

Sayyed, S. G., Ryu, M., Kulkarni, O. P., Schmid, H., Lichtnekert, J., Grüner, S., Green, L., Mattei, P., Hartmann, G., & Anders, H.-J. (2011). An orally active chemokine receptor CCR2 antagonist prevents glomerulosclerosis and renal failure in type 2 diabetes. *Kidney International*, *80*(1), 68–78. https://doi.org/10.1038/ki.2011.102

Scarim, A. L., Arnush, M., Hill, J. R., Marshall, C. A., Baldwin, A., McDaniel, M. L., & Corbett, J. A. (1997). Evidence for the presence of type I IL-1 receptors on beta-cells of islets of Langerhans. *Biochimica Et Biophysica Acta*, *1361*(3), 313–320. https://doi.org/10.1016/s0925-4439(97)00039-2

Schauer, P. R., Kashyap, S. R., Wolski, K., Brethauer, S. A., Kirwan, J. P., Pothier, C. E., Thomas, S., Abood, B., Nissen, S. E., & Bhatt, D. L. (2012). Bariatric surgery versus intensive medical therapy in obese patients with diabetes. *The New England Journal of Medicine*, *366*(17), 1567–1576. https://doi.org/10.1056/NEJMoa1200225

Schecter, A. D., Calderon, T. M., Berman, A. B., McManus, C. M., Fallon, J. T., Rossikhina, M., Zhao, W., Christ, G., Berman, J. W., & Taubman, M. B. (2000). Human vascular smooth muscle cells possess functional CCR5. *The Journal of Biological Chemistry*, *275*(8), 5466–5471. https://doi.org/10.1074/jbc.275.8.5466

Scherer, P. E., Williams, S., Fogliano, M., Baldini, G., & Lodish, H. F. (1995). A novel serum protein similar to C1q, produced exclusively in adipocytes. *The Journal of Biological Chemistry*, *270*(45), 26746–26749. https://doi.org/10.1074/jbc.270.45.26746

Schmidt, F. M., Weschenfelder, J., Sander, C., Minkwitz, J., Thormann, J., Chittka, T., Mergl, R., Kirkby, K. C., Faßhauer, M., Stumvoll, M., Holdt, L. M., Teupser, D., Hegerl, U., & Himmerich, H. (2015). Inflammatory Cytokines in General and Central Obesity and Modulating Effects of Physical Activity. *PLoS ONE*, *10*(3), e0121971. https://doi.org/10.1371/journal.pone.0121971

Scholtz, S., Miras, A. D., Chhina, N., Prechtl, C. G., Sleeth, M. L., Daud, N. M., Ismail, N. A., Durighel, G., Ahmed, A. R., Olbers, T., Vincent, R. P., Alaghband-Zadeh, J., Ghatei, M. A., Waldman, A. D., Frost, G. S., Bell, J. D., le Roux, C. W., & Goldstone, A. P. (2014). Obese patients after gastric bypass surgery have lower brain-hedonic responses to food than after gastric banding. *Gut*, *63*(6), 891–902. https://doi.org/10.1136/gutjnl-2013-305008

Schwartz, M. W., Woods, S. C., Porte, D., Seeley, R. J., & Baskin, D. G. (2000). Central nervous system control of food intake. *Nature*, *404*(6778), Article 6778. https://doi.org/10.1038/35007534

Scrocchi, L. A., Brown, T. J., MaClusky, N., Brubaker, P. L., Auerbach, A. B., Joyner, A. L., & Drucker, D. J. (1996). Glucose intolerance but normal satiety in mice with a null mutation in the glucagon-like peptide 1 receptor gene. *Nature Medicine*, *2*(11), 1254–1258. https://doi.org/10.1038/nm1196-1254

Secher, A., Jelsing, J., Baquero, A. F., Hecksher-Sørensen, J., Cowley, M. A., Dalbøge, L. S., Hansen, G., Grove, K. L., Pyke, C., Raun, K., Schäffer, L., Tang-Christensen, M., Verma, S., Witgen, B. M., Vrang, N., & Bjerre Knudsen, L. (2014). The arcuate nucleus mediates GLP-1 receptor agonist liraglutide-dependent weight loss. *The Journal of Clinical Investigation*, *124*(10), 4473–4488. https://doi.org/10.1172/JCI75276

Segeritz, C.-P., & Vallier, L. (2017). Cell Culture. *Basic Science Methods for Clinical Researchers*, 151–172. https://doi.org/10.1016/B978-0-12-803077-6.00009-6

Sell, H., Laurencikiene, J., Taube, A., Eckardt, K., Cramer, A., Horrighs, A., Arner, P., & Eckel, J. (2009). Chemerin is a novel adipocyte-derived factor inducing insulin resistance in primary human skeletal muscle cells. *Diabetes*, *58*(12), 2731–2740. https://doi.org/10.2337/db09-0277

Seufert, J., Kieffer, T. J., Leech, C. A., Holz, G. G., Moritz, W., Ricordi, C., & Habener, J. F. (1999). Leptin suppression of insulin secretion and gene expression in human pancreatic islets: Implications for the development of adipogenic diabetes mellitus. *The Journal of Clinical Endocrinology and Metabolism*, *84*(2), 670–676. https://doi.org/10.1210/jcem.84.2.5460

Sharma, A., Pillai, M. R. A., Gautam, S., & Hajare, S. N. (2014). MYCOTOXINS | Immunological Techniques for Detection and Analysis. In C. A. Batt & M. L. Tortorello (Eds.), *Encyclopedia of Food Microbiology (Second Edition)* (pp. 869–879). Academic Press. https://doi.org/10.1016/B978-0-12-384730-0.00233-0

Sharma, R. B., O'Donnell, A. C., Stamateris, R. E., Ha, B., McCloskey, K. M., Reynolds, P. R., Arvan, P., & Alonso, L. C. (2015). Insulin demand regulates β cell number via the unfolded protein response. *The Journal of Clinical Investigation*, *125*(10), 3831–3846. https://doi.org/10.1172/JCI79264

Sharp, G. W., Wiedenkeller, D. E., Kaelin, D., Siegel, E. G., & Wollheim, C. B. (1980). Stimulation of adenylate cyclase by Ca2+ and calmodulin in rat islets of langerhans: Explanation for the glucose-induced increase in cyclic AMP levels. *Diabetes*, *29*(1), 74–77. https://doi.org/10.2337/diab.29.1.74

Sherwani, S. I., Khan, H. A., Ekhzaimy, A., Masood, A., & Sakharkar, M. K. (2016). Significance of HbA1c Test in Diagnosis and Prognosis of Diabetic Patients. *Biomarker Insights*, *11*, 95–104. https://doi.org/10.4137/BMI.S38440

Shi, Y.-C., Lau, J., Lin, Z., Zhang, H., Zhai, L., Sperk, G., Heilbronn, R., Mietzsch, M., Weger, S., Huang, X.-F., Enriquez, R. F., Baldock, P. A., Zhang, L., Sainsbury, A., Herzog, H., & Lin, S. (2013). Arcuate NPY controls sympathetic output and BAT function via a relay of tyrosine hydroxylase neurons in the PVN. *Cell Metabolism*, *17*(2), 236–248. https://doi.org/10.1016/j.cmet.2013.01.006

Shibasaki, T., Takahashi, H., Miki, T., Sunaga, Y., Matsumura, K., Yamanaka, M., Zhang, C., Tamamoto, A., Satoh, T., Miyazaki, J.-I., & Seino, S. (2007). Essential role of Epac2/Rap1 signaling in

regulation of insulin granule dynamics by cAMP. *Proceedings of the National Academy of Sciences of the United States of America*, *104*(49), 19333–19338. https://doi.org/10.1073/pnas.0707054104

Shigeto, M., Ramracheya, R., Tarasov, A. I., Cha, C. Y., Chibalina, M. V., Hastoy, B., Philippaert, K., Reinbothe, T., Rorsman, N., Salehi, A., Sones, W. R., Vergari, E., Weston, C., Gorelik, J., Katsura, M., Nikolaev, V. O., Vennekens, R., Zaccolo, M., Galione, A., … Rorsman, P. (2015). GLP-1 stimulates insulin secretion by PKC-dependent TRPM4 and TRPM5 activation. *The Journal of Clinical Investigation*, *125*(12), 4714–4728. https://doi.org/10.1172/JCI81975

Shin, J., Nunomiya, A., Gonda, K., & Nagatomi, R. (2023). Specification of skeletal muscle fiber-type is determined by the calcineurin/NFATc1 signaling pathway during muscle regeneration. *Biochemical and Biophysical Research Communications*, *659*, 20–28. https://doi.org/10.1016/j.bbrc.2023.03.032

Shuai, H., Xu, Y., Ahooghalandari, P., & Tengholm, A. (2021). Glucose-induced cAMP elevation in β-cells involves amplification of constitutive and glucagon-activated GLP-1 receptor signalling. *Acta Physiologica (Oxford, England)*, *231*(4), e13611. https://doi.org/10.1111/apha.13611

Siegel, E. G., Schulze, A., Schmidt, W. E., & Creutzfeldt, W. (1992). Comparison of the effect of GIP and GLP-1 (7-36amide) on insulin release from rat pancreatic islets. *European Journal of Clinical Investigation*, *22*(3), 154–157. https://doi.org/10.1111/j.1365-2362.1992.tb01820.x

Silva, K. R., Liechocki, S., Carneiro, J. R., Claudio-da-Silva, C., Maya-Monteiro, C. M., Borojevic, R., & Baptista, L. S. (2015). Stromal-vascular fraction content and adipose stem cell behavior are altered in morbid obese and post bariatric surgery ex-obese women. *Stem Cell Research & Therapy*, *6*(1), 72. https://doi.org/10.1186/s13287-015-0029-x

Silvestre, R. A., Egido, E. M., Hernández, R., & Marco, J. (2008). Kisspeptin-13 inhibits insulin secretion without affecting glucagon or somatostatin release: Study in the perfused rat pancreas. *The Journal of Endocrinology*, *196*(2), 283–290. https://doi.org/10.1677/JOE-07-0454

Sindhu, S., Kochumon, S., Shenouda, S., Wilson, A., Al-Mulla, F., & Ahmad, R. (2019). The Cooperative Induction of CCL4 in Human Monocytic Cells by TNF-α and Palmitate Requires MyD88 and Involves MAPK/NF-κB Signaling Pathways. *International Journal of Molecular Sciences*, *20*(18), E4658. https://doi.org/10.3390/ijms20184658

Singh, P., Peterson, T. E., Sert-Kuniyoshi, F. H., Glenn, J. A., Davison, D. E., Romero-Corral, A., Pusalavidyasagar, S., Jensen, M. D., & Somers, V. K. (2012). Leptin signaling in adipose tissue: Role in lipid accumulation and weight gain. *Circulation Research*, *111*(5), 599–603. https://doi.org/10.1161/CIRCRESAHA.112.273656

Singh, S., Loke, Y. K., & Furberg, C. D. (2007). Thiazolidinediones and heart failure: A teleo-analysis. *Diabetes Care*, *30*(8), 2148–2153. https://doi.org/10.2337/dc07-0141

Smith, P. A., Sakura, H., Coles, B., Gummerson, N., Proks, P., & Ashcroft, F. M. (1997). Electrogenic arginine transport mediates stimulus-secretion coupling in mouse pancreatic beta-cells. *The Journal of Physiology*, *499*(Pt 3), 625–635.

Soga, T., Ohishi, T., Matsui, T., Saito, T., Matsumoto, M., Takasaki, J., Matsumoto, S.-I., Kamohara, M., Hiyama, H., Yoshida, S., Momose, K., Ueda, Y., Matsushime, H., Kobori, M., & Furuichi, K. (2005). Lysophosphatidylcholine enhances glucose-dependent insulin secretion via an orphan G-protein-coupled receptor. *Biochemical and Biophysical Research Communications*, *326*(4), 744–751. https://doi.org/10.1016/j.bbrc.2004.11.120

Song, T., & Kuang, S. (2019). Adipocyte dedifferentiation in health and diseases. *Clinical Science (London, England : 1979)*, *133*(20), 2107–2119. https://doi.org/10.1042/CS20190128

Sörhede Winzell, M., Magnusson, C., & Ahrén, B. (2005). The apj receptor is expressed in pancreatic islets and its ligand, apelin, inhibits insulin secretion in mice. *Regulatory Peptides*, *131*(1–3), 12–17. https://doi.org/10.1016/j.regpep.2005.05.004

Spijker, H. S., Song, H., Ellenbroek, J. H., Roefs, M. M., Engelse, M. A., Bos, E., Koster, A. J., Rabelink, T. J., Hansen, B. C., Clark, A., Carlotti, F., & de Koning, E. J. P. (2015). Loss of β-Cell Identity

Occurs in Type 2 Diabetes and Is Associated With Islet Amyloid Deposits. *Diabetes*, *64*(8), 2928–2938. https://doi.org/10.2337/db14-1752

Sriram, K., & Insel, P. A. (2018). G Protein-Coupled Receptors as Targets for Approved Drugs: How Many Targets and How Many Drugs? *Molecular Pharmacology*, *93*(4), 251–258. https://doi.org/10.1124/mol.117.111062

Stanik, J., Gasperikova, D., Paskova, M., Barak, L., Javorkova, J., Jancova, E., Ciljakova, M., Hlava, P., Michalek, J., Flanagan, S. E., Pearson, E., Hattersley, A. T., Ellard, S., & Klimes, I. (2007). Prevalence of permanent neonatal diabetes in Slovakia and successful replacement of insulin with sulfonylurea therapy in KCNJ11 and ABCC8 mutation carriers. *The Journal of Clinical Endocrinology and Metabolism*, *92*(4), 1276–1282. https://doi.org/10.1210/jc.2006-2490

Stanley, T. L., Chen, C. Y., Branch, K. L., Makimura, H., & Grinspoon, S. K. (2011). Effects of a growth hormone-releasing hormone analog on endogenous GH pulsatility and insulin sensitivity in healthy men. *The Journal of Clinical Endocrinology and Metabolism*, *96*(1), 150–158. https://doi.org/10.1210/jc.2010-1587

Stanley, T. L., Falutz, J., Mamputu, J.-C., Soulban, G., Potvin, D., & Grinspoon, S. K. (2011). Effects of tesamorelin on inflammatory markers in HIV patients with excess abdominal fat: Relationship with visceral adipose reduction. *AIDS (London, England)*, *25*(10), 1281–1288. https://doi.org/10.1097/QAD.0b013e328347f3f1

Stanley, T. L., Falutz, J., Marsolais, C., Morin, J., Soulban, G., Mamputu, J.-C., Assaad, H., Turner, R., & Grinspoon, S. K. (2012). Reduction in Visceral Adiposity Is Associated With an Improved Metabolic Profile in HIV-Infected Patients Receiving Tesamorelin. *Clinical Infectious Diseases: An Official Publication of the Infectious Diseases Society of America*, *54*(11), 1642–1651. https://doi.org/10.1093/cid/cis251

Stanley, T. L., Feldpausch, M. N., Oh, J., Branch, K. L., Lee, H., Torriani, M., & Grinspoon, S. K. (2014). Effect of tesamorelin on visceral fat and liver fat in HIV-infected patients with abdominal fat

accumulation: A randomized clinical trial. *JAMA*, *312*(4), 380–389. https://doi.org/10.1001/jama.2014.8334

Stelmanska, E., Sledzinski, T., Turyn, J., Presler, M., Korczynska, J., & Swierczynski, J. (2013). Chemerin gene expression is regulated by food restriction and food restriction-refeeding in rat adipose tissue but not in liver. *Regulatory Peptides*, *181*, 22–29. https://doi.org/10.1016/j.regpep.2012.12.001

Stene, L. C., Ulriksen, J., Magnus, P., & Joner, G. (2000). Use of cod liver oil during pregnancy associated with lower risk of Type I diabetes in the offspring. *Diabetologia*, *43*(9), 1093–1098. https://doi.org/10.1007/s001250051499

Stephens, L. A., Thomas, H. E., Ming, L., Grell, M., Darwiche, R., Volodin, L., & Kay, T. W. (1999). Tumor necrosis factor-alpha-activated cell death pathways in NIT-1 insulinoma cells and primary pancreatic beta cells. *Endocrinology*, *140*(7), 3219–3227. https://doi.org/10.1210/endo.140.7.6873

Stewart, F. M., Freeman, D. J., Ramsay, J. E., Greer, I. A., Caslake, M., & Ferrell, W. R. (2007). Longitudinal Assessment of Maternal Endothelial Function and Markers of Inflammation and Placental Function throughout Pregnancy in Lean and Obese Mothers. *The Journal of Clinical Endocrinology & Metabolism*, *92*(3), 969–975. https://doi.org/10.1210/jc.2006-2083

Stone, R. L., & Bernlohr, D. A. (1990). The molecular basis for inhibition of adipose conversion of murine 3T3-L1 cells by retinoic acid. *Differentiation; Research in Biological Diversity*, *45*(2), 119–127. https://doi.org/10.1111/j.1432-0436.1990.tb00465.x

Störmann, S., & Schopohl, J. (2020). Drug treatment strategies for secondary diabetes in patients with acromegaly. *Expert Opinion on Pharmacotherapy*, *21*(15), 1883–1895. https://doi.org/10.1080/14656566.2020.1789098

Sturis, J., Kurland, I. J., Byrne, M. M., Mosekilde, E., Froguel, P., Pilkis, S. J., Bell, G. I., & Polonsky, K. S. (1994). Compensation in pancreatic beta-cell function in subjects with glucokinase mutations. *Diabetes*, *43*(5), 718–723. https://doi.org/10.2337/diab.43.5.718

Suganami, T., Nishida, J., & Ogawa, Y. (2005). A paracrine loop between adipocytes and macrophages aggravates inflammatory changes: Role of free fatty acids and tumor necrosis factor alpha. *Arteriosclerosis, Thrombosis, and Vascular Biology*, *25*(10), 2062–2068. https://doi.org/10.1161/01.ATV.0000183883.72263.13

Suganami, T., Tanimoto-Koyama, K., Nishida, J., Itoh, M., Yuan, X., Mizuarai, S., Kotani, H., Yamaoka, S., Miyake, K., Aoe, S., Kamei, Y., & Ogawa, Y. (2007). Role of the Toll-like receptor 4/NF-kappaB pathway in saturated fatty acid-induced inflammatory changes in the interaction between adipocytes and macrophages. *Arteriosclerosis, Thrombosis, and Vascular Biology*, *27*(1), 84–91. https://doi.org/10.1161/01.ATV.0000251608.09329.9a

Sun, Z., Liu, J., Zeng, X., Huangfu, J., Jiang, Y., Wang, M., & Chen, F. (2011). Protective actions of microalgae against endogenous and exogenous advanced glycation endproducts (AGEs) in human retinal pigment epithelial cells. *Food & Function*, *2*(5), 251–258. https://doi.org/10.1039/C1FO10021A

Sutton, A. K., Myers, M. G., & Olson, D. P. (2016). The Role of PVH Circuits in Leptin Action and Energy Balance. *Annual Review of Physiology*, *78*, 207–221. https://doi.org/10.1146/annurev-physiol-021115-105347

Suzuki, Y., Rahman, M., & Mitsuya, H. (2001). Diverse transcriptional response of CD4+ T cells to stromal cell-derived factor SDF-1: Cell survival promotion and priming effects of SDF-1 on CD4+ T cells. *Journal of Immunology (Baltimore, Md.: 1950)*, *167*(6), 3064–3073. https://doi.org/10.4049/jimmunol.167.6.3064

Svoboda, K. K. H., & Reenstra, W. R. (2002). Approaches To Studying Cellular Signaling: A Primer For Morphologists. *The Anatomical Record*, *269*(2), 123. https://doi.org/10.1002/ar.10074

Swenne, I., Hill, D. J., Strain, A. J., & Milner, R. D. (1987). Effects of human placental lactogen and growth hormone on the production of insulin and somatomedin C/insulin-like growth factor I by human fetal pancreas in tissue culture. *The Journal of Endocrinology*, *113*(2), 297–303. https://doi.org/10.1677/joe.0.1130297

Szabat, M., Page, M. M., Panzhinskiy, E., Skovsø, S., Mojibian, M., Fernandez-Tajes, J., Bruin, J. E., Bround, M. J., Lee, J. T. C., Xu, E. E., Taghizadeh, F., O'Dwyer, S., van de Bunt, M., Moon, K.-M., Sinha, S., Han, J., Fan, Y., Lynn, F. C., Trucco, M., … Johnson, J. D. (2016). Reduced Insulin Production Relieves Endoplasmic Reticulum Stress and Induces β Cell Proliferation. *Cell Metabolism*, *23*(1), 179–193. https://doi.org/10.1016/j.cmet.2015.10.016

Szaszák, M., Christian, F., Rosenthal, W., & Klussmann, E. (2008). Compartmentalized cAMP signalling in regulated exocytic processes in non-neuronal cells. *Cellular Signalling*, *20*(4), 590–601. https://doi.org/10.1016/j.cellsig.2007.10.020

Taberner, P., Flanagan, S. E., Mackay, D. J., Ellard, S., Taverna, M. J., & Ferraro, M. (2016). Clinical and genetic features of Argentinian children with diabetes-onset before 12months of age: Successful transfer from insulin to oral sulfonylurea. *Diabetes Research and Clinical Practice*, *117*, 104–110. https://doi.org/10.1016/j.diabres.2016.04.005

Takahashi, M., Okimura, Y., Iguchi, G., Nishizawa, H., Yamamoto, M., Suda, K., Kitazawa, R., Fujimoto, W., Takahashi, K., Zolotaryov, F. N., Hong, K. S., Kiyonari, H., Abe, T., Kaji, H., Kitazawa, S., Kasuga, M., Chihara, K., & Takahashi, Y. (2011). Chemerin regulates β-cell function in mice. *Scientific Reports*, *1*(1), Article 1. https://doi.org/10.1038/srep00123

Takahashi, M., Takahashi, Y., Takahashi, K., Zolotaryov, F. N., Hong, K. S., Kitazawa, R., Iida, K., Okimura, Y., Kaji, H., Kitazawa, S., Kasuga, M., & Chihara, K. (2008). Chemerin enhances insulin signaling and potentiates insulin-stimulated glucose uptake in 3T3-L1 adipocytes. *FEBS Letters*, *582*(5), 573–578. https://doi.org/10.1016/j.febslet.2008.01.023

Talchai, C., Xuan, S., Lin, H. V., Sussel, L., & Accili, D. (2012). Pancreatic β cell dedifferentiation as a mechanism of diabetic β cell failure. *Cell*, *150*(6), 1223–1234. https://doi.org/10.1016/j.cell.2012.07.029

Tan, P., Pepin, É., & Lavoie, J. L. (2018). Mouse Adipose Tissue Collection and Processing for RNA Analysis. *Journal of Visualized Experiments: JoVE*, *131*, 57026. https://doi.org/10.3791/57026

Tanabe, K., Amo-Shiinoki, K., Hatanaka, M., & Tanizawa, Y. (2017). Interorgan Crosstalk Contributing to β-Cell Dysfunction. *Journal of Diabetes Research*, *2017*, 3605178. https://doi.org/10.1155/2017/3605178

Tang, X., Uhl, S., Zhang, T., Xue, D., Li, B., Vandana, J. J., Acklin, J. A., Bonnycastle, L. L., Narisu, N., Erdos, M. R., Bram, Y., Chandar, V., Chong, A. C. N., Lacko, L. A., Min, Z., Lim, J. K., Borczuk, A. C., Xiang, J., Naji, A., … Chen, S. (2021). SARS-CoV-2 infection induces beta cell transdifferentiation. *Cell Metabolism*, *33*(8), 1577-1591.e7. https://doi.org/10.1016/j.cmet.2021.05.015

Tanizawa, Y., Okuya, S., Ishihara, H., Asano, T., Yada, T., & Oka, Y. (1997). Direct Stimulation of Basal Insulin Secretion by Physiological Concentrations of Leptin in Pancreatic β Cells. *Endocrinology*, *138*(10), 4513–4516. https://doi.org/10.1210/endo.138.10.5576

Tao, X., Zhang, Z., Yang, Z., & Rao, B. (2022). The effects of taurine supplementation on diabetes mellitus in humans: A systematic review and meta-analysis. *Food Chemistry: Molecular Sciences*, *4*, 100106. https://doi.org/10.1016/j.fochms.2022.100106

Tarkowski, A., Bjersing, J., Shestakov, A., & Bokarewa, M. I. (2010). Resistin competes with lipopolysaccharide for binding to toll-like receptor 4. *Journal of Cellular and Molecular Medicine*, *14*(6B), 1419–1431. https://doi.org/10.1111/j.1582-4934.2009.00899.x

Tartaglia, L. A., Dembski, M., Weng, X., Deng, N., Culpepper, J., Devos, R., Richards, G. J., Campfield, L. A., Clark, F. T., Deeds, J., Muir, C., Sanker, S., Moriarty, A., Moore, K. J., Smutko, J. S., Mays, G. G., Wool, E. A., Monroe, C. A., & Tepper, R. I. (1995). Identification and expression cloning of a leptin receptor, OB-R. *Cell*, *83*(7), 1263–1271. https://doi.org/10.1016/0092-8674(95)90151-5

Taylor, R. (2019). Calorie restriction for long-term remission of type 2 diabetes. *Clinical Medicine*, *19*(1), 37–42. https://doi.org/10.7861/clinmedicine.19-1-37

Teta, M., Rankin, M. M., Long, S. Y., Stein, G. M., & Kushner, J. A. (2007). Growth and regeneration of adult beta cells does not involve specialized progenitors. *Developmental Cell*, *12*(5), 817–826. https://doi.org/10.1016/j.devcel.2007.04.011

Thomas, N. J., Lynam, A. L., Hill, A. V., Weedon, M. N., Shields, B. M., Oram, R. A., McDonald, T. J., Hattersley, A. T., & Jones, A. G. (2019). Type 1 diabetes defined by severe insulin deficiency occurs after 30 years of age and is commonly treated as type 2 diabetes. *Diabetologia*, *62*(7), 1167–1172. https://doi.org/10.1007/s00125-019-4863-8

Thorsen, S. U., Eising, S., Mortensen, H. B., Skogstrand, K., Pociot, F., Johannesen, J., Svensson, J., & Registry, the D. C. D. (2014). Systemic Levels of CCL2, CCL3, CCL4 and CXCL8 Differ According to Age, Time Period and Season among Children Newly Diagnosed with type 1 Diabetes and their Healthy Siblings. *Scandinavian Journal of Immunology*, *80*(6), 452–461. https://doi.org/10.1111/sji.12240

Tian, G., Sandler, S., Gylfe, E., & Tengholm, A. (2011). Glucose- and hormone-induced cAMP oscillations in α- and β-cells within intact pancreatic islets. *Diabetes*, *60*(5), 1535–1543. https://doi.org/10.2337/db10-1087

Tian, Q., Stepaniants, S. B., Mao, M., Weng, L., Feetham, M. C., Doyle, M. J., Yi, E. C., Dai, H., Thorsson, V., Eng, J., Goodlett, D., Berger, J. P., Gunter, B., Linseley, P. S., Stoughton, R. B., Aebersold, R., Collins, S. J., Hanlon, W. A., & Hood, L. E. (2004). Integrated Genomic and Proteomic Analyses of Gene Expression in Mammalian Cells *. *Molecular & Cellular Proteomics*, *3*(10), 960–969. https://doi.org/10.1074/mcp.M400055-MCP200

Ticchioni, M., Essafi, M., Jeandel, P. Y., Davi, F., Cassuto, J. P., Deckert, M., & Bernard, A. (2007). Homeostatic chemokines increase survival of B-chronic lymphocytic leukemia cells through inactivation of transcription factor FOXO3a. *Oncogene*, *26*(50), 7081–7091. https://doi.org/10.1038/sj.onc.1210519

Tkachuk, V. A., Bochkov, V. N., Philippova, M. P., Stambolsky, D. V., Kuzmenko, E. S., Sidorova, M. V., Molokoedov, A. S., Spirov, V. G., & Resink, T. J. (1998). Identification of an atypical

lipoprotein-binding protein from human aortic smooth muscle as T-cadherin. *FEBS Letters*, *421*(3), 208–212. https://doi.org/10.1016/s0014-5793(97)01562-7

Toda, Y., Tsukada, J., Misago, M., Kominato, Y., Auron, P. E., & Tanaka, Y. (2002). Autocrine induction of the human pro-IL-1beta gene promoter by IL-1beta in monocytes. *Journal of Immunology (Baltimore, Md.: 1950)*, *168*(4), 1984–1991. https://doi.org/10.4049/jimmunol.168.4.1984

Tomita, T. (2016). Apoptosis in pancreatic β-islet cells in Type 2 diabetes. *Bosnian Journal of Basic Medical Sciences*, *16*(3), 162–179. https://doi.org/10.17305/bjbms.2016.919

Tontonoz, P., Hu, E., Graves, R. A., Budavari, A. I., & Spiegelman, B. M. (1994). mPPAR gamma 2: Tissue-specific regulator of an adipocyte enhancer. *Genes & Development*, *8*(10), 1224–1234. https://doi.org/10.1101/gad.8.10.1224

Tontonoz, P., Hu, E., & Spiegelman, B. M. (1994). Stimulation of adipogenesis in fibroblasts by PPAR gamma 2, a lipid-activated transcription factor. *Cell*, *79*(7), 1147–1156. https://doi.org/10.1016/0092-8674(94)90006-x

Torgerson, J. S., Hauptman, J., Boldrin, M. N., & Sjöström, L. (2004). XENical in the prevention of diabetes in obese subjects (XENDOS) study: A randomized study of orlistat as an adjunct to lifestyle changes for the prevention of type 2 diabetes in obese patients. *Diabetes Care*, *27*(1), 155–161. https://doi.org/10.2337/diacare.27.1.155

Trivett, C., Lees, Z. J., & Freeman, D. J. (2021). Adipose tissue function in healthy pregnancy, gestational diabetes mellitus and pre-eclampsia. *European Journal of Clinical Nutrition*, *75*(12), Article 12. https://doi.org/10.1038/s41430-021-00948-9

Trujillo, M. E., & Scherer, P. E. (2005). Adiponectin – journey from an adipocyte secretory protein to biomarker of the metabolic syndrome. *Journal of Internal Medicine*, *257*(2), 167–175. https://doi.org/10.1111/j.1365-2796.2004.01426.x

Tsai, S.-C., Lin, S.-J., Lin, C.-J., Chou, Y.-C., Lin, J.-H., Yeh, T.-H., Chen, M.-R., Huang, L.-M., Lu, M.-Y., Huang, Y.-C., Chen, H.-Y., & Tsai, C.-H. (2013). Autocrine CCL3 and CCL4 Induced by the

Oncoprotein LMP1 Promote Epstein-Barr Virus-Triggered B Cell Proliferation. *Journal of Virology*, *87*(16), 9041–9052. https://doi.org/10.1128/jvi.00541-13

Tsiloulis, T., & Watt, M. J. (2015). Exercise and the Regulation of Adipose Tissue Metabolism. *Progress in Molecular Biology and Translational Science*, *135*, 175–201. https://doi.org/10.1016/bs.pmbts.2015.06.016

Unger, R. H., Aguilar-Parada, E., Müller, W. A., & Eisentraut, A. M. (1970). Studies of pancreatic alpha cell function in normal and diabetic subjects. *The Journal of Clinical Investigation*, *49*(4), 837–848. https://doi.org/10.1172/JCI106297

Uotani, S., Bjørbaek, C., Tornøe, J., & Flier, J. S. (1999). Functional properties of leptin receptor isoforms: Internalization and degradation of leptin and ligand-induced receptor downregulation. *Diabetes*, *48*(2), 279–286. https://doi.org/10.2337/diabetes.48.2.279

Upadhyaya, C., Jiao, X., Ashton, A., Patel, K., Kossenkov, A. V., & Pestell, R. G. (2020). The G Protein Coupled Receptor CCR5 in Cancer. *Advances in Cancer Research*, *145*, 29–47. https://doi.org/10.1016/bs.acr.2019.11.001

Urakami, T. (2019). Maturity-onset diabetes of the young (MODY): Current perspectives on diagnosis and treatment. *Diabetes, Metabolic Syndrome and Obesity: Targets and Therapy*, *12*, 1047–1056. https://doi.org/10.2147/DMSO.S179793

Valiunas, V., Polosina, Y., Miller, H., Potapova, I., Valiuniene, L., Doronin, S., Mathias, R., Robinson, R., Rosen, M., Cohen, I., & Brink, P. (2005). Connexin-specific cell-to-cell transfer of short interfering RNA by gap junctions. *The Journal of Physiology*, *568*(Pt 2), 459–468. https://doi.org/10.1113/jphysiol.2005.090985

van Loon, L. J. C., Kruijshoop, M., Menheere, P. P. C. A., Wagenmakers, A. J. M., Saris, W. H. M., & Keizer, H. A. (2003). Amino acid ingestion strongly enhances insulin secretion in patients with long-term type 2 diabetes. *Diabetes Care*, *26*(3), 625–630. https://doi.org/10.2337/diacare.26.3.625

Van Schravendijk, C. F. H., Heylen, L., Van den Brande, J. L., & Pipeleers, D. G. (1990). Direct effect of insulin and insulin-like growth factor-I on the secretory activity of rat pancreatic beta cells. *Diabetologia*, *33*(11), 649–653. https://doi.org/10.1007/BF00400565

Vasavada, R. C., Garcia-Ocaña, A., Zawalich, W. S., Sorenson, R. L., Dann, P., Syed, M., Ogren, L., Talamantes, F., & Stewart, A. F. (2000). Targeted expression of placental lactogen in the beta cells of transgenic mice results in beta cell proliferation, islet mass augmentation, and hypoglycemia. *The Journal of Biological Chemistry*, *275*(20), 15399–15406. https://doi.org/10.1074/jbc.275.20.15399

Veldhuis, J. D., Iranmanesh, A., Ho, K. K., Waters, M. J., Johnson, M. L., & Lizarralde, G. (1991). Dual defects in pulsatile growth hormone secretion and clearance subserve the hyposomatotropism of obesity in man. *The Journal of Clinical Endocrinology and Metabolism*, *72*(1), 51–59. https://doi.org/10.1210/jcem-72-1-51

Velloso, L. A., Carneiro, E. M., Crepaldi, S. C., Boschero, A. C., & Saad, M. J. (1995). Glucose- and insulin-induced phosphorylation of the insulin receptor and its primary substrates IRS-1 and IRS-2 in rat pancreatic islets. *FEBS Letters*, *377*(3), 353–357. https://doi.org/10.1016/0014-5793(95)01370-9

Verspohl, E. J., & Ammon, H. P. (1980). Evidence for presence of insulin receptors in rat islets of Langerhans. *The Journal of Clinical Investigation*, *65*(5), 1230–1237. https://doi.org/10.1172/JCI109778

Verspohl, E. J., & Herrmann, K. (1996). Involvement of G proteins in the effect of carbachol and cholecystokinin in rat pancreatic islets. *The American Journal of Physiology*, *271*(1 Pt 1), E65-72. https://doi.org/10.1152/ajpendo.1996.271.1.E65

Vikman, J., & Ahrén, B. (2009). Inhibitory effect of kisspeptins on insulin secretion from isolated mouse islets. *Diabetes, Obesity & Metabolism*, *11 Suppl 4*, 197–201. https://doi.org/10.1111/j.1463-1326.2009.01116.x

Villalpando, S., Cazevieille, C., Fernandez, A., Lamb, N. J., & Hani, E.-H. (2016). Type II PKAs are anchored to mature insulin secretory granules in INS-1 β-cells and required for cAMP-dependent potentiation of exocytosis. *Biochimie*, *125*, 32–41. https://doi.org/10.1016/j.biochi.2016.02.008

Wacker, D., Stevens, R. C., & Roth, B. L. (2017). How Ligands Illuminate GPCR Molecular Pharmacology. *Cell*, *170*(3), 414–427. https://doi.org/10.1016/j.cell.2017.07.009

Wang, J., Hanada, K., Staus, D. P., Makara, M. A., Dahal, G. R., Chen, Q., Ahles, A., Engelhardt, S., & Rockman, H. A. (2017). Gαi is required for carvedilol-induced β1 adrenergic receptor β-arrestin biased signaling. *Nature Communications*, *8*(1), 1706. https://doi.org/10.1038/s41467-017-01855-z

Wang, K., Cui, X., Li, F., Xia, L., Wei, T., Liu, J., Fu, W., Yang, J., Hong, T., & Wei, R. (2023). Glucagon receptor blockage inhibits β-cell dedifferentiation through FoxO1. *American Journal of Physiology. Endocrinology and Metabolism*, *324*(1), E97–E113. https://doi.org/10.1152/ajpendo.00101.2022

Wang, M., Lin, T., Wang, Y., Gao, S., Yang, Z., Hong, X., & Chen, G. (2017). CXCL12 suppresses cisplatin-induced apoptosis through activation of JAK2/STAT3 signaling in human non-small-cell lung cancer cells. *OncoTargets and Therapy*, *10*, 3215–3224. https://doi.org/10.2147/OTT.S133055

Wang, P., Fiaschi-Taesch, N. M., Vasavada, R. C., Scott, D. K., García-Ocaña, A., & Stewart, A. F. (2015). Diabetes mellitus—Advances and challenges in human β-cell proliferation. *Nature Reviews. Endocrinology*, *11*(4), 201–212. https://doi.org/10.1038/nrendo.2015.9

Wang, Y., Rimm, E. B., Stampfer, M. J., Willett, W. C., & Hu, F. B. (2005). Comparison of abdominal adiposity and overall obesity in predicting risk of type 2 diabetes among men. *The American Journal of Clinical Nutrition*, *81*(3), 555–563. https://doi.org/10.1093/ajcn/81.3.555

Warnotte, C., Gilon, P., Nenquin, M., & Henquin, J. C. (1994). Mechanisms of the stimulation of insulin release by saturated fatty acids. A study of palmitate effects in mouse beta-cells. *Diabetes*, *43*(5), 703–711. https://doi.org/10.2337/diab.43.5.703

Warshauer, J. T., Bluestone, J. A., & Anderson, M. S. (2020). New frontiers in the treatment of Type 1 diabetes. *Cell Metabolism*, *31*(1), 46–61. https://doi.org/10.1016/j.cmet.2019.11.017

Washington University School of Medicine. (2013). *Effect of Maraviroc on Metabolic Function in Obese Subjects (Phase I)* (Clinical Trial Registration NCT01133210). clinicaltrials.gov. https://clinicaltrials.gov/study/NCT01133210

Wasserman, D. H., Spalding, J. A., Lacy, D. B., Colburn, C. A., Goldstein, R. E., & Cherrington, A. D. (1989). Glucagon is a primary controller of hepatic glycogenolysis and gluconeogenesis during muscular work. *The American Journal of Physiology*, *257*(1 Pt 1), E108-117. https://doi.org/10.1152/ajpendo.1989.257.1.E108

Watson, M. L., Macrae, K., Marley, A. E., & Hundal, H. S. (2011). Chronic Effects of Palmitate Overload on Nutrient-Induced Insulin Secretion and Autocrine Signalling in Pancreatic MIN6 Beta Cells. *PLOS ONE*, *6*(10), e25975. https://doi.org/10.1371/journal.pone.0025975

Wei, J., Hanna, T., Suda, N., Karsenty, G., & Ducy, P. (2014). Osteocalcin promotes β-cell proliferation during development and adulthood through Gprc6a. *Diabetes*, *63*(3), 1021–1031. https://doi.org/10.2337/db13-0887

Wei, T., Cui, X., Jiang, Y., Wang, K., Wang, D., Li, F., Lin, X., Gu, L., Yang, K., Yang, J., Hong, T., & Wei, R. (2023). Glucagon Acting at the GLP-1 Receptor Contributes to β-Cell Regeneration Induced by Glucagon Receptor Antagonism in Diabetic Mice. *Diabetes*, *72*(5), 599–610. https://doi.org/10.2337/db22-0784

Weir, G. C., Laybutt, D. R., Kaneto, H., Bonner-Weir, S., & Sharma, A. (2001). Beta-cell adaptation and decompensation during the progression of diabetes. *Diabetes*, *50*(suppl_1), S154. https://doi.org/10.2337/diabetes.50.2007.S154

Weisberg, S. P., Hunter, D., Huber, R., Lemieux, J., Slaymaker, S., Vaddi, K., Charo, I., Leibel, R. L., & Ferrante, A. W. (2006). CCR2 modulates inflammatory and metabolic effects of high-fat feeding. *Journal of Clinical Investigation*, *116*(1), 115–124. https://doi.org/10.1172/JCI24335

Weisberg, S. P., McCann, D., Desai, M., Rosenbaum, M., Leibel, R. L., & Ferrante, A. W. (2003). Obesity is associated with macrophage accumulation in adipose tissue. *The Journal of Clinical Investigation*, *112*(12), 1796–1808. https://doi.org/10.1172/JCI19246

Wen, F., Yang, Y., Sun, C., Fang, H., Nie, L., Li, L., Liu, Y., & Yang, Z. (2017). RESISTIN INHIBITS GLUCOSE-STIMULATED INSULIN SECRETION THROUGH MIR-494 BY TARGET ON STXBP5. *Acta Endocrinologica (Bucharest)*, *13*(1), 32–39. https://doi.org/10.4183/aeb.2017.32

Weng, J., Zhou, Z., Guo, L., Zhu, D., Ji, L., Luo, X., Mu, Y., & Jia, W. (2018). Incidence of type 1 diabetes in China, 2010-13: Population based study. *The BMJ*, *360*, j5295. https://doi.org/10.1136/bmj.j5295

Wennerberg, K., & Der, C. J. (2004). Rho-family GTPases: It's not only Rac and Rho (and I like it). *Journal of Cell Science*, *117*(8), 1301–1312. https://doi.org/10.1242/jcs.01118

Werling, M., Olbers, T., Fändriks, L., Bueter, M., Lönroth, H., Stenlöf, K., & le Roux, C. W. (2013). Increased Postprandial Energy Expenditure May Explain Superior Long Term Weight Loss after Roux-en-Y Gastric Bypass Compared to Vertical Banded Gastroplasty. *PLoS ONE*, *8*(4), e60280. https://doi.org/10.1371/journal.pone.0060280

Weyer, C., Funahashi, T., Tanaka, S., Hotta, K., Matsuzawa, Y., Pratley, R. E., & Tataranni, P. A. (2001). Hypoadiponectinemia in obesity and type 2 diabetes: Close association with insulin resistance and hyperinsulinemia. *The Journal of Clinical Endocrinology and Metabolism*, *86*(5), 1930–1935. https://doi.org/10.1210/jcem.86.5.7463

Williams, R., Karuranga, S., Malanda, B., Saeedi, P., Basit, A., Besançon, S., Bommer, C., Esteghamati, A., Ogurtsova, K., Zhang, P., & Colagiuri, S. (2020). Global and regional estimates and projections of diabetes-related health expenditure: Results from the International Diabetes

Federation Diabetes Atlas, 9th edition. *Diabetes Research and Clinical Practice*, *162*. https://doi.org/10.1016/j.diabres.2020.108072

Williams, T., Berelowitz, M., Joffe, S. N., Thorner, M. O., Rivier, J., Vale, W., & Frohman, L. A. (1984). Impaired Growth Hormone Responses to Growth Hormone–Releasing Factor in Obesity. *New England Journal of Medicine*, *311*(22), 1403–1407. https://doi.org/10.1056/NEJM198411293112203

Winzell, M. S., & Ahrén, B. (2007). G-protein-coupled receptors and islet function-implications for treatment of type 2 diabetes. *Pharmacology & Therapeutics*, *116*(3), 437–448. https://doi.org/10.1016/j.pharmthera.2007.08.002

Winzell, M. S., Nogueiras, R., Dieguez, C., & Ahrén, B. (2004). Dual action of adiponectin on insulin secretion in insulin-resistant mice. *Biochemical and Biophysical Research Communications*, *321*(1), 154–160. https://doi.org/10.1016/j.bbrc.2004.06.130

Withers, D. J., Gutierrez, J. S., Towery, H., Burks, D. J., Ren, J.-M., Previs, S., Zhang, Y., Bernal, D., Pons, S., Shulman, G. I., Bonner-Weir, S., & White, M. F. (1998). Disruption of IRS-2 causes type 2 diabetes in mice. *Nature*, *391*(6670), Article 6670. https://doi.org/10.1038/36116

Witkowski, P., Wijkstrom, M., Bachul, P. J., Morgan, K. A., Levy, M., Onaca, N., Chaidarun, S. S., Gardner, T., Shapiro, A. M. J., Posselt, A., Ahmad, S. A., Daffonchio, L., Ruffini, P. A., & Bellin, M. D. (2021). Targeting CXCR1/2 in the first multicenter, double-blinded, randomized trial in autologous islet transplant recipients. *American Journal of Transplantation*, *21*(11), 3714–3724. https://doi.org/10.1111/ajt.16695

Wojtusciszyn, A., Armanet, M., Morel, P., Berney, T., & Bosco, D. (2008). Insulin secretion from human beta cells is heterogeneous and dependent on cell-to-cell contacts. *Diabetologia*, *51*(10), 1843–1852. https://doi.org/10.1007/s00125-008-1103-z

World Health Organisation. (2023). https://www.who.int/news-room/fact-sheets/detail/diabetes

Wortham, M., & Sander, M. (2016). Mechanisms of β-cell functional adaptation to changes in workload. *Diabetes, Obesity & Metabolism*, *18*(Suppl 1), 78–86. https://doi.org/10.1111/dom.12729

Wrede, C. E., Dickson, L. M., Lingohr, M. K., Briaud, I., & Rhodes, C. J. (2002). Protein kinase B/Akt prevents fatty acid-induced apoptosis in pancreatic beta-cells (INS-1). *The Journal of Biological Chemistry*, *277*(51), 49676–49684. https://doi.org/10.1074/jbc.M208756200

Wu, C.-T., Lidsky, P. V., Xiao, Y., Lee, I. T., Cheng, R., Nakayama, T., Jiang, S., Demeter, J., Bevacqua, R. J., Chang, C. A., Whitener, R. L., Stalder, A. K., Zhu, B., Chen, H., Goltsev, Y., Tzankov, A., Nayak, J. V., Nolan, G. P., Matter, M. S., … Jackson, P. K. (2021). SARS-CoV-2 infects human pancreatic β cells and elicits β cell impairment. *Cell Metabolism*, *33*(8), 1565-1576.e5. https://doi.org/10.1016/j.cmet.2021.05.013

Wu, H., Patterson, C. C., Zhang, X., Ghani, R. B. A., Magliano, D. J., Boyko, E. J., Ogle, G. D., & Luk, A. O. Y. (2022). Worldwide estimates of incidence of type 2 diabetes in children and adolescents in 2021. *Diabetes Research and Clinical Practice*, *185*, 109785. https://doi.org/10.1016/j.diabres.2022.109785

Wu, J., Sun, P., Zhang, X., Liu, H., Jiang, H., Zhu, W., & Wang, H. (2012). Inhibition of GPR40 protects MIN6 β cells from palmitate-induced ER stress and apoptosis. *Journal of Cellular Biochemistry*, *113*(4), 1152–1158. https://doi.org/10.1002/jcb.23450

Wyder, L., Vitaliti, A., Schneider, H., Hebbard, L. W., Moritz, D. R., Wittmer, M., Ajmo, M., & Klemenz, R. (2000). Increased expression of H/T-cadherin in tumor-penetrating blood vessels. *Cancer Research*, *60*(17), 4682–4688.

Xiong, X., Sun, X., Wang, Q., Qian, X., Zhang, Y., Pan, X., & Dong, X. C. (2016). SIRT6 protects against palmitate-induced pancreatic β-cell dysfunction and apoptosis. *The Journal of Endocrinology*, *231*(2), 159–165. https://doi.org/10.1530/JOE-16-0317

Xu, G. G., & Rothenberg, P. L. (1998). Insulin receptor signaling in the beta-cell influences insulin gene expression and insulin content: Evidence for autocrine beta-cell regulation. *Diabetes*, *47*(8), 1243–1252. https://doi.org/10.2337/diab.47.8.1243

Xu, G., Stoffers, D. A., Habener, J. F., & Bonner-Weir, S. (1999). Exendin-4 stimulates both beta-cell replication and neogenesis, resulting in increased beta-cell mass and improved glucose tolerance in diabetic rats. *Diabetes*, *48*(12), 2270–2276. https://doi.org/10.2337/diabetes.48.12.2270

Xu, H., Barnes, G. T., Yang, Q., Tan, G., Yang, D., Chou, C. J., Sole, J., Nichols, A., Ross, J. S., Tartaglia, L. A., & Chen, H. (2003). Chronic inflammation in fat plays a crucial role in the development of obesity-related insulin resistance. *The Journal of Clinical Investigation*, *112*(12), 1821–1830. https://doi.org/10.1172/JCI19451

Xue, Y., Liu, C., Xu, Y., Yuan, Q., Xu, K., Mao, X., Chen, G., Wu, X., Brendel, M. D., & Liu, C. (2010). Study on pancreatic islet adaptation and gene expression during pregnancy in rats. *Endocrine*, *37*(1), 83–97. https://doi.org/10.1007/s12020-009-9273-0

Yamamoto, J., Imai, J., Izumi, T., Takahashi, H., Kawana, Y., Takahashi, K., Kodama, S., Kaneko, K., Gao, J., Uno, K., Sawada, S., Asano, T., Kalinichenko, V. V., Susaki, E. A., Kanzaki, M., Ueda, H. R., Ishigaki, Y., Yamada, T., & Katagiri, H. (2017). Neuronal signals regulate obesity induced β-cell proliferation by FoxM1 dependent mechanism. *Nature Communications*, *8*(1), Article 1. https://doi.org/10.1038/s41467-017-01869-7

Yamato, E., Tashiro, F., & Miyazaki, J. (2013). Microarray analysis of novel candidate genes responsible for glucose-stimulated insulin secretion in mouse pancreatic β cell line MIN6. *PloS One*, *8*(4), e61211. https://doi.org/10.1371/journal.pone.0061211

Yamauchi, T., Kamon, J., Ito, Y., Tsuchida, A., Yokomizo, T., Kita, S., Sugiyama, T., Miyagishi, M., Hara, K., Tsunoda, M., Murakami, K., Ohteki, T., Uchida, S., Takekawa, S., Waki, H., Tsuno, N. H., Shibata, Y., Terauchi, Y., Froguel, P., … Kadowaki, T. (2003). Cloning of adiponectin receptors

that mediate antidiabetic metabolic effects. *Nature*, *423*(6941), 762–769. https://doi.org/10.1038/nature01705

Yamauchi, T., Kamon, J., Waki, H., Terauchi, Y., Kubota, N., Hara, K., Mori, Y., Ide, T., Murakami, K., Tsuboyama-Kasaoka, N., Ezaki, O., Akanuma, Y., Gavrilova, O., Vinson, C., Reitman, M. L., Kagechika, H., Shudo, K., Yoda, M., Nakano, Y., … Kadowaki, T. (2001). The fat-derived hormone adiponectin reverses insulin resistance associated with both lipoatrophy and obesity. *Nature Medicine*, *7*(8), 941–946. https://doi.org/10.1038/90984

Yamazaki, H., Tauchi, S., Machann, J., Haueise, T., Yamamoto, Y., Dohke, M., Hanawa, N., Kodama, Y., Katanuma, A., Stefan, N., Fritsche, A., Birkenfeld, A. L., Wagner, R., & Heni, M. (2022). Fat Distribution Patterns and Future Type 2 Diabetes. *Diabetes*, *71*(9), 1937–1945. https://doi.org/10.2337/db22-0315

Yanagida, K., Igarashi, H., Yasuda, D., Kobayashi, D., Ohto-Nakanishi, T., Akahoshi, N., Sekiba, A., Toyoda, T., Ishijima, T., Nakai, Y., Shojima, N., Kubota, N., Abe, K., Kadowaki, T., Ishii, S., & Shimizu, T. (2018). The Gα12/13-coupled receptor LPA4 limits proper adipose tissue expansion and remodeling in diet-induced obesity. *JCI Insight*, *3*(24), e97293, 97293. https://doi.org/10.1172/jci.insight.97293

Yang, B., Li, J., Haller, M. J., Schatz, D. A., & Rong, L. (2022). The progression of secondary diabetes: A review of modeling studies. *Frontiers in Endocrinology*, *13*, 1070979. https://doi.org/10.3389/fendo.2022.1070979

Yang, B. T., Dayeh, T. A., Volkov, P. A., Kirkpatrick, C. L., Malmgren, S., Jing, X., Renström, E., Wollheim, C. B., Nitert, M. D., & Ling, C. (2012). Increased DNA Methylation and Decreased Expression of PDX-1 in Pancreatic Islets from Patients with Type 2 Diabetes. *Molecular Endocrinology*, *26*(7), 1203. https://doi.org/10.1210/me.2012-1004

Yang, C.-H., Ann-Onda, D., Lin, X., Fynch, S., Nadarajah, S., Pappas, E. G., Liu, X., Scott, J. W., Oakhill, J. S., Galic, S., Shi, Y., Moreno-Asso, A., Smith, C., Loudovaris, T., Levinger, I., Eizirik, D. L., Laybutt, D. R., Herzog, H., Thomas, H. E., & Loh, K. (2022). Neuropeptide Y1 receptor

antagonism protects β-cells and improves glycemic control in type 2 diabetes. *Molecular Metabolism*, *55*, 101413. https://doi.org/10.1016/j.molmet.2021.101413

Yang, D.-W., Qian, G.-B., Jiang, M.-J., Wang, P., & Wang, K.-Z. (2019). Inhibition of microRNA-495 suppresses chondrocyte apoptosis through activation of the NF-κB signaling pathway by regulating CCL4 in osteoarthritis. *Gene Therapy*, *26*(6), Article 6. https://doi.org/10.1038/s41434-019-0068-5

Yang, J., Wong, R. K., Park, M., Wu, J., Cook, J. R., York, D. A., Deng, S., Markmann, J., Naji, A., Wolf, B. A., & Gao, Z. (2006). Leucine regulation of glucokinase and ATP synthase sensitizes glucose-induced insulin secretion in pancreatic beta-cells. *Diabetes*, *55*(1), 193–201.

Yang, W., Yang, C., Luo, J., Wei, Y., Wang, W., & Zhong, Y. (2018). Adiponectin promotes preadipocyte differentiation via the PPARγ pathway. *Molecular Medicine Reports*, *17*(1), 428–435. https://doi.org/10.3892/mmr.2017.7881

Yang, Y., Lu, H. L., Zhang, J., Yu, H. Y., Wang, H. W., Zhang, M. X., & Cianflone, K. (2006). Relationships among acylation stimulating protein, adiponectin and complement C3 in lean vs obese type 2 diabetes. *International Journal of Obesity*, *30*(3), Article 3. https://doi.org/10.1038/sj.ijo.0803173

Yano, T., Liu, Z., Donovan, J., Thomas, M. K., & Habener, J. F. (2007). Stromal Cell–Derived Factor-1 (SDF-1)/CXCL12 Attenuates Diabetes in Mice and Promotes Pancreatic β-Cell Survival by Activation of the Prosurvival Kinase Akt. *Diabetes*, *56*(12), 2946–2957. https://doi.org/10.2337/db07-0291

Yatagai, T., Nagasaka, S., Taniguchi, A., Fukushima, M., Nakamura, T., Kuroe, A., Nakai, Y., & Ishibashi, S. (2003). Hypoadiponectinemia is associated with visceral fat accumulation and insulin resistance in Japanese men with type 2 diabetes mellitus. *Metabolism: Clinical and Experimental*, *52*(10), 1274–1278. https://doi.org/10.1016/s0026-0495(03)00195-1

Yue, J. T. Y., Burdett, E., Coy, D. H., Giacca, A., Efendic, S., & Vranic, M. (2012). Somatostatin receptor type 2 antagonism improves glucagon and corticosterone counterregulatory responses to

hypoglycemia in streptozotocin-induced diabetic rats. *Diabetes*, *61*(1), 197–207. https://doi.org/10.2337/db11-0690

Zander, M., Madsbad, S., Madsen, J. L., & Holst, J. J. (2002). Effect of 6-week course of glucagon-like peptide 1 on glycaemic control, insulin sensitivity, and beta-cell function in type 2 diabetes: A parallel-group study. *Lancet (London, England)*, *359*(9309), 824–830. https://doi.org/10.1016/S0140-6736(02)07952-7

Zapata, R. C., Carretero, M., Reis, F. C. G., Chaudry, B. S., Ofrecio, J., Zhang, D., Sasik, R., Ciaraldi, T., Petrascheck, M., & Osborn, O. (2022). Adipocytes control food intake and weight regain via Vacuolar-type H+ ATPase. *Nature Communications*, *13*(1), 5092. https://doi.org/10.1038/s41467-022-32764-5

Zhang, H., Colclough, K., Gloyn, A. L., & Pollin, T. I. (2021). Monogenic diabetes: A gateway to precision medicine in diabetes. *The Journal of Clinical Investigation*, *131*(3), e142244, 142244. https://doi.org/10.1172/JCI142244

Zhang, H., Liu, Y., Yu, B., & Lu, R. (2023). An optimized TRIzol-based method for isolating RNA from adipose tissue. *BioTechniques*, *74*(5), 203–209. https://doi.org/10.2144/btn-2022-0120

Zhang, M., Goforth, P., Bertram, R., Sherman, A., & Satin, L. (2003). The Ca2+ Dynamics of Isolated Mouse β-Cells and Islets: Implications for Mathematical Models. *Biophysical Journal*, *84*(5), 2852–2870.

Zhang, S., & Kuhn, J. R. (2018). *Figure 4, Hemocytometer used for counting cells.* [Text]. WormBook. https://www.ncbi.nlm.nih.gov/books/NBK153594/figure/cellculture_figure4/

Zhang, Y., Han, C., Zhu, W., Yang, G., Peng, X., Mehta, S., Zhang, J., Chen, L., & Liu, Y. (2021). Glucagon Potentiates Insulin Secretion Via β-Cell GCGR at Physiological Concentrations of Glucose. *Cells*, *10*(9), 2495. https://doi.org/10.3390/cells10092495

Zhang, Y., Proenca, R., Maffei, M., Barone, M., Leopold, L., & Friedman, J. M. (1994). Positional cloning of the mouse obese gene and its human homologue. *Nature*, *372*(6505), Article 6505. https://doi.org/10.1038/372425a0

Zhao, P., & Saltiel, A. R. (2020). Interaction of Adipocyte Metabolic and Immune Functions Through TBK1. *Frontiers in Immunology*, *11*, 592949. https://doi.org/10.3389/fimmu.2020.592949

Zhao, X., Hu, H., Wang, C., Bai, L., Wang, Y., Wang, W., & Wang, J. (2019). A comparison of methods for effective differentiation of the frozen-thawed 3T3-L1 cells. *Analytical Biochemistry*, *568*, 57–64. https://doi.org/10.1016/j.ab.2018.12.020

Zheng, Y., Ley, S. H., & Hu, F. B. (2018). Global aetiology and epidemiology of type 2 diabetes mellitus and its complications. *Nature Reviews. Endocrinology*, *14*(2), 88–98. https://doi.org/10.1038/nrendo.2017.151

Zhu, Y., Qi, C., Korenberg, J. R., Chen, X. N., Noya, D., Rao, M. S., & Reddy, J. K. (1995). Structural organization of mouse peroxisome proliferator-activated receptor gamma (mPPAR gamma) gene: Alternative promoter use and different splicing yield two mPPAR gamma isoforms. *Proceedings of the National Academy of Sciences of the United States of America*, *92*(17), 7921–7925.

Zorena, K., Michalska, M., Kurpas, M., Jaskulak, M., Murawska, A., & Rostami, S. (2022). Environmental Factors and the Risk of Developing Type 1 Diabetes-Old Disease and New Data. *Biology*, *11*(4), 608. https://doi.org/10.3390/biology11040608

Abstracts and publications

Alterations in mouse visceral adipose tissue mRNA expression of islet G protein-coupled receptor ligands in obesity. Ashik, T., Lee, V., Atanes, P., & Persaud, S.J. (2022). *Diabetic Medicine: A Journal of the British Diabetic Association, 39*(12), p.e14978. Published.

Acylation of the incretin peptide exendin-4 directly impacts GLP-1 receptor signalling and trafficking. Lucey, M., Ashik, T., Marzook, A., Wang, Y., Goulding, J., Oishi, A., Broichhagen, J., Hodson, D.J., Minnion, J., Elani, Y., Jockers, R., Briddon, S.J., Bloom, S.R., Tomas, A., & Jones, B. (2021). *Molecular Pharmacology, 100*(4), pp.319–334. Published.

High-fat diet-induced up-regulation of chemokine CCL4 in visceral adipose tissue: potential crosstalk with beta cells. Ashik, T., Lee, V., Atanes, P., & Persaud, S.J. (2021). Basic and clinical science posters: Beta cells, islets and stem cells. *Diabetic Medicine, 38*(S1). Published Supplement.

Obesity-induced changes in human islet G protein-coupled receptor expression: Implications for metabolic regulation. Atanes, P., Ashik, T., & Persaud, S.J. (2021). *Pharmacology & Therapeutics, 228*, p.107928. Published.

High-fat diet-induced up-regulation of chemokine CCL4 in visceral adipose tissue: potential crosstalk with beta cells. Ashik, T., Lee, V., Atanes, P., & Persaud, S.J. (2021). *57th EASD Annual Meeting of the European Association for the Study of Diabetes. Diabetologia, 64*(S1), pp.1–380. Published Supplement.

Conference oral presentations and posters

- The European Association for the Study of Diabetes Annual Meeting (2021, 2022 & 2023)
- King's BHF Centre PGR Symposium (2022 & 2023)
- Diabetes UK Professional Conference (2021 & 2022)

- Scientific Meeting of Quebec Society of Lipidology, Nutrition and Metabolism and The Cardiometabolic Health, Diabetes and Obesity Research Network (2023)
- MRC DTP Symposium (2021, 2022 & 2023)
- School of Life Course Sciences Symposium (2021 & 2022)
- Society of Endocrinology BES Conference (2021)

Awards and nominations

- Mitacs Globalink Research Award in partnership with UKRI (2022/23) – Winner
- Diabetes UK Basic Science Poster Award (2022) – Nominee
- School of Life and Population Sciences PGR Best Poster (2021) – Winner
- Faculty PGR Excellence Award (2021) – Nominee
- Lilly Diabetes Basic Science Award (2021) – Nominee